Stem Cells International

Factors Regulating Stem Cell Biology in Development and Disease

Guest Editors: Stefan Liebau, Alexander Kleger, Paul Gadue, Kodandaramireddy Nalapareddy, and Guido von Figura

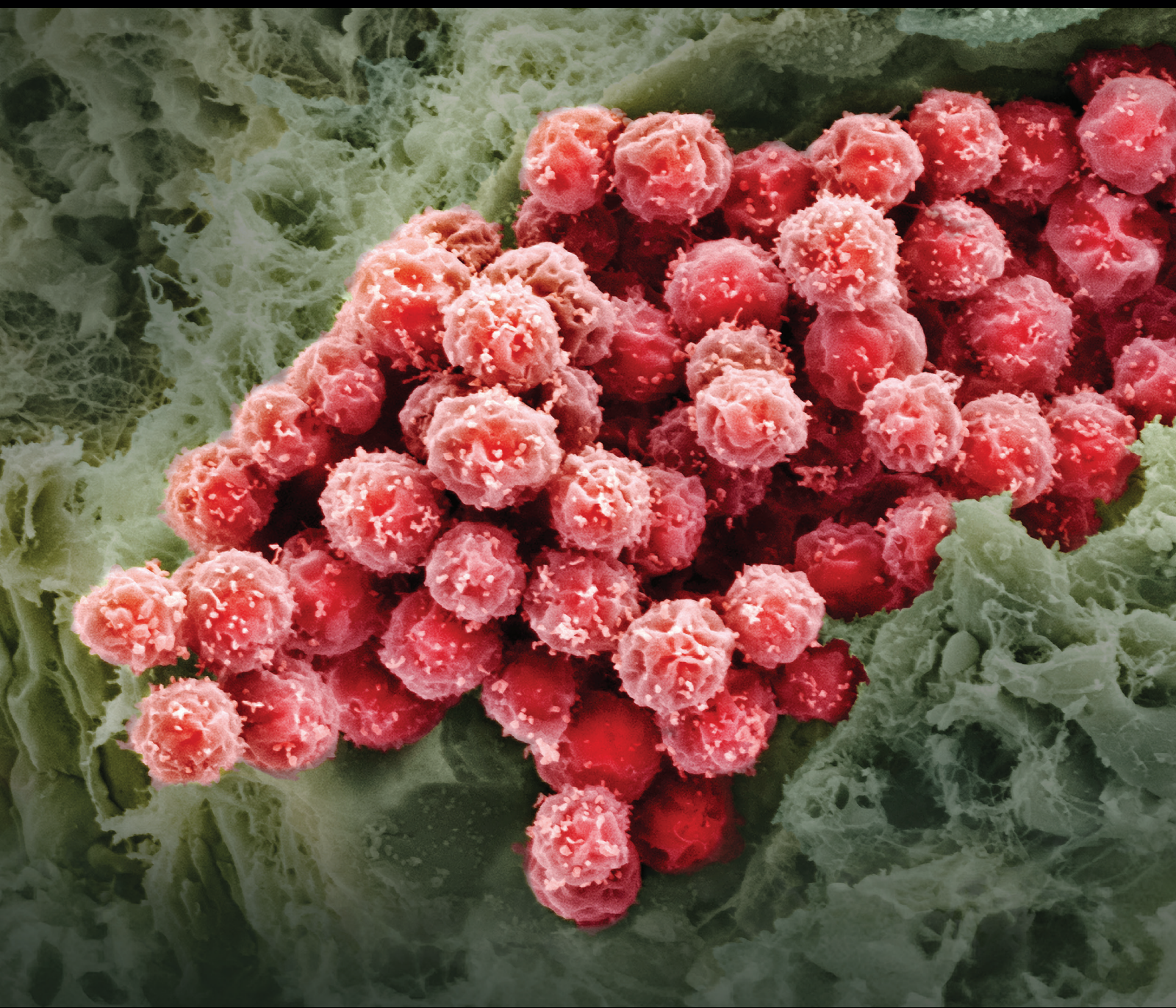

Factors Regulating Stem Cell Biology in Development and Disease

Stem Cells International

Factors Regulating Stem Cell Biology in Development and Disease

Guest Editors: Stefan Liebau, Alexander Kleger, Paul Gadue, Kodandaramireddy Nalapareddy, and Guido von Figura

Editorial Board

Contents

Hindawi Publishing Corporation
Stem Cells International
Volume 2016, Article ID 7170642, 3 pages
http://dx.doi.org/10.1155/2016/7170642

Editorial

Factors Regulating Stem Cell Biology in Development and Disease

Stefan Liebau,[1,2] Paul Gadue,[3] Kodandaramireddy Nalapareddy,[4] Guido von Figura,[5] and Alexander Kleger[6]

[1]*Institute of Neuroanatomy & Developmental Biology, Eberhard Karls University Tübingen, 72074 Tübingen, Germany*
[2]*Center for Neurosensory Systems (ZFN), Eberhard Karls University Tübingen, 72074 Tübingen, Germany*
[3]*Children's Hospital of Philadelphia (CHOP), University of Pennsylvania, 3501 Civic Center Boulevard, Philadelphia, PA 19104, USA*
[4]*Division of Experimental Hematology & Cancer Biology, 3333 Burnet Avenue, Cincinnati, OH 45229, USA*
[5]*II. Medizinische Klinik und Poliklinik, Klinikum rechts der Isar München, Technische Universität München, 81675 Munich, Germany*
[6]*Department of Internal Medicine I, University of Ulm, Albert-Einstein-Allee 11, 89081 Ulm, Germany*

Correspondence should be addressed to Stefan Liebau; stefan.liebau@uni-tuebingen.de

Received 28 September 2015; Accepted 29 September 2015

Stem cells in general are characterized by their ability to self-renew and to differentiate towards various progeny. Great efforts started to give hope since the first discovery of mammalian pluripotency by Stevens and Little, 1954; the field of stem cell research using pluripotent stem cells (PSC) has reached a state of general interest in both science and medicine. Following an overall fast development of *in vivo* and *in vitro* research, stem cells are nowadays regularly implied in developmental and pathomechanistical studies. Their unique ability to generate all cell types of the respective organism allows for the directed differentiation of *in vitro* cultured PSCs into the desired direction. Subsequently, development and function of this differentiated progeny may be investigated in detail. This specifically accounts for the human system where primary materials as well as *in vivo* studies are strongly limited. In addition, the groundbreaking study describing the generation of PSCs from somatic cells by Takahashi and Yamanaka, served as a lift for unlimited use of individual and patient specific stem cell based investigations. Today, these induced pluripotent stem cells (iPSCs) are amongst others utilized to explicitly study human pathomechanisms in a patient specific setting. Moreover, tissue specific stem cell, for example, serving as a cellular reserve and substitute for decayed cells and degenerated tissue, is discussed as a useful source of human tissue and tissue specific cells. Clearly, these adult stem cells have already been successfully used in therapeutic approaches for decades, such as hematopoietic stem cells in bone marrow transplantations.

Numerous studies exploiting stem cells have already been published describing distinct pathomechanisms in rare and common diseases, giving hope for future therapeutic startups.

Moreover, in the current decade, the first reports of using PSCs in therapeutic approaches have been announced and further upcoming clinical trials in several organ systems are approved and ready to start. Nevertheless, it is still crucial to thoroughly understand underlying cellular mechanisms and molecular pathways implied in developmental and pathological surroundings. In that sense, recent reports suggest that "stem cell factors" fulfill additional functions during the stepwise phases of cell lineage commitment. For instance, during germ layer formation, Oct4 and Tbx3 promote mesodermal as well as endodermal fate and limit neuroectoderm differentiation potential. In contrast, Sox2 enhances neuroectoderm specification while restricting mesoderm and endoderm lineage development. Later, these factors are subsequently involved in tissue development. Second, one hallmark of cancer is the ability to reactivate genetic programs known from early development and stem

cells. Interestingly, signalling cascades regulating early patterning in the embryo such as Nodal signalling are again overexpressed during cancer development, and "stem cell factors" can drive dysplasia and tumorigenesis suggesting an intimate link between embryonic cell fate decisions, stem cells, and tumour development.

To that end we have gathered a variety of studies under the umbrella of stem cell development and disease to provide a basis to understand the steps from basic stem cell biology, further going to physiological function during development until disturbances in function leading to pathological symptoms.

On the basis of stem cell biology, M. Nawaz et al. summarize the existing knowledge on stem cell derived extracellular vesicles (EVs). Current knowledge includes that stem cells continuously secrete factors into surrounding compartments serving as autocrine as well as paracrine signal modifiers. Moreover, abundance of EVs has been reported that mimic the phenotypes of the cells from which they originate. They hereby seem to play a role in the exchange of genetic information utilizing persistent bidirectional communication. This implies that EVs could regulate stemness, self-renewal, and differentiation in stem cells and their subpopulations.

A poorly investigated stem cell population is the trophoblast stem cell (TSC), responsible for the generation and function of the fetal placenta. S. J. Arnold et al. thoroughly investigated these TSCs concerning their expression profile *in vivo* and *in vitro*. Using a remarkable set of methods and approaches, they broadly contribute to the knowledge on TSCs and provide a well-defined set of markers and transcriptional signatures of these cells. Moreover, they investigate the time-dependent expression of several genes involved in early differentiation events both on mRNA and protein levels.

In the field of adult mesenchymal stem cells (MSCs), which are still considered as a great hope for a variety of clinical implications, K. C. Elahi et al. briefly discuss both the facts that isolated MSCs are blend of distinct cells and MSCs isolated from different tissues show besides some common features some significant differences. Nevertheless, they point to the fact that these differences could also be a benefit for distinct approaches. For example, subsets of MSCs seem to express distinct and unique sets of surface markers, which might help to find a perfect subpopulation for a respective utilization.

In the system of MSCs, S. Wang et al. provide a study applying transcriptome analyses on Toll-like receptor 3-activated MSCs. TLR3 activity in MSCs was reported to have an impact on MSC function and might therefore be a candidate to understand MSC physiology. Nevertheless, long noncoding RNAs (lncRNAs) were thought to play a role in this system. S. Wang et al. now give a thorough overview on involved lncRNAs using genome-wide transcriptome arrays which might be useful for further studies in TLR3-activated MSCs.

In terms of MSC differentiation signals, J. Chen et al. contribute a study describing the impact of TGFß/Smad signaling for chondrogenic differentiation. Here they explore the role of exogenous heparin sulfate (HS) in terms of its underlying molecular mechanism in MSC chondrogenesis. They applied HS both alone and in combination with TGF-ß and thereby modified TGF-ß receptor expression and ratios, also having an impact on Smad 2/3 activity.

In the neural system, enteric clusters of neurons are crucial to uphold gastrointestinal movement and regulation. Here, P. H. Neckel et al. provide new information on the transcriptome of enteric neural system (ENS) progenitor cells. They report on differentially regulated genes compared in proliferating and differentiating ENSs involved in pathways such as cell cycle, apoptosis, proliferation, or differentiation.

Besides the expected differences in cell cycle regulation they also reported on marked inactivation of the canonical Wnt-pathway after induction of differentiation.

In a second study on the enteric nervous system, K. Nothelfer et al. further extend the knowledge about the Wnt-Fzd-pathway in the ENS. They investigated the expression of the Wnt receptor frizzled-4 in the human ENS of small and large intestines and found a significant abundance of frizzled-4 in a subpopulation of enteric neuronal and glial cells. Moreover they observe a copositivity of frizzled-4 with neural progenitor markers nestin and p75ntr, implying a role of frizzled-4 during the development of the ENS.

On the reverse developmental pathway describing the reprogramming of somatic cells to induced pluripotent stem cells, a huge number of mechanisms and transcription factors are involved in the turn of maturity to pluripotency. Here, it was already reported that T-box transcription factors play distinct roles in the pluripotency network itself as well as during early steps of development. In this respect, M. Klingenstein et al. provide evidence that although Tbx3 is positively promoting iPS cell reprogramming, it still is not crucial for the generation or persistence of iPS cells. This information might fill a gap of knowledge concerning factors involved in both pluripotency and in early steps of cell fate determination, cell development, and adult function.

Signaling pathways and underlying factors represent the crucial set to upkeep stemness *in vivo* and *in vitro*. Nevertheless, during recent years it has become evident that these factors and their balance are also involved in early cell fate choice. In a summary on pluripotency factors, C. Weidgang et al. summarize current knowledge about the role of these factors not only in pluripotent conditions, but also during early cell fate determination, namely, the exit from pluripotency. Herein, a thorough and well-defined overview is provided as useful germ layer-related classifier of pluripotency factors.

Organ development occurs in a cell but also niche-dependent manner. Herein, the developing pancreas gives a bona fide example where pancreatic epithelial cells develop in branching morphogenesis while receiving important signaling input from the overlying mesenchyme. H. A. Russ and colleagues complemented a transgenic mouse model to label the pancreatic mesenchyme with subsequent proteomic analysis. Thereby, three potentially important factors for pancreatic development were identified, which the authors validated in directed differentiation efforts of human embryonic stem cells. Taken together, analyzing the proteome of supporting tissues in mouse models may aid to identify novel regulators of pancreatic differentiation of human pluripotent

stems cells and thereby improve purity of currently available protocols.

Pancreatic development occurs in a stepwise and tightly regulated manner, a process strongly dependent on a transcription factor orchestra including Pdx1, Prrx1, or Sox9. M. Reichert and colleagues shed light on the role of such factors during initiation of pancreatic cancer. Herein, the authors outline the stepwise onset of various pancreatic cancer progenitor lesions and put the governing factors in both a developmental and cancerous context. In that sense they develop a model for developmental factors regulating acinar and duct cell transformation, to date the most critical and earliest event of pancreatic cancer onset.

Following this track, E. Hessmann and colleagues identified the Nfatc4-Sox9 axis as a critical driver of acinar cell plasticity and pancreatic cancer initiation. Oncogenic Kras requires secondary hits to drive premalignant lesions in the pancreas toward carcinogenesis. Herein, developmental pathways such as the epidermal growth factor signaling axis are sufficient to pass this premalignant border. The authors complemented acinar explant cultures with immunohistochemical methods and chromatin immunoprecipitation analysis to identify the fact that Nftac4 is activated by EGFR signaling and initiates acinar to ductal metaplasia by direct transcriptional activation of Sox9. Thereby, the authors provide additional evidence supporting a Janus face of Sox9 during development and cancer in the pancreas.

Finally, M. Quante et al. developed a novel 3D culture system to study cancerous and normal intestinal tissue in a niche-dependent context. The complementation of intestinal but also premalignant Barrett epithelium derived organoid cultures with various matrices and cocultured cell types enabled the group to study niche-dependent effects in the gastrointestinal tract. In turn, myofibroblasts but also neurons from the enteric nervous system boosted organoid growth and enhanced survival. The developed platform provides unique access to modulate and mimic cancerous growth *in vitro* and at the same time to study niche-dependence in self-renewing (cancer) stem cells.

Taken together, the current special issue provides a unique disquisition on embryonic and somatic stem cells in healthy but also diseased tissues and the impact of stem cell factors and niche-effects on their differentiation and self-renewal capacity. Again, the parallel lines between embryonic development and cancer onset, governed by similar factors in different contexts, become evident and disclose the importance to understand both similarities and discrepancies of these processes.

Stefan Liebau
Paul Gadue
Kodandaramireddy Nalapareddy
Guido von Figura
Alexander Kleger

Hindawi Publishing Corporation
Stem Cells International
Volume 2016, Article ID 1520136, 10 pages
http://dx.doi.org/10.1155/2016/1520136

Research Article

Exogenous Heparan Sulfate Enhances the TGF-β3-Induced Chondrogenesis in Human Mesenchymal Stem Cells by Activating TGF-β/Smad Signaling

Juan Chen,[1,2] Yongqian Wang,[3] Chong Chen,[4] Chengjie Lian,[5] Taifeng Zhou,[4] Bo Gao,[5] Zizhao Wu,[5] and Caixia Xu[1]

[1]*Research Center for Translational Medicine, The First Affiliated Hospital of Sun Yat-sen University, Guangzhou 510080, China*
[2]*School of Life Sciences, Sun Yat-sen University, Guangzhou 510275, China*
[3]*Department of Musculoskeletal Oncology, The First Affiliated Hospital of Sun Yat-sen University, Guangzhou 510080, China*
[4]*Department of Orthopedic Surgery, The First Affiliated Hospital of Sun Yat-sen University, Guangzhou 510080, China*
[5]*Department of Spine Surgery, Sun Yat-sen Memorial Hospital, Guangzhou 510120, China*

Correspondence should be addressed to Caixia Xu; xucx3@mail.sysu.edu.cn

Received 26 May 2015; Revised 21 July 2015; Accepted 10 August 2015

Academic Editor: Alexander Kleger

Heparan sulfate (HS) interacts with growth factors and has been implicated in regulating chondrogenesis. However, the effect of HS on TGF-β-mediated mesenchymal stem cell (MSC) chondrogenesis and molecular mechanisms remains unknown. In this study, we explored the effects of exogenous HS alone and in combination with TGF-β3 on chondrogenic differentiation of human MSCs and possible signal mechanisms. The results indicated that HS alone had no obvious effects on chondrogenic differentiation of human MSCs and TGF-β/Smad2/3 signal pathways. However, the combined TGF-β3/HS treatment resulted in a significant increase in GAG synthesis, cartilage matrix protein secretion, and cartilage-specific gene expression compared to cells treated with TGF-β3 alone. Furthermore, HS inhibited type III TGF-β receptors (TβRIII) expression and increased TGF-β3-mediated ratio of the type II (TβRII) to the type I (TβRI) TGF-β receptors and phosphorylation levels of Smad2/3. The inhibitor of the TGF-β/Smad signal, SB431542, not only completely inhibited HS-stimulated TGF-β3-mediated Smad2/3 phosphorylation but also completely inhibited the effects of HS on TGF-β3-induced chondrogenic differentiation. These results demonstrate exogenous HS enhances TGF-β3-induced chondrogenic differentiation of human MSCs by activating TGF-β/Smad2/3 signaling.

1. Introduction

Mesenchymal stem cells (MSCs), because of their extensive proliferative capacity and strong chondrogenic potential, represent a promising cell source for cartilage repair [1, 2]. Effective chondrogenic induction of MSCs for the repair of cartilage damage remains a great challenge. A lot of research has focused on the factors and molecular mechanisms enhancing chondrogenic potential of MSCs [3, 4]. Among the factors, growth factors play important roles in regulating chondrogenesis [5]. Transforming growth factor-β3 (TGF-β3), a member of TGF-β superfamily, is the most extensively used growth factor for inducing differentiation of MSCs [6]. Studies have demonstrated that TGF-β3 stimulates cartilage formation both in vitro and in vivo, producing more collagen II and aggrecan in MSC cultures than either TGF-β1 or TGF-β2 [5, 7].

TGF-β enhances the expression of chondrogenic markers by activating typical TGF-β/Smad signaling. TGF-β signaling is initiated through the sequential activation of two serine/threonine kinase receptors: the type II (TβRII) and the type I (TβRI) TGF-β receptors. The TGF-β ligand, binding to TβRII, phosphorylates and activates TβRI to form a large ligand-receptor complex, which then activates downstream Smad2/3 molecule and induce TGF-β-dependent transcriptional programs [8]. The type III TGF-β receptor (TβRIII),

also named betaglycan, is a widely expressed heparan sulfate (HS) and chondroitin sulfate (CS) proteoglycan that is believed to be a coreceptor for TGF-β [9]. TβRIII modulates TGF-β signaling by binding and presenting TGF-βs ligand to TβRII [10, 11].

Recently, there is increasing evidence that extracellular matrix (ECM), as a major component of cell niche, plays a central role in MSCs proliferation and differentiation through the regulation of the growth factor interactions between the ECM and cells [12, 13]. Heparan sulfates (HSs) are highly sulfated glycosaminoglycans (GAGs) [14, 15]. In vivo, they covalently attach to different core proteins to form heparan sulfate proteoglycans (HSPGs), which exist on the cell surfaces or in the ECM of multiple tissues, including developing and mature cartilage [16, 17]. Studies have demonstrated that HSPGs play key roles in cartilage development and skeletal growth [18–20]. HS chains in HSPG interactions with a variety of chondroregulatory molecules have been implicated in regulating chondrogenesis through various signaling pathways, including fibroblast growth factors (FGFs), bone morphogenetic proteins (BMPs), TGF-βs, Wnt, and Hedgehog [20]. TGF-βs are important chondroregulatory factors that have been shown to interact with HS [21]. Chen et al. reported that HSPGs might play an important role in regulating TGF-β through the regulation of latent transforming growth factor-β-binding protein (LTBP1) assemblies [22]. Cell-surface HS proteoglycans have been shown to modulate TGF-β responsiveness in epithelial cells and other cell types [10]. However, the direct role of exogenous HS in TGF-β-mediated chondrogenesis of MSCs and corresponding molecular mechanisms remains to be demonstrated.

We used an in vitro human MSC (hMSC) chondrogenic differentiation model to study the role of exogenous HS in TGF-β3-induced chondrogenesis and TGF-β/Smad signaling. Our results suggest that exogenous HS clearly potentiates TGF-β3-induced chondrogenic differentiation of hMSCs by modulating the expression mode of TGF-β receptors and by activating the downstream Smad signaling pathway.

2. Materials and Methods

2.1. Cell Isolation and Culture. The Ethics Committee of the First Affiliated Hospital of Sun Yat-sen University approved this study, and all the subjects provided written informed consent. The bone marrow samples are from three healthy volunteer donors with an age range of 18 to 22 years. They have no physical disease. hMSCs were isolated and purified by the following method of density gradient centrifugation [23]. Briefly, the bone marrow samples were added to Ficoll-Paque (1.077 g/mL) (TBD, Tianjin, China) and centrifuged for 20 min at 500 g. The mononuclear cells were resuspended in low-glucose Dulbecco's modified Eagle medium (L-DMEM) (Gibco, Invitrogen Corporation, NY, USA) supplemented with 10% fetal bovine serum (FBS) (Gibco, Invitrogen Corporation, Uruguay) and were incubated at 37°C under 5% CO_2. After 48 h, nonadherent cells were removed by changing the medium. Cells were passaged in culture when 80–90% confluence was reached. We used cells from passage 3 to passage 6 in our experiments.

2.2. Chondrogenic Differentiation of hMSCs in Pellet Culture. Human MSCs were harvested and resuspended at 2×10^7 cells/mL, according to the following procedure [24]. Cell droplets ($4 \times 10^5/20\ \mu$L) were divided into four groups. Group 1 (C group) was maintained in the chondrogenic control medium consisting of high-glucose DMEM (H-DMEM), supplemented with 50 μg/mL vitamin C, 100 nM dexamethasone, 1 mM sodium pyruvate, 40 μg/mL proline, and ITS+ Universal Culture Supplement Premix (BD Biosciences, NY, USA) (final concentrations: 6.25 μg/mL bovine insulin, 6.25 μg/mL transferrin, 6.25 μg/mL selenous acid, 5.33 μg/mL linoleic acid, and 1.25 mg/mL bovine serum albumin (BSA)). Group 2 (HS group) was maintained in the control medium, supplemented with 100 μg/mL HS (Sigma-Aldrich, St. Louis, USA). Group 3 (T group) was maintained in the control medium, supplemented with 10 ng/mL TGF-β3 (PeproTech, Rocky Hill, USA). Group 4 (T + HS group) was maintained in the control medium, supplemented with 100 μg/mL HS and 10 ng/mL TGF-β3. Cell droplets were incubated at 37°C/5% CO_2. The medium was changed every 3 days, and induced cartilage tissues were harvested on days 3, 7, 14, and 21.

2.3. Quantitative Analysis of Glycosaminoglycan (GAG). The harvested cartilage balls were washed and then digested in phosphate-buffered saline (PBS) solution containing 0.03% papain, 5 mM cysteine hydrochloride, and 10 mM EDTA-Na2 for 16 h at 65°C. The DNA concentration was measured using the Hoechst 33258 binding assay. Briefly, an aliquot of the lysate was reacted with 0.7 μg/mL Hoechst 33258 solution (Sigma-Aldrich, St. Louis, USA) for 10 min and then was measured using a SpectraMax M5 Microplate Reader (Molecular Devices, Sunnyvale, CA, USA) at 340 nm for excitation and 465 nm for emission. The 1,9-dimethylmethylene blue (DMMB) (Sigma-Aldrich, St. Louis, USA) dye binding assay was used for detecting GAG concentration. Similarly, an aliquot of the lysate was reacted with DMMB solution for 10 min in the absence of light, and the absorbance at 525 nm was measured using a Varioskan Flash Multimode Reader (Thermo Scientific, Waltham, MA, USA). GAG content was normalized against DNA content.

2.4. Histology and Immunohistochemistry. The different groups of chondrogenic pellets were harvested on day 7 after chondrogenic induction. The pellets were fixed in 4% paraformaldehyde for 1 day and embedded in paraffin. Paraffin sections (4 μm thick) were deparaffinized using xylene, rehydrated through a graded series of washes in ethanol, and finally rinsed in PBS. Sections were stained with hematoxylin and eosin (HE) (Sigma-Aldrich, St. Louis, USA) for cartilage structure and 0.1% Alcian blue (AB) (Sigma-Aldrich, St. Louis, USA) for proteoglycan. For immunohistochemistry, rehydrated sections were treated with a pepsin solution at 37°C for 10 min, incubated with 3% H_2O_2 for 10 min and with blocking serum for 15 min, and then were allowed to react overnight with rabbit anti-human collagen type II polyclonal antibodies (Abzoom Biolabs, Dallas, TX, USA), diluted at 1 : 1000 at a temperature of 4°C. Afterwards, biotinylated goat anti-rabbit IgG (EarthOx, SFO, USA) was applied for 30 min. Sections were incubated

Table 1: Primers used for real-time PCR.

Gene	Forward primer (5′ to 3′)	Reverse primer (5′ to 3′)
GAPDH	5′-AGAAAAACCTGCCAAATATGATGAC-3′	5′-TGGGTGTCGCTGTTGAAGTC-3′
Col2A1	5′-GGCAATAGCAGGTTCACGTACA-3′	5′-CGATAACAGTCTTGCCCCACTT-3′
ACAN	5′-TGCATTCCACGAAGCTAACCTT-3′	5′-GACGCCTCGCCTTCTTGAA-3′
SOX9	5′-AGCGAACGCACATCAAGAC-3′	5′-GCTGTAGTGTGGGAGGTTGAA-3′
TβRI	5′-ATTACCAACTGCCTTATTATGA-3′	5′-CATTACTCTCAAGGCTTCAC-3′
TβRII	5′-ATGGAGGCCCAGAAAGATG-3′	5′-GACTGCACCGTTGTTGTCAG-3′
TβRIII	5′-GTGTTCCCTCCAAAGTGCAAC-3′	5′-AGCTCGATGATGTGTACTTCCT-3′

GAPDH: glyceraldehyde-3-phosphate dehydrogenase; COL2A1: collagen type II; ACAN: aggrecan; SOX9: SRY (sex determining region Y)-box 9; TβRI/II/III: recombinant human transforming growth factor-β receptor type I/II/III.

with peroxide-conjugated streptavidin working solution and stained with 3,3′-diaminobenzidine tetrahydrochloride (DAB) (Jinshan Jinqiao, Beijing, China), and staining was visualized using an Axio observer Z1 microscope (Zeiss, Göttingen, Germany).

For fluorescent immunohistochemistry staining, tissue sections were microwaved in a 10 mM citrate buffer, blocked for 1 h with PBS containing 5% BSA, and reacted overnight with the appropriate primary antibodies (human TβRI antibody (Santa Cruz, Dallas, USA); human TβRII antibody (RD Systems); and human TβRIII antibody (Santa Cruz, Dallas, USA)), diluted at 1 : 50 at 4°C. Tissue sections were incubated then with fluorescein isothiocyanate (FITC) conjugated secondary antibodies (diluted 1 : 100) for 1 h at room temperature. Finally, sections were stained with (4′,6-diamidino-2-phenylindole) DAPI (1 mg/mL), covered with glycerol, and examined using a Zeiss LSM 710 confocal microscope (Carl Zeiss, Heidelberg, Germany).

2.5. RNA Extraction and Real-Time PCR Analysis. Total RNA was extracted from pellets using an RNAsimple Total RNA Kit (Tiangen, China) and reverse transcribed into cDNA using a PrimeScript RT Reagent Kit (Takara, Osaka, Japan) at day 7 after chondrogenic induction. Real-time polymerase chain reaction (PCR) was performed in triplicate using a Bio-Rad real-time PCR Detection System with iQ 5 optical system software (Bio-Rad Laboratories, Hercules, CA, USA) and SYBR Green I Master Mix (Takara, Osaka, Japan). Expression of the following genes was analyzed: aggrecan (ACAN); collagen type II, alpha 1 (COL2A1); SRY (sex determining region Y)-box 9 (SOX9); TβRI; TβRII; and TβRIII. The level of expression of the glyceraldehyde-3-phosphate dehydrogenase (GAPDH) gene was used as an internal control. The primer sequences are listed in Table 1. The relative expression levels for each target gene were calculated using the $2^{-\Delta\Delta CT}$ method.

2.6. Western Blot. After 24 h of chondrogenic induction, proteins were extracted from the pellets with radioimmunoprecipitation assay (RIPA) lysis buffer containing protease and phosphatase (CWBio, Beijing, China). The protein concentration was then measured with a bicinchoninic acid assay using a BCA Protein Assay Kit (CWBio, Beijing, PR China) and conserved at –80°C. For the western blot, equal amounts of proteins were separated by sodium dodecyl sulfate polyacrylamide gel electrophoresis and transferred onto a polyvinylidene difluoride (PVDF) membrane (Millipore, Boston, USA) at 250 mM for 100 minutes using a PowerPac Basic electrophoresis apparatus (Bio-Rad, Hercules, USA). The PVDF membranes were blocked for 1 h with 5% skim milk/Tris-buffered saline containing 0.1% Tween-20 (TBST) and then were incubated overnight at 4°C with the appropriate primary antibodies: rabbit anti-phospho-Smad2 (Ser465/467)/Smad3 (Ser423/425) (Cell Signaling), rabbit anti-Smad2/3 (Cell Signaling, Danvers, USA), and anti-GAPDH monoclonal antibody (EarthOx, SFO, USA). All the primary antibodies were applied at a 1 : 1000 dilution. After the primary antibody reaction, target proteins were detected using HRP-conjugated goat anti-rabbit IgG (diluted 1 : 10,000) for 1 h. The immune complexes were then detected using SuperSignal West Pico Chemiluminescent Substrate (Pierce, NY, USA) and they were visualized via the Image Quant Las4000mini (GE Healthcare, UK). The protein levels in the phosphorylated Smad2/3 were quantified and normalized to the total Smad2/3 quantities.

2.7. Inhibition of TGF-β/Smad Signaling. To assess the role of the TGF-β/Smad signaling in HS regulation of TGF-β3-induced hMSCs chondrogenic differentiation, the cells were treated with or without SB431542 (Sigma-Aldrich, St. Louis, USA) 2 h before stimulation by either 10 ng/mL of TGF-β3 alone or 100 μg/mL HS combined with 10 ng/mL TGF-β3. SB431542 is a selective inhibitor of activin receptor-like kinase ALK5 (TβRI), whereas Smad2 and Smad3 are substrates for ALK5. SB431542 has been demonstrated as being the specific inhibitor for TGF-β/Smad pathway [25]. After 7 days of chondrogenic induction, the cells were collected, and phospho-Smad2 (Ser465/467)/Smad3 (Ser423/425) antibodies were detected by western blot. The chondrogenic differentiation ability of hMSCs was assayed by immunohistochemistry staining for collagen type II and by real-time PCR for chondrogenic genes expression.

2.8. Statistical Analysis. All quantitative data were presented as mean values ± standard errors (SE). Statistical analysis, consisting of one-way ANOVA followed by a LSD t-test, was performed using SPSS 16.0 statistical software (SPSS,

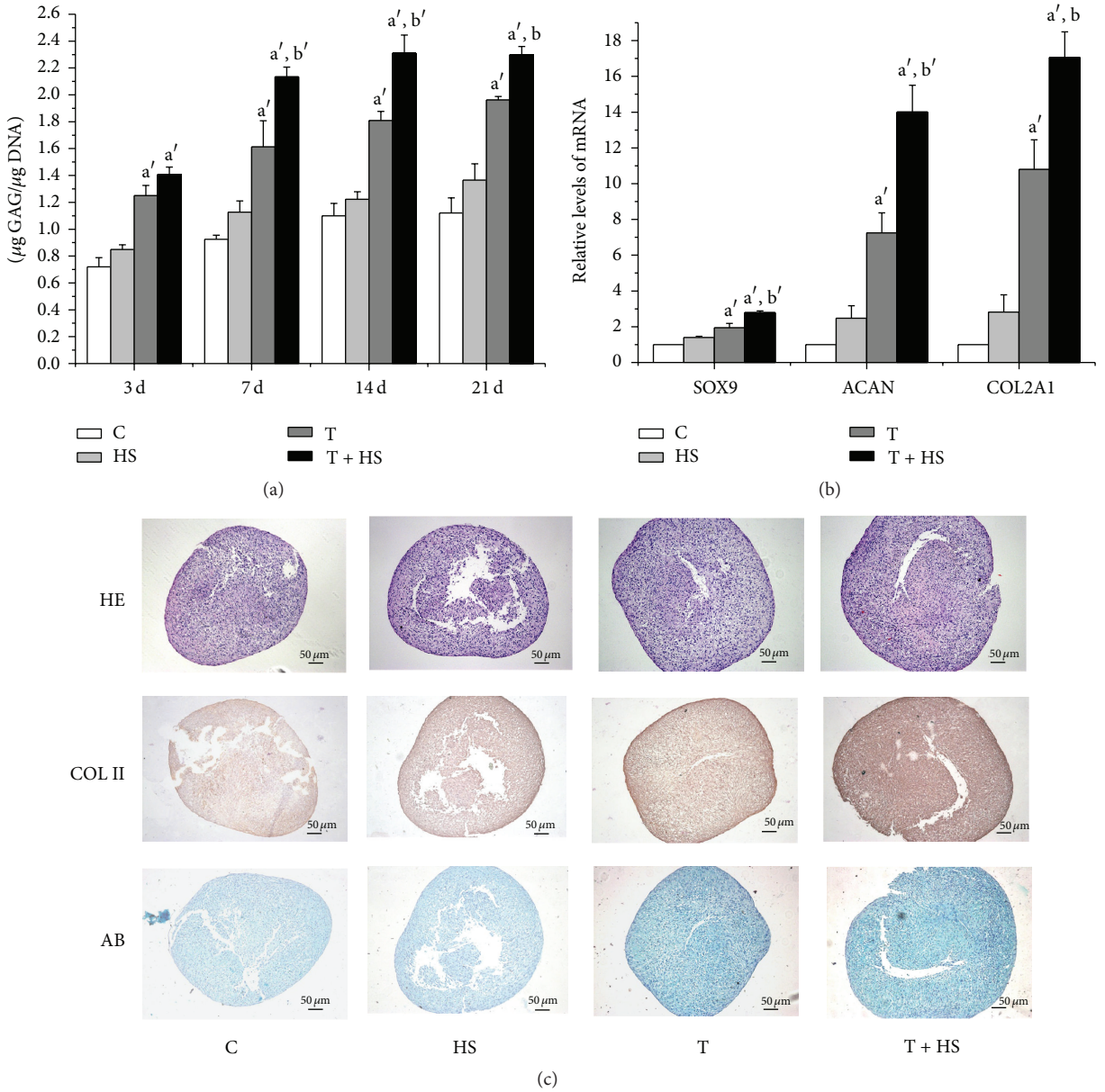

Figure 1: Heparan sulfate promotes TGF-β3-induced chondrogenic differentiation of hMSCs. Cells were cultured in control medium (C), heparan sulfate (HS), TGF-β3 (T), or heparan sulfate together with TGF-β3 (T + HS) for 21 days ($n = 4$). (a) Glycosaminoglycan (GAG) quantification at days 3, 7, 14, and 21. $^{a'}P < 0.01$ versus C group, $^{b}P < 0.05$ versus T group, and $^{b'}P < 0.01$ versus T group. (b) Real-time PCR analysis of cartilage-specific genes SRY (sex determining region Y)-box 9 (SOX9), aggrecan (ACAN), and collagen type II (COL2A1) at day 7. $^{a'}P < 0.01$ versus C group, $^{b}P < 0.05$ versus T group, and $^{b'}P < 0.01$ versus T group. (c) Hematoxylin and eosin (HE) staining for cartilage structure, Alcian blue staining for proteoglycan, and immunohistochemistry for collagen type II at day 7. Scale bar = 50 μm.

Chicago, IL, USA). $P < 0.05$ was chosen as the threshold of significance.

3. Results

3.1. HS Promotes TGF-β3-Induced Chondrogenic Differentiation of hMSCs. HS alone did not elevate the synthesis of GAG greatly at different time points (Figure 1(a); $P > 0.05$). Cartilage-specific gene expression (Figure 1(b); $P > 0.05$) and proteoglycan and collagen type II secretion (Figure 1(c)) were also not elevated significantly compared with that of the untreated controls. The cells treated with TGF-β3 produced more GAG (Figure 1(a); $P < 0.01$) at days 3, 7, 14, and 21 and more cartilage matrix proteins (Figure 1(c)), as well as increased cartilage-specific gene expression (Figure 1(b); $P < 0.01$), compared to the control cells. Interestingly, the addition of TGF-β3 together with HS results in significant increases in GAG synthesis (Figure 1(a); $P < 0.01$ at days 7 and 14 and $P < 0.05$ at day 21), cartilage-specific gene expression of SOX9 ($P < 0.01$), ACAN ($P < 0.01$), and

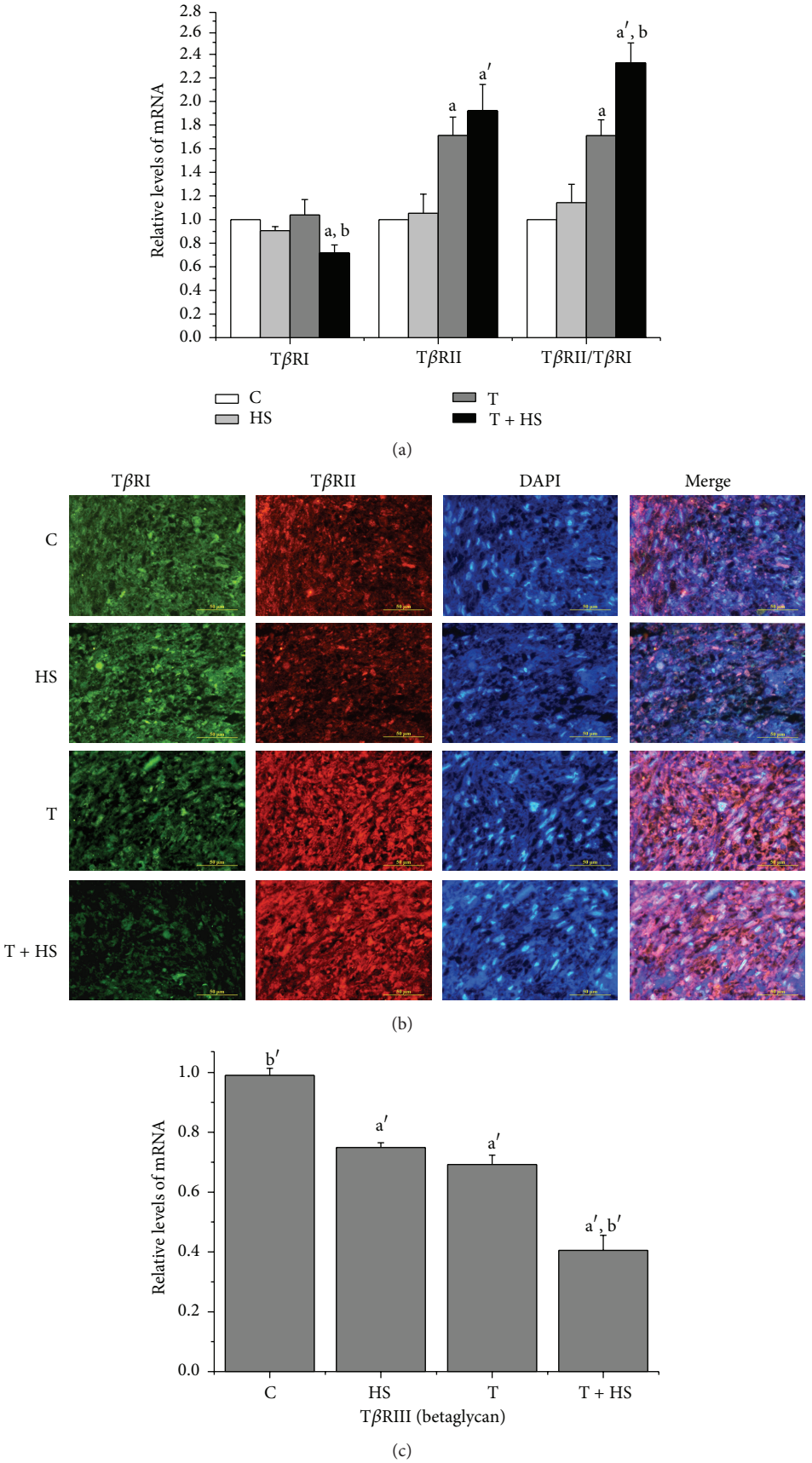

Figure 2: Continued.

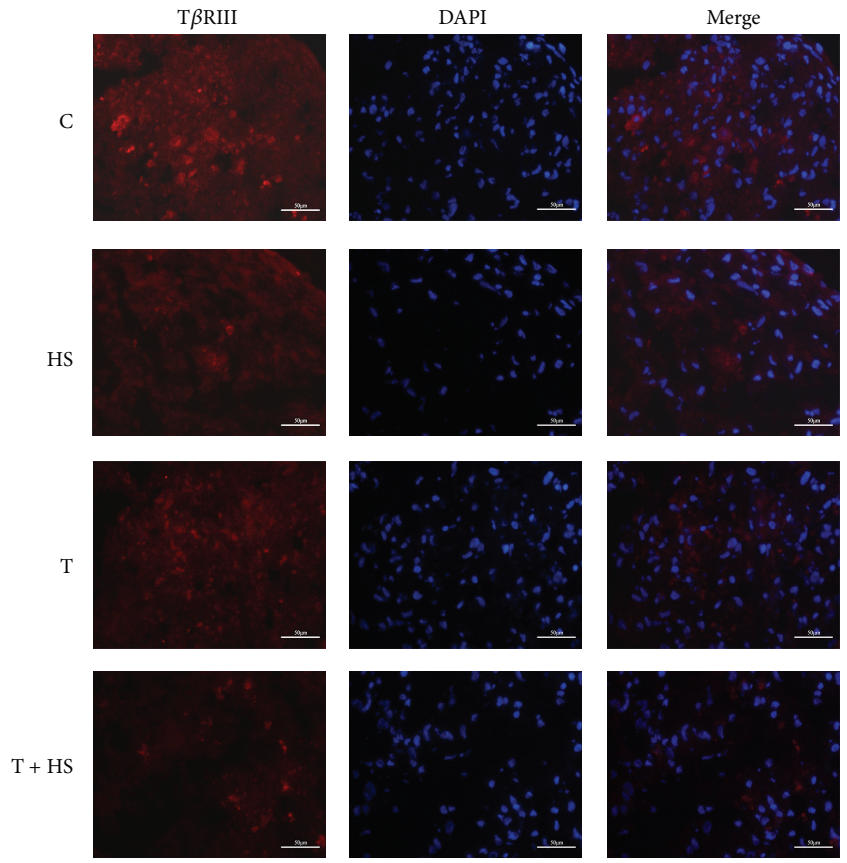

(d)

Figure 2: HS modulates expression mode of TGF-β receptors. Cells were cultured in four different media (C, HS, T, and T + HS) for 7 days. ($n = 3$) (a) mRNA expression of TβRI and TβRII and ratio of TβRII to TβRI by real-time RT-PCR. $^{a}P < 0.05$ versus C group, $^{a'}P < 0.01$ versus C group, and $^{b}P < 0.05$ versus T group. (b) The expressions of TβRI and TβRII are visualized by immunofluorescence staining using anti-TβRI (green) and anti-TβRII (red) antibodies. Nuclei are counterstained using DAPI (blue). The far right panels show merged images. Scale bar = 50 μm. (c) mRNA expression of TβRIII by real-time RT-PCR assay. $^{a'}P < 0.01$ versus C group, $^{b'}P < 0.01$ versus T group. (d) The expressions of TβRIII are visualized by immunofluorescence staining using anti-TβRIII (red) antibodies. Nuclei are counterstained using DAPI (blue). The far right panels show merged images. Scale bar = 50 μm.

COL2A1 ($P < 0.05$) (Figure 1(b)), and cartilage matrix-protein secretion (Figure 1(c)), as compared to the cells treated with TGF-β3 alone. These results show that HS enhances TGF-β3-induced chondrogenic differentiation of hMSCs.

3.2. HS Modulates the Expression Mode of TGF-β Receptors. There was no difference between the TβRI mRNA levels and the protein expression of the cells treated with HS alone or TGF-β3 alone and those of the untreated control cultures (Figure 2(a); $P > 0.05$) (Figure 2(b)). However, the combination of TGF-β3/HS treatment decreased TβRI mRNA levels (Figure 2(a); $P < 0.05$) and TβRI protein expression (Figure 2(b)) compared to those of the other groups. The HS treatment alone did not increase the expression of the TβRII gene (Figure 2(a); $P > 0.05$) or the protein expression (Figure 2(b)) compared to that of the untreated control cultures. Both the TGF-β3 treatment alone and the combined TGF-β3/HS treatment enhanced the mRNA levels of the TβRII gene (Figure 2(a); $P < 0.05$) and TβRII expression (Figure 2(b)) compared to those of the control. There was no obvious difference in TβRII gene levels (Figure 2(a); $P > 0.05$) or TβRII expression (Figure 2(b)) between the TGF-β3 treatment alone and the combined TGF-β3/HS treatment. Analysis of the ratio of TβRII to TβRI levels revealed that the ratio of cells treated was higher in the TGF-β3-only treatment and the combined TGF-β3/HS treatment than in the controls (Figure 2(a); $P < 0.05$ and $P < 0.01$, resp.). TβRII/TβRI levels increased dramatically in the combined TGF-β3/HS treatment compared to those of the TGF-β3-only treatment (Figure 2(a); $P < 0.05$). For TβRIII, the HS alone or TGF-β3 alone treatment and the combination of TGF-β3/HS treatment decreased TβRIII mRNA levels (Figure 2(c); $P < 0.01$) and TβRIII protein expression (Figure 2(d)) compared

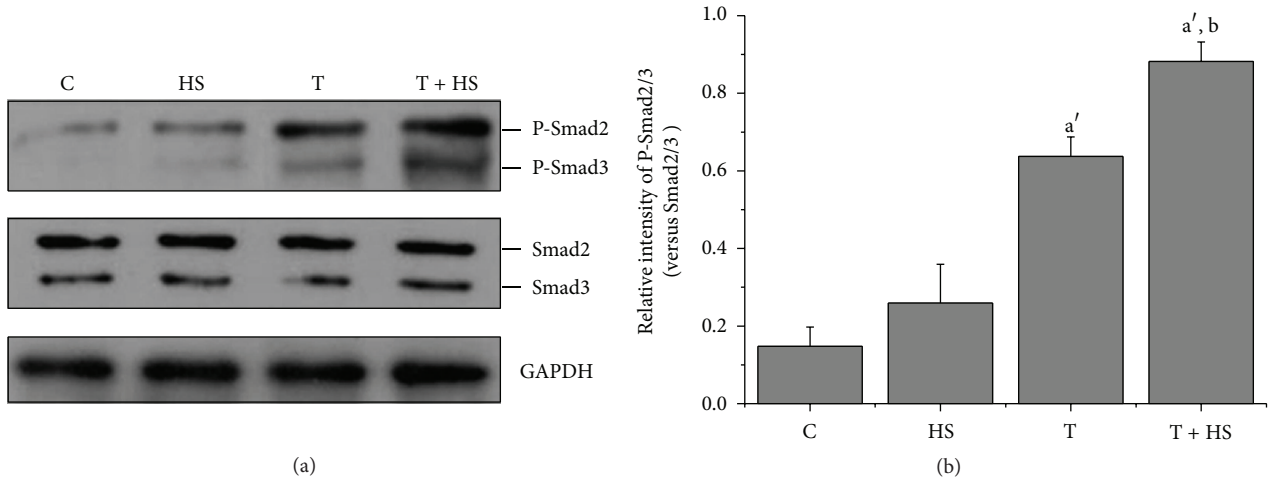

Figure 3: HS strengthens TGF-β3-mediated Smad2/3 phosphorylation. Cells were cultured in four different media (C, HS, T, and T + HS) and were harvested at 24 h. (a) Western blot for protein levels of P-Smad2/3, total Smad2/3, and GAPDH. (b) Quantification of protein levels of P-Smad2/3 normalized to total levels of Smad2/3. Error bars represent the means ± SD, $n = 3$. $^{a'}P < 0.01$ versus C group, $^{b}P < 0.05$ versus T group.

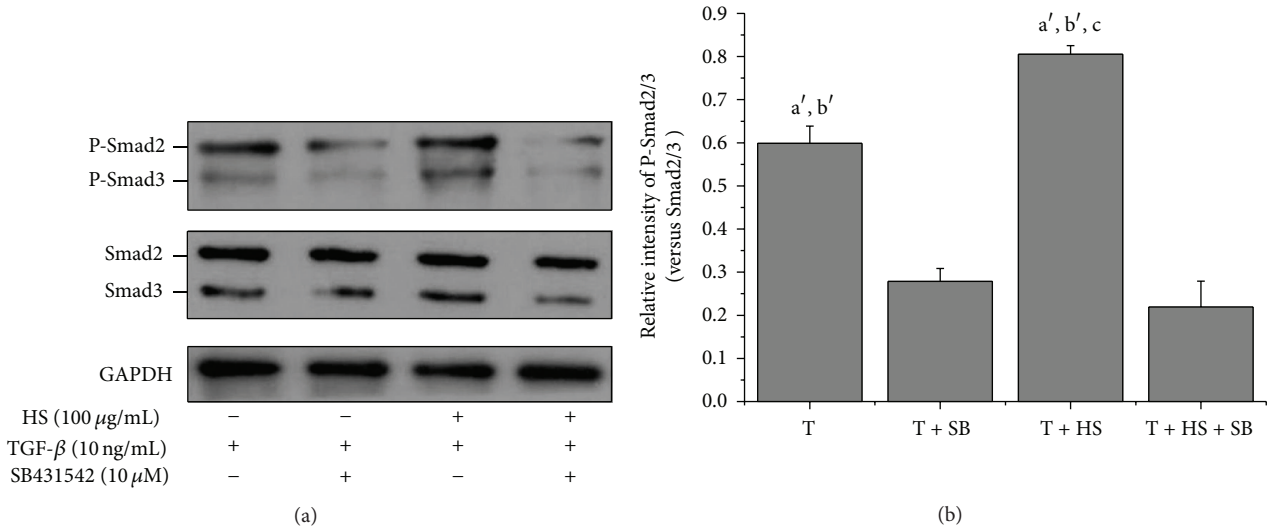

Figure 4: SB431542 blocks HS-activated TGF-β3-mediated Smad2/3 phosphorylation. Cells were cultured in control medium supplemented with TGF-β3 (T), SB431542 treated for 2 h before treatment with TGF-β3 (T + SB), TGF-β3 together with HS (T + HS), or SB431542 treated for 2 h before treatment with TGF-β3 together with HS (T + HS + SB). Samples were harvested at 24 h. (a) Western blot for protein levels of P-Smad2/3, total Smad2/3, and GAPDH. (b) Quantification of protein levels of P-Smad2/3 normalized to total levels of Smad2/3. Error bars represent the means ± SD, $n = 3$. $^{a'}P < 0.01$ versus T + SB group, $^{b'}P < 0.01$ versus T + HS + SB group, and $^{c}P < 0.05$ versus T group.

to those of the control. TβRIII levels decreased obviously in the combined TGF-β3/HS treatment compared to those of the HS alone or TGF-β3 alone treatment (Figure 2(c); $P < 0.01$) (Figure 2(d)).

3.3. HS Strengthens TGF-β3-Mediated Phosphorylation of Smad2/3. As shown in Figure 3, HS alone did not affect the expression of phospho-Smad2/3. However, both the TGF-β3-only treatment and the combined TGF-β3/HS treatment strongly activated the phosphorylation of Smad2/3. It is worth noting that HS further enhanced phospho-Smad2/3 activation induced by TGF-β3.

3.4. SB431542 Blocks HS-Activated TGF-β3-Mediated Phosphorylation of Smad2/3. SB431542 inhibited TGF-β3-activated Smad2/3 phosphorylation and completely inhibited HS-enhanced TGF-β3-activated Smad2/3 phosphorylation (Figure 4(a)). There was no statistical difference between the phosphor-Smad2/3 levels of the cells treated with TGF-β3 in the presence of SB431542 (T + SB) or in those treated with TGF-β3 and HS in the presence of SB431542 (T + HS + SB) (Figure 4(b); $P > 0.05$).

3.5. SB431542 Inhibits HS-Enhanced TGF-β3-Induced Chondrogenic Differentiation of hMSCs. The RT-PCR analysis

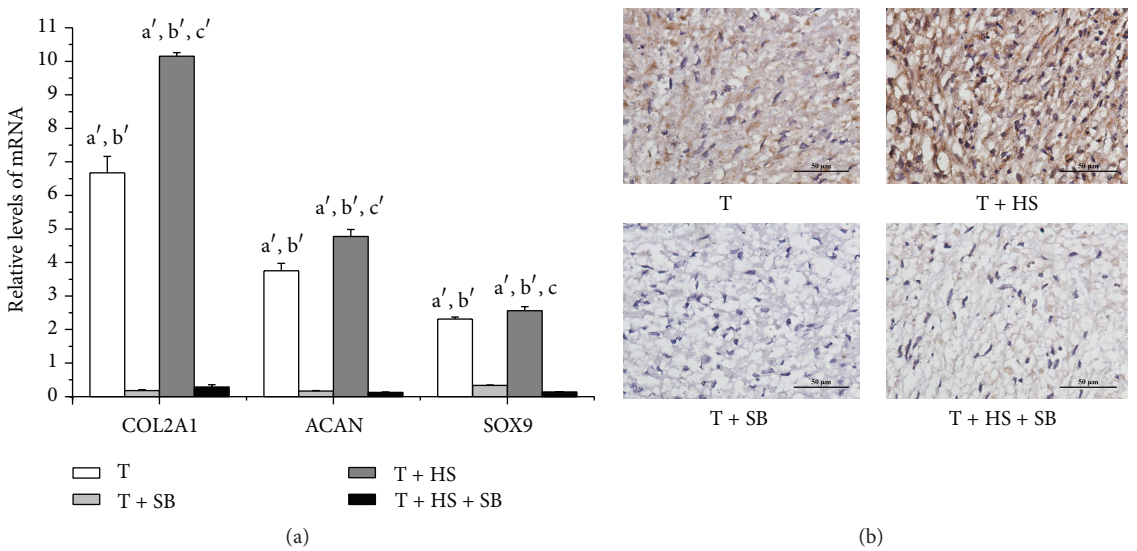

Figure 5: SB431542 inhibits HS-enhanced TGF-β3-induced chondrogenic differentiation of hMSCs. Cells were cultured in four different media (T, T + HS, T + HS, and T + HS + SB) for 7 days. (a) mRNA levels of SOX9, ACAN, and COL2A1 are measured by real-time PCR. Error bars represent the means ± SD, $n = 4$. $^{a'}P < 0.01$ versus T + SB group, $^{b'}P < 0.01$ versus T + HS + SB group, $^{c}P < 0.05$ versus T group, and $^{c'}P < 0.01$ versus T group. (b) Immunohistochemistry staining for collagen type II. $n = 3$, scale bar = 50 μm.

showed that the combined TGF-β3/HS treatment significantly increased cartilage-specific gene (SOX9, ACAN, and COL2A1) expression when compared to that of the cells treated with TGF-β3 alone (Figure 5(a); $P < 0.01$) (Figure 1(b); $P < 0.01$). The expression of cartilage-specific genes decreased in the T + SB and T + HS + SB groups as compared to that of either the T or T + HS groups (Figure 5(a); $P < 0.01$). There was no statistically significant difference in the expression levels of SOX9, ACAN, and COL2A1 between the T + SB group and T + HS + SB group (Figure 5(b); $P > 0.05$). Immunohistochemistry for collagen type II showed similar results, with the expression of collagen type II that was enhanced by TGF-β3 completely inhibited by SB431542 (Figure 5(b)).

4. Discussion

HS-stimulated cartilage nodule formation and growth in micromass cultures of chick limb bud mesenchyme have been reported [26]. However, our results showed that exogenous HS alone did not strongly induce chondrogenesis of MSCs in vitro (Figure 1). The discord may be due to MSCs being more original compared to the cells derived from chick limb bud mesenchyme. Our results also confirmed the findings of other studies, which demonstrated that TGF-β3 induced chondrogenic differentiation of MSCs [7]. Interestingly, we found that HS significantly enhanced TGF-β3-induced chondrogenic differentiation and cartilage-specific gene expression of hMSCs (Figure 1). Fisher et al. reported that exogenous HS enhances the ability of bone morphogenetic protein 2 (BMP-2), another important member of the TGF-β superfamily, to promote chondrogenic differentiation in micromass cultures of limb mesenchymal cell [27]. Based on these studies, perlecan, a HSPG in the ECM, was complexed with collagen II to construct a biomimetic material. The resulting material was able to bind more BMP-2 than a type II collagen scaffold, leading to enhanced chondrogenic differentiation [28]. Our results further demonstrate the important role of HS in regulating the chondrogenic activity of the TGF-β superfamily. They also provide an experimental basis for HS or HSPG as biomimetic biomaterials or drug interacting with TGF-β for cartilage tissue engineering.

HS might regulate signaling-molecule response by modulating the interactions between growth factors with their receptors [27]. To explore the molecular mechanism by which HS enhances TGF-β3-induced chondrogenic differentiation and to determine whether HS increased TGF-β signaling, we observed the effect of HS on TGF-β3-mediated TβR (I, II, and III) expression and phosphorylation of Smad2/3. The results showed that HS modulated the TGF-β3-induced expression of TGF-β receptors, decreased TβRIII expression (Figure 2) but increased the ratio of TβRII to TβRI (Figure 2), and increased Smad2/3 phosphorylation (Figure 3). The results indicate that exogenous HS modulates the interactions between TGF-β3 with its receptors and activates downstream Smad2/3 signal pathway. A previous study reported that increasing the ratio of TβRII to TβRI in the TGF-β receptor/ligand complex provided a positive signal to augment TGF-β-induced cellular responses [10]. It is possible that HS increases the ratio of TGF-β3 binding to TβRII and TβRI and activates TGF-β/Smad2/3 signaling. There are two possible mechanisms in which exogenous HS modulates the interactions between TGF-β3 with its receptors. The binding of HS to TGF-β3 might directly facilitate the interaction of TGF-β3 with its receptors [29]. Alternately, exogenous HS inhibited endogenous HSPGs, TβRIII (betaglycan) expression (Figures 2(c) and 2(d)). It has been reported that TβRIII with larger HSPGs negatively modulates TGF-β-induced cellular

responses by regulating the ratio of TGF-β binding to TβRII and TβRI [9, 10]. That may explain HS-induced promotion of TGF-β3-induced chondrogenic differentiation of MSCs.

Although Smad2/3 is a primary TGF-β signaling pathway for initiating chondrogenic differentiation, other pathways, such as the P38 pathway, are also activated by TGF-β during chondrogenesis [30]. Our study further showed that SB431542, a TGF-β signaling inhibitor, not only completely inhibited HS-stimulated, TGF-β3-mediated Smad2/3 phosphorylation (Figure 4) but also completely inhibited the effects of HS on TGF-β3-induced chondrogenic differentiation (Figure 5). These results demonstrated that TGF-β/Smad2/3 signaling is an exclusive and unique pathway, by which HS potentiates the TGF-β3-induced chondrogenic differentiation of MSCs.

5. Conclusions

This study demonstrated that exogenous HS enhanced TGF-β3-induced chondrogenic differentiation of hMSCs by facilitating interaction of TGF-β3 with its receptors and further activating downstream Smad2/3 signaling. These findings provide a potential strategy for the use of HS or HSPG as biomimetic biomaterials or drugs that cooperate with TGF-β for cartilage tissue engineering. Further research is required to explore the roles of TβRIII (betaglycan) in modulating TGF-β-induced chondrogenesis of MSCs by regulating the interaction of TGF-β3 with TβRII and TβRI. The corresponding experiments are in progress.

Conflict of Interests

The authors declare that there is no conflict of interests regarding the publication of this paper.

Authors' Contribution

Juan Chen and Yongqian Wang contributed equally to this paper.

Acknowledgments

This research was supported by grants from the National Natural Science Foundation of China (no. 81472039) and Fundamental Research Funds for the Central Universities, Young Teachers Fund of Sun Yat-sen University (13YKPY23).

References

[1] M. B. Eslaminejad, "Mesenchymal stem cells as a potent cell source for articular cartilage regeneration," *World Journal of Stem Cells*, vol. 6, no. 3, pp. 344–354, 2014.

[2] T. A. E. Ahmed and M. T. Hincke, "Mesenchymal stem cell-based tissue engineering strategies for repair of articular cartilage," *Histology and Histopathology*, vol. 29, no. 6, pp. 669–689, 2014.

[3] S. E. Bulman, V. Barron, C. M. Coleman, and F. Barry, "Enhancing the mesenchymal stem cell therapeutic response: cell localization and support for cartilage repair," *Tissue Engineering—Part B: Reviews*, vol. 19, no. 1, pp. 58–68, 2013.

[4] A. Mobasheri, G. Kalamegam, G. Musumeci, and M. E. Batt, "Chondrocyte and mesenchymal stem cell-based therapies for cartilage repair in osteoarthritis and related orthopaedic conditions," *Maturitas*, vol. 78, no. 3, pp. 188–198, 2014.

[5] J. L. Puetzer, J. N. Petitte, and E. G. Loboa, "Comparative review of growth factors for induction of three-dimensional *in vitro* chondrogenesis in human mesenchymal stem cells isolated from bone marrow and adipose tissue," *Tissue Engineering Part B: Reviews*, vol. 16, no. 4, pp. 435–444, 2010.

[6] C. Cicione, E. Muiños-López, T. Hermida-Gómez, I. Fuentes-Boquete, S. Díaz-Prado, and F. J. Blanco, "Alternative protocols to induce chondrogenic differentiation: transforming growth factor-β superfamily," *Cell and Tissue Banking*, vol. 16, no. 2, pp. 195–207, 2015.

[7] Q. O. Tang, K. Shakib, M. Heliotis et al., "TGF-β3: a potential biological therapy for enhancing chondrogenesis," *Expert Opinion on Biological Therapy*, vol. 9, no. 6, pp. 689–701, 2009.

[8] Y. G. Shi and J. Massagué, "Mechanisms of TGF-β signaling from cell membrane to the nucleus," *Cell*, vol. 113, no. 6, pp. 685–700, 2003.

[9] O. Eickelberg, M. Centrella, M. Reiss, M. Kashgarian, and R. G. Wells, "Betaglycan inhibits TGF-β signaling by preventing type I-type II receptor complex formation: glycosaminoglycan modifications alter betaglycan function," *The Journal of Biological Chemistry*, vol. 277, no. 1, pp. 823–829, 2002.

[10] C.-L. Chen, S. H. Shuan, and S. H. Jung, "Cellular heparan sulfate negatively modulates transforming growth factor-β1 (TGF-β1) responsiveness in epithelial cells," *The Journal of Biological Chemistry*, vol. 281, no. 17, pp. 11506–11514, 2006.

[11] M. Bilandzic and K. L. Stenvers, "Betaglycan: a multifunctional accessory," *Molecular and Cellular Endocrinology*, vol. 339, no. 1-2, pp. 180–189, 2011.

[12] X.-D. Chen, "Extracellular matrix provides an optimal niche for the maintenance and propagation of mesenchymal stem cells," *Birth Defects Research Part C: Embryo Today: Reviews*, vol. 90, no. 1, pp. 45–54, 2010.

[13] R. K. Okolicsanyi, L. R. Griffiths, and L. M. Haupt, "Mesenchymal stem cells, neural lineage potential, heparan sulfate proteoglycans and the matrix," *Developmental Biology*, vol. 388, no. 1, pp. 1–10, 2014.

[14] B. Mulloy and M. J. Forster, "Conformation and dynamics of heparin and heparan sulfate," *Glycobiology*, vol. 10, no. 11, pp. 1147–1156, 2000.

[15] N. S. Gandhi and R. L. Mancera, "The structure of glycosaminoglycans and their interactions with proteins," *Chemical Biology and Drug Design*, vol. 72, no. 6, pp. 455–482, 2008.

[16] X. Lin, "Functions of heparan sulfate proteoglycans in cell signaling during development," *Development*, vol. 131, no. 24, pp. 6009–6021, 2004.

[17] M. C. Farach-Carson, J. T. Hecht, and D. D. Carson, "Heparan sulfate proteoglycans: key players in cartilage biology," *Critical Reviews in Eukaryotic Gene Expression*, vol. 15, no. 1, pp. 29–48, 2005.

[18] K. Jochmann, V. Bachvarova, and A. Vortkamp, "Heparan sulfate as a regulator of endochondral ossification and osteochondroma development," *Matrix Biology*, vol. 34, pp. 55–63, 2014.

[19] J. Huegel, F. Sgariglia, M. Enomoto-Iwamoto, E. Koyama, J. P. Dormans, and M. Pacifici, "Heparan sulfate in skeletal development, growth, and pathology: the case of hereditary multiple exostoses," *Developmental Dynamics*, vol. 242, no. 9, pp. 1021–1032, 2013.

[20] C. B. Kirn-Safran, R. R. Gomes, A. J. Brown, and D. D. Carson, "Heparan sulfate proteoglycans: coordinators of multiple signaling pathways during chondrogenesis," *Birth Defects Research Part C: Embryo Today: Reviews*, vol. 72, no. 1, pp. 69–88, 2004.

[21] C. C. Rider, "Heparin/heparan sulphate binding in the TGF-β cytokine superfamily," *Biochemical Society Transactions*, vol. 34, no. 3, pp. 458–460, 2006.

[22] Q. Chen, P. Sivakumar, C. Barley et al., "Potential role for heparan sulfate proteoglycans in regulation of transforming growth factor-β (TGF-β) by modulating assembly of latent TGF-β-binding protein-1," *The Journal of Biological Chemistry*, vol. 282, no. 36, pp. 26418–26430, 2007.

[23] J. Zhou, C. Xu, G. Wu et al., "In vitro generation of osteochondral differentiation of human marrow mesenchymal stem cells in novel collagen-hydroxyapatite layered scaffolds," *Acta Biomaterialia*, vol. 7, no. 11, pp. 3999–4006, 2011.

[24] L. Zhang, P. Su, C. Xu, J. Yang, W. Yu, and D. Huang, "Chondrogenic differentiation of human mesenchymal stem cells: a comparison between micromass and pellet culture systems," *Biotechnology Letters*, vol. 32, no. 9, pp. 1339–1346, 2010.

[25] G. J. Inman, F. J. Nicolás, J. F. Callahan et al., "SB-431542 is a potent and specific inhibitor of transforming growth factor-β superfamily type I activin receptor-like kinase (ALK) receptors ALK4, ALK5, and ALK7," *Molecular Pharmacology*, vol. 62, no. 1, pp. 65–74, 2002.

[26] J. D. S. Antonio, B. M. Winston, and R. S. Tuan, "Regulation of chondrogenesis by heparan sulfate and structurally related glycosaminoglycans," *Developmental Biology*, vol. 123, no. 1, pp. 17–24, 1987.

[27] M. C. Fisher, Y. Li, M. R. Seghatoleslami, C. N. Dealy, and R. A. Kosher, "Heparan sulfate proteoglycans including syndecan-3 modulate BMP activity during limb cartilage differentiation," *Matrix Biology*, vol. 25, no. 1, pp. 27–39, 2006.

[28] W. Yang, R. R. Gomes, A. J. Brown et al., "Chondrogenic differentiation on perlecan domain I, collagen II, and bone morphogenetic protein-2-based matrices," *Tissue Engineering*, vol. 12, no. 7, pp. 2009–2024, 2006.

[29] J. S. Park, D. G. Woo, H. N. Yang, H. J. Lim, H.-M. Chung, and K.-H. Park, "Heparin-bound transforming growth factor-β3 enhances neocartilage formation by rabbit mesenchymal stem cells," *Transplantation*, vol. 85, no. 4, pp. 589–596, 2008.

[30] L. A. McMahon, P. J. Prendergast, and V. A. Campbell, "A comparison of the involvement of p38, ERK1/2 and PI3K in growth factor-induced chondrogenic differentiation of mesenchymal stem cells," *Biochemical and Biophysical Research Communications*, vol. 368, no. 4, pp. 990–995, 2008.

Hindawi Publishing Corporation
Stem Cells International
Volume 2016, Article ID 5646384, 9 pages
http://dx.doi.org/10.1155/2016/5646384

Review Article

Human Mesenchymal Stromal Cells from Different Sources Diverge in Their Expression of Cell Surface Proteins and Display Distinct Differentiation Patterns

Kourosch C. Elahi,[1] Gerd Klein,[2] Meltem Avci-Adali,[3] Karl D. Sievert,[4] Sheila MacNeil,[5] and Wilhelm K. Aicher[1]

[1]*KFO273, Department of Urology, University of Tübingen Hospital, 72076 Tübingen, Germany*
[2]*Department of Medicine II, SCeNT, Center for Medical Research, University of Tübingen, 72072 Tübingen, Germany*
[3]*Department of Thoracic, Cardiac and Vascular Surgery, University Hospital of Tübingen, 72076 Tübingen, Germany*
[4]*Department of Urology & Andrology, Paracelsus Medical University, Salzburg General Hospital, 5020 Salzburg, Austria*
[5]*Department of Materials Science & Engineering, Kroto Research Institute, University of Sheffield, Sheffield S3 7HQ, UK*

Correspondence should be addressed to Wilhelm K. Aicher; aicher@uni-tuebingen.de

Received 15 May 2015; Revised 3 August 2015; Accepted 3 August 2015

Academic Editor: Kodandaramireddy Nalapareddy

When germ-free cell cultures became a laboratory routine, hopes were high for using this novel technology for treatment of diseases or replacement of cells in patients suffering from injury, inflammation, or cancer or even refreshing cells in the elderly. Today, more than 50 years after the first successful bone marrow transplantation, clinical application of hematopoietic stem cells is a routine procedure, saving the lives of many every day. However, transplanting other than hematopoietic stem and progenitor cells is still limited to a few applications, and it mainly applies to mesenchymal stromal cells (MSCs) isolated from bone marrow. But research progressed and different trials explore the clinical potential of human MSCs isolated from bone marrow but also from other tissues including adipose tissue. Recently, MSCs isolated from bone marrow (bmMSCs) were shown to be a blend of distinct cells and MSCs isolated from different tissues show besides some common features also some significant differences. This includes the expression of distinct antigens on subsets of MSCs, which was utilized recently to define and separate functionally different subsets from bulk MSCs. We therefore briefly discuss differences found in subsets of human bmMSCs and in MSCs isolated from some other sources and touch upon how this could be utilized for cell-based therapies.

1. Introduction

The MSCs have been described for the first time as colony forming fibroblasts (CFU-F), a rare population of cells residing in the bone marrow of guinea-pigs or mice [1, 2]. Other researchers isolated MSCs from bone marrow of rabbits [3], rats [4], pigs [5], and other species. Human bmMSCs were described in the late nineties as well [6] and at the same time a breakthrough study investigated the expression of typical cell surface markers and the proliferation and differentiation properties of human MSCs in more detail [7]. In the last 20 years, a huge number of studies investigated phenotypic features and facts of MSCs. In July 2015, a web search yielded more than 357 000 hits for the term "mesenchymal stem cell" (Google Scholar; Table 1). At the same time PubMed listed about 35 000 citations, and Web of Science listed about 134 000 publications for this term.

When the biological properties of MSCs were explored in more detail, questions arose whether these cells met the criterion of a true *stem* cell [8]. To qualify as a stem cell, these cells must be able to self-renew, most likely by symmetric cell division to produce two daughter cells with the same stem cell qualities. At the same time, by asymmetric cell division or after specific activation, stem cells must be able to generate more mature progenitor cells or differentiated effector cells (Figure 1). Nowadays, experts agree that MSCs may generate upon appropriate stimulation quite different mature cells including osteoblasts, chondrocytes, tenocytes, adipocytes,

Table 1: Overview of studies published regarding MSCs using the term "stem cell" or "stromal cell" in the last 20 years accessed by a web search in July 2015 (Google Scholar). It seems that the term "stem cell" became more popular although the "stemness" was only shown in a more strict sense for MSCs involved in osteogenesis and bone repair.

Search Year	Hits MSC as "stem" cell	Hits MSC as "stromal" cell
1995–2000	12,000	12,100
2000–2005	41,000	21,700
2005–2010	156,000	38,200
2010–2015	148,000	33,600

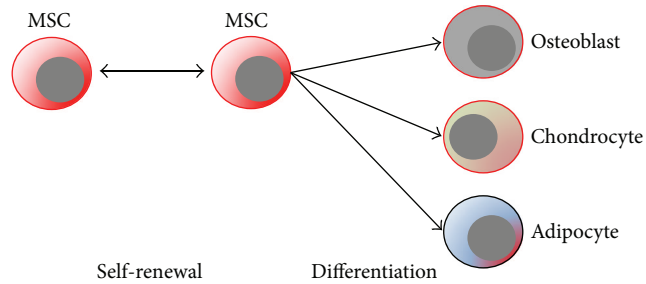

Figure 1: Overview on self-renewal or differentiation of stem cells in their respective stem cell niche.

smooth muscle cells, and stromal cells of the bone marrow [9]. They display differentiation capacities and therefore qualify as multipotent progenitor cells (Figure 1). To qualify as stem cells, self-renewal has to be shown as well [10].

Expansion of MSCs was shown to be limited to a few passages of in vitro culture and the cells underwent replicative senescence [11]. Changes in the differentiation potential of MSCs after in vitro expansion were noted and chondrogenic clones especially disappeared early on [12]. Therefore, available in vitro protocols for expansion of MSCs do not yield true *stem* cells. MSCs were also investigated for stem cell qualities in vivo. By consecutive transplantation, MSCs were able to maintain their osteogenic progenitor potential and spontaneous heterotopic ossification was observed [13]. Spontaneous generation of cartilaginous or adipose tissue was not observed experimentally after heterotopic implantation of MSCs suggesting that at least bmMSCs are self-renewing stem cells for skeletal tissue regeneration, but not stem cells for regeneration of cartilage, fat, and other tissues [13]. Therefore, in a strict sense the term mesenchymal *stem* cell applies only for osteogenesis or bone regeneration and consequently, for general purposes, the term mesenchymal *stromal* cell is preferred nowadays.

2. Sources for Mesenchymal Stromal Cells

Mesenchymal stromal cells have been described in and have been isolated from many different adult tissues, including bone marrow, adipose tissue, inner organs, and blood vessels and from rather "young sources" such as amniotic fluid, amniotic membrane, umbilical cord, or placenta [2, 14–22]. In order to be able to discriminate MSCs from fibroblasts and other adherently growing cells, a group of experts suggested defining bmMSCs by expression of a set of cell surface markers, a trilineage differentiation potential (osteogenic, chondrogenic, and adipogenic), and fibroblast-like appearance in in vitro culture [23] (Figure 2). There is ample experimental evidence that MSCs isolated from tissues other than bone marrow share these features and generate upon stimulation osteoblasts, chondrocytes, adipocytes, and other cells in vitro as well [24–29]. However, until now, there is no experimental evidence that MSC preparations from any source contain progenitor cells that spontaneously generate fat or cartilage after transplantation to ectopic sites.

In avascular tissues such as cartilage, MSC-like cells meeting the inclusion criteria defined by the consensus conference were detected as well [31–33]. Their relation to MSCs derived from vascularized tissues, blood vessels, or serum is a matter of debate for quite some years now [34]. Still, to our momentary knowledge MSCs and MSC-like cells from different sources share characteristics including those features used to define the adult MSCs [23]. However, exploring MSCs from different sources in more detail revealed significant differences (see below).

In an adult organism and in sharp contrast to hematopoietic stem and progenitor cells [35] or spermatogonial stem cells [36], MSCs do not have stringent requirements for a stem cell niche [8], but they attach well to fibronectin, collagens, laminins, and other extracellular matrix proteins [37, 38]. MSCs were shown to appear upon adaptive transfer at several sites in a healthy recipient, and only a few cells home to bone marrow [39, 40]. Up to now, differences between the homing of MSCs to bone marrow and MSCs detected in other locations or trapped in the veins of the lung after intravenous injection of MSCs are not completely understood [40]. Moreover, the overall efficacy of homing or grafting of MSCs is low, but some MSCs applied by intravenous injection are found even at sites of injury [40]. At the same time, mobilization of MSCs occurs upon hypoxia or after injury, indicating a correlation between the migratory capacities of MSC and local wound repair [41]. A strong affinity of MSCs to a defined and specialized niche would possibly hinder the main function of these multipotent repair cells and prevent their migration to damaged sites [42, 43].

3. Differences in the Transcriptome of MSCs from Different Sources

Prima vista MSCs from different tissues share key characteristics such as fibroblast-like appearance in vitro, trilineage differentiation capacity, expression of certain cell surface antigens (e.g., CD73, CD90, and CD105), and lack of expression of others (e.g., CD11b, CD14, CD19, CD34, CD45, CD78, and MHC class II; Figure 2) [23, 29, 44]. Most of the studies investigating the expression of marker genes of MSCs have been performed with cells after in vitro expansion and cell culture conditions showed significant influence on the transcriptome of MSCs. For instance, bmMSCs can be isolated

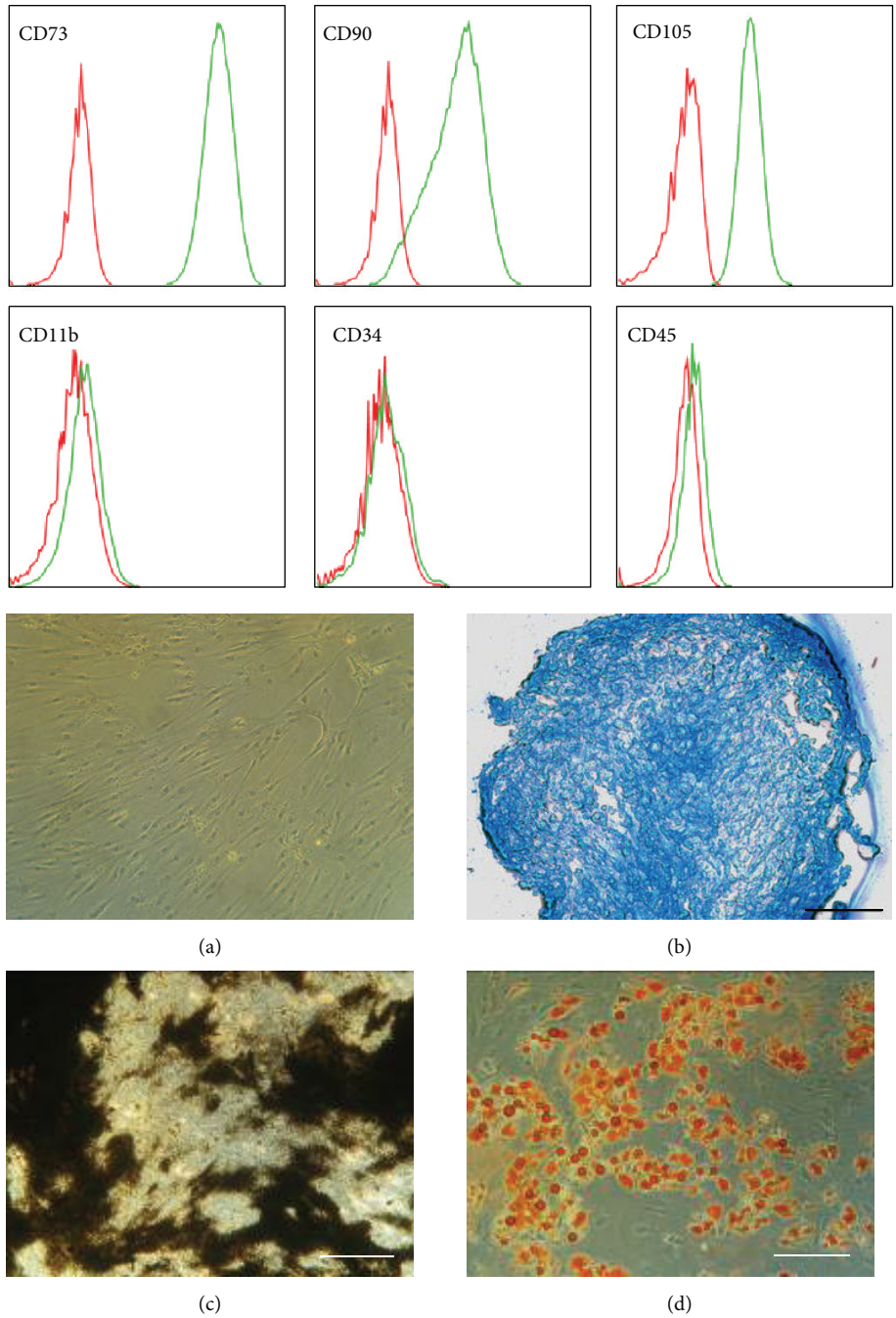

Figure 2: Human mesenchymal stromal cells from bone marrow (bmMSCs) are defined by their expression of CD73, CD90, and CD105, by lack of expression of a series of other cell surface markers such as CD11b, CD34, and CD45, and by a fibroblastoid appearance (a) and trilineage differentiation to generate chondrocytes (b), osteoblasts (c), or adipocytes (d) (for further details see [23]).

and explored ex vivo without time-consuming procedures and without proteolytic digestion [45]. Human bmMSCs express ex vivo the receptor for nerve growth factor (CD271), but its expression is lost by expansion of the cells in vitro [30, 46]. Comparably, expression of CD34 on MSCs from adipose tissue (atMSCs) is detected on cells ex vivo. However, it is variable and depends on the cell culture conditions [28]. Therefore, a comparison of the transcriptome of freshly isolated MSCs from different sources seems biased at least to some extent by methods employed for isolation and preparation of the cells. Furthermore, the transcriptome of MSCs from different sources is probably influenced after expansion at least to some degree by the cell culture conditions as well.

In early passages of in vitro expansion, MSCs from different sources maintain some distinct features. This statement is supported by several studies. The proliferating ability and the gene expression of human bmMSCs and atMSCs were compared [47]. The elevated proliferative capacity of atMSCs was

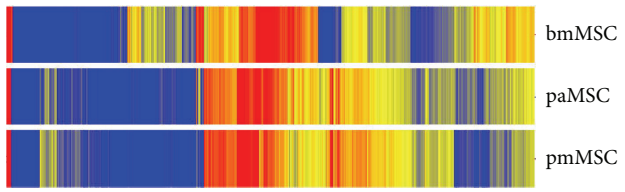

Figure 3: Comparing the total transcriptome of human MSCs from bone marrow (bmMSCs), from the amniotic site of human term placenta (paMSC), and from the maternal, endometrial part of human term placenta (pmMSC) in the second passage of in vitro expansion. MSCs from placenta are similar, but bmMSCs are clearly different from placenta derived MSCs.

associated with an elevated expression of transcription factor *Dickkopf* (DKK) 1. The DKK family of genes encodes soluble factors that participate in the development of mesenchymal tissues and interact with the Wnt-regulated pathway. Overall, the transcriptome of human bmMSCs and atMSCs appeared highly similar but several factors accounting for about 1% of all genes investigated are expressed at significantly different levels [47]. This highly similar gene expression profile was taken as evidence that MSCs in all tissues might be derived from a common mesenchymal precursor. Another study investigated the gene expression in neonatal MSCs isolated from umbilical cord blood (ucb-MSCs) from different donors with published gene-array data [48]. Again, bmMSCs appeared highly similar to ucb-MSCs, and the expression of five transcripts (genes) had not been reported in MSCs before (MGC3047, MGC17528, MGC3278, FLJ12442, and AGENCOURT_6683145) [48]. This study was extended by exploring the transcriptome of ucb-MSCs compared to MSCs isolated from the corresponding umbilical cord, where MSCs are found enriched in Wharton's jelly [49]. In this case, from a total of 13,699 genes investigated 1,870 were transcribed at significantly different levels representing 6% of all annotations computed [49].

When comparing the MSCs from amniotic sites of human term placenta with MSCs from the maternal, endometrial site of the placenta, differences were noted in the transcriptome and more than 100 genes were expressed significantly different (Figure 3). In these gene-array experiments human bmMSCs served as controls, and the differences in their transcriptome compared to both the placenta-derived MSCs from the amniotic site (paMSCs, i.e., fetal MSCs) and placenta-derived MSCs from the endometrial site (pmMSCs, i.e., maternal MSCs) are obvious even to a layperson (Figure 3). We recently confirmed that paMSCs and pmMSCs can be separated with simple methods at a sufficient efficacy as the lengths of the telomeres in paMSCs were significantly longer compared to the corresponding pmMSCs after measuring only a few samples [50]. This finding supports earlier studies reporting on higher and extended mitotic activity of neonatal MSCs, a distinct differentiation potential, and extended life span in vitro [51].

A comparison of the transcriptome of MSCs over time during in vitro expansion revealed that at least within early passages the transcriptome was stable and did not change significantly between cells in their third compared to the sixth passage of culture. At the same time, the expression of a set of core genes was preserved in bmMSCs and all neonatal MSCs were investigated, as were the differences found between bmMSCs and different MSCs from neonatal tissues [52].

Others report on significant differences in the transcriptome of bmMSCs compared to islet-derived precursor cells (IdPCs) [19] which met the minimal criteria set for bmMSCs [23]. Differences in their transcriptomes yielded distinct patterns for factors associated with gland, muscular, ectodermal, and nervous system development [19]. The differences between the transcriptomes can be associated with the differences in the origin of the cells during embryonic development: bmMSCs are derived from limb anlagen and IdPCs are derived from trunk anlagen. However, in this study bmMSCs and IdPCs were expanded in slightly different media [19]. Therefore, a bias regarding cell culture conditions cannot be excluded.

However, small differences in the transcriptome reported between MSCs from different sources do have a noticeable impact on the behaviour of the cells. Recently, we found a significant difference between bmMSCs and placenta-derived MSCs (pMSCs) not only in the expression of the cell surface molecule CD146 and the membrane-anchored alkaline phosphatase [53], but also in the expression of transcription factor Runx2 [50], a gene associated with bone development. In Runx2-targeted mice ($Runx2^{-/-}$) endochondral ossification is completely absent as differentiation of MSCs to osteoblasts requires this transcription factor [54]. Therefore, differences in ossification observed in bmMSCs compared to pMSCs not only depend on a distinct expression of alkaline phosphatase in bmMSCs but also correlate with significant differences of regulatory factors in these cell types. At present, it can be only speculated whether the differences in expression of transcription factors influence the homing of bmMSCs versus pMSCs, atMSCs, or other MSCs [19, 50]. Of note, differences in expression of integrin components, for instance, between bmMSCs and atMSCs, have been reported, and for atMSC specific marker genes were defined [27]. Furthermore, there is compelling evidence that MSCs isolated from different sources but expanded under identical conditions share key features as defined by the so-called minimal criteria [23], but small differences in the expression of a few genes yield a significantly different type of cells when it comes to regulation of proliferation or differentiation of bmMSCs compared to MSCs from other sources [50, 52, 55]. Therefore, preselection of the best source of MSCs and possibly even preselection of subsets of MSCs may become an issue in the context of clinical applications.

Studies exploring the total transcriptome of the cells followed by bioinformatics and systems biology confirm that MSCs from different sources are very closely related cells. In this sense, the minimal criteria defined almost a decade ago seem to not only describe these cells in a correct way but also discriminate the MSCs from other progenitor cells including the hematopoietic progenitor cells or endothelial progenitor cells, found sometimes in the same niche efficiently [23].

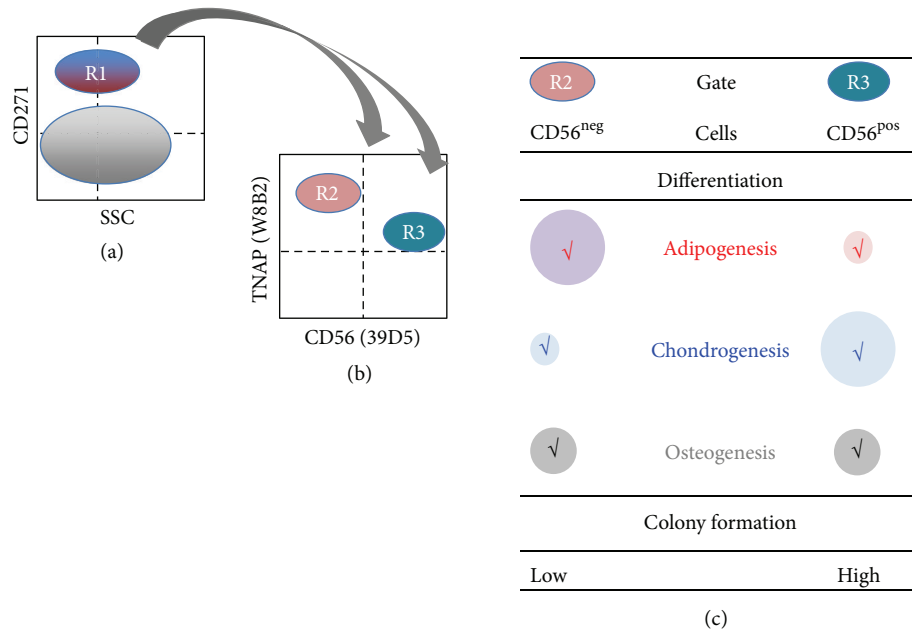

FIGURE 4: Schematic draft of the experimental strategy to define and functionally characterize subsets of human bmMSCs. MSCs were sorted by fluorescence-activated cell sorting (FACS) (left panel). From the mononuclear cells the CD271+ subset, which is gated in R1, was further subdivided by staining with two additional antibodies to TNAP and CD56 positive cells (gates R2 and R3, middle panel). The populations defined by R2 or R3 were expanded in separate cultures and their proliferation and differentiation were compared (right panel) (for further details see [30]).

4. Differences in MSC Subsets from Bone Marrow

In routine procedures most laboratories isolate bulk MSC populations and enrich mesenchymal stromal cells by a combination of plastic adherence followed by expansion of the cells in media preferring proliferation of MSCs [7]. Alternatively, MSCs can be isolated from bone marrow, peripheral blood, or amniotic fluid by simple gradient centrifugation and subsequently a given subset can be isolated using monoclonal antibodies to detect specific cell surface antigens expressed on some [30] but not on all MSCs [30, 45, 56]. For separation of such subsets magnetic-activated cell sorting (MACS) or fluorescence-activated cell sorting (FACS) is used. Accordingly, some of the proliferation- and differentiation-competent human bmMSCs showed expression of the receptor for nerve growth factor (CD271) and the tissue nonspecific alkaline phosphatase (TNAP), previously referred to as mesenchymal stem cell antigen- (MSCA-) 1 [30, 45]. The CD271+ subset was further subdivided using monoclonal antibodies including anti-CD56 clone 39D5. Upon expansion of the CD271+ TNAP+ CD56+ and the CD271+ TNAP+ CD56− MSC subsets in individual cultures, an interesting functional difference was observed: the CD56+ cells were proliferative and more chondrogenic, but less adipogenic compared to the corresponding CD56− cells (Figure 4). This study provided evidence that even a preselected subset of bmMSCs such as the CD271+ mesenchymal cells can be further subdivided in smaller fractions. It also supports the hypothesis that bmMSCs are ex vivo blend of cells. Accordingly, CD90+, VCAM-1+, and CD271+ bmMSCs represent another distinct bmMSC subset of cells [57, 58]. Other monoclonal antibodies defined other MSC subsets [45] and some of these antigens were characterized on MSCs in more detail recently [59]. Moreover, a population of bmMSCs with low expression of the PDGF receptor alpha (PDGFRα) was considered as the primary mesenchymal stromal cell [60]. Interestingly, PDGFRα+, CD51+, and nestin+ MSCs were shown to play a key role for generating a stem cell niche for hematopoiesis [61, 62], a feature of human bmMSCs previously associated with expression of CD146 [63].

However, nowadays not all MSC subsets as defined by monoclonal antibodies ex vivo or in vitro can be associated with functional differences, and the differences between such subsets were defined by in vitro tests. Moreover, homing experiments with bulk bmMSCs followed by detection of MSCs at sites different from bone marrow in the recipient are not definitive proof that bmMSC subsets represent cells with distinct physiological tasks as homing of MSCs can be a passive trapping in irrelevant tissues.

Due to technical limitations it is not well studied if comparable subsets of cells can be defined ex vivo in MSCs from more niches such as adipose tissue, placenta, and perivascular sites in inner organs or others. It might be that *the mesenchymal stem cell* is only present in adult bone marrow and other niches contain progenitor MSCs with a distinct tissue specificity. Alternatively, *the niche* for MSCs may be the bone marrow harbouring or attracting stem cell-like MSCs and distinct subsets of MSCs. Thus, after i.v. injection the stem cell-like MSCs and distinct MSC subsets will primarily migrate to bone marrow of the recipient. However, albeit with low efficacy, they also appear at other sites of a recipient.

Inflammation and processes of tissue repair will then modulate the homing of MSCs and attract those MSC subsets needed for local regeneration.

5. MSC Subsets and Translation in Clinical Applications

The multipotent MSCs are an attractive cellular tool for regenerative medicine and tissue engineering [9] and more than 350 clinical trials involving MSCs are reported in the web-based registry ClinicalTrials.gov. Most studies reported focus on musculoskeletal tissues, circulation and ischemia, gastrointestinal conditions, and the nervous system [64]. Application of MSCs in clinical trials has been considered rather safe but some concerns remain [65, 66]. A recent study pointed out that in less than half of all clinical cellular trials reported to the FDA a tumorigenicity test of the cells employed was performed [67]. Other questions arise from the investigations performed during preclinical studies [68]. However, nowadays there is considerable experience with application of MSCs to treat graft-versus-host disease (GvHD). If MSCs would have a considerable risk to generate tumours or other adverse types of cells, one would expect that such significant problems come to the surface especially in patients after bone marrow transplantation and immune suppression [69].

One important concern for the safety of patients is of course the expansion of MSCs in vitro. Here an enormous variability of protocols exists and in particular studies utilizing cells from industrial sources rarely disclose the exact methods employed in cell production. For preclinical trials and more so for clinical safety and feasibility studies standardized methods or open publication of all procedures involved in cell production would be advantageous [64].

Applying bulk MSCs in a clinical context has technical advantages. The preparation of cells does not involve additional steps for selection or adaptation of the MSCs and many cells can be produced. As outlined above, MSCs prepared by standard procedures (attachment to plastic, preferred outgrowth by choice of medium) contain distinct subsets of cells. Applying, for instance, bmMSCs to treat muscular defects may yield local ossification, sometimes called heterotopic ossification [13, 70]. In this context, a selection of less osteogenic MSCs may help to avoid adverse effects. This can be done by changing the source of MSCs, for instance, by taking MSCs from adipose tissue or term placenta rather than bone marrow to regenerate muscle tissue or vasculature or by depleting the MSCs from the osteogenic subset. A significant correlation between expression of alkaline phosphatase—an enzyme needed for mineralization of bony tissue—Runx2—the key regulator of osteogenic differentiation of mesenchymal precursor cells—and CD146 was reported [22, 50] and using an antibody to CD146 allowed to separate more osteogenic from less osteogenic cells. A method to select more adipogenic or chondrogenic MSCs has been reported recently as well [30] (Figure 4). When used in a clinical context, determination or selection of MSC subsets by antibodies and flow cytometry will require standards for the technology applied [28, 37, 71], as in some cases small subsets of cells have to be defined [45]. Cell culture conditions influence the expression of cell surface antigens [28, 37], and even monoclonal antibodies yield variable results including false positive staining depending on the exact experimental conditions [72].

6. Conclusions

Bulk MSCs have been applied to ameliorate graft-versus-host disease or to treat autoimmune diseases for more than a decade now. Therefore, their clinical use is considered to be very safe. However, in this context it is important to recall that the route of application (i.v.) used for immunosuppression by MSCs may help to select the type of MSCs needed in the hematopoietic niche in bone marrow or in the blood system, because MSCs not matching the respective niches will be either trapped somewhere else or will be discarded. In contrast, the mechanisms contributing to the correct homing of MSCs to bone marrow or sites of tissue regeneration or other natural selective processes may not work well or not work at all in cases of a local administration of the cells, for instance, in the heart, in muscles, or in inner organs. Therefore, as there is no natural selection process for MSCs applied locally, a technical preselection could enrich the MSC subset needed clinically, as local application of a blend of MSCs may contain many unwanted cells. Some of the strategies to select or deplete subsets of MSCs have been discussed in this review. Nevertheless, today our knowledge on functional differences of MSC subsets is still not complete.

Conflict of Interests

The authors declare that there is no conflict of interests regarding the publication of this paper.

Acknowledgments

The authors express their great gratitude to Mrs. Tanja Abruzzese for her excellent experimental expertise and to Chaim Goziga for helping in preparation of the artwork, and the DFG (KFO273) and the European Commission (COST Action BM1209 *ReST*) for financial support.

References

[1] A. J. Friedenstein, R. K. Chailakhjan, and K. S. Lalykina, "The development of fibroblast colonies in monolayer cultures of guinea-pig bone marrow and spleen cells," *Cell and Tissue Kinetics*, vol. 3, no. 4, pp. 393–403, 1970.

[2] A. J. Friedenstein, J. F. Gorskaja, and N. N. Kulagina, "Fibroblast precursors in normal and irradiated mouse hematopoietic organs," *Experimental Hematology*, vol. 4, no. 5, pp. 267–274, 1976.

[3] S. Wakitani, T. Goto, S. J. Pineda et al., "Mesenchymal cell-based repair of large, full-thickness defects of articular cartilage," *The Journal of Bone & Joint Surgery—American Volume*, vol. 76, no. 4, pp. 579–592, 1994.

[4] E. J. Schwarz, G. M. Alexander, D. J. Prockop, and S. A. Azizi, "Multipotential marrow stromal cells transduced to produce L-DOPA: engraftment in a rat model of Parkinson disease," *Human Gene Therapy*, vol. 10, no. 15, pp. 2539–2549, 1999.

[5] H. A. Awad, D. L. Butler, G. P. Boivin et al., "Autologous mesenchymal stem cell-mediated repair of tendon," *Tissue Engineering*, vol. 5, no. 3, pp. 267–277, 1999.

[6] M. K. Majumdar, M. A. Thiede, J. D. Mosca, M. Moorman, and S. L. Gerson, "Phenotypic and functional comparison of cultures of marrow-derived mesenchymal stem cells (MSCs) and stromal cells," *Journal of Cellular Physiology*, vol. 176, no. 1, pp. 57–66, 1998.

[7] M. F. Pittenger, A. M. Mackay, S. C. Beck et al., "Multilineage potential of adult human mesenchymal stem cells," *Science*, vol. 284, no. 5411, pp. 143–147, 1999.

[8] C. M. Kolf, E. Cho, and R. S. Tuan, "Mesenchymal stromal cells. Biology of adult mesenchymal stem cells: regulation of niche, self-renewal and differentiation," *Arthritis Research & Therapy*, vol. 9, no. 1, article 204, 2007.

[9] A. I. Caplan, "Mesenchymal stem cells: cell-based reconstructive therapy in orthopedics," *Tissue Engineering*, vol. 11, no. 7-8, pp. 1198–1211, 2005.

[10] H. Shenghui, D. Nakada, and S. J. Morrison, "Mechanisms of stem cell self-renewal," *Annual Review of Cell and Developmental Biology*, vol. 25, pp. 377–406, 2009.

[11] W. Wagner, P. Horn, M. Castoldi et al., "Replicative senescence of mesenchymal stem cells: a continuous and organized process," *PLoS ONE*, vol. 3, no. 5, Article ID e2213, 2008.

[12] A. Muraglia, R. Cancedda, and R. Quarto, "Clonal mesenchymal progenitors from human bone marrow differentiate in vitro according to a hierarchical model," *Journal of Cell Science*, vol. 113, no. 7, pp. 1161–1166, 2000.

[13] P. Bianco, X. Cao, P. S. Frenette et al., "The meaning, the sense and the significance: translating the science of mesenchymal stem cells into medicine," *Nature Medicine*, vol. 19, no. 1, pp. 35–42, 2013.

[14] L. da Silva Meirelles, P. C. Chagastelles, and N. B. Nardi, "Mesenchymal stem cells reside in virtually all post-natal organs and tissues," *Journal of Cell Science*, vol. 119, part 11, pp. 2204–2213, 2006.

[15] P. De Coppi, A. Callegari, A. Chiavegato et al., "Amniotic fluid and bone marrow derived mesenchymal stem cells can be converted to smooth muscle cells in the cryo-injured rat bladder and prevent compensatory hypertrophy of surviving smooth muscle cells," *Journal of Urology*, vol. 177, no. 1, pp. 369–376, 2007.

[16] P. S. In't Anker, S. A. Scherjon, C. K.-V. der Keur et al., "Isolation of mesenchymal stem cells of fetal or maternal origin from human placenta," *Stem Cells*, vol. 22, no. 7, pp. 1338–1345, 2004.

[17] O. K. Lee, T. K. Kuo, W.-M. Chen, K.-D. Lee, S.-L. Hsieh, and T.-H. Chen, "Isolation of multipotent mesenchymal stem cells from umbilical cord blood," *Blood*, vol. 103, no. 5, pp. 1669–1675, 2004.

[18] K. Bieback, S. Kern, H. Klüter, and H. Eichler, "Critical parameters for the isolation of mesenchymal stem cells from umbilical cord blood," *Stem Cells*, vol. 22, no. 4, pp. 625–634, 2004.

[19] C. Limbert, R. Ebert, T. Schilling et al., "Functional signature of human islet-derived precursor cells compared to bone marrow-derived mesenchymal stem cells," *Stem Cells and Development*, vol. 19, no. 5, pp. 679–691, 2010.

[20] D. T. Covas, R. A. Panepucci, A. M. Fontes et al., "Multipotent mesenchymal stromal cells obtained from diverse human tissues share functional properties and gene-expression profile with $CD146^{+}$ perivascular cells and fibroblasts," *Experimental Hematology*, vol. 36, no. 5, pp. 642–654, 2008.

[21] O. Parolini, F. Alviano, G. P. Bagnara et al., "Concise review: isolation and characterization of cells from human term placenta: outcome of the First International Workshop on Placenta Derived Stem Cells," *Stem Cells*, vol. 26, no. 2, pp. 300–311, 2008.

[22] G. Pilz, C. Ulrich, T. Abruzzese et al., "Human term placenta-derived mesenchymal stromal cells are less prone to osteogenic differentiation than bone marrow-derived mesenchymal stromal cells," *Stem Cells and Development*, vol. 20, pp. 635–646, 2010.

[23] M. Dominici, K. Le Blanc, I. Müller et al., "Minimal criteria for defining multipotent mesenchymal stromal cells. The International Society for Cellular Therapy position statement," *Cytotherapy*, vol. 8, no. 4, pp. 315–317, 2006.

[24] M. Crisan, S. Yap, L. Casteilla et al., "A perivascular origin for mesenchymal stem cells in multiple human organs," *Cell Stem Cell*, vol. 3, no. 3, pp. 301–313, 2008.

[25] E. Schipani and H. M. Kronenberg, *Adult Mesenchymal Stem Cells*, Harvard Stem Cell Institute, Cambridge, Mass, USA, 2008.

[26] A. C. W. Zannettino, S. Paton, A. Arthur et al., "Multipotential human adipose-derived stromal stem cells exhibit a perivascular phenotype in vitro and in vivo," *Journal of Cellular Physiology*, vol. 214, no. 2, pp. 413–421, 2008.

[27] P. A. Zuk, M. Zhu, H. Mizuno et al., "Multilineage cells from human adipose tissue: implications for cell-based therapies," *Tissue Engineering*, vol. 7, no. 2, pp. 211–228, 2001.

[28] J. B. Mitchell, K. McIntosh, S. Zvonic et al., "Immunophenotype of human adipose-derived cells: temporal changes in stromal-associated and stem cell-associated markers," *Stem Cells*, vol. 24, no. 2, pp. 376–385, 2006.

[29] W. K. Aicher, H.-J. Bühring, M. Hart, B. Rolauffs, A. Badke, and G. Klein, "Regeneration of cartilage and bone by defined subsets of mesenchymal stromal cells—potential and pitfalls," *Advanced Drug Delivery Reviews*, vol. 63, no. 4, pp. 342–351, 2011.

[30] V. L. Battula, S. Treml, P. M. Bareiss et al., "Isolation of functionally distinct mesenchymal stem cell subsets using antibodies against CD56, CD271, and mesenchymal stem cell antigen-1," *Haematologica*, vol. 94, no. 2, pp. 173–184, 2009.

[31] C. De Bari, F. Dell'Accio, P. Tylzanowski, and F. P. Luyten, "Multipotent mesenchymal stem cells from adult human synovial membrane," *Arthritis and Rheumatism*, vol. 44, no. 8, pp. 1928–1942, 2001.

[32] G. P. Dowthwaite, J. C. Bishop, S. N. Redman et al., "The surface of articular cartilage contains a progenitor cell populations," *Journal of Cell Science*, vol. 117, no. 6, pp. 889–897, 2004.

[33] K. Benz, C. Stippich, C. Freudigmann, J. A. Mollenhauer, and W. K. Aicher, "Maintenance of 'stem cell' features of cartilage cell sub-populations during in vitro propagation," *Journal of Translational Medicine*, vol. 11, article 27, 2013.

[34] A. I. Caplan, "All MSCs are pericytes?" *Cell Stem Cell*, vol. 3, no. 3, pp. 229–230, 2008.

[35] A. Wilson and A. Trumpp, "Bone-marrow haematopoietic-stem-cell niches," *Nature Reviews Immunology*, vol. 6, no. 2, pp. 93–106, 2006.

[36] J. F. Smith, P. Yango, E. Altman et al., "Testicular niche required for human spermatogonial stem cell expansion," *Stem Cells Translational Medicine*, vol. 3, no. 9, pp. 1043–1054, 2014.

[37] K. Warstat, D. Meckbach, M. Weis-Klemm et al., "TGF-β enhances the integrin $\alpha 2\beta 1$-mediated attachment of mesenchymal stem cells to type i collagen," *Stem Cells and Development*, vol. 19, no. 5, pp. 645–656, 2010.

[38] S. Dånmark, A. Finne-Wistrand, A.-C. Albertsson, M. Patarroyo, and K. Mustafa, "Integrin-mediated adhesion of human mesenchymal stem cells to extracellular matrix proteins adsorbed to polymer surfaces," *Biomedical Materials*, vol. 7, no. 3, Article ID 035011, 2012.

[39] R. F. Wynn, C. A. Hart, C. Corradi-Perini et al., "A small proportion of mesenchymal stem cells strongly expresses functionally active CXCR4 receptor capable of promoting migration to bone marrow," *Blood*, vol. 104, no. 9, pp. 2643–2645, 2004.

[40] J. M. Karp and G. S. Leng Teo, "Mesenchymal stem cell homing: the devil is in the details," *Cell Stem Cell*, vol. 4, no. 3, pp. 206–216, 2009.

[41] G. Y. Rochefort, B. Delorme, A. Lopez et al., "Multipotential mesenchymal stem cells are mobilized into peripheral blood by hypoxia," *Stem Cells*, vol. 24, no. 10, pp. 2202–2208, 2006.

[42] J. M. Fox, G. Chamberlain, B. A. Ashton, and J. Middleton, "Recent advances into the understanding of mesenchymal stem cell trafficking," *British Journal of Haematology*, vol. 137, no. 6, pp. 491–502, 2007.

[43] G. S. L. Teo, Z. Yang, C. V. Carman, J. M. Karp, and C. P. Lin, "Intravital imaging of mesenchymal stem cell trafficking and association with platelets and neutrophils," *Stem Cells*, vol. 33, no. 1, pp. 265–277, 2014.

[44] A. G. Via, A. Frizziero, and F. Oliva, "Biological properties of mesenchymal Stem Cells from different sources," *Muscles, Ligaments and Tendons Journal*, vol. 2, no. 3, pp. 154–162, 2012.

[45] H.-J. Büuhring, V. L. Battula, S. Treml, B. Schewe, L. Kanz, and W. Vogel, "Novel markers for the prospective isolation of human MSC," *Annals of the New York Academy of Sciences*, vol. 1106, pp. 262–271, 2007.

[46] E. Jones, A. English, S. M. Churchman et al., "Large-scale extraction and characterization of CD271+ multipotential stromal cells from trabecular bone in health and osteoarthritis: implications for bone regeneration strategies based on uncultured or minimally cultured multipotential stromal cells," *Arthritis and Rheumatism*, vol. 62, no. 7, pp. 1944–1954, 2010.

[47] R. H. Lee, B. Kim, I. Choi et al., "Characterization and expression analysis of mesenchymal stem cells from human bone marrow and adipose tissue," *Cellular Physiology and Biochemistry*, vol. 14, no. 4–6, pp. 311–324, 2004.

[48] J. A. Jeong, S. H. Hong, E. J. Gang et al., "Differential gene expression profiling of human umbilical cord blood-derived mesenchymal stem cells by DNA microarray," *Stem Cells*, vol. 23, no. 4, pp. 584–593, 2005.

[49] M. Secco, Y. B. Moreira, E. Zucconi et al., "Gene expression profile of mesenchymal stem cells from paired umbilical cord units: cord is different from blood," *Stem Cell Reviews & Reports*, vol. 5, no. 4, pp. 387–401, 2009.

[50] C. Ulrich, T. Abruzzese, J. K. Maerz et al., "Human placenta-derived CD146-positive mesenchymal stromal cells display a distinct osteogenic differentiation potential," *Stem Cells and Development*, vol. 24, no. 13, pp. 1558–1569, 2015.

[51] S. Barlow, G. Brooke, K. Chatterjee et al., "Comparison of human placenta- and bone marrow-derived multipotent mesenchymal stem cells," *Stem Cells and Development*, vol. 17, no. 6, pp. 1095–1107, 2008.

[52] M.-S. Tsai, S.-M. Hwang, K.-D. Chen et al., "Functional network analysis of the transcriptomes of mesenchymal stem cells derived from amniotic fluid, amniotic membrane, cord blood, and bone marrow," *Stem Cells*, vol. 25, no. 10, pp. 2511–2523, 2007.

[53] G. A. Pilz, C. Ulrich, M. Ruh et al., "Human term placenta-derived mesenchymal stromal cells are less prone to osteogenic differentiation than bone marrow-derived mesenchymal stromal cells," *Stem Cells and Development*, vol. 20, no. 4, pp. 635–646, 2011.

[54] T. Takarada, E. Hinoi, R. Nakazato et al., "An analysis of skeletal development in osteoblast-specific and chondrocyte-specific runt-related transcription factor-2 (Runx2) knockout mice," *Journal of Bone and Mineral Research*, vol. 28, no. 10, pp. 2064–2069, 2013.

[55] C. Pendleton, Q. Li, D. A. Chesler, K. Yuan, H. Guerrero-Cazares, and A. Quinones-Hinojosa, "Mesenchymal stem cells derived from adipose tissue vs bone marrow: in vitro comparison of their tropism towards gliomas," *PLoS ONE*, vol. 8, no. 3, Article ID e58198, 2013.

[56] W. Vogel, F. Grünebach, C. A. Messam, L. Kanz, W. Brugger, and H.-J. Bühring, "Heterogeneity among human bone marrow-derived mesenchymal stem cells and neural progenitor cells," *Haematologica*, vol. 88, no. 2, pp. 126–133, 2003.

[57] Y. Mabuchi, S. Morikawa, S. Harada et al., "LNGFR(+), THY-1(+), VCAM-1(hi+) cells reveal functionally distinct subpopulations in mesenchymal stem cells," *Stem Cell Reports*, vol. 1, no. 2, pp. 152–165, 2013.

[58] Y. Mabuchi, D. D. Houlihan, C. Akazawa, H. Okano, and Y. Matsuzaki, "Prospective isolation of murine and human bone marrow mesenchymal stem cells based on surface markers," *Stem Cells International*, vol. 2013, Article ID 507301, 7 pages, 2013.

[59] K. Sivasubramaniyan, A. Harichandan, S. Schumann et al., "Prospective isolation of mesenchymal stem cells from human bone marrow using novel antibodies directed against Sushi domain containing 2," *Stem Cells and Development*, vol. 22, no. 13, pp. 1944–1954, 2013.

[60] H. Li, R. Ghazanfari, D. Zacharaki et al., "Low/negative expression of PDGFR-α identifies the candidate primary mesenchymal stromal cells in adult human bone marrow," *Stem Cell Reports*, vol. 3, no. 6, pp. 965–974, 2014.

[61] S. Pinho, J. Lacombe, M. Hanoun et al., "PDGFRα and CD51 mark human Nestin$^+$ sphere-forming mesenchymal stem cells capable of hematopoietic progenitor cell expansion," *The Journal of Experimental Medicine*, vol. 210, no. 7, pp. 1351–1367, 2013.

[62] S. Méndez-Ferrer, T. V. Michurina, F. Ferraro et al., "Mesenchymal and haematopoietic stem cells form a unique bone marrow niche," *Nature*, vol. 466, no. 7308, pp. 829–834, 2010.

[63] B. Sacchetti, A. Funari, S. Michienzi et al., "Self-renewing osteoprogenitors in bone marrow sinusoids can organize a hematopoietic microenvironment," *Cell*, vol. 131, no. 2, pp. 324–336, 2007.

[64] M. L. Hart, J. Brun, K. Lutz, B. Rolauffs, and W. K. Aicher, "Do we need standarized, GMP-compliant cell culture procedures for pre-clinical in vitro studies involving mesenchymal stem/stromal cells?" *Journal of Tissue Science & Engineering*, vol. 5, pp. 135–139, 2014.

[65] N. Kim and S.-G. Cho, "Clinical applications of mesenchymal stem cells," *Korean Journal of Internal Medicine*, vol. 28, no. 4, pp. 387–402, 2013.

[66] Y. Wang, Z.-B. Han, Y.-P. Song, and Z. C. Han, "Safety of mesenchymal stem cells for clinical application," *Stem Cells International*, vol. 2012, Article ID 652034, 4 pages, 2012.

[67] A. M. Bailey, "Balancing tissue and tumor formation in regenerative medicine," *Science Translational Medicine*, vol. 4, no. 147, Article ID 147fs28, 2012.

[68] F. Baron and R. Storb, "Mesenchymal stromal cells: a new tool against graft-versus-host disease?" *Biology of Blood and Marrow Transplantation*, vol. 18, no. 6, pp. 822–840, 2012.

[69] M. Introna, G. Lucchini, E. Dander et al., "Treatment of graft versus host disease with mesenchymal stromal cells: a phase I study on 40 adult and pediatric patients," *Biology of Blood and Marrow Transplantation*, vol. 20, no. 3, pp. 375–381, 2014.

[70] M. Breitbach, T. Bostani, W. Roell et al., "Potential risks of bone marrow cell transplantation into infarcted hearts," *Blood*, vol. 110, no. 4, pp. 1362–1369, 2007.

[71] W. C. Hines, Y. Su, I. Kuhn, K. Polyak, and M. J. Bissell, "Sorting out the FACS: a devil in the details," *Cell Reports*, vol. 6, no. 5, pp. 779–781, 2014.

[72] G. A. Pilz, J. Braun, C. Ulrich et al., "Human mesenchymal stromal cells express CD14 cross-reactive epitopes," *Cytometry A*, vol. 79, no. 8, pp. 635–645, 2011.

Hindawi Publishing Corporation
Stem Cells International
Volume 2016, Article ID 6838253, 16 pages
http://dx.doi.org/10.1155/2016/6838253

Review Article

Pluripotency Factors on Their Lineage Move

Clair E. Weidgang,[1,2] Thomas Seufferlein,[1] Alexander Kleger,[1] and Martin Mueller[1]

[1]*Department of Internal Medicine I, Ulm University Hospital, 89069 Ulm, Germany*
[2]*Department of Anesthesiology, Ulm University Hospital, 89069 Ulm, Germany*

Correspondence should be addressed to Clair E. Weidgang; clair.weidgang@uni-ulm.de and Alexander Kleger; alexander.kleger@uniklinik-ulm.de

Received 14 May 2015; Revised 30 July 2015; Accepted 3 August 2015

Academic Editor: Kodandaramireddy Nalapareddy

Pluripotent stem cells are characterised by continuous self-renewal while maintaining the potential to differentiate into cells of all three germ layers. Regulatory networks of maintaining pluripotency have been described in great detail and, similarly, there is great knowledge on key players that regulate their differentiation. Interestingly, pluripotency has various shades with distinct developmental potential, an observation that coined the term of a ground state of pluripotency. A precise interplay of signalling axes regulates ground state conditions and acts in concert with a combination of key transcription factors. The balance between these transcription factors greatly influences the integrity of the pluripotency network and latest research suggests that minute changes in their expression can strengthen but also collapse the network. Moreover, recent studies reveal different facets of these core factors in balancing a controlled and directed exit from pluripotency. Thereby, subsets of pluripotency-maintaining factors have been shown to adopt new roles during lineage specification and have been globally defined towards neuroectodermal and mesendodermal sets of embryonic stem cell genes. However, detailed underlying insights into how these transcription factors orchestrate cell fate decisions remain largely elusive. Our group and others unravelled complex interactions in the regulation of this controlled exit. Herein, we summarise recent findings and discuss the potential mechanisms involved.

1. Introduction

Pluripotency represents three essential features: first the capacity of indefinite self-renewal, second the ability of giving rise to differentiated progeny of nearly all lineages of the mature organism, and last the generation of chimeric embryos upon injection into the inner cell mass (ICM) of a blastocyst [1]. The complexity of the regulatory networks, which maintain pluripotency, has previously been described [2]. Complex interactions between signalling axes precisely regulate various states of pluripotency, such as the ground and the primed state, and act in concert with a combination of key transcription factors (TFs). Vice versa, we have gained a great body of knowledge on key players guiding pluripotent stem cells (PSCs) towards differentiation [3, 4]. In line, regulatory networks both in PSCs and in the developing organism are tightly balanced as small changes can break down the entire pluripotency network leading to differentiation [3]. In recent years, studies have revealed novel facets of these core factors balancing a controlled exit of pluripotency and guiding early steps of differentiation [5]. Herein, subsets of pluripotency-maintaining factors have been shown to adopt new roles during lineage specification and have been grouped into neuroectodermal and mesendodermal sets of embryonic stem cell genes [5]. Accordingly, for example, Nanog, Tbx3, Klf5, and Oct3/4 regulate the exit towards mesendoderm while Sox2 regulates differentiation towards a neuroectodermal fate [5]. However, detailed underlying mechanisms of how these TFs orchestrate cell fate decisions remain largely elusive. Aiming to close this gap of knowledge, we have recently studied the mechanism of Tbx3 to regulate mesendodermal fate. Briefly, we have defined novel facets of Tbx3 which directly activates core regulators of the mesendodermal lineage and indirectly induces differentiation via a paracrine Nodal signalling loop [6]. Thus, our data illustrate the dual complexity of pluripotency TFs to gate fate determination.

In turn, the current review will at first give a brief insight into essential signalling pathways and TFs maintaining the self-renewal state. Secondly, we will summarise recent findings of pluripotency-associated factors that have an important impact on early lineage specification processes.

2. ESC Pluripotency and Its Signalling Pathways

Most of the knowledge on pluripotency has been obtained using mouse embryonic stem cells (mESCs) as a research tool [8–11]. *In vitro* pluripotency has various shades mirroring distinct *in vivo* counterparts, an observation which has led to the definition of two pluripotency states: naïve and primed [12–14]. Herein, the early ICM of the blastocyst requires a maturation step to obtain clonal pluripotent colonies, while E4 and E4.5 preimplantation epiblast cells from the blastocyst robustly give rise to naïve pluripotent cells capable of single-cell culture [15]. To capture naïve pluripotency *in vitro*, cells isolated from the ICM are cultured serum-free in the presence of leukaemia inhibitory factor (LIF) and bone morphogenetic protein (BMP) or under LIF/2i-culture conditions (outlined below) [16, 17]. In contrast, cells derived from the postimplantation epiblast are not any longer single-cell culture permissive and require distinct signalling input such as FGF- (fibroblast growth factor-) supplementation to remain within the pluripotent state. These cells are *in vitro* referred to as epiblast stem cells (EpiSCs). They are characterised by primed pluripotency and exhibit a slightly reduced differential potential, thus surrogating a more advanced pregastrulation stage [18, 19]. A large body of knowledge has been gained in the past years, deciphering signalling axes with an impact on the pluripotent state. Basically, the mitogen-activated protein kinase (MAPK) signalling pathway and glycogen synthase kinase 3 (GSK3) signalling pathway negatively influence pluripotency, while LIF/STAT3 (signal transducer and activator of transcription 3) and BMP/SMAD (mothers against decapentaplegic) signalling are complementary beneficial [16, 17].

2.1. LIF/STAT3 Signalling. mESCs are commonly retained in the pluripotent state by culturing them on a feeder layer composed of mouse inactivated fibroblasts (MEFs) in the presence of the cytokine LIF [20–22]. LIF functions via a complex signalling axis and finally activates core TFs, such as octamer binding transcription factor 3/4 (Oct3/4), sex determining region Y- (SRY-) box 2 (Sox2), and Nanog, which orchestrate the self-renewal state [23, 24]. *In vivo*, their expression levels overlap both in the ICM and in the epiblast [24], hence being able to interact and activate pluripotency-associated genes, while repressing lineage specific differentiation programmes. LIF signals via three different pathways. However, its key effect in sustaining the pluripotent state is implemented by activating the TF STAT3 via phosphorylation [25]. STAT3, the crucial downstream target of LIF, directly binds the distal enhancers of Oct3/4 and Nanog [26] and further pluripotency TFs [27] such as Krüppel-like factor 4 (as Klf4) [28]. Thereby it modulates their expression levels for propagation of the murine pluripotent phenotype. In the absence of LIF signalling, mESCs differentiate to the mesodermal and endodermal lineage [29]. Therefore, LIF limits mESC differentiation towards mesendoderm in favour of maintaining the pluripotent state in a closely regulated balance with BMP signalling [16]. Despite its essential role in self-renewal *in vivo* and *in vitro*, LIF also participates in regulating a differentiation programme driven by the extracellular-signal-regulated kinase (ERK). The ERK signalling cascade promotes early differentiation *in vitro* and *in vivo* [30, 31]. Thus, LIF seems to modulate stem cell fate between self-renewal and lineage specification by regulating expression levels of STAT3 and ERK [32]. In summary, LIF represents a critical component in maintaining the self-renewal state in mESC culture by activating pluripotency-associated TFs. Of note, LIF-dependence can be overcome at least temporarily by chemical inhibition of MAPK and GSK3 signalling ("2i") but still remains beneficial, an observation establishing LIF-2i as the gold standard of serum-free mESC culture (Figure 1) [15, 33, 34].

2.2. BMP Signalling. In a serum-free cell culture LIF is solely not able to maintain mESC pluripotency [16]. BMP4 is a secreted signalling molecule belonging to the transforming growth factor beta (TGFβ) family and represents an attested ectoderm-antagonist [16, 35, 36]. BMP4 (and BMP2) successfully replaces serum requirements resulting in propagation of pluripotency and inhibition of multilineage differentiation in the presence of LIF. In the absence of LIF, BMP promotes mesodermal differentiation [37] at the expense of the neural lineage [38] (Figure 1). Further, the BMP pathway also has the potential to promote differentiation of mESCs into the trophoblast lineage via caudal type homeobox 2 (Cdx2) when cultured under defined conditions [39].

In the preimplantation embryo, BMP4 becomes induced in the ICM of the early blastocyst while its expression peaks in the epiblast of the E4.5 blastocyst and decreases afterwards. This decrease of BMP signalling in the postimplantation epiblast coincides with the upregulation of Nodal/Activin signalling and subsequent target gene expression such as Lefty1 and Lefty2 pointing at opposing roles of Nodal and BMP signals at various developmental stages [15, 40–42]. This *in vivo* observation matches the requirement of low-dose Nodal/Activin signalling to maintain the primed state of pluripotency [43]. The opposing effects of Nodal and BMP signalling are obviously relevant not only for lineage commitment but also for fine tuning BMP signalling in the naïve state involving an intracellular mechanism via SMAD7 to modulate SMAD1/SMAD5 levels [4, 40, 44]. In summary, LIF is dependent on BMP signalling in a serum-free mESC culture, while both signalling axes are strongly dependent on a precise dosage regulation as any imbalance between both pathways drives exit from pluripotency to various fates. In the absence of LIF, BMP signalling directs mESCs towards the mesendoderm and trophoblast lineage [45, 46].

2.3. Small Molecules Capture Ground State Pluripotency. Previously, the Smith Laboratory identified two small molecules, PD0325901 (PD03) and CHIR99021 (CHIR), which can substitute for LIF and BMP under defined culture conditions to facilitate ground state pluripotency in mESC (2i conditions)

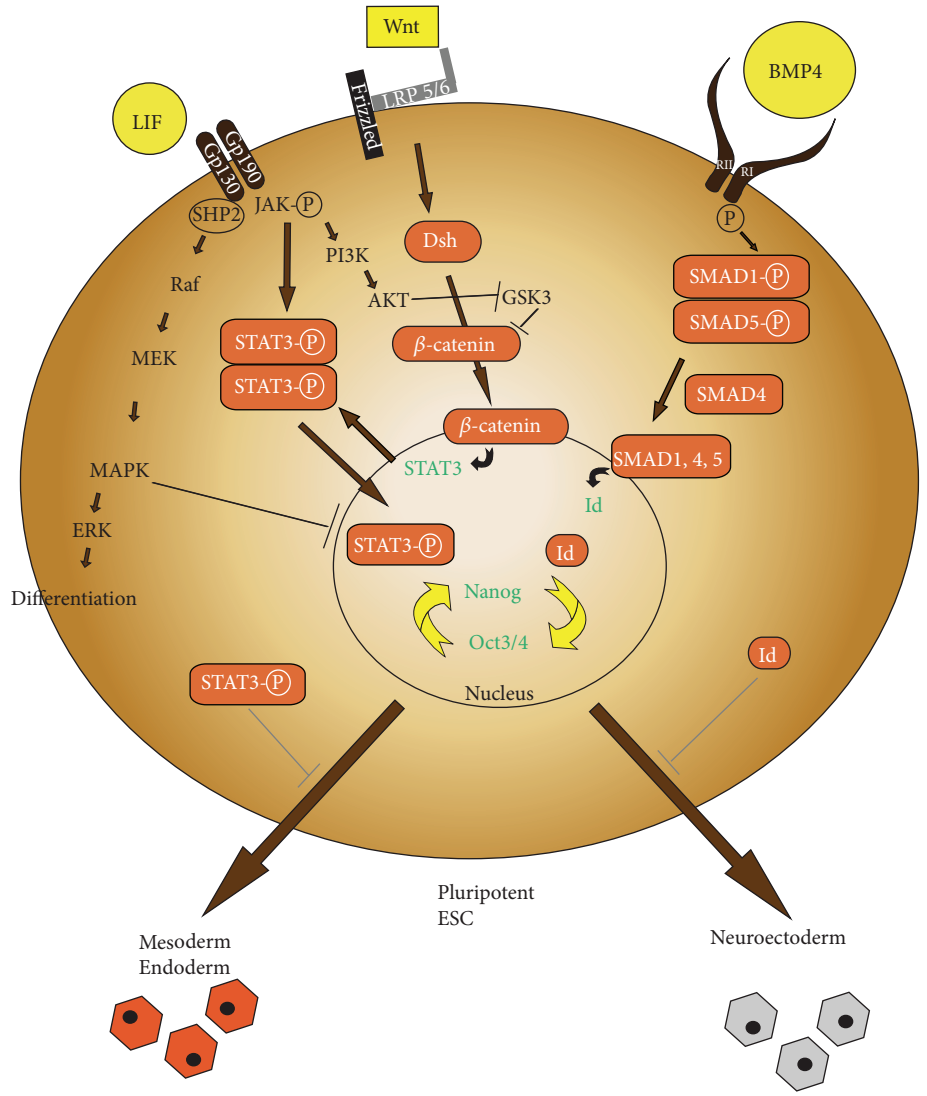

Figure 1: Signalling pathways regulating pluripotency in mESCs. A schematic representation of the main extrinsic pathways (LIF, BMP, and WNT) regulating pluripotency in mESCs. Upon LIF binding to its receptor, Gp130 phosphorylates JAK, which in turn phosphorylates STAT3. Phosphorylated STAT3 operates as a transcription factor which sustains the pluripotency state in mESCs and further inhibits endodermal and mesodermal differentiation. LIF further inhibits GSK3 via PI3K. GSK3 stabilises the self-renewal state by reducing the ubiquitin dependent degradation of β-catenin. WNT proteins bind the Frizzled receptor which in turn forms a complex with LRP5/6 protein and signal downstream via Dsh and β-catenin. β-catenin accumulates in the cytoplasm and nucleus resulting in STAT3 transcription. STAT3 is activated through JAK phosphorylation. Upon BMP4-receptor complex formation, BMP RI phosphorylates SMAD1 and SMAD5 which then interacts with SMAD4 resulting in Id gene transcription and maintenance of the pluripotency state. Image modified after Hao [7]. Dsh: dishevelled, ERK: extracellular receptor kinase, Id: inhibitor of differentiation, JAK: Janus kinase, and mESCs: murine embryoid stem cells. LIF: leukaemia inhibitory factor, MAPK: mitogen-activated protein kinase, Oct3/4: octamer binding transcription factor 3/4, PI3K: phosphatidylinositide 3′-kinase, SMAD1/4/5: mothers against decapentaplegic homolog 1/4/5, STAT3: signal transducers and activators of transcription 3, RI: receptor type I, RII: receptor type II, and WNT: wingless-related MMTV integration site family.

[17]. PD03 inhibits MEK, a downstream target of FGF signalling, important for trophectodermal lineage differentiation in early embryos [47]. Further, mESC pluripotency and particularly viability is promoted by increased WNT (wingless-type MMTV integration site family) signalling via CHIR, a specific GSK3 inhibitor [17, 48]. Nuclear expression level of β-catenin, the core effector of WNT signalling [49], is regulated by a multiprotein destruction complex [50]. Herein, GSK3 inhibition stabilises the self-renewal state by diminishing ubiquitin dependent degradation of β-catenin and repressing Tcf3, a known transcriptional repressor of target genes [34]. Tcf3 cooccupies and represses Oct3/4, Sox2, Nanog, and estrogen-related receptor β (Esrrb) [51–54], suggesting its role as a crucial regulator of the transcriptional control of pluripotency in mESCs. Regarding WNT signalling and its impact on mESC pluripotency, β-catenin

interacts with Oct3/4 [34, 55] and Sox2 [56, 57] and is activated by Nanog via Dickkopf-related protein 1 (Dkk1) repression [58] to reinforce the self-renewal state. Despite its role in maintaining pluripotency, canonical WNT/β-catenin signalling participates in body axis patterning, primitive streak and extraembryonic lineage formation, and mesoderm specification through Brachyury [59–63]. In summary, inhibition of MAPK and GSK3 signalling together with LIF-supplementation under serum-free culture conditions is capable of capturing naïve pluripotency robustly from various preimplantation stages and can preserve ground state conditions with erased lineage fates [15, 33].

3. Lineage Specific Classification of Pluripotency Transcription Factors

Despite acting during mESC self-renewal, pluripotency-associated factors also connect the transition from pluripotency towards lineage specification [4, 5]. The pluripotent state is maintained by a unique network of directly interacting TFs (including Oct3/4, Sox2, Nanog, Tbx3, and Klf4/5). These TFs either inhibit target gene expression levels required for lineage differentiation or sustain the expression of one another [64–66]. However, upon differentiation, controlled mesendodermal and neuroectodermal commitment requires the reorganisation of the circuit to allow onset of lineage specific programmes. Herein, extracellular clues, such as WNT, BMP, and TGFβ, further impact and regulate cell fate choice [67]. Interestingly, certain pluripotency factors are not simply downregulated but instead their expression is either sustained or even upregulated for a short time window during pluripotency exit [4, 5]. This does not occur randomly but instead is lineage and factor specific: Basically, we can distinguish three groups: mesendoderm-class genes (e.g., Kf4/5, Nanog, Oct3/4, and Tbx3), neuroectoderm-class genes (e.g., Sox2), and extraembryonic-class genes (e.g., spalt-like transcription factor 4 (Sall4)) [5]. Mechanistically, TFs bind asymmetrically in regulatory regions on the one hand promoting the respective lineage but on the other hand repressing the other, thus ensuring tightly regulated cell fate choices. In the following sections, we aim to discuss pluripotency factors, which have recently been shown to have such a dual function, namely, pluripotency and early cell fate choice [68].

However, before continuing we want to briefly summarise the earliest embryonic cell fate decisions for better comprehension (Figure 2). The zygote represents the earliest stage of the early mammalian embryo. From here, the cells undergo several series of cleavage divisions producing the morula [69]. Subsequently, the first cell decision occurs during the transition from morula to blastocyst by differentiating into two distinct lineages. The outer cell layer of the blastocyst forms the trophectoderm, whereas the inner cells develop to the ICM [70]. The trophectoderm proliferates further into the extraembryonic ectoderm and trophoblast, later giving rise to the placenta. Prior to implantation the ICM undergoes the second cell fate decision by differentiating into either the epiblast (later forming the primitive ectoderm and subsequently giving rise to the three germ layers among others) or the primitive endoderm [69]. The primitive endoderm cells form both visceral and parietal endoderm and finally give rise to the yolk sac [71]. Prior to mouse gastrulation, the initially symmetrical embryo is prepatterned by regional distinctions in gene expression profiles and levels of signalling pathways along the embryonic axes [4]. The formation of the primitive streak as the first obvious sign of germ layer formation is driven by gradients of growth factor signalling such as Nodal and canonical WNT at the posterior pole of the embryo, accompanied by the expression of early differentiation marker genes [4, 40]. The regulatory events that define the timing and site of gastrulation initiation still remain rather unclear. The formation of a transient precursor cell population located in the region of the anterior primitive streak reflects one of the earliest events during gastrulation. Definitive endoderm and anterior mesoderm derivatives, including cardiovascular and head mesenchyme progenitors, originate from these precursors. Notably, this cell population, referred to as mesendoderm, is marked by the expression of marker genes such as Eomesodermin (Eomes), Forkhead-Box-Protein A2 (Foxa2), Chordin (Chrd), Goosecoid (Gsc), and LIM-homeobox 1 (Lhx1) [72].

3.1. Mesendodermal-Class Genes

3.1.1. Octamer Binding Transcription Factor 3/4 (Oct3/4): Indispensable for Lineage and Pluripotency. Oct3/4 has gained much attention as the key regulator of mESC pluripotency *in vitro* and *in vivo* [73]. Oct3/4 belongs to the POU family and, as a master regulator of pluripotency, it functions in a complex, consisting of Nanog, Oct3/4, and Sox2 [74]. Hereby, it crucially balances gene expression levels of the pluripotency circuitry [75]. STAT3 is able to directly bind and regulate Oct3/4 to maintain self-renewal [26]. Also, both have been shown to activate similar target genes [3]. Previous work describes Oct3/4 as a gatekeeper both for maintaining self-renewal and also in modulating stem cell fate choice in a dose-dependent manner [76]. In this respect, the Chambers Laboratory demonstrated that low Oct3/4 levels, as seen in heterozygous mESCs, were sufficient to maintain mESC pluripotency [77]. This was especially due to elevated promoter binding of Oct3/4 to pluripotency-associated factors (e.g., Esrrb, Klf4, Nanog, and Tbx3) and increased WNT signalling and LIF sensitivity. In contrast, elevated Oct3/4 levels destabilised the pluripotency network resulting in FGF-dependent differentiation [77]. In this sense, alternate partners of Oct3/4 can define the switch between pluripotency and lineage commitment: while in the pluripotent state Oct3/4 sustains Sox2 expression, the switch to activate Sox17 instead marks a critical event during mesendodermal differentiation. This process is triggered not only by a change in target gene expression but in a noncell autonomous manner by the secretion of paracrine factors further favouring mesendodermal differentiation [78, 79]. Moreover, Hogan et al. analysed the impact of Oct3/4 on regulating mESC differentiation based on previous knowledge that mESCs differentiation is the result of an interplay between transcriptional regulation and chromatin organisation [80, 81]. In this regard, exit from pluripotency was facilitated through intermittent

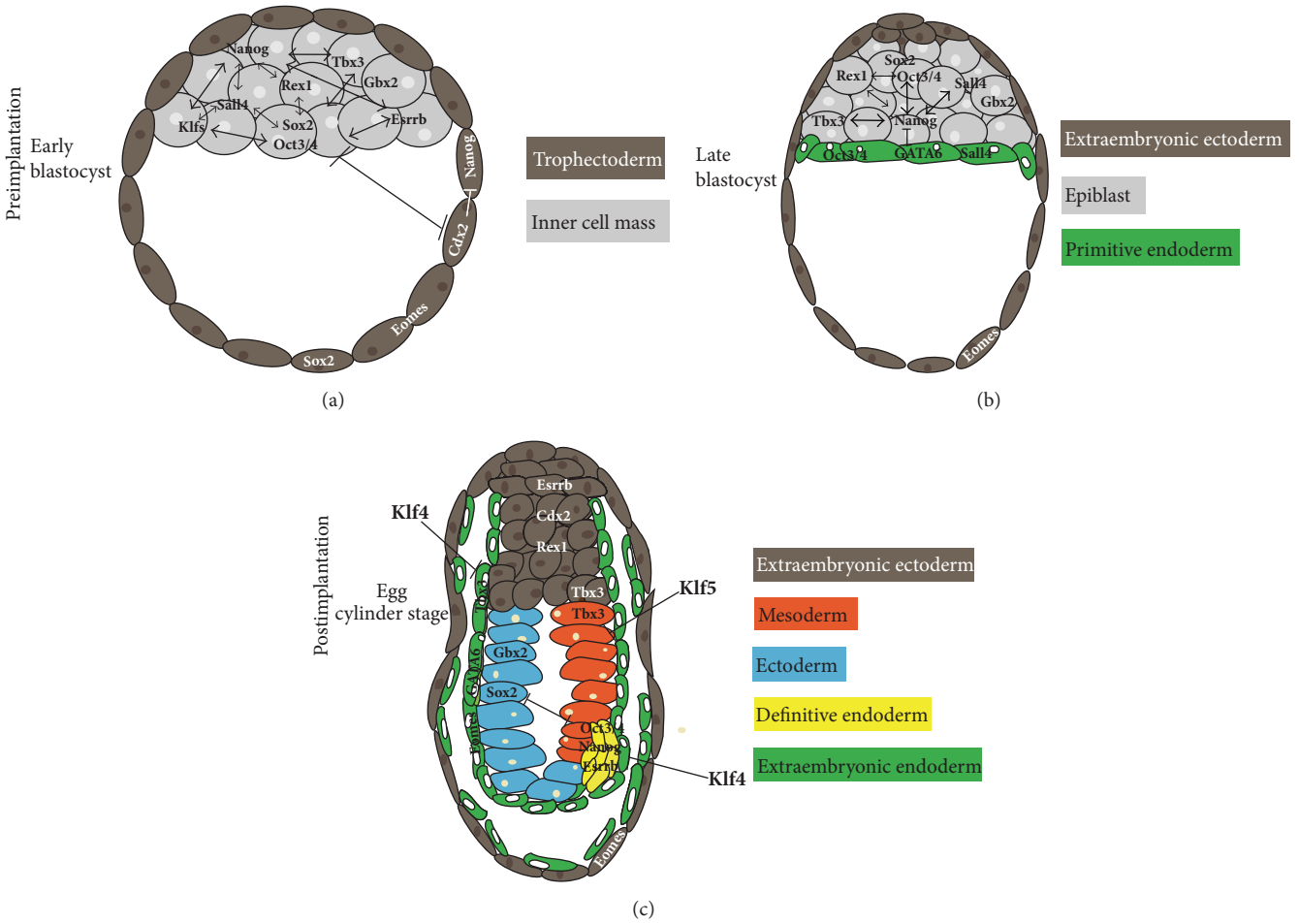

Figure 2: Pluripotency factor expression during early embryonic development. Pluripotency factors are expressed throughout the pluripotency state and subsequently govern early lineage decisions in mouse. (a) The early blastocyst consists of the ICM and the outer trophectoderm. Pluripotency factors are expressed in the ICM, however, interacting with trophectodermal genes for proper lineage development. (b) At the late blastocyst stage, the ICM segregates into the epiblast, notably exhibiting slightly different gene expression patterns, and into the extraembryonic endoderm, later giving rise to yolk sac. Further, the trophectoderm has formed the extraembryonic ectoderm lineage which will generate the placenta. (c) After implantation, the primitive ectoderm, which has origins in the epiblast, forms the four embryo-derived stem cell lineages (ectoderm, mesoderm, endoderm, and germ lineage). Notably, pluripotency factors guide early embryonic decision according to their expression profile, respectively. ICM: inner cell mass.

homologous pairing of the Oct3/4 allele. This was mediated by a locus initially described as the Oct/Sox-binding element within the Oct3/4 promoter region. Besides, Oct3/4 is also known to undergo alternative promoter binding at the stage when loss of pluripotency occurs towards differentiation [82].

In the embryo, Oct3/4 maintains the ICM and guides proper trophectoderm segregation upon differentiation. As Cdx2 expression promotes the trophectoderm lineage [83], it is not surprising that Oct3/4 was identified as a negative regulator of Cdx2 [84]. The Oct3/4-Cdx2 complex (possibly together with Sall4 as mentioned below) specifies lineage formation in the early embryos by reciprocal inhibition *in vivo* and *in vitro* [85] (Figure 2). *In vivo*, Oct3/4 guides mesendodermal differentiation and further suppresses neuroectodermal gene expression programmes [5, 86]. Preceding mouse development, Oct3/4 is expressed in the primitive endoderm [87] (Figure 2). Conditional deletion of Oct3/4 *in vitro* promotes mESCs to commit towards the trophectoderm lineage via Cdx2 and Eomes [3, 73, 84, 88]. Oct3/4-deficient mouse embryos develop to the blastocyst stage but fail to form a consistent pluripotent ICM resulting in embryonic lethality due to differentiation into the extraembryonic trophoblast lineage [73]. Thus, the acquisition of ICM identity is supposed to be dependent on Oct3/4 functions [84]. Indeed, a recent study revealed a transient ICM formation in Oct3/4-deficient embryos, due to elevated Nanog expression levels [89]. Moreover, these embryos were lacking a functional primitive endoderm; however, this was rescued by stage specific supplementation of FGF4 [89]. This study was able to reveal a critical role of Oct3/4 facilitating early lineage decisions in ICM cells towards either epiblast or primitive endoderm by attenuating Nanog expression levels and further promoting

primitive endoderm formation in an FGF-dependent manner [89]. However, due to its importance in governing lineage decisions in the early blastocyst, it is not possible to date to isolate mESCs from Oct3/4-deficient embryos [73].

Taken together, Oct3/4 belongs to key pluripotency TFs, which maintains mESC pluripotency. Its tightly regulated expression levels drive proper mESC differentiation towards mesoderm and primitive endoderm [3] by repressing the neuroectodermal lineage fate [90]. Molecularly, this gatekeeper function is exerted by alternate partnering and changes in cobound factors to orchestra cell fate choice by alternating target gene binding.

3.1.2. T-Box Transcription Factor 3 (Tbx3): Bystander in Pluripotency or Just Cell Fate Regulator? Several studies have highlighted Tbx3 to function during mESC self-renewal [2–4, 65]. Briefly, the PI3K-AKT signalling pathway stimulates Tbx3 resulting in upregulated key pluripotency factor expression levels (Oct3/4, Nanog, and Sox2). To balance accurate pluripotency levels, Tbx3 expression is antagonised by the MAPK pathway [2]. It is also able to drive the expression of key pluripotency markers by direct promoter binding through Nanog [65]. In addition, Tbx3 acts as a downstream activator of WNT signalling [91]. WNT sustains the pluripotent state together with LIF, although, in the absence of LIF, WNT promotes cell differentiation towards primitive endoderm via Tbx3 [91, 92]. Hence, Tbx3 has been widely believed to belong to the inner core of the pluripotency circuitry, with loss of Tbx3 leading to differentiation. In marked contrast, we have recently identified fluctuating Tbx3 levels in mESCs: "Tbx3-low" cells resemble the gastrulating epiblast *in vivo* but retain the capacity to switch back to a Tbx3-high state. Moreover, we could show that Tbx3 is dispensable for the induction and maintenance of naïve pluripotency. Taken together, we delineate novel facets of Tbx3 action in pluripotency and show an involvement of Tbx3 in the transition from the naïve embryonic state to the prepatterned epiblast-like state. These purely mESC-derived data are further fostered by the observation of *in vivo* heterogeneity of Tbx3 in the ICM (Russell, Liebau, Kleger, unpublished data).

However, Tbx3 also fulfills a lineage specifying role, thus being classified as a mesendodermal-class gene [5] (Figure 3). We showed that Tbx3 is dynamically expressed during specification of the mesendoderm lineages in differentiating mESCs *in vitro* and in developing mouse and *Xenopus* embryos *in vivo* [4]. Nodal patterns the preimplantation embryo by interacting with the epiblast and the extraembryonic tissues [93]. Tbx3 overexpression promotes mesendodermal specification by activating crucial lineage specifying factors and by enhancing paracrine Nodal/SMAD2 signalling. Also, Tbx3 expression has also been detected in the visceral endoderm lineage. Therefore we suggest that Tbx3 may promote mesodermal lineage formation by activating Nodal via visceral endodermal cells expressing Tbx3 (Figure 2). Tbx3 is highly enriched in definitive endoderm progenitor cells [94] and it is involved in endoderm patterning together with chromatin-modifying enzymes [95]. The underlying mechanism includes spatial reorganisation of chromatin, leading to sensitisation for definitive endoderm promoting

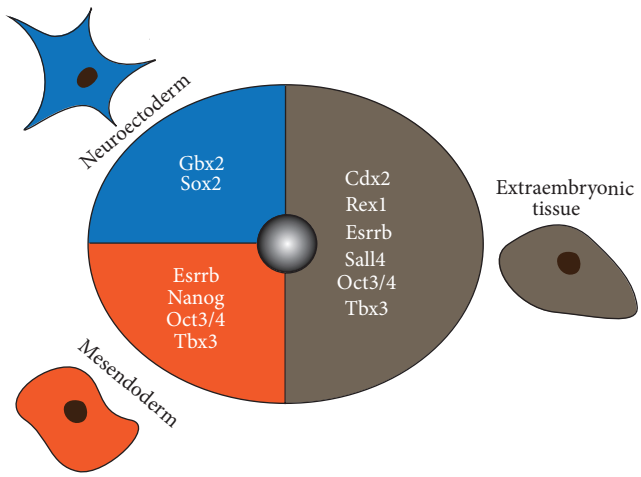

Figure 3: Spatial classifications of pluripotency factors. Upon exit of pluripotency core pluripotency factors get committed to distinct lineages and arising tissues, thus playing a crucial role in directing early lineage decisions in mouse. This image illustrates their spatial classification in the early embryo: neuroectoderm is mainly promoted by Gbx2 and Sox2 and mesendoderm especially by Esrrb, Nanog, Oct3/4, and Tbx3. Further, the extraembryonic tissue is induced by Cdx2, Rex1, Esrrb, Sall4, Oct3/4, and Tbx3. Cdx2: caudal type homeobox 2, Esrrb: estrogen-related receptor β, Gbx2: gastrulation brain homeobox 2, Tbx3: T-box transcription factor 3, Oct3/4: octamer binding transcription factor 3/4, Rex1: Zfp42, Sall4: Sal-like 4, and Sox2: SRY- (sex determining region Y-) box 2.

signals by enabling the histone demethylase Jmjd3 to transiently bind the two T-box factors: Tbx3 and Eomes.

In summary, Tbx3 is embedded in the core pluripotency networks to sustain stemness but also strongly directs early embryonic development by either transcriptional activation of differentiating gene programmes or modification of chromatin structures.

3.1.3. Krüppel-Like Family (Klf): The Transcriptional Lineage Inhibitors. Klfs (Klf2, Klf4, and Klf5) are conserved zinc-finger-containing TFs implicated in various biological processes, such as proliferation, differentiation, and development [96]. In the early embryo they are already expressed in the ICM [97] (Figure 2). Klfs are indispensable for self-renewal by forming a tightly regulated molecular circuitry [64, 98]. Klf4 and Klf5 especially transcriptionally regulate expression of Nanog [98], a known inhibitor of differentiation during pluripotency [99, 100]. However, Klf2 is mainly regulated by Oct3/4, whereas Klf4 is regulated by LIF/STAT3 and additionally by Oct3/4. Klf5 is solely activated by LIF/STAT3 leading to ground state mESC pluripotency [101]. Previous reports suggest that LIF/STAT3 regulate Nanog and indirectly the core regulatory complex consisting of Nanog, Oct3/4, and Sox2 through activation of Klf4, Klf5, and Sall4 [29]. Despite their close relationship Klf4 and Klf5, they often exert opposite effects in regulating gene transcription and cellular proliferation *in vitro* and *in vivo* [102]. Klf4 is a negative regulator of mESC proliferation, whereas Klf5 acts as an activator. Also, Klf5 and Klf4 abrogate the mutual promoter effects [103]. In

summary, the propagation of the LIF/STAT3 reinforced self-renewal state by Nanog is mediated by members of the Klf family. Their overexpression reinforces the pluripotent state in the absence of LIF [64, 104, 105], whereas their inactivation in mESCs induces spontaneous differentiation [29]. However, due to structural and functional overlaps, Klfs are able to compensate for each other. This was noticable as a triple knockdown abolished Nanog promoter activity and led to differentiation of mESCs [98], whereas single knockdowns did not exhibit a specific phenotype [98, 106].

However, Klfs do not just ensure the self-renewal state but are also critical components in regulating lineage specification in the early embryo. Recent work showed that Klf4 negatively regulates the visceral lineage (especially via GATA-binding factors 4 and 6 (GATA 4/6)) and definitive endoderm (especially via Sox17), whereas Klf5 primarily suppresses mesodermal differentiation (T, Mixl1 (mix paired-like homeobox 1)) (Figure 2) [107]. Thus, mESC pluripotency is ensured by additive inhibitory effects of Klf4 and Klf5. When we look at previous findings, Klf levels drop rapidly upon onset of lineage specification, resulting in a diminished lineage inhibition and subsequently in endodermal and mesodermal lineage formation [29]. Thus, mESCs are primed upon the drop of Klfs expression levels and prepared for early lineage differentiation. *In vivo*, Klf4-null mice survive early developmental stages but die shortly after birth due to tissue abnormalities within the smooth and cardiac muscle and basal membrane formation problems which primarily is due to a defective GATA4 regulation [108, 109]. A lacking gastrulation phenotype in Klf4-deficient mouse embryos suggests compensatory mechanisms by the Klf family. In contrast, Klf5-deficient embryos fail to develop further than the blastocyst stage due to reduced Oct3/4 and Nanog expression levels [64, 110]. Taken together, Klfs exert a great impact in sustaining the self-renewal state by either interacting with core pluripotency activating genes or inhibiting differentiation. However, the inhibition of endodermal structures primarily by Klf4 and mesodermal structures by its counterpart Klf5 does not just safeguard the self-renewal state but balances accurate differentiation onset in the early mouse embryo and in differentiating PSCs (Figure 2).

3.1.4. Nanog: Various Facets during Differentiation and Self-Renewal. Nanog, the homeodomain TF, acts together with Oct3/4 and Sox2 to maintain the pluripotency network through the Oct/Sox-motif [74, 98, 111, 112]. Nanog is also able to sustain self-renewal independently from the LIF/STAT3 pathway [113], albeit at a reduced self-renewal capacity [74]. Most robust self-renewal state is promoted under continuous Nanog overexpression and LIF stimulation [114]. However, while Nanog has previously been shown to be dispensable for mESC culture, it mainly functions in stabilising the pluripotency network [115]. Previous studies hypothesised that a switch from monoallelic Nanog expression, in a LIF/serum setting, to a biallelic manner in 2i conditions results in higher expression levels. Of note, this hypothesis was disproved by recent results illustrating a steady biallelic expression of Nanog [116, 117]. Despite direct transcriptional regulation of pluripotency target genes, Nanog sustains the self-renewal state by inhibiting several differential processes in mESCs. First, a population of early mesoderm-specified progenitors was identified, normally present in mESCs and promoted by the BMP pathway. These primed mESCs express pluripotency-associated TFs such as Oct3/4 and Rex1 but are actually specified to the mesodermal fate. In the presence of LIF, Nanog is able to respecify mesoderm-specified progenitors back to pluripotent mESCs [118]. A second mechanism of blocking the progression of mesoderm is a direct inhibition of SMAD1 via STAT3 activation in a LIF-containing setting [119], which has also been demonstrated for Oct3/4 [120], suggesting their cooperative function to sustain self-renewal.

Similarly, Nanog functions as an important determinant during cell fate decisions at the blastocyst stage *in vivo* [121]. Here, it is downregulated by Cdx2 in the trophectoderm [85], whereas it is highly expressed in the ICM [122, 123]. The early ICM of the blastocyst gives rise to the epiblast and primitive endoderm progenitors as a first sign of lineage choice occurring in the ICM. In the unrestricted, early ICM of the blastocyst, Nanog expression is dependent on transcriptional binding of Oct3/4, Sox2, and Esrrb [112, 124], while, in the later derived epiblast, Nanog promoter binding changes now being dependent on Activin A signalling via SMAD2 [123, 125, 126]. We know that Nanog is essential for both epiblast and primitive endoderm formation (Figure 2). GATA6 is crucial in the primitive endoderm lineage *in vivo* and *in vitro* [113, 127–129] and is transcriptionally repressed by Nanog in epiblast-engaged cells [130]. However, recent studies showed primitive endoderm to require epiblast cells for proper differentiation, whereby Nanog signals through FGF/ERK signalling (FGF4) resulting in upregulated GATA4 and Sox17 expression levels [121]. This observation has been recently fostered by live-time imaging data using a Nanog-reporter system *in vivo*, where Nanog expression marks an irreversible commitment between the epiblast and the primitive endodermal lineage, while rarely unidirectional conversions from primitive endoderm to epiblast occur [131].

Elegant studies from the Vallier Laboratory combined PSCs and developing mouse embryos to uncover the transcriptional network around Nanog during pluripotency and lineage commitment [132]. Herein, SMAD2/3 controls the self-renewal state by interacting with core TFs, such as Oct3/4 and Nanog. Notably, endodermal differential programmes were also shown to be downstream of SMAD2/3, demonstrating an opposing function of SMAD2/3. As SMAD2/3 and Nanog are involved in both processes, SMAD2/3 may be guided by distinct genes like Nanog to achieve tissue specific functions [133]. Further, during primitive streak formation initial pluripotent differentiation inhibitors rapidly decline beginning with Sox2. This enables Nanog to form complexes with SMAD2/3, which promote Eomes expression levels. Eomes further diminishes pluripotent signals thereby ensuring sufficient Nanog expression. Subsequently, Nanog expression levels decline making room for SMAD2/3 and Eomes thereby directing primitive streak cells towards endodermal fate and coincidently inhibiting mesoderm formation [134]. This observation receives further support from another recent study showing that Nanog cooperates with Activin/SMAD in recruiting histone modifiers such

as Dpy30, a subunit of the COMPASS methyltransferase complex, thus regulating differentiation-linked genes [132].

In line with these data, Nanog has been classified as a mesendodermal-class gene, like Oct3/4 and Tbx3 [5] (Figure 3). All these genes reveal overlapping gene expression levels and lineage specifying patterns, albeit we are still lacking evidence demonstrating their mutual relationship during early lineage decisions [5, 74]. Inconsistent data has been published regarding the Nanog-lacking phenotype. Initially, Nanog deficiency was reported to result in a failure of epiblast formation and, concomitantly, mESCs lost their pluripotent fate and differentiated into trophectoderm [113]. However, this phenotype was not clearly replicable in recent studies [130]. Instead, Nanog-deficient embryos reveal upregulated GATA6 expression levels and few GATA4-positive cells [130]. Therefore, Nanog mutant ICMs do not undergo apoptosis suggesting a stabilising role of GATA6 in this regard [130]. In summary, Nanog shows multiple facets in regulating mESC pluripotency or by specifying lineage formation in the early mouse embryo.

3.2. Neuroectoderm-Class Genes

3.2.1. Sex Determining Region Y- (SRY-) Box 2 (Sox2): The Neuroectodermal Embryonic Stem Cell Gene. Another master regulator of mESC pluripotency is Sox2, a member of the HMG (high-mobility group) box proteins. Sox2 maintains stemness by directly interacting with Oct3/4 in a reciprocal fashion. Both share the ability to bind to a unique promoter region, the Oct/Sox-motif [135]. This highly conserved Oct/Sox-element is critical for transcriptional regulation of pluripotency and located on different genes in undifferentiated mESCs, such as Oct3/4, Sox2, and Nanog [112]. The proper modulation of these target genes preserves the self-renewal state [88]. Notably, Niwas group showed that Sox2 was dispensable for activating the Oct/Sox-element [88]. Instead, Sox2 is important in activating pluripotency-associated genes, which in turn regulate Oct3/4 resulting in stable Oct3/4 expression levels. Both activate FGF4 expression in the ICM and epiblast [136] and in turn FGF4 controls ICM maintenance and subsequently interacts with Cdx2 and Eomes while promoting trophectoderm maturation [85, 137].

During early lineage decisions, Sox2 is broadly expressed in the ICM and the trophectoderm and later even in the epiblast and in the primitive endoderm [138, 139] (Figure 2). Interestingly, Sox2 knockout studies indicated stable or even low Oct3/4 and Nanog expression levels and at the same time surprisingly low trophectoderm gene (Eomes, FGF4) expression levels [139], resulting in embryonic lethality due to defective epiblast development during the peri-implantation stage. Stable Nanog and Oct3/4 levels seem unusual, as Sox2 is a central member of the pluripotency-maintaining protein complex. Nevertheless, this effect could be explained by autoregulatory functions, which Sox2 has in common with Oct3/4, Nanog, Sall4, and Klfs [98]. *In vitro*, upon reduction of Sox2 levels, mESCs differentiate towards trophectoderm indicating its impact in sustaining the pluripotent state. Thus, trophectoderm differentiation could result from a secondary loss of Oct3/4 levels due to Sox2 reduction [88]. Heterozygous Sox2 knockout mutations in mouse show severe alterations in brain and neural cells [140], thus gaining insight into the promoted germ layer. Sox2 induces neuroectodermal gene expression [5] by specifically repressing Oct3/4, which vice versa participates in cell fate choice by promoting the mesendodermal lineage [86] (Figure 2). In summary, Sox2 is embedded in the pluripotency network by interacting with key pluripotent genes. However, upon onset of differentiation, Sox2 promotes neuroectodermal lineage allocation by transcriptional repression of Oct3/4 (Figure 3).

3.2.2. Gastrulation Brain Homeobox 2 (Gbx2): Another Ectodermal Player? The TF Gbx2 is a direct downstream target of LIF/STAT3. Its overexpression is able to substitute for LIF in mESCs and to maintain self-renewal in a STAT3 deprived mESC culture [141]. Notably, Gbx2 is able to push primed EpiSCs back into the pluripotent state [141]. Nonetheless, its impact on pluripotency just seems to have a supporting character, as shown by *in vitro* knockdown studies, where the pluripotent state was not fully impaired [141]. This is in line with *in vivo* studies, which do not show morphological abnormalities in the blastocyst [141]. In the mouse embryo, Gbx2 is expressed in the ICM and, together with Rex1 (Zfp42), diminishes during primitive ectoderm formation [142] (Figure 2). Notably, at gastrulation stage, Gbx2 is present in all three germ layers [143] but subsequently gets upregulated in the neural ectoderm and underlying mesoderm and finally is limited to the CNS (central nervous system) [144] (Figure 2). In line, Gbx2 knockout mice show abnormalities in hindbrain development, neural crest patterning, and cardiovascular and craniofacial defects and die soon after birth [143, 145].

Taken together, although Gbx2 lies downstream of LIF/STAT3, it seems to be dispensable for mESC culture and ICM integrity. However, during early developmental steps, Gbx2 is committed to the ectodermal lineage fate (Figure 3) [146].

3.3. Extraembryonic-Class Genes

3.3.1. Spalt-Like Transcription Factor 4 (Sall4). The transcriptional network in preimplantation embryos was recently extended by the spalt-like gene family member Sall4. Sall4 directly interacts with Nanog and cooccupies several gene sites, including their own promoters, forming autoregulatory loops. Together, they are suggested to function as a Sall4/Nanog-complex maintaining pluripotency by reciprocal regulation. The physical relationship was suggested to be similar to the Oct3/4-Sox2 interaction encountered on many loci in mESCs [147]. Besides, in the ICM and the epiblast, Sall4 expression occurs simultaneously to Oct3/4 and Sox2 expression [148], revealing another contribution to the transcriptional network. This was confirmed by verifying Sall4 occupation on the Oct/Sox-element *in vitro* and *in vivo* [149] and by gene profiling analyses illustrating Sall4 cooccupying the same target genes as Sox2 in mESCs [149]. Independently, Sall4 can modulate Oct3/4 expression levels, the master TF of pluripotency, and vice versa, indicating its critical role in maintaining stemness [150]. In summary, Sall4 contributes to the transcriptional network by direct interaction with

the key players, Nanog, Oct3/4, and Sox2, to maintain the self-renewal state. Moreover, Sall4 can also be recruited to the promoters of Klf2 and Klf5, although its role contributing to mESC pluripotency through the Klf family requires further studying. Another possible mechanism supporting Sall4 mediated pluripotency could be the recruitment of the strong transcriptional repressor complex NuRD (nucleosome remodelling and deacetylase) [151]. Both Sall4 and NuRD are expressed in mESCs and are involved in maintaining stemness. As Sall4 associates with the NuRD complex, both genes could act together in sustaining pluripotency. But due to lacking evidence this hypothesis remains an assumption.

At the blastocyst stage, Sall4 regulates the ICM development to the two blastocyst-derived stem cell lineages: epiblast and extraembryonic endoderm (Figure 2). GATA6 is important in defining the extraembryonic endoderm, although GATA6 mutants exhibit lineage specific defects, a short time after blastocyst formation. Thus, GATA6 does not seem to be a core component for primitive endoderm initiation but rather for its maturation [152]. In this regard, studies exhibited Sall4 to regulate extraembryonic endoderm genes, such as GATA4, GATA6, Sox7, and Sox17 [153]. So it can be concluded that Sall4 contributes to the transcriptional network maintaining mESC pluripotency mediated by direct interaction with crucial TFs [154]. In line with this, it is not surprising that Sall4 overexpression leads to primitive endoderm differentiation [154] and further may support Oct3/4 in this matter [87]. Also, similar to Oct3/4, Sall4 knockdown mESCs are becoming alkaline phosphatase (AP) negative and tend to differentiate towards the trophoblast lineage [148, 154]. It is feasible that Sall4 cooperates with Oct3/4 to suppress trophectoderm lineage allocation [155]. Sall4-null mice are lethal during peri-implantation [156, 157], whereas heterozygous mice exhibit anorectal tract abnormalities, heart defects, skeletal defects, and anencephaly [157].

Taken together, Sall4 is broadly connected within the pluripotency network and has a major role in driving early lineage decisions especially towards the extraembryonic lineage (Figure 3).

3.3.2. Estrogen-Related Receptor β (Esrrb). The estrogen-related receptor beta (Esrrb), a member of the nuclear orphan receptor family, is a core pluripotency member of sustaining naïve pluripotency and is deeply embedded in the self-renewal network interacting with several pivotal TFs [158]. It transcriptionally interacts with Nanog in a reciprocal manner [51] and apart from overlapping target gene profiles. Esrrb is able to substitute for Nanog in mESCs [159]. Further, Esrrb binds promoters of the master pluripotency factor Oct3/4 [160] and other TFs such as Klf2 [161] and Rex1 [160]. It acts independently of LIF/STAT3 [51]. Despite its expression levels being directly modulated by the transcriptional repressor Tcf3, Esrrb mediates self-renewal effects upon GSK3 inhibition and is also able to stabilise β-catenin levels. Thus, in the presence of a MEK inhibitor, for example, by the small molecule PD03, Esrrb overexpression can replace GSK3 inhibition maintaining self-renewal in mESCs [51, 159]. Indeed, mESCs depleted from Esrrb and cultured in the absence of LIF undergo morphological changes, reduction of AP activity resulting in spontaneous differentiation [51, 162]. *In vivo*, Esrrb deletion leads to embryonic lethality during midgestation due to placenta defects [163]. This is in line with previous studies, which indicated the presence of Esrrb in the trophoblast lineage [164]. Surprisingly these embryos survive throughout gastrulation exhibiting no defects in the ICM and epiblast [163]. Thus, we presume that Esrrb can be compensated by other factors in this complex transcriptional network maintaining pluripotency.

Regarding its expression profile in the ICM and trophoblast (Figure 2) and the fact that Esrrb enhances Cdx2 expression levels, it is also fair to assume that Esrrb acts as an important factor in regulating lineage decisions in the early blastocyst. As we know, overexpressed pluripotency factors promote differentiation. This was also shown for Esrrb, as overexpressed mESCs are prone to differentiate towards the endodermal lineage [165, 166]. Further investigations are necessary to clarify molecular mechanisms to date, but regarding its attested role in trophoblast specification we classified Esrrb to be an extraembryonic-class gene (Figure 3).

3.3.3. Rex1 (Zfp42). Several studies have successfully used all-trans retinoic acid (RA) to induce mESC differentiation [167]. The stem cell marker Rex1 reduces RA-induced differentiation thereby sustaining the self-renewal state [168–170]. During mESC pluripotency, Rex1 activity is up- or down-regulated by Oct3/4 depending on its expression levels [171]. Also Sox2, another key pluripotency factor, is able to transactivate Rex1 via Nanog [169]. Nonetheless, Rex1 is dispensable for mESC pluripotency [172].

Endogenously, Rex1 is expressed in the ICM and in trophoblast lineages [173] (Figure 2). Notably, unlike Oct3/4, Rex1 is not present in all cells of the ICM. A previous study illustrated two different subpopulations: both were positive for Oct3/4 but only one of them was Rex1-positive [174]. Notably, they were able to convert into each other upon LIF stimulation. The group double positive ($Rex1^+/Oct3/4^+$) developed into primitive ectoderm and participated in chimera formation, whereas the other group, $Rex1^-/Oct3/4^+$, induced somatic differentiation, indicating the existence of primed subcultures in ICM which are guided by Rex1 to develop into either epiblast cells or primitive endoderm [174].

Overexpression of Rex1 in mESCs surprisingly results in impaired self-renewal [175] and *in vivo* delayed development through early cleavage divisions [176]. However, homozygous Rex1 knockout in mESCs causes spontaneous differentiation into all three primary germ layers [168, 170, 177], indicating that Rex1 can at least reduce RA associated differentiation. To date, there is neither a noticeable phenotype regarding Rex1-deficient mESCs nor mice. *In vivo* experiments displayed Rex1-deficient mice to be fertile and viable but their offspring die at late gestation [172]. All in all, as the pluripotency factor Rex1 seems to drive lineage segregation at the early blastocyst stage especially towards the extraembryonic lineage, we decided to position it in this section (Figure 3).

3.4. Epigenetic Modulations

Methyl-Binding Domain Protein 3 (Mbd3). Epigenetically, transcriptional sustainment of mESC pluripotency is modulated

by chromatin remodelling including histone modifications and DNA methylation. Pluripotency is maintained by a balance between LIF/STAT3 activation and a repression through NuRD [178]. NuRD mediated silencing in mESCs plays a critical role in early lineage commitment into all three germ layers [179]. Mbd3 is the key subunit of the NuRD repressor complex network [180]. A recent publication demonstrated Mbd3 to be dispensable for maintaining mESC pluripotency. Also, its expression seems to diminish upon fertilisation, therefore being absent during the early preimplantation period, and is upregulated towards the late morula/blastocyst stage [181]. However, according to previous work, Mbd3 exhibits a critical role repressing the trophectoderm lineage in order to ensure mESC propagation and subsequently proper differentiation of the epiblast [182]. Additionally, NuRD mediated mESC self-renewal was shown to function through epigenetic modulation of the WNT pathway [183].

As epigenetic modifications occur during ICM and primary germ layer formation, it is not surprising that Mbd3 deletion in mice leads to early embryonic lethality [184], thus being indispensable for early embryonic development.

4. Conclusion

Naïve pluripotency implies the ability of unlimited self-renewal and regeneration. Its complex regulatory circuity has been studied extensively. Key players such as Oct3/4, Nanog, and Sox2 are complemented by many TFs forming a tightly regulated network that sustains the self-renewal state by inhibiting genes required for differentiation. Upon withdrawal of stemness-inducing signals, pluripotency factor expression levels decline, giving differentiation factors the opportunity to induce lineage allocation. These cell fate decisions are essential for developmental processes into the primary germ layers.

Interestingly, several members of these pluripotency-associated factors have been identified to exert dual functions during early embryogenesis, by also governing the transition of pluripotency towards early lineage commitment. Here, TFs initially maintaining pluripotency by activating self-renewal gene programmes undergo a molecular switch resulting in enhanced expression levels of differentiation inducing genes. In this regard, the TFs were classified into mesendoderm-, neuroectoderm-, and extraembryonic-class genes (Figure 3). Notably, mesendoderm-class genes inhibit neuroectoderm and vice versa to promote the appropriate lineage. Although both the pluripotency circuitry and early lineage commitment mechanisms have been studied in great detail, there is still a broad gap of knowledge regarding the distinct regulatory complexes governing these events. By understanding the interplay of factors and signalling pathways involved in the early embryonic development, basic as well as clinical science would be able to profit broadly in terms of developmental steps and pathomechanistical events. Summarising, TFs interact in network in a spatial and temporal manner to exit pluripotency and establish different lineages in the early embryo.

Conflict of Interests

The authors declare that there is no conflict of interests regarding the publication of this paper.

Acknowledgments

This study was funded by the Deutsche Forschungsgemeinschaft (DFG, KL 2544/1-1), Boehringer-Ingelheim BIU (C1 to Alexander Kleger), Else-Kröner-Fresenius-Stiftung (2011_A200; to Alexander Kleger and Stefan Liebau), and BMBF (Systar to Alexander Kleger). Alexander Kleger is indebted to the Baden-Württemberg Stiftung for the financial support of this research project by the Eliteprogramme for Postdocs. Alexander Kleger is an Else-Kröner-Fresenius Memorial Fellow. Clair E. Weidgang was supported by the International Graduate School in Molecular Medicine within the "Promotionsprogramm for Experimental Medicine," Ulm University.

References

[1] J. Wray, T. Kalkan, and A. G. Smith, "The ground state of pluripotency," *Biochemical Society Transactions*, vol. 38, no. 4, pp. 1027–1032, 2010.

[2] H. Niwa, K. Ogawa, D. Shimosato, and K. Adachi, "A parallel circuit of LIF signalling pathways maintains pluripotency of mouse ES cells," *Nature*, vol. 460, no. 7251, pp. 118–122, 2009.

[3] H. Niwa, J.-I. Miyazaki, and A. G. Smith, "Quantitative expression of Oct-3/4 defines differentiation, dedifferentiation or self-renewal of ES cells," *Nature Genetics*, vol. 24, no. 4, pp. 372–376, 2000.

[4] C. E. Weidgang, R. Russell, P. R. Tata et al., "TBX3 directs cell-fate decision toward mesendoderm," *Stem Cell Reports*, vol. 1, pp. 248–265, 2013.

[5] M. Thomson, S. J. Liu, L.-N. Zou, Z. Smith, A. Meissner, and S. Ramanathan, "Pluripotency factors in embryonic stem cells regulate differentiation into germ layers," *Cell*, vol. 145, no. 6, pp. 875–889, 2011.

[6] M. Bertolessi, L. Linta, T. Seufferlein, A. Kleger, and S. Liebau, "A fresh look on T-box factor action in early embryogenesis (T-box factors in early development)," *Stem Cells and Development*, vol. 24, no. 16, pp. 1833–1851, 2015.

[7] J. Hao, T.-G. Li, X. Qi, D.-F. Zhao, and G.-Q. Zhao, "WNT/β-catenin pathway up-regulates Stat3 and converges on LIF to prevent differentiation of mouse embryonic stem cells," *Developmental Biology*, vol. 290, no. 1, pp. 81–91, 2006.

[8] S. I. Kim, F. Oceguera-Yanez, R. Hirohata et al., "KLF4 N-terminal variance modulates induced reprogramming to pluripotency," *Stem Cell Reports*, vol. 4, no. 4, pp. 727–743, 2015.

[9] G. Nagamatsu, S. Saito, K. Takubo, and T. Suda, "Integrative analysis of the acquisition of pluripotency in PGCs reveals the mutually exclusive roles of blimp-1 and AKT signaling," *Stem Cell Reports*, vol. 5, no. 1, pp. 111–124, 2015.

[10] A. Waghray, N. Saiz, A. Jayaprakash et al., "Tbx3 controls Dppa3 levels and exit frompluripotency toward mesoderm," *Stem Cell Reports*, vol. 5, no. 1, pp. 97–110, 2015.

[11] T. Wu, H. Pinto, Y. Kamikawa, and M. Donohoe, "The BET family member BRD4 interacts with OCT4 and regulates pluripotency gene expression," *Stem Cell Reports*, vol. 4, pp. 390–403, 2015.

[12] Y. Chen, K. Blair, and A. Smith, "Robust self-renewal of rat embryonic stem cells requires fine-tuning of glycogen synthase kinase-3 inhibition," *Stem Cell Reports*, vol. 1, no. 3, pp. 209–217, 2013.

[13] H. G. Leitch, J. Nichols, P. Humphreys et al., "Rebuilding pluripotency from primordial germ cells," *Stem Cell Reports*, vol. 1, no. 1, pp. 66–78, 2013.

[14] J. Nichols and A. Smith, "Naive and primed pluripotent states," *Cell Stem Cell*, vol. 4, no. 6, pp. 487–492, 2009.

[15] T. Boroviak, R. Loos, P. Bertone, A. Smith, and J. Nichols, "The ability of inner-cell-mass cells to self-renew as embryonic stem cells is acquired following epiblast specification," *Nature Cell Biology*, vol. 16, no. 6, pp. 516–528, 2014.

[16] Q.-L. Ying, J. Nichols, I. Chambers, and A. Smith, "BMP induction of Id proteins suppresses differentiation and sustains embryonic stem cell self-renewal in collaboration with STAT3," *Cell*, vol. 115, no. 3, pp. 281–292, 2003.

[17] Q.-L. Ying, J. Wray, J. Nichols et al., "The ground state of embryonic stem cell self-renewal," *Nature*, vol. 453, no. 7194, pp. 519–523, 2008.

[18] M. Müller, J. Schröer, N. Azoitei et al., "A time frame permissive for Protein Kinase D2 activity to direct angiogenesis in mouse embryonic stem cells," *Scientific Reports*, vol. 5, Article ID 11742, 2015.

[19] M. Sugimoto, M. Kondo, Y. Koga et al., "A simple and robust method for establishing homogeneous mouse epiblast stem cell lines by wnt inhibition," *Stem Cell Reports*, vol. 4, no. 4, pp. 744–757, 2015.

[20] C. Dani, I. Chambers, S. Johnstone et al., "Paracrine induction of stem cell renewal by LIF-deficient cells: a new ES cell regulatory pathway," *Developmental Biology*, vol. 203, no. 1, pp. 149–162, 1998.

[21] C. L. Stewart, P. Kaspar, L. J. Brunet et al., "Blastocyst implantation depends on maternal expression of leukaemia inhibitory factor," *Nature*, vol. 359, no. 6390, pp. 76–79, 1992.

[22] R. L. Williams, D. J. Hilton, S. Pease et al., "Myeloid leukaemia inhibitory factor maintains the developmental potential of embryonic stem cells," *Nature*, vol. 336, no. 6200, pp. 684–687, 1988.

[23] I. Chambers and A. Smith, "Self-renewal of teratocarcinoma and embryonic stem cells," *Oncogene*, vol. 23, no. 43, pp. 7150–7160, 2004.

[24] H. Niwa, "How is pluripotency determined and maintained?" *Development*, vol. 134, no. 4, pp. 635–646, 2007.

[25] H. Niwa, T. Burdon, I. Chambers, and A. Smith, "Self-renewal of pluripotent embryonic stem cells is mediated via activation of STAT3," *Genes and Development*, vol. 12, no. 13, pp. 2048–2060, 1998.

[26] D. V. Do, J. Ueda, D. M. Messerschmidt et al., "A genetic and developmental pathway from $STAT_3$ to the OCT_4-NANOG circuit is essential for maintenance of ICM lineages in vivo," *Genes and Development*, vol. 27, no. 12, pp. 1378–1390, 2013.

[27] P. Cartwright, C. McLean, A. Sheppard, D. Rivett, K. Jones, and S. Dalton, "LIF/STAT3 controls ES cell self-renewal and pluripotency by a Myc-dependent mechanism," *Development*, vol. 132, no. 5, pp. 885–896, 2005.

[28] G. Martello, P. Bertone, and A. Smith, "Identification of the missing pluripotency mediator downstream of leukaemia inhibitory factor," *The EMBO Journal*, vol. 32, no. 19, pp. 2561–2574, 2013.

[29] P.-Y. Bourillot, I. Aksoy, V. Schreiber et al., "Novel STAT3 target genes exert distinct roles in the inhibition of mesoderm and endoderm differentiation in cooperation with Nanog," *Stem Cells*, vol. 27, no. 8, pp. 1760–1771, 2009.

[30] T. Kunath, M. K. Saba-El-Leil, M. Almousailleakh, J. Wray, S. Meloche, and A. Smith, "FGF stimulation of the Erk1/2 signalling cascade triggers transition of pluripotent embryonic stem cells from self-renewal to lineage commitment," *Development*, vol. 134, no. 16, pp. 2895–2902, 2007.

[31] J. Nichols, J. Silva, M. Roode, and A. Smith, "Suppression of Erk signalling promotes ground state pluripotency in the mouse embryo," *Development*, vol. 136, no. 19, pp. 3215–3222, 2009.

[32] R. J. Chan, S. A. Johnson, Y. Li, M. C. Yoder, and G.-S. Feng, "A definitive role of Shp-2 tyrosine phosphatase in mediating embryonic stem cell differentiation and hematopoiesis," *Blood*, vol. 102, no. 6, pp. 2074–2080, 2003.

[33] H. Marks, T. Kalkan, R. Menafra et al., "The transcriptional and epigenomic foundations of ground state pluripotency," *Cell*, vol. 149, no. 3, pp. 590–604, 2012.

[34] J. Wray, T. Kalkan, S. Gomez-Lopez et al., "Inhibition of glycogen synthase kinase-3 alleviates Tcf3 repression of the pluripotency network and increases embryonic stem cell resistance to differentiation," *Nature Cell Biology*, vol. 13, pp. 838–845, 2011.

[35] H. Kuroda, L. Fuentealba, A. Ikeda, B. Reversade, and E. M. De Robertis, "Default neural induction: neuralization of dissociated *Xenopus* cells is mediated by Ras/MAPK activation," *Genes and Development*, vol. 19, no. 9, pp. 1022–1027, 2005.

[36] S. I. Wilson, A. Rydström, T. Trimborn et al., "The status of Wnt signalling regulates neural and epidermal fates in the chick embryo," *Nature*, vol. 411, no. 6835, pp. 325–330, 2001.

[37] B. M. Johansson and M. V. Wiles, "Evidence for involvement of activin A and bone morphogenetic protein 4 in mammalian mesoderm and hematopoietic development," *Molecular and Cellular Biology*, vol. 15, no. 1, pp. 141–151, 1995.

[38] M. F. A. Finley, S. Devata, and J. E. Huettner, "BMP-4 inhibits neural differentiation of murine embryonic stem cells," *Journal of Neurobiology*, vol. 40, no. 3, pp. 271–287, 1999.

[39] Y. Hayashi, M. K. Furue, S. Tanaka et al., "BMP4 induction of trophoblast from mouse embryonic stem cells in defined culture conditions on laminin," *In Vitro Cellular and Developmental Biology—Animal*, vol. 46, no. 5, pp. 416–430, 2010.

[40] S. J. Arnold and E. J. Robertson, "Making a commitment: cell lineage allocation and axis patterning in the early mouse embryo," *Nature Reviews Molecular Cell Biology*, vol. 10, no. 2, pp. 91–103, 2009.

[41] K. Katsu, D. Tokumori, N. Tatsumi, A. Suzuki, and Y. Yokouchi, "BMP inhibition by DAN in Hensen's node is a critical step for the establishment of left-right asymmetry in the chick embryo," *Developmental Biology*, vol. 363, no. 1, pp. 15–26, 2012.

[42] Y.-J. Luo and Y.-H. Su, "Opposing nodal and BMP signals regulate left-right asymmetry in the sea urchin larva," *PLoS Biology*, vol. 10, no. 10, Article ID e1001402, 2012.

[43] S. Frank, M. Zhang, H. R. Schöler, and B. Greber, "Small molecule-assisted, line-independent maintenance of human pluripotent stem cells in defined conditions," *PLoS ONE*, vol. 7, no. 7, Article ID e41958, 2012.

[44] K. E. Galvin, E. D. Travis, D. Yee, T. Magnuson, and J. L. Vivian, "Nodal signaling regulates the bone morphogenic protein pluripotency pathway in mouse embryonic stem cells," *The Journal of Biological Chemistry*, vol. 285, no. 26, pp. 19747–19756, 2010.

[45] B. Lichtner, P. Knaus, H. Lehrach, and J. Adjaye, "BMP10 as a potent inducer of trophoblast differentiation in human embryonic and induced pluripotent stem cells," *Biomaterials*, vol. 34, no. 38, pp. 9789–9802, 2013.

[46] M. C. Nostro, X. Cheng, G. M. Keller, and P. Gadue, "Wnt, activin, and BMP signaling regulate distinct stages in the developmental pathway from embryonic stem cells to blood," *Cell Stem Cell*, vol. 2, no. 1, pp. 60–71, 2008.

[47] A. Leunda-Casi, R. de Hertogh, and S. Pampfer, "Control of trophectoderm differentiation by inner cell mass-derived fibroblast growth factor-4 in mouse blastocysts and corrective effect of FGF-4 on high glucose-induced trophoblast disruption," *Molecular Reproduction and Development*, vol. 60, no. 1, pp. 38–46, 2001.

[48] N. Sato, L. Meijer, L. Skaltsounis, P. Greengard, and A. H. Brivanlou, "Maintenance of pluripotency in human and mouse embryonic stem cells through activation of Wnt signaling by a pharmacological GSK-3-specific inhibitor," *Nature Medicine*, vol. 10, no. 1, pp. 55–63, 2004.

[49] R. A. Cavallo, R. T. Cox, M. M. Moline et al., "*Drosophila* Tcf and Groucho interact to repress wingless signalling activity," *Nature*, vol. 395, no. 6702, pp. 604–608, 1998.

[50] J. L. Stamos and W. I. Weis, "The β-catenin destruction complex," *Cold Spring Harbor Perspectives in Biology*, vol. 5, 2013.

[51] G. Martello, T. Sugimoto, E. Diamanti et al., "Esrrb is a pivotal target of the Gsk3/Tcf3 axis regulating embryonic stem cell self-renewal," *Cell Stem Cell*, vol. 11, no. 4, pp. 491–504, 2012.

[52] L. Pereira, F. Yi, and B. J. Merrill, "Repression of Nanog gene transcription by Tcf3 limits embryonic stem cell self-renewal," *Molecular and Cellular Biology*, vol. 26, no. 20, pp. 7479–7491, 2006.

[53] H. Xu, C. Baroukh, R. Dannenfelser et al., "ESCAPE: database for integrating high-content published data collected from human and mouse embryonic stem cells," *Database*, vol. 2013, Article ID bat045, 2013.

[54] F. Yi, L. Pereira, J. A. Hoffman et al., "Opposing effects of Tcf3 and Tcf1 control Wnt stimulation of embryonic stem cell self-renewal," *Nature Cell Biology*, vol. 13, no. 7, pp. 762–770, 2011.

[55] K. F. Kelly, D. Y. Ng, G. Jayakumaran, G. A. Wood, H. Koide, and B. W. Doble, "Beta-catenin enhances Oct-4 activity and reinforces pluripotency through a TCF-independent mechanism," *Cell Stem Cell*, vol. 8, no. 2, pp. 214–227, 2011.

[56] E. Seo, U. Basu-Roy, J. Zavadil, C. Basilico, and A. Mansukhani, "Distinct functions of Sox2 control self-renewal and differentiation in the osteoblast lineage," *Molecular and Cellular Biology*, vol. 31, no. 22, pp. 4593–4608, 2011.

[57] X. Ye, F. Wu, C. Wu et al., "β-catenin, a Sox2 binding partner, regulates the DNA binding and transcriptional activity of Sox2 in breast cancer cells," *Cellular Signalling*, vol. 26, no. 3, pp. 492–501, 2014.

[58] L. Marucci, E. Pedone, U. Di Vicino, B. Sanuy-Escribano, M. Isalan, and M. P. Cosma, "β-Catenin Fluctuates in mouse ESCs and is essential for Nanog-mediated reprogramming of somatic cells to pluripotency," *Cell Reports*, vol. 8, no. 6, pp. 1686–1696, 2014.

[59] S. J. Arnold, J. Stappert, A. Bauer, A. Kispert, B. G. Herrmann, and R. Kemler, "Brachyury is a target gene of the Wnt/β-catenin signaling pathway," *Mechanisms of Development*, vol. 91, no. 1-2, pp. 249–258, 2000.

[60] H. Haegel, L. Larue, M. Ohsugi, L. Fedorov, K. Herrenknecht, and R. Kemler, "Lack of β-catenin affects mouse development at gastrulation," *Development*, vol. 121, no. 11, pp. 3529–3537, 1995.

[61] S. He, D. Pant, A. Schiffmacher, A. Meece, and C. L. Keefer, "Lymphoid enhancer factor 1-mediated Wnt signaling promotes the initiation of trophoblast lineage differentiation in mouse embryonic stem cells," *Stem Cells*, vol. 26, no. 4, pp. 842–849, 2008.

[62] J. Huelsken, R. Vogel, V. Brinkmann, B. Erdmann, C. Birchmeier, and W. Birchmeier, "Requirement for β-catenin in anterior-posterior axis formation in mice," *Journal of Cell Biology*, vol. 148, no. 3, pp. 567–578, 2000.

[63] O. G. Kelly, K. I. Pinson, and W. C. Skarnes, "The Wnt co-receptors Lrp5 and Lrp6 are essential for gastrulation in mice," *Development*, vol. 131, no. 12, pp. 2803–2815, 2004.

[64] M. Ema, D. Mori, H. Niwa et al., "Krüppel-like factor 5 is essential for blastocyst development and the normal self-renewal of mouse ESCs," *Cell Stem Cell*, vol. 3, no. 5, pp. 555–567, 2008.

[65] J. Han, P. Yuan, H. Yang et al., "Tbx3 improves the germ-line competency of induced pluripotent stem cells," *Nature*, vol. 463, no. 7284, pp. 1096–1100, 2010.

[66] B. Schuettengruber and G. Cavalli, "Recruitment of polycomb group complexes and their role in the dynamic regulation of cell fate choice," *Development*, vol. 136, no. 21, pp. 3531–3542, 2009.

[67] K. Takahashi and S. Yamanaka, "Induction of pluripotent stem cells from mouse embryonic and adult fibroblast cultures by defined factors," *Cell*, vol. 126, no. 4, pp. 663–676, 2006.

[68] S.-J. Dunn, G. Martello, B. Yordanov, S. Emmott, and A. G. Smith, "Defining an essential transcription factor program for naïve pluripotency," *Science*, vol. 344, no. 6188, pp. 1156–1160, 2014.

[69] M. Zernicka-Goetz, "Patterning of the embryo: the first spatial decisions in the life of a mouse," *Development*, vol. 129, no. 4, pp. 815–829, 2002.

[70] A. J. Copp, "Interaction between inner cell mass and trophectoderm of the mouse blastocyst. II. The fate of the polar trophectoderm," *Journal of Embryology and Experimental Morphology*, vol. 51, pp. 109–120, 1979.

[71] P. Murray and D. Edgar, "Regulation of the differentiation and behaviour of extra-embryonic endodermal cells by basement membranes," *Journal of Cell Science*, vol. 114, no. 5, pp. 931–939, 2001.

[72] S. Tada, T. Era, C. Furusawa et al., "Characterization of mesendoderm: a diverging point of the definitive endoderm and mesoderm in embryonic stem cell differentiation culture," *Development*, vol. 132, no. 19, pp. 4363–4374, 2005.

[73] J. Nichols, B. Zevnik, K. Anastassiadis et al., "Formation of pluripotent stem cells in the mammalian embryo depends on the POU transcription factor Oct4," *Cell*, vol. 95, no. 3, pp. 379–391, 1998.

[74] D. J. Rodda, J.-L. Chew, L.-H. Lim et al., "Transcriptional regulation of nanog by OCT4 and SOX2," *Journal of Biological Chemistry*, vol. 280, no. 26, pp. 24731–24737, 2005.

[75] M. Pesce and H. R. Schöler, "Oct-4: gatekeeper in the beginnings of mammalian development," *Stem Cells*, vol. 19, no. 4, pp. 271–278, 2001.

[76] A. Radzisheuskaya, G. Le Bin Chia, R. L. dos Santos et al., "A defined Oct4 level governs cell state transitions of pluripotency entry and differentiation into all embryonic lineages," *Nature Cell Biology*, vol. 15, no. 6, pp. 579–590, 2013.

[77] V. Karwacki-Neisius, J. Göke, R. Osorno et al., "Reduced Oct4 expression directs a robust pluripotent state with distinct signaling activity and increased enhancer occupancy by Oct4 and Nanog," *Cell Stem Cell*, vol. 12, no. 5, pp. 531–545, 2013.

[78] I. Aksoy, R. Jauch, J. Chen et al., "Oct4 switches partnering from Sox2 to Sox17 to reinterpret the enhancer code and specify endoderm," *The EMBO Journal*, vol. 32, no. 7, pp. 938–953, 2013.

[79] S. Stefanovic, N. Abboud, S. Désilets, D. Nury, C. Cowan, and M. Pucéat, "Interplay of Oct4 with Sox2 and Sox17: a molecular switch from stem cell pluripotency to specifying a cardiac fate," *Journal of Cell Biology*, vol. 186, no. 5, pp. 665–673, 2009.

[80] M. Hogan, D. Parfitt, C. Zepeda-Mendoza, M. Shen, and D. Spector, "Transient pairing of homologous Oct4 alleles accompanies the onset of embryonic stem cell differentiation," *Cell Stem Cell*, vol. 16, no. 3, pp. 275–288, 2015.

[81] M. R. Hübner, M. A. Eckersley-Maslin, and D. L. Spector, "Chromatin organization and transcriptional regulation," *Current Opinion in Genetics & Development*, vol. 23, no. 2, pp. 89–95, 2013.

[82] Z. Wei, Y. Yang, P. Zhang et al., "Klf4 interacts directly with Oct4 and Sox2 to promote reprogramming," *Stem Cells*, vol. 27, no. 12, pp. 2969–2978, 2009.

[83] K. Deb, M. Sivaguru, H. Y. Yong, and R. M. Roberts, "Cdx2 gene expression and trophectoderm lineage specification in mouse embryos," *Science*, vol. 311, no. 5763, pp. 992–996, 2006.

[84] H. Niwa, Y. Toyooka, D. Shimosato et al., "Interaction between Oct3/4 and Cdx2 determines trophectoderm differentiation," *Cell*, vol. 123, no. 5, pp. 917–929, 2005.

[85] D. Strumpf, C.-A. Mao, Y. Yamanaka et al., "Cdx2 is required for correct cell fate specification and differentiation of trophectoderm in the mouse blastocyst," *Development*, vol. 132, no. 9, pp. 2093–2102, 2005.

[86] Y. Li, W. Yu, A. J. Cooney, R. J. Schwartz, and Y. Liu, "Brief report: Oct4 and canonical Wnt signaling regulate the cardiac lineage factor Mesp1 through a Tcf/Lef-Oct4 composite element," *Stem Cells*, vol. 31, no. 6, pp. 1213–1217, 2013.

[87] T. Frum, M. Halbisen, C. Wang, H. Amiri, P. Robson, and A. Ralston, "Oct4 Cell-autonomously promotes primitive endoderm development in the mouse blastocyst," *Developmental Cell*, vol. 25, no. 6, pp. 610–622, 2013.

[88] S. Masui, Y. Nakatake, Y. Toyooka et al., "Pluripotency governed by Sox2 via regulation of Oct3/4 expression in mouse embryonic stem cells," *Nature Cell Biology*, vol. 9, no. 6, pp. 625–635, 2007.

[89] G. C. Le Bin, S. Muñoz-Descalzo, A. Kurowski et al., "Oct4 is required for lineage priming in the developing inner cell mass of the mouse blastocyst," *Development*, vol. 141, no. 5, pp. 1001–1010, 2014.

[90] G. Tiscornia and J. C. Izpisúa Belmonte, "MicroRNAs in embryonic stem cell function and fate," *Genes and Development*, vol. 24, no. 24, pp. 2732–2741, 2010.

[91] F. D. Price, H. Yin, A. Jones, W. Van Ijcken, F. Grosveld, and M. A. Rudnicki, "Canonical Wnt signaling induces a primitive endoderm metastable state in mouse embryonic stem cells," *Stem Cells*, vol. 31, no. 4, pp. 752–764, 2013.

[92] C.-A. Renard, C. Labalette, C. Armengol et al., "Tbx3 is a downstream target of the Wnt/β-catenin pathway and a critical mediator of β-catenin survival functions in liver cancer," *Cancer Research*, vol. 67, no. 3, pp. 901–910, 2007.

[93] J. Brennan, C. C. Lu, D. P. Norris, T. A. Rodriguez, R. S. P. Beddington, and E. J. Robertson, "Nodal signalling in the epiblast patterns the early mouse embryo," *Nature*, vol. 411, no. 6840, pp. 965–969, 2001.

[94] X. Cheng, L. Ying, L. Lu et al., "Self-renewing endodermal progenitor lines generated from human pluripotent stem cells," *Cell Stem Cell*, vol. 10, no. 4, pp. 371–384, 2012.

[95] A. E. R. Kartikasari, J. X. Zhou, M. S. Kanji et al., "The histone demethylase Jmjd3 sequentially associates with the transcription factors Tbx3 and Eomes to drive endoderm differentiation," *The EMBO Journal*, vol. 32, no. 10, pp. 1393–1408, 2013.

[96] R. Pearson, J. Fleetwood, S. Eaton, M. Crossley, and S. Bao, "Krüppel-like transcription factors: a functional family," *International Journal of Biochemistry and Cell Biology*, vol. 40, no. 10, pp. 1996–2001, 2008.

[97] K. Kurimoto, Y. Yabuta, Y. Ohinata et al., "An improved single-cell cDNA amplification method for efficient high-density oligonucleotide microarray analysis," *Nucleic Acids Research*, vol. 34, no. 5, article e42, 2006.

[98] J. Jiang, Y.-S. Chan, Y.-H. Loh et al., "A core Klf circuitry regulates self-renewal of embryonic stem cells," *Nature Cell Biology*, vol. 10, no. 3, pp. 353–360, 2008.

[99] C. Chazaud, Y. Yamanaka, T. Pawson, and J. Rossant, "Early lineage segregation between epiblast and primitive endoderm in mouse blastocysts through the Grb2-MAPK pathway," *Developmental Cell*, vol. 10, no. 5, pp. 615–624, 2006.

[100] P. Zhang, R. Andrianakos, Y. Yang, C. Liu, and W. Lu, "Kruppel-like factor 4 (Klf4) prevents embryonic stem (ES) cell differentiation by regulating Nanog gene expression," *Journal of Biological Chemistry*, vol. 285, no. 12, pp. 9180–9189, 2010.

[101] J. Hall, G. Guo, J. Wray et al., "Oct4 and LIF/Stat3 additively induce Krüppel factors to sustain embryonic stem cell self-renewal," *Cell Stem Cell*, vol. 5, no. 6, pp. 597–609, 2009.

[102] A. M. Ghaleb, M. O. Nandan, S. Chanchevalap, W. B. Dalton, I. M. Hisamuddin, and V. W. Yang, "Krüppel-like factors 4 and 5: the yin and yang regulators of cellular proliferation," *Cell Research*, vol. 15, no. 2, pp. 92–96, 2005.

[103] D. T. Dang, W. Zhao, C. S. Mahatan, D. E. Geiman, and V. W. Yang, "Opposing effects of Kruppel-like factor 4 (gut-enriched Kruppel-like factor) and Kruppel-like factor 5 (intestinal-enriched Kruppel-like factor) on the promoter of the Kruppel-like factor 4 gene," *Nucleic Acids Research*, vol. 30, pp. 2736–2741, 2002.

[104] Y. Li, J. McClintick, L. Zhong, H. J. Edenberg, M. C. Yoder, and R. J. Chan, "Murine embryonic stem cell differentiation is promoted by SOCS-3 and inhibited by the zinc finger transcription factor Klf4," *Blood*, vol. 105, no. 2, pp. 635–637, 2005.

[105] S. Parisi, F. Passaro, L. Aloia et al., "Klf5 is involved in self-renewal of mouse embryonic stem cells," *Journal of Cell Science*, vol. 121, no. 16, pp. 2629–2634, 2008.

[106] M. Nakagawa, M. Koyanagi, K. Tanabe et al., "Generation of induced pluripotent stem cells without Myc from mouse and human fibroblasts," *Nature Biotechnology*, vol. 26, no. 1, pp. 101–106, 2008.

[107] I. Aksoy, V. Giudice, E. Delahaye et al., "Klf4 and Klf5 differentially inhibit mesoderm and endoderm differentiation in embryonic stem cells," *Nature Communications*, vol. 5, article 3719, 2014.

[108] J. A. Segre, C. Bauer, and E. Fuchs, "Klf4 is a transcription factor required for establishing the barrier function of the skin," *Nature Genetics*, vol. 22, no. 4, pp. 356–360, 1999.

[109] T. Yoshida, Q. Gan, A. S. Franke et al., "Smooth and cardiac muscle-selective knock-out of Krüppel-like factor 4 causes postnatal death and growth retardation," *The Journal of Biological Chemistry*, vol. 285, no. 27, pp. 21175–21184, 2010.

[110] S.-C. J. Lin, M. A. Wani, J. A. Whitsett, and J. M. Wells, "Klf5 regulates lineage formation in the pre-implantation mouse embryo," *Development*, vol. 137, no. 23, pp. 3953–3963, 2010.

[111] A. Gagliardi, N. P. Mullin, Z. Ying Tan et al., "A direct physical interaction between Nanog and Sox2 regulates embryonic stem cell self-renewal," *The EMBO Journal*, vol. 32, no. 16, pp. 2231–2247, 2013.

[112] T. Kuroda, M. Tada, H. Kubota et al., "Octamer and sox elements are required for transcriptional cis regulation of Nanog gene expression," *Molecular and Cellular Biology*, vol. 25, no. 6, pp. 2475–2485, 2005.

[113] K. Mitsui, Y. Tokuzawa, H. Itoh et al., "The homeoprotein nanog is required for maintenance of pluripotency in mouse epiblast and ES cells," *Cell*, vol. 113, no. 5, pp. 631–642, 2003.

[114] I. Chambers, D. Colby, M. Robertson et al., "Functional expression cloning of Nanog, a pluripotency sustaining factor in embryonic stem cells," *Cell*, vol. 113, no. 5, pp. 643–655, 2003.

[115] I. Chambers, J. Silva, D. Colby et al., "Nanog safeguards pluripotency and mediates germline development," *Nature*, vol. 450, no. 7173, pp. 1230–1234, 2007.

[116] D. A. Faddah, H. Wang, A. W. Cheng, Y. Katz, Y. Buganim, and R. Jaenisch, "Single-cell analysis reveals that expression of nanog is biallelic and equally variable as that of other pluripotency factors in mouse ESCs," *Cell Stem Cell*, vol. 13, no. 1, pp. 23–29, 2013.

[117] A. Filipczyk, K. Gkatzis, J. Fu et al., "Biallelic expression of nanog protein in mouse embryonic stem cells," *Cell Stem Cell*, vol. 13, no. 1, pp. 12–13, 2013.

[118] A. Suzuki, Á. Raya, Y. Kawakami et al., "Maintenance of embryonic stem cell pluripotency by Nanog-mediated reversal of mesoderm specification," *Nature Clinical Practice Cardiovascular Medicine*, vol. 3, supplement 1, pp. S114–S122, 2006.

[119] A. Suzuki, Á. Raya, Y. Kawakami et al., "Nanog binds to Smad1 and blocks bone morphogenetic protein-induced differentiation of embryonic stem cells," *Proceedings of the National Academy of Sciences of the United States of America*, vol. 103, no. 27, pp. 10294–10299, 2006.

[120] X. Chen, H. Xu, P. Yuan et al., "Integration of external signaling pathways with the core transcriptional network in embryonic stem cells," *Cell*, vol. 133, no. 6, pp. 1106–1117, 2008.

[121] D. M. Messerschmidt and R. Kemler, "Nanog is required for primitive endoderm formation through a non-cell autonomous mechanism," *Developmental Biology*, vol. 344, no. 1, pp. 129–137, 2010.

[122] H. Ochiai, T. Sugawara, T. Sakuma, and T. Yamamoto, "Stochastic promoter activation affects Nanog expression variability in mouse embryonic stem cells," *Scientific Reports*, vol. 4, article 7125, 2014.

[123] L. T. Sun, S. Yamaguchi, K. Hirano, T. Ichisaka, T. Kuroda, and T. Tada, "Nanog co-regulated by Nodal/Smad2 and Oct4 is required for pluripotency in developing mouse epiblast," *Developmental Biology*, vol. 392, no. 2, pp. 182–192, 2014.

[124] D. L. C. van den Berg, W. Zhang, A. Yates et al., "Estrogen-related receptor beta interacts with Oct4 to positively regulate Nanog gene expression," *Molecular and Cellular Biology*, vol. 28, no. 19, pp. 5986–5995, 2008.

[125] M. Sakaki-Yumoto, J. Liu, M. Ramalho-Santos, N. Yoshida, and R. Derynck, "Smad2 is essential for maintenance of the human and mouse primed pluripotent stem cell state," *The Journal of Biological Chemistry*, vol. 288, no. 25, pp. 18546–18560, 2013.

[126] L. Vallier, S. Mendjan, S. Brown et al., "Activin/Nodal signalling maintains pluripotency by controlling Nanog expression," *Development*, vol. 136, no. 8, pp. 1339–1349, 2009.

[127] S. Bessonnard, L. D. Mot, D. Gonze et al., "Gata6, Nanog and Erk signaling control cell fate in the inner cell mass through a tristable regulatory network," *Development*, vol. 141, no. 19, pp. 3637–3648, 2014.

[128] K. Q. Cai, C. D. Capo-Chichi, M. E. Rula, D.-H. Yang, and X.-X. M. Xu, "Dynamic GATA6 expression in primitive endoderm formation and maturation in early mouse embryogenesis," *Developmental Dynamics*, vol. 237, no. 10, pp. 2820–2829, 2008.

[129] S. A. Morris, R. T. Y. Teo, H. Li, P. Robson, D. M. Glover, and M. Zernicka-Goetz, "Origin and formation of the first two distinct cell types of the inner cell mass in the mouse embryo," *Proceedings of the National Academy of Sciences of the United States of America*, vol. 107, no. 14, pp. 6364–6369, 2010.

[130] S. Frankenberg, F. Gerbe, S. Bessonnard et al., "Primitive endoderm differentiates via a three-step mechanism involving Nanog and RTK signaling," *Developmental Cell*, vol. 21, no. 6, pp. 1005–1013, 2011.

[131] P. Xenopoulos, M. Kang, A. Puliafito, S. Di Talia, and A. Hadjantonakis, "Heterogeneities in nanog expression drive stable commitment to pluripotency in the mouse blastocyst," *Cell Reports*, vol. 10, no. 9, pp. 1508–1520, 2015.

[132] A. Bertero, P. Madrigal, A. Galli et al., "Activin/Nodal signaling and NANOG orchestrate human embryonic stem cell fate decisions by controlling the H3K4me3 chromatin mark," *Genes & Development*, vol. 29, no. 7, pp. 702–717, 2015.

[133] S. Brown, T. E. O. Adrian, S. Pauklin et al., "Activin/nodal signaling controls divergent transcriptional networks in human embryonic stem cells and in endoderm progenitors," *Stem Cells*, vol. 29, no. 8, pp. 1176–1185, 2011.

[134] A. K. K. Teo, S. J. Arnold, M. W. B. Trotter et al., "Pluripotency factors regulate definitive endoderm specification through eomesodermin," *Genes and Development*, vol. 25, no. 3, pp. 238–250, 2011.

[135] J.-L. Chew, Y.-H. Loh, W. Zhang et al., "Reciprocal transcriptional regulation of Pou5f1 and Sox2 via the Oct4/Sox2 complex in embryonic stem cells," *Molecular and Cellular Biology*, vol. 25, no. 14, pp. 6031–6046, 2005.

[136] H. Yuan, N. Corbi, C. Basilico, and L. Dailey, "Developmental-specific activity of the FGF-4 enhancer requires the synergistic action of Sox2 and Oct-3," *Genes and Development*, vol. 9, no. 21, pp. 2635–2645, 1995.

[137] A. P. Russ, S. Wattler, W. H. Colledge et al., "Eomesodermin is required for mouse trophoblast development and mesoderm formation," *Nature*, vol. 404, no. 6773, pp. 95–99, 2000.

[138] A. A. Avilion, S. K. Nicolis, L. H. Pevny, L. Perez, N. Vivian, and R. Lovell-Badge, "Multipotent cell lineages in early mouse development depend on SOX2 function," *Genes and Development*, vol. 17, no. 1, pp. 126–140, 2003.

[139] M. Keramari, J. Razavi, K. A. Ingman et al., "Sox2 is essential for formation of trophectoderm in the preimplantation embryo," *PLoS ONE*, vol. 5, no. 11, Article ID e13952, 2010.

[140] A. L. M. Ferri, M. Cavallaro, D. Braida et al., "Sox2 deficiency causes neurodegeneration and impaired neurogenesis in the adult mouse brain," *Development*, vol. 131, no. 15, pp. 3805–3819, 2004.

[141] C.-I. Tai and Q.-L. Ying, "Gbx2, a LIF/Stat3 target, promotes reprogramming to and retention of the pluripotent ground state," *Journal of Cell Science*, vol. 126, no. 5, pp. 1093–1098, 2013.

[142] J. Rathjen, J.-A. Lake, M. D. Bettess, J. M. Washington, G. Chapman, and P. D. Rathjen, "Formation of a primitive ectoderm like cell population, EPL cells, from ES cells in response to biologically derived factors," *Journal of Cell Science*, vol. 112, no. 5, pp. 601–612, 1999.

[143] K. M. Wassarman, M. Lewandoski, K. Campbell et al., "Specification of the anterior hindbrain and establishment of a normal mid/hindbrain organizer is dependent on Gbx2 gene function," *Development*, vol. 124, no. 15, pp. 2923–2934, 1997.

[144] A. Bulfone, L. Puelles, M. H. Porteus, M. A. Frohman, G. R. Martin, and J. L. R. Rubenstein, "Spatially restricted expression of Dlx-1, Dlx-2 (Tes-1), Gbx-2, and Wnt-3 in the embryonic day 12.5 mouse forebrain defines potential transverse and longitudinal segmental boundaries," *Journal of Neuroscience*, vol. 13, no. 7, pp. 3155–3172, 1993.

[145] N. A. Byrd and E. N. Meyers, "Loss of Gbx2 results in neural crest cell patterning and pharyngeal arch artery defects in the mouse embryo," *Developmental Biology*, vol. 284, no. 1, pp. 233–245, 2005.

[146] J. Y. H. Li and A. L. Joyner, "*Otx2* and *Gbx2* are required for refinement and not induction of mid-hindbrain gene expression," *Development*, vol. 128, no. 24, pp. 4979–4991, 2001.

[147] Q. Wu, X. Chen, J. Zhang et al., "Sall4 interacts with Nanog and co-occupies Nanog genomic sites in embryonic stem cells," *The Journal of Biological Chemistry*, vol. 281, no. 34, pp. 24090–24094, 2006.

[148] U. Elling, C. Klasen, T. Eisenberger, K. Anlag, and M. Treier, "Murine inner cell mass-derived lineages depend on Sall4 function," *Proceedings of the National Academy of Sciences of the United States of America*, vol. 103, no. 44, pp. 16319–16324, 2006.

[149] N. Tanimura, M. Saito, M. Ebisuya, E. Nishida, and F. Ishikawa, "Stemness-related factor Sall4 interacts with transcription factors Oct-3/4 and Sox2 and occupies Oct-Sox elements in mouse embryonic stem cells," *The Journal of Biological Chemistry*, vol. 288, no. 7, pp. 5027–5038, 2013.

[150] J. Yang, C. Gao, L. Chai, and Y. Ma, "A novel SALL4/OCT4 transcriptional feedback network for pluripotency of embryonic stem cells," *PLoS ONE*, vol. 5, no. 5, Article ID e10766, 2010.

[151] J. Lu, H. Jeong, N. Kong et al., "Stem cell factor SALL4 represses the transcriptions of PTEN and SALL1 through an epigenetic repressor complex," *PLoS ONE*, vol. 4, no. 5, Article ID e5577, 2009.

[152] M. Koutsourakis, A. Langeveld, R. Patient, R. Beddington, and F. Grosveld, "The transcription factor GATA6 is essential for early extraembryonic development," *Development*, vol. 126, no. 4, pp. 723–732, 1999.

[153] C. Y. Lim, W.-L. Tam, J. Zhang et al., "Sall4 regulates distinct transcription circuitries in different blastocyst-derived stem cell lineages," *Cell Stem Cell*, vol. 3, no. 5, pp. 543–554, 2008.

[154] J. Zhang, W.-L. Tam, G. Q. Tong et al., "Sall4 modulates embryonic stem cell pluripotency and early embryonic development by the transcriptional regulation of Pou5f1," *Nature Cell Biology*, vol. 8, no. 10, pp. 1114–1123, 2006.

[155] S. Yuri, S. Fujimura, K. Nimura et al., "Sall4 is essential for stabilization, but not for pluripotency, of embryonic stem cells by repressing aberrant trophectoderm gene expression," *Stem Cells*, vol. 27, no. 4, pp. 796–805, 2009.

[156] M. Sakaki-Yumoto, C. Kobayashi, A. Sato et al., "The murine homolog of *SALL4*, a causative gene in Okihiro syndrome, is essential for embryonic stem cell proliferation, and cooperates with *Sall*1 in anorectal, heart, brain and kidney development," *Development*, vol. 133, no. 15, pp. 3005–3013, 2006.

[157] M. Warren, W. Wang, S. Spiden et al., "A Sall4 mutant mouse model useful for studying the role of Sall4 in early embryonic development and organogenesis," *Genesis*, vol. 45, no. 1, pp. 51–58, 2007.

[158] B. Feng, J. Jiang, P. Kraus et al., "Reprogramming of fibroblasts into induced pluripotent stem cells with orphan nuclear receptor Esrrb," *Nature Cell Biology*, vol. 11, no. 2, pp. 197–203, 2009.

[159] N. Festuccia, R. Osorno, F. Halbritter et al., "Esrrb is a direct Nanog target gene that can substitute for Nanog function in pluripotent cells," *Cell Stem Cell*, vol. 11, no. 4, pp. 477–490, 2012.

[160] X. Zhang, J. Zhang, T. Wang, M. A. Esteban, and D. Pei, "Esrrb activates Oct4 transcription and sustains self-renewal and pluripotency in embryonic stem cells," *The Journal of Biological Chemistry*, vol. 283, no. 51, pp. 35825–35833, 2008.

[161] J.-C. Yeo, J. Jiang, Z.-Y. Tan et al., "Klf2 is an essential factor that sustains ground state pluripotency," *Cell Stem Cell*, vol. 14, no. 6, pp. 864–872, 2014.

[162] N. Ivanova, R. Dobrin, R. Lu et al., "Dissecting self-renewal in stem cells with RNA interference," *Nature*, vol. 442, no. 7102, pp. 533–538, 2006.

[163] J. Luo, R. Sladek, J.-A. Bader, A. Matthyssen, J. Rossant, and V. Giguère, "Placental abnormalities in mouse embryos lacking the orphan nuclear receptor ERR-β," *Nature*, vol. 388, no. 6644, pp. 778–782, 1997.

[164] Y. Ohinata and T. Tsukiyama, "Establishment of trophoblast stem cells under defined culture conditions in mice," *PLoS ONE*, vol. 9, no. 9, Article ID e107308, 2014.

[165] K. M. Loh and B. Lim, "A precarious balance: pluripotency factors as lineage specifiers," *Cell Stem Cell*, vol. 8, no. 4, pp. 363–369, 2011.

[166] K. Uranishi, T. Akagi, C. Sun, H. Koide, and T. Yokota, "Dax1 associates with Esrrb and regulates its function in embryonic stem cells," *Molecular and Cellular Biology*, vol. 33, no. 10, pp. 2056–2066, 2013.

[167] J. Rohwedel, K. Guan, and A. M. Wobus, "Induction of cellular differentiation by retinoic acid in vitro," *Cells Tissues Organs*, vol. 165, no. 3-4, pp. 190–202, 1999.

[168] K. B. Scotland, S. Chen, R. Sylvester, and L. J. Gudas, "Analysis of Rex1 (zfp42) function in embryonic stem cell differentiation," *Developmental Dynamics*, vol. 238, no. 8, pp. 1863–1877, 2009.

[169] W. Shi, H. Wang, G. Pan, Y. Geng, Y. Guo, and D. Pei, "Regulation of the pluripotency marker Rex-1 by Nanog and Sox2," *Journal of Biological Chemistry*, vol. 281, no. 33, pp. 23319–23325, 2006.

[170] J. R. Thompson and L. J. Gudas, "Retinoic acid induces parietal endoderm but not primitive endoderm and visceral endoderm differentiation in F9 teratocarcinoma stem cells with a targeted deletion of the Rex-1 (Zfp-42) gene," *Molecular and Cellular Endocrinology*, vol. 195, no. 1-2, pp. 119–133, 2002.

[171] E. Ben-Shushan, J. R. Thompson, L. J. Gudas, and Y. Bergman, "Rex-1, a gene encoding a transcription factor expressed in the early embryo, is regulated via Oct-3/4 and Oct-6 binding to an octamer site and a novel protein, Rox-1, binding to an adjacent site," *Molecular and Cellular Biology*, vol. 18, no. 4, pp. 1866–1878, 1998.

[172] S. Masui, S. Ohtsuka, R. Yagi, K. Takahashi, M. S. H. Ko, and H. Niwa, "Rex1/Zfp42 is dispensable for pluripotency in mouse ES cells," *BMC Developmental Biology*, vol. 8, article 45, 2008.

[173] M. B. Rogers, B. A. Hosler, and L. J. Gudas, "Specific expression of a retinoic acid-regulated, zinc-finger gene, Rex-1, in preimplantation embryos, trophoblast and spermatocytes," *Development*, vol. 113, no. 3, pp. 815–824, 1991.

[174] Y. Toyooka, D. Shimosato, K. Murakami, K. Takahashi, and H. Niwa, "Identification and characterization of subpopulations in undifferentiated ES cell culture," *Development*, vol. 135, no. 5, pp. 909–918, 2008.

[175] J.-Z. Zhang, W. Gao, H.-B. Yang, B. Zhang, Z.-Y. Zhu, and Y.-F. Xue, "Screening for genes essential for mouse embryonic stem cell self-renewal using a subtractive RNA interference library," *Stem Cells*, vol. 24, no. 12, pp. 2661–2668, 2006.

[176] M. Climent, S. Alonso-Martin, R. Pérez-Palacios et al., "Functional analysis of rex1 during preimplantation development," *Stem Cells and Development*, vol. 22, no. 3, pp. 459–472, 2013.

[177] D. Guallar, R. Pérez-Palacios, M. Climent et al., "Expression of endogenous retroviruses is negatively regulated by the pluripotency marker Rex1/Zfp42," *Nucleic Acids Research*, vol. 40, no. 18, pp. 8993–9007, 2012.

[178] G. Hu and P. A. Wade, "NuRD and pluripotency: a complex balancing act," *Cell Stem Cell*, vol. 10, no. 5, pp. 497–503, 2012.

[179] K. Kaji, I. M. Caballero, R. MacLeod, J. Nichols, V. A. Wilson, and B. Hendrich, "The NuRD component Mbd3 is required for pluripotency of embryonic stem cells," *Nature Cell Biology*, vol. 8, no. 3, pp. 285–292, 2006.

[180] J. Ramírez and J. Hagman, "The Mi-2/NuRD complex: a critical epigenetic regulator of hematopoietic development, differentiation and cancer," *Epigenetics*, vol. 4, no. 8, pp. 532–536, 2009.

[181] Y. Rais, A. Zviran, S. Geula et al., "Deterministic direct reprogramming of somatic cells to pluripotency," *Nature*, vol. 502, no. 7469, pp. 65–70, 2013.

[182] D. Zhu, J. Fang, Y. Li, and J. Zhang, "Mbd3, a component of NuRD/Mi-2 complex, helps maintain pluripotency of mouse embryonic stem cells by repressing trophectoderm differentiation," *PLoS ONE*, vol. 4, no. 11, Article ID e7684, 2009.

[183] J. J. Kim, O. Khalid, S. Vo, H.-H. Sun, D. T. W. Wong, and Y. Kim, "A novel regulatory factor recruits the nucleosome remodeling complex to wingless integrated (Wnt) signaling gene promoters in mouse embryonic stem cells," *The Journal of Biological Chemistry*, vol. 287, no. 49, pp. 41103–41117, 2012.

[184] B. Hendrich, J. Guy, B. Ramsahoye, V. A. Wilson, and A. Bird, "Closely related proteins MBD2 and MBD3 play distinctive but interacting roles in mouse development," *Genes & Development*, vol. 15, no. 6, pp. 710–723, 2001.

Hindawi Publishing Corporation
Stem Cells International
Volume 2016, Article ID 9076823, 12 pages
http://dx.doi.org/10.1155/2016/9076823

Research Article

Expression of the Wnt Receptor Frizzled-4 in the Human Enteric Nervous System of Infants

Katharina Nothelfer,[1] Florian Obermayr,[2] Nadine Belz,[1] Ellen Reinartz,[1] Petra M. Bareiss,[1] Hans-Jörg Bühring,[3] Rudi Beschorner,[4] and Lothar Just[1]

[1]*Institute of Clinical Anatomy and Cell Analysis, University of Tübingen, Tübingen, Germany*
[2]*Department of Pediatric Surgery and Pediatric Urology, University Children's Hospital Tübingen, Tübingen, Germany*
[3]*Division of Hematology, Immunology, Oncology, Rheumatology and Pulmonology, Department of Internal Medicine II, University of Tübingen, Tübingen, Germany*
[4]*Institute for Pathology and Neuropathology, Department of Neuropathology, University of Tübingen, Tübingen, Germany*

Correspondence should be addressed to Lothar Just; ljust@anatom.uni-tuebingen.de

Received 15 May 2015; Accepted 12 July 2015

Academic Editor: Kodandaramireddy Nalapareddy

The Wnt signalling pathway plays a crucial role in the development of the nervous system. This signalling cascade is initiated upon binding of the secreted Wnt ligand to a member of the family of frizzled receptors. In the present study, we analysed the presence of frizzled-4 in the enteric nervous system of human infants. Frizzled-4 could be identified by immunohistochemistry in a subpopulation of enteric neuronal and glial cells in the small and large intestine. Detection of frizzled-4 in the tunica muscularis by RT-PCR confirmed this receptor's expression on the mRNA level. Interestingly, we observed distinct cell populations that co-expressed frizzled-4 with the intermediate filament protein nestin and the neurotrophin receptor $p75^{NTR}$, which have been reported to be expressed in neural progenitor cells. Flow cytometry analysis revealed that 60% of $p75^{NTR}$ positive cells of the tunica muscularis were positive for frizzled-4. Additionally, in pathological samples of Hirschsprung's disease, the expression of this Wnt receptor correlated with the number of myenteric ganglion cells and decreased from normoganglionic to aganglionic areas of large intestine. The expression pattern of frizzled-4 indicates that this Wnt receptor could be involved in postnatal development and/or function of the enteric nervous system.

1. Introduction

Neurons and glial cells of the peripheral nervous system derive from neural crest stem cells (NCSCs) [1]. Following a distinct and well defined spatiotemporal pattern, NCSCs migrate out of the neural tube into embryonic tissue, including the developing gut. They enter the primitive foregut by embryonic day (E) 9.5 in mice and migrate in a rostral-to-caudal direction in order to colonize the entire gut by E14.5 [2, 3]. In humans migration of enteric neural crest cells takes place between gestational week 4 and gestational week 7 [4]. During their journey along the gut a proportion of cells continues to proliferate, while others begin to differentiate [5] into neurons and glial cells in order to generate a complex neural network that coordinates bowel motility and is involved in regulation of its secretory activity, blood flow, and modulation of the immune system [6, 7]. Impairment of ENS development leads to incomplete colonization of the gut by NCSCs, resulting in peristaltic dysregulation, intestinal obstruction, and enterocolitis as observed in Hirschsprung's disease (HSCR) [8–10]. Much effort has been put into research investigating the genetic regulation of neural crest development and its derivatives during the last decades. This resulted in the identification of several major pathways regulating NCSC induction, migration, differentiation, and interconnection of developing neurons and glial cells [3, 11]. Wnt signalling has been reported to play a central role in these developmental processes in many model organisms. In concert with members of the bone morphogenic protein (BMP) family and fibroblast growth factors, Wnts regulate neural

crest induction and specification. In addition, migration of neural crest cells is dependent on the Wnt signalling pathway [12, 13].

The Wnt signalling cascade is initiated by binding of Wnt to members of the frizzled transmembrane receptor family and results in activation of pathways like the β-catenin-dependent pathway or the planar cell polarity- (PCP-) dependent pathway, both of which have been shown to be involved in early neural crest development. Recently, the PCP pathway has been demonstrated to be additionally involved in regulating neural interconnection during ENS development [14]. However, while the importance of Wnt-frizzled interaction is well established for early neural crest development, its role in regulating postnatal neural crest derivatives is largely unknown.

Interestingly, there is evidence that neurogenesis continues in postnatal mice *in vivo* upon stimulation with serotonin or following injury [15–17]. A subpopulation of cells of the postnatal ENS has been attributed with stem cell like properties, although this niche is not well characterized yet. Nestin, the low-affinity nerve growth factor receptor $p75^{NTR}$, and CD49b (alpha2-integrin) have been suggested to represent markers for this population of enteric neural stem and progenitor cells [18].

Of the frizzled receptor family members, frizzled-4 has previously been shown to be of particular interest with respect to its role in the regulation of stem cell maintenance, neuroprotection, and cell migration in the CNS [19–21]. In the present study, we examined the expression of this Wnt receptor in the enteric nervous system of infants by immunohistochemistry, RT-PCR, and flow cytometry analysis. In order to characterize the frizzled-4 positive cell population we performed colabelling experiments with various neural markers that are expressed in neural and putative progenitor cells of the ENS.

2. Materials and Methods

2.1. Human Gut Samples. Human gut samples from small and large intestine were obtained from infant male and female patients at the age of 4 weeks to 10 months, who underwent surgical enterostoma removal after treatment for necrotizing enterocolitis or anorectal malformations. In addition, tissue was collected from Hirschsprung's disease patients, who underwent a transanal endorectal pull-through procedure (Table 1). All samples were collected according to the guidelines and after approval of the Local Ethical Committee at the University of Tübingen and with the consent of the patient's parents.

Table 1: Human gut samples.

Sample number	Gender	Patient age	Tissue	Pathology
1	Male	5 months	Colon	Normoganglionic
2	Female	2 months	Ileum	Normoganglionic
3	Female	5 months	Sigma	Normoganglionic
4	Male	2 months	Ileum	Normoganglionic
5	Male	10 months	Colon	Normoganglionic
6	Female	3 months	Sigma	Normoganglionic
7	Male	6 months	Sigma	Normoganglionic
8	Female	4 months	Ileocaecal	Normoganglionic
9	Male	7 months	Colon	Normoganglionic
10	Male	4 weeks	Colon	Hirschsprung
11	Male	6 weeks	Colon	Hirschsprung
12	Male	7 months	Colon	Hirschsprung

2.2. Immunohistochemistry. Immunohistochemistry was performed on 14 μm thick cryosections. Tissue slides were fixed in 4% (w/v) paraformaldehyde in phosphate-buffered saline (PBS, pH 7.4) for 20 min at room temperature and subsequently rinsed three times in PBS. Slides, which were stained with the ABC-detection system (Vector Labs, Peterborough, UK), were additionally pretreated in 3% (v/v) hydrogen peroxide PBS solution for 10 min to block endogenous peroxidases. After incubation with serum containing blocking buffer (PBS containing 0.1% (w/v) BSA, 4% (v/v) goat serum, and 0.3% (v/v) Triton X-100) for 30 min, sections were incubated with primary antibodies diluted in PBS, 0.1% (w/v) BSA, and 0.1% (v/v) Triton X-100 overnight at 4°C. Primary antibodies and concentrations are listed in Table 2. Following three washes with PBS, the sections were incubated with secondary antibodies for 30 min at room temperature in the same buffer. Detection was performed with either fluorochrome-conjugated secondary antibodies (1 : 400, goat anti-rabbit IgG-Cy3 (Dianova, Hamburg, Germany); goat anti-mouse IgG-Cy3 (Dianova, Hamburg, Germany); goat anti-mouse IgG-Alexa 488 (Life Technologies, Darmstadt, Germany)) or biotinylated secondary antibodies (1 : 400, swine anti-rabbit IgG-biotin and rabbit anti-mouse IgG-biotin (Dako, Hamburg, Germany)) when using the ABC-detection system. Incubation of the AB reagent was performed according to the manufacturer and visualization of the ABC system was carried out with 3-3′diaminobenzidine (DAB, Sigma, Taufkirchen, Germany) and hydrogen peroxide solution. For fluorescence detection, the sections and cells were washed three times in PBS and additionally stained with DAPI (4′-6-diamidino-2-phenylindole, 0.2 μg/mL) PBS solution for 10 min. Stained sections were dried, embedded in Kaiser's gelatin (Merck, Darmstadt, Germany), and photographed on an inverted microscope (Axiovert, Zeiss, Jena, Germany).

2.3. RNA Isolation and RT-PCR. Human gut samples were mechanically dissected with the visual aid of a stereomicroscope. After disposure of residual fat and mesenteric tissue, the tunica muscularis was peeled off the submucosal and mucosal layers and thoroughly minced. Total RNA was isolated from human tunica muscularis using the RNeasy Mini Kit (Qiagen, Hilden, Germany) according to the manufacturer's instructions. Possible contaminating genomic DNA was removed by treatment with DNase I (Life Technologies, Darmstadt, Germany). Reverse transcriptase

Table 2: Primary antibodies used for cell analysis.

Primary antibodies	Species	Dilution	Manufacturer
α-smooth muscle actin	Rabbit	1 : 100	Spring Bioscience, Pleasanton, USA
c-kit	Rabbit	1 : 500	Dako, Hamburg, Germany
Fzd4 (clone CH3A4)*	Mouse	Undiluted	In-house (HJB)
Fzd4 PE (clone CH3A4)*	Mouse	1 : 50	Biolegend, San Diego, USA
GFAP	Rabbit	1 : 400	Dako, Hamburg, Germany
Nestin	Rabbit	1 : 1000	Abcam, Cambridge, UK
$p75^{NTR}$	Rabbit	1 : 500	Promega, Madison, USA
$p75^{NTR}$ APC	Rabbit	1 : 50	Miltenyi, Bergisch Gladbach, Germany
Peripherin	Rabbit	1 : 200	Merck Millipore, Darmstadt, Germany

*Monoclonal mouse anti-human antibody CH3A4 against frizzled-4 was raised by immunization with the retinoblastoma cell line WERI-RB-1 and specificity for frizzled-4 was verified by the selective recognition of HEK-293 cells transfected with human frizzled-4. This molecule was clustered to CD344 at the HCDM workshop in Quebec, Canada (http://www.hcdm.org/).

PCR (RT-PCR) reaction containing oligo-$(dT)_{23}$ anchored mRNA primers (Sigma-Aldrich, Taufkirchen, Germany), Superscript II Reverse Transcriptase enzyme, and RNase Out was performed according to the supplier's protocol (Life Technologies, Darmstadt, Germany).

To amplify the frizzled-4 receptor and the housekeeping gene GAPDH, the following primer pairs (Sigma-Aldrich, Taufkirchen, Germany) were used.

Frizzled-4 (product size: 605 bp):

5′-CTCGGCTACAACGTGACCAAGAT-3′,
5′-AATATGATGGGGCGCTCAGGGTA-3′;

GAPDH (product size: 452 bp):

5′-ACCACAGTCCATGCCATCAC-3′,
5′-TCCACCACCCTGTTGCTGTA-3′.

The PCR reaction mixture was incubated at 95°C for 5 min, followed by 35 cycles of 95°C for 30 s, annealing temperatures (T_{An}) for 40 s and 72°C for 40 s, and a final cycle with a prolonged elongation time of 10 min at 72°C. The primer-specific annealing temperatures were as follows: T_{An} (frizzled-4) = 58°C and T_{An} (GAPDH) = 60°C. Amplified PCR products were analyzed by electrophoresis on a 1% (w/v) agarose gel (Roth, Karlsruhe, Germany) in 1x TBE buffer (Tris base, boric acid, and EDTA) at 100 V. The products were visualized with ethidium bromide (2 μg/mL) on U.V. light. The size of each PCR product was estimated by using a 100 bp DNA ladder standard (Life Technologies, Darmstadt, Germany). The RT step was omitted as a control for possible contamination of DNase-treated samples with residual genomic DNA (negative control).

2.4. Flow Cytometry. Cells used for flow cytometry analysis were obtained from human tissue by digestion of the tunica muscularis with 750 U/mL Collagenase XI (Sigma, Taufkirchen, Germany) and 0.5% w/v Dispase II (Roche, Mannheim, Germany) in HBSS with Ca^{2+}/Mg^{2+}. The digestion was carried out for a maximum of 1 h at 37°C, in order to avoid digestion of surface epitopes. Tissue residues were discarded and the supernatant was centrifuged for 7 min at 210 g, washed twice with HBSS, and filtered through a 40 μm cell strainer. The resulting cell pellet was resuspended in 20 μL blocking buffer (polyglobin (Talecris Biotherapeutics, Frankfurt am Main, Germany) diluted 1 : 10 in DPBS/0.5% BSA (0.5% (w/v) BSA in Dulbecco's PBS without Ca^{2+}/Mg^{2+})) and incubated on ice for 10 min. Subsequently, cells were diluted with DPBS/0.5% (w/v) BSA to a concentration of 2×10^5 cells per 50 μL and antibodies were added for 15 min on ice. $P75^{NTR}$ was detected with rabbit anti-$p75^{NTR}$-APC (CD271, Miltenyi, Bergisch Gladbach, Germany, 1 : 50). Staining of frizzled-4 was achieved either by incubation with a mouse anti-frizzled-4 antibody (25 μL/10^4 cells, undiluted hybridoma supernatant) followed by a rabbit anti-mouse IgG-FITC secondary antibody (Dako, Hamburg, Germany, 1 : 15) or by using a mouse anti-frizzled-4 PE-conjugated antibody (Biolegend, San Diego, USA, 1 : 50). All stainings were compared according to isotype controls (rabbit IgG-APC (Miltenyi, Bergisch Gladbach, Germany, 1 : 50), mouse IgG (Biozol, Eching, Germany, 1 : 1000), and mouse IgG-PE (Biolegend, San Diego, USA, 1 : 50)), and no differences in the amount and intensity of frizzled-4 staining were observed between the two different staining procedures. Following incubation with the antibodies, cells were washed with DPBS/0.5% (v/v) BSA and centrifuged for 7 min and 210 g at 4°C. The resulting pellet was resuspended in DPBS/0.5%BSA and acquired on a FACSCanto II system (BD Bioscience, Heidelberg, Germany). Data was analysed using FlowJo software.

3. Results

In the present study, we analysed the expression of the Wnt receptor frizzled-4 in the enteric nervous system of human infants aged between 4 weeks and 10 months. First, immunohistochemical staining processes for frizzled-4 glycoprotein were performed on cryostat sections from small and large intestine. Positive cells could be observed in all layers of the gut wall (Figures 1, 2, and 3). RT-PCR analysis of mRNA isolated from the tunica muscularis confirmed the presence of frizzled-4 receptor mRNA (Figure 4). To further characterize the positive cell population, coimmunostaining processes

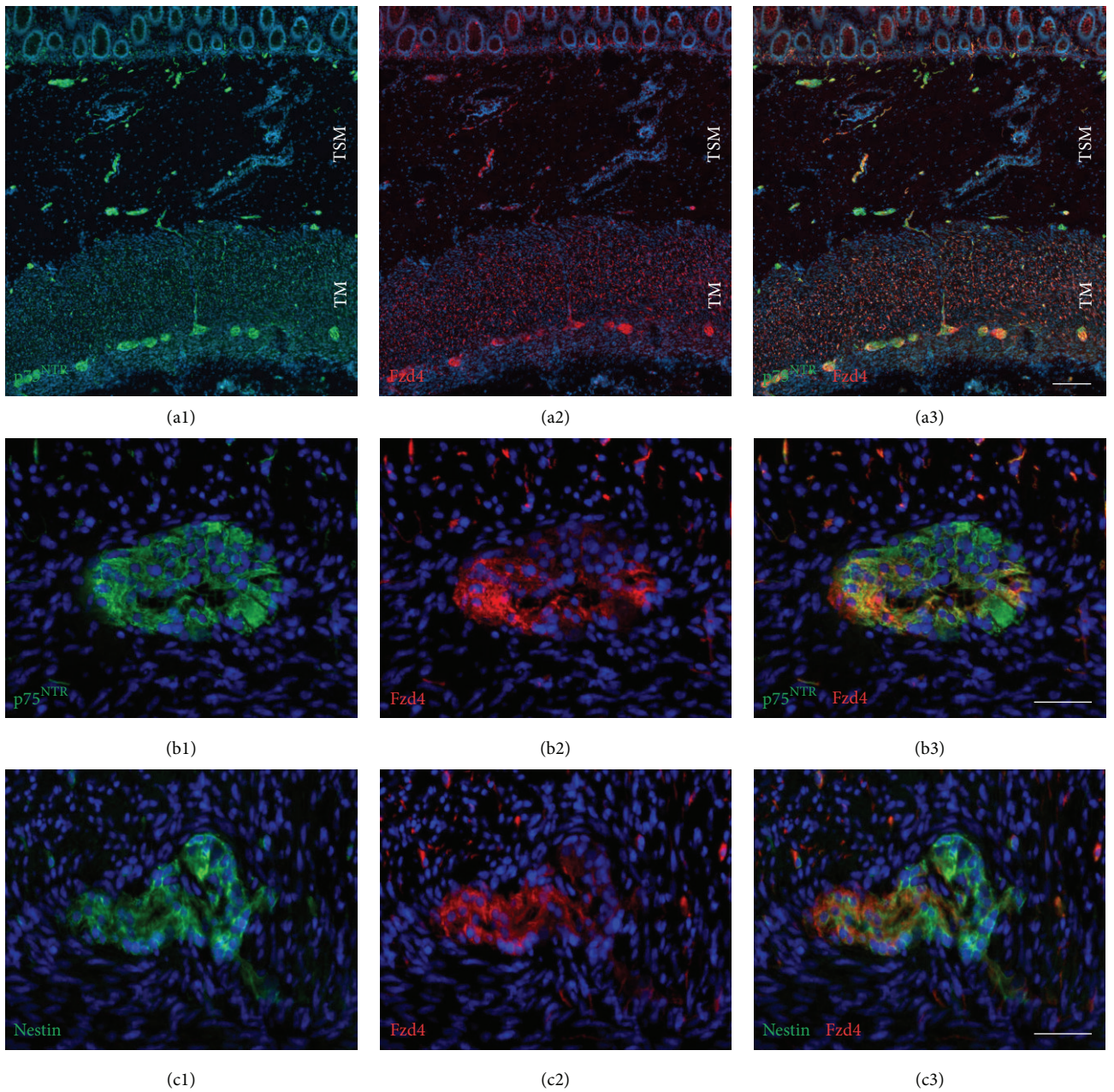

Figure 1: The Wnt receptor frizzled-4 is expressed in neural cells in all layers of the gut wall. Immunohistochemical analysis for frizzled-4 (Fzd4), $p75^{NTR}$, and nestin expression on cryostat sections of human colon (sample number 1). ((a1)–(a3)) Overview of combined $p75^{NTR}$ (green) and Fzd4 (red) immunostaining; $p75^{NTR}$ (a1); Fzd4 (a2); merge (a3); DAPI (blue); tunica muscularis (TM); tela submucosa (TSM); scale bar: 200 μm. ((b1)–(b3)) Higher magnification of combined $p75^{NTR}$ (green) and Fzd4 (red) immunostaining of myenteric ganglia; $p75^{NTR}$ (b1); Fzd4 (b2); merge (b3); DAPI (blue); scale bar: 50 μm. ((c1)–(c3)) Combined nestin (green) and Fzd4 (red) immunostaining of myenteric ganglia; nestin (c1); Fzd4 (c2); merge (c3); DAPI (blue); scale bar: 50 μm.

of frizzled-4 with peripherin and GFAP were performed. As shown in Figures 2 and 7 this Wnt receptor is expressed at various intensities in subpopulations of enteric neurons and glial cells (Figures 2 and 7). Frizzled-4 immunopositive neural extensions were observed in the tunica muscularis, tela submucosa, and the lamina propria mucosae (Figures 1, 2, and 3). Notably, the base of the epithelial crypts was also surrounded by frizzled-4 positive neural extensions (Figure 3). Moreover, the Wnt receptor was costained in cell populations expressing the intermediate filament nestin and the neurotrophin receptor $p75^{NTR}$ (Figures 1, 2, and 7). Interestingly, the amount of $p75^{NTR}$ positive cells that coexpressed frizzled-4 per ganglia was highly variable, even in the same gut area. Frizzled-4 was not found in smooth muscle cells of tunica muscularis, tunica mucosa, or the wall of blood vessels and was also absent in interstitial cells of Cajal, which were stained with c-kit (Figure 2).

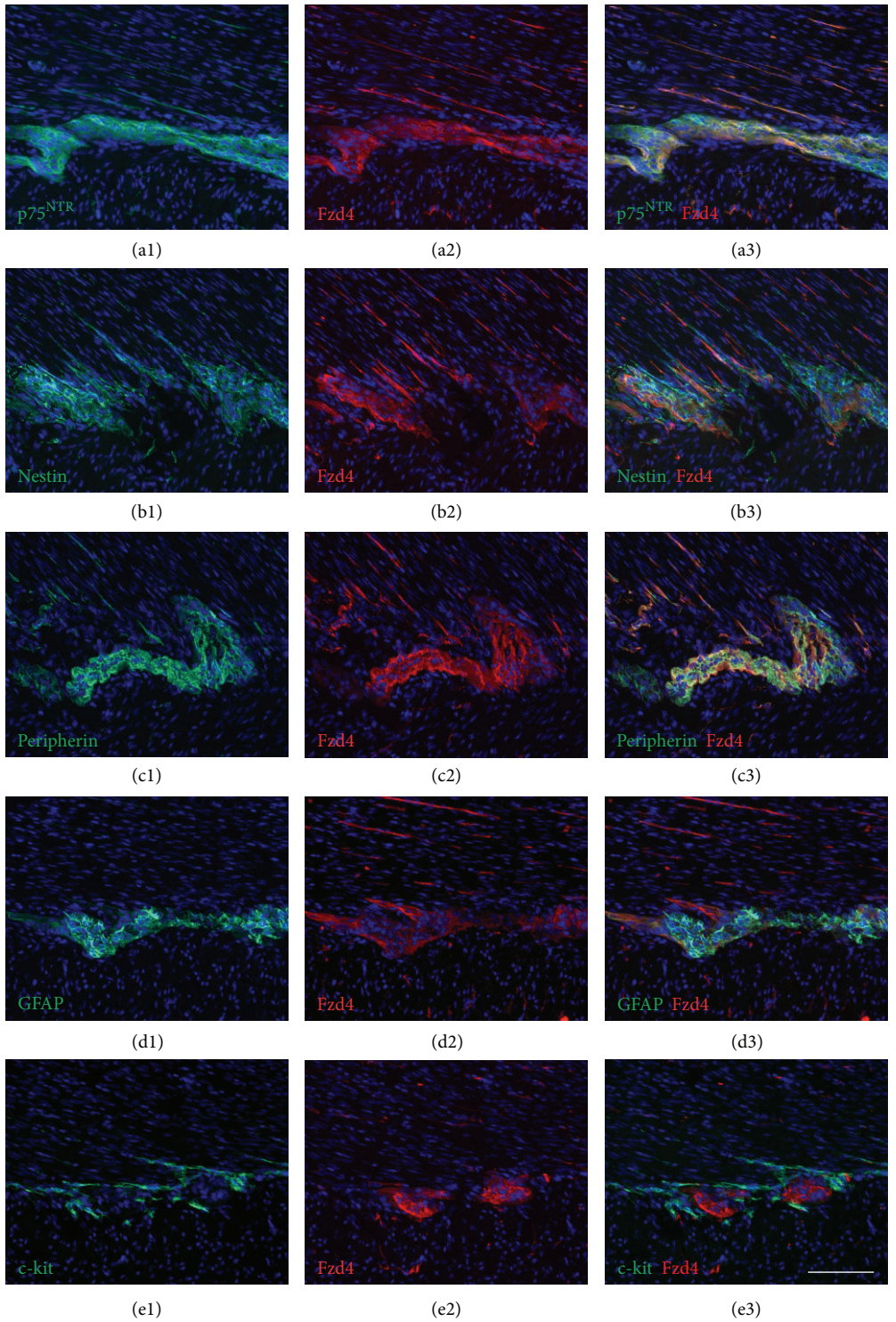

Figure 2: Frizzled-4 is detected in a subpopulation of neural cells. Immunofluorescence for frizzled-4 (Fzd4), $p75^{NTR}$, nestin, peripherin, GFAP, and c-kit on cryostat sections of human ileum (sample number 2). ((a1)–(a3)) Combined $p75^{NTR}$ (green) and Fzd4 (red) immunostaining of myenteric ganglia; $p75^{NTR}$ (a1); Fzd4 (a2); merge (a3); DAPI (blue). ((b1)–(b3)) Combined nestin (green) and Fzd4 (red) immunostaining of myenteric ganglia; nestin (b1); Fzd4 (b2); merge (b3); DAPI (blue). ((c1)–(c3)) Combined peripherin (green) and Fzd4 (red) immunostaining of myenteric ganglia; peripherin (c1); Fzd4 (c2); merge (c3); DAPI (blue). (d1–d3) Combined GFAP (green) and Fzd4 (red) immunostaining of myenteric ganglia; GFAP (d1); Fzd4 (d2); merge (d3); DAPI (blue). ((e1)–(e3)) Combined c-kit (green) and Fzd4 (red) immunostaining of myenteric ganglia; c-kit (e1); Fzd4 (e2); merge (e3); DAPI (blue); scale bar (a–e): 100 μm.

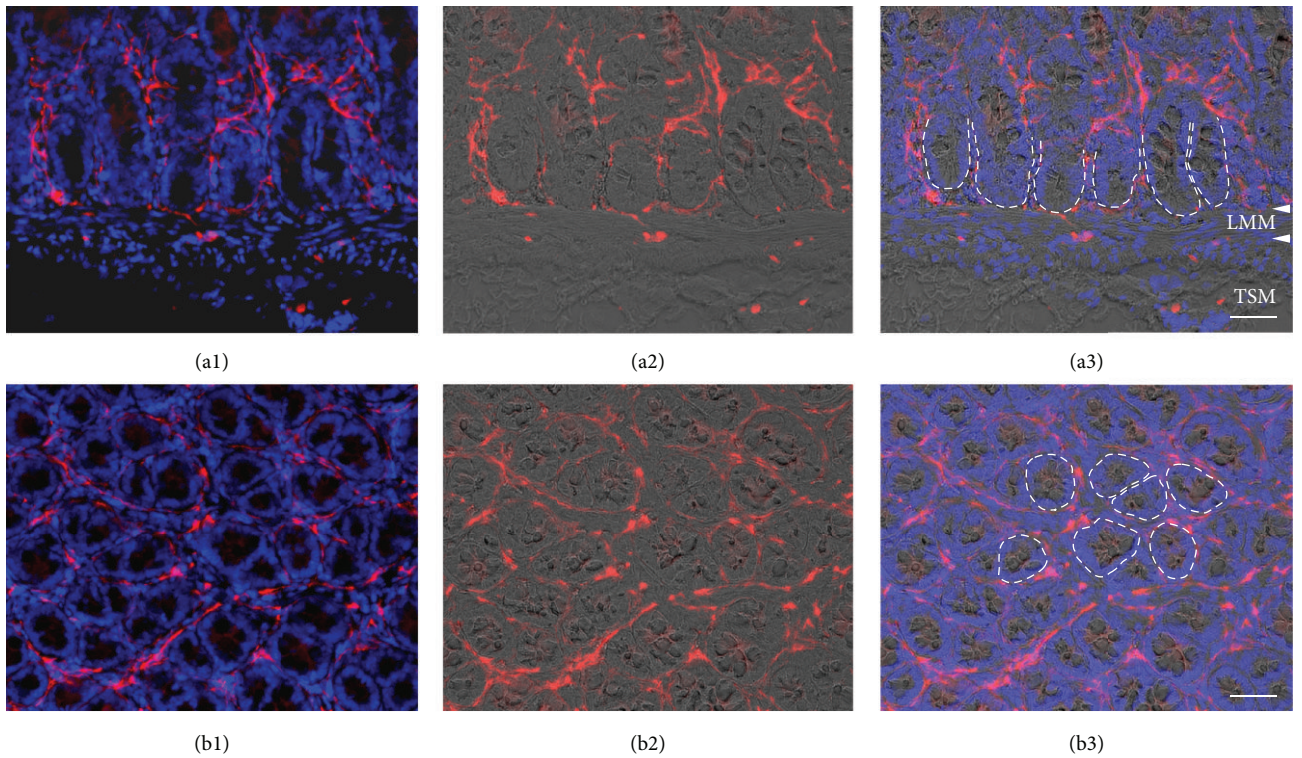

Figure 3: Epithelial crypts of the mucosa are surrounded by frizzled-4 positive neural extensions. Immunofluorescence of frizzled-4 (Fzd4) on cryostat sections of human ileum; (sample number 2). ((a1)–(a3)) Sagittal section. Combined Fzd4 (red) and DAPI (blue) fluorescence staining (a1); combined Fzd4 fluorescence (red) and brightfield view (a2); merge (a3). The broken lines mark the border between epithelial cells of the crypt base and the lamina propria mucosae. The white arrowheads indicate the borders of the lamina muscularis mucosae (LMM) to the lamina propria mucosae and the tela submucosa (TSM); scale bar: 50 μm. ((b1)–(b3)) Horizontal section of the crypt region. Combined Fzd4 (red) and DAPI (blue) fluorescence staining (b1); combined Fzd4 (red) fluorescence and brightfield view (b2); merge (b3). The broken lines mark the border between epithelial cells of some crypts and the lamina propria mucosae; scale bar (a, b): 50 μm.

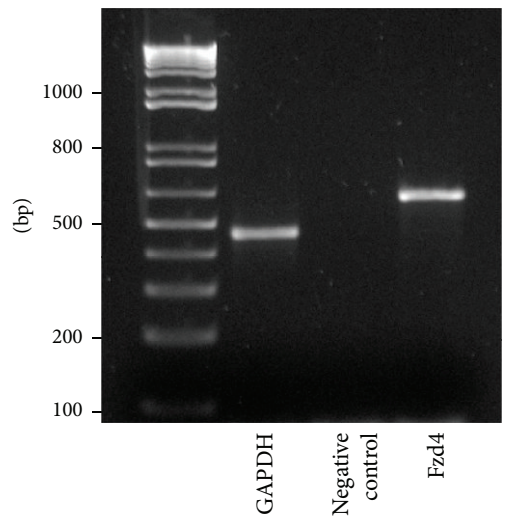

Figure 4: Identification of frizzled-4 (Fzd4) mRNA by RT-PCR. Total RNA was isolated from tunica muscularis. Respective primer pairs were used for detection of Fzd4 (605 bp) and the housekeeping gene GAPDH (452 bp). Isolated RNA without subsequent reverse transcriptase step served as negative control.

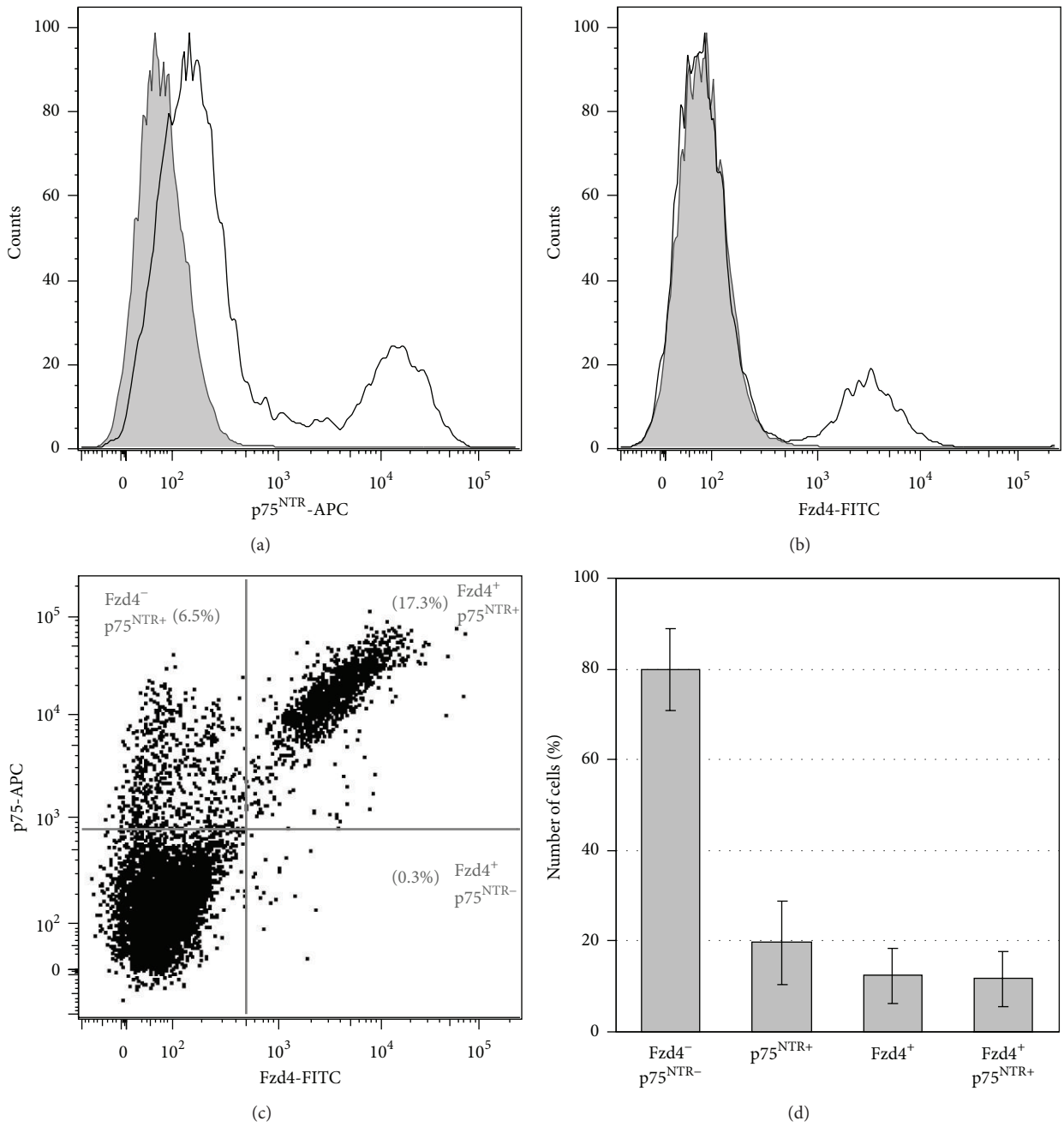

Figure 5: A distinct frizzled-4 positive cell population is observed by flow cytometry. Flow cytometry analysis of $p75^{NTR}$ and frizzled-4 (Fzd4) expression on cells isolated from tunica muscularis (sample numbers 3, 5–9). (a, b) Histograms for $p75^{NTR}$-APC and Fzd4-FITC in comparison to respective isotype controls. The isotype control staining is shown as gray filled histogram. (c) Representative dot plot of $p75^{NTR}$-APC and Fzd4-FITC costained cells. Numbers indicate the percentage of stained cells in each gate. (d) Quantification of the percentages of unstained, $p75^{NTR}$ Fzd4 positive, and $p75^{NTR}$/Fzd4 costained cells from six independent experiments. Data are expressed as mean percentage ± SD of the total cell number.

In summary, we have shown by immunohistochemistry that frizzled-4 is expressed in a subpopulation of enteric nervous system cells, which are positive for peripherin, GFAP, and $p75^{NTR}$.

In order to quantify the frizzled-4 positive cell population, enzymatically digested and immunolabeled cells isolated from tunica muscularis were stained with frizzled-4 antibody and analysed by flow cytometry (Figure 5). Using this approach, a distinct cell population could be detected in six independent experiments: 12.3% ± 5.9% (mean ± SD) of the analysed cells stained positive for frizzled-4 in comparison to 19.7% ± 9.2% (mean ± SD) of cells that were positive for the neurotrophin receptor $p75^{NTR}$. Indeed, colabelling experiments demonstrated that 60.0% ± 16.2%

Figure 6: Overview of immunostained section sliced from "Swiss-rolled" tissue of Hirschsprung's disease. Cryostat section from large intestine diagnosed with Hirschsprung's disease (sample number 10) was immunostained for peripherin; scale bar: 5 mm. The center of the "Swiss-rolled" tissue marks the distal end of resected intestinal segment. In the microscopic view at the upper left corner normoganglionic, hypoglanglionic, and aganglionic areas are marked by an unbroken, broken, and dotted line, respectively.

(mean ± SD) of $p75^{NTR}$ positive cells expressed the Wnt receptor, whereas almost all cells found positive for frizzled-4 also expressed $p75^{NTR}$ (93.3% ± 8.9% (mean ± SD)). Hence, we could identify a double-positive subpopulation of $p75^{NTR+}$ frizzled-4^{+} cells, which is clearly distinguishable from the frizzled-4 negative population.

Next, we investigated the Wnt receptor expression pattern in gut samples of three patients presenting with Hirschsprung's disease. In Figure 6, a representative overview of a peripherin stained cryosection is shown, which was sliced from a "Swiss rolled" tissue of Hirschsprung's disease (Figure 6). In these sections, the size and number of ganglia typically decreased from oral to anal. The rudimentary expression of peripherin in the myenteric plexus at the anal (aganglionic) end represents peripherin expression in myenteric nerve fibers [22]. Immunohistochemical analysis of frizzled-4 in comparison to nestin, $p75^{NTR}$, peripherin, and GFAP revealed that, in line with the other markers, the expression of frizzled-4 declined from normoganglionic to aganglionic areas of the large intestine (Figures 7 and 8).

4. Discussion

Wnt signalling plays an important role in the development of the peripheral nervous system. It induces and specifies the neural crest and is involved in processes regulating neural crest cell migration and formation of neuronal interconnections in the developing gut [12–14].

Among the ten identified frizzled-Wnt receptors, only frizzled-4 is able to strongly bind Norrin. Norrin is known to regulate vascular development of the inner ear and retina [23] but has also been attributed to mediate neuroprotective effects to retinal ganglion cells [20]. In humans it is associated with Norrie disease, a genetic disorder that primarily affects the eye and leads to blindness and to progressive hearing loss in a proportion of patients. Although no gastrointestinal symptoms were described in affected humans, the Norrin-frizzled-4 interaction is suspected to play an important role in colonic mucosa regeneration and colonic tumorigenesis [24].

In addition, frizzled-4 knockout mice suffer from esophageal dysfunction, apart from progressive cerebellar and auditory degeneration [25]. While the authors ascribed changes in esophageal motility rather to muscular maldevelopment and described the lower gastrointestinal ENS to be unaffected in frizzled-4 knockout mice, subtle changes in ENS architecture and the impact on the function of the gut beyond the stomach were not investigated in detail. The fact that the knockout of frizzled genes can lead to profound neurogenic abnormalities of gastrointestinal tract motility, while ENS architecture appears to be almost normal, has been impressively demonstrated by Sasselli et al. [14]. In these experiments, the loss of frizzled-3 led to developmental deficits in the ENS network and resulted in a gastrointestinal

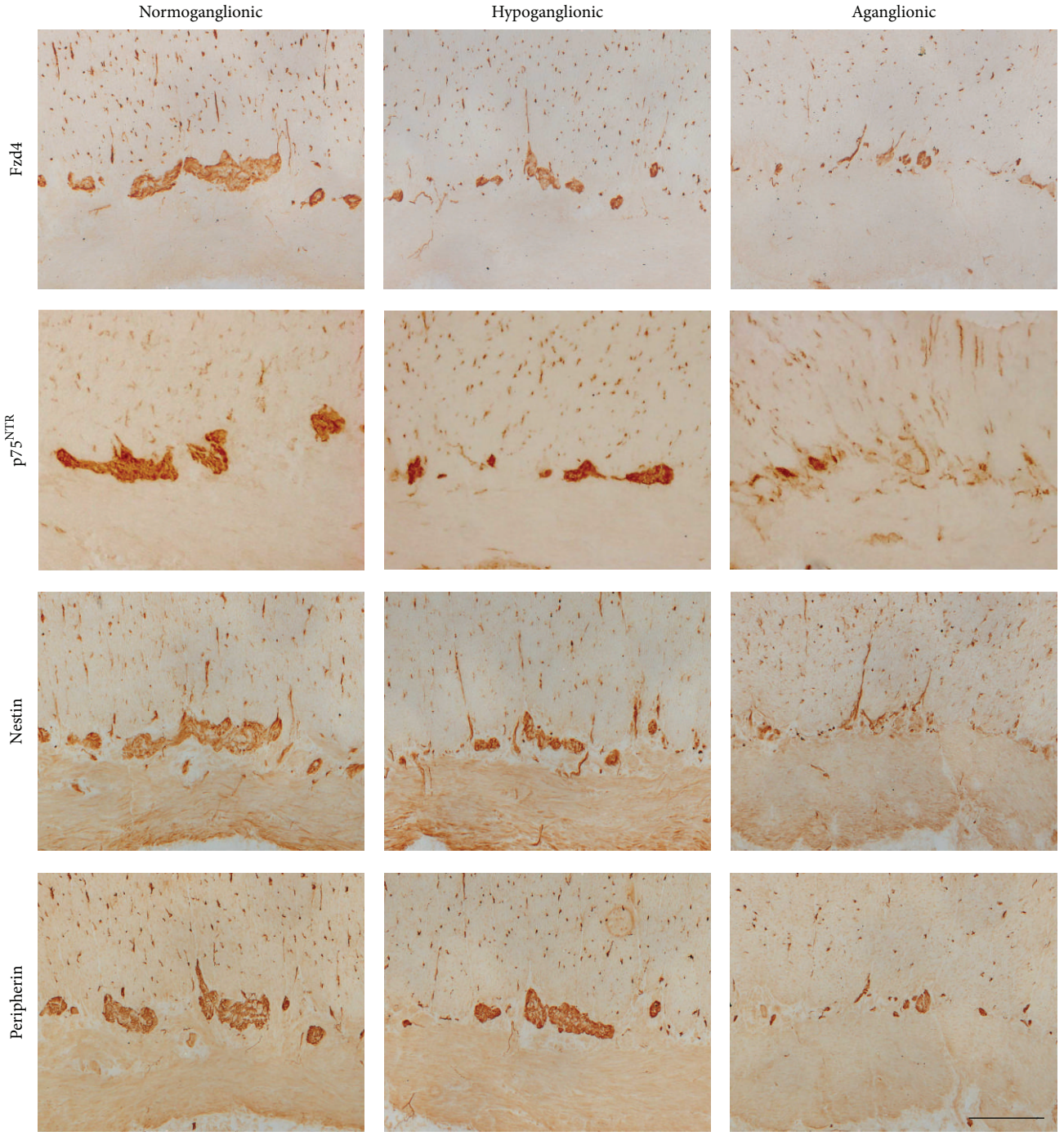

FIGURE 7: The expression of frizzled-4 in Hirschsprung's disease decreases from being oral to anal. Immunohistochemical analysis for frizzled-4 (Fzd4) in comparison to $p75^{NTR}$, nestin, and peripherin on cryostat sections from large intestine diagnosed with Hirschsprung's disease (sample number 10). Microscopic brightfield views were taken from normoganglionic, hypoganglionic, and aganglionic areas, respectively; scale bar: 200 μm.

dysmotility. While the importance of Wnt signalling in neural crest and ENS development is well established, the role of this pathway in the postnatal ENS is largely unknown. Recently, preliminary data indicate an anti-inflammatory activity of Wnt signalling in the postnatal enteric nervous system of rats [26].

In our study, we analyzed the expression pattern of frizzled-4 in normal infant human gut tissue, as well as tissue collected from patients suffering from Hirschsprung's disease. Immunohistochemical analysis revealed that frizzled-4 is expressed in neural cells within the gastrointestinal tract. Subpopulations of peripherin expressing neurons and GFAP positive glial cells were stained with various intensities. In contrast, frizzled-4 was expressed neither in enteric smooth muscle nor in interstitial cells of Cajal. Interestingly, frizzled-4 expression was also observed in cell populations that

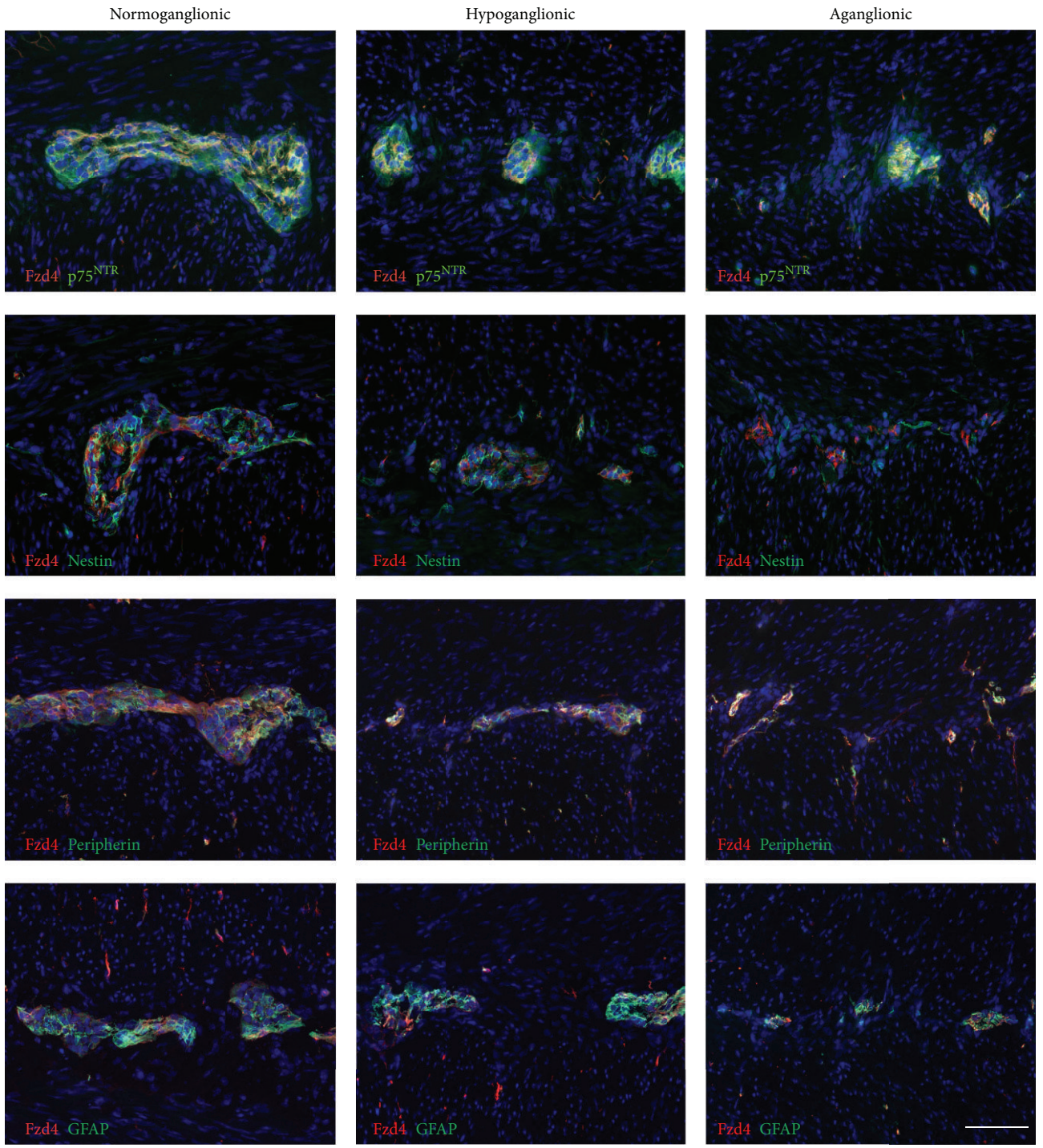

FIGURE 8: Coimmunostaining processes reveal the parallel decrease of frizzled-4 with other neural markers in Hirschsprung's disease. Immunofluorescence for frizzled-4 (Fzd4, red) in combination with $p75^{NTR}$, nestin, peripherin, and GFAP (green) on cryostat sections from large intestine diagnosed with Hirschsprung's disease (sample number 10); cell nuclei were visualized with DAPI (blue). Fluorescence views were taken from normoganglionic, hypoglanglionic, and aganglionic area, respectively; scale bar: 100 μm.

stained positive for the intermediate filament nestin and the cell surface antigen $p75^{NTR}$. Together with CD49b, these proteins have been proposed to be expressed in ENS progenitor or stem cells [18]. Indeed, some evidence supports that neurogenesis also takes place in the postnatal gut. Regeneration of the ENS has been demonstrated to take place in mice *in vivo* upon 5-HT stimulation or following injury of the gut [15–17]. In addition, the ability to isolate and propagate cells of the postnatal ENS of rodents and men indicates the persistence of progenitor or stem cell like neural cell

types in the postnatal intestine [27–30]. In this context, the identification of suitable markers for isolation of these neural progenitor cells is of crucial importance for the development of cell based therapies. Intriguingly, our flow cytometry experiments showed that >93% of frizzled-4 expressing cells were also positive for $p75^{NTR}$, whereas frizzled-4 positive cells represent only about 60% of the $p75^{NTR}$ cell pool. Thus, the frizzled-4 antibody recognizes a subpopulation of $p75^{NTR}$ positive cells and might represent an interesting marker for the isolation and characterization of these distinct cell populations. However, further experiments will be necessary to investigate and compare the cell biological properties of $Fzd4^{+}/p75^{NTR+}$ and $Fzd4^{-}/p75^{NTR+}$ cells.

Interestingly, our immunohistological findings demonstrate that the epithelial crypts are surrounded by frizzled-4 positive neural extension. The intestinal crypt harbors the epithelial stem compartment that is strongly regulated by the Wnt signalling pathway [31]. The close localization of ENS cell extensions to this compartment indicates that the epithelial stem cell niche might influence the enteric nervous system by secreted Wnt pathway agonists such as Wnt3a or R-spondin.

Diagnostic procedures use specific antibodies to identify diseases such as Hirschsprung's disease. However, the identification of enteric ganglion cells can be challenging in human tissue, especially if immature ganglion cells are present in newborns, where these cells can be easily confused with endothelial cells and cells of mesenchymal or immunological origin [32]. In addition, in primary diagnostic suction biopsies specimens usually only include the submucosal plexus and are often of small size, making a precise diagnosis difficult. Therefore, immunohistochemical analysis, using several antibodies targeted at various neuronal and glial antigens, has been proposed to increase sensitivity and specificity of the diagnostic procedure. In this study, we evaluated the frizzled-4 expression pattern in comparison to other cell markers in the various segments of the colon of patients suffering from Hirschsprung's disease. Immunohistochemistry was performed for $p75^{NTR}$, nestin, GFAP, peripherin, and frizzled-4 in the normally ganglionated gut, the transition zone, and the aganglionic segment of the colon. In the examined tissues, the number of frizzled-4 positive cells declined from normoganglionic to aganglionic areas of large intestine, in accordance with the other neural markers. Whether frizzled-4 might be useful as a putative diagnostic marker for the diagnosis of Hirschsprung's disease has to be investigated in a larger cohort of patients.

5. Conclusion

In the present study, we analysed the expression of the Wnt receptor frizzled-4 in the enteric nervous system of human small and large intestine. Frizzled-4 was identified in a distinct subpopulation of enteric neurons and glia as well as nestin and $p75^{NTR}$ positive cells in all layers of gut wall. In pathological human samples of Hirschsprung's disease the expression of this Wnt receptor decreased from normoganglionic to aganglionic areas of large intestine. The expression pattern of frizzled-4 indicates that the Wnt signalling pathway might be involved in the postnatal development and/or function of the enteric nervous system. Additional studies are necessary to characterize the frizzled-4 positive cell population in more detail and to elucidate the biological role of this Wnt receptor in the postnatal human enteric system.

Conflict of Interests

The authors declare that there is no conflict of interests regarding the publication of this paper.

Authors' Contribution

Katharina Nothelfer and Florian Obermayr contributed equally to the work.

Acknowledgments

The authors would like to thank Susanne Stachon for her excellent technical assistance. The project was supported by a grant from the German Federal Ministry for Education and Research (01GN0967).

References

[1] N. M. Le Douarin and E. Dupin, "Multipotentiality of the neural crest," *Current Opinion in Genetics & Development*, vol. 13, no. 5, pp. 529–536, 2003.

[2] C. Nishiyama, T. Uesaka, T. Manabe et al., "Trans-mesenteric neural crest cells are the principal source of the colonic enteric nervous system," *Nature Neuroscience*, vol. 15, no. 9, pp. 1211–1218, 2012.

[3] F. Obermayr, R. Hotta, H. Enomoto, and H. M. Young, "Development and developmental disorders of the enteric nervous system," *Nature Reviews Gastroenterology & Hepatology*, vol. 10, no. 1, pp. 43–57, 2012.

[4] A. S. Wallace and A. J. Burns, "Development of the enteric nervous system, smooth muscle and interstitial cells of Cajal in the human gastrointestinal tract," *Cell and Tissue Research*, vol. 319, no. 3, pp. 367–382, 2005.

[5] H. M. Young, A. J. Bergner, M. J. Simpson et al., "Colonizing while migrating: how do individual enteric neural crest cells behave?" *BMC Biology*, vol. 12, no. 1, p. 23, 2014.

[6] J. B. Furness, "The enteric nervous system and neurogastroenterology," *Nature Reviews Gastroenterology & Hepatology*, vol. 9, no. 5, pp. 286–294, 2012.

[7] M. Schemann, "Control of gastrointestinal motility by the 'gut brain'—the enteric nervous system," *Journal of Pediatric Gastroenterology & Nutrition*, vol. 41, supplement 1, pp. S4–S6, 2005.

[8] C. E. Gariepy, "Developmental disorders of the enteric nervous system: genetic and molecular bases," *Journal of Pediatric Gastroenterology and Nutrition*, vol. 39, no. 1, pp. 5–11, 2004.

[9] D. Newgreen and H. M. Young, "Enteric nervous system: development and developmental disturbances—Part 2," *Pediatric and Developmental Pathology*, vol. 5, no. 4, pp. 329–349, 2002.

[10] D. Newgreen and H. M. Young, "Enteric nervous system: development and developmental disturbances—part 1," *Pediatric and Developmental Pathology*, vol. 5, no. 3, pp. 224–247, 2002.

[11] T. A. Heanue and V. Pachnis, "Enteric nervous system development and Hirschsprung's disease: advances in genetic and stem cell studies," *Nature Reviews Neuroscience*, vol. 8, no. 6, pp. 466–479, 2007.

[12] R. Mayor and E. Theveneau, "The role of the non-canonical Wnt-planar cell polarity pathway in neural crest migration," *Biochemical Journal*, vol. 457, no. 1, pp. 19–26, 2014.

[13] T. Sauka-Spengler and M. Bronner-Fraser, "A gene regulatory network orchestrates neural crest formation," *Nature Reviews Molecular Cell Biology*, vol. 9, no. 7, pp. 557–568, 2008.

[14] V. Sasselli, W. Boesmans, P. V. Berghe, F. Tissir, A. M. Goffinet, and V. Pachnis, "Planar cell polarity genes control the connectivity of enteric neurons," *The Journal of Clinical Investigation*, vol. 123, no. 4, pp. 1763–1772, 2013.

[15] N. M. Joseph, S. He, E. Quintana, Y. Kim, G. Núñez, and S. J. Morrison, "Enteric glia are multipotent in culture but primarily form glia in the adult rodent gut," *Journal of Clinical Investigation*, vol. 121, no. 9, pp. 3398–3411, 2011.

[16] C. Laranjeira, K. Sandgren, N. Kessaris et al., "Glial cells in the mouse enteric nervous system can undergo neurogenesis in response to injury," *The Journal of Clinical Investigation*, vol. 121, no. 9, pp. 3412–3424, 2011.

[17] M. T. Liu, Y. H. Kuan, J. Wang, R. Hen, and M. D. Gershon, "5-HT4 receptor-mediated neuroprotection and neurogenesis in the enteric nervous system of adult mice," *The Journal of Neuroscience*, vol. 29, no. 31, pp. 9683–9699, 2009.

[18] L. Becker, J. Peterson, S. Kulkarni, and P. J. Pasricha, "Ex vivo neurogenesis within enteric ganglia occurs in a PTEN dependent manner," *PLoS ONE*, vol. 8, no. 3, Article ID e59452, 2013.

[19] C. Y. Logan and R. Nusse, "The Wnt signaling pathway in development and disease," *Annual Review of Cell and Developmental Biology*, vol. 20, no. 1, pp. 781–810, 2004.

[20] R. Seitz, S. Hackl, T. Seibuchner, E. R. Tamm, and A. Ohlmann, "Norrin mediates neuroprotective effects on retinal ganglion cells via activation of the Wnt/beta-catenin signaling pathway and the induction of neuroprotective growth factors in Muller cells," *Journal of Neuroscience*, vol. 30, no. 17, pp. 5998–6010, 2010.

[21] G. Abbruzzese, A. Gorny, L. T. Kaufmann et al., "The Wnt receptor Frizzled-4 modulates ADAM13 metalloprotease activity," *Journal of Cell Science*, vol. 128, no. 6, pp. 1139–1149, 2015.

[22] R. Beschorner, M. Mittelbronn, K. Bekure, and R. Meyermann, "Problems in fast intraoperative diagnosis in Hirschsprung's disease," *Folia Neuropathologica*, vol. 42, no. 4, pp. 191–195, 2004.

[23] H. L. Rehm, D. S. Zhang, M. C. Brown et al., "Vascular defects and sensorineural deafness in a mouse model of Norrie disease," *The Journal of Neuroscience*, vol. 22, no. 11, pp. 4286–4292, 2002.

[24] K. Planutis, M. Planutiene, M. Moyer, A. V. Nguyen, C. A. Pérez, and R. F. Holcombe, "Regulation of norrin receptor frizzled-4 by Wnt2 in colon-derived cells," *BMC Cell Biology*, vol. 8, no. 1, article 12, 2007.

[25] Y. Wang, D. Huso, H. Cahill, D. Ryugo, and J. Nathans, "Progressive cerebellar, auditory, and esophageal dysfunction caused by targeted disruption of the frizzled-4 gene," *The Journal of Neuroscience*, vol. 21, no. 13, pp. 4761–4771, 2001.

[26] R. Di Liddo, T. Bertalot, A. Schuster et al., "Anti-inflammatory activity of Wnt signaling in enteric nervous system: in vitro preliminary evidences in rat primary cultures," *Journal of Neuroinflammation*, vol. 12, no. 1, p. 23, 2015.

[27] N. Bondurand, D. Natarajan, N. Thapar, C. Atkins, and V. Pachnis, "Neuron and glia generating progenitors of the mammalian enteric nervous system isolated from foetal and postnatal gut cultures," *Development*, vol. 130, no. 25, pp. 6387–6400, 2003.

[28] G. M. Kruger, J. T. Mosher, S. Bixby, N. Joseph, T. Iwashita, and S. J. Morrison, "Neural crest stem cells persist in the adult gut but undergo changes in self-renewal, neuronal subtype potential, and factor responsiveness," *Neuron*, vol. 35, no. 4, pp. 657–669, 2002.

[29] M. Metzger, P. M. Bareiss, T. Danker et al., "Expansion and differentiation of neural progenitors derived from the human adult enteric nervous system," *Gastroenterology*, vol. 137, no. 6, pp. 2063.e4–2073.e4, 2009.

[30] M. Metzger, C. Caldwell, A. J. Barlow, A. J. Burns, and N. Thapar, "Enteric nervous system stem cells derived from human gut mucosa for the treatment of aganglionic gut disorders," *Gastroenterology*, vol. 136, no. 7, pp. 2214–2225.e3, 2009.

[31] H. Clevers, "The intestinal crypt, a prototype stem cell compartment," *Cell*, vol. 154, no. 2, pp. 274–284, 2013.

[32] S. K. Holland, R. B. Hessler, M. D. Reid-Nicholson, P. Ramalingam, and J. R. Lee, "Utilization of peripherin and S-100 immunohistochemistry in the diagnosis of Hirschsprung disease," *Modern Pathology*, vol. 23, no. 9, pp. 1173–1179, 2010.

Hindawi Publishing Corporation
Stem Cells International
Volume 2016, Article ID 3710836, 16 pages
http://dx.doi.org/10.1155/2016/3710836

Research Article

Three-Dimensional Gastrointestinal Organoid Culture in Combination with Nerves or Fibroblasts: A Method to Characterize the Gastrointestinal Stem Cell Niche

Agnieszka Pastuła,[1] Moritz Middelhoff,[1] Anna Brandtner,[1] Moritz Tobiasch,[1] Bettina Höhl,[1] Andreas H. Nuber,[1] Ihsan Ekin Demir,[2] Steffi Neupert,[1] Patrick Kollmann,[3] Gemma Mazzuoli-Weber,[3] and Michael Quante[1]

[1]*II. Medizinische Klinik, Klinikum rechts der Isar, Technische Universität München, 181675 München, Germany*
[2]*Chirurgische Klinik und Poliklinik, Klinikum rechts der Isar, Technische Universität München, 281675 München, Germany*
[3]*Lehrstuhl für Humanbiologie, Technische Universität München, 385350 Freising, Germany*

Correspondence should be addressed to Michael Quante; michael.quante@lrz.tum.de

Received 12 May 2015; Revised 6 July 2015; Accepted 9 July 2015

Academic Editor: Kodandaramireddy Nalapareddy

The gastrointestinal epithelium is characterized by a high turnover of cells and intestinal stem cells predominantly reside at the bottom of crypts and their progeny serve to maintain normal intestinal homeostasis. Accumulating evidence demonstrates the pivotal role of a niche surrounding intestinal stem cells in crypts, which consists of cellular and soluble components and creates an environment constantly influencing the fate of stem cells. Here we describe different 3D culture systems to culture gastrointestinal epithelium that should enable us to study the stem cell niche *in vitro* in the future: organoid culture and multilayered systems such as organotypic cell culture and culture of intestinal tissue fragments *ex vivo*. These methods mimic the *in vivo* situation *in vitro* by creating 3D culture conditions that reflect the physiological situation of intestinal crypts. Modifications of the composition of the culture media as well as coculturing epithelial organoids with previously described cellular components such as myofibroblasts, collagen, and neurons show the impact of the methods applied to investigate niche interactions *in vitro*. We further present a novel method to isolate labeled nerves from the enteric nervous system using Dclk1-CreGFP mice.

1. Introduction

Adult tissue stem cells are necessary for tissue homeostasis and regeneration after injury, but under certain conditions they may undergo malignant transformation and give rise to cancer. This hypothesis has been widely studied *in vivo* but *in vitro* methods to analyze the underlying factors and the interaction of the epithelium and stroma are missing. A common and distinct feature of most adult stem cells is their localization [1], as they reside within a specific and protected anatomical location called stem cell niche. Such a niche is composed of cellular components surrounding stem cells, extracellular matrix (ECM), and soluble factors. It is thought that the primary function of this stem cell niche is stem cell retention with controlled symmetric and asymmetric divisions. Anchorage of stem cells is mediated by their contact with the ECM and relies on adherens junctions [2, 3]. The cellular part of the niche contains stromal cells such as the osteoblastic cells in bone marrow, Sertoli cells in germ line stem cell niche, or pericryptal fibroblasts in the intestine [1, 4]. As the gastrointestinal epithelium is prone to inflammation and carcinogenesis, it is important to decipher regulatory mechanisms of the intestinal stem cell niche not only in physiology, but also during inflammation and carcinogenesis.

The intestine is an organ with a high epithelial cell turnover comprising a self-renewal every two to seven days

in the context of normal tissue homeostasis [5], making it a perfect model to study the impact of the niche on proliferation and differentiation of stem cells. This plasticity originates from the presence of multipotent intestinal stem cells (ISC), which reside in crypts or gastrointestinal glands [5]. *Lgr5*-positive (and *Prom1*-/*Sox9*-positive) rapid cycling stem cells reside at the crypt base, hence also called crypt base columnar cells (CBC), and the four cell lineages of the intestinal crypt were shown to be derived from these stem cells [6]. Surrounded by endothelial cells (vascular and lymphatic endothelium), pericytes, cells of the immune system, fibroblasts, and neurons, ISCs are constantly modulated by the release of cytokines, chemokines, growth factors, and neurotransmitters and may thereby be modified towards a carcinogenic fate [7, 8]. The maintenance and proliferation of stem cells is highly dependent on modulations of signaling pathways such as Wnt, Notch, BMP, or Hedgehog [8]. Recently, Paneth cells were shown to be an important component of the intestinal stem cell niche [9]; however depletion of this cell type in mouse did not alter significantly the crypt phenotype [10]. That would suggest that niche factors are provided by stromal cells.

A great majority of *in vitro* studies in biomedical research are dominated by the application of two dimensional (2D) cell culture models. However, the latter poorly reflect cellular heterogeneity and cellular behavior of tissues *in vivo*. Moreover, 2D cell culture does not allow studying the communication between different cell types or ECM-cell interaction. In the biomedical research there is growing interest for the application of three-dimensional (3D) cell culture systems. Recently, the 3D culture of mouse intestinal crypts has been developed, which is known as minigut culture or organoid culture [11]. The crypt culture recapitulates the cellular diversity of the intestinal epithelium. Furthermore, in the intestinal organoid culture crypt and villus domains can be identified, thus resembling proliferating and differentiated compartments in the intestine *in vivo*. As it is possible to add stromal cells to the organoid culture, it is a promising physiologically relevant model to study the niche factors *ex vivo*. Here we propose to study the niche factors utilizing nerves and fibroblasts as niche cells for intestinal and cardia crypt organoids *in vitro*.

2. Methods

2.1. Animals. Animal experiments were approved by the local committee of animal welfare. For SI crypt isolation tissue from C57BL/6 mice (Jackson laboratories) was used. For the isolation of intestinal myofibroblasts wild type C57BL/6J mice at the age of 4 weeks–2 years were used. Dclk1-CreGFP mice were crossed to Rosa26-mTomato/mGFP (R26-TGFP) reporter strains as previously described [12]. Mice employed for neuronal coculture were aged between 7 and 10 days and transgenic ubiquitously expressing the protein *Dclk1Cre* in *Dclk1*-positive cells and their lineages, combined with the reporter protein-complex $Tom^{fl/fl}GFP$. To obtain Barrett organoid cardia cells, tissues from pL2-IL-1b mice at the age of one year were isolated. The pL2-IL-1beta mice carry the EBV-L2-IL-1β transgene, overexpressing the human IL-1beta in the esophageal and squamous forestomach mucosa. The mice show esophagitis which progresses to metaplasia and dysplasia at an older age (~12 months) [13]. Additionally, for cardia and intestinal crypt culture Lgr5-CreTMG mice with an inducible Cre and stable GFP expression in Lgr5-positive cells at the age of 60 and 32 weeks respectively, were employed [6].

2.2. Intestinal Organoid Culture (Intestinal Crypts). The small intestine (SI) of mice was taken out and washed in PBS (Life Technologies), removing all fat and adjacent tissue. It was opened longitudinally and washed in PBS to remove all remaining food residues. The SI tissue was cut into ca. 3–5 cm long parts, which were stored in a petri dish containing cold PBS + 10% fetal bovine serum (FBS) (Life Technologies), referred to later as PBS/FBS. The intestine parts were flattened on a petri dish and the villi were scraped off using a cover glass. This step was repeated on the inside and outside of the SI parts. These SI parts were cut with a scalpel into 2–4 mm pieces and transferred into 20 mL PBS/FBS in a 50 mL falcon tube. The tissue samples were allowed to sediment and the supernatant was removed. Additional 10 mL of PBS/FBS was added to wash the tissue and the supernatant was removed. These steps were repeated until the supernatant was clear (approx. 5 times). The remaining tissue was digested in PBS + EDTA (2 mM) for 15 min at 4°C on a shaker. After digestion the supernatant was removed. The tissue was resuspended in 10 mL PBS/FBS and filtered through a 70 μm cell strainer (BD Biosciences) into a new 50 mL falcon tube. This step was repeated several times (~4 times). To pellet the crypts they were centrifuged for 8 min, 800 rpm at 4°C. The supernatant was removed as completely as possible, 150–200 μL Matrigel was added to the pellet avoiding air bubbles. 50 μL Matrigel was plated in every well of a pre-warmed 24-well plate. In every well 0.5 mL of crypt culture medium (CM) was added, which is composed of advanced DMEM/F12 (Life Technologies), supplemented with serum-free B27 (1 : 50, Life Technologies), N2 (1 : 100, Life Technologies), N-acetylcysteine (50 mM, Sigma), recombinant murine epithelial growth factor (EGF 50 ng/mL, Peprotech), Noggin (100 ng/mL, Peprotech), R-Spondin (1 μg/mL, Peprotech), Glutamax-I Supplement (1 : 100, Life Technologies), Penicillin/Streptomycin (500 μg/mL, Life Technologies), and HEPES (10 μM, Life Technologies) (see Table 1). The cultures were incubated in a humidified incubator at 37°C and 5% CO_2.

After 1 day, growth of the isolated crypts can be monitored. After 2-3 days SI crypts start budding, resembling the crypt-villus structure in the intestine. The medium was changed every second day. Approximately every week the crypts can be split 1 : 2 to 1 : 4, depending on the number and size of the crypts. To passage the organoids, the medium was replaced by 0.5 mL ice-cold medium (CM without growth factors, also described as complete medium), pipetted up and down a few times to disrupt the Matrigel, and put in a new 15 mL falcon. Disrupted crypts should no longer be visible by eye. They were pelleted at 800 rpm for 5 min at 4°C and the appropriate amount of Matrigel was added to the pellet. The Matrigel drops are plated again into a 24-well plate and the crypt culture medium was added.

Table 1: Composition of standard media applied in the described methods.

Culture conditions	Composition
Crypt medium (CM)	Advanced DMEM/F12 + HEPES + Pen/Strep + Glutamax + growth supplements (B27, N2) + ENR (EGF, R-Spondin, and Noggin) + N-acetylcysteine
Cardia medium (CaM)	Wnt-conditioned advanced DMEM/F12 + HEPES + Pen/Strep + Glutamax + growth supplements (B27, N2) + ENR (EGF, R-Spondin, and Noggin) + N-acetylcysteine

2.3. Isolation of Intestinal Myofibroblasts. Intestinal myofibroblasts were isolated using the explant technique. The murine small intestine was harvested and cut into 2-3 mm fragments. The tissue fragments were washed in a cold washing solution that was composed of Hanks' Balanced Salt Solution (HBSS) (Life Technologies), 1% Penicillin/Streptomycin (Life Technologies), and 50 μg/mL Gentamicin (Life Technologies) and incubated in 1 mM Dithiothreitol (DTT) for 15 min at room temperature. Afterwards, the tissue fragments were incubated in 1 mM EDTA for 30 min at 37°C with occasional stirring. After washing with HBSS, incubation with 1 mM EDTA was repeated. Then the tissue fragments were washed and incubated with 1 mg/mL collagenase type I (Sigma) for 30 min at 37°C. After washing with a solution containing HBSS, 10% FBS (Life Technologies), and 1% Penicillin/Streptomycin, the tissue fragments were plated and cultured in a medium containing RPMI1640 (Life Technologies), 10% FBS, 1% Penicillin/ Streptomycin, and 100 μg/mL Normocin (Invivogen). The myofibroblasts migrate out of the tissue fragments and adhere to the culture plate.

2.4. Crypt-Fibroblast Coculture in Organotypic Cell Culture System (OTC). Myofibroblasts and crypts were isolated as stated above from 6-week–8-month-old mice ($n = 3$ for the 2-day cultures and $n = 4$ for the 7-day cultures), expanded, and then used for the experiment. Acellular and cellular matrix were prepared as previously published [14], with minor modifications. 900 μL of acellular matrix was pipetted on a transwell (24 mm transwell with 3.0 μm pore polycarbonate membrane insert, Corning), which was placed into a 6-well transwell carrier (Organogenesis). After the solidification, 450 μL of cellular matrix containing intestinal myofibroblasts was poured. After the stabilization of the matrix, 450 μL of cellular matrix containing intestinal crypts was poured on the top. Per well 7.5 mL medium containing RPMI1640 (Life Technologies), 10% FBS (Life Technologies), 1% Penicillin/Streptomycin (Life Technologies), and 330 ng/mL R-Spondin (Peprotech) were added. At day 0 cells were seeded. R-Spondin was added to the medium only at day 0. At days 2 and 7 the culture was fixed in formalin, dehydrated, and embedded in paraffin. On the cut paraffin slides H&E, Ki-67 (Abcam), and α-SMA (Abcam) staining were performed. Total number of crypts was quantified on slides that were stained for H&E. Disintegrated crypts were counted as nonviable. Survival was defined as percentage of viable crypts.

2.5. Tissue Culture Ex Vivo. Small intestine was harvested from 5-week-old mice, cut into small pieces, embedded in a matrix, and cultured. The method was performed as previously published [15], with exception of the composition of the acellular bottom layer and cell-containing layer, which were prepared according to the protocol for organotypic cell culture [14]. The culture was performed in a transwell (24 mm transwell with 3.0 μm pore polycarbonate membrane insert, Corning) that was placed into a 6-well transwell carrier (Organogenesis). The culture medium was composed of Ham's F12 (Life Technologies), 20% FBS (Life Technologies), and 50 μg/mL Gentamicin (Life Technologies) and it was exchanged after one week. 1 mL of medium was added per well. After two weeks, the culture was fixed in formalin and embedded in paraffin and PAS staining was performed.

2.6. Influence of the Extracellular Matrix on Phenotype of Intestinal Organoids. Small intestinal crypts from three wild type 7-week–17-month-old mice were isolated and cultured in Matrigel as described above. For the experiment, crypts were seeded either in Matrigel or in a cellular matrix, which was prepared as previously published [14] with the exception of FBS, which was not added. The crypts were mixed with the cellular matrix and 50 μL of matrix was seeded per well in a 24-well plate. Crypts were seeded at day 0 and the culture medium was the same as previously published [16]. Analysis and fixation in formalin were performed at day 2. Sections were stained for Ki-67 (Abcam).

2.7. Cardia Organoid Culture. The harvested stomach was opened along the large curvature and flushed with cold PBS + 10% FBS to remove food residues. To isolate the tissue of the squamocolumnar junction (SCJ), the opened stomach was put flat on a hard surface inside out; the tissue of interest was dissected, washed in PBS, chopped into small pieces, and transferred into 20 mL PBS buffer substituted with EDTA and ethylene glycol tetraacetic acid (EGTA, final concentration 2 mM). To detach the individual tissue layers, the harvested tissue was incubated for 45 min on a shaker at 4°C. Following incubation the supernatant was removed and 10 mL PBS with 10% FBS was added. Analogous to the isolation of intestinal crypts, further disruption of the tissue was accomplished using the shearing forces of pipetting. The fragments were passed through a 70 μm cell strainer (BD Biosciences). The cell suspension was spun down at 600 rpm for 5 min. The pellet was resuspended in Matrigel and seeded onto a preheated 24-well plate with drops of 50 μL Matrigel in each well. For long-term cultures, the organoids were cultured in Wnt-conditioned intestinal crypt culture medium (0.5 mL per well), which was added freshly every second day. Wnt-CM (later referred to as cardia medium, CaM) was derived from L-Wnt3a cell line (ATCC) that was cultured in the medium

composed of advanced DMEM/F12 (Life Technologies), HEPES (10 μM, Life Technologies), Penicillin/Streptomycin (500 μg/mL, Life Technologies), and Glutamax-I Supplement (1 : 100, Life Technologies). Cardia organoids typically need Wnt3a for growth and long-term survival as an additional growth factor [17]. For efficient expansion of the organoids, they have to be passaged after 7 and 10 days in culture with the same procedure as intestinal organoids. The cultures were fixed in formalin at day 10, dehydrated, and embedded in paraffin. After cutting paraffin slides, hematoxylin and eosin (H&E), periodic acid–Schiff (PAS), Ki-67 (Abcam), and α-SMA (Abcam) staining were performed.

2.8. Isolation of Neuronal Tissue and Coculture. Neuronal tissue is derived from the myenteric plexus by removing the seromuscular layer of the prepared small intestine (adapted from [18, 19]). During the isolation process, isolated tissue was kept on ice in minimum essential medium (MEM, Life Technologies). The obtained tissue was digested for ca. 45–80 min at 37°C in HBSS containing collagenase type II (1 μg/μL, Worthington). Using a microscope, the digestion process was carefully monitored for its progress. After the first incubation period, insufficiently digested plexi were separated and digested for another 15 min. The obtained small fragments were then carefully disrupted using injection syringes (Sterican 23 G × 1 1/4″ or 20 G × 1 1/2″). To stop the digestion process HBSS supplemented with 10% FBS was added. The cell suspension was centrifuged (600 rpm, 5 min) and, after another washing step with HBSS/FBS, resuspended in advanced DMEM/F12 (Life Technologies). For growth and differentiation of neurons, cells were plated in Matrigel together with cardia organoids and cultured in neurobasal complete medium (NBM), which is composed of neurobasal medium (Life Technologies), nerve growth factor (NGF, 1 : 1000, Life Technologies), serum-free B27 (1 : 50, Life Technologies), N2 (1 : 100, Life Technologies), N-acetylcysteine (50 mM, Sigma), recombinant murine epithelial growth factor (EGF 50 ng/mL, Peprotech), Noggin (100 ng/mL, Peprotech), R-Spondin (1 μg/mL, Peprotech), Glutamax-I Supplement (1 : 100, Life Technologies), Penicillin/Streptomycin (500 μg/mL, Life Technologies), and HEPES (10 μM, Life Technologies). Medium was changed every other day. Cocultures were incubated in a humidified incubator at 37°C and 5% CO_2.

2.9. Calcium Imaging. Ca^{2+}-imaging allows visualizing alterations of intracellular $[Ca^{2+}]_i$ visible by using fluorescent dyes that change the intensity of their fluorescence depending on the $[Ca^{2+}]_i$. Although the direct contribution of Ca^{2+} to the neuronal membrane potential is limited, it has been shown that membrane potential events are closely linked to changes in $[Ca^{2+}]_i$ [20, 21]. Therefore the Ca^{2+} indicator Fluo-4 AM (Invitrogen) was used to detect activation of the neurons in the cocultures. The cells were incubated in 10 μM Fluo-4 AM for 20 minutes, followed by a 20 min wash out. During the Ca^{2+}-imaging experiments cells were continuously perfused with Krebs solution [22] at 37°C, which was constantly fumigated with carbogen (95% oxygen and 5% CO_2). To ensure a neuronal staining that was stable for several hours we added 1.25 mM probenecid (Sigma) to the Krebs solution used for the experiments. Probenecid is an inhibitor of organic anion transporters eliminating dyes and indicators from the cytoplasm [23]. The changes in fluorescence were determined using a digital camera (AxioCam Hsm, Zeiss) and the Zeiss Axio Vision software in combination with an inverted microscope (Axio Observer A1, Zeiss). The frame rate of the recording was 2 Hz, which is sufficient to reveal neuronal activation. For viability testing we applied 100 μM nicotine (Sigma) via pressure application (PDES-2L, npi electronic GmbH, Tamm, Germany) through a pulled glass pipette (tip diameter ca. 5 μm). Nicotine acts as an agonist at the nicotinergic acetylcholine receptor and therefore is suitable as a viability test for cultured enteric neurons [24]. To quantify the changes in fluorescence upon nicotinic activation of acetylcholine receptors, we assigned the resting light intensity (RLI) in the regions of interest.

2.10. Reverse Transcription Polymerase Chain Reaction (RT-PCR). RNA was isolated using the RNeasy Mini Kit (Qiagen). Residual genomic DNA was eliminated by DNase digestion on the column (Qiagen). cDNA was generated by the Reverse Transcription Kit (Promega). The primers applied were α-SMA (fw 5′ CGCTGTCAGGAACCCTGAGA 3′, rv 5′ ATGAGGTAGTCGGTGAGATC 3′), β-actin (fw 5′ CCCTGAACCCTAAGGCCAACC 3′, rv 5′ ACCCCGTCTCCGGAGTCCATC 3′), E-cadherin (fw 5′ ACCACTGCCCTCGTAATCGAA 3′, rv 5′ CGTCCTGCCAATCCTGATGAA 3′), Lgr5 (fw 5′ GACGCTGGGTTATTTCAAGTTCAA 3′, rv 5′ CAGCCAGCTACCAAATAGGTGCTC 3′), villin 1 (fw 5′ GACGTTTTCACTGCCAATACCA 3′, rv 5′ CCCAAGGCCCTAGTGAAGTCTT 3′), and vimentin (fw 5′ AACACCCGCACCAAC 3′, rv 5′ TCCGGTACTCGTTTGACT 3′).

2.11. Organoid/Enteroid Evaluation and Statistical Analysis. Proliferation and growth of organoids can be evaluated *in vitro* in several ways; we here applied the determination of the diameter and the circumference of the organoids per passage and compared the means on a timeline. The cardia organoids were measured at day 7 and day 10 using Axio Vision software (Zeiss) and ImageJ. Evaluation of the growth of intestinal crypts in organotypic cell culture system was based on the analysis of H&E staining: diameter of crypts after 2 and 7 days of culture was measured. The statistical analysis was performed using GraphPad Prism. Comparing of two groups was performed using an unpaired two-tailed *t*-test. A standard deviation of $P < 0.05$ was statistical significant.

3. Results

3.1. 3D Cell Culture Systems to Study the Stem Cell Niche in the Gastrointestinal Tract. In order to analyze the stem cell niche *in vitro* we analyzed three different *in vitro* culture systems to ideally mimic the *in vivo* situation and still be able to understand the impact of the different cellular and acellular factors.

The tissue culture *ex vivo* system is based on embedding whole tissue fragments in a matrix. Here we modulated a previously published tissue culture *ex vivo* system [15], utilizing an additional acellular layer and a cell-containing layer that were prepared according to the protocol for the originally published OTC system [14] (Figure 1(a)). The culture was performed in transwells as described above. Firstly an acellular layer was poured, which mimics the basement membrane. Then a cellular layer containing tissue fragments was poured. The medium was added only to the outer dish, which created an air-liquid interface and leads to better oxygenation of the culture. Of note, addition of R-Spondin (which is crucial for organoid culture) was not necessary; however we observed increased efficiency of growing epithelium after the addition of R-Spondin (not shown), similarly as it was previously reported [15]. Although this type of culture preserves a native stromal niche (indicated by arrowhead, Figure 1(a)) and can be analyzed after formalin fixation and paraffin embedding by immunohistochemistry, it does not represent a direct tool to analyze epithelial-stromal interaction *in vitro* without the use of genetically modified mouse models and certainly not for human material.

In contrast to the tissue culture *ex vivo* both OTC and organoid culture enable combining and therefore analyzing distinct cell types. In the OTC system epithelial and stromal cells are embedded in separate matrix layers. Since multilayer and multicellular OTC systems [14] seem to provide gradients of nutrients (feeding from the bottom) and they seem to mimic the structure of an organ much better than organoid cultures, we tested the suitability of OTC as a novel model to study the intestinal stem cell niche with murine intestinal crypts isolated from B6 WT mice. We cultured intestinal crypts in a multilayer OTC system (Figure 1(b)) similarly to the tissue culture *ex vivo*; the culture was performed in a transwell. Firstly, the acellular layer was poured; then a cellular layer with intestinal myofibroblasts was added. On the top, another cellular layer containing crypts was placed. Medium was added only to the outer dish (feeding from the bottom) thus enabling an air-liquid interface with crypts occasionally being directed to the open surface.

In contrast, in the enteroid/organoid culture cells are embedded in Matrigel and cultured in a "Matrigel drop" (Figure 1(c)). Culture medium contains growth factors such as R-Spondin, EGF, and Noggin, which are necessary to maintain growth and structure of the crypts. It has been defined that crypts from the intestine should be named enteroids as soon they form a budding "minigut" and only the combination of these cells with other cell types allows the term organoids. The combination of other cell types such as fibroblasts and nerves with the enteroid system mimics a specific *in vivo* situation and can be called organoid [25]. Although the organoid culture represents a physiologically relevant cell culture system and it has been shown that small intestinal crypts in an organoid culture system contain a crypt and villus domain [11], it has limitations. The organoid culture system does, for example, not recapitulate the gradient of nutrients, which is present along crypt-villus axis *in vivo*.

3.2. Characterization of Small Intestinal Organoids and Small Intestinal Myofibroblasts. In order to characterize small intestinal organoids, the culture was fixed in formalin, embedded in paraffin, and stained. H&E staining showed that an intestinal organoid is composed of a monolayer of polarized columnar epithelial cells (Figure 2(a), left). Moreover small intestinal organoids contain lumen and are characterized by the presence of buds. PAS staining revealed presence of mucus producing cells and the secretion of mucus into the lumen (Figure 2(a), middle). Besides differentiated zones characterized, for example, by the presence of mucus producing cells, in small intestinal organoids proliferative zones can be distinguished as can be seen from Ki-67 staining (Figure 2(a), right). Cells with proliferative activity seemed not to be randomly distributed, but rather accumulated in areas where buds grew (Figure 2(a), right). Moreover, small intestinal organoids expressed Lgr5, a marker of intestinal stem cells (Figure 2(b)), and we demonstrate Lgr5-positive cells isolated from an Lgr5 CreTM mouse in which all LgR5 expressing cells also have GFP expression in the intestinal organoids (Figure 2(b)). Myofibroblasts isolated from small intestine and cultured *in vitro* were elongated and spindle-like (Figure 2(c)). To confirm the lineage identity of small intestinal organoids and small intestinal myofibroblasts, RT-PCR for the epithelial cell markers E-cadherin and villin as well as mesenchymal cell markers such as α-SMA and vimentin was performed. The data revealed that small intestinal organoids were positive for E-cadherin and villin and negative for α-SMA and vimentin, thus confirming their epithelial lineage identity (Figure 2(d)). Small intestinal myofibroblasts expressed α-SMA and vimentin and were negative for epithelial cell markers, thus confirming their stromal cell identity (Figure 2(d)).

3.3. Fibroblasts Improve Organoid Culture Survival. To study the role of fibroblasts as a niche factor for ISCs, small intestinal crypts were cultured together with intestinal myofibroblasts in an OTC system (Figure 1(b)) and compared to the crypt monoculture. For the monoculture, the same matrix was used but with the only change that the myofibroblasts were not added to the cellular layer. After 7 days of the cultivation we observed increased macroscopic visibility of the coculture when compared to the monoculture (Figure 3(a)). Both crypt OTC monoculture and crypt OTC coculture contained mucus producing cells and proliferating cells as demonstrated by PAS and Ki-67 staining (Figure 3(b)). Proliferating cells were not homogenously distributed, but proliferating compartments could be distinguished especially in the coculture. α-SMA staining confirmed the presence of underlying spindle-shape myofibroblasts in the crypt OTC coculture (Figure 3(b), with adjacent magnification). To check whether the myofibroblasts influence crypt growth over the time, the diameter of crypts at day 2 and day 7 was measured from cultures that were fixed in formalin, embedded in paraffin, and stained for H&E. Although we did not detect significant changes in crypt size between monoculture and coculture at day 2, we observed that at day 7 crypt diameter in the monoculture was ~100 μm, whereas in the coculture it was ~400 μm (Figure 3(c)), suggesting

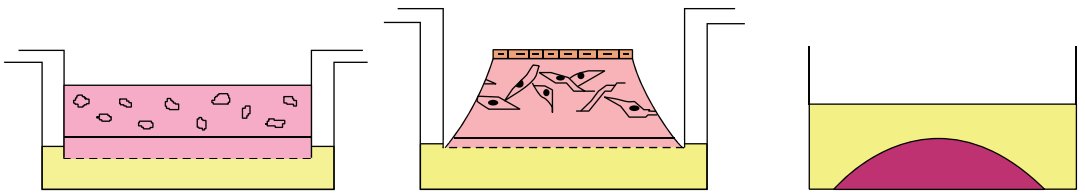

(a) (b) (c)

	Tissue culture *ex vivo*	Organotypic cell culture	Organoid culture
Matrix	Matrigel + collagen	Matrigel + collagen	Matrigel
Layers	Two	Three	One
Oxygenation	Air-liquid interface	Air-liquid interface	No air-liquid interface
Nutrients	Gradient	Gradient	No gradient
Medium	RPMI, 20% FBS (R-Spo)	RPMI, 10% FBS (R-Spo)	Serum-free, R-Spo, EGF, Noggin
Cell types	Tissue microenvironment	Two	One or more

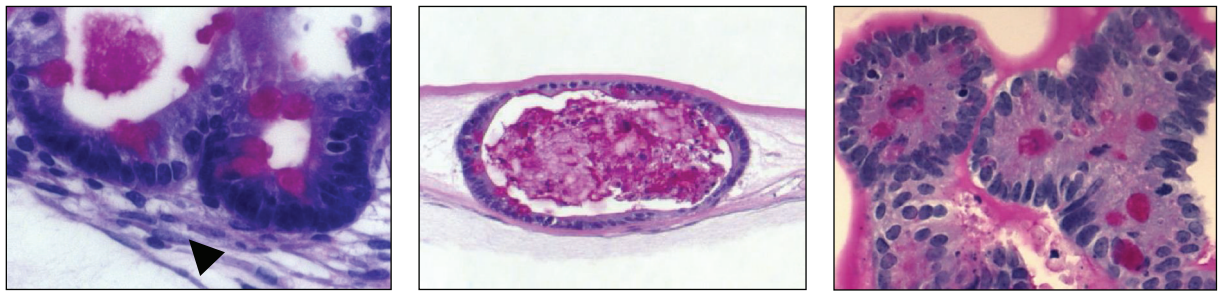

Figure 1: Summary of three-dimensional methods to culture intestinal epithelium. (a) Tissue culture *ex vivo*. Arrowhead indicates stromal cells. (b) Organotypic cell culture. (c) Organoid culture. PAS staining. R-Spo, R-Spondin.

that myofibroblasts improve growth of the crypts. To further investigate the influence of myofibroblasts on the crypts, analysis of the organoid survival was performed, which relied on the quantification of viable crypts based on the H&E staining. A viable crypt was defined as a crypt with intact epithelial cell monolayer, while a nonviable crypt was defined as an accumulation of cellular detritus (Figure 3(d), lower). In the crypt OTC monoculture 30% of crypts were viable, whereas in the crypt OTC coculture 90% of crypts were viable (Figure 3(d), upper), indicating that myofibroblasts improve organoid culture survival and thus supporting the hypothesis that myofibroblasts provide some niche factors for ISCs.

3.4. Collagen Modulates the Phenotype of Intestinal Crypts. Interestingly, crypts cultured in the OTC system almost did not have buds, which are a characteristic feature of 3D intestinal tissue cultures, as shown by crypts that were cultured in the organoid system (Figure 4(a)). Since the extracellular matrix was shown to alter the phenotype of normal mammary epithelium [26] and given that matrix composition of OTC differs from that one used in organoid culture of intestinal crypts, we hypothesized that the extracellular matrix might contribute to shaping the phenotype of the normal intestinal epithelium. To test this hypothesis, we utilized the organoid culture system and embedded crypts in the OTC cellular matrix. To exclude the potential effect of an air-liquid interface and the effect of serum, the culture was performed in a 24-well plate (identically as the organoid culture) [11, 27] and without addition of serum into the cellular matrix. In control conditions (crypts seeded in Matrigel) approximately 70% crypts contained buds, while in the OTC cellular matrix only 40% crypts were budding (Figure 4(c)), suggesting that collagen reduces the formation of buds. Although crypts in OTC cellular matrix showed a decreased number of buds, they contained proliferating cells, as revealed by Ki-67 staining (Figure 4(b)).

3.5. Isolating Distinct Neurons from the Enteric Nervous System for In Vitro Culture. As described above, the nervous system is thought to have an important function in intestinal epithelial stem cell regulation and in the development of neoplasia [12, 28, 29]. Upon surgical or pharmacological denervation of the stomach, our collaborators and we recently demonstrated that carcinogenesis in the denervated part of the stomach was depending on innervation [17]. At the same time, this was correlated with a downregulation of Wnt3a in the stem cell niche of the denervated part of the stomach.

We recently generated a BAC transgenic mouse line that expresses constitutive Cre-recombinase under the control of the Dclk1 gene locus [12]. We subsequently crossed Dclk1-Cre mice to a Tomato/GFP reporter mouse line (B6.129S4-Gt(ROSA)26Sortm4(ACTB-tdTomato-EGFP)Luo/J), in which membrane targeted Tomato (RFP) is replaced by membrane targeted Green fluorescent protein

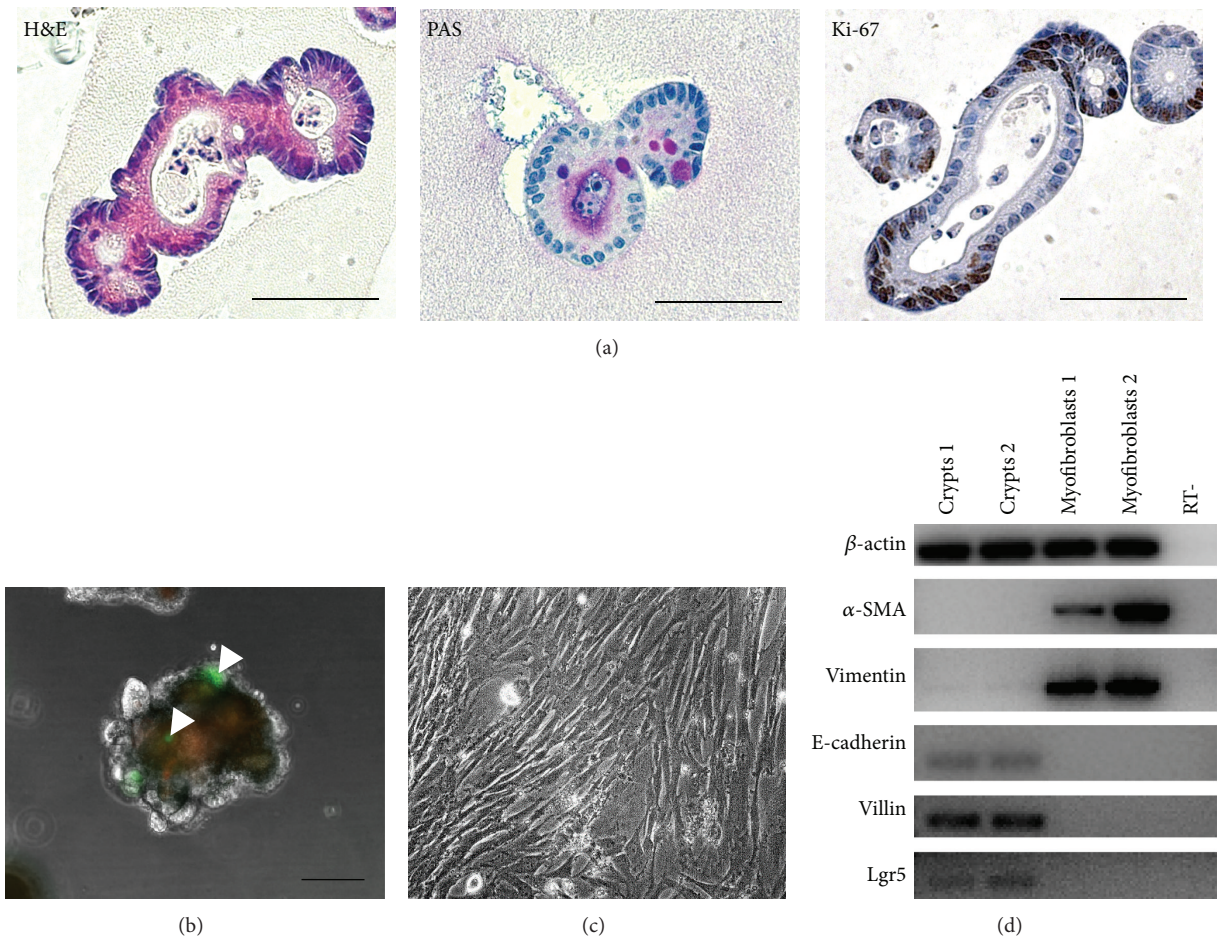

Figure 2: Characterization of small intestinal organoids and small intestinal myofibroblasts used to reconstruct intestinal stem cell niche *ex vivo*. (a) H&E staining, PAS staining, and Ki-67 staining of small intestine organoids. Scale bar, 50 μm. (b) Lgr5-GFP-positive epithelial cells in cultured conditions (marked with arrowheads). Scale bar, 100 μm. (c) Morphology of small intestine myofibroblasts, phase contrast microscopy. (d) Confirmation of the purity of small intestine organoids and small intestine myofibroblasts by Reverse-Transcription PCR. RT- (reaction without the addition of reverse transcriptase) served as the negative control.

(GFP) upon Cre-mediated recombination. Interestingly, in this mouse line with constitutive active Cre expression from embryogenesis on, we observed lineage tracing in nerve-like structures throughout the entire gut (Figures 5(a)–5(d)). Within the Dclk1 lineage, we frequently observed enteric GFAP+ glial cells and PGP9.5+ nerves and ganglia (Figures 5(e)–5(f)), suggesting that the Dclk1 lineage labels parts of the enteric nervous system (ENS), which has been shown to modulate responses to injury [30].

Subsequently, we established a neuron-organoid coculture model as a novel method to examine the role of nerves on the intestinal stem cell niche [12] in health and disease such as Barrett esophagus, for which we also recently developed a new mouse model [13], which allows us to isolate mouse Barrett epithelial organoids. Using our robust organoid culture model, we cultured and cocultured organoids from Barrett epithelium of the mouse in different media as described above.

Similar to the characterization of the cultured small intestinal crypts, H&E staining showed that cardia organoids are composed of a monolayer of polarized columnar epithelial cells (Figure 6(a)). Moreover the organoids contain lumen and are characterized by the presence of mucus producing cells and the secretion of mucus into the lumen (Figure 6(a), PAS staining). Besides differentiated zones characterized, for example, by the presence of mucus producing cells, in cardia organoids proliferative zones also can be distinguished as can be seen from Ki-67 staining (Figure 6(a)). Cells with proliferative activity seemed not to be randomly distributed, but rather accumulated in expanding areas of the organoids (Figure 6(a)). To verify the purity of the isolated cardia organoids, α-SMA showed to be predominantly negative except only few positive fibroblasts adjacent to proliferative epithelium (Figure 6(a)). To prove the presence of stem cells in our cardia organoids, we demonstrate the presence of Lgr5-CreTM-GFP labeled epithelial cells in cultured conditions (see Figure 6(b)).

For isolation of neurons from the enteric nervous system, 7–10-day-old pups were used from *Dclk1.Cre.GFP-Tom*$^{fl/fl}$*GFP* mice, as described above (Figure 6(c)). This figure

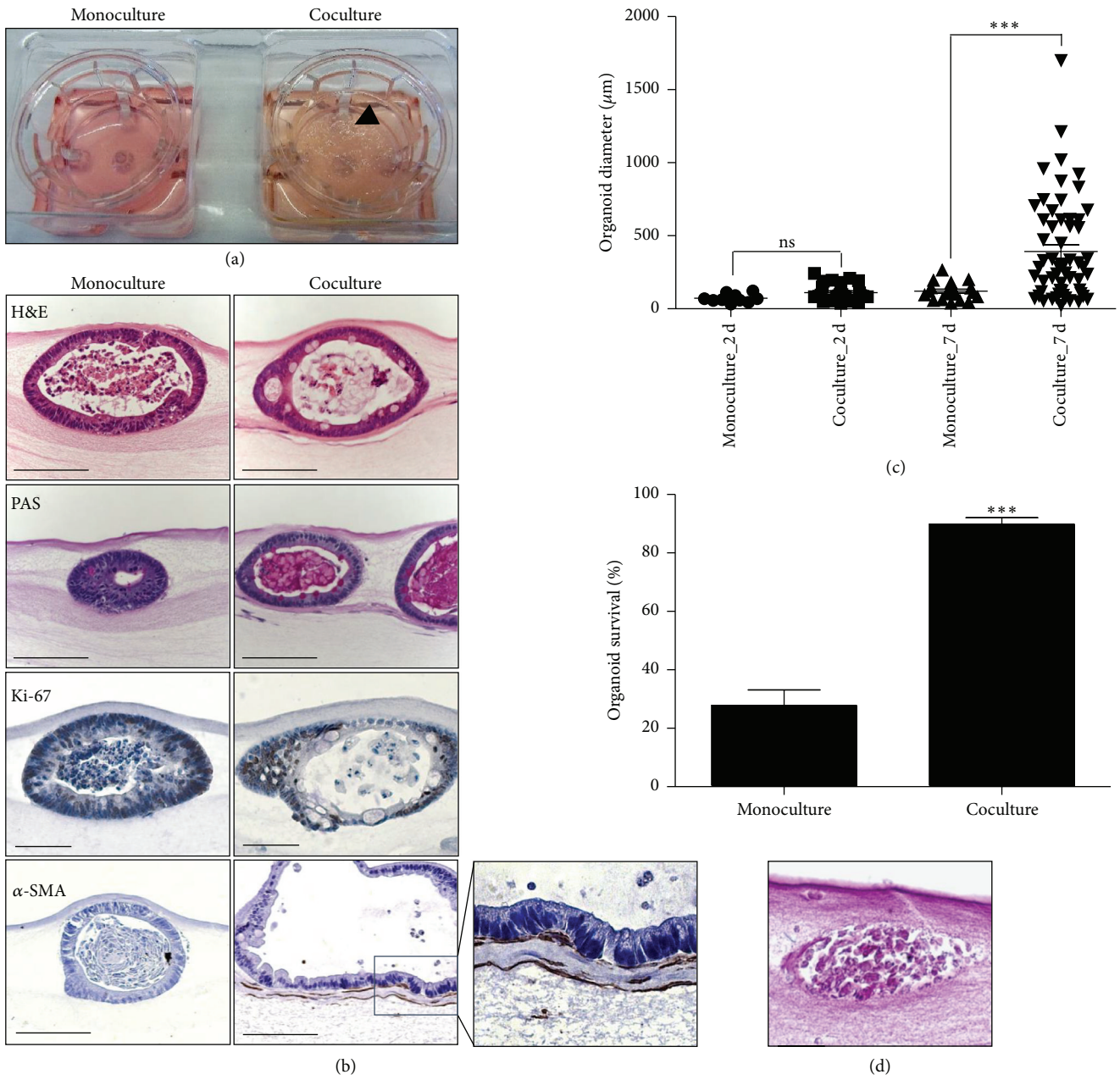

FIGURE 3: Fibroblasts improve organoid growth and organoid culture survival. (a) Macroscopic image of the crypt monoculture and coculture in an organotypic cell culture system at day 7. (b) Characterization of the crypt monoculture (left panel) and coculture (right panel) in an organotypic cell culture system at day 7 by immunohistochemistry staining: H&E (scale bar 100 μm), PAS (scale bar 100 μm), Ki-67 (scale bar 50 μm), and α-SMA staining (scale bar 100 μm), with adjacent magnification. (c) Organoid diameter measured on H&E slides from crypt monoculture and coculture in organotypic cell culture system after 2 and 7 days of culture. Each dot represents a single organoid. $P < 0.0001$ (one-way ANOVA with Bonferroni comparison). (d) Lower, example of a nonviable crypt in organotypic cell culture system, H&E staining. Scale bar, 25 μm. Upper, survival of crypts in an organotypic cell culture system, for the monoculture 169 crypts were quantified; for the coculture 213 crypts were quantified. $P < 0.0001$, two-tailed t-test.

demonstrates the pure isolation of neuronal structures from the gut, which then could be cultured with cardia organoids from the Barrett model. As additional proof of nerves showing the positive lineage, a beta-III Tubulin staining was performed of neurons cultured *in vitro*, which almost exclusively labeled neurons (Figure 6(d)). Using the Dclk1 lineage reporter we were therefore able to specifically isolate ENS neurites and grow them in 3D coculture conditions (Figure 6(e)). Neurons showed prominent neurite outgrowth and were physiologically active till day 10 of culture as demonstrated by utilizing Ca-imaging (Figures 6(f) and 6(g)). The analysis of the RLI showed an abrupt increase upon

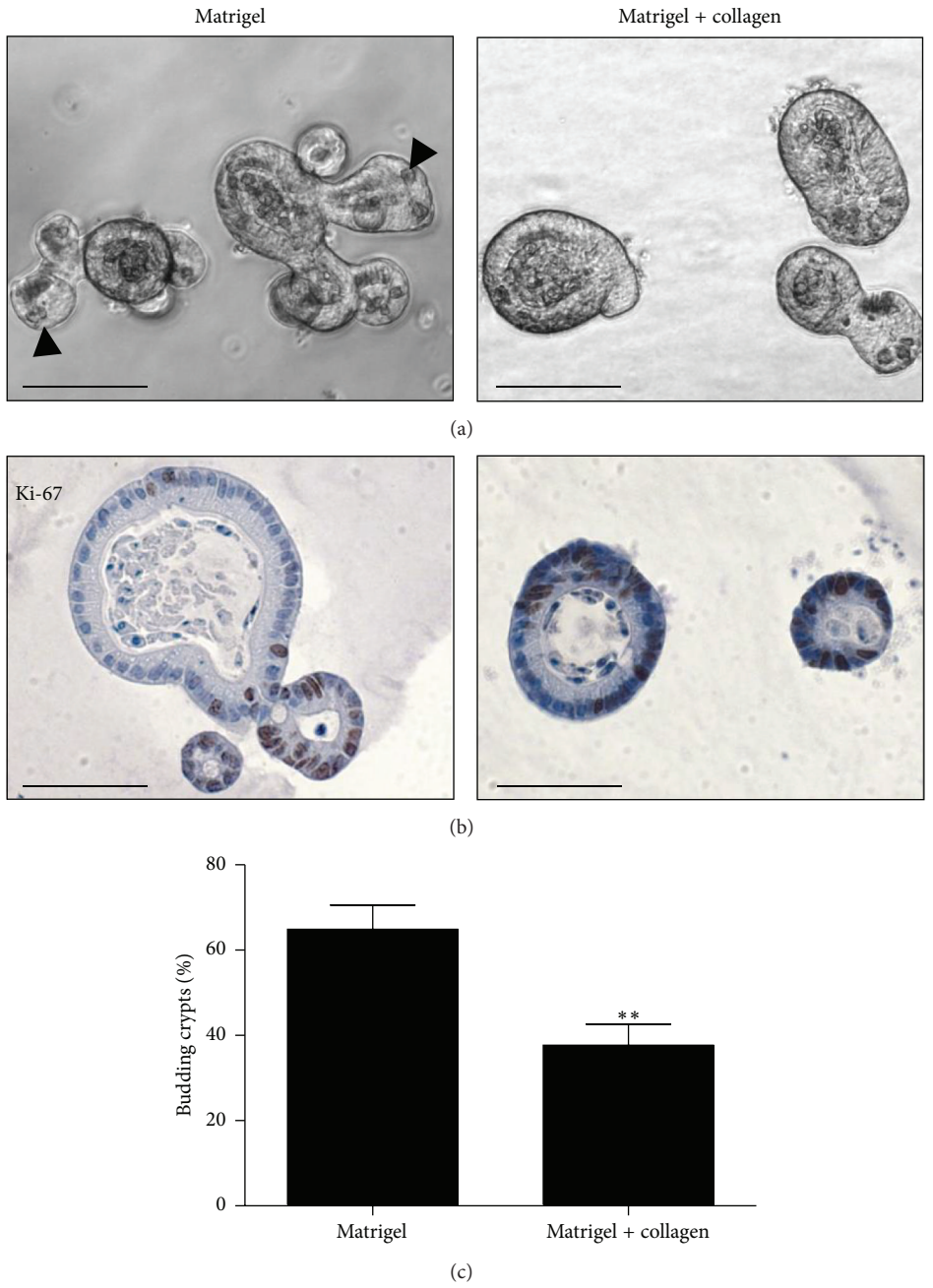

Figure 4: Collagen modulates the phenotype of small intestine organoids. (a) Morphology of small intestine organoids cultured in the presence of EGF, Noggin, and R-Spondin. Arrowheads indicate buds. Scale bar, 100 μm. (b) Ki-67 staining of small intestine organoids, scale bar, 50 μm. (c) Collagen reduces budding of small intestine organoids. In total 1700–1800 crypts were quantified per condition. $P = 0.0045$, two-tailed t-test.

stimulation of neurons with nicotine, subsequently showing a decrease of RLI over time in the regions of interest (ROI) in the absence of nicotine (Figure 6(g)).

3.6. Neurons Enhance Growth of Murine Cardia Organoids. Comparing different conditions of organoid cultures with and without neurons and variations in the culture media, we observed significant differences between the cultures with and without neurons as described previously [12]. We compared organoid cultures of Barrett epithelium isolated from Barrett esophagus from pL2-IL-1b mice [13] cultivated with CM, Wnt-conditioned CaM, and the coculture with neurons in NBM, the normal organoid cultures in CM being the control groups at seven days and ten days (for composition of media, see Table 1). The comparison of cardia organoids in Wnt-conditioned medium and cocultured with

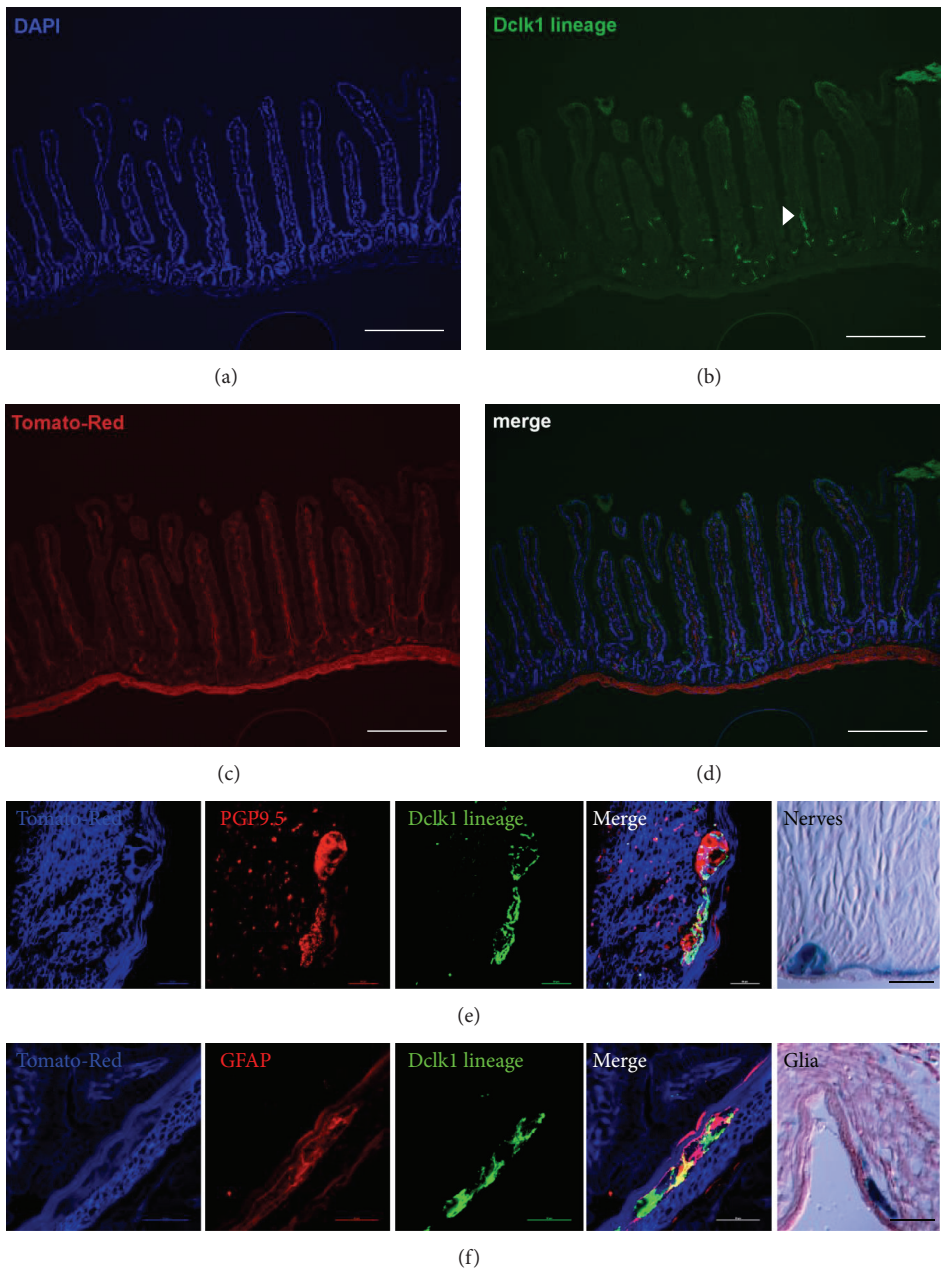

Figure 5: Positive Dclk1 lineage shown in the enteric nervous system with GFP labeled neurons. Immunofluorescence of small intestine from *Dclk1.Cre.GFP-Tom*$^{fl/fl}$*GFP* mice. (a) DAPI for cell nuclei. (b) Positive GFP-fluorescence in neurons (*Dclk1.Cre.GFP-Tom*$^{fl/fl}$*GFP* label recombined cells of the Dclk1 lineage from birth on) invading organoids and single Dclk1-positive cells in epithelium, arrowhead indicating lineage of Dclk1-positive neurons, (c) Tom-Red ubiquitously expressed as marker protein complex. (d) Merge of (a)–(c), scale bars 100 μm. (e) Cultured neurons identified by positive GFP-fluorescence and overlapping with PGP9.5 staining as proof of lineage, last panel demonstrating lacZ stained neuronal structures next to smooth musculature within the GI tract, scale bar, 50 μm. (f) Overlapping fluorescence with GFAP as proof of lineage of glia within myenteric plexus, last panel showing lacZ stained glia within myenteric plexus, scale bar, 50 μm.

neurons remained of special interest, as the role of nerves and the Wnt signaling was recently investigated intensively in gastrointestinal tumorigenesis [17].

Interestingly, the means ± SEM (standard error of the mean) of the groups showed highly significant differences already after seven days of culture (see Table 2), in total three experiments per group and point in time were performed. The size of the organoids cultivated in CaM (Wnt-conditioned medium) compared to CM showed significantly larger organoids after seven and ten days applying both methods of measuring organoid size ($P < 0.0001$). The same result is shown for the comparison of organoids in CM compared to organoids in NBM with neurons in coculture (NBM + N) ($P < 0.0001$). Organoids in NBM

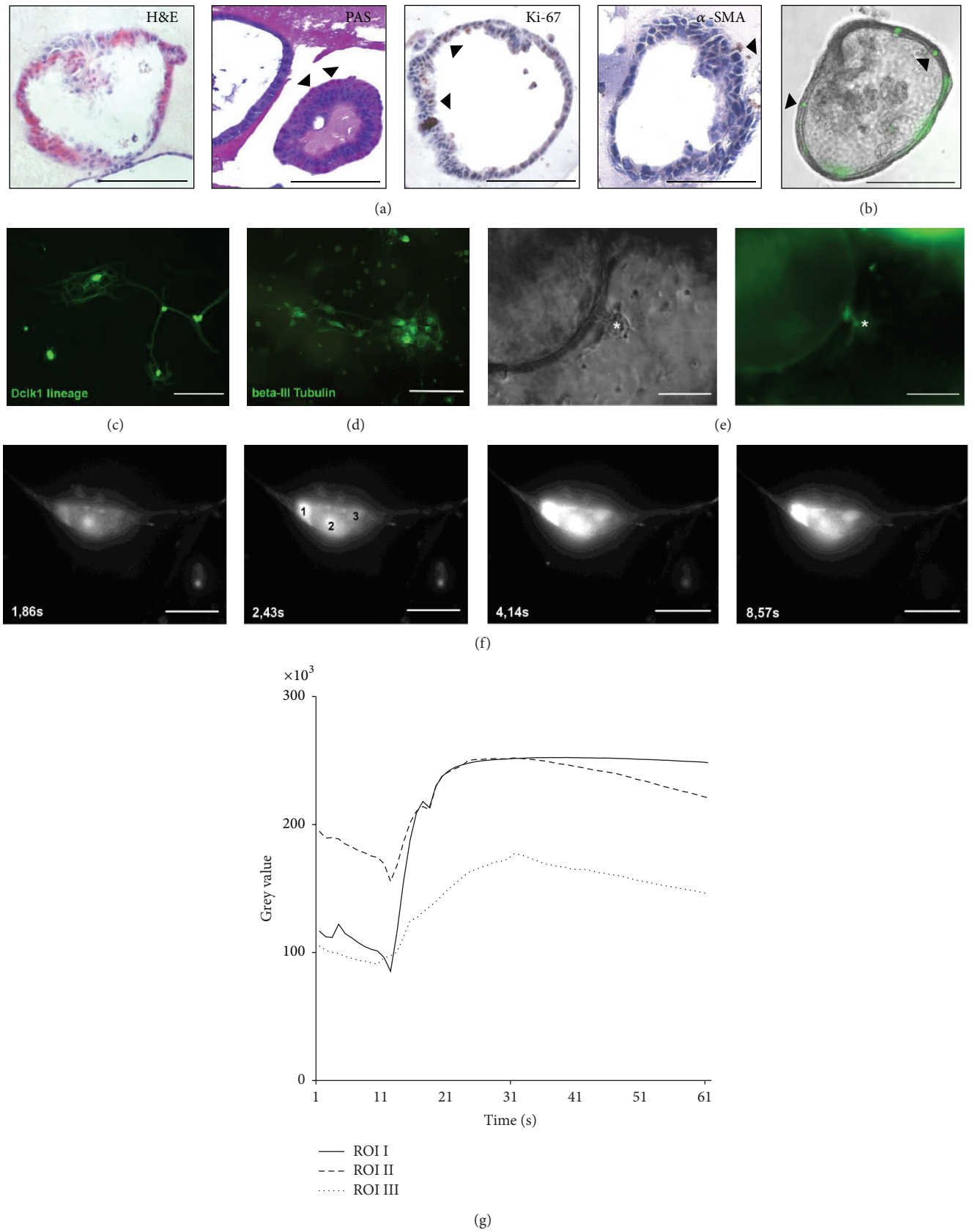

Figure 6: Continued.

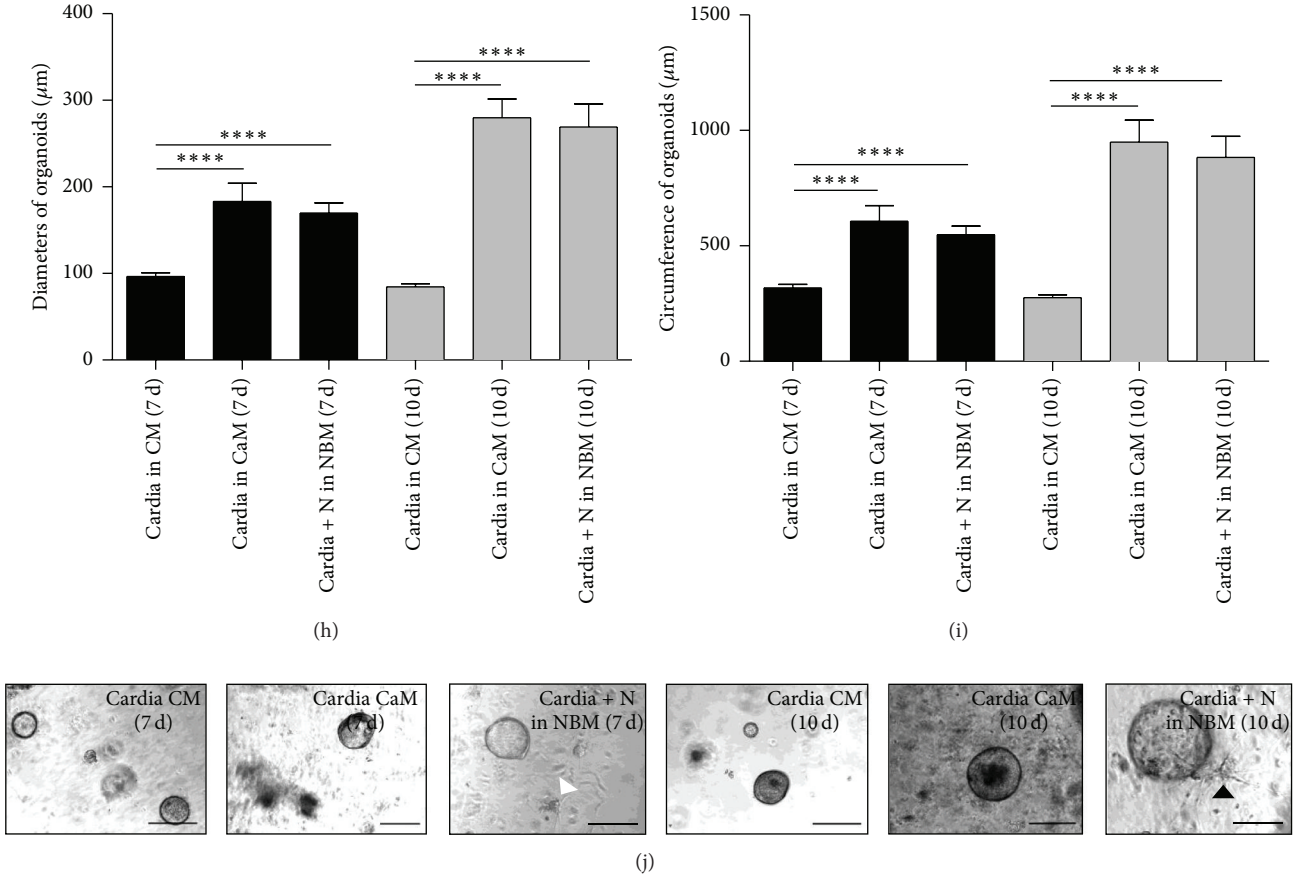

Figure 6: Cardia organoid cultures and cocultures with neurons as a model to investigate the gastrointestinal stem cell niche. (a) IHC for H&E, PAS, Ki-67, and α-SMA for further characterization of the method, arrowheads indicating positive stained cells, scale bars, 100 μm. (b) Light microscopy of Lgr5-GFP-positive organoid, scale bar, 50 μm. (c) Immunofluorescence of Dclk1-labeled neurons in cultured conditions (NBM). (d) Cultured neurons (NBM) stained with beta-III Tubulin, scale bar, 100 μm. (e) Cocultured neuron with cardia organoid, light microscopy and immunofluorescence, *Dclk1-labeled neuron (green fluorescence) neighboring crypt wall, scale bar, 100 μm. (f) Ca-imaging of neuron in cocultured conditions (NBM), different points in time beginning from application of nicotinic acid to Fluo-4-labeled neurons, brightening of neuron indicating Ca-influx. Scale bar, 50 μm. (g) Analysis of the RLI of stimulated neuron, ROI I, ROI II, and ROI III measuring different regions of the neuron as indicated in (f), picture 2 (regions labeled 1, 2, and 3). ((h), (i)) Analysis of organoids and cocultured neurons in different conditions, distribution of mean diameters and circumferences per group and point in time and standard error of the mean (SEM) (CM = crypt medium, CaM = Wnt-conditioned cardia medium, NBM = cocultured neurons in neurobasal complete medium, groups compared at 7 d and 10 d), measured in μm; comparison of average organoid growth between groups applying two-tailed t-test (*level of statistical significance, $^{****}P < 0.0001$), $n = 3$ experiments per group and point in time. (j) Representative light microscopic image of each group and point in time (arrowheads indicating neurons), scale bar, 100 μm.

cocultured with neurons compared with organoids cultured in CaM did not show any significant differences in size at both day 7 and day 10 (Figures 6(h) and 6(i), examples of cultured and cocultured organoids shown in Figure 6(j)). Interestingly, the organoid count over time reached a 1.5–2-fold increase in number of organoids per well already at day 4 of culture in both CaM conditions and cocultures with nerves compared to the control group cultured in CM (data not shown), although organoid count balanced at day 10 of culture for all conditions compared. Additionally, judging from the analysis of the diameters and circumferences, the latter are feasible to calculate from the diameters (Table 2).

4. Conclusions

Here we describe the utilization and modification of distinct 3D culture methods that can be used to analyze the role and function of different stem cell niche components *in vitro*. The basic element of each 3D cell culture is a matrix, which plays a scaffolding role for the cells and tissues, similarly to ECM that is present in organs *in vivo*. Examples of the matrices used in 3D cell biology are the following: Matrigel, collagen, and Hydrogel [31–35]. 3D cell cultures have shown altered gene expression profiling when compared to 2D [36]. Here we describe the modification and establishment of three distinct 3D cell culture methods to study the adult gastrointestinal

Table 2: Measurements of organoid size and circumference at 7 d and 10 d in μm, $n = 3$ experiments.

	Mean ± SEM (Diameter)	Mean ± SEM (Circumference)	n (Measurements)
Cardia in CM (7 d)	96.54 ± 4.316	318.5 ± 14.67	93
Cardia in CaM (7 d)	183.3 ± 20.74	606.8 ± 66.98	79
Cardia + N in NBM (7 d)	169.7 ± 11.76	548.3 ± 37.37	96
Cardia in CM (10 d)	84.40 ± 3.850	275.8 ± 12.44	77
Cardia in CaM (10 d)	279.9 ± 21.67	949.4 ± 94.87	60
Cardia + N in NBM (10 d)	269.1 ± 26.72	883.2 ± 90.80	79

SEM = standard error of the mean.

epithelium in order to evaluate their potential to study niche factors: (1) tissue culture *ex vivo*, (2) organotypic cell culture (OTC), and (3) organoid culture (see Figure 1). We further performed cocultures with adult mouse fibroblasts, collagen, or adult murine neurons, and our data show that cellular components of an *in vitro* niche, represented here by myofibroblasts and neurons, support growth of epithelial organoids that contain stem cells; however the precise mechanisms of interaction may be subject to further investigation.

The tissue culture *ex vivo* is characterized by the highest biological complexity from all of these methods. It preserves stem cells and their native niche and any manipulations in tissue culture *ex vivo* will affect the whole stem cell niche unit. Nevertheless, this culture method does not allow a specific analysis of distinct components of the stem cell niche and therefore we provide here a novel aspect to split those different components such as adult pericryptal fibroblasts, collagen, and adult nerves from the ENS into distinct separate coculture assays. Both OTC and organoid culture fulfill these criteria. The advantage of OTC compared to organoid culture, however, is the feature of an air-liquid interface as recently described as a cellular differentiation factor [37], and handling for the immunohistochemistry purposes, even given the fact that OTC requires a lot of cells. In the adult mouse intestine, the epithelium is surrounded by a layer of subepithelial myofibroblasts [38] and likely the heterogeneity of myofibroblasts correlates with the gradient of crucial niche factors (e.g., Wnt ligands, BMPs) that determine the proliferation and differentiation zones in the crypt-villus unit [39]. Based on their anatomical location, subepithelial myofibroblasts were hypothesized to be a cellular component of the intestinal epithelial niche and to regulate self-renewal and differentiation of ISCs [40]. Cocultures in which cells of human origin were utilized have shown that a certain type of infant fibroblasts can increase the longevity of human organoid/enteroid cultures [33, 34]. Here we demonstrate that adult murine pericryptal fibroblasts do also affect crypt size and survival in an organotypic culture setting with a direct epithelial mesenchymal cell contact, suggesting again that fibroblasts represent niche cells for intestinal stem cell and their differentiation capacities.

As another example, we demonstrate that normal intestinal crypts exhibit reduced budding when cultured in matrix composed of collagen and Matrigel (cellular matrix used for OTC). Since Matrigel already contains collagen, the cellular matrix for OTC is characterized by an increased concentration of collagen that is likely leading to an increased stiffness of the matrix. Our results confirm previous findings that collagen can modify the matrix of the organoid culture [41] and suggest that increased collagen concentration has a major impact on the growth conditions of intestinal organoids as it restricts formation of buds and should therefore be considered as a caveat in future analysis of organoid culture systems.

Accumulating studies have pointed to the importance of nerves in the regulation of the intestinal stem cell niche [12, 17, 42, 43]. A role for nerves in the development of neoplasia has also been postulated [17, 28, 29]. Nerve fibers were shown to support carcinogenesis by either mechanical aspects, being an anatomical structure used as guidance for tumor growth by perineural tumor invasion, or functional aspects, comprising neurotransmitters influencing local vascularization, migratory activity of neighboring cells, or the neoneurogenesis itself [29, 44, 45]. Interestingly, upon surgical or pharmacological denervation of the stomach, it was shown that the denervated part of the stomach had a markedly reduced tumor incidence and progression in different mouse models of gastric cancer [17]. At the same time, this was correlated with a downregulation of Wnt3a in the stem cell niche of the denervated part of the stomach. Here we present a novel method to isolate distinct enteric nerves from the mouse ENS identified by the Dclk1-Cre-Tom/GFP lineage and perform cocultures of nerves with cardia organoids *in vitro* (Figures 5 and 6).

We previously demonstrated that intestinal [12] and gastric [17] organoids can be cocultured with neurons. Here we demonstrate that when culturing cardia organoids, that specifically depend on Wnt signaling in the 3D monoculture system, upon coculture with nerves these are apparently able to replace Wnt signaling. The Wnt pathway represents a fundamental signaling pathway for ISCs and dysregulations of this pathway lead to intestinal cancer [46]. Our analysis of cultures and cocultures of predominantly circular cardia organoids from our Barrett esophagus mouse model demonstrates some interesting details about the interaction of neurons within the intestinal niche. Organoids cultured in Wnt-conditioned medium compared to standard crypt medium already showed a significant difference of organoid growth after seven and ten days (see Table 2, Figures 6(h) and 6(i)), applying both the measurement of diameters and circumferences for growth determination. The coculture with neurons

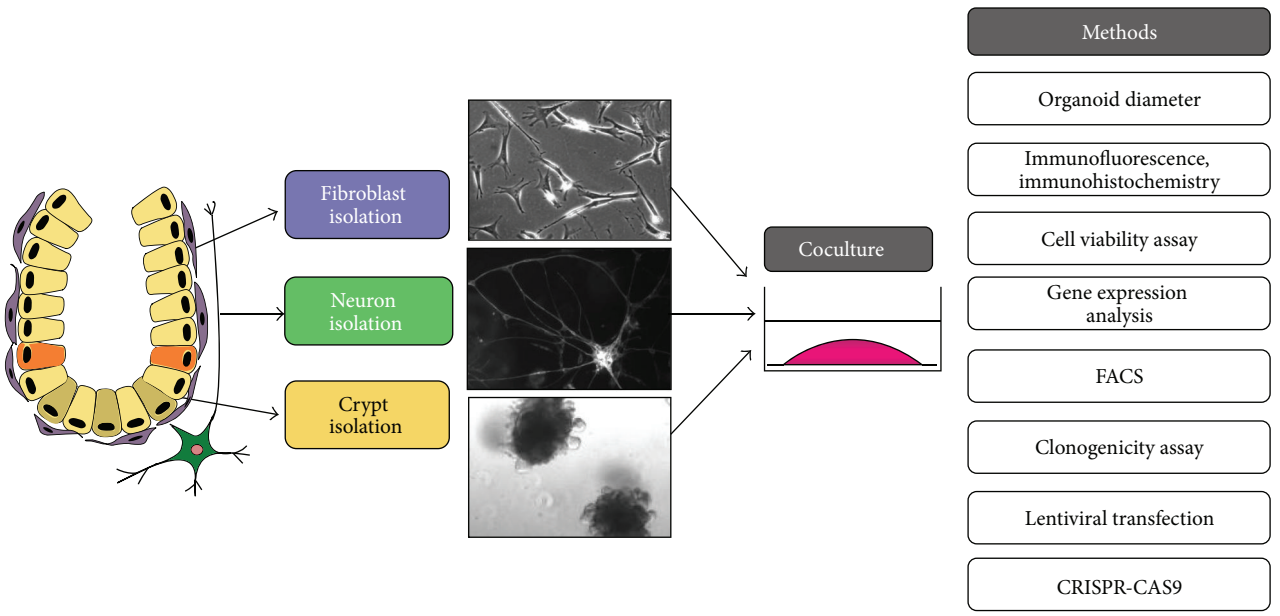

Figure 7: Reconstruction of stem cell niche in the intestine *in vitro* and proposed workflow. Intestinal crypts and stromal cells (neurons and/or myofibroblasts) are isolated and combined together in three-dimensional system such as organoid culture. Role of stromal cells as stem cell niche can be analyzed, for example, by the measurement of organoid diameter, cell viability assay, clonogenicity assay, gene expression analysis, and different types of staining. Identification of stem cell markers and individual cell types can be analyzed by FACS. In addition, genetic manipulations in organoids can be performed by lentiviral transfection and CRISPR-CASP9 system.

also showed a highly significant difference of organoid growth compared to standard crypt medium after seven and ten days without any supplement of Wnt. The same effect is reflected in the 1.5–2-fold increase in organoid count per well in both Wnt-conditioned monoculture and neuronal coculture compared to standard monoculture. Interestingly, there was no significant difference in growth and organoid count between organoids cultured in Wnt-conditioned medium or cocultured with neurons, neither at day 7 nor at day 10. Using calcium imaging we showed that the cocultured neurons were alive and physiologically active during the observation period, which is underlined by these significant differences of organoid growth between control and cocultured group.

Judging from these results, in the absence of Wnt it is most likely the neuronal influence on organoids that promotes organoid growth, which may implicate that neurons and their transmitters replace the effect of Wnt signaling. This argues for a neuronal signaling, which creates a proliferative environment and supports organoid growth stronger than the usually applied growth factors used in standard crypt medium, which was already postulated and shown by Zhao and colleges to possibly exist [17]. In their study, gastric organoid growth was markedly promoted if cocultured with neurons and without neurons but upon stimulation with pilocarpine (an unspecific muscarinic receptor agonist), and Wnt target genes such as *Lgr5*, *Cd44*, and *Sox9* were shown to be elevated [17]. In future studies it remains to be elucidated which factors lead to an increase of organoid growth in the neuronal coculture compared to Wnt-conditioned medium. Neurons are rich sources of neurotrophic factors including nerve growth factor (NGF), GDNF family of ligands (such as GDNF, artemin, and neurturin), or transforming growth factor beta 1 [47]. It is imaginable that these factors may substantially promote the maintenance and growth of organoids or of the stem cell niche in the stomach. In our experiments we applied NGF within the neurobasal medium, so that it remains to be clarified if the effect we describe here is due to this single neurotrophic factor or others. Our observations also imply that enteric neurons may have similar trophic functions in the maintenance of epithelial integrity in the gut, as it is known for enteric glia cells [48]. Thus we strongly support future emphasis on investigating pathways of the interaction between neurons and intestinal stem cells to characterize the composition of the cancer stem cell niche, fostering the development of therapeutics directing the origin of malignancy as putative therapeutic targets.

Currently, a broad spectrum of downstream methods is available in order to analyze the organoids, for example, immunohistochemistry and immunofluorescence [11, 49], the CRISP-Cas9 system [50, 51], organoid transduction with retroviral construct [52], or a clonogenicity assay [53] (see Figure 7). In combination with the culture of intestinal fragments *ex vivo* [15], in which the specific local niche is preserved, we suggest these types of cultures as reliable physiologically relevant 3D models to analyze a mesenchymal-epithelial cross talk in the intestinal stem cell niche and identify underlying mechanism of early tumorigenesis. Although our results so far do not allow any basic conclusions on the specific role of these components in a stem cell niche, the presented coculture methods point to an important function of stromal cell types in the described 3D culture conditions.

Conflict of Interests

The authors declare no conflict of interests.

Authors' Contribution

Agnieszka Pastuła and Moritz Middelhoff equally contributed to this paper.

Acknowledgments

Agnieszka Pastuła received Laura Bassi Award and the Leonhard-Lorenz-Stiftung Award by the Technical University of Munich. Michael Quante was supported by the Max-Eder Program of the Deutsche Krebshilfe.

References

[1] J. Voog and D. L. Jones, "Stem cells and the niche: a dynamic duo," *Cell Stem Cell*, vol. 6, no. 2, pp. 103–115, 2010.

[2] M. R. Walker, K. K. Patel, and T. S. Stappenbeck, "The stem cell niche," *Journal of Pathology*, vol. 217, no. 2, pp. 169–180, 2009.

[3] E. Fuchs, T. Tumbar, and G. Guasch, "Socializing with the neighbors: stem cells and their niche," *Cell*, vol. 116, no. 6, pp. 769–778, 2004.

[4] J. Zhang, C. Niu, L. Ye et al., "Identification of the haematopoietic stem cell niche and control of the niche size," *Nature*, vol. 425, no. 6960, pp. 836–841, 2003.

[5] M. Brittan and N. A. Wright, "Gastrointestinal stem cells," *The Journal of Pathology*, vol. 197, no. 4, pp. 492–509, 2002.

[6] N. Barker, J. H. van Es, J. Kuipers et al., "Identification of stem cells in small intestine and colon by marker gene Lgr5," *Nature*, vol. 449, no. 7165, pp. 1003–1007, 2007.

[7] D. Hanahan and R. A. Weinberg, "Hallmarks of cancer: the next generation," *Cell*, vol. 144, no. 5, pp. 646–674, 2011.

[8] M. Quante, J. Varga, T. C. Wang, and F. R. Greten, "The gastrointestinal tumor microenvironment," *Gastroenterology*, vol. 145, no. 1, pp. 63–78, 2013.

[9] T. Sato, J. H. van Es, H. J. Snippert et al., "Paneth cells constitute the niche for Lgr5 stem cells in intestinal crypts," *Nature*, vol. 469, no. 7330, pp. 415–418, 2011.

[10] A. Durand, B. Donahue, G. Peignon et al., "Functional intestinal stem cells after Paneth cell ablation induced by the loss of transcription factor Math1 (Atoh1)," *Proceedings of the National Academy of Sciences of the United States of America*, vol. 109, no. 23, pp. 8965–8970, 2012.

[11] T. Sato, R. G. Vries, H. J. Snippert et al., "Single Lgr5 stem cells build crypt-villus structures in vitro without a mesenchymal niche," *Nature*, vol. 459, no. 7244, pp. 262–265, 2009.

[12] C. B. Westphalen, S. Asfaha, Y. Hayakawa et al., "Long-lived intestinal tuft cells serve as colon cancer-initiating cells," *The Journal of Clinical Investigation*, vol. 124, no. 3, pp. 1283–1295, 2014.

[13] M. Quante, G. Bhagat, J. A. Abrams et al., "Bile acid and inflammation activate gastric cardia stem cells in a mouse model of barrett-like metaplasia," *Cancer Cell*, vol. 21, no. 1, pp. 36–51, 2012.

[14] J. Kalabis, G. S. Wong, M. E. Vega et al., "Isolation and characterization of mouse and human esophageal epithelial cells in 3D organotypic culture," *Nature Protocols*, vol. 7, no. 2, pp. 235–246, 2012.

[15] A. Ootani, X. Li, E. Sangiorgi et al., "Sustained in vitro intestinal epithelial culture within a Wnt-dependent stem cell niche," *Nature Medicine*, vol. 15, no. 6, pp. 701–706, 2009.

[16] A. Pastula and M. Quante, "Isolation and 3-dimensional culture of primary murine intestinal epithelial cells," *Bio-Protocol*, vol. 4, no. 10, 2014.

[17] C. M. Zhao, Y. Hayakawa, Y. Kodama et al., "Denervation suppresses gastric tumorigenesis," *Science Translational Medicine*, vol. 6, no. 250, Article ID 250ra115, 2014.

[18] I. E. Demir, E. Tieftrunk, K. H. Schäfer, H. Friess, and G. O. Ceyhan, "Simulating pancreatic neuroplasticity: *in vitro* dual-neuron plasticity assay," *The Journal of Visualized Experiments*, no. 86, 2014.

[19] K.-H. Schäfer, M. J. Saffrey, G. Burnstock, and P. Mestres-Ventura, "A new method for the isolation of myenteric plexus from the newborn rat gastrointestinal tract," *Brain Research Protocols*, vol. 1, no. 2, pp. 109–113, 1997.

[20] P. V. Berghe, R. Bisschops, and J. Tack, "Imaging of neuronal activity in the gut," *Current Opinion in Pharmacology*, vol. 1, no. 6, pp. 563–567, 2001.

[21] K. Michel, M. Michaelis, G. Mazzuoli, K. Mueller, P. Vanden Berghe, and M. Schemann, "Fast calcium and voltage-sensitive dye imaging in enteric neurones reveal calcium peaks associated with single action potential discharge," *The Journal of Physiology*, vol. 589, no. 24, pp. 5941–5947, 2011.

[22] G. Mazzuoli and M. Schemann, "Multifunctional rapidly adapting mechanosensitive enteric neurons (RAMEN) in the myenteric plexus of the guinea pig ileum," *Journal of Physiology*, vol. 587, no. 19, pp. 4681–4694, 2009.

[23] F. Di Virgilio, T. H. Steinberg, and S. C. Silverstein, "Inhibition of Fura-2 sequestration and secretion with organic anion transport blockers," *Cell Calcium*, vol. 11, no. 2-3, pp. 57–62, 1990.

[24] E. M. Kugler, G. Mazzuoli, I. E. Demir, G. O. Ceyhan, F. Zeller, and M. Schemann, "Activity of protease-activated receptors in primary cultured human myenteric neurons," *Frontiers in Neuroscience*, vol. 6, article 133, 2012.

[25] M. Stelzner, M. Helmrath, J. C. Dunn et al., "A nomenclature for intestinal in vitro cultures," *American Journal of Physiology: Gastrointestinal and Liver Physiology*, vol. 302, no. 12, pp. G1359–G1363, 2012.

[26] L. Kass, J. T. Erler, M. Dembo, and V. M. Weaver, "Mammary epithelial cell: influence of extracellular matrix composition and organization during development and tumorigenesis," *International Journal of Biochemistry and Cell Biology*, vol. 39, no. 11, pp. 1987–1994, 2007.

[27] A. Pastuła and M. Quante, "Isolation and 3-dimensional culture of primary murine intestinal epithelial cells," *Bio-Protocol*, vol. 4, no. 10, Article ID e1125, 2014, http://www.bio-protocol.org/e1125.

[28] G. E. Ayala, H. Dai, M. Powell et al., "Cancer-related axonogenesis and neurogenesis in prostate cancer," *Clinical Cancer Research*, vol. 14, no. 23, pp. 7593–7603, 2008.

[29] I. E. Demir, H. Friess, and G. O. Ceyhan, "Nerve-cancer interactions in the stromal biology of pancreatic cancer," *Frontiers in Physiology*, vol. 3, article 97, 2012.

[30] M. D. Gershon, "Nerves, reflexes, and the enteric nervous system: pathogenesis of the irritable bowel syndrome," *Journal of Clinical Gastroenterology*, vol. 39, no. 5, pp. S184–S193, 2005.

[31] J. Lee, M. J. Cuddihy, and N. A. Kotov, "Three-dimensional cell culture matrices: state of the art," *Tissue Engineering, Part B: Reviews*, vol. 14, no. 1, pp. 61–86, 2008.

[32] M. W. Tibbitt and K. S. Anseth, "Hydrogels as extracellular matrix mimics for 3D cell culture," *Biotechnology and Bioengineering*, vol. 103, no. 4, pp. 655–663, 2009.

[33] N. Lahar, N. Y. Lei, J. Wang et al., "Intestinal subepithelial myofibroblasts support the growth of intestinal epithelial stem cells," *PLoS ONE*, vol. 9, no. 1, Article ID e84651, 2014.

[34] N. Lahar, N. Y. Lei, J. Wang et al., "Intestinal subepithelial myofibroblasts support *in vitro* and *in vivo* growth of human small intestinal epithelium," *PLoS ONE*, vol. 6, no. 11, Article ID e26898, 2011.

[35] Z. Jabaji, C. M. Sears, G. J. Brinkley et al., "Use of collagen gel as an alternative extracellular matrix for the in vitro and in vivo growth of murine small intestinal epithelium," *Tissue Engineering Part C: Methods*, vol. 19, no. 12, pp. 961–969, 2013.

[36] M. J. Bissell, D. C. Radisky, A. Rizki, V. M. Weaver, and O. W. Petersen, "The organizing principle: microenvironmental influences in the normal and malignant breast," *Differentiation*, vol. 70, no. 9-10, pp. 537–546, 2002.

[37] X. Wang, Y. Yamamoto, L. H. Wilson et al., "Cloning and variation of ground state intestinal stem cells," *Nature*, vol. 522, no. 7555, pp. 173–178, 2015.

[38] D. L. Worthley, Y. Si, M. Quante, M. Churchill, S. Mukherjee, and T. C. Wang, "Bone marrow cells as precursors of the tumor stroma," *Experimental Cell Research*, vol. 319, no. 11, pp. 1650–1656, 2013.

[39] D. W. Powell, I. V. Pinchuk, J. I. Saada, X. Chen, and R. C. Mifflin, "Mesenchymal cells of the intestinal lamina propria," *Annual Review of Physiology*, vol. 73, pp. 213–237, 2011.

[40] D. L. Worthley, M. Churchill, J. T. Compton et al., "Gremlin 1 identifies a skeletal stem cell with bone, cartilage, and reticular stromal potential," *Cell*, vol. 160, no. 1-2, pp. 269–284, 2015.

[41] Z. Jabaji, G. J. Brinkley, H. A. Khalil et al., "Type I collagen as an extracellular matrix for the in vitro growth of human small intestinal epithelium," *PLoS ONE*, vol. 9, no. 9, Article ID e107814, 2014.

[42] Y. Katayama, M. Battista, W.-M. Kao et al., "Signals from the sympathetic nervous system regulate hematopoietic stem cell egress from bone marrow," *Cell*, vol. 124, no. 2, pp. 407–421, 2006.

[43] J. Larsson and D. Scadden, "Nervous activity in a stem cell niche," *Cell*, vol. 124, no. 2, pp. 253–255, 2006.

[44] M. Mancino, E. Ametller, P. Gascón, and V. Almendro, "The neuronal influence on tumor progression," *Biochimica et Biophysica Acta: Reviews on Cancer*, vol. 1816, no. 2, pp. 105–118, 2011.

[45] H. Dai, R. Li, T. Wheeler et al., "Enhanced survival in perineural invasion of pancreatic cancer: an in vitro approach," *Human Pathology*, vol. 38, no. 2, pp. 299–307, 2007.

[46] T. Reya and H. Clevers, "Wnt signalling in stem cells and cancer," *Nature*, vol. 434, no. 7035, pp. 843–850, 2005.

[47] I. E. Demir, K.-H. Schäfer, E. Tieftrunk, H. Friess, and G. O. Ceyhan, "Neural plasticity in the gastrointestinal tract: chronic inflammation, neurotrophic signals, and hypersensitivity," *Acta Neuropathologica*, vol. 125, no. 4, pp. 491–509, 2013.

[48] M. Neunlist, M. Rolli-Derkinderen, R. Latorre et al., "Enteric glial cells: recent developments and future directions," *Gastroenterology*, vol. 147, no. 6, pp. 1230–1237, 2014.

[49] A. Calon, E. Lonardo, A. Berenguer-Llergo et al., "Stromal gene expression defines poor-prognosis subtypes in colorectal cancer," *Nature Genetics*, vol. 47, pp. 320–329, 2015.

[50] M. Matano, S. Date, M. Shimokawa et al., "Modeling colorectal cancer using CRISPR-Cas9–mediated engineering of human intestinal organoids," *Nature Medicine*, 2015.

[51] J. Drost, R. H. van Jaarsveld, B. Ponsioen et al., "Sequential cancer mutations in cultured human intestinal stem cells," *Nature*, vol. 521, no. 7550, pp. 43–47, 2015.

[52] B.-K. Koo, D. E. Stange, T. Sato et al., "Controlled gene expression in primary Lgr5 organoid cultures," *Nature Methods*, vol. 9, no. 1, pp. 81–83, 2012.

[53] A. L. Farrall, P. Riemer, M. Leushacke et al., "Wnt and BMP signals control intestinal adenoma cell fates," *International Journal of Cancer*, vol. 131, no. 10, pp. 2242–2252, 2012.

Hindawi Publishing Corporation
Stem Cells International
Volume 2016, Article ID 9695827, 13 pages
http://dx.doi.org/10.1155/2016/9695827

Research Article

Comparative Microarray Analysis of Proliferating and Differentiating Murine ENS Progenitor Cells

Peter Helmut Neckel, Roland Mohr, Ying Zhang, Bernhard Hirt, and Lothar Just

Institute of Clinical Anatomy and Cell Analysis, University of Tübingen, Österbergstrasse 3, 72074 Tübingen, Germany

Correspondence should be addressed to Lothar Just; ljust@anatom.uni-tuebingen.de

Received 15 May 2015; Accepted 12 July 2015

Academic Editor: Kodandaramireddy Nalapareddy

Postnatal neural progenitor cells of the enteric nervous system are a potential source for future cell replacement therapies of developmental dysplasia like Hirschsprung's disease. However, little is known about the molecular mechanisms driving the homeostasis and differentiation of this cell pool. In this work, we conducted Affymetrix GeneChip experiments to identify differences in gene regulation between proliferation and early differentiation of enteric neural progenitors from neonatal mice. We detected a total of 1333 regulated genes that were linked to different groups of cellular mechanisms involved in cell cycle, apoptosis, neural proliferation, and differentiation. As expected, we found an augmented inhibition in the gene expression of cell cycle progression as well as an enhanced mRNA expression of neuronal and glial differentiation markers. We further found a marked inactivation of the canonical Wnt pathway after the induction of cellular differentiation. Taken together, these data demonstrate the various molecular mechanisms taking place during the proliferation and early differentiation of enteric neural progenitor cells.

1. Introduction

The enteric nervous system (ENS) is a largely autonomous and highly complex neuronal network found in the gastrointestinal tract. Its two major plexuses are integrated into the layered anatomy of the gut wall and, together with central modulating influences, exert control over gastrointestinal motility, secretion, ion-homeostasis, and immunological mechanisms [1]. In order to achieve this variety of functions, the ENS is composed of a multitude of different neuronal and glial cell types and closely interacts with smooth muscle cells and myogenic pacemaker cells called interstitial cells of Cajal. Furthermore, a population of neural stem or progenitor cells in the ENS has been identified in rodents [2, 3] and humans that retain their proliferative capacity throughout adult life even into old age [4, 5]. It is therefore not surprising that the correct functioning of the ENS as well as the regulation on enteric neural progenitor cells is subjected to the influence of a myriad of transmitters, neurotrophic and growth factors, signalling molecules, and extracellular matrix components, which are not exclusively expressed by neural cell types [6]. Likewise, the control of the development of the ENS is equally complex and mutations in its genetic program can lead to fatal dysplasia like Hirschsprung's disease (HCSR) [7, 8].

HSCR is hallmarked by an aganglionic distal bowel leading to life-threatening disturbances in intestinal motility. Today's therapeutic gold standard, the surgical resection of the affected gut segments, is nevertheless associated with problematic long-term outcomes with regard to continence [9]. In order to improve the therapeutic success, the use of autologous enteric neural stem cells was proposed [10]. This concept relies on the *in vitro* expansion of enteric neural stem cells derived from small biopsy materials. However, we are just beginning to understand the molecular mechanisms that underlie neural stem cell biology and how this knowledge can be used for optimizing *in vitro* culture conditions [11, 12].

Genome-wide gene-expression analyses are a useful tool to examine the genetic programs and cellular interactions and have been widely used to identify potential markers or signalling mechanisms especially in CNS neurospheres or cancer tissues. Further, gene-expression assays have also helped to unravel genetic prepositions associated with HSCR

[13, 14], though little effort has so far been put into characterizing the genetic profile of enteric neural stem cells *in vitro* [15].

Here, we used an Affymetrix microarray analysis to evaluate the genetic expression profile of proliferating murine enteric neural stem cells and its changes during the early differentiation *in vitro*.

2. Materials and Methods

2.1. Cell Culturing. Cell culturing was conducted as described previously [15]. The handling of animals was in accordance to the institutional guidelines of the University of Tuebingen, which conform to the international guidelines.

Neonatal (P0) C57BL/6 mice without regard to sex were decapitated and the whole gut was removed. After removal of adherent mesentery the longitudinal and circular muscle layers containing myenteric plexus could be stripped as a whole from the small intestine. Tissue was chopped and incubated in collagenase type XI (750 U/mL; Sigma-Aldrich, Taufkirchen, Germany) and dispase II (250 μg/mL; Roche Diagnostics, Mannheim, Germany) dissolved in Hanks' balanced salt solution with Ca^{2+}/Mg^{2+} (HBSS; PAA, Pasching, Austria) for 30 min at 37°C. During enzymatic dissociation the tissue was carefully triturated every 10 min with a fire polished 1 mL pipette tip. Prior to the first trituration step, cell suspension was treated with 0.05% (w/v) DNAse I (Sigma-Aldrich). After 30 min, tissue dissociation was stopped by adding fetal calf serum (FCS; PAA) to a final concentration of 10% (v/v) to the medium. Undigested larger tissue pieces were removed with a 40 μm cell strainer (BD Biosciences, Franklin Lakes, NJ, USA). Residual enzymes were removed during two washing steps in HBSS at 200 g. After dissociation, cells were resuspended in proliferation culture medium (Dulbecco's modified Eagle's medium with Ham's F12 medium (DMEM/F12; 1 : 1; PAA)) containing N2 supplement (1 : 100; Invitrogen, Darmstadt, Germany), penicillin (100 U/mL; PAA), streptomycin (100 μg/mL; PAA), L-glutamine (2 mM; PAA), epidermal growth factor (EGF; 20 ng/mL; Sigma-Aldrich), and fibroblast growth factor (FGF; 20 ng/mL; Sigma-Aldrich). Cells were seeded into 6-well plates (BD Biosciences) in a concentration of 2.5×10^4 cells/cm^2. Only once before seeding, the medium was supplemented with B27 (1 : 50; Invitrogen). EGF and FGF were added daily and culture medium was exchanged every 3 days. All cultivation steps were conducted in a humidified incubator at 37°C and 5% CO_2. An overview of the following cell culture protocol is shown in Figure 1. During proliferation phase of the culture, cells formed spheroid-like bodies termed enterospheres. After 5 days of proliferation, free-floating enterospheres were picked and transferred to petri dishes (Ø 60 mm; Greiner Bio One, Frickenhausen, Germany) in 5 mL fresh proliferation medium and proliferation was continued for further 4 days.

Single free-floating enterospheres (50 enterospheres/dish) were picked again, washed 3 times in Tris buffer, and transferred into new petri dishes containing either proliferation medium or differentiation medium. Differentiation medium consists of DMEM/F12 containing N2 supplement (1 : 100), penicillin (100 U/mL), streptomycin (100 μg/mL), L-glutamine (2 mM), and ascorbic acid-2-phosphate (200 μM; Sigma-Aldrich).

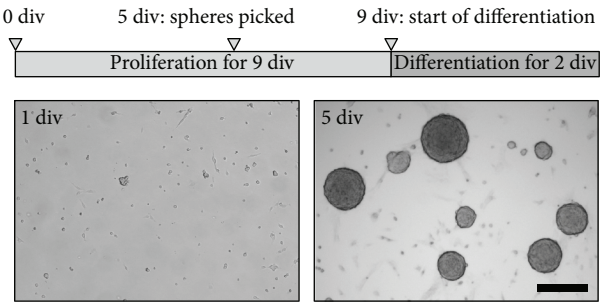

Figure 1: Time schedule of enterosphere culture. The timeline illustrates the schedule of *in vitro* culture. Cells were isolated at 0 div (days *in vitro*) and proliferated for 5 days. Spheres were then picked and again proliferated for 4 days. At 9 div, enterospheres were picked, washed, transferred to differentiation medium, and incubated for 2 days before gene expression analyses were carried out. The micrographs show proliferating enterospheres after 1 and 5 div. Scale bar: 200 μm.

Enterospheres were proliferated or differentiated for 2 more days, thereby forming the two experimental groups "proliferation" and "differentiation." The difference in expression between those two groups (differentiation versus proliferation) was successively compared by microarray analysis as described below.

2.2. Affymetrix Microarray Analysis. Affymetrix microarray analysis was conducted similar to previously published data in three independent experiments, each with cell cultures prepared from 2 pups from the same litter [15]. In each experiment, free-floating enterospheres were picked as described above in order to diminish the fraction of adhesive fibroblasts and smooth muscle cells.

Total RNA of enterospheres of both groups was extracted using the RNeasy Micro Kit (Qiagen). RNA quality was evaluated on Agilent 2100 Bioanalyzer with RNA integrity numbers (RIN) of the samples in this study being in the range from 8 to 10. RIN numbers higher than 8 are considered optimal for downstream application [16].

Double-stranded cDNA was synthesized from 100 ng of total RNA, subsequently linearly amplified, and biotinylated using the GeneChip WT cDNA Synthesis and Amplification Kit (Affymetrix, Santa Clara, CA, USA) according to the manufacturer's instructions. 15 μg of labeled and fragmented cDNA was hybridized to GeneChip Mouse Gene 1.0 ST arrays (Affymetrix). After hybridization, the arrays were stained and washed in a Fluidics Station 450 (Affymetrix) with the recommended washing procedure. Biotinylated cDNA bound to target molecules was detected with streptavidin-coupled phycoerythrin, biotinylated anti-streptavidin IgG antibodies and again streptavidin-coupled phycoerythrin according to the protocol. Arrays were scanned using the GCS3000 GeneChip Scanner (Affymetrix) and AGCC 3.0 software. Scanned images were subjected to visual inspection

to check for hybridization artifacts and proper grid alignment and analyzed with Expression Console 1.0 (Affymetrix) to generate report files for quality control.

Normalization of raw data was performed by the Partek Software 6.6, applying an RMA (Robust Multichip Average) algorithm. Significance was calculated using a t-test without multiple testing correction (Partek), selecting all transcripts with a minimum change in expression level of 1.5-fold together with a p value less than 0.05.

3. Results

In this study, we investigated the changes of the genetic expression profile that occur during the transition from proliferating to differentiating enteric neural progenitor cells *in vitro*. Therefore, we generated enterospheres by 9 day *in vitro* cultures, which then could be picked and either proliferated or differentiated for two more days (Figure 1). mRNA was subsequently extracted and gene expression of these two groups was analysed by Affymetrix microarray analysis.

Analysis of mRNA expression was performed on a GeneChip Mouse Gene 1.0 ST array that determines the expression profile of 28.853 genes. Each gene was interrogated by a median of 27 probes that are spread along the full gene.

In total, the gene chip detected 1454 transcripts to be at least 1.5-fold differentially expressed between proliferating and differentiating enterospheres. 1333 of these transcripts code for already identified proteins. 541 genes were found to be upregulated and 792 genes were found to be downregulated in comparison to proliferating enterospheres (see Supplementary Table 1 of the Supplementary Material available online at http://dx.doi.org/10.1155/2016/9695827).

We used the ingenuity pathway analysis software (IPA) and data mining with the science literature search engine http://www.ncbi.nlm.nih.gov/pubmed/ to divide the genes into different groups according to their function during cellular development. The largest functional group contained 171 genes related to cell cycle and apoptosis (Table 1, Supplementary Table 2). Here, we identified especially different cyclin proteins and cell division cycle proteins that were mainly downregulated. Further, we found several genes that are linked to neural development as well as genes regulating neural stem cell proliferation and differentiation. Furthermore, we also detected neuronal and glial differentiation markers and numerous genes involved in synapse formation (Table 2). It is noteworthy that we also identified a group of genes that are known to be involved in the differentiation of smooth muscle cells (Table 3) as well as in extracellular matrix components (Table 4). Additionally, we found regulated genes related to canonical Wnt signalling indicating a deactivation of this pathway during ENS progenitor cell differentiation (Figure 2, Table 5).

4. Discussion

The proliferation and differentiation of enteric neural progenitor cells during embryonic and postnatal development are controlled by a complex interplay of various intrinsic

Table 1: Selected genes related to cell cycle.

Gene	Encoded protein	Fold change	Cell cycle
AURKA	Aurora kinase A	−2.712	**STOP**
AURKB	Aurora kinase B	−4.146	**STOP**
CCNA2	Cyclin A2	−4.652	**STOP**
CCNB1	Cyclin B1	−5.752 −5.820 −5.857	**STOP**
CCNB2	Cyclin B2	−3.392	**STOP**
CCND1	Cyclin D1	−2.476	**STOP**
CCND3	Cyclin D3	−1.539	**STOP**
CCNE1	Cyclin E1	−1.777	**STOP**
CCNE2	Cyclin E2	−2.847	**STOP**
CCNF	Cyclin F	−3.211	**STOP**
CDC6	Cell division cycle 6	−1.936	**STOP**
CDC20	Cell division cycle 20	−3.113	**STOP**
CDC25B	Cell division cycle 25B	−1.636	**STOP**
CDC25C	Cell division cycle 25C	−2.414	**STOP**
CDC45	Cell division cycle 45	−1.769	**STOP**
CDCA2	Cell division cycle associated 2	−3.461	**STOP**
CDCA3	Cell division cycle associated 3	−3.003	**STOP**
CDCA5	Cell division cycle associated 5	−3.053	**STOP**
CDCA7L	Cell division cycle associated 7-like	−4.123	**STOP**
CDCA8	Cell division cycle associated 8	−3.467	**STOP**
CDK1	Cyclin-dependent kinase 1	−3.227	**STOP**
CDK15	Cyclin-dependent kinase 15	1.618	*GO*
CDK19	Cyclin-dependent kinase 19	1.619	*GO*
CDK5R1	Cyclin-dependent kinase 5, regulatory subunit 1 (p35)	1.597	—
CENPA	Centromere protein A	−1.895	**STOP**
CENPE	Centromere protein E, 312 kDa	−4.140	**STOP**
CENPF	Centromere protein F, 350/400 kDa	−3.927	**STOP**
CENPI	Centromere protein I	−2.899	**STOP**
CENPK	Centromere protein K	−2.813	**STOP**
CENPL	Centromere protein L	−1.864	**STOP**
CENPM	Centromere protein M	−3.407	**STOP**
CENPN	Centromere protein N	−2.465	**STOP**
CENPU	Centromere protein U	−1.624	**STOP**
SKA1	Spindle and kinetochore associated complex subunit 1	−1.532	**STOP**
SKA2	Spindle and kinetochore associated complex subunit 2	−1.582	**STOP**
SKA3	Spindle and kinetochore associated complex subunit 3	−3.490	**STOP**
SKP2	S-phase kinase-associated protein 2, E3 ubiquitin protein ligase	−1.845	**STOP**
SPC25	SPC25, NDC80 kinetochore complex component	−4.148	**STOP**

Table 2: Neural differentiation/development.

Gene	Encoded protein	Fold change
	Neural stem cells	
ABCG2	ATP-binding cassette, subfamily G (WHITE), member 2 (junior blood group)	−1.526
ASPM	asp (abnormal spindle) homolog, microcephaly associated (*Drosophila*)	−4.911
CDT1	Chromatin licensing and DNA replication factor 1	−1.528
EGFL7	EGF-like-domain, multiple 7	3.132
EPHA2	EPH receptor A2	−1.529
ETV4	ets variant 4	−1.934
ETV5	ets variant 5	−2.844
		−2.651
FABP7	Fatty acid binding protein 7, brain	−2.095
	Neural differentiation	
ATOH8	Atonal homolog 8 (*Drosophila*)	1.932
AXL	AXL receptor tyrosine kinase	2.015
CRIM1	Cysteine-rich transmembrane BMP regulator 1 (chordin-like)	1.999
CRLF1	Cytokine receptor-like factor 1	2.382
DAB1	Dab, reelin signal transducer, homolog 1 (*Drosophila*)	−2.297
ELK3	ELK3, ETS-domain protein (SRF accessory protein 2)	−1.613
ESCO2	Establishment of sister chromatid cohesion N-acetyltransferase 2	−4.767
GAP43	Growth associated protein 43	1.613
GLDN	Gliomedin	5.809
HMOX1	Heme oxygenase (decycling) 1	1.884
KLF9	Kruppel-like factor 9	1.592
Lmo3	LIM domain only 3	1.542
MAP6	Microtubule-associated protein 6	1.874
MYRF	Myelin regulatory factor	2.527
NEUROD4	Neuronal differentiation 4	2.036
OLIG1	Oligodendrocyte transcription factor 1	2.660
Pvr	Poliovirus receptor	1.768
RGS4	Regulator of G-protein signaling 4	1.955
S1PR1	Sphingosine-1-phosphate receptor 1	5.073
SOCS2	Suppressor of cytokine signaling 2	2.052
		2.335
WIPF1	WAS/WASL interacting protein family, member 1	1.587
	Neural differentiation markers	
CALB2	Calbindin 2	1.616
CNP	2′,3′-Cyclic nucleotide 3′-phosphodiesterase	1.732
GFAP	Glial fibrillary acidic protein	2.239
MBP	Myelin basic protein	1.768
Mturn	Maturin, neural progenitor differentiation regulator homolog (*Xenopus*)	1.853
OMG	Oligodendrocyte myelin glycoprotein	−1.822
OPALIN	Oligodendrocytic myelin paranodal and inner loop protein	39.246
PLP1	Proteolipid protein 1	1.630
S100B	S100 calcium binding protein B	−1.675
TUBB2A	Tubulin, beta 2A class IIa	1.608
TUBB2B	Tubulin, beta 2B class IIb	1.535
TUBB3	Tubulin, beta 3 class III	1.976

Table 2: Continued.

Gene	Encoded protein	Fold change
	Synapse and neurotransmitters	
ABAT	4-Aminobutyrate aminotransferase	−1.512
ADRA1D	Adrenoceptor alpha 1D	1.803
ADRA2A	Adrenoceptor alpha 2A	2.900
ADRA2B	Adrenoceptor alpha 2B	−2.093
CHRM2	Cholinergic receptor, muscarinic 2	1.635
CHRM3	Cholinergic receptor, muscarinic 3	−1.715
CHRNA7	Cholinergic receptor, nicotinic, alpha 7 (neuronal)	1.772
COMT	Catechol-O-methyltransferase	1.515
DDC	DOPA decarboxylase (aromatic L-amino acid decarboxylase)	1.711
DNM3	Dynamin 3	2.643
EPHA5	EPH receptor A5	2.076
GRIA3	Glutamate receptor, ionotropic, AMPA 3	−1.528
GRIA4	Glutamate receptor, ionotropic, AMPA 4	−1.997
GRIK2	Glutamate receptor, ionotropic, kainate 2	−1.565
GRM5	Glutamate receptor, metabotropic 5	−1.600
HTR1B	5-Hydroxytryptamine (serotonin) receptor 1B, G-protein-coupled	−2.377
HTR2B	5-Hydroxytryptamine (serotonin) receptor 2B, G-protein-coupled	2.205
LRRTM2	Leucine-rich repeat transmembrane neuronal 2	3.665
LRRTM3	Leucine-rich repeat transmembrane neuronal 3	2.210
NTM	Neurotrimin	1.820
PENK	Proenkephalin	3.478
PRR7	Proline rich 7 (synaptic)	1.788
SLC10A4	Solute carrier family 10, member 4	1.824
		1.867
SLITRK2	SLIT and NTRK-like family, member 2	−2.414
SLITRK6	SLIT and NTRK-like family, member 6	1.672
STON2	Stonin 2	4.054
STXBP3	Syntaxin-binding protein 3	1.730
Stxbp3b	Syntaxin-binding protein 3B	1.637
SV2C	Synaptic vesicle glycoprotein 2C	1.929
SYT6	Synaptotagmin VI	2.571
	Neurite outgrowth	
ATF3	Activating transcription factor 3	2.579
DOK4	Docking protein 4	4.937
FEZ2	Fasciculation and elongation protein zeta 2 (zygin II)	1.547
NAV2	Neuron navigator 2	1.647
NRCAM	Neuronal cell adhesion molecule	2.496
PLXNB3	Plexin B3	1.739
RGMA	Repulsive guidance molecule family member a	1.552
RNF165	Ring finger protein 165	−1.548
ROBO2	Roundabout, axon guidance receptor, homolog 2 (*Drosophila*)	−2.211
SEMA3B	Sema domain, immunoglobulin domain (Ig), short basic domain, secreted (semaphorin) 3B	3.692
SEMA3E	Sema domain, immunoglobulin domain (Ig), short basic domain, secreted (semaphorin) 3E	2.877
SEMA4F	Sema domain, immunoglobulin domain (Ig), transmembrane domain (TM) and short cytoplasmic domain, (semaphorin) 4F	4.891
SEMA6A	Sema domain, transmembrane domain (TM), and cytoplasmic domain (semaphorin) 6A	−1.707
SRGAP1	SLIT-ROBO Rho GTPase activating protein 1	1.524
UNC5B	unc-5 homolog B (*C. elegans*)	−1.927

Table 2: Continued.

Gene	Encoded protein	Fold change
	Growth factors	
ARTN	Artemin	2.423
FGF2	Fibroblast growth factor 2 (basic)	2.264
FGF5	Fibroblast growth factor 5	7.704
GDF10	Growth differentiation factor 10	−2.361
GDF11	Growth differentiation factor 11	1.604
GDNF	Glial cell derived neurotrophic factor	4.325
GFRA3	GDNF family receptor alpha 3	1.707
MET	MET protooncogene, receptor tyrosine kinase	6.680
NGFR	Nerve growth factor receptor	1.728
NTRK3	Neurotrophic tyrosine kinase, receptor, type 3	−1.575
SNX16	Sorting nexin 16	1.641
SPHK1	Sphingosine kinase 1	1.704
SPRY1	Sprouty homolog 1, antagonist of FGF signaling (*Drosophila*)	−1.647

and extrinsic factors. Their exact timing is crucial for proper migration and proliferation of neural crest cells and for their differentiation into the various neural cell types that compose the complex neural structures of the ENS. Although research in recent years extended our understanding of ENS development and its pathologies [13], there are still many genes and processes unknown. Particularly, factors regulating neural progenitor proliferation and differentiation in the developing and postnatal gut as well as cellular and molecular interaction systems remain largely elusive. Here, we used *in vitro* cultures of enteric neural progenitor cells derived from murine tunica muscularis to scan for molecular programs and signalling pathways acting on cell proliferation and early differentiation.

Our experiment aimed to elucidate gene regulations in enterospheres that occur while ENS progenitor cells leave their proliferative state and begin to differentiate into more defined and specific cell types. The results of the Affymetrix gene expression analysis showed the up- and downregulation of overall 1333 known genes that code for already identified proteins. 171 of these genes could be linked to cell proliferation (Table 1, Supplementary Table 1). Amongst them we detected genes coding for proteins related to the kinetochore complex (like NSL1 [17], NUF2 [18], SKA1-3 [19], and ZWILCH [20]), cyclin proteins [21], cyclin-dependent kinases (CDK) [22], and several types of centromere proteins. The regulation of 145 of these genes strongly indicates a slowdown of cell cycle progression as it was intended by the experimental deprivation of growth factor supplementation by the end of the proliferation phase (see Section 3). Interestingly, betacellulin (BTC) was upregulated nearly 6-fold although it was reported to promote cellular proliferation in the neural stem cell niche [23]. Nonetheless, the vast majority of genes including all regulated cyclins, cell division cycle proteins, and kinetochore proteins were found to be downregulated.

We also checked the regulated genes for apoptosis markers to see whether the stop in proliferation was related to cell death (Supplementary Table 2). Since only 3 of 12 apoptotic genes were regulated in the direction that indicates apoptosis, it is unlikely that apoptosis played a leading role in the interruption of proliferation. Still, the effect and regulation of apoptosis during enteric sphere cultures are an important cornerstone of understanding enteric neural progenitors in culture and *in vivo* and require further investigation. Together, on a broad basis, this dataset provides strong evidence that this cell culture design is applicable to decreasing the proliferative rate of enteric neural progenitor cells without inducing cell death or apoptosis in an appreciable quantity.

To further evaluate the proliferative conditions of cell types present in enterospheres, we focused on different cell specific markers of neural progenitors as well as neurons, glial, or smooth muscle cells. We consider this complex cellular composition of the enterospheres an advantage compared to more purified neural crest derived neurospheres as we are able to capture complex interactions and secretion mechanisms between cell types that might also play an important role *in vivo*. Interestingly, we found 8 genes involved in adult central or embryonic neural stem cells homeostasis (Table 2). The majority of genes like EPHA2 [24] are regulated in a way that suggests that neural stem cells exit the proliferative cell cycle to enter differentiation programs. This idea was supported by the upregulation of numerous genes that drive neuronal and glial differentiation like NEUROD4 [25] or OLIG1 [26]. In this context, we identified several upregulated genes involved in proper myelination. As enteric and central glia cells are known to temporally express myelin-related proteins during development, it is conceivable that this regulation is part of the early glial differentiation program [27]. Moreover, also typical markers of differentiated neurons (class III beta-tubulin, CALB2 [28]) and enteric glia (GFAP [29]) were found to be upregulated. Intriguingly, S100B, a common glia cell marker, was downregulated contrasting the rest of our data. Again, this might be due to the complex differentiation program of enteric glia, in which S100B plays a role at later stages.

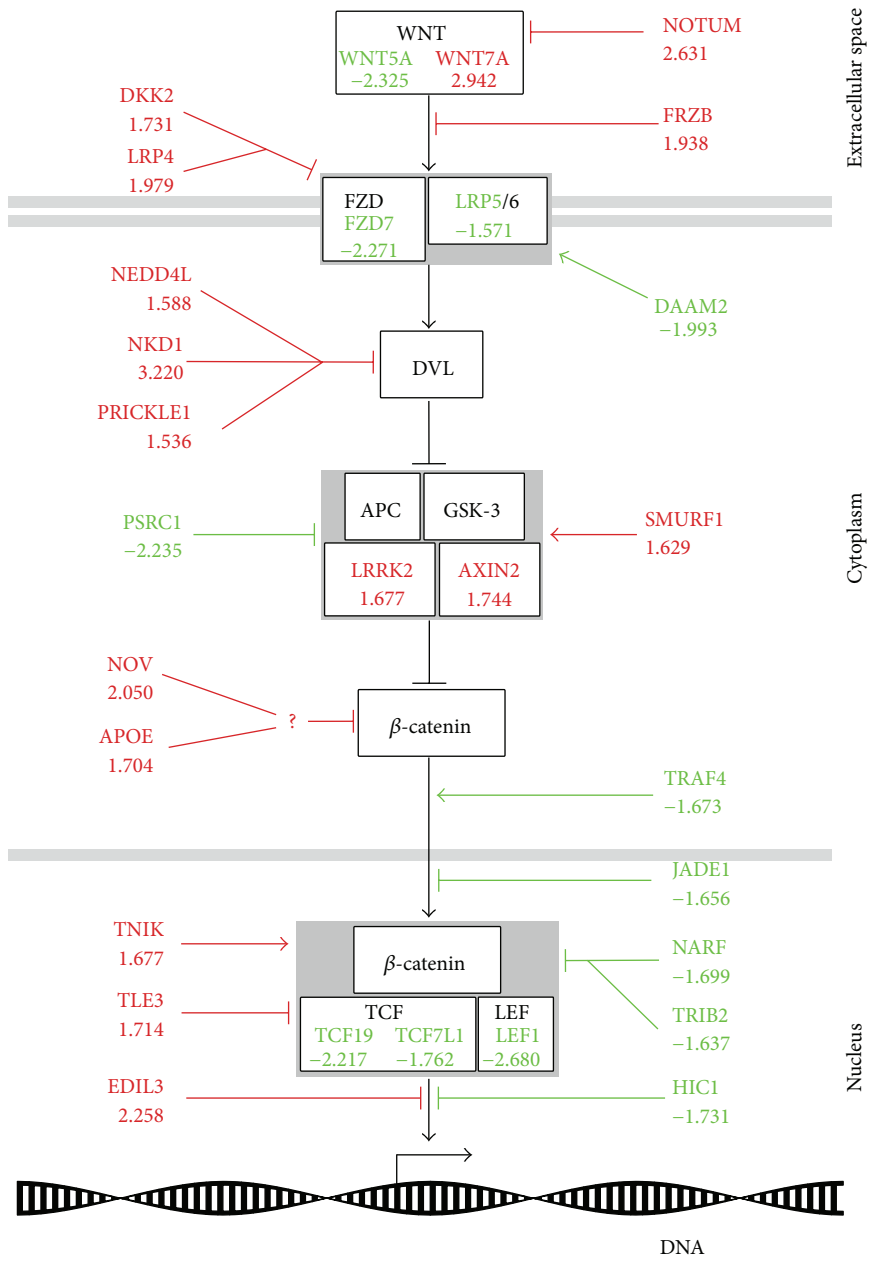

Figure 2: Detected regulatory influences on the canonical Wnt pathway. Scheme of the canonical Wnt pathway. Pointy arrowheads indicate an activating, blunt arrowheads, an inhibitory influence. The fold-change in expression of genes is written under the respective gene acronyms and colours indicate a general upregulation (red) or downregulation (green). For detailed explanation of the signalling cascade and regulated genes, see text.

Furthermore, the establishment of neuronal cell communication was strongly regulated. Here, we found an increased expression of genes related to synaptogenesis (LRRTM2 and 3 [30], neurotrimin [31]) and to SNARE or vesicle protein function (STXBP3, SV2C [32], and SYT6 [33]). We also identified a number of genes involved in transmitter metabolism (COMT, DDC) as well as neurotransmitter receptor like 5-HT, glutamate, and adrenergic receptors. However, the regulation of those genes was highly variable shedding light on the intricacy of synapse formation in the developing enteric nervous system. This complexity is carried on by genes related to axon sprouting and guidance like semaphorins [34] or RGMa [35].

Additionally, we found that regulated genes directly involved in the differentiation of muscle cells and/or enteric pacemaker cells called interstitial cells of Cajal (Table 3). Particularly interesting is the upregulation of a number of genes known to drive smooth muscle differentiation like ARID5B [36], FOSL2 [36] and genes that are expressed in differentiated smooth muscle cells in the intestine like AFAP1 [37], ENPP2 [38], and CNN1 [39] as well as various myosin and actin isoforms. These data confirm the

Table 3: Differentiation of smooth muscle cells/ICCs.

Gene	Encoded protein	Fold change
	Smooth muscle cells	
ACTA2	Actin, alpha 2, smooth muscle, aorta	1.693
ACTG2	Actin, gamma 2, smooth muscle, enteric	2.336
ACTN1	Actinin, alpha 1	−1.724
AEBP1	AE binding protein 1	2.702
AFAP1	Actin filament associated protein 1	1.638
ARID5B	AT-rich interactive domain 5B (MRF1-like)	1.521
Cald1	Caldesmon 1	−1.535
CNN1	Calponin 1, basic, smooth muscle	1.652
ENG	Endoglin	−1.552
ENPP1	Ectonucleotide pyrophosphatase/phosphodiesterase 1	−1.522
ENPP2	Ectonucleotide pyrophosphatase/phosphodiesterase 2	2.959
ENTPD1	Ectonucleoside triphosphate diphosphohydrolase 1	1.636
FOSL2	FOS-like antigen 2	2.566
GAMT	Guanidinoacetate N-methyltransferase	1.725
MYO1E	Myosin IE	1.569
MYO5A	Myosin VA (heavy chain 12, myoxin)	1.680
MYO7B	Myosin VIIB	1.710
MYO18A	Myosin XVIIIA	1.994
MYPN	Myopalladin	1.570
NEB	Nebulin	1.569
Nebl	Nebulette	2.378
NUP210	Nucleoporin 210 kDa	−1.838
RBM24	RNA binding motif protein 24	1.548
SMTN	Smoothelin	−1.778
SSPN	Sarcospan	1.603
TAGLN	Transgelin	2.706
	ICC	
GUCY1A3	Guanylate cyclase 1, soluble, alpha 3	−1.876
GUCY1B3	Guanylate cyclase 1, soluble, beta 3	−2.008
KIT	v-kit Hardy-Zuckerman 4 feline sarcoma viral oncogene homolog	−1.798
KITLG	KIT ligand	−1.541

fact that cultured spheroids are composed of different cell types present in the intestinal tunica muscularis and further indicate that deprivation of growth factors induces differentiation of smooth muscle cells resembling molecular processes in the developing gut. In fact, we among others were previously able to confirm the presence of smooth muscle cells derived from enterosphere culture by BrdU-immunolabeling costudies [4]. However, it is noteworthy that a few genes related to muscular differentiation (endoglin [40], smoothelin [41], NUP210 [42], caldesmon 1 [43], and ACTN1 [44]) were downregulated contrasting the expression pattern observed in the majority of regulated genes. This hints to complex regulatory mechanisms controlling the myogenic differentiation program in which these genes are not required at all or in a different temporal sequence not mapped by our experimental design. It is further remarkable that five markers expressed in interstitial cells of Cajal (ICC) including KIT [45] were downregulated.

Moreover, the regulation of 43 extracellular matrix proteins like collagens, integrins, proteoglycans, and matrix metallopeptidases points to a reconstruction of extracellular environment that has been discussed to influence neural stem cell behaviour [46] (Table 4). Taken together, these results illustrate the ongoing genetic programs during early differentiation of enterospheres.

Within the dataset, it was of special interest to find particularly many regulated genes related to the canonical Wnt pathway (Table 5). The involvement of canonical Wnt signalling has frequently been shown in the regulation of various stem cell niches, like intestinal epithelium or CNS derived neural stem cells. However, these studies exhibited different and partly contradicting outcomes, which strongly hint to the variable functions of canonical Wnt signals in different tissues during embryonic and postnatal development. In previous work, we found regulation of several Wnt-related genes in the context of thyroid hormone dependent differentiation of enteric neural progenitor cells indicating a potential role of the canonical Wnt pathway activation during the proliferation of this progenitor cell pool [15]. Canonical Wnt signalling has frequently been reviewed in the literature—just recently by Ring et al. [47]. In brief, secreted Wnt proteins bind to frizzled receptors (FZD) complexed with low density lipoprotein receptor-related protein 5/6 (LRP5/6) coreceptors. Thereafter, the scaffolding protein disheveled (DVL) is recruited to FZD and inhibits the β-catenin destruction complex (AXIN2, APC, and GSK-3β). Therefore, β-catenin accumulates in the cytoplasm and translocates to the nucleus where it binds to TCF/LEF transcription factors to initiate Wnt target gene expression. Interestingly, our current data strongly indicate that the canonical Wnt pathway is switched off during the first two days of enteric progenitor differentiation on several levels of the signalling cascade (Figure 2). On the one hand we identified a downregulation of activating parts of the signalling cascade itself like the receptor proteins FZD7 and LRP5 or the transcription factors TCF19, TCF7L1, and LEF1. On the other hand, inactivating elements of the pathway like parts of the β-catenin destruction complex AXIN2 and LRRK2 [48] were upregulated. We also found numerous modulators of the signalling cascade. It is of interest that the majority of those genes are reported to inhibit the signalling process extracellularly or on receptor level (Notum [49], FRZB [50], DKK2 [51], and LRP4 [52]), in the cytoplasm (NEDD4L [53], NKD1 [54], PRICKLE1 [55], NOV [56], and APOE [57]), or in the nucleus (TLE3 [58], EDIL3 [59]). Furthermore, we identified target genes of the canonical Wnt pathway that were either upregulated (e.g., AXIN2 that exerts a negative feedback on the pathway) or downregulated like the cell cycle progression genes CCND1 and SPRY4 [60]. We also found a lower expression of SPRY2 [61], a Wnt target gene and known inhibitor of GDNF signalling [62], in the differentiation group. Together with a strong upregulation of

Table 4: ECM.

Gene	Encoded protein	Fold change
CHSY3	Chondroitin sulfate synthase 3	−1.645
COL6A5	Collagen, type VI, alpha 5	1.527
COL12A1	Collagen, type XII, alpha 1	−1.973
COL14A1	Collagen, type XIV, alpha 1	6.135
COL16A1	Collagen, type XVI, alpha 1	1.666
COL18A1	Collagen, type XVIII, alpha 1	1.595
COL27A1	Collagen, type XXVII, alpha 1	1.522
COLGALT2	Collagen beta(1-O)galactosyltransferase 2	−1.564
CSPG4	Chondroitin sulfate proteoglycan 4	−2.952
CSPG5	Chondroitin sulfate proteoglycan 5 (neuroglycan C)	−1.585
CYR61	Cysteine-rich, angiogenic inducer, 61	1.748
ECM1	Extracellular matrix protein 1	2.580
HSPG2	Heparan sulfate proteoglycan 2	1.923
ITGA1	Integrin, alpha 1	−1.665
ITGA4	Integrin, alpha 4 (antigen CD49D, alpha 4 subunit of VLA-4 receptor)	−2.324
ITGA7	Integrin, alpha 7	4.203
ITGA8	Integrin, alpha 8	−2.262
ITGA11	Integrin, alpha 11	1.762
ITGB3	Integrin, beta 3 (platelet glycoprotein IIIa, antigen CD61)	−5.342
ITGB4	Integrin, beta 4	1.567
KRT80	Keratin 80	2.833
LAMA4	Laminin, alpha 4	−1.537
LAMA5	Laminin, alpha 5	1.684
LOX	Lysyl oxidase	3.250
LOXL4	Lysyl oxidase-like 4	2.427
		2.417
MATN2	Matrilin 2	2.570
MMP2	Matrix metallopeptidase 2 (gelatinase A, 72 kDa gelatinase, 72 kDa type IV collagenase)	1.668
MMP9	Matrix metallopeptidase 9 (gelatinase B, 92 kDa gelatinase, 92 kDa type IV collagenase)	−5.557
MMP15	Matrix metallopeptidase 15 (membrane-inserted)	−2.017
MMP16	Matrix metallopeptidase 16 (membrane-inserted)	−1.634
MMP17	Matrix metallopeptidase 17 (membrane-inserted)	1.612
MMP19	Matrix metallopeptidase 19	3.236
MMP28	Matrix metallopeptidase 28	1.956
NDST3	N-deacetylase/N-sulfotransferase (heparan glucosaminyl) 3	−5.557
P4HA1	Prolyl 4-hydroxylase, alpha polypeptide I	−1.958
PLOD3	Procollagen-lysine, 2-oxoglutarate 5-dioxygenase 3	2.250
UGDH	UDP-glucose 6-dehydrogenase	1.529

GDNF itself by 4.325-fold, this might drive enteric progenitor cells into neural differentiation [12].

Taken together, it is conceivable that canonical Wnt signalling plays a role in the maintenance of the enteric progenitor pool during proliferation and is switched off at the beginning of differentiation conditions. Indeed, our previous gene expression analyses [15] as well as recently published cell culture experiments [63] and yet unpublished *in vitro* analyses strongly support this hypothesis.

5. Conclusion

This study focused on the changes in gene expression of enteric neural progenitor cells occurring within the first two days of transition from a proliferative state to differentiation *in vitro*. Using microarray analysis, we found a marked inhibition of cell cycle progression in general as well as strong evidence for neural stem cells differentiation into enteric neurons and glia cells. These findings were substantiated

Table 5: Wnt.

Gene	Encoded protein	Fold change
	Wnt signaling cascade	
FZD7	Frizzled class receptor 7	−2.271
LEF1	Lymphoid enhancer-binding factor 1	−2.680
LRP5	Low density lipoprotein receptor-related protein 5	−1.571
LRRK2	Leucine-rich repeat kinase 2	1.677
TCF19	Transcription factor 19	−2.217
F7L1	Transcription factor 7-like 1 (T-cell specific, HMG-box)	−1.762
WNT5A	Wingless-type MMTV integration site family, member 5A	−2.325
WNT7B	Wingless-type MMTV integration site family, member 7B	2.942
	Target gene	
ARL4C	ADP-ribosylation factor-like 4C	2.179
AXIN2	Axin 2	1.744
CCND1	Cyclin D1	−2.476
CSRNP1	Cysteine-serine-rich nuclear protein 1	1.822
RACGAP1	Rac GTPase activating protein 1	−3.201
SPRY2	Sprouty homolog 2 (*Drosophila*)	−1.771
SPRY4	Sprouty homolog 4 (*Drosophila*)	−2.771
WISP1	WNT1 inducible signaling pathway protein 1	2.489
	Wnt antagonists/inhibitors	
APOE	Apolipoprotein E	1.704
DKK2	Dickkopf WNT signaling pathway inhibitor 2	1.731
EDIL3	EGF-like repeats and discoidin I-like domains 3	2.258
FRZB	Frizzled-related protein	1.938
HIC1	Hypermethylated in cancer 1	−1.731
JADE1	Jade family PHD finger 1	−1.656
LRP4	Low density lipoprotein receptor-related protein 4	1.979
NARF	Nuclear prelamin A recognition factor	−1.699
NEDD4L	Neural precursor cell expressed, developmentally downregulated 4-like, E3 ubiquitin protein ligase	1.588
NKD1	Naked cuticle homolog 1 (*Drosophila*)	3.220
NOTUM	Notum pectinacetylesterase homolog (*Drosophila*)	2.631
NOV	Nephroblastoma overexpressed	2.050
PRICKLE1	Prickle homolog 1 (*Drosophila*)	1.536
TLE3	Transducin-like enhancer of split 3	1.714
TRIB2	Tribbles pseudokinase 2	−1.637
	Wnt activators	
DAAM2	Dishevelled associated activator of morphogenesis 2	−1.993
PSRC1	Proline/serine-rich coiled-coil 1	−2.235
TNIK	TRAF2 and NCK interacting kinase	1.677
TRAF4	TNF receptor-associated factor 4	−1.673

by the upregulation of genes related to synapse formation and neural connectivity. Most interesting, we found that this transition from enteric neural progenitor proliferation to differentiation was accompanied by a considerable inactivation of the canonical Wnt signalling pathway. This, together with previous work, strongly indicates that canonical Wnt activation is one of the driving mechanisms of enteric neural progenitor proliferation and thus might play a role in the homeostasis of this cell pool *in vivo* and *in vitro*.

Conflict of Interests

The authors declare that there is no conflict of interests regarding the publication of this paper.

Authors' Contribution

Peter Helmut Neckel and Roland Mohr contributed equally to this work.

Acknowledgments

The project was supported by a grant from the German Federal Ministry for Education and Research (01GN0967). The authors would like to thank Andrea Wizenmann, Andreas Mack, and Sven Poths for their helpful advice.

References

[1] J. B. Furness, "The enteric nervous system and neurogastroenterology," *Nature Reviews Gastroenterology & Hepatology*, vol. 9, no. 5, pp. 286–294, 2012.

[2] D. Natarajan, M. Grigoriou, C. V. Marcos-Gutierrez, C. Atkins, and V. Pachnis, "Multipotential progenitors of the mammalian enteric nervous system capable of colonising aganglionic bowel in organ culture," *Development*, vol. 126, no. 1, pp. 157–168, 1999.

[3] G. M. Kruger, J. T. Mosher, S. Bixby, N. Joseph, T. Iwashita, and S. J. Morrison, "Neural crest stem cells persist in the adult gut but undergo changes in self-renewal, neuronal subtype potential, and factor responsiveness," *Neuron*, vol. 35, no. 4, pp. 657–669, 2002.

[4] M. Metzger, P. M. Bareiss, T. Danker et al., "Expansion and differentiation of neural progenitors derived from the human adult enteric nervous system," *Gastroenterology*, vol. 137, no. 6, pp. 2063.e4–2073.e4, 2009.

[5] M. Metzger, C. Caldwell, A. J. Barlow, A. J. Burns, and N. Thapar, "Enteric nervous system stem cells derived from human gut mucosa for the treatment of aganglionic gut disorders," *Gastroenterology*, vol. 136, no. 7, pp. 2214.e3–2225.e3, 2009.

[6] M. J. Saffrey, "Cellular changes in the enteric nervous system during ageing," *Developmental Biology*, vol. 382, no. 1, pp. 344–355, 2013.

[7] M. D. Gershon, "Developmental determinants of the independence and complexity of the enteric nervous system," *Trends in Neurosciences*, vol. 33, no. 10, pp. 446–456, 2010.

[8] F. Obermayr, R. Hotta, H. Enomoto, and H. M. Young, "Development and developmental disorders of the enteric nervous system," *Nature Reviews Gastroenterology and Hepatology*, vol. 10, no. 1, pp. 43–57, 2013.

[9] R. J. Rintala and M. P. Pakarinen, "Long-term outcomes of Hirschsprung's disease," *Seminars in Pediatric Surgery*, vol. 21, no. 4, pp. 336–343, 2012.

[10] T. A. Heanue and V. Pachnis, "Enteric nervous system development and Hirschsprung's disease: advances in genetic and stem cell studies," *Nature Reviews Neuroscience*, vol. 8, no. 6, pp. 466–479, 2007.

[11] L. Becker, J. Peterson, S. Kulkarni, and P. J. Pasricha, "Ex vivo neurogenesis within enteric ganglia occurs in a PTEN dependent manner," *PLoS ONE*, vol. 8, no. 3, Article ID e59452, 2013.

[12] T. Uesaka, M. Nagashimada, and H. Enomoto, "GDNF signaling levels control migration and neuronal differentiation of enteric ganglion precursors," *The Journal of Neuroscience*, vol. 33, no. 41, pp. 16372–16382, 2013.

[13] T. A. Heanue and V. Pachnis, "Expression profiling the developing mammalian enteric nervous system identifies marker and candidate Hirschsprung disease genes," *Proceedings of the National Academy of Sciences of the United States of America*, vol. 103, no. 18, pp. 6919–6924, 2006.

[14] B. P. S. Vohra, K. Tsuji, M. Nagashimada et al., "Differential gene expression and functional analysis implicate novel mechanisms in enteric nervous system precursor migration and neuritogenesis," *Developmental Biology*, vol. 298, no. 1, pp. 259–271, 2006.

[15] R. Mohr, P. Neckel, Y. Zhang et al., "Molecular and cell biological effects of 3,5,3′-triiodothyronine on progenitor cells of the enteric nervous system in vitro," *Stem Cell Research*, vol. 11, no. 3, pp. 1191–1205, 2013.

[16] S. Fleige and M. W. Pfaffl, "RNA integrity and the effect on the real-time qRT-PCR performance," *Molecular Aspects of Medicine*, vol. 27, no. 2-3, pp. 126–139, 2006.

[17] S. L. Kline, I. M. Cheeseman, T. Hori, T. Fukagawa, and A. Desai, "The human Mis12 complex is required for kinetochore assembly and proper chromosome segregation," *The Journal of Cell Biology*, vol. 173, no. 1, pp. 9–17, 2006.

[18] E. D. Salmon, D. Cimini, L. A. Cameron, and J. G. DeLuca, "Merotelic kinetochores in mammalian tissue cells," *Philosophical Transactions of the Royal Society B: Biological Sciences*, vol. 360, no. 1455, pp. 553–568, 2005.

[19] A. A. Ye and T. J. Maresca, "Cell division: kinetochores SKAdaddle," *Current Biology*, vol. 23, no. 3, pp. R122–R124, 2013.

[20] Y. Lu, Z. Wang, L. Ge, N. Chen, and H. Liu, "The RZZ complex and the spindle assembly checkpoint," *Cell Structure and Function*, vol. 34, no. 1, pp. 31–45, 2009.

[21] D. G. Johnson and C. L. Walker, "Cyclins and cell cycle checkpoints," *Annual Review of Pharmacology and Toxicology*, vol. 39, pp. 295–312, 1999.

[22] M. Malumbres, E. Harlow, T. Hunt et al., "Cyclin-dependent kinases: a family portrait," *Nature Cell Biology*, vol. 11, no. 11, pp. 1275–1276, 2009.

[23] M. V. Gómez-Gaviro, C. E. Scott, A. K. Sesay et al., "Betacellulin promotes cell proliferation in the neural stem cell niche and stimulates neurogenesis," *Proceedings of the National Academy of Sciences of the United States of America*, vol. 109, no. 4, pp. 1317–1322, 2012.

[24] K. Khodosevich, Y. Watanabe, and H. Monyer, "EphA4 preserves postnatal and adult neural stem cells in an undifferentiated state *in vivo*," *Journal of Cell Science*, vol. 124, no. 8, pp. 1268–1279, 2011.

[25] E. Abranches, M. Silva, L. Pradier et al., "Neural differentiation of embryonic stem cells in vitro: a road map to neurogenesis in the embryo," *PLoS ONE*, vol. 4, no. 7, Article ID e6286, 2009.

[26] V. Balasubramaniyan, N. Timmer, B. Kust, E. Boddeke, and S. Copray, "Transient expression of Olig1 initiates the differentiation of neural stem cells into oligodendrocyte progenitor cells," *Stem Cells*, vol. 22, no. 6, pp. 878–882, 2004.

[27] M. Kolatsi-Joannou, X. Z. Li, T. Suda, H. T. Yuan, and A. S. Woolf, "In early development of the rat mRNA for the major myelin protein P_0 is expressed in nonsensory areas of the embryonic inner ear, notochord, enteric nervous system, and olfactory ensheathing cells," *Developmental Dynamics*, vol. 222, no. 1, pp. 40–51, 2001.

[28] M. I. Morris, D. B.-D. Soglio, A. Ouimet, A. Aspirot, and N. Patey, "A study of calretinin in Hirschsprung pathology, particularly in total colonic aganglionosis," *Journal of Pediatric Surgery*, vol. 48, no. 5, pp. 1037–1043, 2013.

[29] K. R. Jessen and R. Mirsky, "Glial cells in the enteric nervous system contain glial fibrillary acidic protein," *Nature*, vol. 286, no. 5774, pp. 736–737, 1980.

[30] T. J. Siddiqui, R. Pancaroglu, Y. Kang, A. Rooyakkers, and A. M. Craig, "LRRTMs and neuroligins bind neurexins with a differential code to cooperate in glutamate synapse development," *The Journal of Neuroscience*, vol. 30, no. 22, pp. 7495–7506, 2010.

[31] S. Chen, O. Gil, Y. Q. Ren, G. Zanazzi, J. L. Salzer, and D. E. Hillman, "Neurotrimin expression during cerebellar development suggests roles in axon fasciculation and synaptogenesis," *Journal of Neurocytology*, vol. 30, no. 11, pp. 927–937, 2002.

[32] R. Janz and T. C. Südhof, "SV2C is a synaptic vesicle protein with an unusually restricted localization: anatomy of a synaptic vesicle protein family," *Neuroscience*, vol. 94, no. 4, pp. 1279–1290, 1999.

[33] B. Marquèze, F. Berton, and M. Seagar, "Synaptotagmins in membrane traffic: which vesicles do the tagmins tag?" *Biochimie*, vol. 82, no. 5, pp. 409–420, 2000.

[34] B. C. Jongbloets and R. J. Pasterkamp, "Semaphorin signalling during development," *Development*, vol. 141, no. 17, pp. 3292–3297, 2014.

[35] M. Metzger, S. Conrad, T. Skutella, and L. Just, "RGMa inhibits neurite outgrowth of neuronal progenitors from murine enteric nervous system via the neogenin receptor *in vitro*," *Journal of Neurochemistry*, vol. 103, no. 6, pp. 2665–2678, 2007.

[36] J. M. Spin, S. Nallamshetty, R. Tabibiazar et al., "Transcriptional profiling of *in vitro* smooth muscle cell differentiation identifies specific patterns of gene and pathway activation," *Physiological Genomics*, vol. 19, pp. 292–302, 2005.

[37] J. M. Baisden, Y. Qian, H. M. Zot, and D. C. Flynn, "The actin filament-associated protein AFAP-110 is an adaptor protein that modulates changes in actin filament integrity," *Oncogene*, vol. 20, no. 44, pp. 6435–6447, 2001.

[38] L. E. Peri, K. M. Sanders, and V. N. Mutafova-Yambolieva, "Differential expression of genes related to purinergic signaling in smooth muscle cells, PDGFRα-positive cells, and interstitial cells of Cajal in the murine colon," *Neurogastroenterology & Motility*, vol. 25, no. 9, pp. e609–e620, 2013.

[39] S. J. Winder, B. G. Allen, O. Clément-Chomienne, and M. P. Walsh, "Regulation of smooth muscle actin—myosin interaction and force by calponin," *Acta Physiologica Scandinavica*, vol. 164, no. 4, pp. 415–426, 1998.

[40] M. L. Mancini, J. M. Verdi, B. A. Conley et al., "Endoglin is required for myogenic differentiation potential of neural crest stem cells," *Developmental Biology*, vol. 308, no. 2, pp. 520–533, 2007.

[41] F. T. L. van der Loop, G. Schaart, E. D. J. Timmer, F. C. S. Ramaekers, and G. J. J. M. van Eys, "Smoothelin, a novel cytoskeletal protein specific for smooth muscle cells," *The Journal of Cell Biology*, vol. 134, no. 2, pp. 401–411, 1996.

[42] M. A. D'Angelo, J. S. Gomez-Cavazos, A. Mei, D. H. Lackner, and M. W. Hetzer, "A change in nuclear pore complex composition regulates cell differentiation," *Developmental Cell*, vol. 22, no. 2, pp. 446–458, 2012.

[43] J. J.-C. Lin, Y. Li, R. D. Eppinga, Q. Wang, and J.-P. Jin, "Chapter 1: roles of caldesmon in cell motility and actin cytoskeleton remodeling," *International Review of Cell and Molecular Biology*, vol. 274, pp. 1–68, 2009.

[44] S. B. Marston and C. W. J. Smith, "The thin filaments of smooth muscles," *Journal of Muscle Research and Cell Motility*, vol. 6, no. 6, pp. 669–708, 1985.

[45] K. M. Sanders and S. M. Ward, "Kit mutants and gastrointestinal physiology," *The Journal of Physiology*, vol. 578, no. 1, pp. 33–42, 2007.

[46] L. S. Campos, "Neurospheres: insights into neural stem cell biology," *Journal of Neuroscience Research*, vol. 78, no. 6, pp. 761–769, 2004.

[47] A. Ring, Y.-M. Kim, and M. Kahn, "Wnt/catenin signaling in adult stem cell physiology and disease," *Stem Cell Reviews and Reports*, vol. 10, no. 4, pp. 512–525, 2014.

[48] D. C. Berwick and K. Harvey, "LRRK2: an éminence grise of Wnt-mediated neurogenesis?" *Frontiers in Cellular Neuroscience*, vol. 7, article 82, 2013.

[49] S. Kakugawa, P. F. Langton, M. Zebisch et al., "Notum deacylates Wnt proteins to suppress signalling activity," *Nature*, vol. 519, no. 7542, pp. 187–192, 2015.

[50] Y. Mii and M. Taira, "Secreted Wnt 'inhibitors' are not just inhibitors: regulation of extracellular Wnt by secreted Frizzled-related proteins," *Development Growth & Differentiation*, vol. 53, no. 8, pp. 911–923, 2011.

[51] Y. Kawano and R. Kypta, "Secreted antagonists of the Wnt signalling pathway," *Journal of Cell Science*, vol. 116, part 13, pp. 2627–2634, 2003.

[52] A. Ohazama, E. B. Johnson, M. S. Ota et al., "Lrp4 modulates extracellular integration of cell signaling pathways in development," *PLoS ONE*, vol. 3, no. 12, Article ID e4092, 2008.

[53] Y. Ding, Y. Zhang, C. Xu, Q.-H. Tao, and Y.-G. Chen, "HECT domain-containing E_3 ubiquitin ligase $NEDD_4L$ negatively regulates Wnt signaling by targeting dishevelled for proteasomal degradation," *The Journal of Biological Chemistry*, vol. 288, no. 12, pp. 8289–8298, 2013.

[54] A. Ishikawa, S. Kitajima, Y. Takahashi et al., "Mouse Nkd1, a Wnt antagonist, exhibits oscillatory gene expression in the PSM under the control of Notch signaling," *Mechanisms of Development*, vol. 121, no. 12, pp. 1443–1453, 2004.

[55] D. W. Chan, C.-Y. Chan, J. W. P. Yam, Y.-P. Ching, and I. O. L. Ng, "Prickle-1 negatively regulates Wnt/β-catenin pathway by promoting Dishevelled ubiquitination/degradation in liver cancer," *Gastroenterology*, vol. 131, no. 4, pp. 1218–1227, 2006.

[56] K. Sakamoto, S. Yamaguchi, R. Ando et al., "The nephroblastoma overexpressed gene (NOV/ccn3) protein associates with Notch1 extracellular domain and inhibits myoblast differentiation via Notch signaling pathway," *The Journal of Biological Chemistry*, vol. 277, no. 33, pp. 29399–29405, 2002.

[57] A. Caruso, M. Motolese, L. Iacovelli et al., "Inhibition of the canonical Wnt signaling pathway by apolipoprotein E_4 in PC12 cells," *Journal of Neurochemistry*, vol. 98, no. 2, pp. 364–371, 2006.

[58] A. J. Hanson, H. A. Wallace, T. J. Freeman, R. D. Beauchamp, L. A. Lee, and E. Lee, "XIAP monoubiquitylates Groucho/TLE to promote canonical Wnt signaling," *Molecular Cell*, vol. 45, no. 5, pp. 619–628, 2012.

[59] A. Takai, H. Inomata, A. Arakawa, R. Yakura, M. Matsuo-Takasaki, and Y. Sasai, "Anterior neural development requires Del1, a matrix-associated protein that attenuates canonical Wnt signaling via the Ror2 pathway," *Development*, vol. 137, no. 19, pp. 3293–3302, 2010.

[60] Y. Katoh and M. Katoh, "FGF signaling inhibitor, SPRY4, is evolutionarily conserved target of WNT signaling pathway in progenitor cells," *International Journal of Molecular Medicine*, vol. 17, no. 3, pp. 529–532, 2006.

[61] P. Ordóñez-Morán, A. Irmisch, A. Barbáchano et al., "SPROUTY2 is a β-catenin and FOXO3a target gene indicative of poor prognosis in colon cancer," *Oncogene*, vol. 33, no. 15, pp. 1975–1985, 2014.

[62] T. Taketomi, D. Yoshiga, K. Taniguchi et al., "Loss of mammalian *Sprouty2* leads to enteric neuronal hyperplasia and esophageal achalasia," *Nature Neuroscience*, vol. 8, no. 7, pp. 855–857, 2005.

[63] R. Di Liddo, T. Bertalot, A. Schuster et al., "Anti-inflammatory activity of Wnt signaling in enteric nervous system: *in vitro* preliminary evidences in rat primary cultures," *Journal of Neuroinflammation*, vol. 12, no. 1, p. 23, 2015.

Hindawi Publishing Corporation
Stem Cells International
Volume 2016, Article ID 6759343, 7 pages
http://dx.doi.org/10.1155/2016/6759343

Research Article

TBX3 Knockdown Decreases Reprogramming Efficiency of Human Cells

Moritz Klingenstein,[1] Stefanie Raab,[1] Kevin Achberger,[1] Alexander Kleger,[2] Stefan Liebau,[1] and Leonhard Linta[1]

[1]*Institute of Neuroanatomy, Eberhard Karls University Tübingen, 72074 Tübingen, Germany*
[2]*Department of Internal Medicine I, Ulm University, 89081 Ulm, Germany*

Correspondence should be addressed to Alexander Kleger; alexander.kleger@uni-ulm.de, Stefan Liebau; stefan.liebau@uni-tuebingen.de, and Leonhard Linta; leonhard.linta@uni-tuebingen.de

Received 24 April 2015; Accepted 2 July 2015

Academic Editor: Su-Chun Zhang

TBX3 is a member of the T-box transcription factor family and is involved in the core pluripotency network. Despite this role in the pluripotency network, its contribution to the reprogramming process during the generation of human induced pluripotent stem cells remains elusive. In this respect, we performed reprogramming experiments applying *TBX3* knockdown in human fibroblasts and keratinocytes. Knockdown of *TBX3* in both somatic cell types decreased the reprogramming efficiencies in comparison to control cells but with unchanged reprogramming kinetics. The resulting iPSCs were indistinguishable from control cells and displayed a normal *in vitro* differentiation capacity by generating cells of all three germ layers comparable to the controls.

1. Introduction

Pluripotent embryonic stem cells (ESCs) are isolated from the inner cell mass of early embryos. Pluripotency is defined by a high and indefinite proliferative potential and the capacity to differentiate into cells of the three germ layers, subsequently able to generate all cell types and tissues of an organism. The possibility of culturing and investigating ESCs has led to a good understanding of the pluripotency network, but also of various signaling pathways involved in cell differentiation events [1, 2]. The pluripotency network is comprised of numerous transcription factors, interconnected with each other by regulatory feedback loops. Basically, it keeps the expression of stem cell genes active and represses genes involved in differentiation [3, 4]. These transcription factors have such a dominant role in cell function that the overexpression of a few factors is able to force a somatic cell back into a pluripotent state. In this way, somatic cells are reprogrammed into induced pluripotent stem cells (iPSCs) by overexpression of *OCT4*, *SOX2*, *KLF4,* or other related factors [5, 6]. The discovery of this reprogramming technique has not just widened the understanding of the pluripotency network but is also an invaluable tool to generate donor and patient specific stem cells for disease modeling and for future therapeutic strategies [7–12].

The T-box transcription factor family is involved in a variety of processes including differentiation and pluripotency. In the pluripotency circuitry, TBX3 has been shown to interact with the core pluripotency factors NANOG, OCT4, and SOX2, to maintain the stem cell state and to inhibit differentiation. Depletion of Tbx3 leads to differentiation of murine pluripotent stem cells [13]. Moreover, Tbx3 upholds pluripotency by acting as a downstream activator of WNT signaling and plays a role in the reprogramming process by direct binding and activation of the Oct4 promoter. During early differentiation processes, Tbx3 is involved in mesendodermal differentiation, heart development, and limb formation [14]. Additionally, Tbx3 is highly expressed in definite endoderm progenitors and together with Jmjd3 and Eomes promotes the formation of the endoderm [15]. In that respect, Tbx3 was classified as one of the mesendoderm pluripotency transcription factors.

Based on these findings, we applied a knockdown of *TBX3* in human somatic cells to investigate the role of TBX3 in the reprogramming process.

2. Materials and Methods

2.1. Keratinocyte and Fibroblast Cultivation. The cultivation of keratinocytes from plucked human hair was mainly performed according to [16]. In brief, keratinocytes were cultured on 20 μg/mL collagen IV (Sigma-Aldrich) coated dishes in EpiLife medium with HKGS supplement (both from Gibco) until they reached ~70% confluency.

Human foreskin fibroblasts (HFFs) (System Biosciences) were cultivated in Dulbecco's modified Eagle's medium (DMEM) supplemented with 10% fetal bovine serum (FBS) and 1% Glutamax, 1% nonessential amino acids (NEAA), and 1% antibiotic-antimycotic (all from Life Technologies).

2.2. Lentivirus Production, Infection, and Selection. 4×10^6 Lenti-X 293T cells (Clontech) were transfected with 8 μg DNA of plasmid pRRL.PPT.SF.hOKSMco.idTom.pre FRT [17], or TRIPZ Human TBX3 shRNA (V2THS_135043, GE Healthcare) together with 2 μg pMD2.G and 5.5 μg of psPAX2 vector DNA (Addgene 12259 and 12260 from Didier Trono) using 1 μg/mL polyethylenimine (PEI). Lenti-X Concentrator Kit (Clontech) was used to concentrate the viral supernatant collected after two and four days. Virus pellets were resuspended in EpiLife with HKGS supplement. Spinfection with 1000 g for 30 min was used to transduce TRIPZ TBX3 lentivirus into the cells on two consecutive days with a medium change after 4 h, respectively. Infected cells were selected by puromycin (1 μg/mL) treatment for two days.

2.3. Feeder Cells, Reprogramming of Keratinocytes and Fibroblasts. Rat embryonic fibroblasts (REFs) from embryonic day 14 were generated according to the protocol previously described in [18] and were cultured in DMEM containing 10% fetal bovine serum (FBS), 1% Glutamax, 1% NEAA, and 1% antibiotic-antimycotic (all from Life Technologies). REFs were treated with 7.5 μg/mL mitomycin C (Biomol) for 2.5 hours for mitotic inactivation.

Keratinocytes and fibroblasts were infected as mentioned above over two days with 5×10^8 lentiviral particles in the appropriate medium containing 8 μg/mL polybrene (Sigma-Aldrich). 1 μg/mL doxycycline was added to the keratinocytes and fibroblasts depending on the condition from the first day of infection.

Two days after infection, keratinocytes and fibroblasts were detached using TrypLE Express (Life Technologies) and were seeded on 1.5×10^5 mitotic inactive REF cells in iPSC medium (DMEM F12 supplemented with 20% knockout serum replacement, 1% antibiotic-antimycotic, 1% NEAA, 1% Glutamax, 100 μM β-mercaptoethanol, 10 μM Y-27632, 50 μg/mL ascorbic acid, and 10 ng/mL FGF2). Incubation conditions for reprogramming cells were 37°C, 5% CO_2, and 5% O_2. Reprogramming cells were cultured on feeder cells until iPSC colonies were clearly visible and were then mechanically picked and transferred onto Matrigel-coated (Corning) cell culture dishes for feeder-free culture.

2.4. Human iPSC Culture, Germ Layer Differentiation. iPSCs were cultivated under feeder-free conditions in FTDA medium according to [19]. For further passaging and germ layer differentiation, iPSCs were detached using ReLeSR (Stemcell Technologies) according to the manufacturer's manual. To form embryoid bodies, detached cell clumps were cultured in suspension using ultralow attachment flasks (Corning) for 7 days. After seeding on Matrigel-coated dishes, the embryoid bodies were cultured two additional weeks adherently. iPSC medium was used for germ layer differentiation.

2.5. Immunocytochemistry and Alkaline Phosphatase Staining. Cells were fixed for 15 minutes with 4% paraformaldehyde (PFA) and 10% sucrose. Pluripotency staining was performed using StemLight Pluripotency Antibody Kit according to the manufacturer's recommended conditions (Cell Signaling) with Alexa secondary antibodies (all from Abcam). For germ layer differentiation immunocytochemistry stainings, fixed cells were permeabilized with 0.2% Triton-X for 5 minutes, followed by blocking with 5% bovine serum albumin (BSA) for 60 minutes. Antibodies were used as described below: mouse anti-DESMIN (DAKO, 1 : 500), goat anti-SOX17 (R&D Systems, 1 : 500), rabbit anti-TUBB3 (Covance, 1 : 2000), and Alexa secondary antibodies (all from Abcam). Cells were mounted with ProLong Gold Antifade Reagent with 4′,6-diamidino-2-phenylindole (DAPI) (Life Technologies).

Cells for alkaline phosphatase (AP) staining were fixed in 4% PFA for two minutes. Nitroblue tetrazolium/5-bromo-4-chloro-3-indolyl phosphate (NBT/BCIP) solution was prepared according to the manufacturer's protocol (Sigma-Aldrich). The cells were incubated with the substrate solution for 20 minutes and the reaction was stopped with phosphate-buffered saline (PBS). Pictures were taken under artificial light with a normal camera with particular caution on the same acquisition settings and exposure time. Colony numbers were counted manually or quantified with the ImageJ software by measuring the total intensity in the well area after subtraction of the background value.

2.6. Quantitative Reverse Transcription Polymerase Chain Reaction. Total RNA was isolated from cell lysates using RNeasy MiniKit (Qiagen). QuantiTect primer assays were used for all experiments (Qiagen, Supplementary Table 1 in Supplementary Material available online at http://dx.doi.org/10.1155/2016/6759343).

PCR was performed on a StepOne instrument (Applied Biosciences) using QuantiFast SYBR Green RT-PCR Kit (Qiagen) according to the manufacturer's protocol. Relative gene expression was calculated as a ratio of target gene concentration to the housekeeping gene hydroxymethylbilane synthase (*HMBS*) concentration.

3. Results

3.1. Reprogramming of Human TBX3 Knockdown Cells. To rule out cell type specific effects in our experimental setup, we chose somatic cells which originate from different germ layers: mesodermal human foreskin fibroblasts (HFFs) and

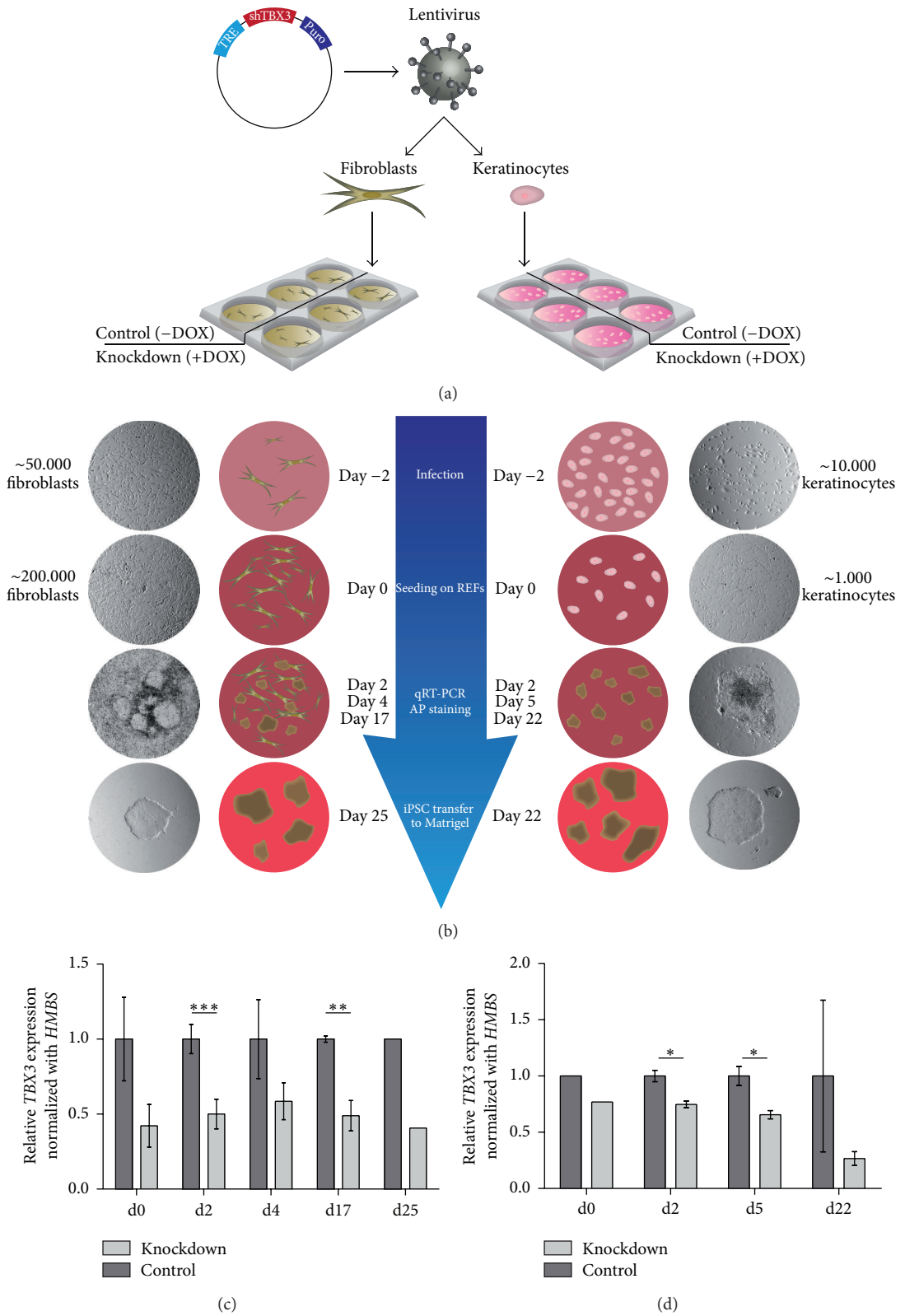

Figure 1: Reprogramming fibroblasts and keratinocytes with a *TBX3* knockdown. (a) Infection of fibroblasts and keratinocytes with a TRIPZ Human *TBX3* shRNA lentivirus, inducible via doxycycline addition. (b) Reprogramming time scheme with fibroblasts (left) and keratinocytes (right) along with starting cell numbers and experiment time points. (c) *TBX3* knockdown during reprogramming of fibroblasts at day 0 (seeding infected cells on feeder layer), day 2, day 4, day 17, and day 25 (last day on feeder cells before transfer to feeder-free system on Matrigel). Control is not treated with doxycycline. (d) *TBX3* knockdown during reprogramming of keratinocytes at day 0 (seeding infected cells on feeder layer), day 2, day 5, and day 22 (last day on feeder cells before transfer to feeder-free system on Matrigel). Control is not treated with doxycycline.

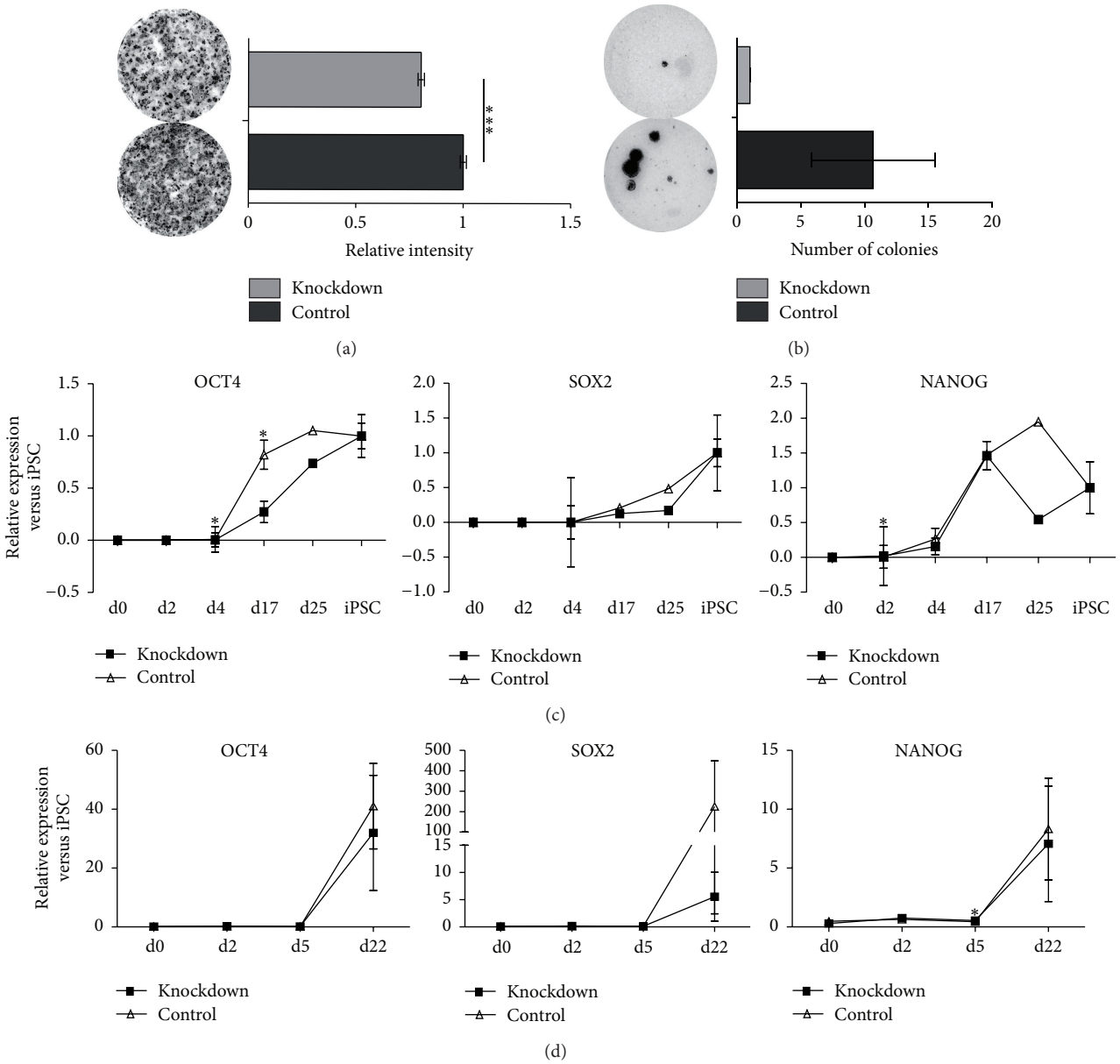

Figure 2: *TBX3* knockdown in fibroblasts and keratinocytes during reprogramming causes decreased reprogramming efficiency. (a) Alkaline phosphatase (AP) staining at day 17 of fibroblast reprogramming with a highly significant reduction (23%) of iPSC colonies. (b) Alkaline phosphatase (AP) staining at day 22 of keratinocyte reprogramming with a reduction (91%) of iPSC colonies. (c) Relative expression of *OCT4*, *SOX2,* and *NANOG* during fibroblast reprogramming. (d) Relative expression of *OCT4, SOX2,* and *NANOG* during keratinocyte reprogramming.

ectodermal human hair follicle keratinocytes. First, we infected both cell types with a lentiviral vector containing a puromycin resistance for selection of infected cells as well as a doxycycline (DOX) inducible shRNA directed against *TBX3* (Figure 1(a)). After successful puromycin selection, cells were either treated with doxycycline (+DOX) or left untreated as a control (−DOX). Subsequently, a defined number of all cell types were infected with a reprogramming lentivirus, containing *OCT4*, *SOX2*, *KLF4,* and C-*MYC*. After two days, infected cells were transferred onto mitotically inactivated feeder cells (rat embryonic fibroblasts). At indicated time points, RNA samples were collected and alkaline phosphatase (AP) stainings were performed (Figure 1(b)). *TBX3* knockdown efficiency was traced throughout the reprogramming process by qRT-PCR. For HFFs, the knockdown was ~50% (Figure 1(c)) while keratinocytes displayed an initial knockdown of approximately 30% showing an increase at later time points (Figure 1(d)). However, it must be taken into account that all measured cell populations contained a considerable amount of rat feeder cells. Due to the highly conserved

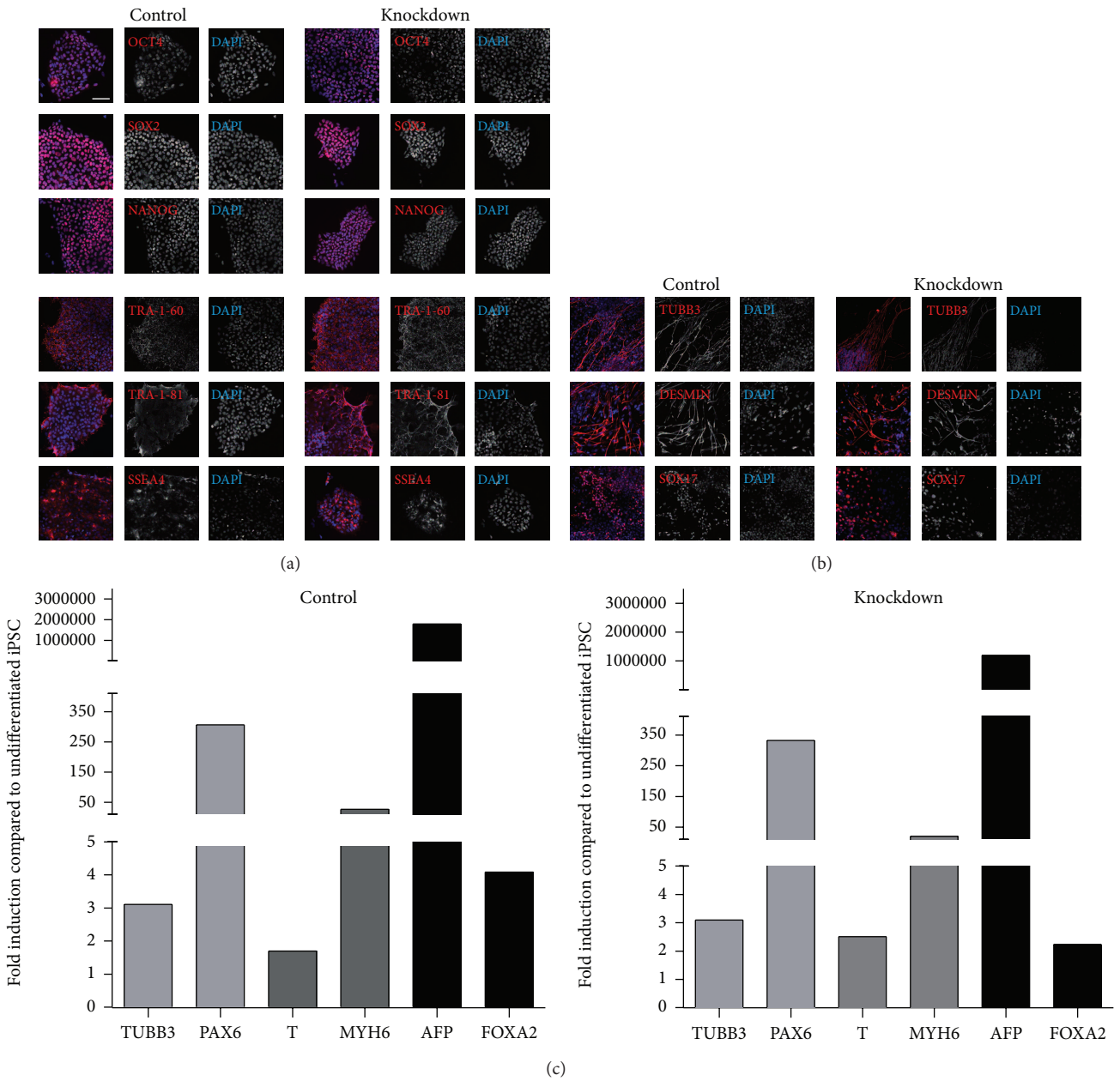

Figure 3: Reprogrammed fibroblasts under *TBX3* knockdown have the same stem cell properties as control iPSCs. (a) Pluripotency staining of iPSCs generated from fibroblasts is positive for the pluripotency markers OCT4, SOX2, and NANOG as well as for the surface markers TRA-1-60, TRA-1-81, and SSEA4. (b) Immunocytochemistry of germ layer differentiation shows positive staining for ectoderm (TUBB3), mesoderm (DESMIN), and endoderm (SOX17) for *TBX3* knockdown and control, respectively. (c) Expression of ectodermal genes (*TUBB3, PAX6*), mesodermal genes (*T, MYH6*), and endodermal genes (*AFP, FOXA2*) in germ layer differentiation shows pluripotent differentiation potential of the generated iPSCs in both control and *TBX3* knockdown cells. Scale bar: 100 μm.

sequence in both species, the feeder cells partly contribute to the measured *TBX3* levels. Therefore, knockdown efficiency in the reprogramming cells might be considerably higher.

3.2. TBX3 Knockdown Reduces Reprogramming Efficiency. At the end of the reprogramming process, when large iPS colonies were clearly visible, AP stainings were performed and the stained areas were measured. In both cell types, the reduced levels of *TBX3* led to a reduced number of colonies, 23% in HFF (highly significant) and 91% in keratinocytes (Figures 2(a) and 2(b)). Of note, only a very low number of keratinocytes were infected and reprogrammed (due to slow proliferation after infection) leading to a highly reduced number of iPS colonies compared to HFFs which divide continuously and fast during the reprogramming process. Neither colony size nor colony morphology was noticeably altered in knockdown cultures. The reduced reprogramming efficiency was confirmed by qRT-PCR. The RNA levels of

OCT4, *SOX2,* and *NANOG* were additionally reduced in both TBX3 knockdown cell types, most probably due to the lower number of reprogrammed cells (Figures 2(c) and 2(d)). In later passage iPSCs, RNA levels for *OCT4*, *SOX2,* and *NANOG* levels were comparable to control cultures. Additionally, knockdown cells at later passages displayed a comparable growth speed (not shown) and colony morphology. To generally test the full pluripotent capacity of the knockdown iPSCs, we analyzed later passage HFF derived iPSCs in more detail in terms of pluripotency factor expression and differentiation potential. iPSCs were positive for the transcription factors OCT4, SOX2, and NANOG as well as the surface antigens TRA-1-60, TRA-1-81, and SSEA4 in immunofluorescence staining (Figure 3(a)), comparable to the control cells. In an *in vitro* differentiation experiment, knockdown iPSCs generated cells positive for TUBB3 as an ectodermal marker, DESMIN as a mesodermal marker, and SOX17 as an endodermal marker as shown by immunofluorescence staining (Figure 3(b)). This ability to differentiate into all three germ layers could be underlined by qRT-PCR (Figure 3(c)). Comparable expression levels for different differentiation markers between knockdown and control cells showed that the knockdown does not lead to an altered germ layer preference or diminished differentiation potential. Taken together, the *TBX3* knockdown significantly reduced the reprogramming efficiency but the still arising iPSCs were comparable to control iPSCs.

4. Discussion

TBX3 is a core member of the pluripotency network of transcription factors which keeps ESCs and iPSCs in the pluripotent state. Therefore, we were interested if a knockdown of *TBX3* expression would affect the reprogramming process or alter the resulting stem cells in their characteristics. For this, we used two human cell types, fibroblasts and keratinocytes, containing an inducible shRNA directed against *TBX3*. Reprogramming of these cells did not show altered reprogramming kinetics but a reduced reprogramming efficiency compared to control cells. This result was similar for both tested cell types. The number of arising colonies was significantly smaller than in control AP stainings. RNA levels of pluripotency factors were also reduced during the reprogramming process, indicating lower pluripotent cell numbers. Fully reprogrammed cells of later passages, however, did not exhibit altered RNA levels of pluripotency factors. They were also comparable to controls in stem cell marker immunofluorescence stainings. After induction of differentiation, they expressed markers of the three germ layers in a ratio comparable to control cells, without altered germ layer preference. This stays in contrast to a previous study indicating that *TBX3* knockdown inhibits neural rosette formation [20]. However, since we solely investigated RNA levels and not the appearance of neural rosettes, a disturbed rosette morphology cannot be excluded. Interestingly, we found that although the knockdown of *TBX3* was very constant throughout the reprogramming process, in later passage iPSCs it was not visible any more. Here, we suppose that the shRNA does not reduce the very low expression levels any further or that iPSCs may be able to silence the shRNA expression after several passages.

In the future, studies could investigate if the reduction of reprogramming efficiency, as observed with *TBX3* knockdown cells, will also be present in *TBX3* depleted cells or if these cells even fail to be reprogrammed at all. If stable iPSCs can be obtained in this way, their differentiation behavior should be studied in detail since TBX3 is well known to also have important contributions in certain differentiation pathways.

Conflict of Interests

The authors declare that there is no conflict of interests regarding the publication of this paper.

Authors' Contribution

Stefanie Raab and Moritz Klingenstein contributed equally to this paper.

Acknowledgments

The authors would like to thank Clara Misbah for the technical assistance. This study was funded by the Deutsche Forschungsgemeinschaft (Stefan Liebau BO1718/4-1), the Forschungskern SyStaR to Alexander Kleger, BIU (Böhringer Ingelheim Ulm to Alexander Kleger), and the Else-Kröner-Fresenius-Stiftung (2011_A200, to Alexander Kleger and Stefan Liebau). Alexander Kleger is indebted to the Baden-Württemberg Stiftung for the financial support of this research project by the Eliteprogramme for Postdocs. Alexander Kleger is also an Else-Kröner-Fresenius Memorial Fellow. Leonhard Linta is supported by a fortüne junior grant of the Faculty of Medicine Tübingen (2248-0-0).

References

[1] Y. Tanaka, E. Hysolli, J. Su et al., "Transcriptome signature and regulation in human somatic cell reprogramming," *Stem Cell Reports*, vol. 4, no. 6, pp. 1125–1139, 2015.

[2] E. A. Mason, J. C. Mar, A. L. Laslett et al., "Gene expression variability as a unifying element of the pluripotency network," *Stem Cell Reports*, vol. 3, no. 2, pp. 365–377, 2014.

[3] G. Martello and A. Smith, "The nature of embryonic stem cells," *Annual Review of Cell and Developmental Biology*, vol. 30, no. 1, pp. 647–675, 2014.

[4] V. Karwacki-Neisius, J. Göke, R. Osorno et al., "Reduced Oct4 expression directs a robust pluripotent state with distinct signaling activity and increased enhancer occupancy by Oct4 and Nanog," *Cell Stem Cell*, vol. 12, no. 5, pp. 531–545, 2013.

[5] K. Takahashi and S. Yamanaka, "Induction of pluripotent stem cells from mouse embryonic and adult fibroblast cultures by defined factors," *Cell*, vol. 126, no. 4, pp. 663–676, 2006.

[6] K. Takahashi, K. Tanabe, M. Ohnuki et al., "Induction of pluripotent stem cells from adult human fibroblasts by defined factors," *Cell*, vol. 131, no. 5, pp. 861–872, 2007.

[7] Q. Feng, N. Shabrani, J. N. Thon et al., "Scalable generation of universal platelets from human induced pluripotent stem cells," *Stem Cell Reports*, vol. 3, no. 5, pp. 817–831, 2014.

[8] H. Kamao, M. Mandai, S. Okamoto et al., "Characterization of human induced pluripotent stem cell-derived retinal pigment epithelium cell sheets aiming for clinical application," *Stem Cell Reports*, vol. 2, no. 2, pp. 205–218, 2014.

[9] L. Linta, M. Stockmann, T. M. Boeckers, A. Kleger, and S. Liebau, "The potential of iPS cells in synucleinopathy research," *Stem Cells International*, vol. 2012, Article ID 629230, 6 pages, 2012.

[10] M. Rao, "IPSC-based cell therapy: an important step forward," *Stem Cell Reports*, vol. 1, no. 4, pp. 281–282, 2013.

[11] F. A. Soares, M. Sheldon, M. Rao, C. Mummery, and L. Vallier, "International coordination of large-scale human induced pluripotent stem cell initiatives: wellcome Trust and ISSCR workshops white paper," *Stem Cell Reports*, vol. 3, no. 6, pp. 931–939, 2014.

[12] L. Ye, C. Swingen, and J. Zhang, "Induced pluripotent stem cells and their potential for basic and clinical sciences," *Current Cardiology Reviews*, vol. 9, no. 1, pp. 63–72, 2013.

[13] J. Han, P. Yuan, H. Yang et al., "*Tbx3* improves the germ-line competency of induced pluripotent stem cells," *Nature*, vol. 463, no. 7284, pp. 1096–1100, 2010.

[14] C. E. Weidgang, R. Russell, P. R. Tata et al., "TBX3 directs cell-fate decision toward mesendoderm," *Stem Cell Reports*, vol. 1, no. 3, pp. 248–265, 2013.

[15] A. E. R. Kartikasari, J. X. Zhou, M. S. Kanji et al., "The histone demethylase Jmjd3 sequentially associates with the transcription factors Tbx3 and Eomes to drive endoderm differentiation," *The EMBO Journal*, vol. 32, no. 10, pp. 1393–1408, 2013.

[16] T. Aasen, A. Raya, M. J. Barrero et al., "Efficient and rapid generation of induced pluripotent stem cells from human keratinocytes," *Nature Biotechnology*, vol. 26, no. 11, pp. 1276–1284, 2008.

[17] E. Warlich, J. Kuehle, T. Cantz et al., "Lentiviral vector design and imaging approaches to visualize the early stages of cellular reprogramming," *Molecular Therapy*, vol. 19, no. 4, pp. 782–789, 2011.

[18] L. Linta, M. Stockmann, K. N. Kleinhans et al., "Rat embryonic fibroblasts improve reprogramming of human keratinocytes into induced pluripotent stem cells," *Stem Cells and Development*, vol. 21, no. 6, pp. 965–976, 2012.

[19] S. Frank, M. Zhang, H. R. Schöler, and B. Greber, "Small molecule-assisted, line-independent maintenance of human pluripotent stem cells in defined conditions," *PLoS ONE*, vol. 7, no. 7, Article ID e41958, 2012.

[20] T. Esmailpour and T. Huang, "TBX3 promotes human embryonic stem cell proliferation and neuroepithelial differentiation in a differentiation stage-dependent manner," *Stem Cells*, vol. 30, no. 10, pp. 2152–2163, 2012.

Hindawi Publishing Corporation
Stem Cells International
Volume 2016, Article ID 5272498, 11 pages
http://dx.doi.org/10.1155/2016/5272498

Research Article

NFATc4 Regulates *Sox9* Gene Expression in Acinar Cell Plasticity and Pancreatic Cancer Initiation

Elisabeth Hessmann,[1] Jin-San Zhang,[2,3] Nai-Ming Chen,[1] Marie Hasselluhn,[1] Geou-Yarh Liou,[4] Peter Storz,[4] Volker Ellenrieder,[1] Daniel D. Billadeau,[2] and Alexander Koenig[1,2]

[1]*Department of Gastroenterology and Gastrointestinal Oncology, University Medical Center Göttingen, Robert-Koch Street 40, 37075 Göttingen, Germany*
[2]*Schulze Center for Novel Therapeutics, Division of Oncology Research, Mayo Clinic, 200 1st Street SW No. W4, Rochester, MN 55905, USA*
[3]*School of Pharmaceutical Sciences and Key Laboratory of Biotechnology and Pharmaceutical Engineering, Wenzhou Medical University, Wenzhou, Zhejiang, China*
[4]*Department of Cancer Biology, Mayo Clinic Cancer Center, 4500 San Pablo Road, Jacksonville, FL 32224, USA*

Correspondence should be addressed to Alexander Koenig; alexander.koenig@med.uni-goettingen.de

Received 15 May 2015; Accepted 12 July 2015

Academic Editor: Silvia Brunelli

Acinar transdifferentiation toward a duct-like phenotype constitutes the defining response of acinar cells to external stress signals and is considered to be the initial step in pancreatic carcinogenesis. Despite the requirement for oncogenic Kras in pancreatic cancer (PDAC) development, oncogenic Kras is not sufficient to drive pancreatic carcinogenesis beyond the level of premalignancy. Instead, secondary events, such as inflammation-induced signaling activation of the epidermal growth factor (EGFR) or induction of Sox9 expression, are required for tumor formation. Herein, we aimed to dissect the mechanism that links EGFR signaling to Sox9 gene expression during acinar-to-ductal metaplasia in pancreatic tissue adaptation and PDAC initiation. We show that the inflammatory transcription factor NFATc4 is highly induced and localizes in the nucleus in response to inflammation-induced EGFR signaling. Moreover, we demonstrate that NFATc4 drives acinar-to-ductal conversion and PDAC initiation through direct transcriptional induction of *Sox9*. Therefore, strategies designed to disrupt NFATc4 induction might be beneficial in the prevention or therapy of PDAC.

1. Introduction

Pancreatic ductal adenocarcinoma (PDAC) is among the most aggressive human malignancies with a 5-year survival rate of less than 7% [1]. PDAC arises from well-defined precursor lesions, with pancreatic intraepithelial neoplasia (PanIN) being the best described [2, 3]. Oncogenic mutations of the *Kras* gene represent the defining molecular alteration in pancreatic carcinogenesis and can be detected in early PanIN lesions and in more than 90% of advanced human PDAC, leading to the current dogma that this genetic event is required for PDAC initiation and progression [4, 5]. Lineage-tracing studies have demonstrated that acinar cells expressing oncogenic Kras lose their grape-like structure and undergo a de- and transdifferentiation process termed acinar-to-ductal metaplasia (ADM) to generate metaplastic lesions with a duct-like phenotype [4, 5]. Characteristically, dedifferentiation of mature exocrine pancreatic cells involves a gene expression profile that highly resembles the one found in the embryonic pancreas [6, 7], including activation of Notch signaling or induction of the sex-determining region Y-box 9 (Sox9) transcription factor [6, 8]. Importantly, the progenitor-like characteristics of metaplastic acinar cells make them more susceptible to Kras-induced oncogenesis [6, 9]. In fact, oncogenic Kras hijacks the acinar redifferentiation process that occurs in regenerative pancreatic tissue and

instead promotes a transition from metaplastic cells to PanIN precursor lesions that eventually progress to invasive PDAC [10, 11].

Significantly, ADM formation and neoplastic progression in the context of Kras mutation occur with a low penetrance and a long latency, unless secondary events arise which drive pancreatic carcinogenesis beyond the stage of premalignancy [2, 3, 5]. Inflammatory environmental cues are well appreciated to promote pancreatic carcinogenesis on the background of oncogenic Kras mutations [5], thus reflecting epidemiologic studies characterizing chronic pancreatitis as the major risk factor for PDAC development [12]. Examination of chronic pancreatitis patient samples revealed an upregulation of epidermal growth factor receptor expression in metaplastic pancreatic lesions [13–15]. Interestingly, transgenic EGFR ligand overexpression promoted the formation of pancreatic metaplasia [16, 17], whereas EGFR inactivation utilizing genetic or pharmacological approaches suppressed acinar-to-ductal transdifferentiation by oncogenic Kras activation and inflammation [9, 18]. Taken together, these data suggest that EGFR activation is required for inflammation-driven acinar dedifferentiation and PDAC initiation. Nevertheless, the exact molecular mechanisms that link EGFR activation to acinar transdifferentiation remain elusive.

Herein we sought to determine how inflammatory signaling pathways in metaplastic pancreatic cells bridge EGFR activation to transcriptional induction of key mediators of acinar cell dedifferentiation. In particular, we sought to characterize the impact of NFATc4 (nuclear factor of activated T-cells 4) on transcriptional activation of the ductal fate determinant *Sox9* during acinar-ductal transdifferentiation. We show that NFATc4 gene expression is highly induced during EGFR-stimulated acinar-to-ductal conversion in acinar explants and is required for duct formation and the expression of Sox9 in this *in vitro* system. Moreover, we show that NFATc4 protein is expressed in metaplastic areas during inflammation-induced pancreatic carcinogenesis using mouse models and human tissues. Importantly, genetic or pharmacological inactivation of NFATc4 abrogates transcriptional activation of *Sox9* and hinders development of metaplastic pancreatic lesions.

2. Materials and Methods

2.1. Animals. Generation and characterization of *pdx1-Cre* and *LSL-Kras^{G12D}* animals have been described previously [2, 19]. Mouse strains were interbred to obtain *Kras^{G12D}*; *pdx1-Cre* animals. All strains had a C57Bl/6 background. For genotyping, PCRs were performed following digestion of tail cuts by using PCR buffer with nonionic detergents (PBND) and protein kinase (Applichem, Darmstadt, Germany). For induction of chronic pancreatitis, 8-week-old mice were subjected to caerulein (50 μg/kg, 3 times/week) or dimethyl sulfoxide (DMSO) treatment for 4 weeks. All animal experiments were performed using protocols approved by the Institutional Animal Care and Use Committee at the Philipps University Marburg in Germany.

2.2. Acinar Cell Isolation. Acinar cell isolation was performed as described previously [17]. Briefly, the whole pancreas was dissected and incubated at 37°C in a collagenase I-containing solution. The minced pancreas was passed through a 105 μm nylon filter to isolate acinar cells. After repetitive washing steps acinar cells were exposed to culture solution containing 30% fetal calf serum for a short time. Then cells were cultured in collagen supplemented with 1% heat-inactivated fetal bovine serum and, unless indicated otherwise, treated with DMSO and/or ddH_2O, CsA (1 μM), TGFα (50 ng/mL), or EGF (20 ng/mL). Ducts were counted after indicated time points using brightfield microscopy and Hoechst 33324 staining to show cell viability.

2.3. Cell Lines and Transfections. The acinar cell line 266-6 was obtained from Jemal et al. [20]. Primary tumor cells from *Kras^{G12D}*; *p53$^{\Delta/wt}$*; *pdx1-Cre* and *Kras^{G12D}*; *p53$^{\Delta/wt}$*; *EGFR$^{-/-}$*; *pdx1-Cre* mice were a kind gift from Jens Siveke, TU Munich, Germany. Cells were cultured in Dulbecco's modified Eagle medium (DMEM, Gibco, Darmstadt, Germany) supplemented with 10% fetal calf serum (Gibco) or in serum-containing DMEM supplemented with 1% nonessential amino acids, respectively. For EGF and TGFβ treatment, cells were starved in serum-free medium for 24 h and afterwards stimulated with EGF (20 ng/mL) or with TGFβ (10 ng/mL) as indicated.

For NFATc4 shRNA delivery in acinar cell explants, NFATc4 shRNAs (#1 5′-CGAGGTGGAGTCTGAACTTAA-3′; #2 5′-GCCAGACTCTAAAGTGGTGTT-3′) or control shRNAs (5′-CCTAAGGTTAAGTCGCCCTCG-3′) were infected using a lentiviral infection system as previously described [21]. For transfection of 266-6 acinar cells, NFATc4 siRNA was obtained from Life Technologies (5′-ccaguccaggucuacuuuutt-3′). Cells were transfected with NFATc4 siRNA for 48 h, using lipofectamine 2000 (Invitrogen). The constitutive active EGFR construct was obtained from Martin Privalsky. For reexpression of constitutive active EGFR, cells were transfected with either 3 μg of EGFR or a control vector utilizing lipofectamine 2000 (Invitrogen).

2.4. RNA Isolation and Quantitative Real-Time PCR Analysis. For RNA isolation from acinar cells, solidified collagen was dissolved using collagenase I (Sigma). RNA from cell lines and acinar cells was isolated utilizing the RNeasy Mini Kit (Qiagen, Hilden, Germany) and first-strand complementary DNA was synthesized from 1 μg of total RNA using random primers and the Omniscript Reverse Transcriptase Kit (Qiagen). RPLP0 was used as a housekeeping gene for normalization of gene expression. Mouse specific primers with the following sequences were used for expression analysis: NFATc1 (forward: 5′-tgggagatggaagcaaagac-3′; reverse: 5′-atagaaactgacttggacggg-3′), NFATc2 (forward: 5′-aagaggaaacgaagtcagcc-3′ reverse: 5′-tgggtgctgtgggtaatatg-3′) NFATc3 (forward: 5′-gaaactgaaggtagccgagg-3′ reverse: 5′-ctggtaaaatgcatgaggtcg-3′), NFATc4 (forward: 5′-tcttcaggacctctgccctа-3′; reverse: 5′-agcctaggagcttgaccaca-3′), Sox9 (forward: 5′-cgtgcagcacaagaaagacca-3′; reverse: 5′-gcagcgccttgaagatagcat-3′), cytokeratin 19 (forward: 5′-cctcccgcgattacaaccact-3′;

reverse: 5′-ggcgagcattgtcaatctgt-3′), cytokeratin 6 (forward: 5′-gagcagatcaagaccctcaac-3′; reverse: 5′-aaacataggctccaggttctg-3′), EGFR (forward: 5′-acactgctggtgttgctgac; reverse: 5′-cccaaggaccacttcacagt-3′), and RPLP0 (forward: 5′-tgacatcgtctttaaaccccg-3′; reverse: 5′-tgtctgctcccacaatgaag-3′).

2.5. Protein Isolation and Immunoblotting. For protein isolation from cell lines, whole cell lysates were prepared using lysis buffer (50 mmol/L HEPES, pH 7.5–7.9, 150 mmol/L NaCl, 1 mmol/L ethylene glycol-bis(β-aminoethylether)-N,N,N′,N′-tetraacetic acid, 10% glycerin, 1% Triton X-100, 100 mmol/L NaF, and 10 mmol/L $Na_4P_2O_7\times$ 10 H_2O) containing protease inhibitors. For immunoblot analysis 20 μg of protein extracts was electrophoresed through 10% sodium dodecyl sulfate/polyacrylamide gels and transferred onto nitrocellulose membranes (Millipore, Darmstadt, Germany). Protein detection was performed using the following antibodies: NFATc4 (Abcam, ab62613, 1 : 1000) and β-actin (Sigma, 1 : 20000).

2.6. Histological Evaluation and Immunohistochemistry. Human chronic pancreatitis samples were obtained from 9 different patients and were derived from the Institute of Pathology of the Philipps University Marburg in accordance with the ethical regulations of the institute. For immunohistochemistry, formalin-fixed, paraffin-embedded tissue was sectioned (4 μm). H&E staining and immunohistochemistry were performed as described previously [22]. The following antibodies were used: NFATc4 (Santa Cruz, sc13036), EGFR (Abcam, ab52894), pEGFR (Santa Cruz, sc101668), and Sox9 (Abcam, ab26414).

2.7. Chromatin Immunoprecipitation (ChIP). ChIP analysis in 266-6 cells was performed as described previously [23]. Briefly, cells were cross-linked in medium containing 1% formaldehyde for 10 minutes at room temperature. Cross-linking was terminated utilizing 2.5 mol/L glycine. Cells were washed and harvested in ice-cold PBS. Nuclear lysates were obtained and DNA was sheered to fragments of 500 base pairs by sonication. The following antibodies were added to precleared chromatin for overnight incubation at 4°C: NFATc4 (Abcam, ab62613, 4 μg), H3K4me3 (Cell Signalling 9727s, 2 μg), RNA-polymerase II (Millipore, 05-623, 2 μg), rabbit IgG (Santa Cruz, sc-2027, 2 μg), and mouse IgG (Santa Cruz, sc-2025, 2 μg). Protein A or G agarose was added and incubated for 2 hours. Beads were washed as described before [23] and reversion was performed using RNAse A (R4642, Sigma), protein kinase, and 5 mol/L sodium dodecyl sulfate overnight at 65°C. DNA was isolated using a phenol-chloroform protocol and analyzed via qRT-PCR utilizing Sox9 primers with the following sequences: +370 (forward: 5′-cgcgtatgaatctcctggac-3′, reverse: 5′-ggtgttctccgtgtccg-3′) and −825 (forward: 5′-ccgggaaaggacttgtcag-3′, reverse: 5′-tctggttcaacgaagctgg-3′).

3. Results

3.1. NFATc4 Is Highly Induced during EGFR-Mediated Acinar-to-Ductal Metaplasia. In addition to its pivotal role in PDAC initiation, acinar-to-ductal metaplasia represents a cellular adaptation process of the acinar cell in response to external stress signals which prevents stress-mediated cell death and can result in a stepwise regeneration program that reconstitutes pancreatic tissue integrity [24–26]. Either acute or chronic pancreatic inflammation results in the formation of metaplastic pancreatic lesions that can redifferentiate into acinar cells in a permissive cellular context [27]. Metaplastic lesions of chronic pancreatitis patients regularly express high levels of the epidermal growth factor receptor (EGFR) family and their natural ligands EGF and TGFα [12, 13, 16]. Recent reports have indicated that EGFR activation integrates external inflammatory cues into intracellular programs that mediate acinar cell adaptation and dedifferentiation [9, 17, 18, 28]. Accordingly, in an *in vitro* approach utilizing acinar cell explants from wildtype mice, activation of EGFR signaling by stimulation with TGFα strongly promoted transdifferentiation of explanted acinar cells into cells with duct-like characteristics (Figure 1(a)). The striking transdifferentiation behavior of pancreatic acinar cells in response to EGFR signaling activation is based on stepwise dedifferentiation processes of acinar cells and subsequent activation of ductal initiation programs [9, 18]. This crucial regulation of cellular plasticity is at least partially mediated by spatially and temporally controlled activation of the nuclear factor of activated T-cell (NFAT) family of transcription factors [22]. NFAT is a critical mediator of Ca^{2+}/calcineurin signaling. NFAT functions were initially recognized in T-cell activation, where it regulates vital cellular functions related to adaptation and differentiation [29]. Importantly, expression and function of NFAT proteins are by no means limited to immune cells. Rather, cellular adaptation in several tissues has been attributed to NFAT-dependent signaling and transcription [30, 31]. In pancreatic acinar cells, basal expression levels of the four Ca^{2+}/calcineurin-responsive NFAT family members were low (Figure 1(b)). Strikingly, TGFα stimulation of the acinar cell explants resulted in a time-dependent rise of NFATc1 and NFATc4 mRNA levels, while the expression of NFATc2 and NFATc3 was not altered (Figure 1(b)), consistent with previous reports suggesting that NFAT proteins do not have redundant functions [32]. The most prominent response to TGFα treatment was observed for NFATc4, suggesting that activation of this particular isoform might be essential during EGFR signaling-dependent acinar-to-ductal transdifferentiation (Figure 1(b)). To test whether EGFR signaling is required for NFATc4 activation, we utilized primary PDAC cells from *Kras*^{G12D}; *p53*$^{\Delta/wt}$; *EGFR*$^{-/-}$; *pdx1-Cre* mice with a homozygous deletion of EGFR. As shown in Figures 1(c) and 1(d), NFATc4 expression is low in EGFR depleted cells but is inducible in response to transient overexpression of constitutive active EGFR (Figures 1(c) and 1(d)). However, the induction of cellular plasticity in pancreatic exocrine cells has also been reported following treatment with the inflammatory cytokine TGFβ [33] and TGFβ treatment of pancreatic tumor cells promotes a transdifferentiation program leading to epithelial to mesenchymal transition (EMT) [33]. Most strikingly, TGFβ stimulation of primary PDAC cells obtained from *Kras*^{G12D}; *p53*$^{\Delta/wt}$; *pdx1-Cre* mice resulted in the induction of several NFAT genes, including robust induction of

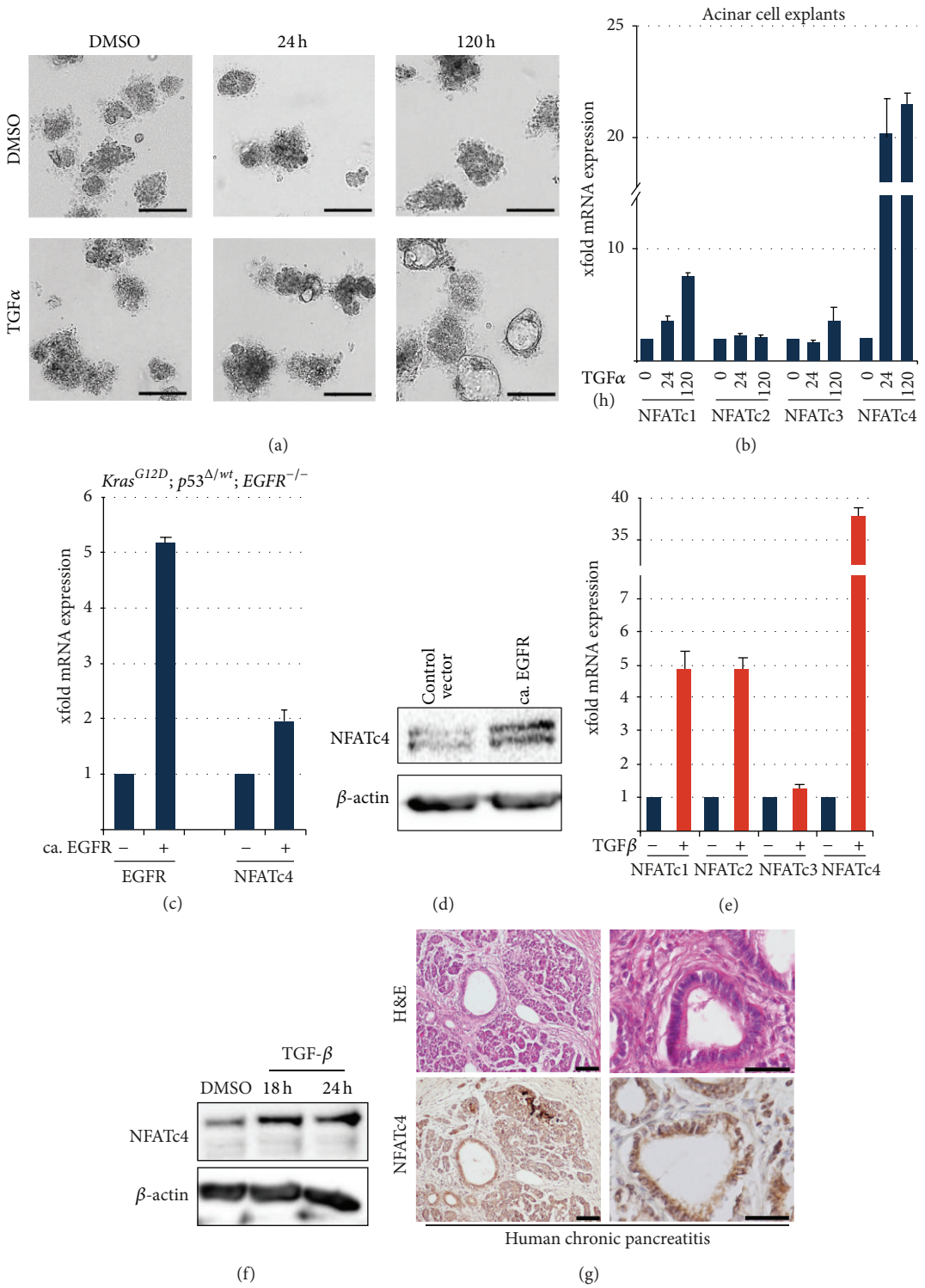

Figure 1: NFATc4 is induced in acinar cell transdifferentiation. (a) Light microscopy shows morphology of acinar cell extracts from wildtype mice in response to TGFα for the indicated time points (scale bar represents 100 μm). (b) qRT-PCR to detect mRNA expression of NFAT isoforms in transdifferentiating acinar cells of wildtype mice in response to TGFα. (c)-(d) NFATc4 mRNA (c) and protein (d) expression levels in $Kras^{G12D}$; $p53^{\Delta/wt}$; $EGFR^{-/-}$; *pdx1-Cre* mice were determined after transient overexpression of a control vector or constitutive EGFR, respectively. NFATc4 mRNA expression following EGFR overexpression was normalized to control (means ± SD). (e) qRT-PCR reveals mRNA expression of NFAT isoforms in primary tumor cells from $Kras^{G12D}$; $p53^{\Delta/wt}$; *pdx1-Cre* mice following TGFβ treatment for 24 hours. (f) Western Blot analysis in primary tumor cells from $Kras^{G12D}$; $p53^{\Delta/wt}$; *pdx1-Cre* mice upon TGFβ treatment. β-actin was utilized as a loading control. (g) Representative H&E staining and immunohistochemistry were performed in human chronic pancreatitis samples. Scale bar represents 100 μm. Asterisks indicate NFATc4 positive nuclei.

NFATc4 mRNA and protein (Figures 1(e) and 1(f)). Lastly, we observed increased NFATc4 staining in the nuclei of cells within the metaplastic areas of a tissue from a patient with chronic pancreatitis (Figure 1(g)). Taken together, these data are consistent with the notion that NFATc4 is induced during the process of ADM in a mouse explant model and in human pancreatic tissue.

3.2. NFATc4 Is Involved in EGFR-Mediated Acinar-to-Ductal Metaplasia. To test whether induction of NFATc4 is crucial for acinar-to-ductal conversion, we cotreated acinar cell explants with TGFα and cyclosporin A (CsA), a clinically used calcineurin inhibitor which prevents NFAT activation. Inhibition of calcineurin-NFAT signaling significantly attenuated acinar-to-ductal conversion, even in the presence of EGFR activation (Figure 2(a)). Consequently, duct formation was inhibited and cytokeratin 19 expression was decreased following CsA treatment (Figures 2(b) and 2(c)). Since pharmacological inhibition of calcineurin neither specifically inhibits the NFAT signaling pathway nor targets individual members of the NFAT family, we extended our analysis and genetically depleted NFATc4 in acinar cell explants using two specific NFATc4 shRNAs (Figure 2(d)). Importantly, depletion of NFATc4 expression significantly reduced TGFα-mediated duct formation in this ADM assay (Figures 2(d) and 2(e)). Consistent with the reduced duct-forming capacity of NFATc4-depleted acinar explants, we found diminished expression of cytokeratins 6 and 19, two marker genes that are induced during the process of acinar-to-ductal differentiation (Figures 2(f)–2(h)). Taken together, these data implicate NFATc4 as a critical EGFR-induced transcription factor involved in acinar cell reprogramming.

3.3. NFATc4 Is Induced during Pancreatic Cancer Initiation. Acinar-to-ductal transdifferentiation is not limited to the physiological mechanisms of cellular adaptation, but it is now appreciated for its pivotal role in PDAC initiation [8]. Importantly, progression of inflammation-driven ADM to neoplastic lesions requires oncogenic mutation of *Kras* ($Kras^{G12D}$) in the metaplastic epithelial cell to block acinar redifferentiation and reconstitution of normal pancreatic architecture [34]. Hence, inflammation-induced EGFR signaling cooperates with oncogenic *Kras* mutation to promote pancreatic carcinogenesis [9, 22]. To examine whether NFATc4 activation is involved in PDAC initiation, we took advantage of an *in vivo* model of inflammation-driven pancreatic carcinogenesis. Specifically, we utilized a genetically engineered mouse model (GEMM) harboring a pancreas specific *Kras* mutation ($Kras^{G12D}$; *pdx1-Cre* mice) and treated these animals with caerulein, a well-established inducer of pancreatic inflammation [22, 30, 34]. A 4-week treatment regimen led to severe exocrine pancreatic injury with disordered acinar structure and induction of acinar-to-ductal metaplasia and early PanIN lesions as a result of increased acinar cell plasticity and initiation of pancreatic carcinogenesis (Figure 3(a)). Importantly, EGFR expression was remarkably induced in metaplastic exocrine cells upon pancreatic inflammation, visualized by enhanced cytosolic localization of its active phosphorylated form in caerulein-treated mice (Figure 3(a)). As reported previously, the metaplastic areas were characterized by strong induction of nuclear Sox9 expression, a pivotal marker of cellular reprogramming (Figure 3(a)), while the control group displayed only low cytosolic expression of the transcription factor. Strikingly, metaplastic areas and PanIN lesions with high EGFR, pEGFR, and Sox9 expressions also showed a dramatic increase of NFATc4 expression (Figure 3(a)). Consistent with our analyses in human chronic pancreatitis samples, NFATc4 expression in ADM areas in response to caerulein administration was predominantly detected in the nucleus, thus indicating activity of the transcription factor.

3.4. EGFR Signaling Involves NFATc4-Dependent Transcriptional Activation of Sox9. The formation and maintenance of pancreatic metaplastic lesions depend on the expression and activation of transcription factors that drive acinar transdifferentiation toward a duct-like phenotype. Recently, *Sox9* was implicated in cellular plasticity upon PDAC initiation and progression [8, 22, 35]. In accordance with these observations, acinar cell explants showed an increase of Sox9 mRNA expression following EGFR activation (Figure 3(b)), suggesting that Sox9 expression during acinar cell conversion is regulated at the transcription level. The concomitant expression of NFATc4 and Sox9 in metaplastic pancreatic cells suggests a mechanistic connection of both transcription factors. This assumption is further strengthened by the fact that genetic depletion of NFATc4 expression not only alters duct formation in the ADM model but also abrogated expression of Sox9 mRNA (Figure 3(b)). Moreover, TGFβ-mediated time-dependent induction of NFATc4 expression in primary tumor cells from $Kras^{G12D}$; $p53^{\Delta/wt}$; *pdx1-Cre* mice correlated with increased Sox9 expression (Figures 3(c) and 3(d)). Together, our data identify *Sox9* as an NFATc4 target gene and implicate that both transcription factors functionally cooperate to drive the transdifferentiation processes in the pancreas.

To further scrutinize the mechanistic correlation of NFATc4 and Sox9 expression, we performed chromatin immunoprecipitation (ChIP) analysis in the acinar cell line 266-6 upon activation of EGFR signaling and in primary tumor cells from $Kras^{G12D}$; $p53^{\Delta/wt}$; *pdx1-Cre* mice upon TGFβ treatment. In both cell systems, EGFR activation as well as TGFβ treatment resulted in an increased recruitment of NFATc4 to the *Sox9* promoter (Figures 4(a) and 4(b)), which correlated with enhanced occupancy of H3K4me3 and RNA-polymerase II on the *Sox9* promoter, indicating its transcriptional activity (Figures 4(c) and 4(d)). Both increased NFATc4 binding to the *Sox9* promoter and the enhanced promoter activity upon extracellular stimulation suggest a critical involvement of NFATc4 in the transcriptional regulation of Sox9. To verify this hypothesis, we genetically depleted NFATc4 expression in 266-6 acinar cells and investigated the impact of NFATc4 deficiency on EGFR-mediated Sox9 expression. Significantly, loss of NFATc4 significantly diminished EGFR-dependent induction of Sox9 expression in 266-6 acinar cells (Figures 4(e) and 4(f)).

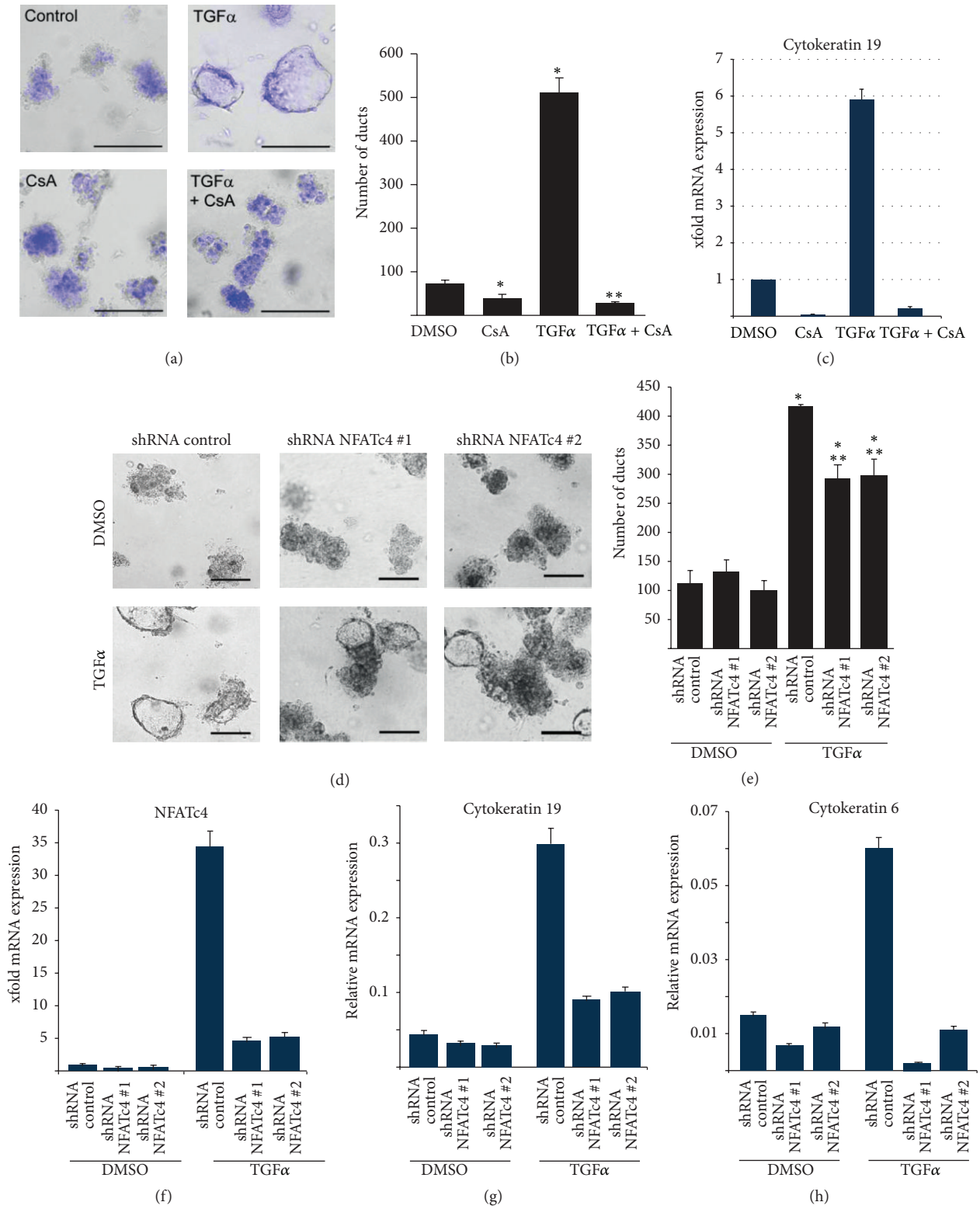

Figure 2: NFATc4 is required for acinar-to-ductal transdifferentiation in the pancreas. (a) Brightfield microscopy reveals acinar cell morphology upon TGFα and/or CsA treatment for 5 days (scale bars indicate 100 μm). Hoechst 33342 was used to stain alive cells embedded in collagen at day 5. (b) Quantification of duct formation was performed five days after acinar cell extraction from wildtype mice. (c) qRT-PCR shows cytokeratin 19 expression in acinar cell explants upon indicated treatments for 5 days. (d)–(h) Acinar cells from wildtype mice were subjected to two different NFATc4 shRNAs or shRNA controls and were stimulated with TGFα for 5 days. (d) Brightfield microscopy was conducted to determine acinar cell morphology (scale bars indicate 100 μm). (e) Quantification of duct formation was performed on day 5 following acinar cell extraction. (f)–(h) mRNA expression levels of the indicated genes were detected on day 5 following acinar cell extraction.

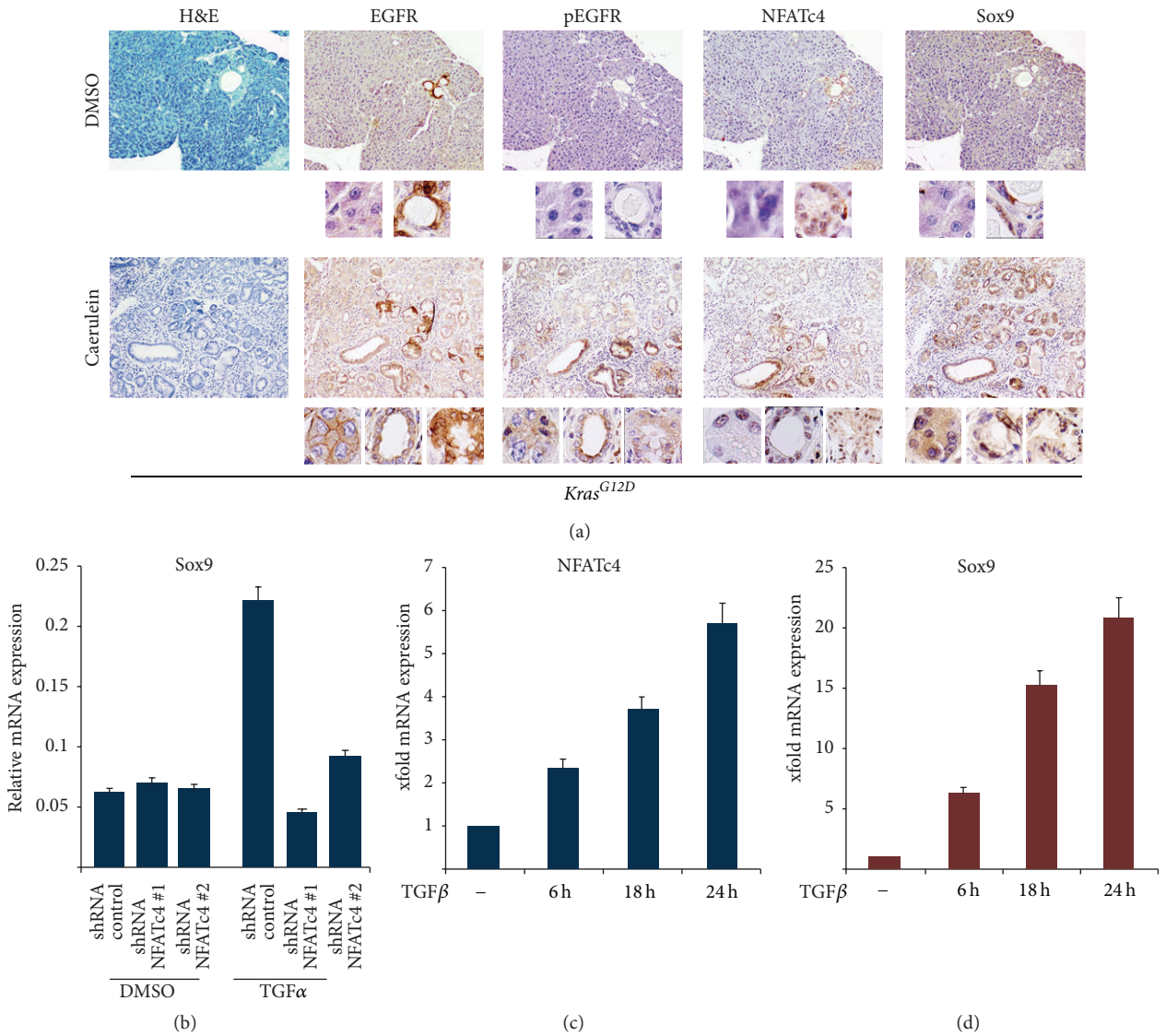

Figure 3: NFATc4 activation in metaplastic cells is associated with transcriptional induction of *Sox9*. (a) H&E staining as well as immunohistochemistry in 3-month-old $Kras^{G12D}$; *pdx1-Cre* mice following a four-week spanning treatment with caerulein or DMSO. The black boxes beyond the immunohistochemical staining display representative magnifications of normal acinar cells (left boxes), ADM (right box for the control group, middle box for the caerulein-treated mice), and PanIN lesions (right boxes in the caerulein cohort). (b) qRT-PCR reveals Sox9 mRNA expression in acinar cell explants from wildtype mice following genetic depletion of NFATc4 and TGFα stimulation for 5 days. (c)-(d) Primary pancreatic tumor cells from $Kras^{G12D}$; $p53^{\Delta/wt}$; *pdx1-Cre* mice were treated with TGFβ for the indicated time points. mRNA expression of NFATc4 (c) and Sox9 (d) was determined by using qRT-PCR.

Taken together, these data suggest that EGFR-stimulated NFATc4 gene expression and activation constitute a prerequisite for the transcriptional induction of *Sox9* and the process of acinar-to-ductal transdifferentiation.

4. Discussion

Acinar-to-ductal transdifferentiation represents a mechanism of cellular reprogramming in response to external stress signals, thus initiating pancreatic regeneration of damaged epithelial cells [36]. In the presence of an oncogenic Kras mutation, the function of ADM shifts from a preserver of pancreatic tissue integrity to a driver of neoplastic progression toward frank adenocarcinoma [34]. ADM induction and progression to neoplastic precursor lesions are closely linked to inflammation-induced activation of EGFR signaling [9, 17, 18]. Importantly, EGFR-mediated induction of ADM involves activation of genes that promote and maintain the ductal phenotype [37]. For instance, EGFR activation in response to epithelial injury has been shown to induce Sox9 expression in urothelial cancer [37], suggesting the involvement of an EGFR-Sox9 axis in malignant development and progression. The prominent function of Sox9 in tumorigenesis is also reflected in the pancreas, where Sox9

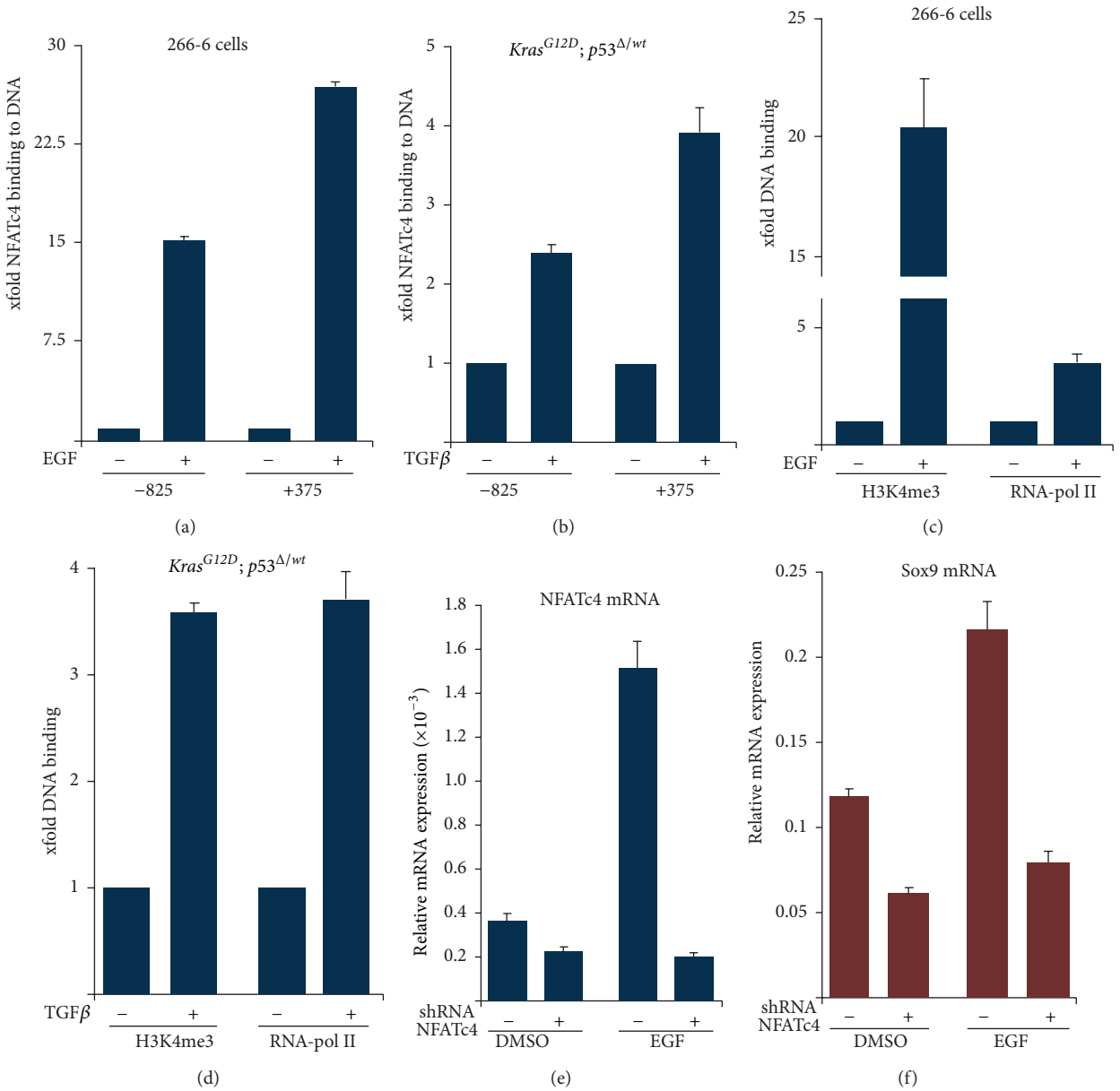

Figure 4: Sox9 represents a transcriptional NFATc4 target in metaplastic pancreatic cells. (a)–(d) ChIP analyses in 266-6 cells ((a) and (c)) and in primary tumor cells from *Kras*^{G12D}; *p53*$^{\Delta/wt}$; *pdx1-Cre* mice ((b) and (d)) were conducted in the following EGF (3 hours) or TGFβ (24 hours) treatment, respectively. (a)-(b) qRT-PCR was performed to determine NFATc4 occupancy on the *Sox9* promoter regions −825 and +370. Data was normalized to IgG and displayed as xfold binding compared to control. (c)-(d) H4K3me3 and polymerase II enrichment are demonstrated on the Sox9 promoter region +370. Data was normalized to IgG and displayed as xfold binding compared to control. (e)-(f) qRT-PCR to detect NFATc4 (e) and Sox9 (f) mRNA expressions following genetic depletion of NFATc4 and EGF treatment (3 hours).

was described as a central transcription factor during acinar cell dedifferentiation and ductal conversion [8]. While loss of Sox9 during acinar cell dedifferentiation hindered ADM formation and neoplastic progression, ectopic induction of Sox9 accelerated Kras^{G12D}-driven pancreatic carcinogenesis [8]. Although the relevance of an EGFR-Sox9 pathway has been demonstrated in several cellular contexts, the mechanisms linking inflammation-induced EGFR activation to Sox9 induction in PDAC initiation remained elusive. Here we identify the transcription factor NFATc4 as a functional link connecting inflammation-induced EGFR signaling to acinar metaplasia and show that induction of Sox9 in response to EGFR activation requires NFATc4-dependent transcriptional activation of the *Sox9* promoter.

The NFAT family of transcription factors has been reported to be involved in the integration of environmental signals into oncogenic processes that mediate proliferation, differentiation, and adaptation to inflammation in several

cellular contexts [31, 38, 39]. For instance, recent work linked EGFR activation to NFAT-mediated Cox2 expression in colorectal tumorigenesis, thus pointing toward a critical role of the EGFR/NFAT cascade in the integration of inflammatory signals during carcinogenesis and progression [40]. In the pancreas, oncogenic activity has been demonstrated for the isoforms NFATc1 and NFATc2 that both accelerate $Kras^{G12D}$-driven pancreatic carcinogenesis and PDAC progression in mice and humans [23, 31, 41, 42]. Importantly, the oncogenic activity of NFAT transcription factors not only is limited to neoplastic progression, but also comprises PDAC initiation. We recently showed that NFATc1 becomes activated in response to inflammation-induced EGFR signaling and complexes with c-Jun to promote acinar-ductal conversion by transcriptional induction of the *Sox9* gene [22]. Consistently, attenuation of NFATc1 activity using pharmacological or genetic approaches hindered EGFR-mediated promotion of acinar-to-ductal transdifferentiation [22], thus underlining the pivotal function of NFAT transcription factors in acinar cell adaptation and oncogenic conversion.

In comparison to its close relatives NFATc1 and NFATc2, less is known about the role of NFATc4 in pancreatic tissue adaptation and carcinogenesis. Here we show that NFATc4 is induced in an experimental setting of chronic pancreatitis and PDAC initiation and that inhibition of NFATc4 signaling preserves acinar cell morphology and function, indicating that the transcription factor might cooperate with oncogenic Kras signaling to promote pancreatic cancer initiation. The first evidence for a functional link between NFATc4 activation and neoplastic progression came from a study investigating patients with esophageal squamous dysplasia, which showed that enhanced expression levels of NFATc4 were associated with a higher chance of progression towards esophageal cancer [43]. Further underlining the role of NFATc4 in tumorigenesis, non-small lung cell cancer samples which were positively stained for oncogenic Cox2 displayed high expression levels of NFATc4 and the AP1 proteins c-Fos and c-Jun [44]. This is of particular interest, as c-Jun functions as the *bona fide* partner of NFAT transcription factors in pancreatic adaptation and neoplastic progression [22], suggesting that both transcription factors cooperate to drive acinar cell dedifferentiation.

In summary, we describe a novel mechanism of inflammation-induced cellular adaptation during PDAC initiation and propose a model in which NFATc4 links EGFR signaling activation to transcriptional induction of *Sox9* to promote acinar ductal dedifferentiation. Our data complements the wide functional spectrum of NFAT transcription factors in pancreatic adaptation and carcinogenesis and suggests that pharmacological strategies that target NFAT activation might pave the road for new preventive or therapeutic options in PDAC.

5. Conclusion

Pancreatic ductal adenocarcinoma (PDAC) represents a devastating disease with a dismal prognosis that has remained unchanged during the past several decades. Therefore, a better understanding of the molecular mechanisms that control PDAC initiation and progression is urgently needed in order to combat or prevent pancreatic cancer.

Herein we report a novel molecular mechanism that links EGFR signaling to activation of Sox9 during acinar-ductal metaplasia in pancreatic tissue adaptation and PDAC initiation. We identify the inflammatory transcription factor NFATc4 as a critical mediator of inflammation-induced EGFR signaling activation and demonstrate that NFATc4 drives acinar-to-ductal conversion and PDAC initiation through transcriptional induction of *Sox9*. Therefore, strategies designed to disrupt this pathway might be considered for the prevention and therapy of PDAC.

Conflict of Interests

The authors declare that they do not have any conflict of interests.

Authors' Contribution

Daniel D. Billadeau and Alexander Koenig share last authorship.

Acknowledgments

The authors kindly thank Kristina Reutlinger and Sarah Hanheide (both at the Department of Gastroenterology and Gastrointestinal Oncology, University Medical Center Göttingen) for technical support. The authors are grateful to Jens Siveke, TU Munich, Germany, for providing primary tumor cells from $Kras^{G12D}$; $p53^{\Delta/wt}$; *pdx1-Cre* and $Kras^{G12D}$; $p53^{\Delta/wt}$; $EGFR^{-/-}$; *pdx1-Cre* mice. This work was supported by the German Cancer Research Foundation (109423 to Volker Ellenrieder and a Mildred Scheel Fellowship to Alexander Koenig), the Wilhelm Sander Foundation (2013.037.1 to Volker Ellenrieder), a postdoctoral fellowship from the Center of Regenerative Medicine at the Mayo Clinic, Jacksonville (to Geou-Yarh Liou), the National Cancer Institute (R01 CA140182 to Peter Storz), and a National Cancer Institute Pancreas SPORE grant (P50 CA102701 to Daniel D. Billadeau).

References

[1] T. Seufferlein, M. Porzner, T. Becker et al., "S3-guideline exocrine pancreatic cancer," *Zeitschrift für Gastroenterologie*, vol. 51, no. 12, pp. 1395–1440, 2013.

[2] S. R. Hingorani, E. F. Petricoin III, A. Maitra et al., "Preinvasive and invasive ductal pancreatic cancer and its early detection in the mouse," *Cancer Cell*, vol. 4, no. 6, pp. 437–450, 2003.

[3] S. R. Hingorani, L. Wang, A. S. Multani et al., "Trp53R172H and KrasG12D cooperate to promote chromosomal instability and widely metastatic pancreatic ductal adenocarcinoma in mice," *Cancer Cell*, vol. 7, no. 5, pp. 469–483, 2005.

[4] L. Zhu, G. Shi, C. M. Schmidt, R. H. Hruban, and S. F. Konieczny, "Acinar cells contribute to the molecular heterogeneity of pancreatic intraepithelial neoplasia," *The American Journal of Pathology*, vol. 171, no. 1, pp. 263–273, 2007.

[5] C. Guerra, A. J. Schuhmacher, M. Cañamero et al., "Chronic pancreatitis is essential for induction of pancreatic ductal adenocarcinoma by K-Ras oncogenes in adult mice," *Cancer Cell*, vol. 11, no. 3, pp. 291–302, 2007.

[6] Y. Miyamoto, A. Maitra, B. Ghosh et al., "Notch mediates TGFα-induced changes in epithelial differentiation during pancreatic tumorigenesis," *Cancer Cell*, vol. 3, no. 6, pp. 565–576, 2003.

[7] S. Y. Song, M. Gannon, M. K. Washington et al., "Expansion of Pdx1-expressing pancreatic epithelium and islet neogenesis in transgenic mice overexpressing transforming growth factor alpha," *Gastroenterology*, vol. 117, no. 6, pp. 1416–1426, 1999.

[8] J. L. Kopp, G. von Figura, E. Mayes et al., "Identification of Sox9-dependent acinar-to-ductal reprogramming as the principal mechanism for initiation of pancreatic ductal adenocarcinoma," *Cancer Cell*, vol. 22, no. 6, pp. 737–750, 2012.

[9] C. M. Ardito, B. M. Grüner, K. K. Takeuchi et al., "EGF receptor is required for KRAS-induced pancreatic tumorigenesis," *Cancer Cell*, vol. 22, no. 3, pp. 304–317, 2012.

[10] P. A. Pérez-Mancera, C. Guerra, M. Barbacid, and D. A. Tuveson, "What we have learned about pancreatic cancer from mouse models," *Gastroenterology*, vol. 142, no. 5, pp. 1079–1092, 2012.

[11] M. A. Collins, F. Bednar, Y. Zhang et al., "Oncogenic Kras is required for both the initiation and maintenance of pancreatic cancer in mice," *The Journal of Clinical Investigation*, vol. 122, no. 2, pp. 639–653, 2012.

[12] D. Yadav and A. B. Lowenfels, "The epidemiology of pancreatitis and pancreatic cancer," *Gastroenterology*, vol. 144, no. 6, pp. 1252–1261, 2013.

[13] M. Korc, B. Chandrasekar, Y. Yamanaka, H. Friess, M. Buchler, and H. G. Beger, "Overexpression of the epidermal growth factor receptor in human pancreatic cancer is associated with concomitant increases in the levels of epidermal growth factor and transforming growth factor alpha," *Journal of Clinical Investigation*, vol. 90, no. 4, pp. 1352–1360, 1992.

[14] K. Tobita, H. Kijima, S. Dowaki et al., "Epidermal growth factor receptor expression in human pancreatic cancer: significance for liver metastasis," *International Journal of Molecular Medicine*, vol. 11, no. 3, pp. 305–309, 2003.

[15] M.-L. H. Fjällskog, M. H. Lejonklou, K. E. Öberg, B. K. Eriksson, and E. T. Janson, "Expression of molecular targets for tyrosine kinase receptor antagonists in malignant endocrine pancreatic tumors," *Clinical Cancer Research*, vol. 9, no. 4, pp. 1469–1473, 2003.

[16] A. L. Means, K. C. Ray, A. B. Singh et al., "Overexpression of heparin-binding EGF-like growth factor in mouse pancreas results in fibrosis and epithelial metaplasia," *Gastroenterology*, vol. 124, no. 4, pp. 1020–1036, 2003.

[17] A. L. Means, I. M. Meszoely, K. Suzuki et al., "Pancreatic epithelial plasticity mediated by acinar cell transdifferentiation and generation of nestin-positive intermediates," *Development*, vol. 132, no. 16, pp. 3767–3776, 2005.

[18] C. Navas, I. Hernández-Porras, A. J. Schuhmacher, M. Sibilia, C. Guerra, and M. Barbacid, "EGF receptor signaling is essential for k-ras oncogene-driven pancreatic ductal adenocarcinoma," *Cancer Cell*, vol. 22, no. 3, pp. 318–330, 2012.

[19] E. L. Jackson, N. Willis, K. Mercer et al., "Analysis of lung tumor initiation and progression using conditional expression of oncogenic K-ras," *Genes and Development*, vol. 15, no. 24, pp. 3243–3248, 2001.

[20] A. Jemal, R. Siegel, E. Ward, Y. Hao, J. Xu, and M. J. Thun, "Cancer statistics, 2009," *CA: Cancer Journal for Clinicians*, vol. 59, no. 4, pp. 225–249, 2009.

[21] M. Herreros-Villanueva, J.-S. Zhang, A. Koenig et al., "SOX2 promotes dedifferentiation and imparts stem cell-like features to pancreatic cancer cells," *Oncogenesis*, vol. 2, article e61, 2013.

[22] N. Chen, G. Singh, A. Köenig et al., "NFATc1 links EGFR signaling to induction of sox9 transcription and acinar-ductal transdifferentiation in the pancreas," *Gastroenterology*, vol. 148, no. 5, pp. 1024.e9–1034.e9, 2015.

[23] S. Baumgart, E. Glesel, G. Singh et al., "Restricted heterochromatin formation links NFATc2 repressor activity with growth promotion in pancreatic cancer," *Gastroenterology*, vol. 142, no. 2, pp. 388–398.e7, 2012.

[24] V. Fendrich, F. Esni, M. V. R. Garay et al., "Hedgehog signaling is required for effective regeneration of exocrine pancreas," *Gastroenterology*, vol. 135, no. 2, pp. 621–631, 2008.

[25] A. Fukuda, J. P. Morris, and M. Hebrok, "Bmi1 is required for regeneration of the exocrine pancreas in mice," *Gastroenterology*, vol. 143, no. 3, pp. 821.e2–831.e2, 2012.

[26] G. von Figura, J. P. Morris IV, C. V. E. Wright, and M. Hebrok, "Nr5a2 maintains acinar cell differentiation and constrains oncogenic Kras-mediated pancreatic neoplastic initiation," *Gut*, vol. 63, no. 4, pp. 656–664, 2014.

[27] C. Carrière, A. L. Young, J. R. Gunn, D. S. Longnecker, and M. Korc, "Acute pancreatitis markedly accelerates pancreatic cancer progression in mice expressing oncogenic Kras," *Biochemical and Biophysical Research Communications*, vol. 382, no. 3, pp. 561–565, 2009.

[28] I. Rooman and F. X. Real, "Pancreatic ductal adenocarcinoma and acinar cells: a matter of differentiation and development?" *Gut*, vol. 61, no. 3, pp. 449–458, 2012.

[29] J.-P. Shaw, P. J. Utz, D. B. Durand, J. J. Toole, E. A. Emmel, and G. R. Crabtree, "Identification of a putative regulator of early T cell activation genes," *Science*, vol. 241, no. 4862, pp. 202–205, 1988.

[30] G. T. Gurda, S. J. Crozier, B. Ji et al., "Regulator of calcineurin 1 controls growth plasticity of adult pancreas," *Gastroenterology*, vol. 139, no. 2, pp. 609.e6–619.e6, 2010.

[31] S. Baumgart, N.-M. Chen, J. T. Siveke et al., "Inflammation-induced NFATc1-STAT3 transcription complex promotes pancreatic cancer initiation by KrasG12D," *Cancer Discovery*, vol. 4, no. 6, pp. 688–701, 2014.

[32] M. Mancini and A. Toker, "NFAT proteins: emerging roles in cancer progression," *Nature Reviews Cancer*, vol. 9, no. 11, pp. 810–820, 2009.

[33] V. Ellenrieder, A. Buck, A. Harth et al., "KLF11 mediates a critical mechanism in TGF-beta signaling that is inactivated by ERK-MAPK in pancreatic cancer cells," *Gastroenterology*, vol. 127, no. 2, pp. 607–620, 2004.

[34] C. Guerra, M. Collado, C. Navas et al., "Pancreatitis-induced inflammation contributes to pancreatic cancer by inhibiting oncogene-induced senescence," *Cancer Cell*, vol. 19, no. 6, pp. 728–739, 2011.

[35] A. Fukuda and T. Chiba, "Sox9-dependent acinar-to-ductal reprogramming is critical for pancreatic intraepithelial neoplasia formation," *Gastroenterology*, vol. 145, no. 4, pp. 904–907, 2013.

[36] A. Maitra and R. H. Hruban, "Pancreatic cancer," *Annual Review of Pathology*, vol. 3, pp. 157–188, 2007.

[37] S. Ling, X. Chang, L. Schultz et al., "An EGFR-ERK-SOX9 signaling cascade links urothelial development and regeneration to cancer," *Cancer Research*, vol. 71, no. 11, pp. 3812–3821, 2011.

[38] G. T. Gurda, L. Guo, S.-H. Lee, J. D. Molkentin, and J. A. Williams, "Cholecystokinin activates pancreatic calcineurin-NFAT signaling in vitro and in vivo," *Molecular Biology of the Cell*, vol. 19, no. 1, pp. 198–206, 2008.

[39] M. Buchholz, A. Schatz, M. Wagner et al., "Overexpression of c-*myc* in pancreatic cancer caused by ectopic activation of NFATc1 and the Ca^{2+}/calcineurin signaling pathway," *The EMBO Journal*, vol. 25, no. 15, pp. 3714–3724, 2006.

[40] T. Cai, X. Li, J. Ding, W. Luo, J. Li, and C. Huang, "A cross-talk between NFAT and NF-κB pathways is crucial for nickel-induced COX-2 expression in beas-2B cells," *Current Cancer Drug Targets*, vol. 11, no. 5, pp. 548–559, 2011.

[41] A. Köenig, T. Linhart, K. Schlengemann et al., "NFAT-induced histone acetylation relay switch promotes c-Myc-dependent growth in pancreatic cancer cells," *Gastroenterology*, vol. 138, no. 3, pp. 1189.e2–1199.e2, 2010.

[42] S. K. Singh, N.-M. Chen, E. Hessmann et al., "Antithetical NFATc1-Sox2 and p53-miR200 signaling networks govern pancreatic cancer cell plasticity," *The EMBO Journal*, vol. 34, no. 4, pp. 517–530, 2015.

[43] N. Joshi, L. L. Johnson, W.-Q. Wei et al., "Gene expression differences in normal esophageal mucosa associated with regression and progression of mild and moderate squamous dysplasia in a high-risk Chinese population," *Cancer Research*, vol. 66, no. 13, pp. 6851–6860, 2006.

[44] X. Zhao, Z. Chen, S. Zhao, and J. He, "Expression and significance of COX-2 and its transcription factors NFAT3 and c-Jun in non-small cell lung cancer," *Zhongguo Fei Ai Za Zhi*, vol. 13, no. 11, pp. 1035–1040, 2010.

Hindawi Publishing Corporation
Stem Cells International
Volume 2016, Article ID 6205485, 11 pages
http://dx.doi.org/10.1155/2016/6205485

Research Article

Transcriptome Analysis of Long Noncoding RNAs in Toll-Like Receptor 3-Activated Mesenchymal Stem Cells

Shihua Wang, Xiaoxia Li, and Robert Chunhua Zhao

Center of Excellence in Tissue Engineering, Institute of Basic Medical Sciences and Peking Union Medical College Hospital, School of Basic Medicine, Peking Union Medical College, Chinese Academy of Medical Sciences, Beijing 100005, China

Correspondence should be addressed to Robert Chunhua Zhao; zhaochunhua@vip.163.com

Received 30 March 2015; Revised 21 May 2015; Accepted 11 June 2015

Academic Editor: Stefan Liebau

Mesenchymal stem cells (MSCs) possess great immunomodulatory capacity which lays the foundation for their therapeutic effects in a variety of diseases. Recently, toll-like receptors (TLR) have been shown to modulate MSC functions; however, the underlying molecular mechanisms are poorly understood. Emerging evidence suggests that long noncoding RNAs (lncRNAs) are an important class of regulators involved in a wide range of biological processes. To explore the potential involvement of lncRNAs in TLR stimulated MSCs, we performed a comprehensive lncRNA and mRNA profiling through microarray. 10.2% of lncRNAs (1733 out of 16967) and 15.1% of mRNA transcripts (1760 out of 11632) were significantly differentially expressed (absolute fold-change ≥5 , P value ≤ 0.05) in TLR3 stimulated MSCs. Furthermore, we characterized the differentially expressed lncRNAs through their classes and length distribution and correlated them with differentially expressed mRNA. Here, we are the first to determine genome-wide lncRNAs expression patterns in TLR3 stimulated MSCs by microarray and this work could provide a comprehensive framework of the transcriptome landscapes of TLR3 stimulated MSCs.

1. Introduction

Mesenchymal stem cells (MSCs) are a type of adult stem cells with the capacity to generate a wide range of cells such as adipocytes, osteoblasts, chondrocytes, and myocytes [1]. Being originally identified from the bone marrow, MSCs now can be isolated from many other tissues including adipose tissue, placenta, and umbilical cord. MSCs also possess potent immunoregulatory abilities through interactions with both the adaptive and the innate immune cells. The immunomodulatory effect of MSCs is mediated by the secretion of soluble factors and/or by cell-cell contact-dependent regulation. These features make MSCs an interesting cell resource for tissue regeneration and cellular therapy.

Recently, the findings of functional toll-like receptors (TLRs) expression on MSC implicate these receptors in modulating MSCs functions [2]. TLRs are pattern recognition receptors involved in the recognition of pathogen-associated molecular patterns (PAMP) by immune cells, initiating both primary and adaptive immune responses [3]. To date, thirteen mammalian TLR analogs have been identified (10 in humans and 13 in mice). Beside their important roles in immunity, TLRs have also been recognized as regulators of stem cells functions, including cell growth, differentiation, and survival. For instance, De Luca et al. showed that TLR1/2 signaling instructed commitment of human hematopoietic stem cells to a myeloid cell fate [4]. Qi et al. demonstrated that both TLR3 and TLR4 promoted differentiation of bone marrow MSCs to osteoblasts [5].

In the field of immunology, recent publications have shown widespread changes in the expression of lncRNAs during the activation of the innate immune response and T cell development, differentiation, and activation [6]. It is well known that TLRs and their specific stimulus activate MyD88-dependent or -independent downstream signaling pathways. However, whether epigenetic regulators such as long noncoding RNA are involved in this process remains unclear. In this study, we determined the TLR expression profile of adipose tissue derived MSCs (AD-MSCs) and the consequences of TLR3 ligation in terms of cytokine secretion by these cells.

To explore the potential involvement of lncRNAs in TLR stimulated MSCs, we performed comprehensive lncRNA and mRNA profiling through microarray. 10.2% of lncRNAs (1733 out of 16967) and 15.1% of mRNA transcripts (1760 out of 11632) were significantly differentially expressed (absolute fold-change ≥5, P value ≤ 0.05) in TLR3 stimulated MSCs. Furthermore, we characterized the differentially expressed lncRNAs through their classes and length distribution and correlated them with differentially expressed mRNA. To the best of our knowledge, this is the first study that links TLR3 with lncRNAs in MSCs.

2. Materials and Methods

2.1. Isolation and Culture of AD-MSCs. Adipose tissues were obtained from patients undergoing tumescent liposuction according to procedures approved by the Ethics Committee at the Chinese Academy of Medical Sciences and Peking Union Medical College. AD-MSCs were isolated and culture-expanded as previously reported [1, 7]. Passage 3 cells were used for the experiments.

2.2. Adipogenic and Osteogenic Differentiation of AD-MSCs. Adipogenic differentiation was induced in high glucose of Dulbecco's Modified Eagle's Medium (H-DMEM) supplemented with 10% FBS, 1 μM dexamethasone, 0.5 mM 3-isobutyl-1-methylxanthine, and 5 μg/mL 0.1 mM l-ascorbic acid. After being cultured in adipocyte induction medium for 4 days, medium was replaced with adipocyte maintaining medium, H-DMEM, with 10% FBS. For osteogenic differentiation, AD-MSCs were cultured in H-DMEM containing 10% FBS, 10 mM β-glycerophosphate, 50 μmM l-ascorbic acid, and 0.01 μM dexamethasone for 14 days.

2.3. ALP and Oil Red O Staining. The procedure of ALP staining was performed according to the manufacturer's instructions of ALP staining kit (Institute of Hematology and Blood Diseases Hospital, Chinese Academy of Medical Sciences). For oil red O staining, cells were washed twice with PBS and fixed with 10% formalin for 10 min at room temperature. After fixation, cells were stained with filtered oil red O solution (stock solution: 3 mg/mL in isopropanol, working solution: 60% oil red O stock solution and 40% distilled water) for 1 h at room temperature. After staining, cells were washed with water to remove unbound dye, visualized by light microscopy, and photographed.

2.4. Real-Time Polymerase Chain Reaction Analysis. Total RNA was extracted with TRIzol (Invitrogen), and cDNA was prepared. Real-time polymerase chain reaction (PCR) was amplified in triplicates according to manufacturer's procedures (TaKaRa). Relative expression of mRNA was evaluated by $2^{-\Delta\Delta Ct}$ method and normalized to the expression of GAPDH.

2.5. Cytokines Production. AD-MSCs were seeded in 12-well plate in culture medium with or without Poly I:C. Supernatants were collected after 24 h and concentrations of IL-1β, IL-4, IL-6, IL-8, IL-10, IL-12, TNF-α, TGFβ, and IFN-γ were determined by enzyme-linked immunosorbent assay (ELISA) (R&D system) according to the manufacturer's instructions.

2.6. Microarray and Data Analysis. Arraystar Human LncRNA Microarray V3.0 is designed for the global profiling of human LncRNAs and protein-coding transcripts, which is updated from the previous microarray V2.0. About 30,586 LncRNAs and 26,109 coding transcripts can be detected by our third-generation LncRNA microarray. The LncRNAs are carefully constructed using the most highly respected public transcriptome databases (Refseq, UCSC knowngenes, Gencode, etc.), as well as landmark publications. Each transcript is represented by a specific exon or splice junction probe which can identify individual transcript accurately. Total RNA was extracted and examined for quality control before array. The OD260/OD280 ratios were approximately 2.0, and the OD260/OD230 ratios were more than 1.8 (Supplementary Table 1 in Supplementary Material available online at http://dx.doi.org/10.1155/2016/6205485). Positive probes for housekeeping genes and negative probes are also printed onto the array for hybridization quality control. (1) RNA labeling and array hybridization are as follows: sample labeling and array hybridization were performed according to the Agilent One-Color Microarray-Based Gene Expression Analysis protocol (Agilent Technology) with minor modifications. Briefly, mRNA was purified from total RNA after removal of rRNA (mRNA-ONLY Eukaryotic mRNA Isolation Kit, Epicentre). Then, each sample was amplified and transcribed into fluorescent cRNA along the entire length of the transcripts without 3′ bias utilizing a random priming method (Arraystar Flash RNA Labeling Kit, Arraystar). The labeled cRNAs were purified by RNeasy Mini Kit (Qiagen). The concentration and specific activity of the labeled cRNAs (pmol Cy3/μg cRNA) were measured by NanoDrop ND-1000. 1 μg of each labeled cRNA was fragmented by adding 5 μL 10× blocking agent and 1 μL of 25× fragmentation buffer and then the mixture was heated at 60°C for 30 min; finally, 25 μL 2× GE hybridization buffer was added to dilute the labeled cRNA. 50 μL of hybridization solution was dispensed into the gasket slide and assembled to the LncRNA expression microarray slide. The slides were incubated for 17 hours at 65°C in an Agilent Hybridization Oven. The hybridized arrays were washed, fixed, and scanned using the Agilent DNA Microarray Scanner (part number G2505C). Quality control for labeling efficiency was shown in Supplementary Table 2.

(2) Data analysis is as follows: slides were scanned at 5 lm/pixel resolution using an Axon GenePix 4000B scanner (Molecular Devices Corporation) piloted by GenePix Pro 6.0 software (Axon). Scanned images (TIFF format) were then imported into NimbleScan software (version 2.5) for grid alignment and expression data analysis. Expression data were normalized through quantile normalization and the Robust Multichip Average (RMA) algorithm included in the NimbleScan software. The probe level files and mRNA level files were generated after normalization. All gene level files were imported into Agilent GeneSpring GX software (version

Table 1: PCR primers specific to TLR-1 and to TLR-10.

Gene	Sense primer (5′~3′)	Antisense primer (5′~3′)
TLR1	CCACGTTCCTAAAGACCTATCCC	CCAAGTGCTTGAGGTTCACAG
TLR2	ATCCTCCAATCAGGCTTCTCT	GGACAGGTCAAGGCTTTTTACA
TLR3	TTGCCTTGTATCTACTTTTGGGG	TCAACACTGTTATGTTTGTGGGT
TLR4	AGACCTGTCCCTGAACCCTAT	CGATGGACTTCTAAACCAGCCA
TLR5	TCCCTGAACTCACGAGTCTTT	GGTTGTCAAGTCCGTAAAATGC
TLR6	TGAATGCAAAAACCCTTCACCT	CCAAGTCGTTTCTATGTGGTTGA
TLR7	CACATACCAGACATCTCCCCA	CCCAGTGGAATAGGTACACAGTT
TLR8	ATGTTCCTTCAGTCGTCAATGC	TTGCTGCACTCTGCAATAACT
TLR9	CTGCCACATGACCATCGAG	GGACAGGGATATGAGGGATTTGG
TLR10	GGTTCTTTTGCGTGATGGAATC	GGTCGTCCCAGAGTAAATCAAC

Table 2: Summary of microarray analysis results.

Probe class	Total	Expressed above background	Differentially expressed*
LncRNA	30586	16967 (55.5%)	1733 (10.2%)
mRNA	26109	11632 (44.5%)	1760 (15.1%)
Combined	56695	28599 (50.4%)	3493 (12.2%)

*Significant differential expression was defined as probes with $P \leq 0.05$ and absolute fold-change ≥5.

11.5.1) and normalized by the quantile method; then, Combat software was used to adjust the normalized intensity to remove batch effects. Hierarchical clustering was performed using Agilent GeneSpring GX software (version 11.5.1). The analysis was performed by KangChen Biotech., Shanghai, China. Agilent Feature Extraction software (version 11.0.1.1) was used to analyze acquired array images. We have four samples; three were control MSCs and one is TLR3-activated MSCs. LncRNAs and mRNAs that have flags in Present or Marginal (all targets value) in at least 2 out of the 3 control MSCs samples were chosen for further data analysis. Differentially expressed LncRNAs and mRNAs with statistical significance between the two groups were identified through *P* value/FDR filtering. Hierarchical clustering and combined analysis were performed using homemade scripts. For gene ontology analysis, Fisher's exact test was used to determine whether the overlap between the differentially expressed gene list and the GO annotation list was greater than that expected by chance. The *P* value denotes the significance of GO term enrichment in the differentially expressed genes.

3. Results

3.1. Characterization of AD-MSCs and the Expression Pattern of TLRs. We isolated and expanded plastic adherent, spindle-like mesenchymal stem cells from adipose tissue (Figure 1(a)). AD-MSCs expressed high levels of CD29, CD44, and CD105 but were persistently negative for CD31, CD34, and HLA-DR (Figure 1(b)). Osteogenic differentiation was detected by Alizarin red staining and ALP activity assay (Figure 1(c)). Adipogenic differentiation was demonstrated by oil red O staining (Figure 1(c)). The expression of TLRs in MSCs remains controversial. PCR primers specific to TLR-1 and to TLR-10 were designed to detect TLRs from total RNA in AD-MSCs (Table 1). RT-PCR results showed that all TLRs were detectable within 33 cycles and that TLR3 has the highest expression level (Figure 1(d)).

3.2. Effect of TLR3 Agonist on Cytokine Expression of AD-MSCs. Since TLR3 had the highest expression level, to evaluate its functionality, we stimulated AD-MSCs with TLR3 agonist (Poly I:C 20 μg/mL) for 24 h and determined its effect on cell proliferation and cytokine secretion. Poly I:C slightly decreased proliferation of AD-MSCs (Figure 2(a)). Flow cytometry analysis of cell cycles showed that Poly I:C stimulated AD-MSCs had enhanced G2 phase (Figure 2(b)). We measured a number of cytokines known to be involved in immunomodulation, including IL-1β, IL-4,IL-6, IL-8, IL-10, IL-12, TNF-α, TGFβ, and IFN-γ. We found that Poly I:C induced upregulation of IL-1β, IL-6, IL-8, and TNF-α as measured by RT-PCR (Figure 2(c)). Enhanced release of these cytokines was also detected by ELISA (Figure 2(d)). Exposure to poly (I:C) also increased the expression of TLR3 (Figure 2(e)).

3.3. Overview of lncRNA and mRNA Profiles in TLR3-Activated AD-MSCs and Control AD-MSCs. To examine the lncRNA expression profiles in AD-MSCs treated with or without TLR3 agonist, we used Arraystar Human LncRNA Microarray V3.0 which contains 30,586 lncRNA probes, collected from RefSeq, UCSC knowngenes, Gencode, and so forth, and 26,109 mRNA probes. The overview of lncRNA expression profiles is summarized in Table 2 and Figure 3(a). Overall, we found that 55.5% of lncRNAs (16967 out of 30586) and 44.5% of protein-coding mRNA transcripts (11632 out of 26109) on the microarray exhibited expression above background. 10.2% of lncRNAs (1733 out of 16967) and 15.1% of protein-coding mRNA transcripts (1760 out of 11632) were significantly differentially expressed (absolute fold-change ≥5, P value ≤ 0.05) between TLR3-activated AD-MSCs

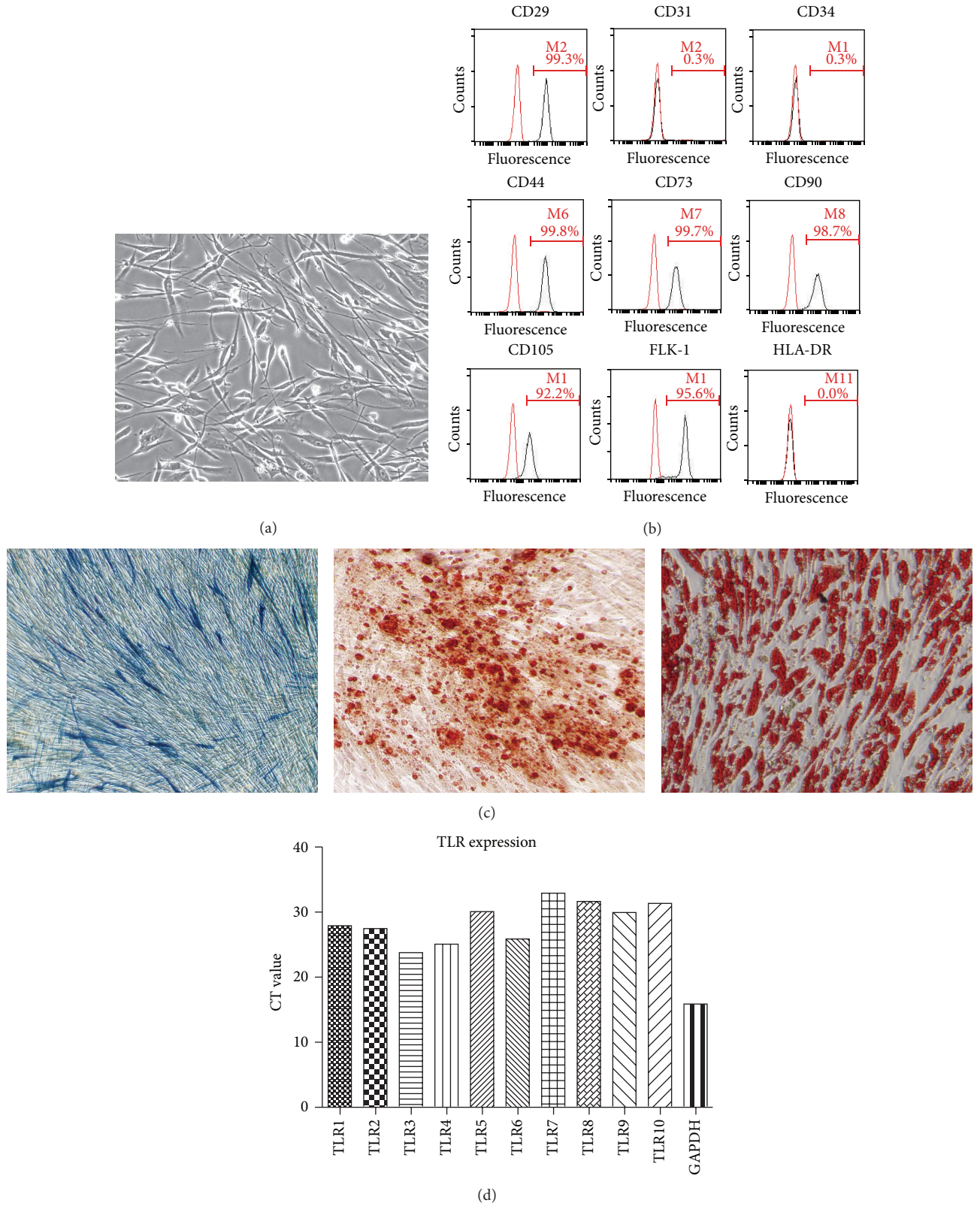

Figure 1: Characterization of AD-MSCs and the expression pattern of TLRs. (a) The cell morphology of AD-MSCs observed under light microscope. (b) Immunophenotype of AD-MSCs. (c) Differentiation capacity of AD-MSCs was demonstrated by ALP staining (left) and Alizarin red staining (centered) for osteoblasts and oil red O staining for adipocytes (right). (d) The expression levels of TLRs were analyzed by real-time PCR.

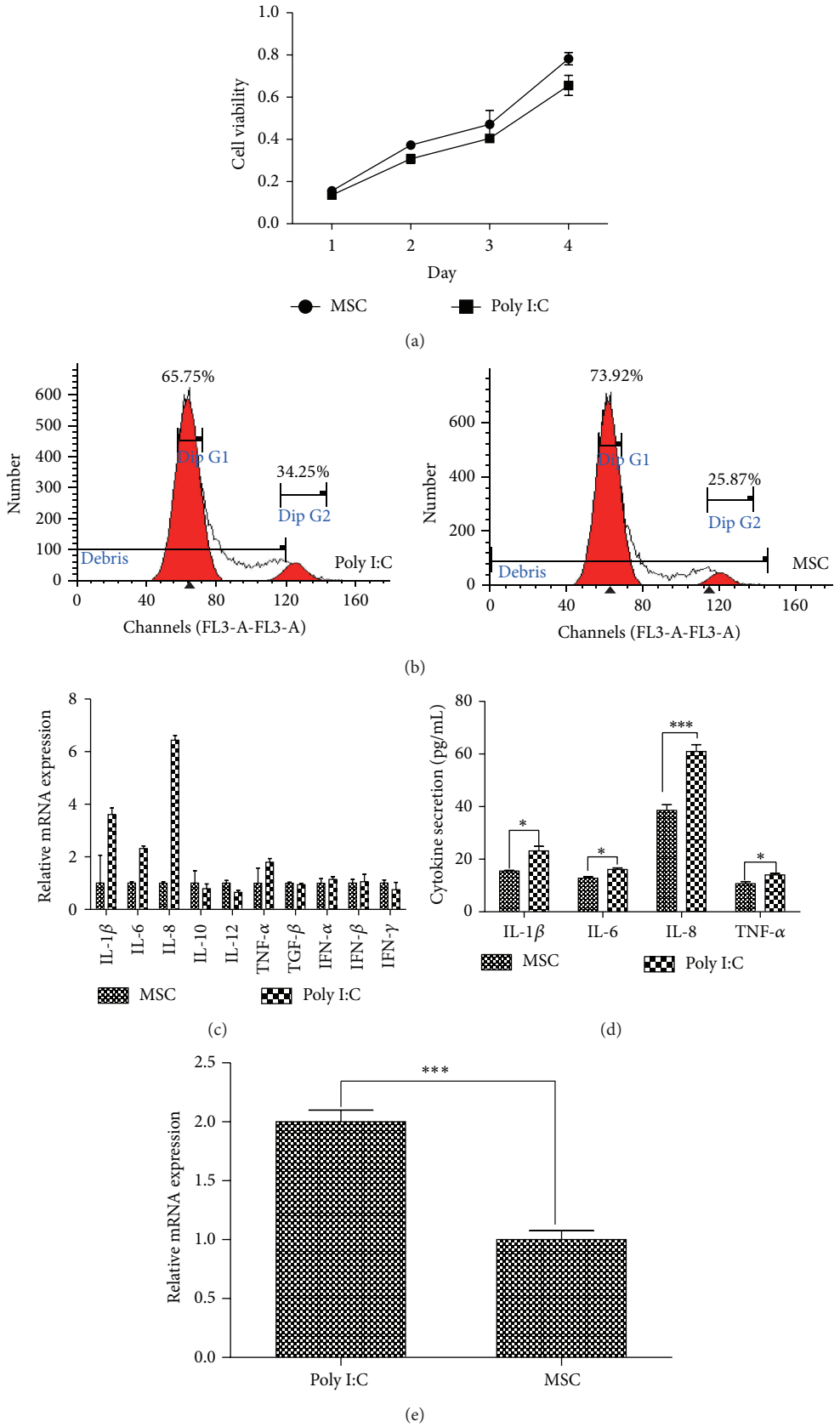

Figure 2: Effect of TLR3 agonist on AD-MSCs. (a) Effect of TLR3 agonist on the proliferation of AD-MSCs. (b) Cell cycle analysis of Poly I:C stimulated AD-MSCs and control AD-MSCs. (c) Cytokine secretion of AD-MSCs after Poly I:C stimulation as detected by RT-PCR. (d) Cytokine secretion of AD-MSCs after Poly I:C stimulation as detected by ELASA. (e) TLR3 expression in Poly I:C stimulated AD-MSCs and control AD-MSCs.

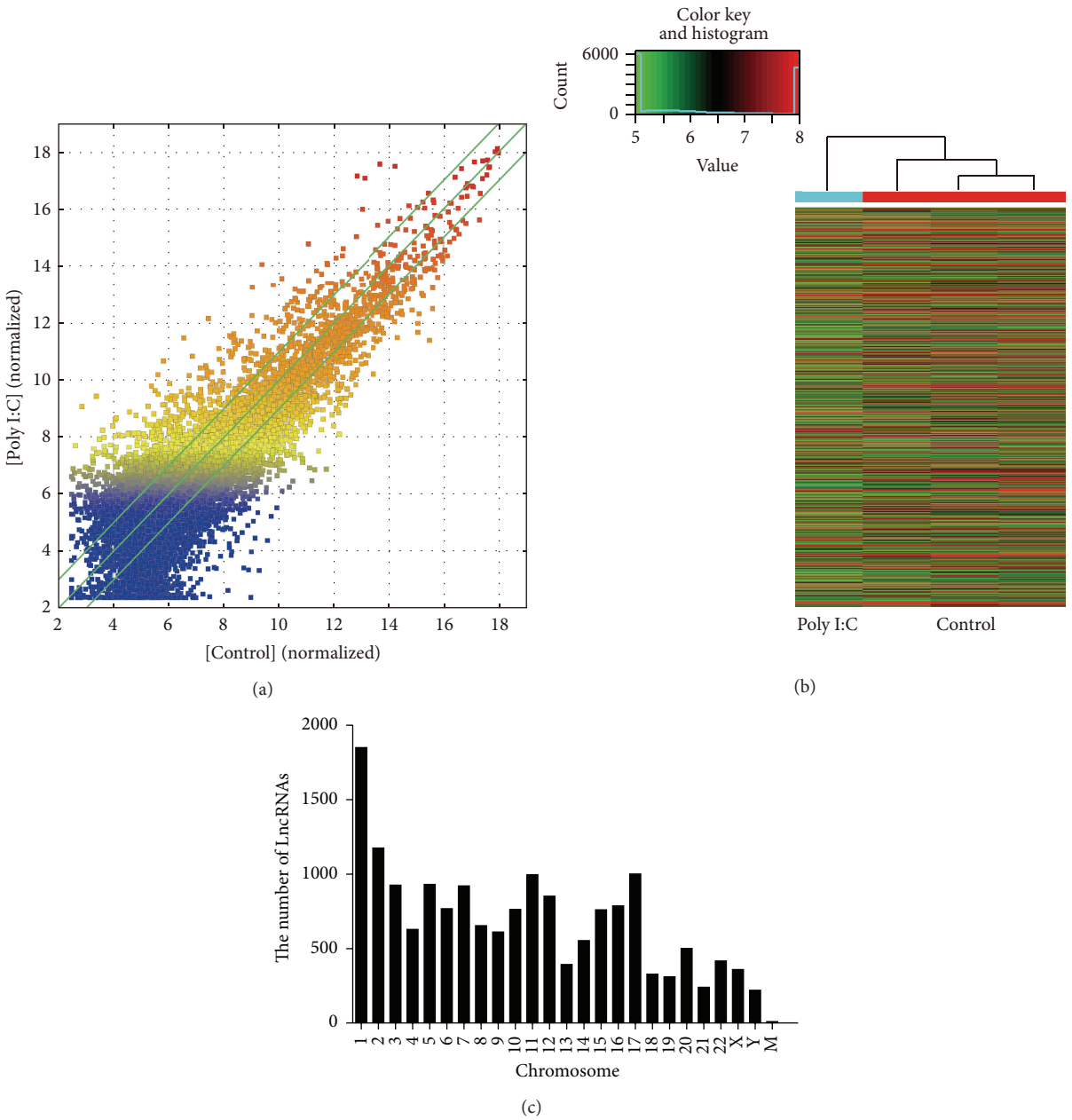

Figure 3: Overview of lncRNA profiles in TLR3-activated AD-MSCs and control AD-MSCs. (a) The scatter plot is a visualization method used for assessing the lncRNA expression variations between TLR3-activated AD-MSCs and control AD-MSCs. The values of the X and Y axes in the scatter plot are the averaged normalized signal values of the group (log 2 scale). The green lines are fold-change lines (the default fold-change given is 2). (b) Hierarchical clustering of lncRNAs in TLR3-activated AD-MSCs and control AD-MSCs. (c) Chromosomal distribution of detected lncRNAs.

and control AD-MSCs. The top 10 up- and downregulated LncRNAs in TLR3-activated AD-MSCs compared to control AD-MSCs were shown in Table 3. Figure 3(b) showed the hierarchical cluster of lncRNAs expression in Poly I:C stimulated AD-MSCs and nonstimulated AD-MSCs. Additionally, statistical analysis showed that the expressed lncRNAs were widely distributed on all chromosomes (Figure 3(c)) and that chr1 had the most expressed lncRNAs, while the mitochondrial genome had the least.

3.4. Characteristics of LncRNAs with Changed Expression in TLR3-Activated AD-MSCs. Among the 7271 differentially expressed LncRNA (absolute fold-change ≥2, P value ≤ 0.05), 2155 lncRNAs were upregulated in experimental group compared to the control group, while 5116 lncRNAs were downregulated. Here, one upregulated lncRNA uc010kun.2 was of particular interest for us because it is located upstream of IL6, a cytokine induced after TLR3 activation in AD-MSCs. Using qPCR, we observed a 2.70-fold upregulation in

Table 3: The top 10 up- and downregulated lncRNAs in TLR3-activated AD-MSCs versus control AD-MSCs.

	Top 10 LncRNAs	Chromosomal localization	RNA length	Start locus	Stop locus	Associated gene name	Relationship
TLR3-activated AD-MSCs versus control AD-MSCs upregulated	NR_052024	Chr20	803	33866708	33872520	EIF6	Sense-overlapping
	NR_037793	Chr14	1853	50065414	50081390	LRR1	Sense-overlapping
	ENST00000577672	Chr1	409	1655950	1667412	SLC35E2	Intronic
	ENST00000430598	Chr15	4279	20613648	20711433		Intergenic
	ENST00000514727	Chr4	442	140036086	140036528		Intergenic
	NR_024596	Cchr11	1129	86014397	86056985	C11orf73	Sense-overlapping
	NR_027653	Chr10	4525	3818187	3827473	KLF6	Sense-overlapping
	uc002xij.3	Chr20	805	37049238	37063962		Intergenic
	ENST00000478666	Chr3	1068	75471569	75484197		Intergenic
	uc010hbj.3	Chr22	1172	51222224	51238065	RABL2B	Bidirectional
TLR3-activated AD-MSCs versus control AD-MSCs downregulated	TCONS_00020653	Chr12	978	130442131	130444607		Intergenic
	ENST00000428453	Chr15	4383	20588367	20711414		Intergenic
	CB112975	Chr13	379	30229248	30229615		Intergenic
	uc009whu.1	Chr1	2772	142853227	142855999		Intergenic
	TCONS_00013	Chr7	1092	22450335	22452159		Intergenic
	ENST00000557155	Chr14	381	85860291	85886396		Intergenic
	ENST00000421735	Chr3	338	50304072	50304803	SEMA3B	Bidirectional
	TCONS_00014720	Chr8	206	59129760	59131635		Intergenic
	ENST00000505736	Chr4	1668	137717876	138133953		Intergenic
	ENST00000568150	Chr16	547	48657346	48778553		Intergenic

uc010kun.2, consistent with microarray analysis results (2.63-fold-change) (Supplementary Figure 1). Table 3 showed the top 10 up- and downregulated lncRNAs in TLR3-activated AD-MSCs versus control AD-MSCs. We classified these differentially expressed LncRNAs into 6 groups: "sense-overlapping," the LncRNA's exon is overlapping a coding transcript exon on the same genomic strand; "intronic," the LncRNA is overlapping the intron of a coding transcript on the same genomic strand; "natural antisense," the LncRNA is transcribed from the antisense strand and overlapping with a coding transcript; "nonoverlapping antisense," the LncRNA is transcribed from the antisense strand without sharing overlapping exons; "bidirectional," the LncRNA is oriented head to head to a coding transcript within 1000 bp; "intergenic": there are no overlapping or bidirectional coding transcripts nearby the LncRNA. Figure 4(a) showed the distribution of the six classes of LncRNAs with changed expression in TLR3-activated AD-MSCs. The lncRNAs are mainly between 200 bp and 3000 bp in length. Figure 4(b) showed the length distribution of differentially expressed lncRNAs. The majority of the differentially expressed lncRNAs have a length between 500 bp and 1000 bp.

3.5. Gene Ontology and Pathway Analysis. GO analysis was performed to determine the gene and gene product enrichment in biological processes, cellular components, and molecular functions (Supplementary Figure 2). We found that the highest enriched GOs targeted by upregulated mRNAs in TLR3-activated MSCs were mRNA metabolic process (ontology: biological process) (Figure 5(a)), intracellular part (ontology: cellular component) (Figure 5(b)), and structural constituent of ribosome (ontology: molecular function) (Figure 5(c)). The highest enriched GOs targeted by the downregulated transcripts in TLR3-activated MSCs were response to external stimulus (ontology: biological process) (Figure 5(d)), ankyrin binding (ontology: cellular component) (Figure 5(e)), and intrinsic to plasma membrane (ontology: molecular function) (Figure 5(f)). Specifically, we analyzed expression of genes associated with immune response (GO:0006955 Figure 6(a)), genes associated with immune response-regulation signaling pathway (GO:0002764 Figure 6(b)), and genes associated with regulation of immune response (GO:0050776 Figure 6(c)). Additionally, other genes associated with immune response (GO:0050778, GO:0042092, GO:0002828, GO:0002920, and GO:0002821) were analyzed (Supplementary Figure 3). Pathway analysis indicated that 38 pathways were upregulated and 31 were downregulated in TLR3-activated MSCs. Figure 7 showed the top 10 of the changed pathways.

4. Discussion

TLRs play an important role in innate and adaptive immunity. The expression and function of multiple TLRs have been described in many cell types, especially in cells of the innate immune system, where they function as sensors of infection or damage [8, 9]. However, conflicting results have been reported because TLRs expressed on different cell types from different species and tissues resulted in different responses [10]. Recently, it has been reported that MSC derived from

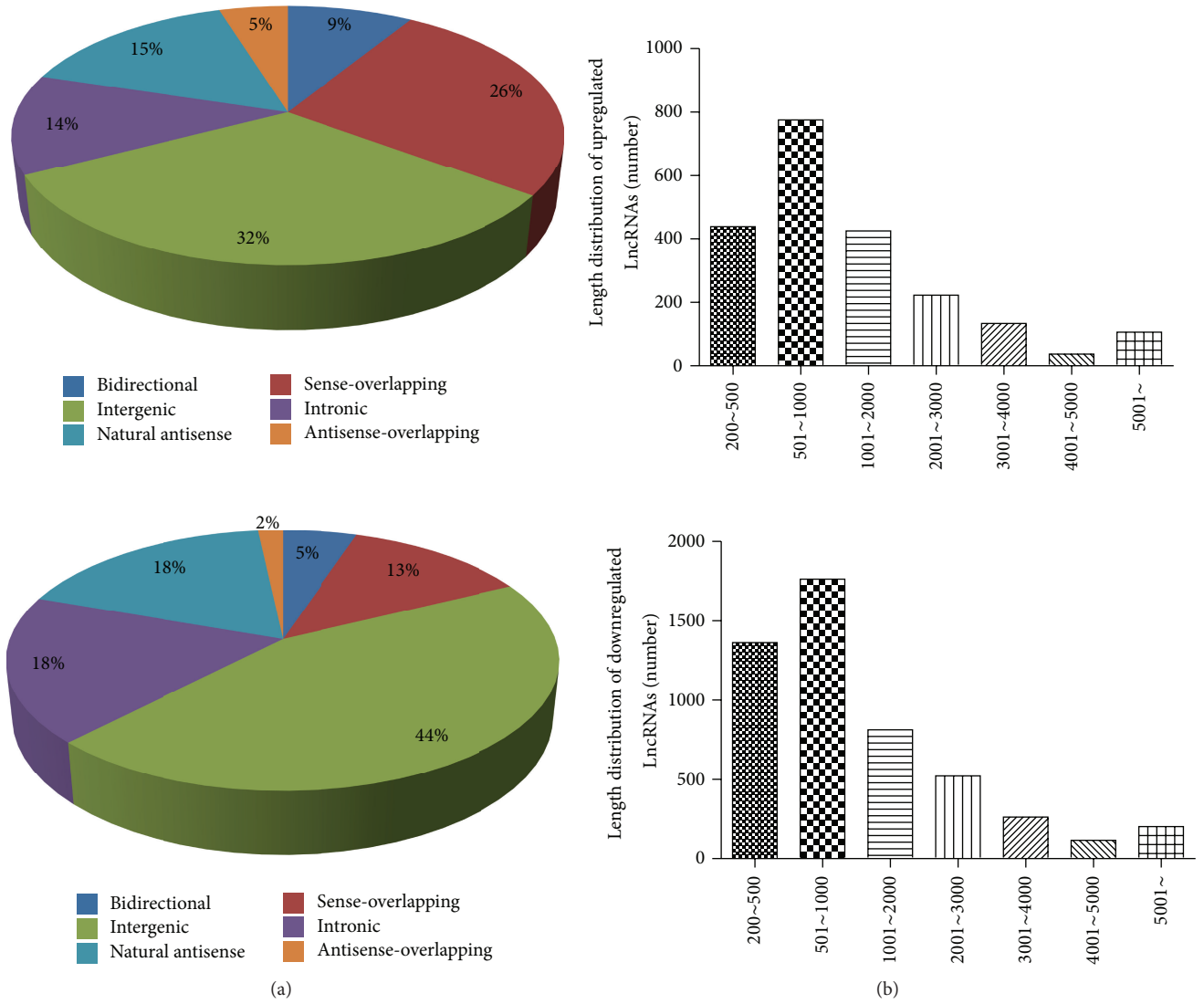

Figure 4: Characteristics of LncRNAs with changed expression in TLR3-activated AD-MSCs. (a) Distribution of various classes of differentially expressed LncRNAs. The ratio of 6 classes (sense overlap LncRNAs, antisense overlap LncRNAs, bidirectional LncRNAs, and intergenic LncRNAs) in total changed LncRNAs was analyzed in TLR3-activated AD-MSCs. (b) Length distribution of differentially expressed lncRNAs in TLR3-activated AD-MSCs.

adult bone marrow also expresses functional TLRs that promote their survival and proinflammatory cytokine secretion [11]. Here, we show that AD-MSCs express 10 types of TLRs and the expression level of TLR3 was the highest. Activation of TLR3 in AD-MSCs leads to enhanced secretion of IL-1β, IL-6, IL-8, and TNF-α.

It is well known that TLRs and their specific stimulus activate MyD88-dependent or -independent downstream signaling pathways. However, whether epigenetic regulators such as long noncoding RNA are involved in this process remains unclear. lncRNAs are over 200 nucleotides in length and are separate from the other known ncRNA subsets. Previous studies have focused primarily on short noncoding RNAs, such as microRNAs, transfer RNAs, and short interfering RNAs. Increasing evidence confirmed lncRNAs to be one of the most important factors controlling gene expression and the aberrant expression of which is involved in a variety of human diseases, including immunological disorders [12, 13]. Guttman et al. were the first to use the intergenic deposition of epigenetic marks to identify 20 lncRNAs induced in lipopolysaccharide- (LPS-) stimulated mouse bone marrow-derived dendritic cells (BMDD) [14]. Later on, several lncRNAs have been identified following activation of monocytes, macrophages, fibroblasts, and dendritic cells [15–18]. The potential importance of lncRNAs in the immune response is only now emerging. Immune-related lncRNAs are generally identified through examination of differential expression in response to activation of immune cells [6]. Here, a major focus of our study was to define the repertoire of lncRNAs in TLR3-activated AD-MSCs. We performed comprehensive lncRNA and mRNA profiling through microarray and found 10.2% of lncRNAs (1733 out of 16967) and 15.1% of mRNA

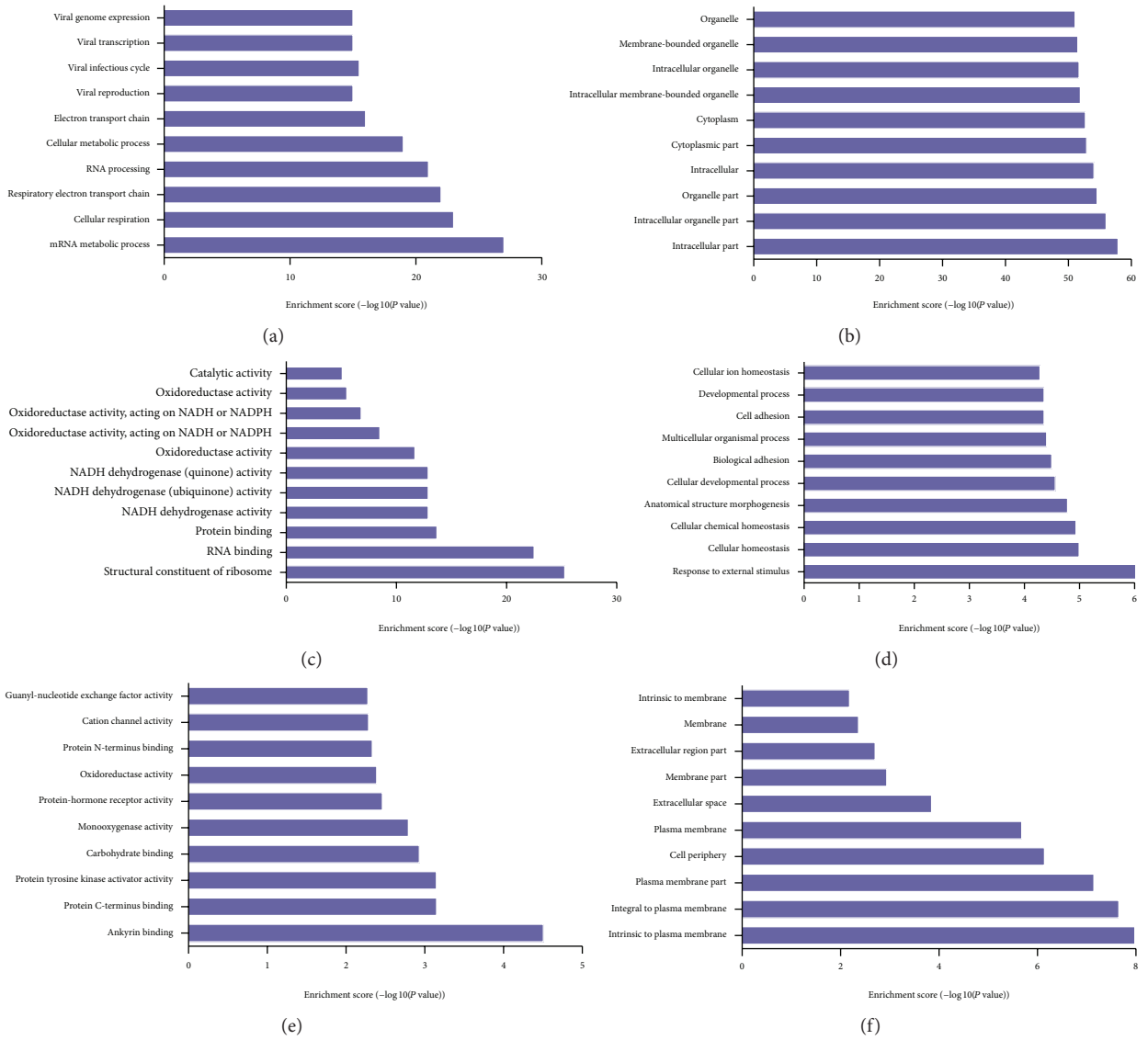

Figure 5: GO term enrichment in the differentially expressed genes. (a, b, c) Genes upregulated in TLR3-activated AD-MSCs. (d, e, f) Genes downregulated in TLR3-activated AD-MSCs.

transcripts (1760 out of 11632) were significantly differentially expressed in TLR3 stimulated MSCs. Furthermore, we characterized the differentially expressed lncRNAs through their classes and length distribution and correlated them with differentially expressed mRNA.

An interesting observation from sequencing data is that many of the immune-related lncRNAs are located close to, or partially overlapping, the 5′ end (upstream) or 3′ end (downstream) of protein-coding genes implicated in the immune response [6, 19]. Here, one upregulated lncRNA uc010kun.2 was of particular interest for us because it is located upstream of IL6, a cytokine induced after TLR3 activation in AD-MSCs. Another lncRNA our data may highlight is lncRNA-Cox7A2. Carpenter et al. indicated that Cox2 and lncRNA-Cox2 regulated by MyD88 and NF-kB were markedly induced after TLR4 stimulation in BMDMs [17]. Here, lncRNA-Cox7A2 is predicted to be associated with Cox7A2, which is also a cytochrome c oxidase subunit.

TLR3 signaling and subsequent inflammatory responses are controlled by a multitude of regulatory molecules. Here, we propose a model whereby TLR3 signaling induces expression changes of lncRNAs which then exert their effects as repressors or activators of genes through interactions with various regulatory complexes. As such, lncRNAs represent a new component of the TLR3 signaling pathway.

In summary, our study was the first to demonstrate that a set of lncRNAs is significantly regulated in AD-MSCs upon stimulation with TLR3, suggesting a role of lncRNAs in the immune response of AD-MSCs. This will provide the basis for the subsequent functional and mechanistic analysis of individual lncRNAs. Currently, the precise functions of the differentially expressed lncRNAs remain largely unknown

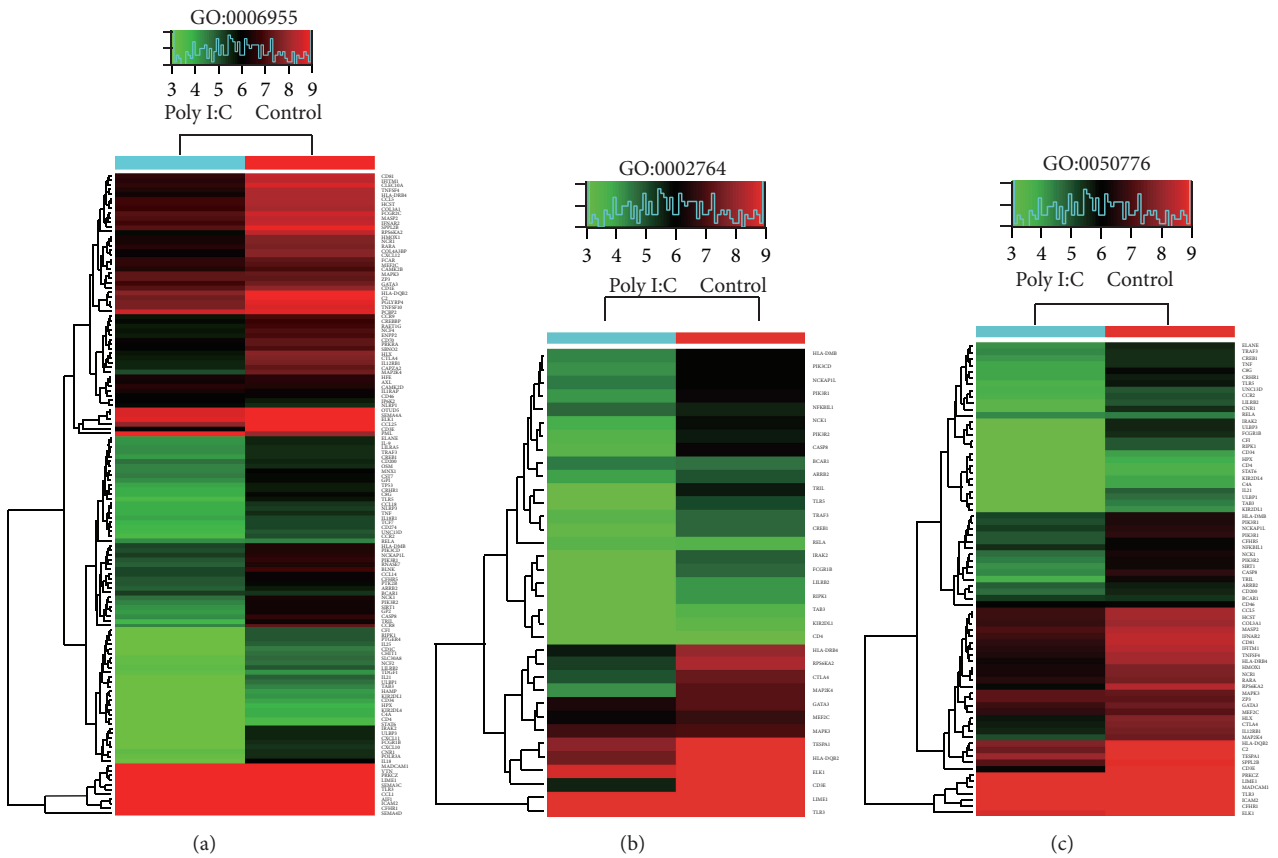

FIGURE 6: Gene ontology analysis of genes (a) associated with immune response GO:0006955, (b) genes associated with immune response-regulation signaling pathway GO:0002764, and (c) genes associated with regulation of immune response GO:0050776.

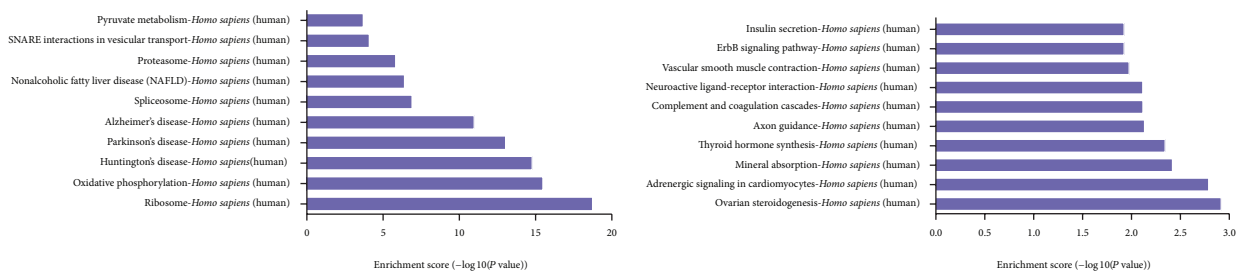

FIGURE 7: Pathway analysis of the differentially expressed genes. (a) Top 10 of the upregulated pathways in TLR3-activated AD-MSCs. (b) Top 10 of the downregulated pathways in TLR3-activated AD-MSCs.

and advances in the understanding of their role will allow us to tackle a range of challenges in AD-MSCs immunomodulatory properties.

Highlights

(1) TLR3 is highly expressed in adipose tissue derived mesenchymal stem cells.

(2) TLR3 agonist Poly I:C promotes secretion of a variety of cytokines.

(3) TLR3-activated AD-MSCs show dynamic changes in lncRNA and mRNA profiles.

Ethical Approval

Adipose tissues and informed consent were obtained from patients undergoing tumescent liposuction according to procedures approved by the Ethics Committee at the Chinese Academy of Medical Sciences and Peking Union Medical College.

Conflict of Interests

The authors have declared that no competing interests exist.

Authors' Contribution

Shihua Wang and Xiaoxia Li contributed equally to this work.

Acknowledgments

This study was supported by grants from National Natural Science Foundation of China (nos. 30830052, 30700321, and 30800429) and Program for Cheung Kong Scholars and Innovative Research Team (PCSIRT) in University (no. IRT0909).

References

[1] R. Lin, S. Wang, and R. C. Zhao, "Exosomes from human adipose-derived mesenchymal stem cells promote migration through Wnt signaling pathway in a breast cancer cell model," *Molecular and Cellular Biochemistry*, vol. 383, no. 1-2, pp. 13–20, 2013.

[2] M. Pevsner-Fischer, V. Morad, M. Cohen-Sfady et al., "Toll-like receptors and their ligands control mesenchymal stem cell functions," *Blood*, vol. 109, no. 4, pp. 1422–1432, 2007.

[3] B. Beutler, "Inferences, questions and possibilities in Toll-like receptor signalling," *Nature*, vol. 430, no. 6996, pp. 257–263, 2004.

[4] K. De Luca, V. Frances-Duvert, M.-J. Asensio et al., "The TLR1/2 agonist PAM_3CSK_4 instructs commitment of human hematopoietic stem cells to a myeloid cell fate," *Leukemia*, vol. 23, no. 11, pp. 2063–2074, 2009.

[5] C. Qi, X. Xiaofeng, and W. Xiaoguang, "Effects of toll-like receptors 3 and 4 in the osteogenesis of stem cells," *Stem Cells International*, vol. 2014, Article ID 917168, 7 pages, 2014.

[6] J. A. Heward and M. A. Lindsay, "Long non-coding RNAs in the regulation of the immune response," *Trends in Immunology*, vol. 35, no. 9, pp. 408–419, 2014.

[7] Y. Cao, Z. Sun, L. Liao, Y. Meng, Q. Han, and R. C. Zhao, "Human adipose tissue-derived stem cells differentiate into endothelial cells in vitro and improve postnatal neovascularization in vivo," *Biochemical and Biophysical Research Communications*, vol. 332, no. 2, pp. 370–379, 2005.

[8] R. Kulkarni, S. Behboudi, and S. Sharif, "Insights into the role of Toll-like receptors in modulation of T cell responses," *Cell and Tissue Research*, vol. 343, no. 1, pp. 141–152, 2011.

[9] P. D. Smith, M. Shimamura, L. C. Musgrove et al., "Cytomegalovirus enhances macrophage TLR expression and MyD88-mediated signal transduction to potentiate inducible inflammatory responses," *The Journal of Immunology*, vol. 193, no. 11, pp. 5604–5612, 2014.

[10] O. DelaRosa and E. Lombardo, "Modulation of adult mesenchymal stem cells activity by toll-like receptors: implications on therapeutic potential," *Mediators of Inflammation*, vol. 2010, Article ID 865601, 9 pages, 2010.

[11] G. Raicevic, M. Najar, B. Stamatopoulos et al., "The source of human mesenchymal stromal cells influences their TLR profile as well as their functional properties," *Cellular Immunology*, vol. 270, no. 2, pp. 207–216, 2011.

[12] L.-L. Chen and G. G. Carmichael, "Decoding the function of nuclear long non-coding RNAs," *Current Opinion in Cell Biology*, vol. 22, no. 3, pp. 357–364, 2010.

[13] M. Turner, A. Galloway, and E. Vigorito, "Noncoding RNA and its associated proteins as regulatory elements of the immune system," *Nature Immunology*, vol. 15, no. 6, pp. 484–491, 2014.

[14] M. Guttman, I. Amit, M. Garber et al., "Chromatin signature reveals over a thousand highly conserved large non-coding RNAs in mammals," *Nature*, vol. 458, no. 7235, pp. 223–227, 2009.

[15] N. A. Rapicavoli, K. Qu, J. Zhang, M. Mikhail, R.-M. Laberge, and H. Y. Chang, "A mammalian pseudogene lncRNA at the interface of inflammation and antiinflammatory therapeutics," *eLife*, vol. 2013, no. 2, Article ID e00762, 2013.

[16] P. Wang, Y. Xue, Y. Han et al., "The STAT3-binding long noncoding RNA lnc-DC controls human dendritic cell differentiation," *Science*, vol. 344, no. 6181, pp. 310–313, 2014.

[17] S. Carpenter, D. Aiello, M. K. Atianand et al., "A long noncoding RNA mediates both activation and repression of immune response genes," *Science*, vol. 341, no. 6147, pp. 789–792, 2013.

[18] R. K. Dave, M. E. Dinger, M. Andrew, M. Askarian-Amiri, D. A. Hume, and S. Kellie, "Regulated expression of *PTPRJ*/CD148 and an antisense long noncoding RNA in macrophages by proinflammatory stimuli," *PLoS ONE*, vol. 8, no. 6, Article ID e68306, 2013.

[19] G. Hu, Q. Tang, S. Sharma et al., "Expression and regulation of intergenic long noncoding RNAs during T cell development and differentiation," *Nature Immunology*, vol. 14, no. 11, pp. 1190–1198, 2013.

Hindawi Publishing Corporation
Stem Cells International
Volume 2016, Article ID 9298535, 8 pages
http://dx.doi.org/10.1155/2016/9298535

Review Article

Developmental Pathways Direct Pancreatic Cancer Initiation from Its Cellular Origin

Maximilian Reichert,[1,2] Karin Blume,[1] Alexander Kleger,[3] Daniel Hartmann,[4] and Guido von Figura[1]

[1] *II. Medizinische Klinik und Poliklinik, Klinikum rechts der Isar München, Technische Universität München, 81675 Munich, Germany*
[2] *Division of Gastroenterology, Perelman School of Medicine, University of Pennsylvania, Philadelphia, PA 19104, USA*
[3] *Department of Internal Medicine I, Ulm University, 89081 Ulm, Germany*
[4] *Chirurgische Klinik und Poliklinik, Klinikum rechts der Isar München, Technische Universität München, 81675 Munich, Germany*

Correspondence should be addressed to Maximilian Reichert; maximilian.reichert@lrz.tum.de
and Guido von Figura; gvfigura@lrz.tum.de

Received 24 April 2015; Accepted 25 June 2015

Academic Editor: Kodandaramireddy Nalapareddy

Pancreatic ductal adenocarcinoma (PDA) is characterized by an extremely poor prognosis, since it is usually diagnosed at advanced stages. In order to employ tools for early detection, a better understanding of the early stages of PDA development from its main precursors, pancreatic intraepithelial neoplasia (PanIN), and intraductal papillary mucinous neoplasm (IPMN) is needed. Recent studies on murine PDA models have identified a different exocrine origin for PanINs and IPMNs. In both processes, developmental pathways direct the initiation of PDA precursors from their cellular ancestors. In this review, the current understanding of early PDA development is summarized.

1. Introduction

The idea that cancer cells share properties of their embryonic predecessors is, scientifically speaking, ancient [1]. Within the last decade, this conception has mostly fueled the work in the field of cancer stem cells. As controversial as this theory might be, it is one way to explain tumor heterogeneity, and solid tumors, especially pancreatic ductal adenocarcinomas (PDA), are heterogeneous [2, 3]. Similar to embryonic development, tumor cells, or at least a subset of them, have the ability to maintain indefinite growth as well as cellular plasticity. Terminal differentiation most likely has to be disadvantageous for tumor cells in order to adapt to the hostile environment within the primary tumor, the circulation, or at the metastatic site.

In the pancreas, different cell types harbor distinct susceptibilities towards oncogenic insults. Recently, new light has been shed on the cell-of-origin question of PDA. Historically PDA was thought to arise from pancreatic ductal epithelium. Instead, murine models revealed that both ductal and acinar cells are capable of transforming into distinct precursor lesions that develop into biologically different PDA subsets [4]. The parent cell transformation in both processes is characterized by dedifferentiation with recapitulation of elements of pancreatic development. Recent data investigating the role of Sox9 in PDA initiation suggest that ductal but also centroacinar cells (CACs) are more refractory to transformation mediated by a mutated *Kras* allele compared to acinar cells [5]. In contrast, Pten loss results in rapid formation of invasive carcinoma, which is preceded by significant expansion of CACs [6]. This suggests that CACs, ductal cells, and acinar cells may have the potential to initiate invasive carcinoma but that each cellular context may require a different repertoire of genetic alterations for tumour initiation. Cell-specific induction of different oncogenic mutations in mice may define morphologically and molecularly distinct tumours, which may help to identify human PDA subtypes that respond differently to therapeutic intervention.

In the following, we will give an overview of pancreas organogenesis and discuss how pancreatic cancer cells

exploit developmental programs during cancer initiation with respect to their cellular origin.

2. Pancreatic Morphogenesis and Lineage Segregation

The development of the murine pancreas is initiated around embryonic day 8.5 (e8.5) after gastrulation, when a pancreatic and duodenal homeobox 1- (Pdx1-) expressing ($Pdx1^+$) population within endodermal gut tube gives rise to both the ventral and dorsal pancreas anlage [7]. A subset of $Pdx1^+$ cells that arises from the ventral foregut eventually loses its Pdx1-expression, eventually, to form the extrahepatic bile duct [8]. Stringent genetic studies in the mouse have demonstrated that Pdx1 ablation leads to pancreatic agenesis [9, 10]. The $Pdx1^+$ multipotent progenitor cells (MPCs), directed by cues from the surrounding mesenchyme, establish distinct cellular lineages in order to produce and drain digestive enzymes as well as maintaining glucose homeostasis [11].

In order to execute these processes, three main lineages are required: the acinar cells, producing a plethora of digestive enzymes; the ductal cells, forming a hierarchical conduit system; and the endocrine cells, organized in the islet of Langerhans, producing hormones like insulin, glucagon, pancreatic polypeptide, somatostatin, and ghrelin. Careful designed genetic lineage-tracing studies using Cre/LoxP technology have provided insight into the spatiotemporal organization of these compartments.

For example, Gu et al. utilized *Pdx1-CreER*^{TM} mice to demonstrate that the $Pdx1^+$ population truly harbors multipotent progenitors since tamoxifen administration at E9.5 labels exocrine, endocrine, and duct cells [7]. Interestingly, it is the number of $Pdx1^+$ progenitor cells that determines the size of the pancreas in the adult mouse, suggesting that it is rather an intrinsic program of the progenitor population than growth compensation limiting organ size, like in other organs, for example, the liver [12]. Besides Pdx1, numerous transcription factors have been employed to investigate pancreatic lineage commitment in the developing embryo. Slightly later than Pdx1 (around e9.5–10.5), Ptf1a (pancreatic transcription factor 1) is expressed in MPCs, further seizing segregation from a duodenal fate while the pancreatic bud evaginates [13]. These two transcription factors are certainly the most prominent members during this early phase of organogenesis, termed primary transition. It is at the end of primary transition, approximately around e12.5, when a primitive trunk epithelium with a continuous lumen as well as tip-structures emerges [14]. This spatial tip-trunk organization was thought to be accompanied by a loss of multipotency of the primitive duct at the beginning of secondary transition [14]. However, more recent studies, employing *Sox9Cre*^{ER} as well as *Hnf1β*^{CreERT2}, with both transcription factors localizing to the trunk, demonstrated that either population still harbors the ability to give rise to the endocrine, acinar, and ductal lineage during secondary transition to a varying degree [15, 16].

In the adult pancreas, under tissue homeostatic conditions, Pdx1 becomes restricted to insulin-producing β-cells maintaining a β-cell-phenotype by repressing an α-cell program [17, 18], while Ptf1a remains expressed exclusively in acinar cells [19]. On the other hand, Sox9 and Hnf1β remain expressed in the ductal tree including intercalated (terminal), intralobular, and interlobular ducts as well as the main duct [20]. Thus, a set of transcription factors defines pancreatic plasticity or differentiation capacity of pancreatic progenitors in a spatiotemporally regulated manner.

The fact that mature pancreatic lineages maintain a certain degree of plasticity becomes evident in nontissue homeostatic conditions, particularly in regeneration and carcinogenesis, and will be discussed in the following section.

3. Pancreatic Cancer and Its Precursors

PDA is characterized by an extremely poor prognosis with a mortality rate almost equaling the incidence rate [21]. The underlying reason for this dismal situation is the limited possibility for early detection of this disease and, therefore, diagnosis is often only made in advanced stages, where only few, insufficient treatment options exist [22]. Thus, a better understanding of the initial steps of PDA development is important in order to develop new tools for early detection. In addition, deciphering the factors important for PDA progression will help to identify novel treatment options.

It is believed that PDA can develop from three established precursor lesions [23]: (i) pancreatic intraepithelial neoplasia (PanIN) and the cystic lesions, (ii) intraductal papillary mucinous neoplasm (IPMN), and (iii) mucinous cystic neoplasm (MCN). These precursor lesions differ in their prevalence; the majority of PDA is thought to arise from PanINs and less frequently from IPMN, whereas MCNs are rare [24]. There is indirect evidence for PanINs as precursors for PDA, which is largely based on the fact that PDA is often associated with advanced PanIN, and both share common tumor promoting genetic alterations. In contrast, cystic lesions can directly be identified as the origin for PDA on histological examination and imaging techniques such as MRI scan or endoscopic ultrasound. The possibility of imaging cystic precursor lesions also offers the chance to detect the precursor before PDA has developed. In fact, probably due to more frequent and better diagnostic imaging as well as physicians' awareness, IPMN lesions are increasingly identified in the pancreas, and ideal management of these patients is still an ongoing debate [25].

Interestingly, PDA that is associated with IPMNs has a much more favorable prognosis than PDA that is thought to arise from PanINs [26–28]. The underlying reasons for this different biological behavior are largely unknown. One possibility could be different genetic mutations during evolution of PDA from its precursors. In fact, whereas a *KRAS* mutation occurs nearly universally during PanIN initiation [29], *KRAS* is less frequently mutated in IPMNs [30, 31]. Instead, IPMNs but not PanINs frequently harbor mutations in *GNAS* and *RNF43* [32–34]. Apart from this difference, common genetic alterations in both precursors are found in *TP53* and *CDKN2A* (reviewed by Xiao [35] and Gnoni et al. [24]).

An additional possibility for the different biology of PanIN and IPMN-associated PDA could be a different cellular origin of the precursors. In line with this hypothesis, recent evidence from genetically engineered mouse models (GEMM) revealed that the cellular origin of PanINs and IPMNs might be different [4, 5]. This work will be discussed below.

4. Mechanisms of PanIN Development from Its Cellular Origin

Whereas there is considerable knowledge about the molecular and genetic events during progression of PanIN lesions, the mechanisms of precursor initiation are still poorly understood. Historically, PDA and its precursors were thought to develop from pancreatic ductal cells because both have a ductal morphology and express ductal markers such as cytokeratin 19 (CK19). However, this assumption was challenged by studies in mice that revealed an acinar source for PanIN lesions [36–38].

4.1. ADM/ADR: The Precursor of the Precursor? That pancreatic acinar cells have a marked plasticity was already noted 30 years ago in pancreatitis studies on rats [39, 40]. In these experiments an acute pancreatitis was induced by repetitive injections of cerulein, a cholecystokinin analogue, which causes autodigestion of the pancreas and a pronounced inflammatory reaction. It was found that in response to this damage acinar cells form a transient duct-like metaplasia before a complete regeneration of the organ occurs. The direct *in vivo* evidence for an acinar source of this acinar to ductal metaplasia (ADM) was brought in 2008 using lineage-tracing techniques on a murine pancreatitis model by Fendrich et al. [41]. Further characterization of ADM has shown that it is not only accompanied by downregulation of acinar and expression of ductal markers (e.g., CK19) but also resembles pancreatic embryonic progenitor cells evidenced by reexpression of pancreatic developmental factors, such as PDX1, Sox9, and Hes1 [41–43]. Following this transient phase in response to an acute damage, the duct-like cells of ADM resume an acinar morphology and expression profile [43, 44]. In contrast to an acute damage, chronic pancreatitis leads to a persistence of ADM [45] and a failure to regenerate the pancreas. However, although acute and chronic pancreatitis can induce duct-like structures originating from pancreatic acinar cells, both are not sufficient to induce PanIN lesions *per se*.

Importantly, an oncogenic mutation in *Kras* can induce ADM from acinar cells that resembles ADM formed in response to pancreatitis [37, 46]. However, the Kras-induced ADM is persistent and not transient and is also termed acinar to ductal reprogramming (ADR) in this context. In addition to ADR, acinar expression of mutant Kras is sufficient to induce PanIN lesions [36–38, 46]. Although direct lineage-tracing evidence is missing, it is suggested that Kras-associated ADR progresses to PanIN lesions [47], in part, because the expression of key signaling pathways in ADR cells is mimicking expression detected in PanIN lesions [48]. Moreover, in mouse models with expression of mutant Kras in the pancreas lesions of acinar to ductal reprogramming precede PanIN development [43, 48]. In addition, PanINs in mice and humans are usually associated with areas of ADM/ADR [48].

4.2. Acinar Cells Give Rise to PanINs. In contrast to mouse models where mutant Kras is activated during pancreatic embryogenesis [49], mutant Kras expressed in mature acinar cells leads to PanIN formation but is insufficient to cause PDA [36–38, 46]. However, when combined with chronic pancreatitis, which is a risk factor for the development of PDA [50], mutant Kras ($Kras^{G12V}$) was able to accelerate precursor formation with progression to cancer [37]. This suggests that inflammation can induce synergistic protumorigenic changes in acinar cells that cooperate with mutant Kras. Pancreatitis experiments in wild-type animals have shown that these changes could comprise reactivation of developmental factors that have been shown to be important for Kras-mediated neoplastic transformation of pancreatic acinar cells which will be discussed in detail below [42, 43].

The above mentioned studies have shown that adult pancreatic acinar cells are capable of forming PanIN lesions in the context of mutant Kras. It is also important to note that ductal cells in CK19 promoter-based expression of mutant Kras were able, albeit at much lower frequency, to form PanIN lesions [51]. In a study by Kopp et al. it was investigated by comparative recombination in adult pancreatic duct/CACs and acinar cells using tamoxifen inducible *Sox9CreER* and $Ptf1a^{CreER}$-mediated recombination of mutant Kras [5]. Interestingly, it was found that pancreatic ductal cells including CACs were virtually incapable of transforming into PanIN lesions, whereas acinar cells readily transformed into PanIN lesions with a >100-fold greater efficiency as compared to ductal cells. Scientists in the field have speculated extensively about the possibility of CACs being the cell of origin of PanIN and PDAC. However, the compartment of CACs is still characterized insufficiently and, hence, the genetic tools to address this question appropriately are missing. Taken together, the most recent findings suggest that this is a very unlikely scenario and strongly support the model that at least in the murine Kras model acinar cells serve as the origin for PanIN lesions. This also prompts the question of which factors are important for acinar cells to transform into ADR/PanIN. Previous studies have taught us that recapitulation of developmental factors is occurring during acinar transformation. One of these is the embryonic transcription factor Sox9 that is expressed in pancreatic progenitor cells and becomes restricted to ductal cells in the adult organ [52]. Kopp et al. investigated if this factor not only is a marker of acinar cells undergoing transformation but also plays an essential function in this process [5]. To test this, Sox9 was deleted from acinar cells expressing oncogenic Kras, which resulted in a complete blockage of PanIN formation (Figure 1). Vice versa, overexpression of Sox9 in the context of oncogenic Kras dramatically catalyzed preneoplastic transformation. Mechanistically, it was shown that ectopic expression of Sox9 alone in acinar cells can erode cell integrity evidenced by downregulation of markers

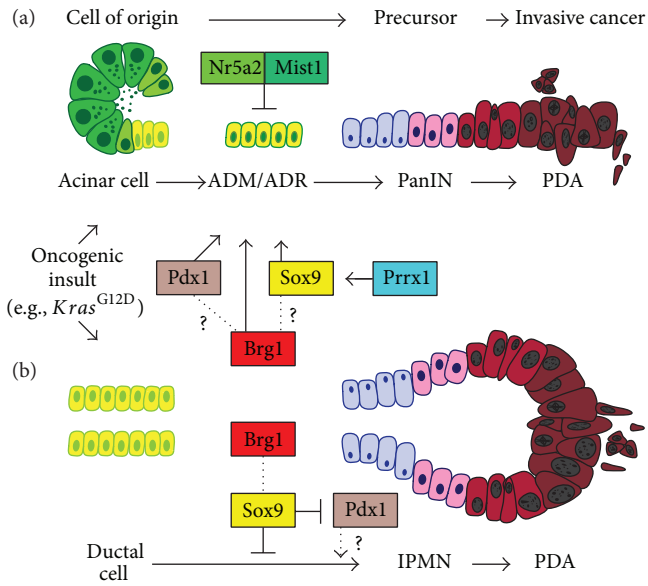

Figure 1: A model for developmental factors regulating acinar and duct cell transformation. (a) Acinar cells undergo acinar to ductal reprogramming (ADM/ADR) on their way to become PanINs and PDA. The ductal reprogramming of acinar cells is inhibited by factors that maintain stable acinar differentiation, such as Mist1 and Nr5a2. Instead, the transcription factors Sox9 and Pdx1 promote ductal reprogramming. Prrx1 and the chromatin remodeler Brg1 also promote ductal reprogramming, possibly by regulating other transcription factors, such as Sox9 or Pdx1. (b) Ductal cells transform into IPMN lesions by undergoing a dedifferentiation step ("ductal retrogression") evidenced by an upregulation of the progenitor marker Pdx1. The chromatin remodeler Brg1 suppresses ductal retrogression by regulating Sox9 expression, which in turn inhibits Pdx1. This points to an opposing function of Brg1 in acinar versus duct cell transformation.

of acinar differentiation, such as Mist1, and concomitant upregulation of the ductal factor CK19 [5]. Interestingly, previous studies have shown that combining mutant Kras with a deletion of Mist1 also accelerates formation of PanIN lesions in the pancreas [53], which further highlights the relevance of a stable acinar differentiation state as a barrier for Kras-mediated transformation (Figure 1).

4.3. Epithelial Cell Plasticity. The notion that loss of acinar cell integrity is a prerequisite for PDA formation is accompanied by the emergence of a developmental program as mentioned above [44]. This phenomenon is not exclusive to pancreatic cancer but also present in other processes involving ADM during pancreatic regeneration in response to pancreatitis [42]. Besides the already mentioned Sox9 and Pdx1, Notch- and Shh-signaling, among others, are reactivated within the acinar compartment after challenging the gland using cerulein [42]. Interestingly, persistent overexpression of Pdx1 within the pancreatic epithelium by transgenic means leads to ADM formation suggesting that Pdx1 has a driving function in acinar cell dedifferentiation [54] (Figure 1). More recently, using an unbiased approach comparing gene expression profiles of the developing pancreas, acute pancreatitis and mutant *Kras*-driven carcinogenesis revealed a transcriptional program shared in these processes [55]. Of note, Prrx1 emerged as the most regulated transcription factor in this system. The *Prrx1* gene encodes two major variants, *Prrx1a* and *Prrx1b*, generated by alternative splicing [56]. Remarkably, PRRX1B is upregulated in ADM as well as PanINs and induces Sox9 expression on a transcriptional level thereby fostering a ductal phenotype [55] (Figure 1). In PDA, both splice variants, Prrx1a and Prrx1b, control differentially epithelial-to-mesenchymal transition (EMT) and the reverse process, mesenchymal-to-epithelial transition (MET) (Takano, Reichert et al. unpublished data). In general, the degree of cellular plasticity is illustrated by the ability to undergo EMT/MET both being critical in embryonic development (EMT type I), tissue regeneration (EMT type II), and cancer (EMT type III) [57]. The two latter types are characterized by an inflammatory response in contrast to EMT type I observed in the embryo [58]. However, all subtypes can be identified by the expression of EMT-transcription factors (EMT-TFs), including Slug, Snail, Twist, and Zeb [59]. Interestingly, Slug has been found to cooperate with Sox9 in promoting tumorigenicity in breast cancer cells [60].

4.4. Acinar Cells in Human Pancreatic Cancer Initiation. In summary, murine studies have identified acinar cells as the origin for PanIN lesions and highlighted the role of developmental factors in this process. An open question remains if these studies in mouse models are applicable to the situation of pancreatic cancer initiation in humans. Although it is impossible to directly prove *in vivo* that acinar cells transform into PanINs in human pancreas, there is some evidence that this process may also be true for human pancreatic carcinogenesis. *In vitro* studies have shown that human pancreatic acinar cells have a comparable plasticity, as their murine equivalents, and readily transdifferentiate into duct-like cells in culture [61]. Shi et al. examined in human pancreas specimens if the initiating oncogenic Kras

mutation can be detected in acinar cells that are in proximity to ADM/PanIN [62]. Although the authors could not detect Kras mutations in acinar cells and isolated areas of ADM, expectedly PanINs but also areas of adjacent ADM exhibited a high frequency of mutant Kras. This data could be interpreted that ADM adjacent to PanIN represents retrograde extensions of the latter and thus would not support an acinar origin for PanINs. However, it is also conceivable that it was impossible to detect mutant Kras in morphologically normal acinar cells, because Kras mutant acinar cells may promptly transdifferentiate into ADM in humans and Kras mutant ADM may have a high propensity to immediate formation of PanIN lesions.

The acinar origin hypothesis is also supported by genome wide association studies that identified frequent single-nucleotide polymorphisms (SNPs) in pancreatic developmental factors that are associated with pancreatic cancer. These developmental factors comprised not only *PDX1* but also the important regulators of acinar differentiation *HNF1A* and *NR5A2* [63, 64]. The role of Nr5a2 in maintaining a stable acinar differentiation state and preventing Kras-driven PanIN formation was subsequently demonstrated in studies in mice [65, 66] (Figure 1). These investigations supported the relevance of the identified SNPs in *NR5A2* as pancreatic cancer susceptibility lesions and further suggest a role of acinar cells in human preneoplastic transformation.

5. Development of IPMN from Its Cellular Origin

Whereas PanINs and PanIN-PDA have been studied in great detail, in part, due to the prevalence of GEMM recapitulating PanIN-PDA formation [67, 68], the molecular properties of IPMN are less well characterized and few suitable mouse models for studying IPMN-PDA progression had been developed [69, 70]. In humans, IPMNs are macroscopically cystic lesions that develop within the pancreatic main and/or branch duct system and show a direct connection to the ducts. This fact and the ductal morphology have led to the assumption of duct cells as the cellular origin for this precursor lesion. However, lineage-tracing studies in murine models had been hampered by the lack of suitable inducible *Cre*-lines that allow recombination specifically in adult duct cells. Therefore, proving a ductal origin of the preneoplastic lesions in mouse models of IPMN had been impossible.

With the recent availability of such duct-specific *Cre*-lines, it was demonstrated in a study on a novel GEMM of IPMN that the preneoplastic lesions in this particular model derive from ductal cells [4]. In an initial experiment, it was shown that embryonic pancreas specific deletion ($Ptf1a^{Cre}$) of Brg1, the catalytic subunit of the SWItch/sucrose non-fermentable (SWI/SNF) chromatin remodeling complexes, in combination with expression of mutant Kras led to the formation of cystic neoplastic lesions in adult mice that resembled human IPMNs [4]. This mouse model faithfully recapitulated human IPMN-PDA development and mirrored the human situation with a less malignant biological behavior as compared with PanIN-PDA. Next, it was interrogated, in this model, whether the IPMN lesions were of ductal or acinar origin by using *Cre*-lines that allow specific recombination of the *Brg1* and mutant *Kras* alleles in adult acinar ($Ptf1a^{CreER}$) or ductal ($Hnf1\beta\text{-}Cre^{ERT2}$) cells [4]. These experiments showed that Brg1 deletion renders adult duct cells sensitive to Kras-mediated transformation evidenced by the occurrence of duct atypia and lesions that resembled IPMNs. In contrast, Brg1 deletion in adult acinar cells in the context of mutant *Kras* did not lead to IPMN formation and, moreover, PanIN formation was blocked. This suggests that Brg1 plays a dual role in PDA precursor development by inhibiting duct transformation to IPMN and promoting acinar transformation to PanIN in the context of an oncogenic stimulus by mutant *Kras* (Figure 1).

This study gave the first experimental evidence that ductal cells can serve as the origin for IPMN lesions and highlighted the relevance of chromatin remodeling in this process. In a subsequent work, Roy et al. investigated the mechanistic basis for this observation [71]. It was found that combination of mutant *Kras* and loss of Brg1 in pancreatic ducts led to a dedifferentiation of mature ductal cells that was termed "ductal retrogression." Ductal retrogression was characterized by a reduced expression of markers of mature ductal differentiation and an upregulation of pancreatic progenitor factors such as Pdx1. One of the downregulated ductal markers was Sox9. Mechanistically it was shown that ectopic expression of Sox9 in the context of combined mutant Kras/Brg1 loss prevented ductal retrogression and IPMN formation (Figure 1). The upregulation of Pdx1 during ductal retrogression mirrors the expression pattern in pancreatic acinar cells during injury or Kras-mediated dedifferentiation. This points to Pdx1 as a unique factor in transformation of both acinar and ductal cells. Therefore, future studies need to explore a functional role of Pdx1 in this process and whether inhibition of this progenitor factor can prevent the formation of both PanIN and IPMN.

6. Conclusions with Translational Aspects

In contrast to some other cancers, embryonic signaling pathways like TGFβ, Wnt-β-catenin, and Hedgehog alone are not sufficient for the initiation of PDA [44]. Although the expression of a primitive ductal program can be launched, an oncogenic insult, most frequently mutated and constitutive active Kras, is required to drive pancreatic cancer progression. Apparently, acinar cells display the highest degree of cellular plasticity in order to adopt an undifferentiated progenitor state upon inflammatory or oncogenic stimuli. At the same time, it is becoming more and more clear that, although morphologically relatively uniform, PDA represents an extremely complex disease. In the field of pancreatic cancer research, we are lagging behind in terms of subtype identification compared to other solid cancer entities, for example, breast cancer. The cell of origin or precursor type leading to PDA has significant impact towards the prognosis of PDA patients. This suggests that not only the genetic makeup of a given cancer cell but its primordial lineage plays an important role. Our knowledge has been fueled to

a large extent by mouse models of pancreatic cancer but in order to address the complexity of this disease, human model systems are needed. For example, Kim et al. used an elegant induced-pluripotency approach to reprogram human PDA cells in order to recapitulate human disease progression [72]. Another study by Boj et al. suggests that an organoidculture system established from surgery specimen or endoscopic biopsy material grown in a three-dimensional matrix might be a useful tool to address this complexity [73]. In addition, this model system harbors the opportunity to test personalized therapies for pancreatic cancer patients, potentially even in real time.

In general, mouse models have significantly contributed to our understanding of virtually all aspects of PDA biology. However, so far we were not able to make use of this knowledge in order to improve PDA patients' care. The recent advances in pancreatic cancer treatment have been generated by not molecular defined strategies but rather pragmatic approaches using extremely toxic chemotherapeutic regimens [74] or increasing the delivery of established cytotoxic drugs [75].

The genetic heterogeneity of PDA and distinct oncogenic susceptibilities of defined compartments within the gland make this disease the opposite of what clinicians call a "chameleon"; one disease with many faces, PDA, instead, might represent numerous diseases with the same appearance. Thus, tailored therapies taking the mutational landscape of the respective tumor into account need to be developed and an even more profound understanding of the cellular plasticity and the regulating genetic factors in pancreatic carcinogenesis is required.

Conflict of Interests

The authors declare that there is no conflict of interests regarding the publication of this paper.

Acknowledgments

The authors express their gratitude to Ben Z. Stanger (University of Pennsylvania) for commenting on the developmental section of this review. This work was supported by the National Pancreas Foundation (Maximilian Reichert), the German Cancer Aid Foundation (Max-Eder Program, Deutsche Krebshilfe 111273 to Maximilian Reichert), and the AGA-Actavis Research Award in Pancreatic Disorders (Maximilian Reichert). Guido von Figura was supported by the Deutsche Forschungsgemeinschaft (FI 1719/1-1 and FI 1719/2-1). Alexander Kleger was supported by the Deutsche Forschungsgemeinschaft (KL 2544/1-1) and the Baden-Württemberg Stiftung (Eliteprogramme for Postdocs). Alexander Kleger is an Elser-Kröner-Fresenius-Memorial Fellow.

References

[1] R. Virchow, "Krankheitswesen und Krankheitsursachen," *Archiv für Pathologische Anatomie und Physiologie und für Klinische Medicin*, vol. 79, no. 2, pp. 185–228, 1880.

[2] N. Waddell, M. Pajic, A.-M. Patch et al., "Whole genomes redefine the mutational landscape of pancreatic cancer," *Nature*, vol. 518, no. 7540, pp. 495–501, 2015.

[3] A. K. Witkiewicz, E. A. McMillan, U. Balaji et al., "Whole-exome sequencing of pancreatic cancer defines genetic diversity and therapeutic targets," *Nature Communications*, vol. 6, article 6744, 2015.

[4] G. von Figura, A. Fukuda, N. Roy et al., "The chromatin regulator Brg1 suppresses formation of intraductal papillary mucinous neoplasm and pancreatic ductal adenocarcinoma," *Nature Cell Biology*, vol. 16, no. 3, pp. 255–267, 2014.

[5] J. L. Kopp, G. von Figura, E. Mayes et al., "Identification of Sox9-dependent acinar-to-ductal reprogramming as the principal mechanism for initiation of pancreatic ductal adenocarcinoma," *Cancer Cell*, vol. 22, no. 6, pp. 737–750, 2012.

[6] B. Z. Stanger, B. Stiles, G. Y. Lauwers et al., "Pten constrains centroacinar cell expansion and malignant transformation in the pancreas," *Cancer Cell*, vol. 8, no. 3, pp. 185–195, 2005.

[7] G. Gu, J. Dubauskaite, and D. A. Melton, "Direct evidence for the pancreatic lineage: NGN3+ cells are islet progenitors and are distinct from duct progenitors," *Development*, vol. 129, no. 10, pp. 2447–2457, 2002.

[8] J. R. Spence, A. W. Lange, S.-C. J. Lin et al., "Sox17 regulates organ lineage segregation of ventral foregut progenitor cells," *Developmental Cell*, vol. 17, no. 1, pp. 62–74, 2009.

[9] J. Jonsson, L. Carlsson, T. Edlund, and H. Edlund, "Insulin-promoter-factor 1 is required for pancreas development in mice," *Nature*, vol. 371, no. 6498, pp. 606–609, 1994.

[10] M. F. Offield, T. L. Jetton, P. A. Labosky et al., "PDX-1 is required for pancreatic outgrowth and differentiation of the rostral duodenum," *Development*, vol. 122, no. 3, pp. 983–995, 1996.

[11] F. C. Pan and C. Wright, "Pancreas organogenesis: from bud to plexus to gland," *Developmental Dynamics*, vol. 240, no. 3, pp. 530–565, 2011.

[12] B. Z. Stanger, A. J. Tanaka, and D. A. Melton, "Organ size is limited by the number of embryonic progenitor cells in the pancreas but not the liver," *Nature*, vol. 445, no. 7130, pp. 886–891, 2007.

[13] Y. Kawaguchi, B. Cooper, M. Gannon, M. Ray, R. J. MacDonald, and C. V. E. Wright, "The role of the transcriptional regulator Ptf1a in converting intestinal to pancreatic progenitors," *Nature Genetics*, vol. 32, no. 1, pp. 128–134, 2002.

[14] Q. Zhou, A. C. Law, J. Rajagopal, W. J. Anderson, P. A. Gray, and D. A. Melton, "A multipotent progenitor domain guides pancreatic organogenesis," *Developmental Cell*, vol. 13, no. 1, pp. 103–114, 2007.

[15] J. L. Kopp, C. L. Dubois, A. E. Schaffer et al., "Sox9+ ductal cells are multipotent progenitors throughout development but do not produce new endocrine cells in the normal or injured adult pancreas," *Development*, vol. 138, no. 4, pp. 653–665, 2011.

[16] M. Solar, C. Cardalda, I. Houbracken et al., "Pancreatic exocrine duct cells give rise to insulin-producing β cells during embryogenesis but not after birth," *Developmental Cell*, vol. 17, no. 6, pp. 849–860, 2009.

[17] T. Gao, B. McKenna, C. Li et al., "Pdx1 maintains β cell identity and function by repressing an α cell program," *Cell Metabolism*, vol. 19, no. 2, pp. 259–271, 2014.

[18] A. E. Schaffer, K. K. Freude, S. B. Nelson, and M. Sander, "Nkx6 transcription factors and Ptf1a function as antagonistic lineage determinants in multipotent pancreatic progenitors," *Developmental Cell*, vol. 18, no. 6, pp. 1022–1029, 2010.

[19] T. Masui, G. H. Swift, M. A. Hale, D. M. Meredith, J. E. Johnson, and R. J. MacDonald, "Transcriptional autoregulation controls pancreatic Ptf1a expression during development and adulthood," *Molecular and Cellular Biology*, vol. 28, no. 17, pp. 5458–5468, 2008.

[20] M. Reichert and A. K. Rustgi, "Pancreatic ductal cells in development, regeneration, and neoplasia," *The Journal of Clinical Investigation*, vol. 121, no. 12, pp. 4572–4578, 2011.

[21] R. Siegel, J. Ma, Z. Zou, and A. Jemal, "Cancer statistics, 2014," *CA: A Cancer Journal for Clinicians*, vol. 64, no. 1, pp. 9–29, 2014.

[22] D. P. Ryan, T. S. Hong, and N. Bardeesy, "Pancreatic adenocarcinoma," *The New England Journal of Medicine*, vol. 371, no. 11, pp. 1039–1049, 2014.

[23] A. Maitra, N. Fukushima, K. Takaori, and R. H. Hruban, "Precursors to invasive pancreatic cancer," *Advances in Anatomic Pathology*, vol. 12, no. 2, pp. 81–91, 2005.

[24] A. Gnoni, A. Licchetta, A. Scarpa et al., "Carcinogenesis of pancreatic adenocarcinoma: precursor lesions," *International Journal of Molecular Sciences*, vol. 14, no. 10, pp. 19731–19762, 2013.

[25] M. Tanaka, C. Fernández-Del Castillo, V. Adsay et al., "International consensus guidelines 2012 for the management of IPMN and MCN of the pancreas," *Pancreatology*, vol. 12, no. 3, pp. 183–197, 2012.

[26] H. Matthaei, A. L. Norris, A. C. Tsiatis et al., "Clinicopathological characteristics and molecular analyses of multifocal intraductal papillary mucinous neoplasms of the pancreas," *Annals of Surgery*, vol. 255, no. 2, pp. 326–333, 2012.

[27] G. A. Poultsides, S. Reddy, J. L. Cameron et al., "Histopathologic basis for the favorable survival after resection of intraductal papillary mucinous neoplasm-associated invasive adenocarcinoma of the pancreas," *Annals of Surgery*, vol. 251, no. 3, pp. 470–476, 2010.

[28] M. Mino-Kenudson, C. Fernández-del Castillo, Y. Baba et al., "Prognosis of invasive intraductal papillary mucinous neoplasm depends on histological and precursor epithelial subtypes," *Gut*, vol. 60, no. 12, pp. 1712–1720, 2011.

[29] M. Kanda, H. Matthaei, J. Wu et al., "Presence of somatic mutations in most early-stage pancreatic intraepithelial neoplasia," *Gastroenterology*, vol. 142, no. 4, pp. 730.e9–733.e9, 2012.

[30] E. Amato, M. D. Molin, A. Mafficini et al., "Targeted next-generation sequencing of cancer genes dissects the molecular profiles of intraductal papillary neoplasms of the pancreas," *The Journal of Pathology*, vol. 233, no. 3, pp. 217–227, 2014.

[31] F. Schönleben, W. Qiu, K. C. Bruckman et al., "BRAF and KRAS gene mutations in intraductal papillary mucinous neoplasm/carcinoma (IPMN/IPMC) of the pancreas," *Cancer Letters*, vol. 249, no. 2, pp. 242–248, 2007.

[32] T. Furukawa, Y. Kuboki, E. Tanji et al., "Whole-exome sequencing uncovers frequent GNAS mutations in intraductal papillary mucinous neoplasms of the pancreas," *Scientific Reports*, vol. 1, article 161, 2011.

[33] J. Wu, Y. Jiao, M. Dal Molin et al., "Whole-exome sequencing of neoplastic cysts of the pancreas reveals recurrent mutations in components of ubiquitin-dependent pathways," *Proceedings of the National Academy of Sciences of the United States of America*, vol. 108, no. 52, pp. 21188–21193, 2011.

[34] J. Wu, H. Matthaei, A. Maitra et al., "Recurrent *GNAS* mutations define an unexpected pathway for pancreatic cyst development," *Science Translational Medicine*, vol. 3, no. 92, Article ID 92ra66, 2011.

[35] S. Y. Xiao, "Intraductal papillary mucinous neoplasm of the pancreas: an update," *Scientifica*, vol. 2012, Article ID 893632, 20 pages, 2012.

[36] J.-P. De La O, L. L. Emerson, J. L. Goodman et al., "Notch and Kras reprogram pancreatic acinar cells to ductal intraepithelial neoplasia," *Proceedings of the National Academy of Sciences of the United States of America*, vol. 105, no. 48, pp. 18907–18912, 2008.

[37] C. Guerra, A. J. Schuhmacher, M. Cañamero et al., "Chronic pancreatitis is essential for induction of pancreatic ductal adenocarcinoma by K-Ras oncogenes in adult mice," *Cancer Cell*, vol. 11, no. 3, pp. 291–302, 2007.

[38] N. Habbe, G. Shi, R. A. Meguid et al., "Spontaneous induction of murine pancreatic intraepithelial neoplasia (mPanIN) by acinar cell targeting of oncogenic Kras in adult mice," *Proceedings of the National Academy of Sciences of the United States of America*, vol. 105, no. 48, pp. 18913–18918, 2008.

[39] H. P. Elsasser, G. Adler, and H. F. Kern, "Time course and cellular source of pancreatic regeneration following acute pancreatitis in the rat," *Pancreas*, vol. 1, no. 5, pp. 421–429, 1986.

[40] S. Willemer, H. P. Elsasser, H. F. Kern, and G. Adler, "Tubular complexes in cerulein- and oleic acid-induced pancreatitis in rats: glycoconjugate pattern, immunocytochemical, and ultrastructural findings," *Pancreas*, vol. 2, no. 6, pp. 669–675, 1987.

[41] V. Fendrich, F. Esni, M. V. R. Garay et al., "Hedgehog signaling is required for effective regeneration of exocrine pancreas," *Gastroenterology*, vol. 135, no. 2, pp. 621–e8, 2008.

[42] J. N. Jensen, E. Cameron, M. V. R. Garay, T. W. Starkey, R. Gianani, and J. Jensen, "Recapitulation of elements of embryonic development in adult mouse pancreatic regeneration," *Gastroenterology*, vol. 128, no. 3, pp. 728–741, 2005.

[43] J. P. T. Morris IV, D. A. Cano, S. Sekine, S. C. Wang, and M. Hebrok, "Beta-catenin blocks Kras-dependent reprogramming of acini into pancreatic cancer precursor lesions in mice," *The Journal of Clinical Investigation*, vol. 120, no. 2, pp. 508–520, 2010.

[44] J. P. Morris, S. C. Wang, and M. Hebrok, "KRAS, Hedgehog, Wnt and the twisted developmental biology of pancreatic ductal adenocarcinoma," *Nature Reviews. Cancer*, vol. 10, no. 10, pp. 683–695, 2010.

[45] O. Strobel, Y. Dor, J. Alsina et al., "In vivo lineage tracing defines the role of acinar-to-ductal transdifferentiation in inflammatory ductal metaplasia," *Gastroenterology*, vol. 133, no. 6, pp. 1999–2009, 2007.

[46] J. P. Morris IV, D. A. Cano, S. Sekine, S. C. Wang, and M. Hebrok, "β-catenin blocks Kras-dependent reprogramming of acini into pancreatic cancer precursor lesions in mice," *Journal of Clinical Investigation*, vol. 120, no. 2, pp. 508–520, 2010.

[47] L. C. Murtaugh, "Pathogenesis of pancreatic cancer: lessons from animal models," *Toxicologic Pathology*, vol. 42, no. 1, pp. 217–228, 2014.

[48] L. Zhu, G. Shi, C. M. Schmidt, R. H. Hruban, and S. F. Konieczny, "Acinar cells contribute to the molecular heterogeneity of pancreatic intraepithelial neoplasia," *The American Journal of Pathology*, vol. 171, no. 1, pp. 263–273, 2007.

[49] S. R. Hingorani, E. F. Petricoin III, A. Maitra et al., "Preinvasive and invasive ductal pancreatic cancer and its early detection in the mouse," *Cancer Cell*, vol. 4, no. 6, pp. 437–450, 2003.

[50] A. B. Lowenfels, P. Maisonneuve, G. Cavallini et al., "Pancreatitis and the risk of pancreatic cancer," *The New England Journal of Medicine*, vol. 328, no. 20, pp. 1433–1437, 1993.

[51] K. C. Ray, K. M. Bell, J. Yan et al., "Epithelial tissues have varying degrees of susceptibility to Kras(G12D)-initiated tumorigenesis in a mouse model," *PLoS ONE*, vol. 6, no. 2, Article ID e16786, 2011.

[52] P. A. Seymour, K. K. Freude, M. N. Tran et al., "SOX9 is required for maintenance of the pancreatic progenitor cell pool," *Proceedings of the National Academy of Sciences of the United States of America*, vol. 104, no. 6, pp. 1865–1870, 2007.

[53] G. Shi, L. Zhu, Y. Sun et al., "Loss of the acinar-restricted transcription factor Mist1 accelerates Kras-induced pancreatic intraepithelial neoplasia," *Gastroenterology*, vol. 136, no. 4, pp. 1368–1378, 2009.

[54] T. Miyatsuka, H. Kaneto, T. Shiraiwa et al., "Persistent expression of PDX-1 in the pancreas causes acinar-to-ductal metaplasia through Stat3 activation," *Genes & Development*, vol. 20, no. 11, pp. 1435–1440, 2006.

[55] M. Reichert, S. Takano, J. Von Burstin et al., "The Prrx1 homeodomain transcription factor plays a central role in pancreatic regeneration and carcinogenesis," *Genes & Development*, vol. 27, no. 3, pp. 288–300, 2013.

[56] R. A. Norris and M. J. Kern, "The identification of Prx1 transcription regulatory domains provides a mechanism for unequal compensation by the Prx1 and Prx2 loci," *Journal of Biological Chemistry*, vol. 276, no. 29, pp. 26829–26837, 2001.

[57] R. Kalluri and R. A. Weinberg, "The basics of epithelial-mesenchymal transition," *The Journal of Clinical Investigation*, vol. 119, no. 6, pp. 1420–1428, 2009.

[58] M. A. Nieto, "Epithelial plasticity: a common theme in embryonic and cancer cells," *Science*, vol. 342, no. 6159, Article ID 1234850, 2013.

[59] T. Brabletz, "To differentiate or not—routes towards metastasis," *Nature Reviews. Cancer*, vol. 12, no. 6, pp. 425–436, 2012.

[60] W. Guo, Z. Keckesova, J. L. Donaher et al., "Slug and Sox9 cooperatively determine the mammary stem cell state," *Cell*, vol. 148, no. 5, pp. 1015–1028, 2012.

[61] I. Houbracken, E. de Waele, J. Lardon et al., "Lineage tracing evidence for transdifferentiation of acinar to duct cells and plasticity of human pancreas," *Gastroenterology*, vol. 141, no. 2, pp. 731.e4–741.e4, 2011.

[62] C. Shi, S.-M. Hong, P. Lim et al., "KRAS2 mutations in human pancreatic acinar-ductal metaplastic lesions are limited to those with PanIN: implications for the human pancreatic cancer cell of origin," *Molecular Cancer Research*, vol. 7, no. 2, pp. 230–236, 2009.

[63] D. Li, E. J. Duell, K. Yu et al., "Pathway analysis of genome-wide association study data highlights pancreatic development genes as susceptibility factors for pancreatic cancer," *Carcinogenesis*, vol. 33, no. 7, pp. 1384–1390, 2012.

[64] G. M. Petersen, L. Amundadottir, C. S. Fuchs et al., "A genome-wide association study identifies pancreatic cancer susceptibility loci on chromosomes 13q22.1, 1q32.1 and 5p15.33," *Nature Genetics*, vol. 42, no. 3, pp. 224–228, 2010.

[65] M. Flandez, J. Cendrowski, M. Cañamero et al., "Nr5a2 heterozygosity sensitises to, and cooperates with, inflammation in KRas(G12V)-driven pancreatic tumourigenesis," *Gut*, vol. 63, no. 4, pp. 647–655, 2014.

[66] G. von Figura, J. P. Morris IV, C. V. E. Wright, and M. Hebrok, "Nr5a2 maintains acinar cell differentiation and constrains oncogenic Kras-mediated pancreatic neoplastic initiation," *Gut*, vol. 63, no. 4, pp. 656–664, 2014.

[67] A. F. Hezel, A. C. Kimmelman, B. Z. Stanger, N. Bardeesy, and R. A. Depinho, "Genetics and biology of pancreatic ductal adenocarcinoma," *Genes & Development*, vol. 20, no. 10, pp. 1218–1249, 2006.

[68] P. K. Mazur and J. T. Siveke, "Genetically engineered mouse models of pancreatic cancer: unravelling tumour biology and progressing translational oncology," *Gut*, vol. 61, no. 10, pp. 1488–1500, 2012.

[69] J. T. Siveke, H. Einwächter, B. Sipos, C. Lubeseder-Martellato, G. Klöppel, and R. M. Schmid, "Concomitant pancreatic activation of Kras(G12D) and Tgfa results in cystic papillary neoplasms reminiscent of human IPMN," *Cancer Cell*, vol. 12, no. 3, pp. 266–279, 2007.

[70] N. Bardeesy, K.-H. Cheng, J. H. Berger et al., "Smad4 is dispensable for normal pancreas development yet critical in progression and tumor biology of pancreas cancer," *Genes and Development*, vol. 20, no. 22, pp. 3130–3146, 2006.

[71] N. Roy, S. Malik, K. E. Villanueva et al., "Brg1 promotes both tumor-suppressive and oncogenic activities at distinct stages of pancreatic cancer formation," *Genes & Development*, vol. 29, no. 6, pp. 658–671, 2015.

[72] J. Kim, J. P. Hoffman, R. K. Alpaugh et al., "An iPSC line from human pancreatic ductal adenocarcinoma undergoes early to invasive stages of pancreatic cancer progression," *Cell Reports*, vol. 3, no. 6, pp. 2088–2099, 2013.

[73] S. F. Boj, C.-I. Hwang, L. A. Baker et al., "Organoid models of human and mouse ductal pancreatic cancer," *Cell*, vol. 160, no. 1-2, pp. 324–338, 2015.

[74] T. Conroy, F. Desseigne, M. Ychou et al., "FOLFIRINOX versus gemcitabine for metastatic pancreatic cancer," *The New England Journal of Medicine*, vol. 364, no. 19, pp. 1817–1825, 2011.

[75] D. D. Von Hoff, T. Ervin, F. P. Arena et al., "Increased survival in pancreatic cancer with nab-paclitaxel plus gemcitabine," *The New England Journal of Medicine*, vol. 369, no. 18, pp. 1691–1703, 2013.

Hindawi Publishing Corporation
Stem Cells International
Volume 2016, Article ID 6183562, 9 pages
http://dx.doi.org/10.1155/2016/6183562

Research Article

Dynamic Proteomic Analysis of Pancreatic Mesenchyme Reveals Novel Factors That Enhance Human Embryonic Stem Cell to Pancreatic Cell Differentiation

Holger A. Russ,[1] Limor Landsman,[1,2] Christopher L. Moss,[3] Roger Higdon,[3,4,5] Renee L. Greer,[1] Kelly Kaihara,[1] Randy Salamon,[3] Eugene Kolker,[3,4,5,6] and Matthias Hebrok[1]

[1]*Diabetes Center, Department of Medicine, University of California, San Francisco, San Francisco, CA 94143, USA*
[2]*Department of Cell and Developmental Biology, Faculty of Medicine, Tel Aviv University, 69978 Tel Aviv, Israel*
[3]*Bioinformatics and High-Throughput Analysis Laboratory and High-Throughput Analysis Core, Center for Developmental Therapeutics, Seattle Children's Research Institute, Seattle, WA 98105, USA*
[4]*Predictive Analytics, Seattle Children's Hospital, Seattle, WA 98105, USA*
[5]*Data-Enabled Life Sciences Alliance (DELSA), Seattle, WA 98105, USA*
[6]*Department of Biomedical Informatics & Medical Education and Pediatrics, Medical School, University of Washington, Seattle, WA 98101, USA*

Correspondence should be addressed to Eugene Kolker; eugene.kolker@seattlechildrens.org and Matthias Hebrok; matthias.hebrok@ucsf.edu

Received 16 March 2015; Accepted 4 May 2015

Academic Editor: Stefan Liebau

Current approaches in human embryonic stem cell (hESC) to pancreatic beta cell differentiation have largely been based on knowledge gained from developmental studies of the epithelial pancreas, while the potential roles of other supporting tissue compartments have not been fully explored. One such tissue is the pancreatic mesenchyme that supports epithelial organogenesis throughout embryogenesis. We hypothesized that detailed characterization of the pancreatic mesenchyme might result in the identification of novel factors not used in current differentiation protocols. Supplementing existing hESC differentiation conditions with such factors might create a more comprehensive simulation of normal development in cell culture. To validate our hypothesis, we took advantage of a novel transgenic mouse model to isolate the pancreatic mesenchyme at distinct embryonic and postnatal stages for subsequent proteomic analysis. Refined sample preparation and analysis conditions across four embryonic and prenatal time points resulted in the identification of 21,498 peptides with high-confidence mapping to 1,502 proteins. Expression analysis of pancreata confirmed the presence of three potentially important factors in cell differentiation: Galectin-1 (LGALS1), Neuroplastin (NPTN), and the Laminin α-2 subunit (LAMA2). Two of the three factors (LGALS1 and LAMA2) increased expression of pancreatic progenitor transcript levels in a published hESC to beta cell differentiation protocol. In addition, LAMA2 partially blocks cell culture induced beta cell dedifferentiation. Summarily, we provide evidence that proteomic analysis of supporting tissues such as the pancreatic mesenchyme allows for the identification of potentially important factors guiding hESC to pancreas differentiation.

1. Introduction

Generation of functional insulin-producing beta cells from human stem cell populations would provide an abundant resource for cell replacement therapies used in the treatment of type 1 diabetic patients. Several cell culture protocols detailing the guided differentiation of hESC [1, 2] and human induced pluripotent stem (iPS) cells [3, 4] into insulin-producing beta-like cells have been generated. However, most approaches have resulted in low numbers of immature, non-functional insulin expressing cells. A possible reason for the failure is the absence of critical factors present during embryonic pancreas development. Current approaches are largely based on knowledge gained from developmental studies into

the pathways and transcriptional programs underlying murine pancreatic epithelium specification [1–4]. In contrast, the contribution of surrounding supportive tissues, including the mesenchyme critical for *in vivo* pancreas formation [3–5], has not been explored fully. Recent evidence underscoring the importance of the mesenchyme comes from coculture experiments demonstrating that mesenchymal cell lines promote the expansion of hESC-derived endocrine progenitors [6]; however, the factors responsible for these effects have not been identified. We hypothesized that a detailed proteomic characterization of factors produced by the pancreatic mesenchyme would result in the identification of proteins that could be added to current ES differentiation protocols to enable a more comprehensive simulation of normal development *in vitro*.

2. Experimental Methods

2.1. Mice. Mice used in this study were maintained according to protocols approved by the University of California, San Francisco, Committee on Laboratory Animal Resource Center. *Nkx3.2 (Bapx1)*-Cre mice were described previously [7]. *R26-YFP*^{flox} (*Gt(ROSA)26Sor*$^{tm1(EYFP)Cos}$) mice were obtained from Jackson Laboratories.

2.2. Sorting. Dissected pancreata were digested in 0.4 mg/mL Collagenase P (Roche) and 0.1 ng/mL DNase (Sigma) diluted in HBSS for 30 min at 37°C and filtered through a 40 mm filter. Following staining with PECAM1-PE (eBioscience, 1 : 200) and/or DAPI to exclude dead cells, cell isolation was performed using FACS Aria (BD).

2.3. Cell Culture. Undifferentiated CyT49 hES cells (ViaCyte, Inc.) were maintained on mouse embryo fibroblast feeder layers (Millipore). Differentiation was carried out as described previously [8]. LGALS1 (1 μg/mL or 5 μg/mL), LAMA2 (5 μg/mL), and Narpin (3 μM) were obtained from Peprotech (USA), Millipore (USA), and Bio Basics (Canada), respectively. Control fibroblast lines were established by culturing sorted YFP$^+$ mesenchymal cells in DMEM containing 10% fetal bovine serum for at least 4 passages. For dedifferentiation analysis, isolated islets were dispersed into single cells by 5–10 min incubation with 0.25% Trypsin (Gibco), followed by cell filtration. Cells were grown for 3 days either on poly-D-Lysine coated-plates (Millipore) or on plates coated overnight with 5 μg/mL human Merosin (Millipore), which is comprised of a mixture of LM211 and LM221.

2.4. Immunofluorescence Analysis. Fixed human cadaver pancreatic tissue (Prodo) was incubated in 30% sucrose solution followed by embedding in OCT (TissueTek), cryopreservation, and sectioning. Dissected mouse pancreatic tissues were fixed with Z-fix (Anatech), incubated in 30% sucrose overnight, and cryopreserved. Tissue sections were stained with primary antibodies, anti-mouse vimentin (1 : 200, Sigma), anti-human vimentin (1 : 50, Calbiochem), anti-YFP/GFP (1 : 500, Abcam), anti-Galectin-1 (1 : 50, RnD Systems), anti-LAMA2 (1 : 200, Enzo), and anti-PDX1 (1 : 200, RnD Systems), followed by staining with AlexaFluor tagged secondary antibodies (1 : 500, Invitrogen) and mounting Vectashield media (Vector). Nuclei were visualized with DAPI. Images were acquired using a Leica SP5 microscope or an InCell Analyzer 2000 for quantification (GE Healthcare). 16 fields from each condition were randomly selected by the InCell Analyzer and imaged for quantification. PDX1 positive nuclei over total nuclei were determined using InCell Developer software (GE Healthcare).

2.5. qPCR Analysis. Total RNA was isolated with TRIZOL (Sigma) and 500 ng was reverse transcribed using the iScript cDNA Kit (Bio-Rad) according to manufacturer's instructions. qPCR analysis was performed on an ABI 7900 HT Fast Real-Time PCR System (Applied Biosystems) using standard protocols. Primer sequences are as follows: LGALS1 ATCGTGTGCAACAGCAAGG and CCTGGTCGAAGGTGATGC; LAMA2 AAAGATCCTTCCAAGAACAAAATC and CGGTCAGCTTCCTGTTCTAAA; NPTN TCTCGCTGTTGCTGGTCTC and CCTCTTCACTGGTGACAATCC; NGN3 AAGTCTACCAAAGCTCACGCG and GCTCATCGCTCTCTATTCTTTTGC; PDX1 AAGTCTACCAAAGCTCACGCG and GTAGGCGCCGCCTGC; TBP TGTGCACAGGAGCCAAGAGT and ATTTTCTTGCTGCCAGTCTGG. Taqman Probes: LAMA2 Mm00550083_m1; ACTB 4352933-0810025.

2.6. MS Methods. Filter-Aided Sample Prep (FASP) was used to lyse cells, digest with trypsin, and recover the tryptic peptides [9]. Peptides were analyzed by nano-LC/MS/MS. Peptides were eluted across a 3-hour gradient on a 20 cm, self-packed C18 capillary column on an Eksigent NanoLC-2D system. Mass spectra were acquired on a Thermo LTQ Velos linear ion-trap mass spectrometer. The 5 highest intensity 2^+ or 3^+ ions from each MS scan were selected for collision induced dissociation (CID).

2.7. Data Analysis. Protein identification and quantitation were carried out using the SPIRE (Systematic Protein Identification and Relative Expression) analysis platform for high-throughput proteomics data analysis [10]. SPIRE employs a novel approach to combining the open source search algorithms X! Tandem and OMSSA to increase the number of peptide and protein identifications and significantly improve statistical assessment of these identifications. SPIRE generates peptide identification probabilities based on a combination of logistic regression models and a randomized protein sequence database search, in this case versus the Uniprot complete mouse proteome. SPIRE uses a newly modified protein ID model to aggregate peptide spectra identifications into protein identifications and generate a false discovery rate threshold value (q-value) for each identified protein. SPIRE also generates quantitation estimates for relative expression analysis based upon spectral counts (number of high-confidence peptide spectrum matches) normalized by total expression in each sample. Visualization of the proteomics expression data was carried out by a combination of heatmaps and hierarchical clustering using R statistical software (R foundation for statistical computing). The protein identifications were mapped to functional keywords in the Gene

Ontology using amiGO [11]. The data were revisualized as separated protein groups based upon these results. Human ES differentiation data are shown as the mean ± SD. Data were evaluated using a two-tailed Student's t-test.

2.8. Targeted Proteomics. Laminin alpha-2 was quantified in samples using selected reaction monitoring (SRM) coupled with stable isotope dilution mass spectrometry (SID-MS) [12]. Two peptides identified in spectral libraries from previous experiments were used as characteristic peptides for Laminin alpha-2. We had these peptides synthesized and isotopically labeled. The highest intensity y-ions for each peptide from the MS/MS spectra in the spectral library were chosen as reporter ions to determine concentration. Calibration curves of reporter ion intensity ratios were determined for the two different synthesized peptides and their isotope-labeled partners. The isotope-labeled synthesized peptide standards were spiked into samples at 0.5 fmol/μL; then absolute concentration of target peptides was determined by fitting isotope ratios of the MS/MS reporter ions to the calibration curve. Skyline analysis software was used to set up inclusion lists for peptide sequences extract peak intensity values and provide spectral libraries [13].

3. Results and Discussion

In our proteomic analysis we employed the previously described *Nkx*3.2-Cre mouse line, which permits specific expression of Cre recombinase in mesenchyme, but not epithelial, endothelial, or neuronal cells of the developing pancreas [5]. This mouse line was used in conjunction with a Rosa26 loxp STOP loxp yellow fluorescence protein (YFP) reporter mouse to isolate pancreatic mesenchymal cells by fluorescence activated cell sorting (FACS) for global proteomic analysis (Figures 1(a) and 1(b)). YFP$^+$ mesenchymal cell aliquots of ~500,000 cells from embryonic day (e)15.5 (peak of Ngn3 expression, a marker for endocrine cell differentiation), e17.5 (islet formation initiated), postnatal day (p)2 (immature beta cells present), and p14 (mature beta cells present) pancreata with purities of 96.8 ± 1.6% (see Figure S1 in Supplementary Material available online at http://dx.doi.org/10.1155/2016/6183562) were sorted under protein-free conditions and snap frozen prior to analysis by tandem MS based shotgun proteomics. Notably, the sample amount obtained was an order of magnitude lower than what is typically employed in such experiments. Given this constraint we used a protocol (Figure 1(c)) that minimizes necessary sample clean-up and resulted in the recovery of 8.6 to 16.3 μg of protein from each aliquot. Aliquots were analyzed in triplicate and protein identification and quantification were carried out using SPIRE software [10] and peptide spectra were matched to the UniProt [14] mouse complete proteome sequence database. Overall, we identified 21,498 high-confidence (greater than 90%) peptide spectrum matches across time points using our approach (Figure 1(d)). Using SPIRE generated false discovery rate (FDR) thresholds of either 1% or 5% resulted in the identification of 842 and 1502 proteins, respectively (Figure 1(d)). Visualization using heatmaps of the normalized spectral counts and hierarchical clustering revealed distinct sets of proteins based on expression changes over time (Figure 2(a)). Further filtering of proteins by Gene Ontology (GO) [11] terms including extracellular matrix (ECM), secretion, adhesion, wingless signaling transduction pathway (WNT), and membrane localization resulted in matches to 143 total proteins. From these, we chose two, Galectin-1 (LGALS1) and Neuroplastin (NPTN) (Figure 2(b)), for further evaluation, based on their expression patterns and information from published studies [15, 16]. Although the approach we employed is an excellent strategy for evaluating a large number of protein candidates, many very low abundance proteins still remain below the detection limit. Given this caveat, we also pursued a targeted approach based on preliminary results suggesting a role for Laminins 211 and 221 containing the α-2 subunit (LAMA2) in beta cell function. We had noted that FACS sorted YFP$^+$ mesenchymal cells revealed a significant enrichment of *Lama2* transcripts compared to whole pancreas. Of note, *Lama2* was not detected in pancreatic endothelial cells (Figure S2A and [17]), suggesting the mesenchyme as the primary source of Laminin α-2 chain in the pancreas. Addition of LAMA2 partially blocks cell culture induced dedifferentiation of beta cells (Figure S2B). mRNA transcript levels for beta cell marker genes *Ins1* and *Mafa* in cultured islets treated with LAMA2 were unchanged compared to fresh islets, while Lysine treated control cultures showed a significant reduction. Glucose transporter *Glut2* gene expression was reduced in both cultured islet groups compared to fresh islets, albeit significantly less in LAMA2 treated cultured islets. In addition, *Hes1*, a marker for beta cell dedifferentiation [18], was less induced in LAMA2 treated islets compared to control cultures (Figure S2B). Collectively, these data indicate a functional role for LAMA2 in supporting the beta cell differentiation state. We designed a selected reaction-monitoring (SRM) assay using two synthesized peptide standards from LAMA2 and determined the mean concentration of protein present in three independent fibroblast cell lines established from sorted YFP$^+$ mesenchymal cells and in two samples of freshly sorted P2 neonatal YFP$^+$ cells to be 0.032 and 0.047 fmol/μL, respectively (Figure 2(c)). Notably, concentrations are an order of magnitude below what is typically detected in shotgun proteomics experiments using the instrumentation employed in this study [19]. Tandem MS and SRM results were confirmed by employing immunofluorescence analysis of lineage-traced YFP$^+$ mesenchymal cells of pancreata from e15.5, e17.5, p2, and p14. As expected, YFP$^+$ cells costain for the mesenchymal marker Vimentin (Vim) that was used as a positive control (Figure 3(a)). These cells also exhibit immune reactivity to an LGALS1 specific antibody, confirming the proteomic identification of this factor in pancreas mesenchyme (Figure 3(b)). Staining by Lama2 revealed an intricate network in close proximity to YFP-labeled mesenchymal cells (Figure 3(c)). We also detected cells positive for the mesenchymal marker VIM or LGALS1 with a typical mesenchymal morphology immediately adjacent to insulin-producing beta cells.

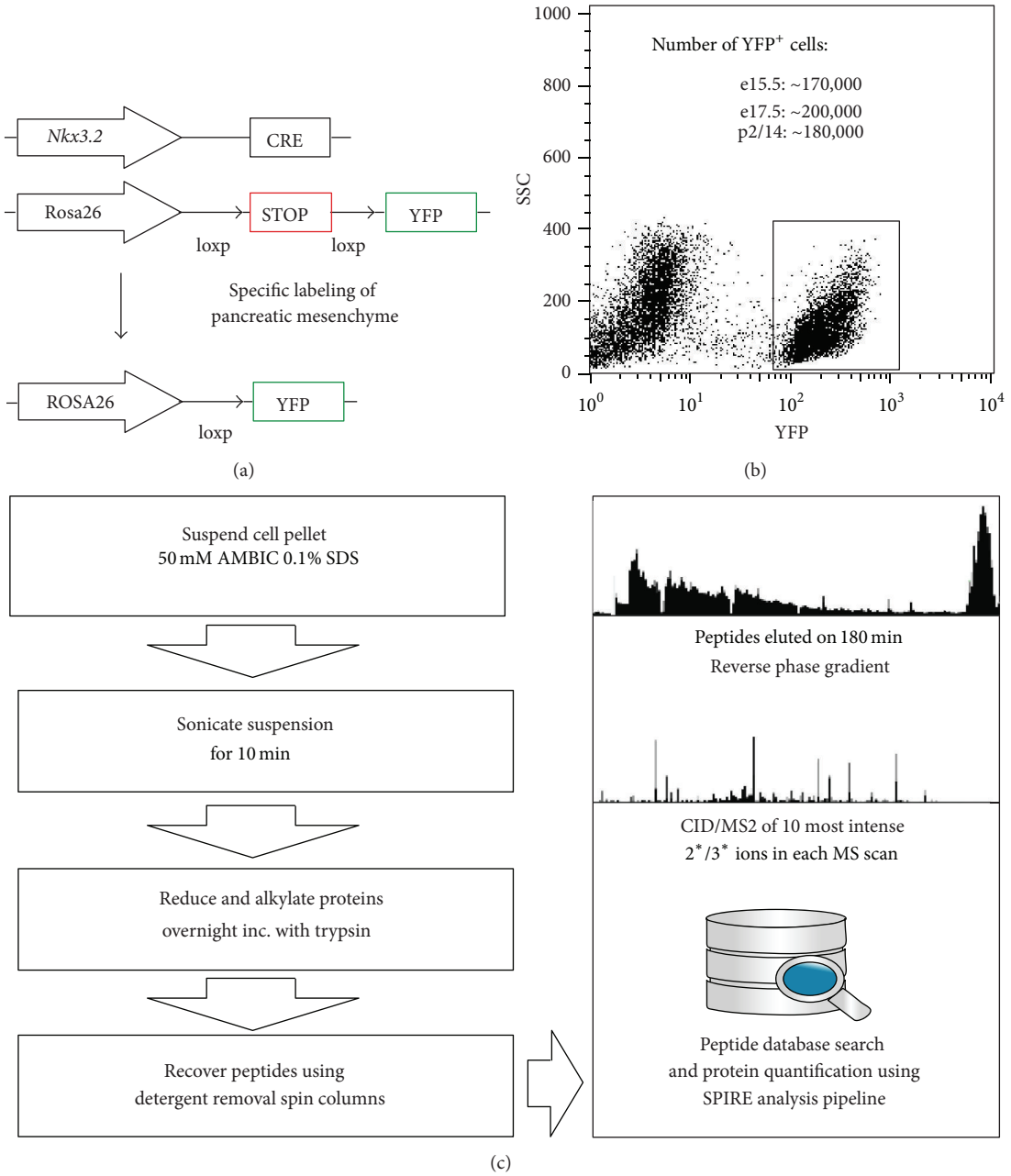

Sample	Peptide ID	Protein ID FDR < 0.05	Protein ID FDR < 0.01
e15.5	2187	171	67
e17.5	9475	493	234
p2	4546	384	172
p14	5290	454	271

(d)

Figure 1: Isolation of pancreatic mesenchyme for proteomic analysis. (a) Schematic representation of transgenic mouse models employed to permanently label pancreatic mesenchymal cells. The mesenchyme specific *Nkx3.2* promoter drives Cre recombinase expression during organogenesis and results in the excision of a loxp site flanked stop sequence. This excision in turn gives rise to constitutive expression of the fluorescence reporter YFP specifically in mesenchymal cells. (b) Representative dot plot of fluorescence activated cell sorting of YFP labeled mesenchymal cells. Approximate numbers of sorted YFP$^+$ cells per litter and postpartum mouse are given in the inset. (c) Schematic illustrating the sample preparation and mass spectrometric analysis. (d) Table with total number of identified peptides per time point and corresponding protein discoveries with false discovery rates (FDR) of 5% and 1%, respectively.

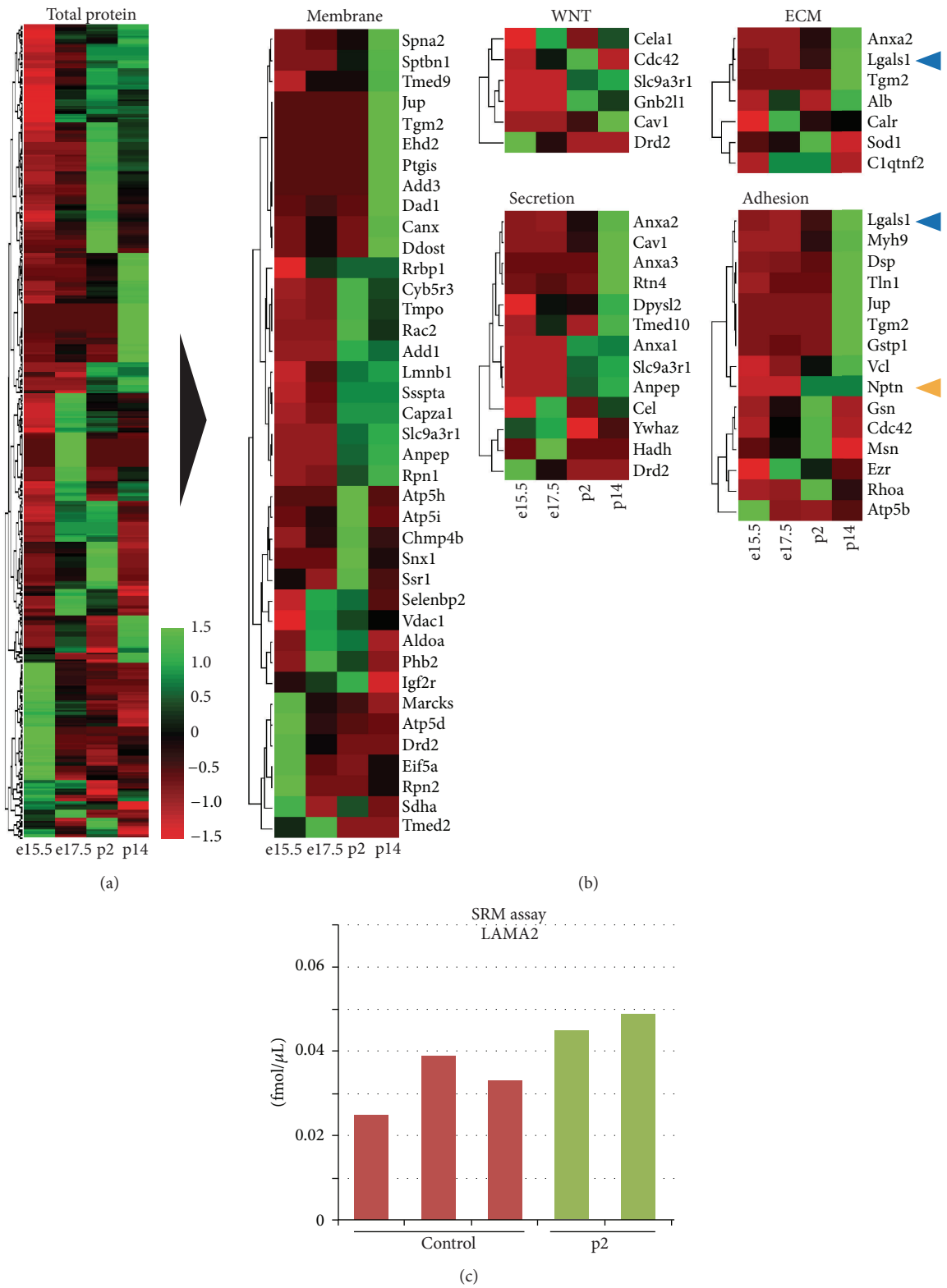

FIGURE 2: Expression pattern analysis of mesenchymal proteome and absolute quantification of candidate protein Laminin α-2. ((a) and (b)) Identified proteins were visualized as heat maps with high and low expression visualized in green or red, respectively. Expression values were normalized to z scores by subtracting raw means and dividing by standard deviations. (a) All proteins with at least 5 peptide spectrum matches are visualized. (b) Proteins were further broken down by GO terms: membrane, WNT pathway, extracellular matrix (ECM), secretion, and adhesion. Two factors, Galectin-1 (LGALS1, blue arrowheads) and Neuroplastin (NPTN, yellow arrowhead), were chosen for further analysis. (c) Absolute quantification of Laminin α-2 chain (LAMA2) in p2 samples by selected reaction monitoring (SRM) revealed a concentration of 0.47 fmol/μL in comparison to 0.30 fmol/μL in control fibroblast samples.

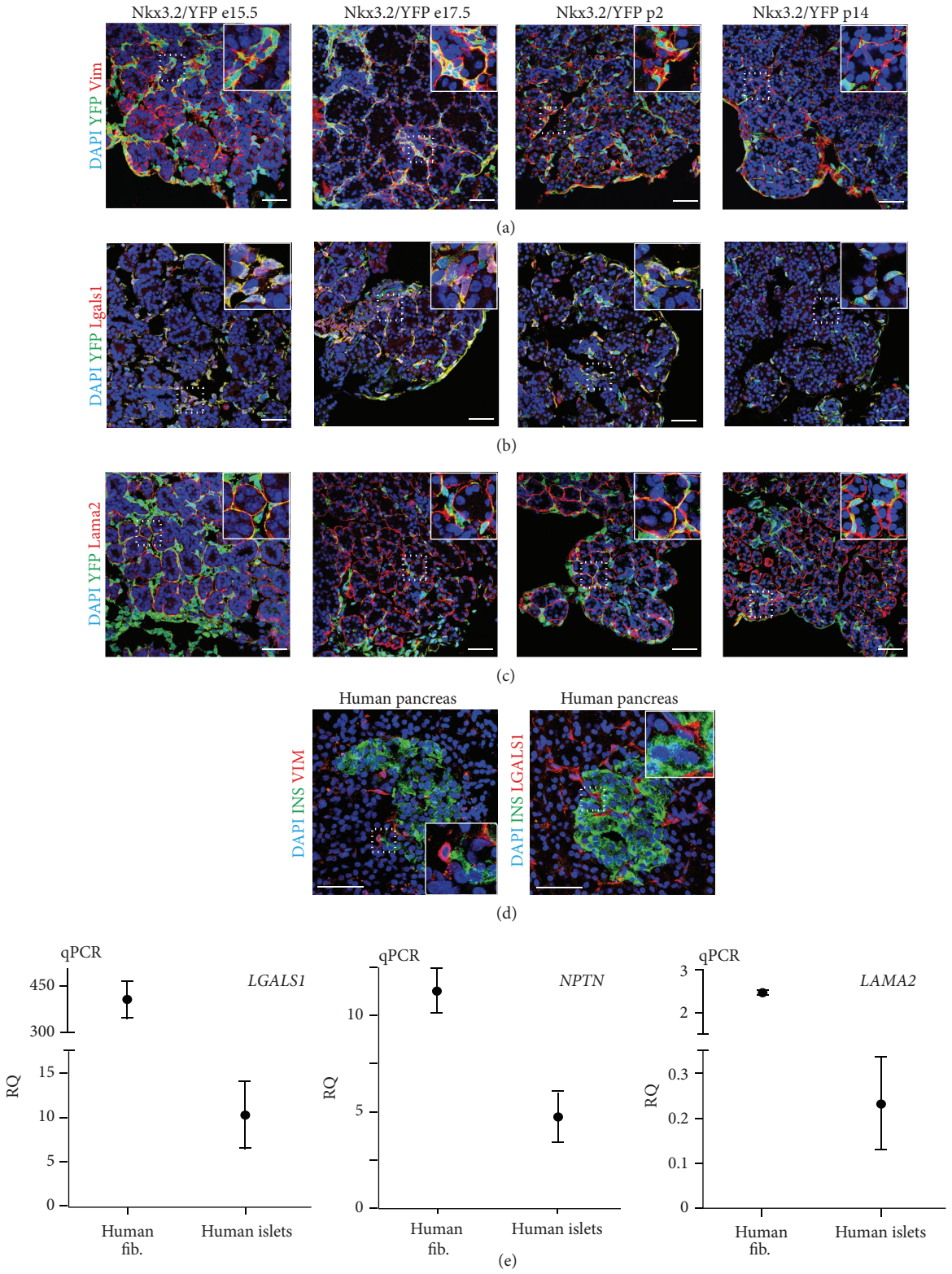

Figure 3: Mesenchymal factors, Galectin-1, Neuroplastin, and Laminin α-2, are expressed in mouse and human pancreata. ((a), (b), and (c)) Coimmunofluorescence analysis of YFP linage-traced transgenic pancreata at e15.5, e17.5, p2, and p14 for coexpression of YFP marker, the common mesenchymal marker Vimentin (Vim, in (a)), Galectin-1 (Lgals1, in (b)), and Laminin α-2 (Lama2, in (c)). Size bar = 50 μm. (d) Healthy human pancreas sections showing vimentin (VIM) and galectin-1 (LGALS1) positive cells with mesenchymal morphology intermingled and in close proximity to insulin expressing beta cells organized in islets of Langerhans. Size bar = 50 μm. (e) Quantitative PCR analysis of Galectin-1 (*LGALS1*), Neuroplastin (*NPTN*), and Laminin α-2 (*LAMA2*) transcripts in human foreskin fibroblasts (n = 2) and purified human islet preparations (n = 5).

These putative mesenchymal cells can be found both surrounding and within islets of healthy human pancreata (Figure 3(d)). Although we could not achieve reliable staining with existing antibodies for LAMA2 in human pancreas sections and NPTN in mouse or human sections, qPCR analysis of purified human islets revealed on average 0.2- and 5-fold expression of the *LAMA2* and *NPTN* transcripts, respectively, over the endogenous control gene TATA box binding protein (*TBP*) (Figure 3(e)). Cultured human fibroblasts expressed on average 2.5- and 11-fold more *LAMA2* and *NPTN*, respectively. *LGALS1* transcripts in cultured human fibroblasts and purified human islets were on average 406- and 10-fold enriched, respectively (Figure 3(e)). These results confirm the presence of the factors identified by proteomic analysis in mouse and human islet tissues.

Next we examined whether our novel factors could promote directed differentiation of hESCs towards pancreatic endocrine cells employing our recently published protocol [8]. Analysis by qPCR revealed very low or undetectable transcript levels for *LAMA2* and *LGALS1* in control differentiated hESC cultures at the pancreatic progenitor stage. In contrast, *NPTN* transcripts levels, albeit lower than in cultured fibroblast or islets, were on average 1.3-fold higher than *TBP* levels (Figure S3). We added recombinant LGALS1 and LAMA2, as well as the peptide Narpin (shown to mimic the binding activity of NPTN *in vitro* [16]), to hESC-derived foregut-like cells for three days to allow further differentiation into pancreatic progenitors (Figure 4(a)). We observed significant differences relative to control cultures in the proliferation of cells treated with either LAMA2 or LGALS1 (Figure 4(b)). We previously showed that mesenchymal cells support proliferation of pancreatic precursors and later staged differentiated endocrine cells *in vivo* [5]. While LGALS1 addition resulted in a significant increase of proliferation, LAMA2 reduced proliferation of pancreatic progenitors. These data indicate discrete effects of individual mesenchyme factors at specific developmental stages and that such might differ from the combined effects of all factors provided by a supportive tissue, like the pancreatic mesenchyme, during development *in vivo*. Pancreatic progenitor marker *PDX-1* mRNA levels were significantly increased in experiments incubated with either LGALS1 or LAMA2 while Narpin incubation did not show any changes (Figure 4(c)). The observed increase in *PDX-1* transcript levels after addition of LGALS was concentration dependent. However, quantification of pancreatic progenitor cells identified by PDX-1 protein expression did not reveal significant changes after treatment with LGALS1, LAMA2, or Narpin (Figure 4(d)), indicating that the factors promote PDX-1 expression without increasing the already high percentage of PDX-1+ cells present under control conditions. In addition, LAMA2 enhanced transcript levels of the endocrine progenitor marker *NGN3* (Figure 4(c)), known to be required for the generation of all hormone positive endocrine cells [20].

In summary our data demonstrate the ability to identify novel factors potentially important in beta cell differentiation using proteomic analysis of the pancreatic mesenchyme. In addition, we show that specific proteins can be quantified by our approach in low abundance samples. Most importantly, we show that two out of three novel factors selected for additional validation can enhance hESC to beta cell differentiation. Our approach described here not only is restricted to the pancreas but also can be easily adopted to better characterize even small numbers of supportive cell types and tissues in differentiation of other lineages and organs. We anticipate that fine-tuning existing hESC differentiation approaches will enable the generation of fully matured beta cells under cell culture conditions.

Conflict of Interests

The authors declare that there is no conflict of interests regarding the publication of this paper.

Authors' Contribution

Conception and design were performed by Holger A. Russ, Eugene Kolker, and Matthias Hebrok. Financial support was from NIH BCBC. Holger A. Russ, Limor Landsman, Renee L. Greer, and Christopher L. Moss contributed to collection and/or assembly of data. Data analysis and interpretation were done by Holger A. Russ, Limor Landsman, Christopher L. Moss, Roger Higdon, Randy Salamon, Renee L. Greer, Kelly Kaihara, Eugene Kolker, and Matthias Hebrok. Holger A. Russ and Roger Higdon contributed to paper writing. Final approval of paper was done by Holger A. Russ, Limor Landsman, Christopher L. Moss, Roger Higdon, Randy Salamon, Renee L. Greer, Kelly Kaihara, Eugene Kolker, and Matthias Hebrok.

Acknowledgments

The authors thank members of the Hebrok and Kolker laboratories for comments and discussion. They would like to thank Dr. Shimon Efrat (Tel Aviv University, Israel) for the kind gift of purified human islet RNA and Dr. Sheng Ding (Gladstone Institute, San Francisco, USA) for human foreskin fibroblasts. Holger A. Russ was supported by a Richard G. Klein fellowship and a JDRF fellowship (3-2012-266). Limor Landsman was supported by an American Diabetes Association Mentorship Award. Image acquisition was supported by the University of California, San Francisco, Diabetes and Endocrinology Research Center (DERC) microscopy coreP30 DK63720. Islet isolation was performed by the University of California, San Francisco, Diabetes and Endocrinology Research Center (DERC) islet core P30 DK63720. Research in Matthias Hebrok's laboratory is supported by funds from a TCPA grant from the Beta Cell Biology Consortium (UO1 DK089541) and a grant from the Leona M. & Harry B. Helmsley Charitable Trust. Research in the lab of Eugene Kolker is supported by the National Science Foundation under the Division of Biological Infrastructure Award 0969929, National Institute of Diabetes and Digestive and Kidney Diseases of the National

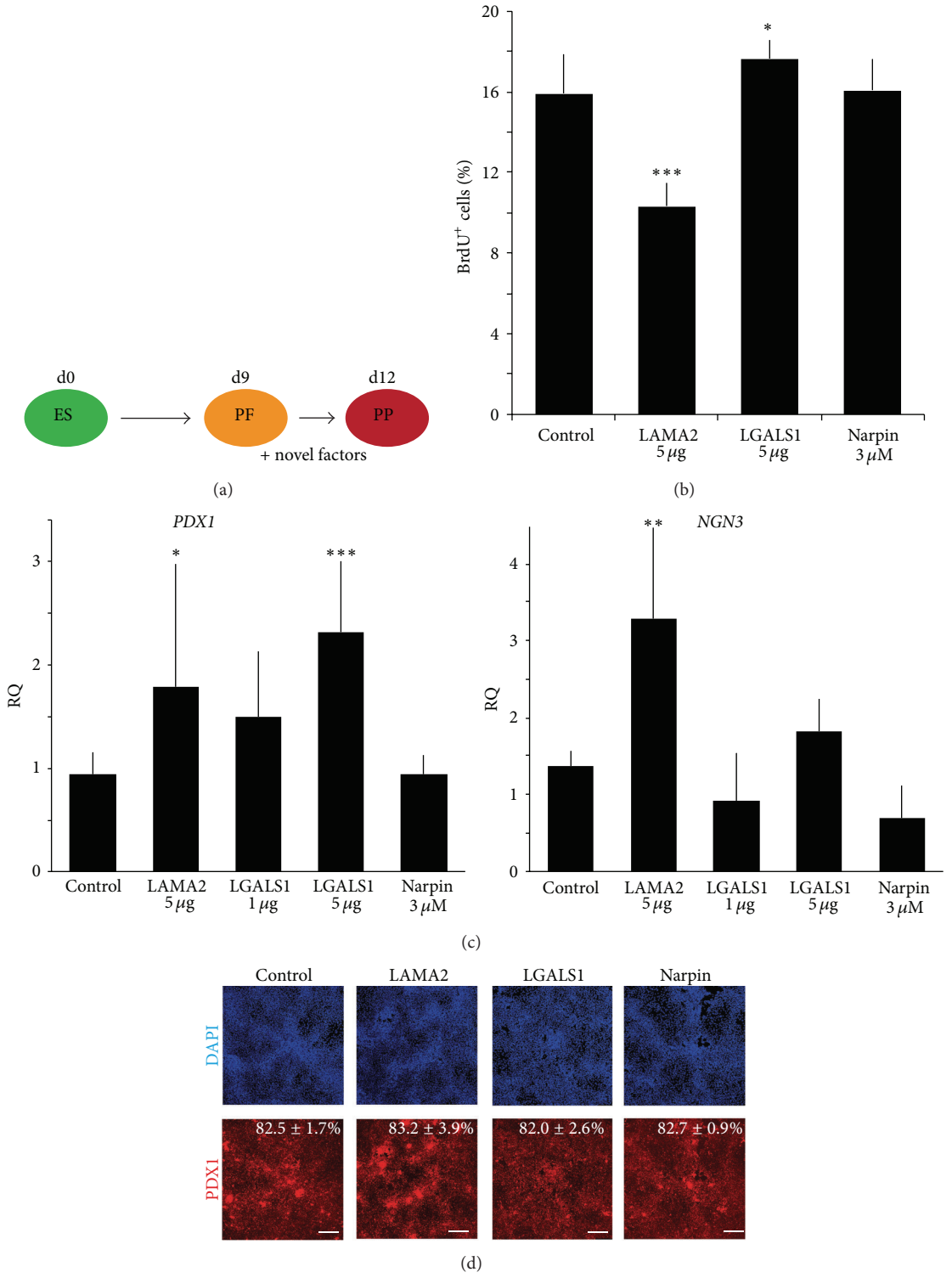

Figure 4: Mesenchymal factors, Laminins containing a α-2 chain and Galectin-1, improve human embryonic stem cell differentiation. (a) Schematic of the experimental setup to test possible effects of novel mesenchymal factors on direct differentiation of human embryonic stem (ES) cells. Factors were added at day 9 to posterior foregut-like (PF) cells for three days before analysis of pancreatic progenitor (PP) cells. (b) Flow cytometric analysis of proliferating cells in control and treated cultures at day 12 after 24-hour incubation with BrdU. Data shown are from 2 independent experiments, $n = 7$. (c) Quantitative PCR analysis for the pancreatic progenitor marker *PDX1* and endocrine marker *NGN3*. Data shown are average ± standard deviation from 3 independent experiments, $n = 5$–8, relative to untreated control cultures at day 12 of differentiation and normalized to the endogenous control gene *TBP*. (d) Quantification of immunofluorescence analysis of PDX1 positive as a percentage of total cells with an InCell Analyzer. Data shown are average ± standard deviation of 16 independent fields assayed in 2 independent experiments. Size bar = 250 μm.

Institutes of Health under Awards U01-DK-089571 and U01-DK-072473, The Robert B. McMillen Foundation, The Gordon and Betty Moore Foundation, and Seattle Children's Research Institute award.

References

[1] K. A. D'Amour, A. G. Bang, S. Eliazer et al., "Production of pancreatic hormone-expressing endocrine cells from human embryonic stem cells," *Nature Biotechnology*, vol. 24, no. 11, pp. 1392–1401, 2006.

[2] D. Van Hoof, K. A. D'Amour, and M. S. German, "Derivation of insulin-producing cells from human embryonic stem cells," *Stem Cell Research*, vol. 3, no. 2-3, pp. 73–87, 2009.

[3] R. Maehr, S. Chen, M. Snitow et al., "Generation of pluripotent stem cells from patients with type 1 diabetes," *Proceedings of the National Academy of Sciences of the United States of America*, vol. 106, no. 37, pp. 15768–15773, 2009.

[4] H. Hua, L. Shang, H. Martinez et al., "iPSC-derived β cells model diabetes due to glucokinase deficiency," *The Journal of Clinical Investigation*, vol. 123, no. 7, pp. 3146–3153, 2013.

[5] L. Landsman, A. Nijagal, T. J. Whitchurch et al., "Pancreatic mesenchyme regulates epithelial organogenesis throughout development," *PLoS Biology*, vol. 9, no. 9, Article ID e1001143, 2011.

[6] J. B. Sneddon, M. Borowiak, and D. A. Melton, "Self-renewal of embryonic-stem-cell-derived progenitors by organ-matched mesenchyme," *Nature*, vol. 491, no. 7426, pp. 765–768, 2012.

[7] M. P. Verzi, M. N. Stanfel, K. A. Moses et al., "Role of the homeodomain transcription factor Bapx1 in mouse distal stomach development," *Gastroenterology*, vol. 136, no. 5, pp. 1701–1710, 2009.

[8] T. Guo, L. Landsman, N. Li, and M. Hebrok, "Factors expressed by murine embryonic pancreatic mesenchyme enhance generation of insulin-producing cells from hESCs," *Diabetes*, vol. 62, no. 5, pp. 1581–1592, 2013.

[9] J. R. Wiśniewski, A. Zougman, N. Nagaraj, and M. Mann, "Universal sample preparation method for proteome analysis," *Nature Methods*, vol. 6, no. 5, pp. 359–362, 2009.

[10] E. Kolker, R. Higdon, P. Morgan et al., "SPIRE: systematic protein investigative research environment," *Journal of Proteomics*, vol. 75, no. 1, pp. 122–126, 2011.

[11] The Gene Ontology Consortium, "Gene ontology annotations and resources," *Nucleic Acids Research*, vol. 41, pp. D530–D535, 2013.

[12] P. Picotti and R. Aebersold, "Selected reaction monitoring-based proteomics: workflows, potential, pitfalls and future directions," *Nature Methods*, vol. 9, no. 6, pp. 555–566, 2012.

[13] B. MacLean, D. M. Tomazela, N. Shulman et al., "Skyline: an open source document editor for creating and analyzing targeted proteomics experiments," *Bioinformatics*, vol. 26, no. 7, Article ID btq054, pp. 966–968, 2010.

[14] M. Y. Galperin and X. M. Fernández-Suárez, "The 2012 nucleic acids research database issue and the online molecular biology database collection," *Nucleic Acids Research*, vol. 40, no. 1, pp. D1–D8, 2012.

[15] M. Y. Lee, S. H. Lee, J. H. Park, and H. J. Han, "Interaction of galectin-1 with caveolae induces mouse embryonic stem cell proliferation through the Src, ERas, Akt and mTOR signaling pathways," *Cellular and Molecular Life Sciences*, vol. 66, no. 8, pp. 1467–1478, 2009.

[16] S. Owczarek, D. Kiryushko, M. H. Larsen et al., "Neuroplastin-55 binds to and signals through the fibroblast growth factor receptor," *The FASEB Journal*, vol. 24, no. 4, pp. 1139–1150, 2010.

[17] G. Nikolova, N. Jabs, I. Konstantinova et al., "The vascular basement membrane: a niche for insulin gene expression and β cell proliferation," *Developmental Cell*, vol. 10, no. 3, pp. 397–405, 2006.

[18] Y. Bar, H. A. Russ, S. Knoller, L. Ouziel-Yahalom, and S. Efrat, "HES-1 is involved in adaptation of adult human β-cells to proliferation *in vitro*," *Diabetes*, vol. 57, no. 9, pp. 2413–2420, 2008.

[19] A. Bauman, R. Higdon, S. Rapson et al., "Design and initial characterization of the SC-200 proteomics standard mixture," *OMICS*, vol. 15, no. 1-2, pp. 73–82, 2011.

[20] G. Gu, J. Dubauskaite, and D. A. Melton, "Direct evidence for the pancreatic lineage: NGN^{3+} cells are islet progenitors and are distinct from duct progenitors," *Development*, vol. 129, no. 10, pp. 2447–2457, 2002.

Hindawi Publishing Corporation
Stem Cells International
Volume 2016, Article ID 1073140, 17 pages
http://dx.doi.org/10.1155/2016/1073140

Review Article

Extracellular Vesicles: Evolving Factors in Stem Cell Biology

Muhammad Nawaz,[1,2] Farah Fatima,[1,2] Krishna C. Vallabhaneni,[3] Patrice Penfornis,[3] Hadi Valadi,[2] Karin Ekström,[4,5] Sharad Kholia,[6] Jason D. Whitt,[3] Joseph D. Fernandes,[3] Radhika Pochampally,[3] Jeremy A. Squire,[1] and Giovanni Camussi[7]

[1]*Department of Pathology and Forensic Medicine, Faculty of Medicine Ribeirao Preto, University of Sao Paulo, Avenue Bandeirantes, 3900 Ribeirao Preto, SP, Brazil*
[2]*Department of Rheumatology and Inflammation Research, University of Gothenburg, Box 480, 405 30 Gothenburg, Sweden*
[3]*Cancer Institute, University of Mississippi Medical Center, Jackson, MS 39216, USA*
[4]*BIOMATCELL VINN Excellence Center of Biomaterials and Cell Therapy, 40530 Gothenburg, Sweden*
[5]*Department of Biomaterials, University of Gothenburg, Box 412, 405 30 Gothenburg, Sweden*
[6]*Cellular and Molecular Immunology Research Centre, School of Human Sciences, London Metropolitan University, London 166-220, UK*
[7]*Department of Medical Sciences and Molecular Biotechnology Center, University of Torino, Corso Dogliotti 14, 10126 Torino, Italy*

Correspondence should be addressed to Muhammad Nawaz; nawaz@usp.br and Giovanni Camussi; giovanni.camussi@unito.it

Received 13 May 2015; Revised 9 July 2015; Accepted 16 July 2015

Academic Editor: Alexander Kleger

Stem cells are proposed to continuously secrete trophic factors that potentially serve as mediators of autocrine and paracrine activities, associated with reprogramming of the tumor microenvironment, tissue regeneration, and repair. Hitherto, significant efforts have been made to understand the level of underlying paracrine activities influenced by stem cell secreted trophic factors, as little is known about these interactions. Recent findings, however, elucidate this role by reporting the effects of stem cell derived extracellular vesicles (EVs) that mimic the phenotypes of the cells from which they originate. Exchange of genetic information utilizing persistent bidirectional communication mediated by stem cell-EVs could regulate stemness, self-renewal, and differentiation in stem cells and their subpopulations. This review therefore discusses stem cell-EVs as evolving communication factors in stem cell biology, focusing on how they regulate cell fates by inducing persistent and prolonged genetic reprogramming of resident cells in a paracrine fashion. In addition, we address the role of stem cell-secreted vesicles in shaping the tumor microenvironment and immunomodulation and in their ability to stimulate endogenous repair processes during tissue damage. Collectively, these functions ensure an enormous potential for future therapies.

1. Introduction

Stem cell technology has recently attracted considerable attention in translational medicine due to the potential that these cells possess in terms of tissue regeneration and repair and as drug delivery tools for which existing therapeutic strategies pose enduring challenges. In recent years, the fields of regenerative and translational medicine have proven to be very attractive owing to the discovery of novel cellular and noncellular therapeutic platforms for tissue repairs and cancer treatments.

This review mainly engages studies carried out on the two major types of stem cell lines: embryonic stem cells (ESCs) and mesenchymal stem cells (MSCs). Nevertheless, several other types of stem cells closely related to their tissue of origin (e.g., adipose stem cells, cancer stem cells) have also been reported.

ESCs are pluripotent cells with the ability to differentiate into cells from any of the three germ layers: mesoderm, endoderm, and ectoderm. They have the capability to self-renew and proliferate limitlessly, but their application in

research and therapy has been limited due to ethical concerns on availability and the risk of forming teratomas.

In the last two decades, more attention has been diverted towards MSCs as they are easily obtainable and show therapeutic promise. MSCs are a nonhematopoietic, heterogeneous population of plastic-adherent cells that exhibit a fibroblast-like morphology. They form distinct colonies when seeded at clonal densities, and their heterogeneity is distinguished through morphological differences, rate of proliferation, and their ability to differentiate [1]. According to the current nomenclature, human MSCs can be identified through their positivity for cell surface markers such as CD73, CD90, and CD105 and the lack of expression of hematopoietic markers such as CD11b or CD34, CD45, CD79 or CD19, and HLA-DR [2]. Furthermore, they must have the ability to differentiate into osteoblasts, chondrocytes, and adipocytes *in vitro* [2]. The biological effects of MSCs depend largely on their ability to secrete trophic factors that stimulate tissue-intrinsic progenitor cell phenotypes [3]. These factors include growth factors, miRNAs, and small vesicles that not only potentially affect the differentiation and regenerative abilities of MSCs but also play a critical role in mediating crosstalk to local and distant tissues through which stem cell populations maintain a stable coexistence [4].

Recent evidence shows that stem cells secrete small vesicles into the extracellular milieu, known as extracellular vesicles (EVs). EVs are submicron vesicles, which based on their size, origin, morphology, and mode of release can be categorized into exosomes (40–200 nm), microvesicles (50–1000 nm), apoptotic bodies (50–5000 nm), or Golgi vesicles (reviewed in [5]). EVs are secreted by a multitude of cell types into various body fluids [6] and can be isolated via several conventional as well as high throughput technologies [5]. They are known to carry a repertoire of mRNAs, miRNAs, DNA, proteins, and lipids that can be transferred to neighboring cells, modifying their phenotype as well as the microenvironment [7, 8]. The molecular signatures of EVs are selective to each cell/tissue type, which makes them ideal source for clinical applications [5].

The biogenesis and secretion of EVs from biologically active cells are a stimulus dependent event that is arising as a result of tumor progression or repair processes. A well-studied process of formation of exosomes is by the fusion of the multivesicular endosome with plasma membrane and release by the process of exocytosis. Conversely, microvesicles are less well characterized in comparison to exosomes and are produced as a result of membrane budding processes and detachment of spherical bodies from discriminatory regions of the plasma membrane (for mechanisms, see [5]). Recently, Golgi vesicles were highlighted, considering them a part of the extracellular vesicle populations as separate entities. Like other vesicles, they may reflect distinct disease states [5], and their role could be hypothesized for underappreciated effectors in stem cell context.

Interestingly, it has been shown recently that MSC exosomes are derived from endocytosed lipid-raft microdomains [9]. Arguably, the knowledge about the mechanisms of biogenesis and origin of EV populations from stem cells could enhance our understanding of the functional relevance and help acquire therapeutic possibilities using stem cell-EVs.

2. Intercellular Communication and Transfer of Biological Information

Cells use several means of communication for the exchange of materials and the transfer of information in order to maintain tissue homeostasis, cell development, repair, and survival. Intercellular communication is therefore considered one of the most important regulatory mechanisms for cell growth, differentiation, and tissue remodeling. This intercellular crosstalk may occur through direct receptor-mediated interaction between cells, or through cellular junctions (i.e., cell fusion). Certain molecules, specific transmembrane proteins, and cell adhesion molecules such as integrins, tetraspanins, and cadherins are known to promote receptor-mediated cellular interactions that are critical in the formation of biological patterns as well as determining cell fates [10, 11]. On the other hand, the direct coupling of the cytoplasm of two cells through gap junctions (GJs) has also been reported to play an essential role in maintaining tissue homeostasis, development, and stem cell differentiation [12, 13].

It has been proposed that normal human adult stem cells do not express gap junctional proteins (i.e., connexins) and do not appear to have gap junctional intercellular communication. However, their differentiated, nonstem cell derivatives do express connexins and therefore utilize GJs for intercellular communication in order to differentiate [14]. Remarkably, bone marrow derived MSCs have been reported to differentiate into cells with a cardiac phenotype in response to signals from neighboring myocytes, as a result of gap junctional intercellular communication [15]. Arguably, the crucial role that these interactions play in the maintenance of tissue integrity in a plethora of different cell types such as endothelial cells, fibroblasts, adipocytes, cardiomyocytes, and neurons is of critical translational importance.

2.1. Tunneling Nanotubes and Intercellular Communication. Recently, a novel mechanism for cellular communication involving long distance intercellular connections called tunneling nanotubes (TNTs) has come to light [16]. TNTs are actin-based cytoplasmic extensions that not only facilitate direct communication between distant cells and intercellular trafficking [17] but also are associated with the transfer of biomolecular cargos such as organelles, Golgi vesicles, plasma membrane components, and even pathogens [18–20]. These functions of TNTs have therefore implicated them in the promotion of various physiological (tissue development and regeneration [21]) as well as pathological processes such as mesothelioma [22].

For instance, extensive spontaneous intercellular exchange of cytosolic materials and organelles, between primary human proximal tubular epithelial cells, was recently reported [23]. Interestingly, this exchange was alleviated significantly on inhibiting TNT genesis, therefore implying the importance of TNTs in renal physiology [23]. Surprisingly, the direct transfer of genetic material between tumor and stromal cells has also been identified to be

mediated through TNTs, exclusive of other forms of cell-cell communication, therefore suggesting a role of TNTs in tissue remodeling as well [24]. A recent study described the nanotubular connections and tubule fragments in multipotent MSCs from human arteries, demonstrating that they interact constitutively through an articulate and dynamic tubule network allowing long-range cell-to-cell communication [25]. This therefore suggests that one mechanism by which MSCs exhibit their protective effects on the heart may be through tubular communication.

2.2. Cell-Cell Communication through Paracrine Secreted Factors. Diffusion of autocrine and paracrine signaling molecules enables cells to communicate in the absence of physical contact. The beneficial effects of stem cells are therefore restricted not only to cell-to-cell contact alone, but also to their transient paracrine actions through the release of a combination of trophic factors including cytokines, chemokines, and growth factors [26–28]. These factors have been shown to have various functional properties such as being antiapoptotic, immunomodulatory, and angiogenic, playing a role in cell-mobilization, evoking responses from resident cells in the extracellular environment, and facilitating collateral remodeling [29]. Through receptor-mediated interactions, these paracrine mechanisms potentially facilitate the homing of stem cells to sites of tissue injury, therefore allowing recipient cells to interact with stem cell factors that may influence the regulation of differentiation and anti-inflammatory responses [26].

Cells could also communicate through secreted extracellular RNAs, which, once transferred from one cell to another, may modulate the phenotype and function of the recipient cells. Furthermore, the exchange of extracellular RNAs between resident cells and MSCs has been implicated in the modulation of cell fate [30]. These extracellular RNAs are secreted, vesicle-encapsulated or in association with proteins that confer protection from degrading enzymes and contribute towards the microenvironmental modulation of cell fate with other extracellular factors such as the extracellular matrix as well as the local biochemical and mechanical niches [31].

2.3. Extracellular Vesicles as Novel Means of Communication. Secreted EVs exhibit novel paracrine mechanisms mediating cell-to-cell communication through receptor-ligand mediated interactions and/or direct fusion with resident cells, resulting in the horizontal transfer of various proteins as well as genetic material (including mRNA [8, 32–34] and miRNA [34]). As paracrine factors, EVs have been reported to induce phenotypic changes in recipient cells and also generate a functional link between stem cells and tissues under various physiological and pathological circumstances (reviewed in [33]).

Recently, it has been demonstrated that EVs released by human adipocytes or adipose tissue-explants are involved in a reciprocal proinflammatory loop between adipocytes and macrophages in a paracrine fashion, with the possibility to aggravate insulin resistance locally or systemically [35]. Moreover, EVs released from osteoblasts serve as a mechanism of communication between osteoblasts and osteoclasts through receptor-ligand interactions to facilitate osteoclast formation that represent a novel mechanism of bone remodeling [36].

Although stem cells have been considered safe for available therapeutic strategies, there are still potential risks and complications that may arise such as culture-induced senescence, immune-mediated rejection, genetic instability, loss of functional properties, and consequent malignant transformations. In this perspective, there is a prospect that stem cell-EVs may overcome these limitations and therefore offer novel and safe cell-free therapeutic opportunities. However, their promise as real clinical applications still awaits further investigations yet to be fully realized.

3. Extracellular Vesicles Mimic Stemlike Phenotypes

Recent data from various different studies have shown stem cell-EVs to traffic stem cell associated transcription factors such as Nanog, Oct-4, HoxB4, and Rex-1 operating at the level of pluripotent stem cells [37]. On top of that, they have also been shown to express MSC markers such as CD105 [38], prominin-1/CD133 [39–41], and KIT [42]. More direct effectors of the stem cell phenotype such as WNT [43, 44], β-catenin [45], and Hedgehog [46] have also been identified on stem cell-EVs together with several other components that may be considered potential factors in stem cell biology (Table 1). Furthermore, ESC-EVs can be harvested from exponentially growing ESCs, therefore suggesting that the mechanism of EV release from ESCs is inherent [37].

Emerging evidence reveals that secreted vesicles from stem cells could mimic a spectrum of stemlike phenotypes. Ratajczak and coworkers provided the first evidence that EVs released from stem cells might modulate the phenotype of recipient cells [37]. In this study, they reported that EVs released from ESCs sustained the maintenance of hematopoietic stem/progenitor cell stemness and multipotency by delivering specific proteins and mRNA, subsequently upregulating the expression of early pluripotent and hematopoietic stem cell genes [37]. A following study further confirmed this by reporting that mRNA-carrying EVs from endothelial progenitors induced a proangiogenic phenotype in quiescent endothelial cells [47]. Moreover, it was recently revealed that EV-mediated mRNA delivery into marrow cells could introduce tissue-specific changes through the induction of transcription in recipient cells [48], further indicating that mRNAs present in stem cell-EVs are functional and have regulatory effects.

Several studies have revealed that the key biological features of stem cells, such as self-renewal, differentiation, and maturation, could be mimicked by stem cell associated EVs [49–53]. Furthermore, stem cell-EVs have been reported to coordinate physiological self-regenerative and repair processes after tissue injury in a paracrine manner. For instance, EVs released from MSCs (MSC-EVs) activate repair processes by transferring miRNAs [54] and promoting angiogenesis [55, 56], therefore suggesting EVs as functional extensions of stem cells.

Table 1: Stem cell signatures expressed and secreted in EVs.

Components	Stem cell type/source	Reference
Nanog, Oct-4, HoxB4 and Rex-1	ESCs	[37]
CD105	CSCs, MSCs	[38, 97]
Prominin-1/CD133	HPCs, melanocytes	[39, 40]
KIT	Mast/stem cells	[42]
WNT	Fibroblasts, DLBCL	[43, 44, 96]
β-catenin	HEK	[45]
Stem-cell antigen-1	MSCs	[97]
TGF-β1	Fibroblasts, epithelial cells	[98]
TIA, TIAR, HuR, Stau1, Stau2, RPS29, and Ago2	MSCs	[54]
KGF	MSCs	[99]
Oct4 and *Sox2* mRNAs	ESCs	[62]
IGF-1R mRNA	MSCs	[100]
DEFA3, HBB, ITGA2B, and ITGB3 mRNAs	HPCs	[101]
VEGF	MSCs	[68]
PDGFR-β, TIMP 1 and 2, sphingomyelin, lactic acid, and glutamic acid	MSCs	[69]
CD34	MSCs	[102]
E-cadherin	MSCs	[103]
Bcl-2	MSCs	[104]
NEP	MSCs	[105]

ESCs: embryonic stem cells, CSCs: cancer stem cells, MSC: mesenchymal stem cells, HPCs: haematopoietic precursor cells, DLBCL: diffuse large B-cell lymphoma, HEK: human embryonic kidney cells, KIT: mast/stem cell growth factor receptor, IGF-1R: growth factor receptor, TGF-β1: transforming growth factor beta 1, KGF: keratinocyte growth factor, ITGA; integrin alpha, VEGF: vascular endothelial growth factor, PDGFR-β: platelet-derived growth factor receptor beta, TIMP: tissue inhibitor of metalloproteinase, and NEP: neprilysin.

Interplay between stem cells and EVs reveals that EVs could transmit multipotential traits and represent several features of MSCs, such as multilineage differentiation, self-renewal, and transcriptional regulation, therefore, inferring their role as evolving factors in stem cell biology.

4. Stem Cell-EVs Contribute to the Cell-Fate Determination

There is sufficient evidence to postulate that EVs carry biological messages from parent cells that interact with recipient cells and influence their normal physiology and therefore their overall fate [33]. In the context of stem cell biology, it is likely that the same principle applies (Figure 1), as biological content from stem cell-EVs has been shown to have the capability to influence and define cell fates of future populations of resident cells, potentially producing long lasting and stable transformation in genetic programs [48, 57]. Furthermore, Quesenberry et al. have also proposed that EV-mediated exchange of genetic information could be an integral element of the continuum model of stem cell biology, in which the differentiation decision of stem cells is conditioned by the cell cycle transit and environmental stimuli [58].

4.1. EV-Mediated miRNA Transport and Cell-Fate Determination. To sustain stemness, a set of transcriptional factors are required to efficiently reprogram and self-renew the pluripotency of recipient cells to enable them to differentiate into various cell types [59]. Indeed, miRNAs are capable of targeting and regulating the expression of stem cell associated transcriptional networks by which they can induce phenotypic transition [60, 61]. In this context, EVs contribute to such reprogramming and phenotypic switching by transferring miRNAs as the delivery of selective sequestered miRNAs in EVs to recipient cells has been reported [34].

For instance, EVs from bone marrow- (BM-) MSCs shuttle the selected pattern of miRNAs to recipient cells targeting genes involved in multiorgan development, cell survival, and differentiation [54]. Furthermore, ESC-EVs induce dedifferentiation and the expression of pluripotency factors in their target cells by selective transfer of mRNA and miRNA, which may initiate an early differentiation process by targeting early transcriptional factors [62]. It has also been reported that telocytes (TCs) secrete EVs loaded with miRNAs that could modulate stem cell fates through continuous posttranscriptional regulatory signals acting back and forth between TCs and stem cells [63]. Moreover, Let-7 miRNA family expressed from human embryonic MSCs has been shown to affect its downstream target hepatic nuclear factor 4 alpha (HNF4A), indicating the possible role of stem cells in differentiation processes through EV-mediated transfer of miRNAs [64]. In addition, several other miRNAs have been identified to potentially contribute to regulatory mechanisms in stem cell biology (Table 2). These reports therefore signify that stem cells may exhibit their biological effects through EV-mediated shuttle of miRNAs for the biological effects mediated by stem cells.

5. Stem Cell-EVs and Tumor Progression

The role of stem cells in tumor progression has been well documented [65]; however, the mechanisms by which cancer stem cell-derived EVs initiate and promote tumor progression are still uncertain. Recent evidence explains the interplay between stem progenitors and their secreted vesicles in tumor progression. For example, it has been reported that EVs positive for the stem cell marker prominin-1 participate in Wnt signaling and mediate prometastatic activity in melanoma cells [40]. In addition, EVs from mast cells express and shuttle KIT protein (mast/stem cell growth factor receptor), which in turn promotes tumor growth in recipient lung adenocarcinoma cells by activating the KIT-SCF signaling pathway [42]. EVs from BM-MSCs have also been shown to express higher levels of oncogenic proteins, cytokines, and adhesion molecules that could be transferred to multiple myeloma cells and modulate tumor growth *in vivo* [66].

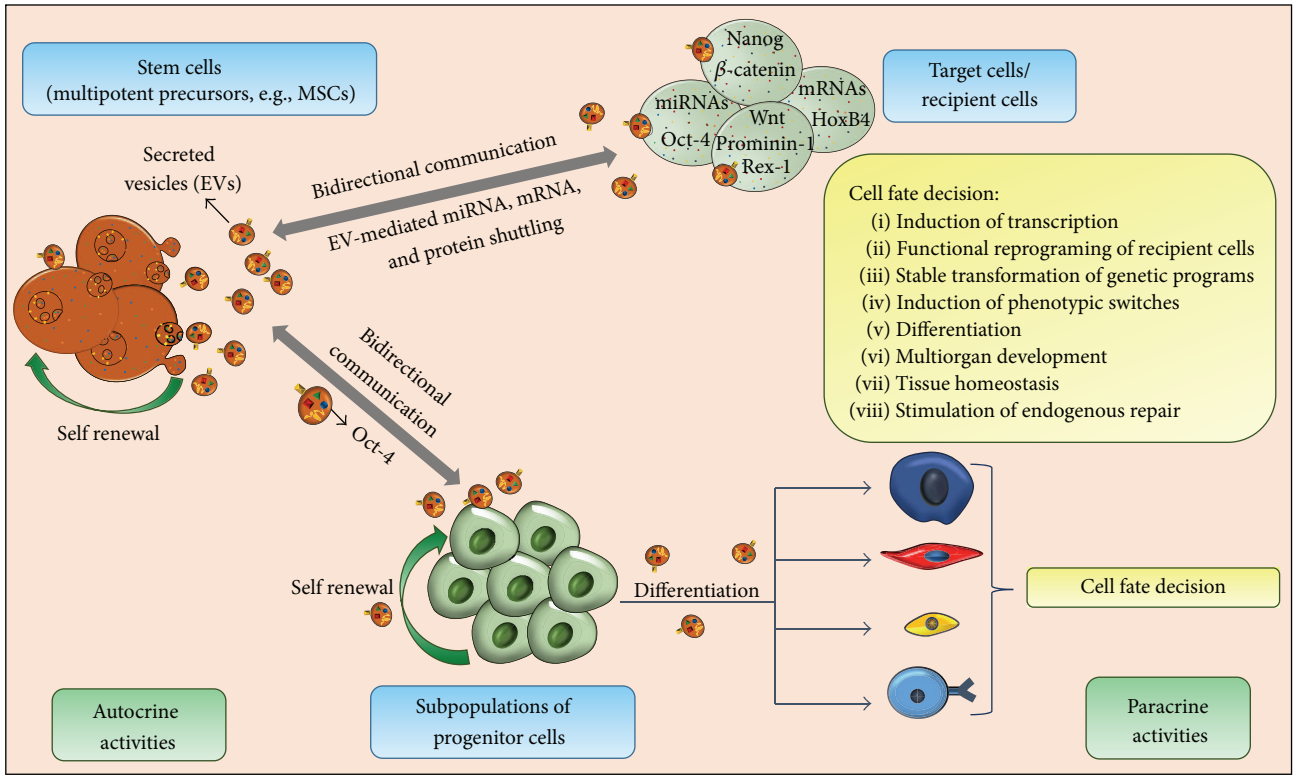

Figure 1: The role played by stem cell-derived EVs in the determination of cell fate. Stem cells use EVs to transfer miRNAs and stem cell effectors in recipient cells, which target the regulatory networks and induce persistent genetic transformation and phenotypic switching of resident cells towards cell-fate determination.

Table 2: Selectively enriched regulatory miRNAs from stem cell-derived EVs.

miRNAs	Stem cell type/source	Reference
miR-199b, miR-218, miR-148a, miR-135b, and miR-221	MSCs	[106]
miR-223, miR-564, miR-451, and miR-142-3p	MSCs	[54]
miRNAs of 290 cluster	ESCs	[62]
let-7 miRNA family	MSCs	[64]
miR-133b	MSCs	[107]
miR-15a	MSCs	[66]
miR148a, miR532-5p, miR378, and let-7f	MSCs	[67]
miRNA-21, 34a	MSCs	[69]
miR-23b	MSCs	[73]
miR-16	MSCs	[74]
miR-140	Preadipocytes	[108]
miR-22	MSCs	[109]
miR-221	MSCs	[70, 110]
miR-210, miR-132, and miR-146a-3p	CPCs	[111]
miR-294	ESCs	[112]

Recently, Eirin et al. reported that adipose MSC (AT-MSC) derived EVs enriched with distinct mRNAs and miRNAs regulate various physiological processes such as angiogenesis, adipogenesis, apoptosis, and proteolysis in recipient cells [67]. Furthermore, EVs from BM-MSCs have been reported to not only transport tumor regulatory miRNAs, antiapoptotic proteins, and metabolites but also enhance the expression of vascular endothelial growth factor (VEGF) through the activation of extracellular signal-regulated kinase 1/2 (ERK1/2) pathway to promote growth of various tumors [68, 69]. In addition, gastric cancer derived MSC-EVs have been shown to deliver deregulated miRNAs to human gastric cancer cells and promote their proliferation and migration [70].

A subset of tumor-initiating cells expressing the MSC marker CD105 in human renal cell carcinoma release EVs that induce angiogenic phenotype in endothelial cells and promote the formation of a premetastatic niche [38, 71]. Furthermore, renal cell carcinoma-derived EVs induce persistent phenotypical changes in MSCs accompanied with enhanced expression of genes associated with cell migration, matrix remodeling, angiogenesis, and tumor growth [71].

To the contrary, various reports also suggest the antitumorigenic effects of EVs from multiple stem cell types. For instance, Bruno et al. have reported that BM-MSCs exert inhibitory effects on tumor growth through the release of EVs [72]. Furthermore, BM-MSC derived EV-mediated transfer

of miRNAs from the bone marrow could promote dormancy in metastatic breast cancer cells [73]. In addition, various studies have reported the antiproliferative effects of MSC-EVs through various mechanisms, for instance, miRNA-mediated VEGF suppression in breast cancer cells [74] and the downregulation of phosphorylation of Akt kinase in bladder tumor cells [75]. Similarly, a study by Fonsato et al. shows that EV-mediated delivery of selected miRNAs from adult human liver stem cells (HLSC) exhibits inhibitory effects on hepatoma growth [76]. On the basis of this information and on various other reports, MSC derived EVs could therefore exert either anti- or protumorigenic effects depending on the tumor type and stage of development [77].

Glioma-associated stem cells (GASCs) produce substantial amounts of EVs that express and mediate glioma-stem cell characteristics [78–80]. For instance, a recent study reported that GASCs exhibit stem cell feature and anchorage-independent growth and are capable of sustaining malignant properties of both glioma cells and glioma-stem cells, mainly through the release of EVs [78]. Furthermore, the cargo (DNA, miRNA, transcripts, and proteins) from GASC derived EVs may influence lineage specific dynamics of the stem cell compartments [81].

MSC-EVs could also be engineered to play a potential role in cancer therapeutics as delivery vehicles. For instance, Munoz et al. successfully reported the delivery of functional anti-miR-9 to glioblastoma (GBM) cells through MSC-EVs, therefore increasing their level of chemosensitivity substantially [79]. In addition, EV-dependent phenotypes of stem cells such as neurosphere growth and endothelial tube formation were attenuated by loading miR-1 into GBM-EVs that were exposed to the glioblastoma microhabitat [80]. Furthermore, a recent study by Katakowski et al. observed that intratumor injection of miR-146 expressing MSC-EVs significantly inhibited glioma xenograft growth [82]. Likewise, Pascucci et al. also reported the potential ability of MSCs to package/incorporate and deliver active drugs such as paclitaxel through EVs to inhibit tumor progression [83]. These studies therefore indicate the potential capability and utility of stem cell-EVs as drug delivery mechanisms for cancer therapy.

5.1. Ways by Which Stem Cell-EVs Influence the Tumor Microenvironment. The principle properties of cancer stem cells (CSCs) are maintained by niches which are anatomically distinct regions within the tumor microenvironment [84]. The premetastatic niche plays a role in dormancy, relapse, and the development of metastasis. It has been hypothesized that EVs from CSCs may behave as metastasomes, helping the implementation of secondary lesions by transmission of the metastatic phenotype via EV-borne tumor RNA signatures to the target organ [85]. Since the construction of a premetastatic niche is an essential early step required for initiated cells to survive and evolve [86], it could be speculated that stem cells may contribute to the construction of premetastatic niches, at least in part, by secreting EVs. This could be supported through the observation of Grange et al., whereby interactions between endothelial cells and CSCs induced phenotypical changes in MSCs and promoted the formation of lung premetastatic niches through the release of EVs [38].

5.1.1. Fibroblastic Differentiation and Stroma. Tumor cells have the ability to efficiently "educate" MSCs to induce changes in the local microenvironment through the release of EVs. For instance, tumor cell-derived EVs have been observed to propagate the construction of the tumor stroma through fibroblastic differentiation of MSCs [87]. Similarly, EVs from ovarian cancer cells have also been reported to induce adipose stromal cells (ASCs) to acquire the characteristics of tumor-supporting myofibroblasts [88]. A similar phenotypic switch was also noted in prostate cancer (PC) EVs whereby they influenced the differentiation of MSCs into proangiogenic and proinvasive myofibroblasts that was associated with disease promotion [89]. In another study, EVs from PC cells induced phenotypic transformation in PC patient ASCs to form prostate-like neoplastic lesions [90]. On top of that, tumor derived EVs can initiate phenotypic differentiation of MSCs into cancer-associated fibroblasts (CAFs) through signaling pathways [91]. These activated CAFs influence tumor progression through the secretion of metalloproteinases-rich EVs that promote cell motility and activate RhoA and Notch signaling in cancer cells [92]. Moreover, these EVs also play a role in chemoresistance and tumor relapse by promoting clonogenicity and growth of CSCs which are inherently resistant to cell death [93].

5.1.2. Crosstalk among Stromal Elements. EV-mediated dynamic crosstalk within the stroma could relocalize the oncogenic factors that can generate a tumor-initiating niche. This can be speculated from the fact that carcinogenesis involves the relocalization of CAFs to the tumor site therefore sustaining metastasis [94]. The general involvement of EVs in intercellular communication suggests that they may also have a role in information exchange within stem cell hierarchies, whereby cancer stemlike cells may transmit signals to their stroma via EVs. Undeniably, it is well known that ESC-EVs transfer mRNAs, miRNAs, and proteins to recipient cells and therefore are important mediators of crosstalk within stem cell niches [95].

Stromal cell-derived EVs can interact with cancer cells and exchange oncogenic signatures present in tumor-associated stroma. For example, intercellular communication mediated by fibroblast-secreted EVs promotes cancer cell motility via autocrine Wnt-planar cell polarity signaling pathway to drive invasive activities [43]. Furthermore, the Wnt3a has been shown to be exported via EVs to neighboring cells which in turn modulates the population equilibrium in the tumor towards progression [96]. Such features are expected to be established very early during tumorigenesis; however, the prolonged intercellular communication could eventually be sustained and ultimately aggravate tumor growth. It could also be anticipated that the tumor microenvironment may host nontumorigenic multipotent stem cells that could likewise support the biological activity of tumor-initiating cells through the release of EVs.

5.1.3. Endothelial Cell Growth and Angiogenesis. Angiogenesis is one of the underlying hallmarks of a developing tumor microenvironment. It is activated by proangiogenic factors such as VEGF thereby promoting tumor growth, invasion, and metastases. In response to hypoxia (a hallmark of developing tumors), MSCs increase EV production, which in turn promotes angiogenesis [113] and endothelial cell growth *in vitro* [114]. This proangiogenic property of stem cell-secreted EVs is reported to be linked with the activation of the ERK signaling pathway therefore increasing the expression of VEGF in tumor cells [68]. Furthermore, AT-MSC derived EVs have also been implicated to influence AT-MSC induced angiogenesis. Interestingly, the platelet-derived growth factor (PDGF) was identified to elicit this effect by stimulating AT-MSCs to release EVs with an enhanced proangiogenic potential [115]. In addition, AT-MSC derived EVs have been shown to interact with endothelial cells as well, thereby stimulating proangiogenic activity in the tumor microenvironment, possibly through the exchange of angiogenic growth factors [116].

EV-assisted targeting of key regulatory signaling pathways in the tumor microenvironment such as Wnt, Hedgehog, and angiogenic pathways (i.e., VEGF) could inhibit tumor growth. A recent study by Gernapudi et al. showed that a critical signaling axis, miR-140/SOX2/SOX9, which regulates differentiation, stemness, and migration in the tumor microenvironment, could be targeted to obstruct tumor progression [108]. Likewise, EV-assisted targeting of the VEGF pathway in the tumor microenvironment could exert antiangiogenic effects and inhibit tumor growth [74]. However, monitoring a complex stromal network in a dynamic tumor microenvironment has been and still remains technically challenging.

In summary, EVs secreted from cancer cells educate MSCs to undergo neoplastic transformation into tumor-associated fibroblasts in local stroma. In addition, EV-mediated dynamic interactions amongst stromal elements and the concomitant recruitment of oncogenic CAFs, growth factors, immune molecules, and several other related mechanisms shape a tumor niche capable of development and growth (Figure 2).

6. Stem Cell-EVs: Emerging Factors in Immunomodulation and Immunotherapy

There is increasing evidence implicating EVs to play a critical role in immune regulatory mechanisms comprising of both immunoactive and suppressive activities [117–119]. Conversely, studies elucidating the role of EVs from immunologically active stem cells are seldom reported in the scientific literature, possibly because their role as potential factors in immunomodulation is still novel. MSCs have been shown to secrete immunologically active EVs, which induce higher expression of anti-inflammatory transcripts such as interleukin 10 (IL10) and transforming growth factor β1 (TGF β1) and attenuated levels of proinflammatory transcripts such as IL1B, IL6, tumor necrosis factor α (TNFα), and IL12P40 [120]. Furthermore, infusion of MSC-EVs significantly enhanced the survival and delayed the rejection of allogenic skin graft in mice with a corresponding increase in regulatory T cells (Tregs) therefore indicating some role of EVs in immunomodulation [120].

Islet derived MSCs have been reported to release immunostimulatory EVs that could activate autoreactive B and T cells in nonobese diabetic (NOD) mice. Furthermore, immunization with EVs also promotes the expansion of transferred diabetogenic T cells and accelerates the effector T cell-mediated destruction of islets suggesting that stem cell-EVs act as autoantigen carriers with the potential to trigger autoimmune responses [97]. On the other hand, human adipose MSC derived EVs have been reported to exert inhibitory effects on the differentiation and activation of T cells followed by reduced T cell proliferation and IFN-γ release, therefore suggesting MSC-EVs to play a potential therapeutic role in the treatment of inflammation-related diseases [121]. Furthermore, EVs from immune cells can also have an effect on MSC cells. For instance, Ekström et al. showed that monocyte-derived EVs can induce increased gene expression of osteogenic markers in human MSCs, indicating that monocyte-derived EVs play a role in bone healing [122].

EVs from acute myeloid leukemia- (AML-) blasts that are positive for the hematopoietic progenitor cell antigen CD34 have been reported to be biologically active. Upon coincubation with natural killer (NK) cells, these AML-blast EVs efficiently downregulated the expression of surface NKG2D (an activator of NK cells) indicating a possible function in mediating immunosuppression in AML [123]. In addition, immunocaptured blast-derived EVs could also serve as biomarkers for AML during the course of therapy as a measure of disease progression or response to therapy.

Using a model of human-into-mouse xenogeneic graft-versus-host disease (x-GVHD), BMSCs were shown to play a role in immunomodulation, mediated by human CD4+ Th1 cells [124]. Notably, recipients treated with BMSCs had elevated levels of exosomes expressing CD73 in the serum that promoted the accumulation of adenosine *ex vivo*. Furthermore, on inhibiting the adenosine A2A receptor, the immunomodulatory property of BMSCs was abrogated, therefore implying a possible role of BMSC-EVs in an adenosine based immunosuppressive mechanism mediated in a paracrine fashion [124]. Recently, MSC-EVs were tested in a human patient to treat GVHD, whereby they were shown to be well tolerated [125]. Interestingly, the EV based treatment resulted in a reduced proinflammatory cytokine response to the patient's peripheral blood mononucleated cells (PBMCs) *in vitro* and the clinical GVHD symptoms improved significantly shortly after the start of the EV therapy [125].

Although initial findings ascertain that EVs could be a promising therapeutic source for the treatment of immune-inflammatory diseases [126, 127], translating this technology into EV-mediated stem cell therapy to achieve promising outcomes with minimized toxic effects and safety risks still needs to be explored.

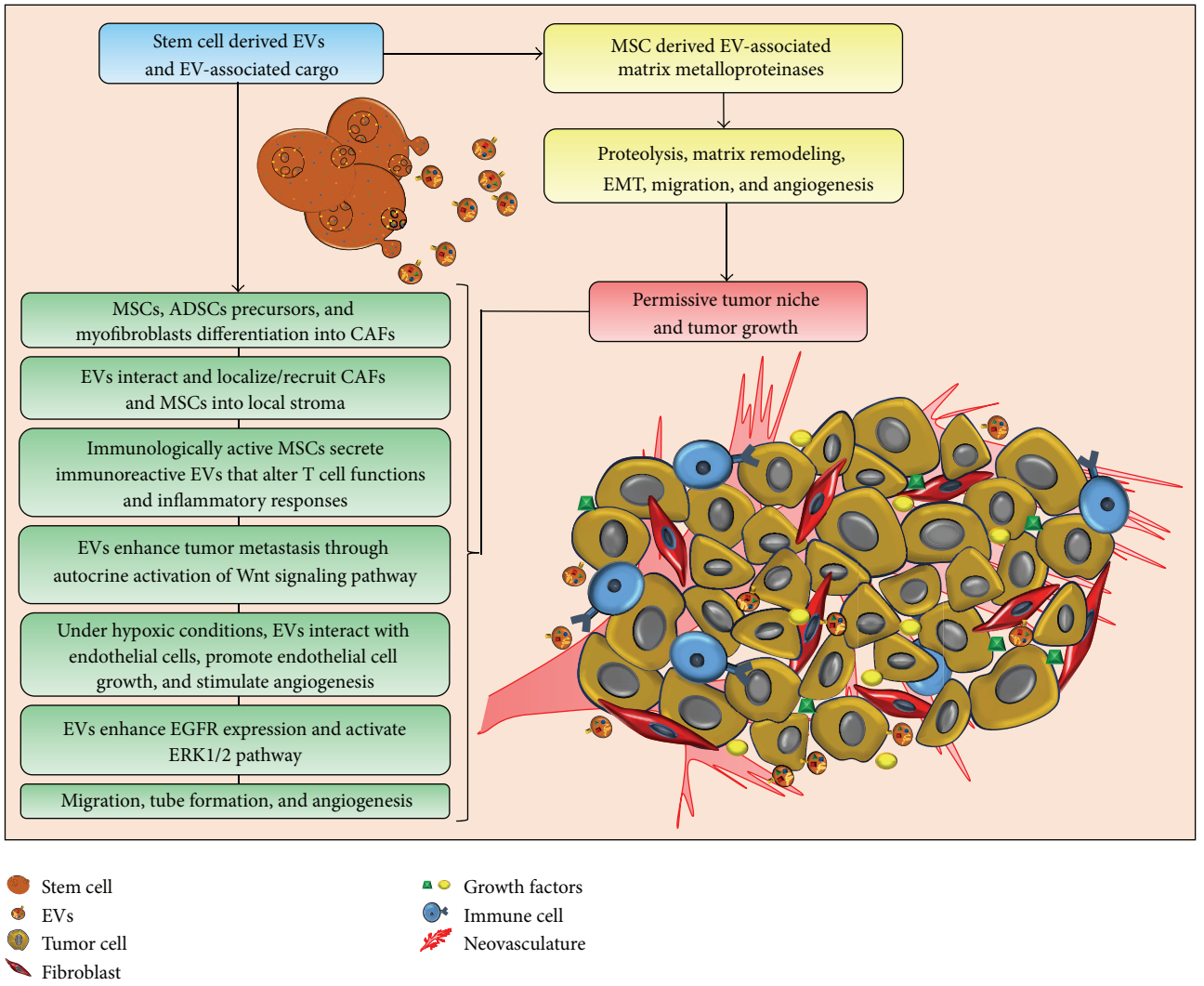

Figure 2: Contribution of stem cell-derived EVs in the construction of the tumor microenvironment. Stem cell-derived EVs influence the presence of cancer-associated fibroblasts (CAFs), inflammatory immune cells, metalloproteinases, angiogenic growth factors, and regulatory RNAs, which shape the tumor microenvironment. Extracellular matrix (ECM) remodeling, endothelial cell growth, cell migration, and angiogenesis generate a permissive tumor niche.

7. Stem Cell-EVs and Tissue Repair

The therapeutic applications of stem cells for the treatment of various injuries and diseases have received considerable attention in recent years. However, investigations into the possibility of utilizing stem cell-EVs in regenerative medicine are still in their early stages. Recently, it has come to light that stem cells, particularly MSCs, use EVs for tissue repair and regeneration through the transfer of transcription factors, anti-inflammatory factors, and growth factors to target cells in a paracrine fashion. In this section, we discuss the regenerative abilities of MSC-EVs to recover vascular functions, repair injuries, and restore tissue homeostasis.

7.1. Stem Cell-EVs: Allies in the Fight against Cardiovascular Diseases. Stem cells have been suggested as an ideal novel therapeutic approach against cardiovascular diseases. However, an important feature of this approach is that EVs subsequently released from stem cells are a newly discovered source of cardiovascular protection. Improved heart function and vessel formation have been attributed to EVs released from stem cells, largely due to their anti-inflammatory and antiapoptotic effects (discussed below). Moreover, their effects can equally be extended towards neovascularization and cardiac regeneration.

Stem cell-EVs participate in the suppression of inflammatory responses in order to enhance cardiac functions. For instance, MSC-EVs mediate cytoprotective actions in a model of pulmonary hypertension by suppressing hyperproliferative pathways such as the signal transducer and activator of transcription 3 (STAT3) pathway as well as upregulating miRNAs that are downregulated during pulmonary hypertension [128]. Moreover, MSC-EVs moderate inflammatory reactions and rapidly ameliorate myocardial

functions during ischemia/reperfusion injury, possibly by restoring bioenergetics, activating PI3K/Akt pathway, and triggering prosurvival signaling [129].

Cardiomyocyte progenitor cells (CPCs) have been shown to stimulate the migration of endothelial cells as well as promoting neovascularization that can potentially improve heart function [130]. Recently, EVs secreted by human CPCs have also been implicated with similar cardioenhancing functions mainly through inhibiting apoptosis, promoting tube formation, and initiating angiogenesis in cardiomyocytic cells [111]. Furthermore, MSC derived EVs also protect cardiac tissue from ischemic injury primarily by enhancing angiogenesis, blood flow recovery, and reducing infarct size [131]. After myocardial infarctions, they are linked with promoting recovery of cardiac functions via the Akt signaling pathway [132].

Ischemic preconditioning can potentiate the protective effects of MSCs during ischemic cardiomyocytes (CMs) injury. This is mainly achieved through the secretion of EVs that deliver miRNAs with antiapoptotic effects [109]. Furthermore, EVs released by the heart after ischemic preconditioning also contribute towards cardioprotection [133]. Interestingly, heat shock proteins have been shown to improve stem cell survival in an ischemic environment. This therefore promotes a prosurvival phenotype in CMs through heat shock factor-1 (HSF-1) and miR-34a interaction that is found to be mediated by EVs [134]. Other than proteins, MSCs are also capable of transferring antiapoptotic miRNAs to CMs via EVs that transcriptionally repress the expression of apoptotic genes, activate cell survival signaling pathway, and ensure cardioprotection [110, 135]. Such delivery of miRNAs could potentiate antiapoptotic effect of MSCs by inhibiting PUMA (p53-upregulated modulator of apoptosis) to promote cardiomyocyte survival [110].

Injured epithelial cells produce TGF-β1-containing EVs with defined genetic information able to activate fibroblasts, which initiate tissue regenerative responses and fibrosis [98]. Cardiac fibrosis is antagonized by stem cell-secreted EVs, exhibiting a substantial protection against myocardial infarction [109]. Furthermore, MSC-EVs have a replacement or cytoprotective effect, thus demonstrating potential therapeutic use in stem cell transplantation for the treatment of pulmonary fibrosis [136]. Notably, ESC-derived EVs can also effectively augment cardiac function in infarcted hearts through enhanced neovascularization, cardiomyocyte survival, and reduced fibrosis after infarction. The underlying basis for this beneficial effect was linked to the delivery of ESC specific miR-294 to CPCs promoting increased survival, cell cycle progression, and proliferation [112]. In addition, CD34+ stem cell-EVs also mediate the transfer of angiogenic factors to the surrounding cells, which may be beneficial in achieving functional recovery after ischemic injury [102]. Therefore, stem cell-EVs from various different tissue locations with their above mentioned healing properties have the potential to act as significant therapeutic agents in the fight against cardiovascular diseases.

7.1.1. Protective and Therapeutic Role against Kidney Injury. MSCs have been implicated in protecting against renal damage through their paracrine effects. By use of a genetic fate-mapping technique, it has been shown that the recovery from acute kidney injury (AKI) depends on the intrinsic regenerative ability of tubular epithelial cells that undergo mesenchymal dedifferentiation and reentry into cell cycle [137]. Experiments performed by Bi et al. show that MSC conditioned medium has the ability to mimic the effects of MSC cells therefore indicating a paracrine form of action [138].

Recent evidence has also demonstrated that MSC-EVs could confer the paracrine actions of their parent cells and therefore contribute towards renal protection as well. For instance, Bruno et al. observed that human MSC-EVs induce recovery in a murine model of AKI in a manner comparable to that of the cell of origin [139]. Furthermore, evidence of mRNAs carried by EVs being translated into proteins has also come to light in both *in vitro* and *in vivo* conditions [139]. For example, Tomasoni et al. reported that MSC-EVs mediated the transfer of human IGF-1R mRNA to murine proximal tubular cells, which was subsequently followed by the enhancement of cell sensitivity to the regenerative actions of IGF-1 [100]. EVs from human umbilical cord-derived MSCs (hUC-MSCs) have also been demonstrated to trigger the ERK 1/2 pathway thereby inducing proliferation of tubular cells and protection against cisplatin-induced apoptosis [140].

EVs from human adult MSCs exhibit protective properties against AKI, largely by inhibiting apoptosis and stimulating proliferation of tubular epithelial cells [141]. This was further confirmed by Bruno et al., who showed, in a cisplatin-induced lethal model of AKI, that MSC-EVs enhanced the survival of mice through the upregulation of antiapoptotic genes and downregulation of proapoptotic genes [142]. This increased expression was attributed partly to EV-mediated miRNA transfer and in part due to the EV-triggered miRNA transcription [143]. Moreover, miRNA-depleted EVs released by Drosha knockdown MSCs failed to protect the kidney from acute injury [144], indicating that miRNA content of EVs is essential for their biological activity.

Using a mouse remnant kidney model, it was shown that BMSC-EVs could have protective effects against renal injury [145]. Furthermore, endothelial progenitor cell-derived EVs exert a protective effect against mesangial cell injury during Thy1.1 glomerulonephritis [146], and HLSC-derived EVs have the potential to influence renal function and morphology, in a manner comparable to the cells of origin [147]. Administration of MSC-EVs might also remarkably protect mice against renal failure, probably by transferring selective patterns of miRNAs from MSC-EVs to target cells and protection against EMT for restoration [148]. Hence, these studies concur on the therapeutic ability of stem cell-EVs and their potential to be applied as treatment for renal diseases in the future.

7.1.2. Recovering Lung and Liver Injuries. EVs from lung cells have been shown to induce the expression of mRNAs coding for lung specific proteins such as Clara cell protein and aquaporin-5 and A-D surfactants in bone marrow cells [149]. Furthermore, this phenomenon is enhanced significantly during lung injury [149].

Acute and chronic lung injuries could in theory be recovered through the paracrine actions of MSC-EVs which confer a stem cell-like phenotype in injured cells for the activation of self-regenerative programs [99]. Moreover, ischemic preconditioning can also potentiate the protective effects of MSCs against endotoxin-induced acute lung injury through the secretion of EVs [150].

HLSC-EVs may also have a role in accelerating the morphological and functional recovery of injured cells during liver damage, mainly through horizontal transfer of specific mRNA subsets to recipient cells [151]. Recently, it has been reported that transplantation of EVs released from hUC-MSCs could reduce the surface fibrous capsules, soften their textures, and alleviate hepatic inflammation in fibrotic liver [103]. Moreover, it was observed that human liver cells undergo typical EMT after induction with recombinant human TGF-β1, whereas MSC-EV treatment reverses the expression of EMT-associated markers [103], indicating that MSC-EVs could prevent liver fibrosis and ameliorate hepatocyte protection through EMT inhibition. Furthermore, MSC-EVs appear to promote hepatic regeneration following drug-induced liver injury, mainly through the activation of proliferative and regenerative responses [152]. This therefore demonstrates the ability of EVs to act as functional messengers of stem cells.

7.1.3. Stem Cell-EVs and Neuroprotection. There are several studies that have recently come to light that associate MSC-EVs with a neuroprotective role along with stem cells. For instance, EV-mediated transfer of miRNAs from MSCs promotes neural plasticity and functional recovery of neurons and astrocytes after treatment for stroke in rats [107]. Furthermore, EV-mediated delivery of miRNAs enhances the expression of glutamate transporters, suggesting an efficient route of therapeutic miRNA delivery to the brain. A recent study by Raisi et al. reported that EVs produced from anti-inflammatory MSCs enhanced sciatic nerve regeneration in rats which could be potentially applied in peripheral nerve cell therapy [153]. In addition, EVs from embryonic cerebrospinal fluid have been reported to carry evolutionarily conserved proteins and miRNAs, which promote neural stem cell proliferation [154].

The protective effects of MSC-EVs were recently observed against glutamate-induced excitotoxicity in rat pheochromocytoma via a PI3K/Akt dependent pathway [104]. Investigation of a possible underlying mechanism for this protection revealed that MSC-EVs were responsible for downregulating Bax expression accompanied by reduced cleavage of caspase-3, upregulation of Bcl-2 expression, and Akt phosphorylation in glutamate-treated cells, therefore providing a prosurvival fate for affected cells [104]. Transplantation of MSC-EVs could therefore be a potential strategy to treat neuronal diseases involving excitotoxicity.

MSC-EVs may also have effects on neurovascular plasticity during traumatic brain injury by inducing endogenous angiogenesis and neurogenesis and reducing neuronal inflammation [155, 156]. Furthermore, a study by Katsuda et al. has reported the role of human AT-MSCs derived EVs as a novel therapeutic approach for Alzheimer's disease (AD) as they were found to be loaded with enzymatically active neprilysin (NEP) that potentially contributes to amyloid-β clearance in the brain [105]. These observations and others therefore support the potential of stem cell-EVs as a means of cell-free therapy against cerebral injuries and neurological diseases.

In summary, stem cells induce regenerative programs in injured tissues of different organs through EV-mediated transfer of anti-inflammatory miRNAs and growth factors. These, in turn, ameliorate the damage (Figure 3) by activating different signaling pathways, which have an antiapoptotic and angiogenic effect therefore significantly restoring the bioenergetics, improving blood flow recovery, and inducing stemlike phenotypes in injured organs.

The ability of EVs to mediate bidirectional intercellular communication suggests that they could not only send information from stem cells to injured cells but also communicate from injured cells back to stem cells. In this regard, the future clinical contributions of EVs could therefore be (1) translocation of regenerative signatures at injured sites to trigger repair process, (2) transmission of signals related to tissue injury towards stem cells, to generate more progeny for maintaining stem cell equilibrium and continuous supplies to injured sites, and (3) EVs from injured tissues that could also stimulate stem cells to acquire features of the injured cells.

8. Concluding Remarks and Future Perspective

Stem cell-EVs provide a new interpretation of stem cell plasticity that is still a hotly debated topic [157]. EV-mediated bidirectional exchange of information between progenitor cells and tissue differentiated cells leads to phenotypic changes that provide evidence of previously uncertain cell plasticity. This could be beneficial to clinical implications of EVs for future regenerative medicine.

Elucidating the contribution of stem cell-EVs in premetastatic niche formation and biological characteristics of the cancerous stromal elements may offer novel targeting opportunities and have prognostic and predictive values. However, monitoring the target complex tumor microenvironment remains a technical challenge.

Moreover, the immunomodulatory features of MSC-EVs could be extended in the treatment of immune diseases, reducing potential safety risks originated from conventional immunotherapy such as susceptibility to infection, immune dysfunction, autoimmune responses, and/or increased risk of developing cancer. Conceivably, EVs from immunoreactive MSCs could be novel therapeutic tools against inflammation-associated diseases [125].

Despite the improvements of surgical procedures in organ transplantation and cell-based therapies in the last decade, current methods present potential complications (i.e., toxicity and organ rejection), which remains dismal for improving long-term survival and reducing mortality. It is therefore necessary to look for alternative and more reliable procedures, which could potentially minimize associated risk factors. In this regard, EV based cell-free therapy could be a preferred option as it would improve patients' outcome considerably, by reducing the complications associated with

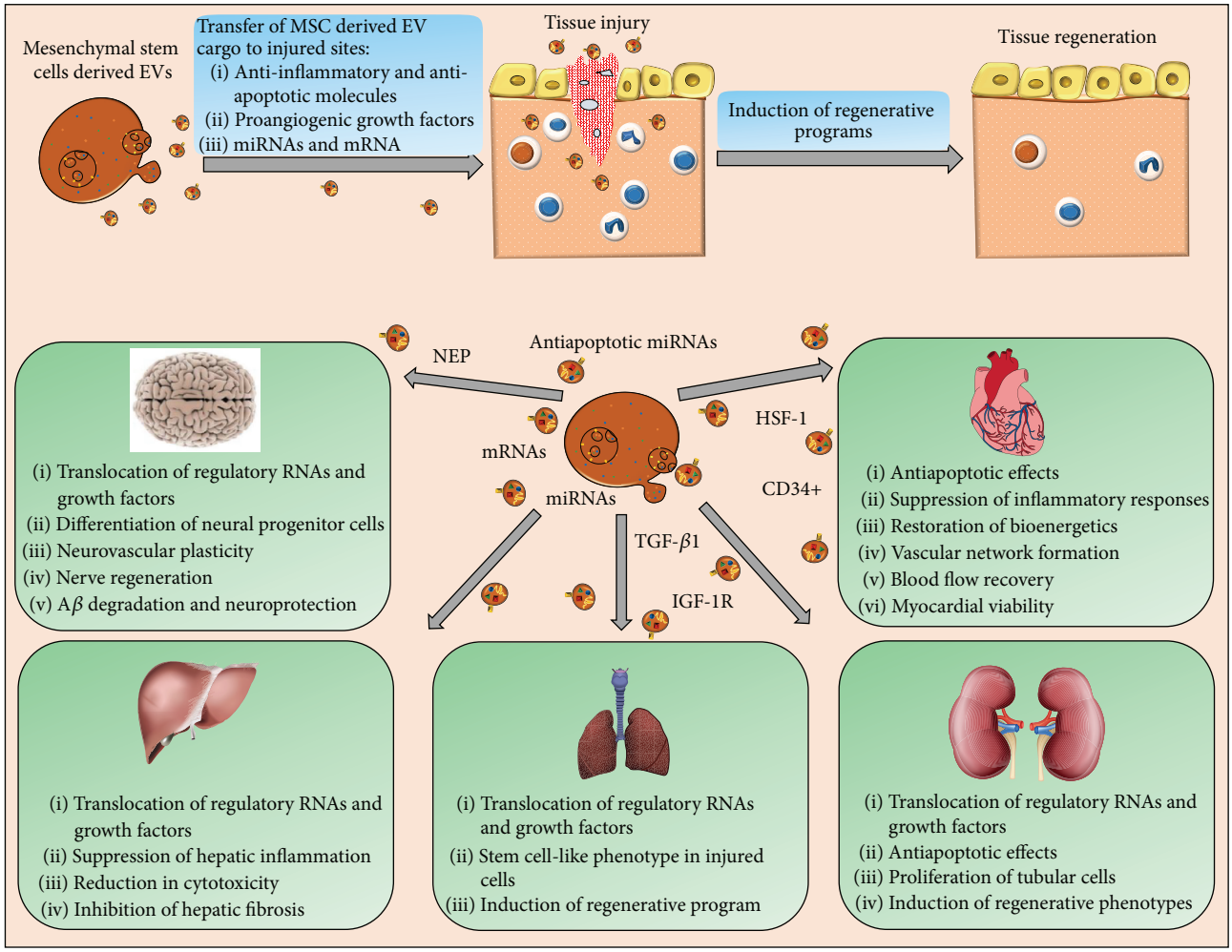

Figure 3: Schematic representation of the regenerative effects of stem cell-derived EVs. MSCs use EVs to ameliorate tissue damage through translocating growth factors, anti-inflammatory, antiapoptotic, and proangiogenic molecules, to sites of injury where they induce and regulate regenerative phenotypes.

cell-based treatments. For instance, ESC-EVs provide a novel cell-free system that uses the immense regenerative power of ES cells while avoiding the risks associated with direct ES or ES-derived cell transplantation and risk of teratomas [112]. Furthermore, EVs have the ability to extend the therapeutic effects and functions of stem cells in both a local and systemic environment. Hence, the administration of stem cell-derived EVs would reduce potential safety risks associated with cellular therapy and/or transplantation surgery.

However, further studies are needed to define whether EVs permanently or transiently change the "genetic fingerprint" of an injured target organ and the consequences of it. Preliminary studies on acute kidney injury indicate a restoration of a persistently normal renal molecular pattern after EV treatment [144]. However, the effect may be dose dependent and increasing doses of EVs may produce unwanted effects as we observed in preliminary experiments with adipose-derived MSCs.

As MSCs have the potential to differentiate into other types of viable replicating cells, replacing their transplantation with administration of MSC-EVs (which mimic similar functions as MSCs) would reduce this possibility and maintain the therapeutic benefits at the same time. However, the mobilization of EVs and homing to specific tissues are still a major concern. Given that EVs express specific membrane receptors and proteins specific to certain cell types [158], it may be possible to identify a potential mechanism to direct EVs as well as stem cells to a particular tissue. Receptor-ligand mediated interactions and homing could also facilitate the cellular uptake of EVs and their associated cargo by recipient injured cells. Furthermore, as a reparatory response, the mobilization of EVs to injured zones could be a result of dynamic interactions among stromal elements. It is quite possible that, in response to an injury or transplant, the enhanced release of EVs could create a gradient that may educate them to mobilize to the site of injury.

Since EVs are more suitable for monitored manufacturing processes, they could be engineered to express and deliver regenerative signatures to target sites. However, a potential

challenge is the lack of standardization of the existing technologies to isolate and characterize EVs for their effective therapeutic utility. Therefore, a combination of different high throughput methods could overcome the potential limitations related to EV detection and characterization [5]. Particularly, the technologies for the isolation and characterization of stem cell-EVs must be improved and optimized [159], ensuring the purity of EVs that is critical for developing cell-free therapeutic strategies using stem cell-EVs in the future.

Conflict of Interests

Authors of this paper declare that there is no potential conflict of interests.

Authors' Contribution

All authors contributed in intellectual discussions and critical review of the paper. Muhammad Nawaz and Giovanni Camussi arranged data and revised the paper for submission.

Acknowledgments

This work was supported by funding from Associazione Italiana per la Ricerca sul Cancro (AIRC) IG2012 no. 12890 to G. Camussi. M. Nawaz, F. Fatima, and J. Squire acknowledge FAPESP, CAPES, and CNPq in Brazil. K. Ekström acknowledge The Swedish Research Council (VR 521-2014-2660) and the BIOMATCELL VINN Excellence Center of Biomaterials and Cell Therapy. The authors searched for original articles in PubMed containing the search terms: "exosomes", "microvesicles", "extracellular vesicles", "mesenchymal stromal cells", "stem cells", and "progenitor cells". All papers identified were English-language, full-text articles. Papers were prioritized on the basis of relevance and the authors apologize to authors of manuscripts that might have been missed.

References

[1] A. J. Friedenstein, K. V. Petrakova, A. I. Kurolesova, and G. P. Frolova, "Heterotopic of bone marrow. Analysis of precursor cells for osteogenic and hematopoietic tissues," *Transplantation*, vol. 6, no. 2, pp. 230–247, 1968.

[2] M. Dominici, K. Le Blanc, I. Mueller et al., "Minimal criteria for defining multipotent mesenchymal stromal cells. The International Society for Cellular Therapy position statement," *Cytotherapy*, vol. 8, no. 4, pp. 315–317, 2006.

[3] A. I. Caplan and J. E. Dennis, "Mesenchymal stem cells as trophic mediators," *Journal of Cellular Biochemistry*, vol. 98, no. 5, pp. 1076–1084, 2006.

[4] K. X. Wang, L. Xu, Y. Rui et al., "The effects of secretion factors from umbilical cord derived mesenchymal stem cells on osteogenic differentiation of mesenchymal stem cells," *PLoS ONE*, vol. 10, no. 3, Article ID e0120593, 2015.

[5] M. Nawaz, G. Camussi, H. Valadi et al., "The emerging role of extracellular vesicles as biomarkers for urogenital cancers," *Nature Reviews Urology*, vol. 11, no. 12, pp. 688–701, 2014.

[6] C. Lässer, V. Seyed Alikhani, K. Ekström et al., "Human saliva, plasma and breast milk exosomes contain RNA: uptake by macrophages," *Journal of Translational Medicine*, vol. 9, article 9, 2011.

[7] G. Camussi, M.-C. Deregibus, S. Bruno, C. Grange, V. Fonsato, and C. Tetta, "Exosome/microvesicle-mediated epigenetic reprogramming of cells," *American Journal of Cancer Research*, vol. 1, no. 1, pp. 98–110, 2011.

[8] M. Nawaz, F. Fatima, B. R. Zanetti et al., "Microvesicles in gliomas and medulloblastomas: an overview," *Journal of Cancer Therapy*, vol. 05, no. 02, pp. 182–191, 2014.

[9] S. S. Tan, Y. Yin, T. Lee et al., "Therapeutic MSC exosomes are derived from lipid raft microdomains in the plasma membrane," *Journal of Extracellular Vesicles*, vol. 2, Article ID 22614, 2013.

[10] R. O. Hynes, "Integrins: versatility, modulation, and signaling in cell adhesion," *Cell*, vol. 69, no. 1, pp. 11–25, 1992.

[11] E. C. Lai, "Notch signaling: control of cell communication and cell fate," *Development*, vol. 131, no. 5, pp. 965–973, 2004.

[12] B. Constantin and L. Cronier, "Involvement of gap junctional communication in myogenesis," *International Review of Cytology*, vol. 196, pp. 1–65, 2000.

[13] P. C. Schiller, G. D'Ippolito, R. Brambilla, B. A. Roos, and G. A. Howard, "Inhibition of gap-junctional communication induces the trans-differentiation of osteoblasts to an adipocytic phenotype in vitro," *Journal of Biological Chemistry*, vol. 276, no. 17, pp. 14133–14138, 2001.

[14] J. E. Trosko, "The role of stem cells and gap junctional intercellular communication in carcinogenesis," *Journal of Biochemistry and Molecular Biology*, vol. 36, no. 1, pp. 43–48, 2003.

[15] M. Xu, M. Wani, Y.-S. Dai et al., "Differentiation of bone marrow stromal cells into the cardiac phenotype requires intercellular communication with myocytes," *Circulation*, vol. 110, no. 17, pp. 2658–2665, 2004.

[16] A. Rustom, R. Saffrich, I. Markovic, P. Walther, and H.-H. Gerdes, "Nanotubular highways for intercellular organelle transport," *Science*, vol. 303, no. 5660, pp. 1007–1010, 2004.

[17] L. Marzo, K. Gousset, and C. Zurzolo, "Multifaceted roles of tunneling nanotubes in intercellular communication," *Frontiers in Physiology*, vol. 3, article 72, 2012.

[18] H.-H. Gerdes, N. V. Bukoreshtliev, and J. F. V. Barroso, "Tunneling nanotubes: a new route for the exchange of components between animal cells," *FEBS Letters*, vol. 581, no. 11, pp. 2194–2201, 2007.

[19] S. Abounit and C. Zurzolo, "Wiring through tunneling nanotubes—from electrical signals to organelle transfer," *Journal of Cell Science*, vol. 125, no. 5, pp. 1089–1098, 2012.

[20] E. Lou, S. Fujisawa, A. Morozov et al., "Tunneling nanotubes provide a unique conduit for intercellular transfer of cellular contents in human malignant pleural mesothelioma," *PLoS ONE*, vol. 7, no. 3, Article ID e33093, 2012.

[21] H.-H. Gerdes, A. Rustom, and X. Wang, "Tunneling nanotubes, an emerging intercellular communication route in development," *Mechanisms of Development*, vol. 130, no. 6–8, pp. 381–387, 2013.

[22] J. W. Ady, S. Desir, V. Thayanithy et al., "Intercellular communication in malignant pleural mesothelioma: properties of tunneling nanotubes," *Frontiers in Physiology*, vol. 5, article 400, 2014.

[23] S. Domhan, L. Ma, A. Tai et al., "Intercellular communication by exchange of cytoplasmic material via tunneling nano-tube like structures in primary human renal epithelial cells," *PLoS ONE*, vol. 6, no. 6, Article ID e21283, 2011.

[24] V. Thayanithy, E. L. Dickson, C. Steer, S. Subramanian, and E. Lou, "Tumor-stromal cross talk: direct cell-to-cell transfer of oncogenic microRNAs via tunneling nanotubes," *Translational Research*, vol. 164, no. 5, pp. 359–365, 2014.

[25] S. Valente, R. Rossi, L. Resta, and G. Pasquinelli, "Exploring the human mesenchymal stem cell tubule communication network through electron microscopy," *Ultrastructural Pathology*, vol. 39, no. 2, pp. 88–94, 2015.

[26] T. J. Burdon, A. Paul, N. Noiseux, S. Prakash, and D. Shum-Tim, "Bone marrow stem cell derived paracrine factors for regenerative medicine: current perspectives and therapeutic potential," *Bone Marrow Research*, vol. 2011, Article ID 207326, 14 pages, 2011.

[27] X. Sun, J. Su, J. Bao et al., "Cytokine combination therapy prediction for bone remodeling in tissue engineering based on the intracellular signaling pathway," *Biomaterials*, vol. 33, no. 33, pp. 8265–8276, 2012.

[28] K. Tsuji and S. Kitamura, "Trophic factors from tissue stem cells for renal regeneration," *Stem Cells International*, vol. 2015, Article ID 537204, 7 pages, 2015.

[29] T. Kinnaird, E. S. Burnett, M. Shou et al., "Local delivery of marrow-derived stromal cells augments collateral perfusion through paracrine mechanisms," *Circulation*, vol. 109, no. 12, pp. 1543–1549, 2004.

[30] L. Guo, R. C. H. Zhao, and Y. Wu, "The role of microRNAs in self-renewal and differentiation of mesenchymal stem cells," *Experimental Hematology*, vol. 39, no. 6, pp. 608–616, 2011.

[31] D. E. Discher, D. J. Mooney, and P. W. Zandstra, "Growth factors, matrices, and forces combine and control stem cells," *Science*, vol. 324, no. 5935, pp. 1673–1677, 2009.

[32] J. Ratajczak, M. Wysoczynski, F. Hayek, A. Janowska-Wieczorek, and M. Z. Ratajczak, "Membrane-derived microvesicles: important and underappreciated mediators of cell-to-cell communication," *Leukemia*, vol. 20, no. 9, pp. 1487–1495, 2006.

[33] G. Camussi, M. C. Deregibus, S. Bruno, V. Cantaluppi, and L. Biancone, "Exosomes/microvesicles as a mechanism of cell-to-cell communication," *Kidney International*, vol. 78, no. 9, pp. 838–848, 2010.

[34] H. Valadi, K. Ekström, A. Bossios, M. Sjöstrand, J. J. Lee, and J. O. Lötvall, "Exosome-mediated transfer of mRNAs and microRNAs is a novel mechanism of genetic exchange between cells," *Nature Cell Biology*, vol. 9, no. 6, pp. 654–659, 2007.

[35] M. E. G. Kranendonk, F. L. J. Visseren, B. W. M. Van Balkom et al., "Human adipocyte extracellular vesicles in reciprocal signaling between adipocytes and macrophages," *Obesity*, vol. 22, no. 5, pp. 1296–1308, 2014.

[36] L. Deng, Y. Wang, Y. Peng et al., "Osteoblast-derived microvesicles: a novel mechanism for communication between osteoblasts and osteoclasts," *Bone*, vol. 79, pp. 37–42, 2015.

[37] J. Ratajczak, K. Miekus, M. Kucia et al., "Embryonic stem cell-derived microvesicles reprogram hematopoietic progenitors: evidence for horizontal transfer of mRNA and protein delivery," *Leukemia*, vol. 20, no. 5, pp. 847–856, 2006.

[38] C. Grange, M. Tapparo, F. Collino et al., "Microvesicles released from human renal cancer stem cells stimulate angiogenesis and formation of lung premetastatic niche," *Cancer Research*, vol. 71, no. 15, pp. 5346–5356, 2011.

[39] N. Bauer, M. Wilsch-Bräuninger, J. Karbanová et al., "Haematopoietic stem cell differentiation promotes the release of prominin-1/CD133-containing membrane vesicles—a role of the endocytic-exocytic pathway," *EMBO Molecular Medicine*, vol. 3, no. 7, pp. 398–409, 2011.

[40] G. Rappa, J. Mercapide, F. Anzanello et al., "Wnt interaction and extracellular release of prominin-1/CD133 in human malignant melanoma cells," *Experimental Cell Research*, vol. 319, no. 6, pp. 810–819, 2013.

[41] H. B. Huttner, P. Janich, M. Köhrmann et al., "The stem cell marker prominin-1/CD133 on membrane particles in human cerebrospinal fluid offers novel approaches for studying central nervous system disease," *Stem Cells*, vol. 26, no. 3, pp. 698–705, 2008.

[42] H. Xiao, C. Lässer, G. Shelke et al., "Mast cell exosomes promote lung adenocarcinoma cell proliferation—role of KIT-stem cell factor signaling," *Cell Communication and Signaling*, vol. 12, article 64, 2014.

[43] V. Luga, L. Zhang, A. M. Viloria-Petit et al., "Exosomes mediate stromal mobilization of autocrine Wnt-PCP signaling in breast cancer cell migration," *Cell*, vol. 151, no. 7, pp. 1542–1556, 2012.

[44] J. C. Gross, V. Chaudhary, K. Bartscherer, and M. Boutros, "Active Wnt proteins are secreted on exosomes," *Nature Cell Biology*, vol. 14, no. 10, pp. 1036–1045, 2012.

[45] A. Chairoungdua, D. L. Smith, P. Pochard, M. Hull, and M. J. Caplan, "Exosome release of β-catenin: a novel mechanism that antagonizes Wnt signaling," *Journal of Cell Biology*, vol. 190, no. 6, pp. 1079–1091, 2010.

[46] A. C. Gradilla, E. González, I. Seijo et al., "Exosomes as Hedgehog carriers in cytoneme-mediated transport and secretion," *Nature Communications*, vol. 5, article 5649, 2014.

[47] M. C. Deregibus, V. Cantaluppi, R. Calogero et al., "Endothelial progenitor cell—derived microvesicles activate an angiogenic program in endothelial cells by a horizontal transfer of mRNA," *Blood*, vol. 110, no. 7, pp. 2440–2448, 2007.

[48] J. M. Aliotta, M. Pereira, K. W. Johnson et al., "Microvesicle entry into marrow cells mediates tissue-specific changes in mRNA by direct delivery of mRNA and induction of transcription," *Experimental Hematology*, vol. 38, no. 3, pp. 233–245, 2010.

[49] R. Nair, L. Santos, S. Awasthi et al., "Extracellular vesicles derived from preosteoblasts influence embryonic stem cell differentiation," *Stem Cells and Development*, vol. 23, no. 14, pp. 1625–1635, 2014.

[50] A. Forterre, A. Jalabert, K. Chikh et al., "Myotube-derived exosomal miRNAs downregulate Sirtuin1 in myoblasts during muscle cell differentiation," *Cell Cycle*, vol. 13, no. 1, pp. 78–89, 2014.

[51] D. S. Mistry, Y. Chen, and G. L. Sen, "Progenitor function in self-renewing human epidermis is maintained by the exosome," *Cell Stem Cell*, vol. 11, no. 1, pp. 127–135, 2012.

[52] J. P. Webber, L. K. Spary, A. J. Sanders et al., "Differentiation of tumour-promoting stromal myofibroblasts by cancer exosomes," *Oncogene*, vol. 34, no. 3, pp. 290–302, 2015.

[53] S. C. McIver, Y.-A. Kang, A. W. Devilbiss et al., "The exosome complex establishes a barricade to erythroid maturation," *Blood*, vol. 124, no. 14, pp. 2285–2297, 2014.

[54] F. Collino, M. C. Deregibus, S. Bruno et al., "Microvesicles derived from adult human bone marrow and tissue specific mesenchymal stem cells shuttle selected pattern of miRNAs," *PLoS ONE*, vol. 5, no. 7, Article ID e11803, 2010.

[55] J. Zhang, J. Guan, X. Niu et al., "Exosomes released from human induced pluripotent stem cells-derived MSCs facilitate cutaneous wound healing by promoting collagen synthesis and angiogenesis," *Journal of Translational Medicine*, vol. 13, no. 1, p. 49, 2015.

[56] A. Shabbir, A. Cox, L. Rodriguez-Menocal, M. Salgado, and E. V. Badiavas, "Mesenchymal stem cell exosomes induce proliferation and migration of normal and chronic wound fibroblasts, and enhance angiogenesis in vitro," *Stem Cells and Development*, vol. 24, no. 14, pp. 1635–1647, 2015.

[57] J. M. Aliotta, M. Pereira, M. Li et al., "Stable cell fate changes in marrow cells induced by lung-derived microvesicles," *Journal of Extracellular Vesicles*, vol. 1, 2012.

[58] P. J. Quesenberry, M. S. Dooner, and J. M. Aliotta, "Stem cell plasticity revisited: the continuum marrow model and phenotypic changes mediated by microvesicles," *Experimental Hematology*, vol. 38, no. 7, pp. 581–592, 2010.

[59] K. Takahashi and S. Yamanaka, "Induction of pluripotent stem cells from mouse embryonic and adult fibroblast cultures by defined factors," *Cell*, vol. 126, no. 4, pp. 663–676, 2006.

[60] Y. Tay, J. Zhang, A. M. Thomson, B. Lim, and I. Rigoutsos, "MicroRNAs to *Nanog*, *Oct4* and *Sox2* coding regions modulate embryonic stem cell differentiation," *Nature*, vol. 455, no. 7216, pp. 1124–1128, 2008.

[61] N. Xu, T. Papagiannakopoulos, G. Pan, J. A. Thomson, and K. S. Kosik, "microRNA-145 regulates OCT4, SOX2, and KLF4 and represses pluripotency in human embryonic stem cells," *Cell*, vol. 137, no. 4, pp. 647–658, 2009.

[62] D. Katsman, E. J. Stackpole, D. R. Domin, and D. B. Farber, "Embryonic stem cell-derived microvesicles induce gene expression changes in Muller cells of the retina," *PLoS ONE*, vol. 7, no. 11, Article ID e50417, 2012.

[63] V. B. Cismasiu and L. M. Popescu, "Telocytes transfer extracellular vesicles loaded with microRNAs to stem cells," *Journal of Cellular and Molecular Medicine*, vol. 19, no. 2, pp. 351–358, 2015.

[64] W. Koh, C. T. Sheng, B. Tan et al., "Analysis of deep sequencing microRNA expression profile from human embryonic stem cells derived mesenchymal stem cells reveals possible role of let-7 microRNA family in downstream targeting of hepatic nuclear factor 4 alpha," *BMC Genomics*, vol. 11, supplement 1, article S6, 2010.

[65] T. Oskarsson, E. Batlle, and J. Massagué, "Metastatic stem cells: sources, niches, and vital pathways," *Cell Stem Cell*, vol. 14, no. 3, pp. 306–321, 2014.

[66] A. M. Roccaro, A. Sacco, P. Maiso et al., "BM mesenchymal stromal cell-derived exosomes facilitate multiple myeloma progression," *Journal of Clinical Investigation*, vol. 123, no. 4, pp. 1542–1555, 2013.

[67] A. Eirin, S. M. Riester, X.-Y. Zhu et al., "microRNA and mRNA cargo of extracellular vesicles from porcine adipose tissue-derived mesenchymal stem cells," *Gene*, vol. 551, no. 1, pp. 55–64, 2014.

[68] W. Zhu, L. Huang, Y. Li et al., "Exosomes derived from human bone marrow mesenchymal stem cells promote tumor growth *in vivo*," *Cancer Letters*, vol. 315, no. 1, pp. 28–37, 2012.

[69] K. C. Vallabhaneni, P. Penfornis, S. Dhule et al., "Extracellular vesicles from bone marrow mesenchymal stem/stromal cells transport tumor regulatory microRNA, proteins, and metabolites," *Oncotarget*, vol. 6, no. 7, pp. 4953–4967, 2015.

[70] M. Wang, C. Zhao, H. Shi et al., "Deregulated microRNAs in gastric cancer tissue-derived mesenchymal stem cells: novel biomarkers and a mechanism for gastric cancer," *British Journal of Cancer*, vol. 110, no. 5, pp. 1199–1210, 2014.

[71] R. S. Lindoso, F. Collino, and G. Camussi, "Extracellular vesicles derived from renal cancer stem cells induce a pro-tumorigenic phenotype in mesenchymal stromal cells," *Oncotarget*, vol. 6, no. 10, pp. 7959–7969, 2015.

[72] S. Bruno, F. Collino, M. C. Deregibus, C. Grange, C. Tetta, and G. Camussi, "Microvesicles derived from human bone marrow mesenchymal stem cells inhibit tumor growth," *Stem Cells and Development*, vol. 22, no. 5, pp. 758–771, 2013.

[73] M. Ono, N. Kosaka, N. Tominaga et al., "Exosomes from bone marrow mesenchymal stem cells contain a microRNA that promotes dormancy in metastatic breast cancer cells," *Science Signaling*, vol. 7, no. 332, p. ra63, 2014.

[74] J.-K. Lee, S.-R. Park, B.-K. Jung et al., "Exosomes derived from mesenchymal stem cells suppress angiogenesis by down-regulating VEGF expression in breast cancer cells," *PLoS ONE*, vol. 8, no. 12, Article ID e84256, 2013.

[75] S. Wu, G.-Q. Ju, T. Du, Y.-J. Zhu, and G.-H. Liu, "Microvesicles derived from human umbilical cord Wharton's jelly mesenchymal stem cells attenuate bladder tumor cell growth in vitro and in vivo," *PLoS ONE*, vol. 8, no. 4, Article ID e61366, 2013.

[76] V. Fonsato, F. Collino, M. B. Herrera et al., "Human liver stem cell-derived microvesicles inhibit hepatoma growth in SCID mice by delivering antitumor microRNAs," *Stem Cells*, vol. 30, no. 9, pp. 1985–1998, 2012.

[77] S. Bruno, F. Collino, A. Iavello, and G. Camussi, "Effects of mesenchymal stromal cell-derived extracellular vesicles on tumor growth," *Frontiers in Immunology*, vol. 5, article 382, 2014.

[78] E. Bourkoula, D. Mangoni, T. Ius et al., "Glioma-associated stem cells: a novel class of tumor-supporting cells able to predict prognosis of human low-grade gliomas," *Stem Cells*, vol. 32, no. 5, pp. 1239–1253, 2014.

[79] J. L. Munoz, S. A. Bliss, S. J. Greco, S. H. Ramkissoon, K. L. Ligon, and P. Rameshwar, "Delivery of functional anti-miR-9 by mesenchymal stem cell-derived exosomes to glioblastoma multiforme cells conferred chemosensitivity," *Molecular Therapy—Nucleic Acids*, vol. 2, article e126, 2013.

[80] A. Bronisz, Y. Wang, M. O. Nowicki et al., "Extracellular vesicles modulate the glioblastoma microenvironment via a tumor suppression signaling network directed by miR-1," *Cancer Research*, vol. 74, no. 3, pp. 738–750, 2014.

[81] I. Nakano, D. Garnier, M. Minata, and J. Rak, "Extracellular vesicles in the biology of brain tumour stem cells—implications for inter-cellular communication, therapy and biomarker development," *Seminars in Cell & Developmental Biology*, vol. 40, pp. 17–26, 2015.

[82] M. Katakowski, B. Buller, X. Zheng et al., "Exosomes from marrow stromal cells expressing miR-146b inhibit glioma growth," *Cancer Letters*, vol. 335, no. 1, pp. 201–204, 2013.

[83] L. Pascucci, V. Coccè, A. Bonomi et al., "Paclitaxel is incorporated by mesenchymal stromal cells and released in exosomes that inhibit *in vitro* tumor growth: a new approach for drug delivery," *Journal of Controlled Release*, vol. 192, pp. 262–270, 2014.

[84] V. Plaks, N. Kong, and Z. Werb, "The cancer stem cell niche: how essential is the niche in regulating stemness of tumor cells?" *Cell Stem Cell*, vol. 16, no. 3, pp. 225–238, 2015.

[85] R. Ghasemi, A. Grassadonia, N. Tinari et al., "Tumor-derived microvesicles: the metastasomes," *Medical Hypotheses*, vol. 80, no. 1, pp. 75–82, 2013.

[86] M. H. Barcellos-Hoff, D. Lyden, and T. C. Wang, "The evolution of the cancer niche during multistage carcinogenesis," *Nature Reviews Cancer*, vol. 13, no. 7, pp. 511–518, 2013.

[87] H. Haga, I. K. Yan, K. Takahashi, J. Wood, A. Zubair, and T. Patel, "Tumour cell-derived extracellular vesicles interact with mesenchymal stem cells to modulate the microenvironment and

enhance cholangiocarcinoma growth," *Journal of Extracellular Vesicles*, vol. 4, Article ID 24900, 2015.

[88] J. A. Cho, H. Park, E. H. Lim et al., "Exosomes from ovarian cancer cells induce adipose tissue-derived mesenchymal stem cells to acquire the physical and functional characteristics of tumor-supporting myofibroblasts," *Gynecologic Oncology*, vol. 123, no. 2, pp. 379–386, 2011.

[89] R. Chowdhury, J. P. Webber, M. Gurney, M. D. Mason, Z. Tabi, and A. Clayton, "Cancer exosomes trigger mesenchymal stem cell differentiation into pro-angiogenic and pro-invasive myofibroblasts," *Oncotarget*, vol. 6, no. 2, pp. 715–731, 2015.

[90] Z. Y. A. Elmageed, Y. Yang, R. Thomas et al., "Neoplastic reprogramming of patient-derived adipose stem cells by prostate cancer cell-associated exosomes," *Stem Cells*, vol. 32, no. 4, pp. 983–997, 2014.

[91] J. Gu, H. Qian, L. Shen et al., "Gastric cancer exosomes trigger differentiation of umbilical cord derived mesenchymal stem cells to carcinoma-associated fibroblasts through TGF-β/smad pathway," *PLoS ONE*, vol. 7, no. 12, Article ID e52465, 2012.

[92] M. Shimoda, S. Principe, H. W. Jackson et al., "Loss of the *Timp* gene family is sufficient for the acquisition of the CAF-like cell state," *Nature Cell Biology*, vol. 16, no. 9, pp. 889–901, 2014.

[93] Y. Hu, C. Yan, L. Mu et al., "Fibroblast-derived exosomes contribute to chemoresistance through priming cancer stem cells in colorectal cancer," *PLoS ONE*, vol. 10, no. 5, Article ID e0125625, 2015.

[94] M. Quante, S. P. Tu, H. Tomita et al., "Bone marrow-derived myofibroblasts contribute to the mesenchymal stem cell niche and promote tumor growth," *Cancer Cell*, vol. 19, no. 2, pp. 257–272, 2011.

[95] A. Yuan, E. L. Farber, A. L. Rapoport et al., "Transfer of microRNAs by embryonic stem cell microvesicles," *PLoS ONE*, vol. 4, no. 3, Article ID e4722, 2009.

[96] R. Koch, M. Demant, T. Aung et al., "Populational equilibrium through exosome-mediated Wnt signaling in tumor progression of diffuse large B-cell lymphoma," *Blood*, vol. 123, no. 14, pp. 2189–2198, 2014.

[97] M. J. Rahman, D. Regn, R. Bashratyan, and Y. D. Dai, "Exosomes released by islet-derived mesenchymal stem cells trigger autoimmune responses in NOD mice," *Diabetes*, vol. 63, no. 3, pp. 1008–1020, 2014.

[98] F. T. Borges, S. A. Melo, B. C. Özdemir et al., "TGF-beta1-containing exosomes from injured epithelial cells activate fibroblasts to initiate tissue regenerative responses and fibrosis," *Journal of the American Society of Nephrology*, vol. 24, no. 3, pp. 385–392, 2013.

[99] Y.-G. Zhu, X.-M. Feng, J. Abbott et al., "Human mesenchymal stem cell microvesicles for treatment of *Escherichia coli* endotoxin-induced acute lung injury in mice," *Stem Cells*, vol. 32, no. 1, pp. 116–125, 2014.

[100] S. Tomasoni, L. Longaretti, C. Rota et al., "Transfer of growth factor receptor mRNA via exosomes unravels the regenerative effect of mesenchymal stem cells," *Stem Cells and Development*, vol. 22, no. 5, pp. 772–780, 2013.

[101] J. Aoki, K. Ohashi, M. Mitsuhashi et al., "Posttransplantation bone marrow assessment by quantifying hematopoietic cell-derived mRNAs in plasma exosomes/microvesicles," *Clinical Chemistry*, vol. 60, no. 4, pp. 675–682, 2014.

[102] S. Sahoo, E. Klychko, T. Thorne et al., "Exosomes from human $CD34^+$ stem cells mediate their proangiogenic paracrine activity," *Circulation Research*, vol. 109, no. 7, pp. 724–728, 2011.

[103] T. Li, Y. Yan, B. Wang et al., "Exosomes derived from human umbilical cord mesenchymal stem cells alleviate liver fibrosis," *Stem Cells and Development*, vol. 22, no. 6, pp. 845–854, 2013.

[104] S.-S. Lin, B. Zhu, Z.-K. Guo et al., "Bone marrow mesenchymal stem cell-derived microvesicles protect rat pheochromocytoma PC12 cells from glutamate-induced injury via a PI3K/Akt dependent pathway," *Neurochemical Research*, vol. 39, no. 5, pp. 922–931, 2014.

[105] T. Katsuda, R. Tsuchiya, N. Kosaka et al., "Human adipose tissue-derived mesenchymal stem cells secrete functional neprilysin-bound exosomes," *Scientific Reports*, vol. 3, article 1197, 2013.

[106] J.-F. Xu, G.-H. Yang, X.-H. Pan et al., "Altered microRNA expression profile in exosomes during osteogenic differentiation of human bone marrow-derived mesenchymal stem cells," *PLoS ONE*, vol. 9, no. 12, Article ID e114627, 2014.

[107] H. Xin, Y. Li, B. Buller et al., "Exosome-mediated transfer of miR-133b from multipotent mesenchymal stromal cells to neural cells contributes to neurite outgrowth," *Stem Cells*, vol. 30, no. 7, pp. 1556–1564, 2012.

[108] R. Gernapudi, Y. Yao, Y. Zhang et al., "Targeting exosomes from preadipocytes inhibits preadipocyte to cancer stem cell signaling in early-stage breast cancer," *Breast Cancer Research and Treatment*, vol. 150, no. 3, pp. 685–695, 2015.

[109] Y. Feng, W. Huang, M. Wani, X. Yu, and M. Ashraf, "Ischemic preconditioning potentiates the protective effect of stem cells through secretion of exosomes by targeting Mecp2 via miR-22," *PLoS ONE*, vol. 9, no. 2, Article ID e88685, 2014.

[110] B. Yu, M. Gong, Y. Wang et al., "Cardiomyocyte protection by GATA-4 gene engineered mesenchymal stem cells is partially mediated by translocation of miR-221 in microvesicles," *PLoS ONE*, vol. 8, no. 8, Article ID e73304, 2013.

[111] L. Barile, V. Lionetti, E. Cervio et al., "Extracellular vesicles from human cardiac progenitor cells inhibit cardiomyocyte apoptosis and improve cardiac function after myocardial infarction," *Cardiovascular Research*, vol. 103, no. 4, pp. 530–541, 2014.

[112] M. Khan, E. Nickoloff, T. Abramova et al., "Embryonic stem cell-derived exosomes promote endogenous repair mechanisms and enhance cardiac function following myocardial infarction," *Circulation Research*, vol. 117, no. 1, pp. 52–64, 2015.

[113] J. Wang, S. Chen, X. Ma et al., "Effects of endothelial progenitor cell-derived microvesicles on hypoxia/reoxygenation-induced endothelial dysfunction and apoptosis," *Oxidative Medicine and Cellular Longevity*, vol. 2013, Article ID 572729, 9 pages, 2013.

[114] X.-Y. Bi, S. Huang, J.-L. Chen, F. Wang, Y. Wang, and Z.-K. Guo, "Exploration of conditions for releasing microvesicle from human bone marrow mesenchymal stem cells," *Zhongguo Shi Yan Xue Ye Xue Za Zhi*, vol. 22, no. 2, pp. 491–495, 2014.

[115] T. Lopatina, S. Bruno, C. Tetta, N. Kalinina, M. Porta, and G. Camussi, "Platelet-derived growth factor regulates the secretion of extracellular vesicles by adipose mesenchymal stem cells and enhances their angiogenic potential," *Cell Communication and Signaling*, vol. 12, article 26, 2014.

[116] L. Pascucci, G. Alessandri, C. Dall'Aglio et al., "Membrane vesicles mediate pro-angiogenic activity of equine adipose-derived mesenchymal stromal cells," *Veterinary Journal*, vol. 202, no. 2, pp. 361–366, 2014.

[117] L. Zitvogel, A. Regnault, A. Lozier et al., "Eradication of established murine tumors using a novel cell-free vaccine: dendritic cell-derived exosomes," *Nature Medicine*, vol. 4, no. 5, pp. 594–600, 1998.

[118] N. M. Mahaweni, M. E. Kaijen-Lambers, J. Dekkers, J. G. Aerts, and J. P. Hegmans, "Tumour-derived exosomes as antigen delivery carriers in dendritic cell-based immunotherapy for malignant mesothelioma," *Journal of Extracellular Vesicles*, vol. 2, 2013.

[119] G. Raposo, H. W. Nijman, W. Stoorvogel et al., "B lymphocytes secrete antigen-presenting vesicles," *Journal of Experimental Medicine*, vol. 183, no. 3, pp. 1161–1172, 1996.

[120] B. Zhang, Y. Yin, R. C. Lai, S. S. Tan, A. B. H. Choo, and S. K. Lim, "Mesenchymal stem cells secrete immunologically active exosomes," *Stem Cells and Development*, vol. 23, no. 11, pp. 1233–1244, 2014.

[121] R. Blazquez, F. M. Sanchez-Margallo, O. de la Rosa et al., "Immunomodulatory potential of human adipose mesenchymal stem cells derived exosomes on in vitro stimulated T cells," *Frontiers in Immunology*, vol. 5, article 556, 2014.

[122] K. Ekström, O. Omar, C. Granéli, X. Wang, F. Vazirisani, and P. Thomsen, "Monocyte exosomes stimulate the osteogenic gene expression of mesenchymal stem cells," *PLoS ONE*, vol. 8, no. 9, Article ID e75227, 2013.

[123] C. S. Hong, L. Muller, M. Boyiadzis, and T. L. Whiteside, "Isolation and characterization of CD34+ blast-derived exosomes in acute myeloid leukemia," *PLoS ONE*, vol. 9, no. 8, Article ID e103310, 2014.

[124] S. Amarnath, J. E. Foley, D. E. Farthing et al., "Bone marrow-derived mesenchymal stromal cells harness purinergenic signaling to tolerize human Th1 cells in vivo," *Stem Cells*, vol. 33, no. 4, pp. 1200–1212, 2015.

[125] L. Kordelas, V. Rebmann, A.-K. Ludwig et al., "MSC-derived exosomes: a novel tool to treat therapy-refractory graft-versus-host disease," *Leukemia*, vol. 28, no. 4, pp. 970–973, 2014.

[126] B. Zhang, Y. Yin, R. C. Lai, and S. K. Lim, "Immunotherapeutic potential of extracellular vesicles," *Frontiers in Immunology*, vol. 5, article 518, 2014.

[127] E. I. Buzas, B. György, G. Nagy, A. Falus, and S. Gay, "Emerging role of extracellular vesicles in inflammatory diseases," *Nature Reviews Rheumatology*, vol. 10, no. 6, pp. 356–364, 2014.

[128] C. Lee, S. A. Mitsialis, M. Aslam et al., "Exosomes mediate the cytoprotective action of mesenchymal stromal cells on hypoxia-induced pulmonary hypertension," *Circulation*, vol. 126, no. 22, pp. 2601–2611, 2012.

[129] F. Arslan, R. C. Lai, M. B. Smeets et al., "Mesenchymal stem cell-derived exosomes increase ATP levels, decrease oxidative stress and activate PI3K/Akt pathway to enhance myocardial viability and prevent adverse remodeling after myocardial ischemia/reperfusion injury," *Stem Cell Research*, vol. 10, no. 3, pp. 301–312, 2013.

[130] K. R. Vrijsen, J. P. G. Sluijter, M. W. L. Schuchardt et al., "Cardiomyocyte progenitor cell-derived exosomes stimulate migration of endothelial cells," *Journal of Cellular and Molecular Medicine*, vol. 14, no. 5, pp. 1064–1070, 2010.

[131] S. Bian, L. Zhang, L. Duan, X. Wang, Y. Min, and H. Yu, "Extracellular vesicles derived from human bone marrow mesenchymal stem cells promote angiogenesis in a rat myocardial infarction model," *Journal of Molecular Medicine*, vol. 92, no. 4, pp. 387–397, 2014.

[132] K. Kang, R. Ma, W. Cai et al., "Exosomes secreted from CXCR4 overexpressing mesenchymal stem cells promote cardioprotection via Akt signaling pathway following myocardial infarction," *Stem Cells International*, vol. 2015, Article ID 659890, 14 pages, 2015.

[133] Z. Giricz, Z. V. Varga, T. Baranyai et al., "Cardioprotection by remote ischemic preconditioning of the rat heart is mediated by extracellular vesicles," *Journal of Molecular and Cellular Cardiology*, vol. 68, pp. 75–78, 2014.

[134] Y. Feng, W. Huang, W. Meng et al., "Heat shock improves Sca-1+ stem cell survival and directs ischemic cardiomyocytes toward a prosurvival phenotype via exosomal transfer: a critical role for HSF1/miR-34a/HSP70 pathway," *Stem Cells*, vol. 32, no. 2, pp. 462–472, 2014.

[135] B. Yu, H. W. Kim, M. Gong et al., "Exosomes secreted from GATA-4 overexpressing mesenchymal stem cells serve as a reservoir of anti-apoptotic microRNAs for cardioprotection," *International Journal of Cardiology*, vol. 182, pp. 349–360, 2015.

[136] M. Choi, T. Ban, and T. Rhim, "Therapeutic use of stem cell transplantation for cell replacement or cytoprotective effect of microvesicle released from mesenchymal stem cell," *Molecules and Cells*, vol. 37, no. 2, pp. 133–139, 2014.

[137] B. D. Humphreys, M. T. Valerius, A. Kobayashi et al., "Intrinsic epithelial cells repair the kidney after injury," *Cell Stem Cell*, vol. 2, no. 3, pp. 284–291, 2008.

[138] B. Bi, R. Schmitt, M. Israilova, H. Nishio, and L. G. Cantley, "Stromal cells protect against acute tubular injury via an endocrine effect," *Journal of the American Society of Nephrology*, vol. 18, no. 9, pp. 2486–2496, 2007.

[139] S. Bruno, C. Grange, M. C. Deregibus et al., "Mesenchymal stem cell-derived microvesicles protect against acute tubular injury," *Journal of the American Society of Nephrology*, vol. 20, no. 5, pp. 1053–1067, 2009.

[140] Y. Zhou, H. Xu, W. Xu et al., "Exosomes released by human umbilical cord mesenchymal stem cells protect against cisplatin-induced renal oxidative stress and apoptosis in vivo and in vitro," *Stem Cell Research and Therapy*, vol. 4, no. 2, article 34, 2013.

[141] S. Gatti, S. Bruno, M. C. Deregibus et al., "Microvesicles derived from human adult mesenchymal stem cells protect against ischaemia-reperfusion-induced acute and chronic kidney injury," *Nephrology Dialysis Transplantation*, vol. 26, no. 5, pp. 1474–1483, 2011.

[142] S. Bruno, C. Grange, F. Collino et al., "Microvesicles derived from mesenchymal stem cells enhance survival in a lethal model of acute kidney injury," *PLoS ONE*, vol. 7, no. 3, Article ID e33115, 2012.

[143] R. S. Lindoso, F. Collino, S. Bruno et al., "Extracellular vesicles released from mesenchymal stromal cells modulate miRNA in renal tubular cells and inhibit ATP depletion injury," *Stem Cells and Development*, vol. 23, no. 15, pp. 1809–1819, 2014.

[144] F. Collino, S. Bruno, D. Incarnato et al., "AKI recovery induced by mesenchymal stromal cell-derived extracellular vesicles carrying MicroRNAs," *Journal of the American Society of Nephrology*, 2015.

[145] J. He, Y. Wang, S. Sun et al., "Bone marrow stem cells-derived microvesicles protect against renal injury in the mouse remnant kidney model," *Nephrology*, vol. 17, no. 5, pp. 493–500, 2012.

[146] V. Cantaluppi, D. Medica, C. Mannari et al., "Endothelial progenitor cell-derived extracellular vesicles protect from complement-mediated mesangial injury in experimental anti-Thy1.1 glomerulonephritis," *Nephrology Dialysis Transplantation*, vol. 30, no. 3, pp. 410–422, 2015.

[147] M. Sanchez, S. Bruno, C. Grange et al., "Human liver stem cells and derived extracellular vesicles improve recovery in a murine model of acute kidney injury," *Stem Cell Research & Therapy*, vol. 5, no. 6, article 124, 2014.

[148] J. He, Y. Wang, X. Lu et al., "Micro-vesicles derived from bone marrow stem cells protect the kidney both in vivo and in vitro by microRNA-dependent repairing," *Nephrology*, vol. 20, no. 9, pp. 591–600, 2015.

[149] J. M. Aliotta, F. M. Sanchez-Guijo, G. J. Dooner et al., "Alteration of marrow cell gene expression, protein production, and engraftment into lung by lung-derived microvesicles: a novel mechanism for phenotype modulation," *Stem Cells*, vol. 25, no. 9, pp. 2245–2256, 2007.

[150] L. Li, S. Jin, and Y. Zhang, "Ischemic preconditioning potentiates the protective effect of mesenchymal stem cells on endotoxin-induced acute lung injury in mice through secretion of exosome," *International Journal of Clinical and Experimental Medicine*, vol. 8, no. 3, pp. 3825–3832, 2015.

[151] M. B. Herrera, V. Fonsato, S. Gatti et al., "Human liver stem cell-derived microvesicles accelerate hepatic regeneration in hepatectomized rats," *Journal of Cellular and Molecular Medicine*, vol. 14, no. 6B, pp. 1605–1618, 2010.

[152] C. Y. Tan, R. C. Lai, W. Wong, Y. Y. Dan, S.-K. Lim, and H. K. Ho, "Mesenchymal stem cell-derived exosomes promote hepatic regeneration in drug-induced liver injury models," *Stem Cell Research and Therapy*, vol. 5, no. 3, article 76, 2014.

[153] A. Raisi, S. Azizi, N. Delirezh, B. Heshmatian, A. A. Farshid, and K. Amini, "The mesenchymal stem cell-derived microvesicles enhance sciatic nerve regeneration in rat: a novel approach in peripheral nerve cell therapy," *Journal of Trauma and Acute Care Surgery*, vol. 76, no. 4, pp. 991–997, 2014.

[154] D. M. Feliciano, S. Zhang, C. M. Nasrallah, S. N. Lisgo, and A. Bordey, "Embryonic cerebrospinal fluid nanovesicles carry evolutionarily conserved molecules and promote neural stem cell amplification," *PLoS ONE*, vol. 9, no. 2, Article ID e88810, 2014.

[155] X. Zhuang, X. Xiang, W. Grizzle et al., "Treatment of brain inflammatory diseases by delivering exosome encapsulated anti-inflammatory drugs from the nasal region to the brain," *Molecular Therapy*, vol. 19, no. 10, pp. 1769–1779, 2011.

[156] Y. Zhang, M. Chopp, Y. Meng et al., "Effect of exosomes derived from multipluripotent mesenchymal stromal cells on functional recovery and neurovascular plasticity in rats after traumatic brain injury," *Journal of Neurosurgery*, vol. 122, no. 4, pp. 856–867, 2015.

[157] P. J. Quesenberry, G. Dooner, M. Dooner, and M. Abedi, "Developmental biology: ignoratio elenchi: red herrings in stem cell research," *Science*, vol. 308, no. 5725, pp. 1121–1122, 2005.

[158] R. J. Simpson, H. Kalra, and S. Mathivanan, "ExoCarta as a resource for exosomal research," *Journal of Extracellular Vesicles*, vol. 1, Article ID 18374, 2012.

[159] D. Kumar, D. Gupta, S. Shankar, and R. K. Srivastava, "Biomolecular characterization of exosomes released from cancer stem cells: possible implications for biomarker and treatment of cancer," *Oncotarget*, vol. 6, no. 5, pp. 3280–3291, 2015.

Hindawi Publishing Corporation
Stem Cells International
Volume 2015, Article ID 218518, 13 pages
http://dx.doi.org/10.1155/2015/218518

Research Article

A Resource for the Transcriptional Signature of Bona Fide Trophoblast Stem Cells and Analysis of Their Embryonic Persistence

Georg Kuales,[1] Matthias Weiss,[1] Oliver Sedelmeier,[1] Dietmar Pfeifer,[2] and Sebastian J. Arnold[1,3,4]

[1]*Renal Department, Centre for Clinical Research, University Medical Centre, Breisacher Strasse 66, 79106 Freiburg, Germany*
[2]*Department of Hematology, Oncology and Stem Cell Transplantation, University Medical Centre, Freiburg, Germany*
[3]*Institute of Experimental and Clinical Pharmacology and Toxicology, University of Freiburg, Freiburg, Germany*
[4]*BIOSS, Centre for Biological Signalling Studies, Albert Ludwigs University, Freiburg, Germany*

Correspondence should be addressed to Sebastian J. Arnold; sebastian.arnold@uniklinik-freiburg.de

Received 25 May 2015; Accepted 22 July 2015

Academic Editor: Valerie Kouskoff

Trophoblast stem cells (TSCs) represent the multipotent progenitors that give rise to the different cells of the embryonic portion of the placenta. Here, we analysed the expression of key TSC transcription factors *Cdx2*, *Eomes*, and *Elf5* in the early developing placenta of mouse embryos and in cultured TSCs and reveal surprising heterogeneity in protein levels. We analysed persistence of TSCs in the early placenta and find that TSCs remain in the chorionic hinge until E9.5 and are lost shortly afterwards. To define the transcriptional signature of bona fide TSCs, we used inducible gain- and loss-of-function alleles of *Eomes* or *Cdx2*, and $Eomes^{GFP}$, to manipulate and monitor the core maintenance factors of TSCs, followed by genome-wide expression profiling. Combinatorial analysis of resulting expression profiles allowed for defining novel TSC marker genes that might functionally contribute to the maintenance of the TSC state. Analyses by qRT-PCR and *in situ* hybridisation validated novel TSC- and chorion-specific marker genes, such as *Bok/Mtd, Cldn26, Duox2, Duoxa2, Nr0b1*, and *Sox21*. Thus, these expression data provide a valuable resource for the transcriptional signature of bona fide and early differentiating TSCs and may contribute to an increased understanding of the transcriptional circuitries that maintain and/or establish stemness of TSCs.

1. Introduction

Trophectoderm (TE) and inner cell mass (ICM) are the first cell lineages that are specified at the 16- to 32-cell (morula) stage around embryonic day 3 (E3.0) of mouse development (reviewed in [1, 2]). Mutual negative feedback inhibition of the two key transcription factors *Cdx2* and *Oct4* establishes the lineages of *Cdx2*-expressing TE and *Oct4*-positive ICM cells [3–6]. Multiple signals, including cell polarity, cell-cell contacts, positional information, and Hippo signalling, converge on the phosphorylation state of Yes-associated protein (YAP). YAP forms a transcriptional complex with TEAD4 to activate *Cdx2* transcription in predominantly outer, peripheral cells of the early embryo, thus priming the TE programme [4–13]. Additional layers of regulation ensure lineage restricted *Cdx2* and *Oct4* expression, such as Notch-signalling, which cooperates with TEAD4 to directly regulate *Cdx2* expression [14]. Similarly, the transcription factor *AP2γ* promotes *Cdx2* expression and downregulates Hippo signalling [15]. GATA3 acts in parallel with CDX2 and downstream of TEAD4 to induce an overlapping set of target genes in the trophoblast lineage [16]. Within the polar TE, which is defined by its vicinity to the ICM at the blastocyst stage (E3.5), a population of trophoblast stem cells (TSCs) is established and maintained by ICM-derived Fgf- and Nodal-signals, to generate the main cellular source for formation of the embryonic part of the placenta [13, 17–20]. Following initial specification of TE fate by *Cdx2*-functions,

additional transcriptional regulators, including *Eomes* [4] and *Elf5* [21], initiate expression in the TE lineage or become specifically restricted to TE cells such as *AP2γ* [22, 23]. Following implantation around E4.5, the polar TE gives rise to the extraembryonic ectoderm (ExE), which contains TSCs, and the ectoplacental cone (EPC), which mediates the embryonic invasion into the decidual wall then connects the embryo to the maternal uterus. TSCs retain their stem cell characteristics, namely, self-renewal capacity and multipotency, only in the polar TE and the ExE while cells of the mural TE lack supportive signalling from the ICM and thus differentiate to primary trophoblast giant cells (TGCs) [17]. TSC maintenance is controlled by transcriptional circuitries involving *Elf5* [24, 25], *Ets2* [26], and *AP2γ* [23, 27], which act in positive feed forward loops to maintain *Cdx2* and/or *Eomes* expression. After E7.5, the core set of TSC marker genes, including *Cdx2*, *Eomes*, *Elf5*, and *Esrrβ*, remain expressed in the chorion in addition to other embryonic and extraembryonic expression domains [24, 28–30].

TSCs can be routinely isolated and cultured from E3.5 blastocysts and E6.5 ExE explants under defined conditions [17]. Assessing the potential to isolate cells with TSC character beyond E6.5, Uy and colleagues have shown that the frequency to obtain TSC clones increases until the 4-somite pair stage (~E8.0 to E8.25) but then rapidly drops and no TSCs can be isolated following the 11-somite pair stage around E8.5 to E8.75 [31]. The T-box transcription factor *Eomes* was previously used to mark TSCs through different developmental stages and expression of an *Eomes*::*GFP* BAC transgene was detected until E14.5 in the outer periphery of the murine placenta [32]. To date it was not clearly shown until which embryonic stage cells with TSC character are maintained in the TSC niche, which is functionally defined by high levels of Fgf and Tgfβ signals [17, 33]. In addition to *Eomes* [34] and *Cdx2* [35], also other transcription factors share essential functions for TSC self-renewal and multipotency including *Elf5* [24], *Esrrβ* [29], *Ets2* [26], *AP2γ* [23, 27, 36], and *Sox2* [37]. A recent report demonstrated that the functional loss of the histone demethylase *Lsd1* in TSCs results in premature migration of TSCs from their niche, demonstrating additional requirements of proper epigenetic regulation for the propagation of TSCs [38, 39].

In addition to their functional importance during TSC maintenance, *Cdx2* [3, 11], *Eomes* [3], *Elf5* [25], *Tead4* [11], *AP2γ* [23], and *Gata3* [16] also evoke lineage conversion from mouse embryonic stem (mES) cells to the TE lineage when overexpressed (reviewed in [40]). While the transcriptional programme involving *Cdx2*, *Eomes*, *Elf5*, *AP2γ*, and *Ets2* is key for the maintenance of the trophoblast stemness state, genetic deletions of each of these transcription factors generate remarkable different embryonic phenotypes. *Cdx2*-deficiency results in implantation defects [41], *Eomes*-deficient embryos show early postimplantation [34], and the deletions of *Elf5* [24], *Ets2* [26, 42, 43], or *AP2γ* [36] lead to postgastrulation lethality. This diversity in loss-of-function phenotypes might indicate differential requirements of these factors for the stemness maintaining regulatory circuitry. Alternatively, different states of TSCs might exist with differential developmental potential and distinct requirements of transcriptional regulation, in analogy to different states of pluripotency, such as that found in naïve or primed pluripotent stem cells [39, 44].

In the current study, we have analysed the endogenous expression of key stemness-maintaining factors, *Cdx2*, *Eomes*, and *Elf5*, in the chorion of gastrulation stage embryos to characterise TSCs by overlapping marker gene expression. We traced *Eomes* expression through later gastrulation stages and demonstrate that it is lost around E9.5 in the region emanating from the chorionic hinge. Surprisingly, TSC markers consistently show heterogenous, partially nonoverlapping expression in different areas of the late TSC niche, potentially indicating different states of TSCs during placental development. The analysis of TSCs cultured under stemness-maintaining conditions additionally revealed heterogeneous TSC marker expression *in vitro*, underscoring our findings from embryonic analyses in the chorion. To determine the transcriptional state that describes undifferentiated, bona fide TSCs and to monitor transcriptional changes during early TSC differentiation, we used genetic tools to manipulate *Eomes* and *Cdx2* expression in TSC cultures followed by genome wide transcriptional profiling. First, we generated TSCs that harbour an $Eomes^{GFP}$ reporter allele, thereby marking *bona fide* TSCs that were enriched by fluorescence activated cell sorting (FACS) and forced towards differentiation by removal of stemness maintaining conditions. Second, we employed TSCs that allow for the inducible deletion of *Eomes* gene function, and third we used inducible expression of key TSC transcriptional regulators *Cdx2* and *Eomes* in mouse ES (mES) cells for the identification of downstream target genes. Resulting differential expression profiles allow for a detailed description of the TSC signature and the changes during early differentiation, which might be directly or indirectly regulated by a combination of Fgf- and Tgfβ-signalling and the key regulatory factors of TSCs, *Cdx2*, and *Eomes*. We used resulting expression profiles to identify novel candidate TSC marker genes at stemness state. To validate this approach, a handful of differentially expressed genes were selected and tested by qRT-PCRs of bona fide TSCs and during early differentiation. Additionally, expression of novel candidates was analysed in the TSC compartment of postimplantation embryos *by in situ* hybridisation analysis. In summary, this study characterises and describes the expression signature of TSCs within the embryo and in cultured TSCs.

2. Materials and Methods

2.1. Cell Culture. Genetically modified TSCs were isolated from E3.5 blastocysts of animals carrying alleles for $Eomes^{GFP}$ [45], $Eomes^{CA}$ [47], and $R26Cre^{ER}$ [58] according to standard protocols [17]. TSCs cultured in stemness maintaining conditions (SMC) were kept in 70% mouse embryonic fibroblast-(MEF-) conditioned TSC-medium (MCM) supplemented with hrFGF4 and heparin (F4H) on MEFs [17]. For differentiation conditions (DC), TSCs were cultured in TSC-medium without MCM and F4H on gelatinized plates without feeder cells [17]. Cre-mediated excision of the conditional $Eomes^{CA}$ allele was induced by administration of 1 μg/mL

4-hydroxytamoxifen (Sigma Aldrich, H7904) to the culture medium for up to 3 days.

To generate mES cells that inducibly express *Cdx2* or *Eomes* in response to doxycycline administration, we performed inducible cassette exchange (ICE) using A2lox.cre mES cells [59] and the p2lox-V5 vector system using gateway cloning (Invitrogen) [48]. Expression was induced by administration of 1 μg/mL doxycycline (Fargon, 137087) to the ES cell culture medium composed of DMEM (Gibco, 11960), 15% ES cell-qualified FBS (Gibco, 16141), 2 mM L-glutamine (Gibco, 25030), 50 U/mL penicillin/50 μg/mL streptomycin (Gibco, 15070), 0.1 mM nonessential amino acids (Gibco, 11140), 1 mM sodium pyruvate (Gibco, 11360), 0.1 mM β-mercaptoethanol (Sigma Aldrich, M7522), and 1,000 U/mL leukemia inhibitory factor (Merck Millipore, ESG1107).

2.2. Flow Cytometry. Single cell suspensions of *Eomes*^{GFP} TSCs cultured in SMC were FACS-purified for GFP^{high} cells using a MoFlo Legacy cell sorter (Beckman Coulter). Selected cells were reseeded in SMC without MEF feeder cells for 24 h before preparation of the RNA.

2.3. Immunofluorescence Staining of E7.5–E14.5 Tissue Sections. Whole decidua (E6.5–E8.5) or placenta (E10.5–E14.5) was isolated from *Eomes*^{GFP} pregnant females on ice, washed in PBS, and fixed in 4% PFA at 4°C for 1 h (E6.5, E7.5) or 3 h (E8.5–E14.5). Fixed tissues were rinsed in PBS and successively transferred to 15% and 30% sucrose dissolved in PBS until samples no longer floated. Tissues were subsequently incubated in embedding medium (7.5% fish skin gelatin, 15% sucrose) for 1 h at 37°C and snap frozen in liquid nitrogen. Frozen blocks were cut at 8 μm sections on a cryostat (CM3050s, Leica), and sections mounted on SuperFrost Plus slides (R. Langenbrinck, 03-0060). Washing steps, blocking, incubation with primary and secondary antibodies, and DAPI staining were performed as described for immunofluorescence on TSCs.

2.4. Immunofluorescence Staining on TSCs. TSC cultures were grown on coverslips coated with 0.1% gelatin, briefly rinsed in PBS, and fixed in 4% PFA for 30 min on ice. Fixed cells were washed with PBS containing 0.1% Tween-20 (PBS-T), blocked for 1 h in PBS-T with 5% bovine serum albumin (BSA-T), and incubated with primary antibodies (Supplementary Table S1 available online at http://dx.doi.org/10.1155/2015/218518) in 5% BSA-T over night at 4°C. After washing off the primary antibodies, samples were incubated for 45 min at RT with conjugated secondary antibodies (Supplementary Table S1) diluted in 5% BSA-T. Cells were counterstained for 10 min at RT with DAPI diluted 1 : 1000 in PBS and mounted with Fluoromount-G. Fluorescent images were captured on a Zeiss Axiovert 200 M, equipped with a 20x Plan-Apochromat objective. Displayed images were eventually merged and brightness adjusted using Adobe Photoshop CS5 software.

2.5. RNA Preparation for Microarray and Quantitative RT-PCR. Total RNA was purified from TSC and ES cell culture dishes using the RNeasy Mini Kit (QIAGEN, 74104) using 350 μL RLT lysis buffer per 6 cm culture dish. On-column DNaseI digestion was applied and RNA eluted in 50 μL RNase free water, yielding concentrations of 179–1.686 ng/μL RNA.

2.6. Microarray and Analysis of Microarray Data. To identify genes overrepresented in TSCs, gene expression datasets obtained from the microarray were sorted for highest negative (*Eomes*^{GFP} TSC differentiation and *Eomes*^{CA}) or positive (induced *Eomes* or *Cdx2* expression) fold changes. Resulting lists from induced *Eomes* deletion or induced *Cdx2* or *Eomes* expression were additionally filtered for genes that were regulated at least 1.5-fold when compared to respective controls. Only genes with p values ≤ 0.05 were considered for further analyses. Finally, median expression values of mES cell- and TSC-based experimental subsets were calculated for each gene. Gene lists were compared by Venn diagrams using the Manteia data mining system (http://manteia.igbmc.fr/).

2.7. Validation by Quantitative RT-PCR and Statistical Analyses. For reverse transcription, the QIAGEN QuantiTect Reverse Transcription Kit (205311) was used according to the protocol with an input of 1.0 μg RNA per sample. Quantitative PCR was carried out in triplicate from three independent experiments, using the Roche Light Cycler 480 (SN: 1126) detection system and the Light Cycler 480 DNA SYBR Green I Master kit (Roche, 04707516001) and the primers listed in Supplementary Table S2. *36B4* and *βcat* served as reference genes. mRNA expression levels over time were calculated relative to day 0 which was set to 1. Statistical analyses were performed using a two-sided Student's t-test and the standard error of the mean was calculated for each dataset consisting of biological triplicates in technical triplicates each, individually.

2.8. Validation by In Situ Hybridization. Deciduae containing embryos were dissected and fixed in 4% PFAin PBS, dehydrated through ethanol series, and embedded in paraffin before 8 μM sections were prepared on a Leica RM2165 microtome. *In situ* hybridization on paraffin sections was performed according to standard protocols [60] using *Bok/Mtd*-, *Cldn26*-, *Cyp26a1*-, *Duox2*-, *Duoxa2*-, *Eomes*-, *Nr0b1*-, and *Sox21*-specific probes. Eosin counterstaining was performed according to standard protocols [60].

2.9. Animals. All mice were housed in the pathogen-free barrier facility of the University Medical Centre Freiburg in accordance with the institutional guidelines and approval by the regional board.

3. Results

3.1. Bona Fide TSCs Are Marked by Coexpression of Eomes, Cdx2, and Elf5 and Are Lost from the Chorionic Hinge around E9.5. To investigate the spatial and temporal distribution of TSCs during placentogenesis, we performed detailed immunofluorescence (IF) staining using antibodies specific for EOMES, CDX2, and ELF5, in combination with a previously described *Eomes*^{GFP} reporter allele [45]. EOMES protein and the GFP-reporter can be detected in the TSC compartment of the extraembryonic ectoderm (ExE),

in the primitive streak (PS), and in the visceral endoderm (VE) during early gastrulation at E6.5 (Figures 1(a)–1(a″)) [45]. One day later, at E7.5 *Eomes* expression is refined to a subregion of the chorion, which we refer to as the chorionic hinge (ChH), and expression is gradually reduced in the remainder of the chorion (Figure 1(b)). CDX2 colocalizes with EOMES within the chorion at E7.5 but, unlike EOMES, the staining intensity shows no gradual changes and is uniform throughout the entire chorion (Figure 1(b′)). CDX2 is additionally found in the extraembryonic mesoderm of the allantois (Figure 1(b′)). Finally, we stained for expression of *Elf5*, which acts in the transcriptional circuitry that maintains TSC stemness by positive feed-forward regulation of *Eomes* and *Cdx2* expression [25]. Strongest ELF5 staining was detected in the ChH and the distal portion of the ectoplacental cone (EPC) facing the ectoplacental cavity while reduced levels are found throughout the remainder of the chorion and the proximal EPC (Figure 1(c)). At E8.5, EOMES expressing cells are remaining within the tip of the ChH, which is detached from the surrounding tissues, while the central part of the chorion has started to fuse with the allantois and the EPC (Figures 1(d)–1(d″)). EOMES-positive cells are almost entirely lost around E9.5 from the forming placenta (Figures 1(e) and 1(e′)) with only little EOMES staining in a region emanating from the former ChH (Figure 1(e′)). Following E10.5 placental EOMES staining could not be detected, apart from single EOMES positive cells that most likely represent placental natural killer cells (Figures 1(e) and 1(f)) [46]. In summary, these detailed marker analyses suggest that EOMES-positive TSCs remain in the chorionic hinge as the functional stem cell niche of TSCs until E9.5 and are not found at later time points.

3.2. TSCs in Culture Show Heterogeneous Staining for Stemness Factors and Can Be Identified by High Levels of the Eomes^{GFP} Reporter Expression. TSCs can be cultured under conditions of continuous stimulation with Fgf- and Tgfβ- growth factors for extended periods of time and multiple passages [17, 33]. However, TSCs *in vitro* exhibit an eminent tendency towards spontaneous differentiation and in stemness-maintaining conditions about 5–10% of TSCs differentiate towards the trophoblast giant cell fate, indicated early by an increase in nuclear and total cell size. TSC cultures thus intrinsically contain heterogeneous cell types to various degrees. To study the degree of heterogeneity in cultured TSCs, we first investigated the coexpression of TSC markers using antibodies against CDX2, EOMES, and ELF5 in TSCs cultured on feeder layers of mouse embryonic fibroblasts (MEF) in the presence of MEF-conditioned TSC-medium (MCM), human recombinant FGF4 (hrFGF4), and heparin (F4H) (Figures 2(a)–2(c)). Double-IF staining for EOMES and CDX2 showed a surprising degree of mutual staining. Predominantly, cells at the periphery of colonies showed strong CDX2 staining, while only very weak EOMES signal could be observed. These CDX2 positive cells exhibited a markedly enlarged nucleus in comparison to CDX2 and EOMES double positive cells, indicating that they may have differentiated from TSCs that normally present as cells with small nuclei and cell bodies. Colabelling for EOMES and CDX2 (Figure 1(a)), as well as EOMES and ELF5 (Figure 1(b)), and CDX2 and ELF5 (Figure 1(c)) was very consistently found in small cells, likely representing bona fide TSCs. In larger, more differentiated cells, the CDX2 signal is only partially overlapping with EOMES and ELF5 (Figures 1(a) and 1(c)), while ELF5- and EOMES-staining are predominantly overlapping in all cell types (Figure 1(b)).

To allow for the analysis of TSCs that harbour a stemness-indicating reporter gene, we generated TSCs from E3.5 blastocysts carrying the *Eomes*^{GFP} knock-in allele [45]. To characterize resulting *Eomes*^{GFP} TSCs, we compared GFP-reporter expression with α-EOMES antibody staining. *Eomes*^{GFP} reporter and EOMES protein expression widely overlap and highest levels of EOMES protein staining were reflected by strongest reporter activity (Figure 2(d)). As an exception, cells undergoing mitosis loose nuclear EOMES staining, while cytoplasmic GFP expression remains clearly detectable. Highest levels of GFP-reporter expression were found in populations of small cells that morphologically qualify for bona fide TSCs. In summary, our marker analysis in cultured TSCs demonstrates that only the combination of multiple stemness markers allows for unambiguous identification of bona fide TSCs. However, the generation of TSCs carrying the *Eomes*^{GFP} allele is a suitable tool for the isolation of pure populations of undifferentiated TSCs (GFP^{high}) that are characterised by high-level expression of *Eomes*.

3.3. Variable Experimental Setups Delineate the Transcriptional Characteristics of Bona Fide TSCs. Eomes^{GFP} TSCs allow for the enrichment of GFP^{high} cells representing fully undifferentiated and thus bona fide TSCs. These should serve as a suitable source to delineate the transcriptional signature of TSC stemness. *Eomes* maintains TSCs in an undifferentiated state and the genetic deletion of *Eomes* prohibits TSC maintenance and induces differentiation [34, 41]. In reverse, the expression of *Eomes* or *Cdx2* (and other factors) in mES cells initiates the transcriptional programme that induces lineage conversion towards the TSC lineage [3]. To define the transcriptional signature of TSCs in their bona fide stemness state downstream of *Eomes* and *Cdx2*, we thus employed three experimental settings followed by genomewide expression analyses (Figure 3). First, we enriched *Eomes*^{GFP} TSCs for GFP^{high} cells and compared cells under stemness maintaining culture conditions with cells that were differentiated by withdrawal of MCM, F4H, and MEFs by gene expression profiling at daily intervals over a period of three days (Figure 3(a)). In the second approach, we induced Cre-mediated gene deletion in TSCs that homozygously carry an *Eomes* conditional allele in combination with a tamoxifen- (Tx-) inducible Cre-estrogen receptor fusion (*Eomes*$^{CA/CA}$; R26Cre^{ERT}) [47] and monitored gene expression at 24 h intervals for three days (Figure 3(b)). The recombination efficiency was monitored by PCR (Figure 3(b′)) and EOMES levels by Western blot, showing that EOMES protein was almost absent for 24 h after Tx-administration (Figure 3(b″)). Third, to identify genes that are positively regulated by *Eomes* or *Cdx2*, we generated mES cells with inducible overexpression of both transcription factors. mES cells with inducible expression were

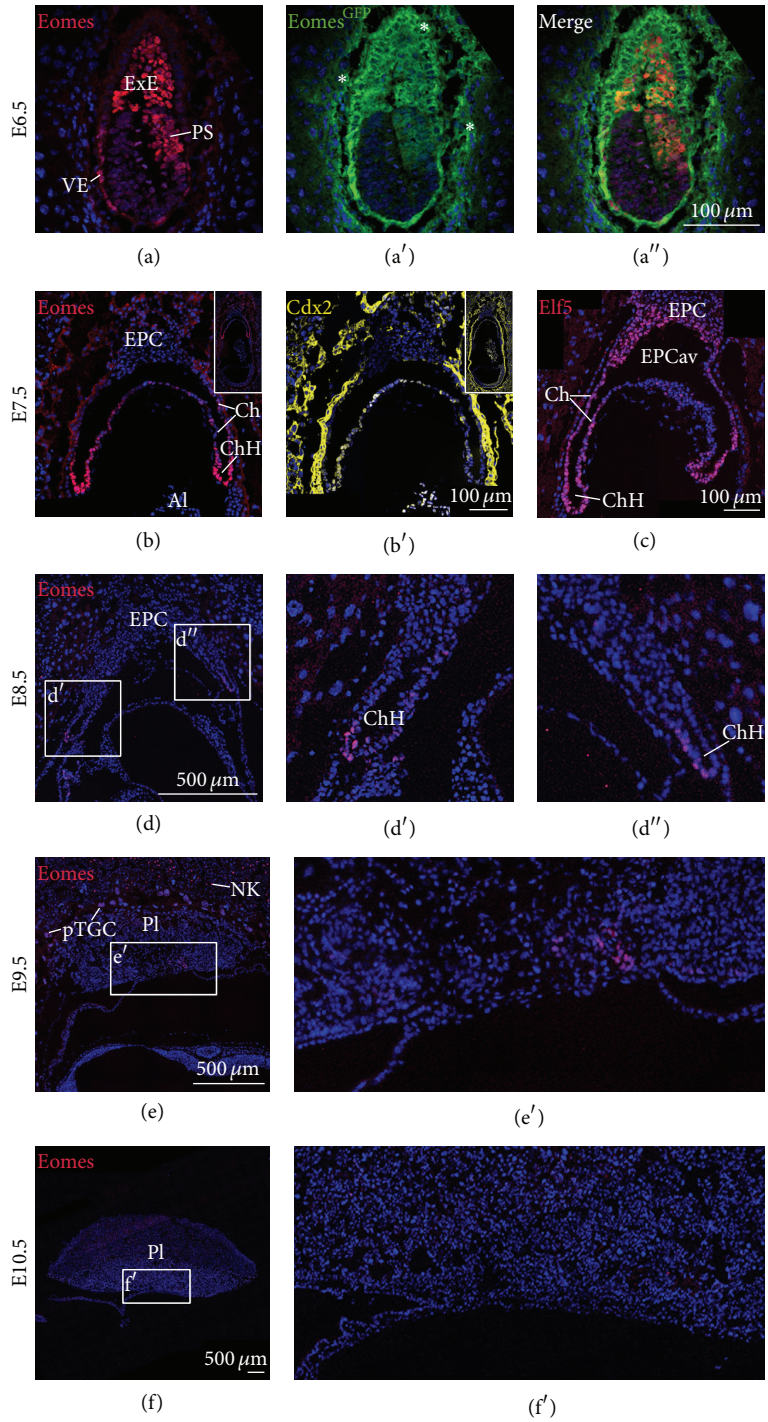

Figure 1: EOMES colocalizes with TSC markers CDX2 and ELF5 in the E7.5 chorionic hinge and expression is lost around E9.5. Immunofluorescence staining shows nuclear EOMES and *Eomes*^{GFP} reporter expression in (a–a″) the visceral endoderm (VE), the primitive streak (PS), and the extraembryonic ectoderm (ExE) at E6.5, (b) within the chorion (Ch) and the chorionic hinge at E7.5, and (d–d″) in the chorion at E8.5. Asterisks in (a′) indicates unspecific signals in extraembryonic tissues. (b and b′) TSC markers EOMES and CDX2 colocalize in cells of the chorion at E7.5. EOMES staining is most prominent in the chorionic hinge and shows a gradient along the chorion, while CDX2 does not show graded reduction along the chorion. (c) ELF5 similarly localizes to the chorion with strongest staining in the chorionic hinge and additionally expands into the ectoplacental cone (EPC) adjacent to the ectoplacental cavity (EPCav). (e, e′) Faint EOMES staining can be detected at E9.5 in the region emanating from the chorionic hinge, and (f, f′) staining is entirely lost at E10.5. (e) EOMES can be additionally found in parietal trophoblast giant cells (pTGC) and natural killer cells (NK) at E9.5. Al, allantois; EPC, ectoplacental cone; EPCav, ectoplacental cavity ExE, extraembryonic ectoderm; Ch, chorion; ChH, chorionic hinge; Pl, placenta; PS, primitive streak; pTGC, parietal trophoblast giant cells VE, visceral endoderm; NK, NK cells.

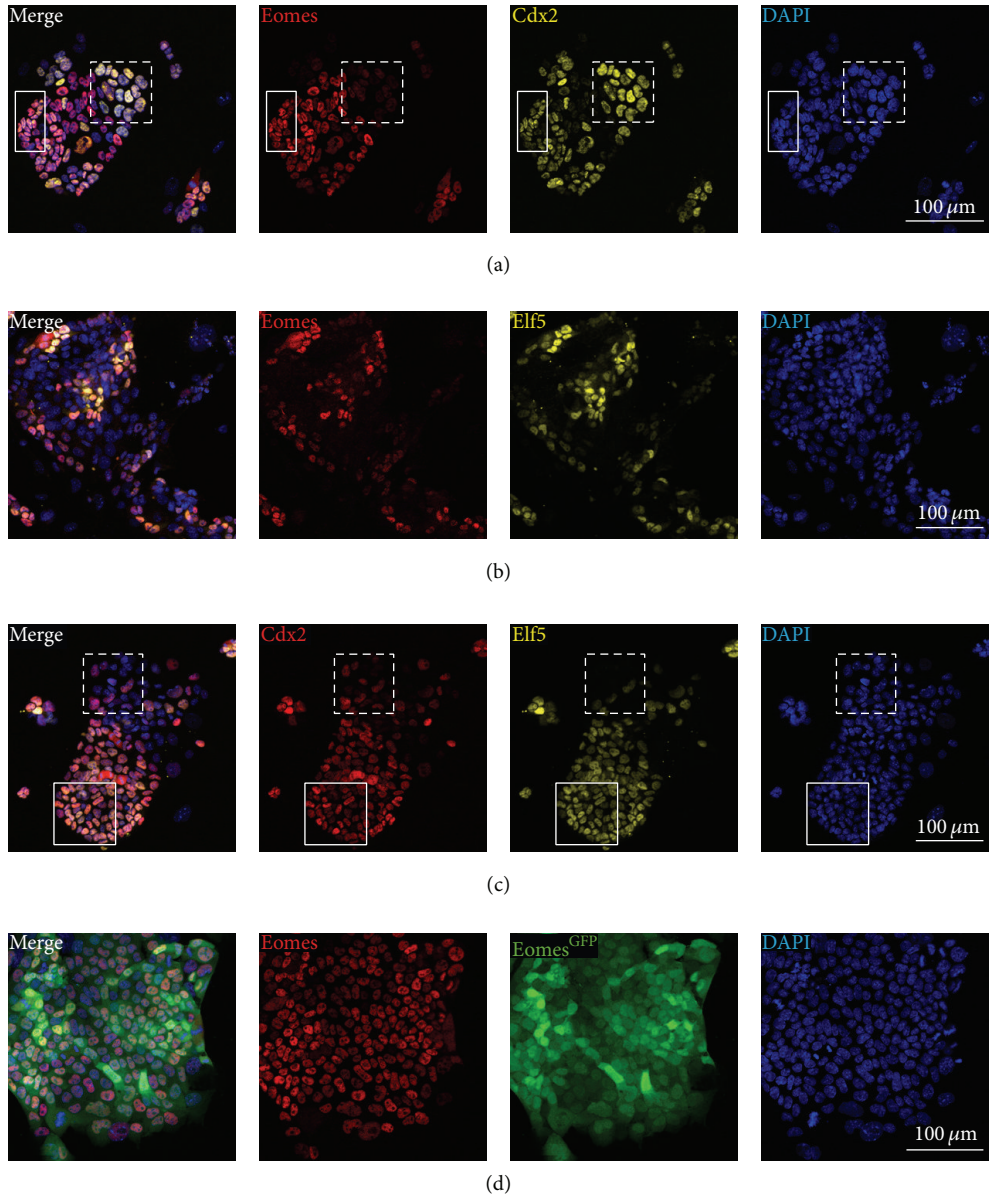

Figure 2: TSCs in culture exhibit heterogeneous patterns of EOMES, CDX2, and ELF5 staining which is recapitulated by *Eomes*^{GFP} reporter expression. Cultured TSCs are colabelled with antibodies against EOMES, CDX2, and ELF5 or the *Eomes*^{GFP} knock-in reporter allele. (a) EOMES staining and CDX2 staining largely overlap in TSCs of small size, which morphologically match undifferentiated TSCs (solid boxed region), but staining diverges in enlarged cells (dashed boxed region). (b) ELF5 and EOMES immunostaining widely labels the same cells, and accordingly (c) ELF5 and CDX2 do not colocalize in enlarged cells ((c), dashed boxed region). (d) EOMES protein levels and *Eomes*^{GFP} reporter expression closely correlate and highest fluorescence intensities are found in cells with strongest EOMES staining.

generated by site-specific introduction of cDNAs including an N-terminal fusion to a V5-tag [48] into the engineered doxycycline-inducible *Hprt* locus of p2lox mES cells using inducible cassette exchange (ICE) [49]. Resulting mES cells allow for temporally regulated and moderate overexpression levels of *Eomes* or *Cdx2* in mES cells as monitored by Western blot (Figures 3(c) and 3(c′)). Expression profiles of mES cells were performed before doxycycline induction and at 24 and 48 h following induced expression to identify the early induced genes downstream of *Eomes* or *Cdx2* that initiate lineage conversion of mES cells towards the TE lineage. All three experimental settings were subsequently used for gene array based transcriptional profiling (see Supplementary Table S3).

3.4. Comparative Expression Profiling Reveals the Transcriptional Signature of TSCs. To reveal the transcriptional signature that constitutes and/or maintains a stable TSC state downstream of the key transcription factors *Eomes* and *Cdx2*, we performed a combined analysis of our independent gene array datasets and identified those genes that showed differential expression in multiple experiments (Figure 4 and

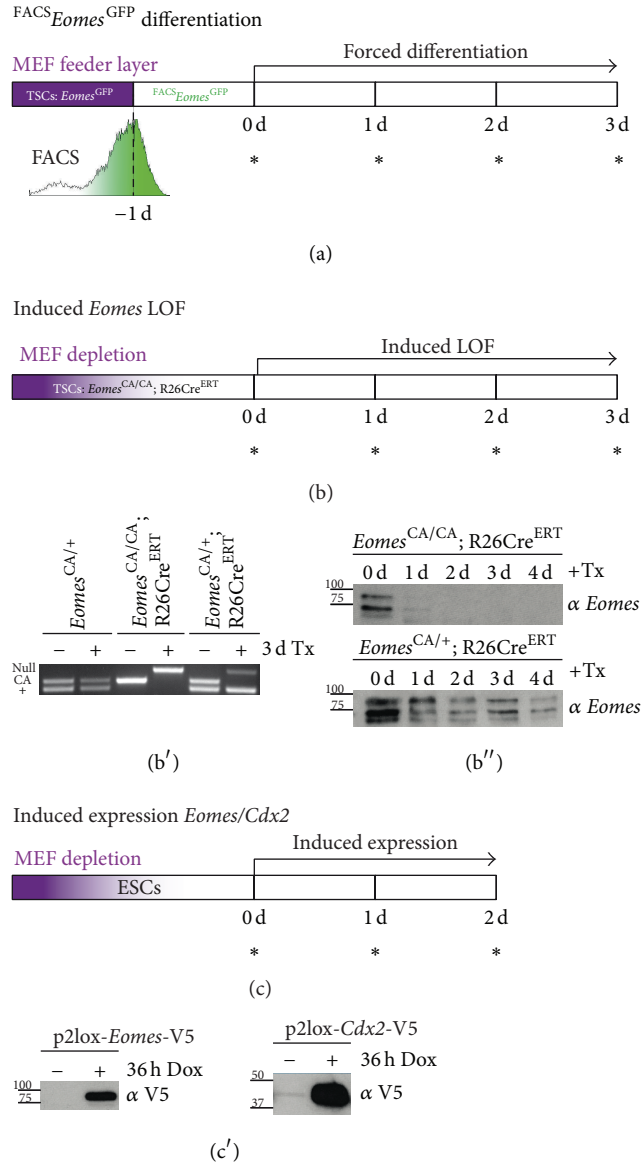

Figure 3: Experimental approaches for the detection and manipulation of the core TSC maintenance factors *Eomes* and *Cdx2*, followed by gene expression profiling. Three complementary experimental approaches were chosen for expression profiling of (a, b) TSCs and (c) mES cells with inducible expression of *Eomes* or *Cdx2*. (a) For the expression profiling of bona fide TSCs and early stages of differentiation, $Eomes^{GFP}$ TSCs were FACS-enriched for GFP^{high} cells and forced towards differentiation by withdrawal of stemness maintaining conditions for 3d. (b) For the identification of *Eomes*-regulated target genes, TSCs harbouring *Eomes* conditional alleles ($Eomes^{CA}$) in combination with a tamoxifen-inducible Cre-estrogen receptor allele ($R26Cre^{ER}$) were used for conditional inactivation *in vitro*. Cells were tamoxifen-treated for 24 h and (b′) Cre-mediated excision was monitored by genotyping PCR, and (b″) presence of EOMES protein was analysed by Western blot. (c) To transcriptionally profile the initiation of *Eomes*- and *Cdx2*-induced target genes during ES cell to TSC conversion, mES cells with doxycycline-regulated expression were induced for 48 h. (c′) The expression of V5-tagged EOMES or CDX2 protein was monitored by Western blot. MEF, mouse embryonic fibroblast; TSC, trophoblast stem cell; asterisks (∗) indicate the different time points of gene expression profiling by gene arrays.

Supplementary Table S4). All experimental interventions resulted in gross changes of differential gene expression that were defined by changes in expression above 1.5-fold with a p value below 0.05 in three biological replicates and a mean level of gene expression above a set background threshold. To identify genes that showed differential expression in multiple experiments, we analysed the intersections of genes that were among (1) the 300 most downregulated genes during differentiation of FACS-enriched $Eomes^{GFP\text{-}high}$ TSCs, (2) the 189 genes that were downregulated following induced *Eomes* deletion, (3) the 300 genes that showed the highest relative expression in TSCs compared to mES cells as assessed by the ratio of median expression values in TSCs to the median expression values in mES cells, (4) the 498 genes that were upregulated in response to induced *Cdx2* expression, and (5) the 147 genes that were upregulated in response to induced

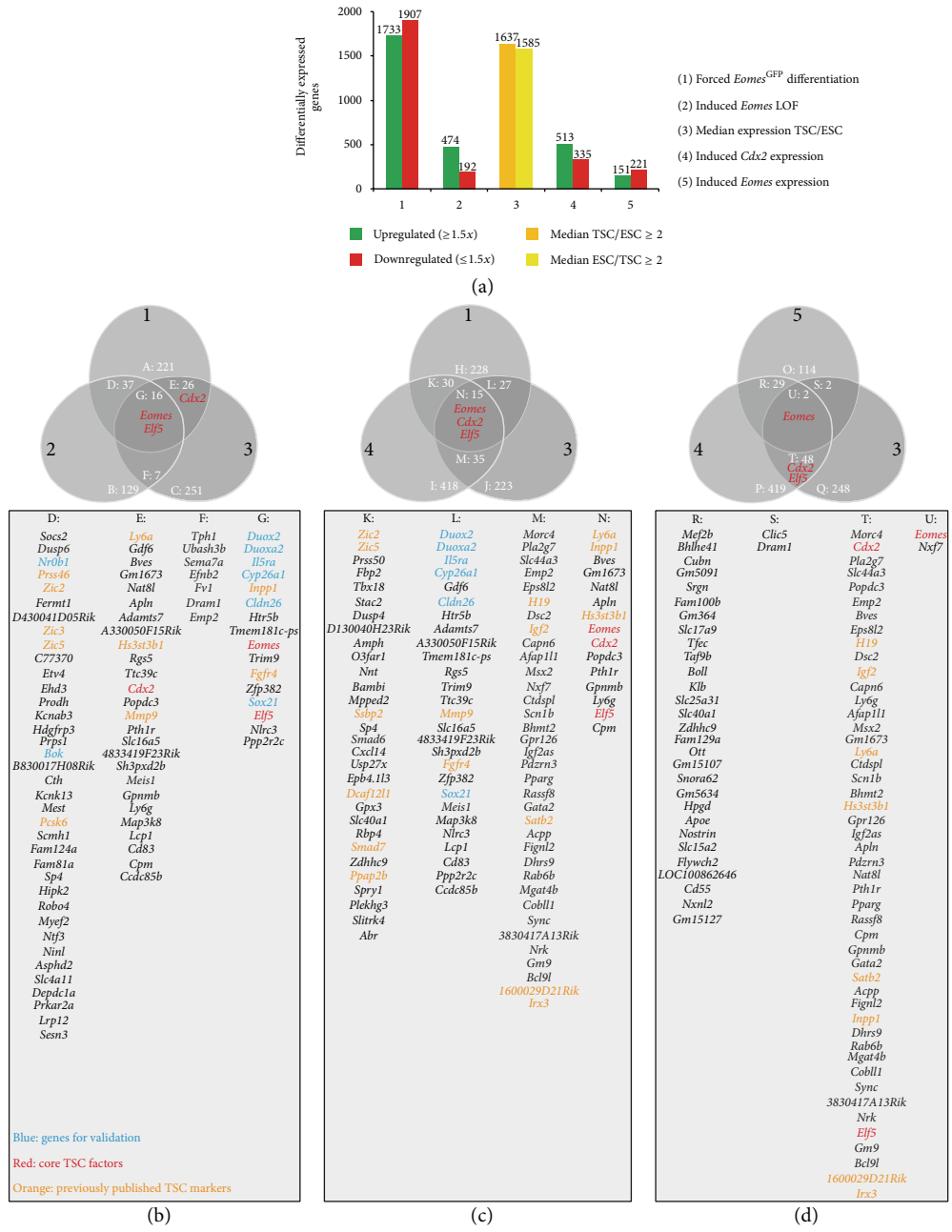

Figure 4: Comparative gene expression analysis reveals candidate TSC marker genes. (a) Genome-wide expression analysis generated five data sets of differentially expressed genes resulting from different experimental settings as shown in Figure 3. (1) The first group contains regulated genes after 3 days of differentiation of *Eomes*$^{\text{GFP-high}}$ FACS-enriched TSCs when compared to undifferentiated *Eomes*$^{\text{GFP-high}}$ TSCs. (2) The second group represents differentially regulated genes 3 days following *Eomes* gene deletion in TSCs (LOF, loss-of-function). (3) The third group comprises genes which show significantly increased or decreased median expression in TSCs versus mES cells, (4, 5) and the fourth and fifth group are differentially expressed genes 2 days after induced expression of *Cdx2* or *Eomes*, respectively. The bar chart indicates numbers of differentially expressed genes for each gene group. (b–d) Venn diagrams indicate groups of intersecting, differentially expressed genes. The genes of resulting groups are listed in the table below each Venn diagram. (b) Comparison between the 300 most strongly downregulated genes in differentiating *Eomes*$^{\text{GFP}}$ FACS-enriched TSCs, the 189 genes downregulated following *Eomes* deletion, and the 300 genes with highest expression ratio between TSCs and mES cells. Of note, *Cdx2*, *Eomes*, and *Elf5* expression levels decrease during TSC differentiation. The loss of *Eomes* function does not significantly reduce *Cdx2* expression after 3d. In (c) the set of differentially regulated genes after *Eomes* gene deletion was exchanged with those 498 genes that were upregulated following *Cdx2*-induction in mES cells. In (d) genes that were induced by *Eomes* or *Cdx2* expression in mES cells were compared to 300 genes with the highest expression ratio in TSCs versus mES cells. Note that *Eomes* is neither significantly upregulating *Elf5* nor *Cdx2* expression. Differences in number of genes listed in (a) and in (b–d) result from genes with multiple transcripts but identical gene symbols. The selected cut-off criteria for genes to be included in datasets were a positive or negative fold change ≥ 1.5 in response to treatment and a p value ≤ 0.05. Genes selected for further analyses are highlighted in blue, core genes of the TSC positive feedback loop in red, and genes that were previously identified as TSC markers in orange.

Eomes expression in mES cells (Figure 4 and Supplementary Table S4). The intersections of differentially expressed genes are represented in Venn diagrams and corresponding groups of genes are listed in tables (Figures 4(b)–4(d) and Supplementary Table S4).

In a first comparative analysis, we investigated the intersection of those genes that were (1) downregulated in differentiating *Eomes*$^{\text{GFP-high}}$ TSCs, (2) downregulated in TSCs following induced deletion of *Eomes*, and (3) presented with a high relative expression in TSCs in comparison to mES cells (Figure 4(b)). 16 genes (group G) matched these criteria and thus were considered candidate *Eomes* target genes, which are lost during differentiation of TSCs. Within this group were the known specific TSC markers, *Elf5,* and *Eomes* itself. Additionally, this group contained novel genes that were not previously described in TSCs, such as *Duox2* and *Duoxa2* or *Cldn26*. *Cdx2* was not included in the intersection, since the deletion of *Eomes* caused only a mild reduction of *Cdx2* within the short time interval of the experiment.

Next, we compared genes that were (1) downregulated during differentiation of *Eomes*$^{\text{GFP-high}}$ TSCs, that were (4) positively regulated by *Cdx2* in mES cells, and that were (3) TSC-specific (Figure 4(c)). The resulting group of 15 genes included *Eomes*, *Elf5*, and *Cdx2* itself.

To compare the early transcriptional changes induced by *Cdx2* or *Eomes* that initiate the conversion of mES cells to TSC-like cells, we analysed the intersecting TSC-specific genes (3) that were upregulated following two days of *Cdx2* (4) or *Eomes* (5) induction (Figure 4(d)). Surprisingly, except for *Eomes*, none of the known TSC factors was significantly upregulated by both *Cdx2* and *Eomes* after two days of induced expression. However, this might reflect the previous observations that *Eomes* is not as effective during the conversion of mES cells to TSCs in comparison to *Cdx2*. While *Cdx2* expression initiates TSC-specific gene expression within 48 hours, including upregulation of *Eomes* and *Elf5, Eomes* expression fails to effectively induce TSC-specific genes within the 2-day interval, despite positive regulation of published *Eomes* targets, such as *Fgf5, Mesp2,* and *Mixl1* [50, 51].

To validate the gene array data of differentially expressed genes, we performed quantitative RT-PCRs for established TSC marker genes and selected genes that were at intersections of differentially regulated genes in more than one experiment. To validate specific expression in bona fide TSCs, we compared expression levels in FACS-enriched *Eomes*$^{\text{GFP-high}}$ TSCs with levels during forced differentiation by removal of stemness maintaining conditions (Figure 5). All tested known and novel TSC marker genes showed highest expression in undifferentiated TSCs and significantly reduced levels following induction of differentiation with changes in expression over a minimum of two magnitudes (Figure 5).

3.5. Novel Marker Genes Label TSCs during Development of the Early Placenta. To generally validate if the approach revealed novel markers for TSCs during embryonic development, candidate genes were further analysed by *in situ* hybridisation

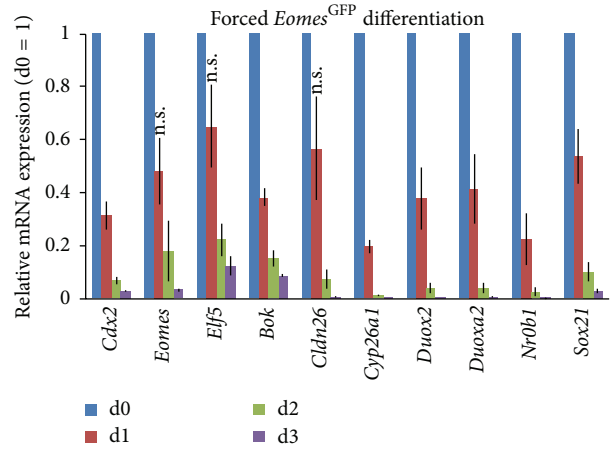

Figure 5: Genes identified by expression arrays and comparative analyses are downregulated during TSC differentiation when validated by qPCR. mRNA expression levels for genes selected by dataset comparisons were quantified at 24 h intervals by qRT-PCR of undifferentiated FACS-enriched *Eomes*$^{\text{GFP-high}}$ TSCs at day 0 (d0) and after forced differentiation for three days (d1–d3). Expression levels are depicted as means of biological triplicates relative to d0, which was set to 1. All genes were significantly (p value ≤ 0.05) downregulated at different time points unless indicated otherwise (n.s., not significant). Error bars indicate the standard error of the mean. p values were calculated according to two-sided Student's t-test. All marker genes show grossly reduced expression during the course of 3 days of differentiation.

using histological sections of E7.5 embryos. We focused on genes with previously unknown functions in the murine TE, such as *Bok/Mtd*, *Duox2*, *Duoxa2*, *Nr0b1*, and *Sox21*. To our knowledge, specific surface markers for TSCs that would allow for antibody-mediated FACS-sorting have not been identified so far. Thus, we additionally analysed expression of the transmembrane protein-coding gene *Cldn26* (*Tmem114*). For *Sox21*, it was shown that it is involved in the regulation of intestinal and pluripotent stem cells and is induced by *Sox2*, an important stem cell factor in both mES cells and TSCs [52, 53]. Accordingly, *Sox21* was also included into the following analysis. Expression of *Cyp26a1* in the trophectoderm was previously described and together with *Eomes* served as a positive control for expression in the chorion. Of the seven tested novel marker genes, six showed expression in entire chorion (*Bok*, *Cldn26*, and *Sox21*) or were more specifically restricted to the chorionic hinge (*Nr0b1*, *Duox2*, and *Duoxa2*) (Figure 6).

In conclusion, the *in situ* hybridisation analysis revealed that the multimodal expression profiling of TSCs in culture serves as a valuable resource for the identification of novel TSC marker genes *in vitro*, but also for TSCs of the developing placenta.

4. Discussion

In the present report we describe a resource for the transcriptional signature of TSCs. We used genetically modified TSCs and mES cells to experimentally interfere with stemness

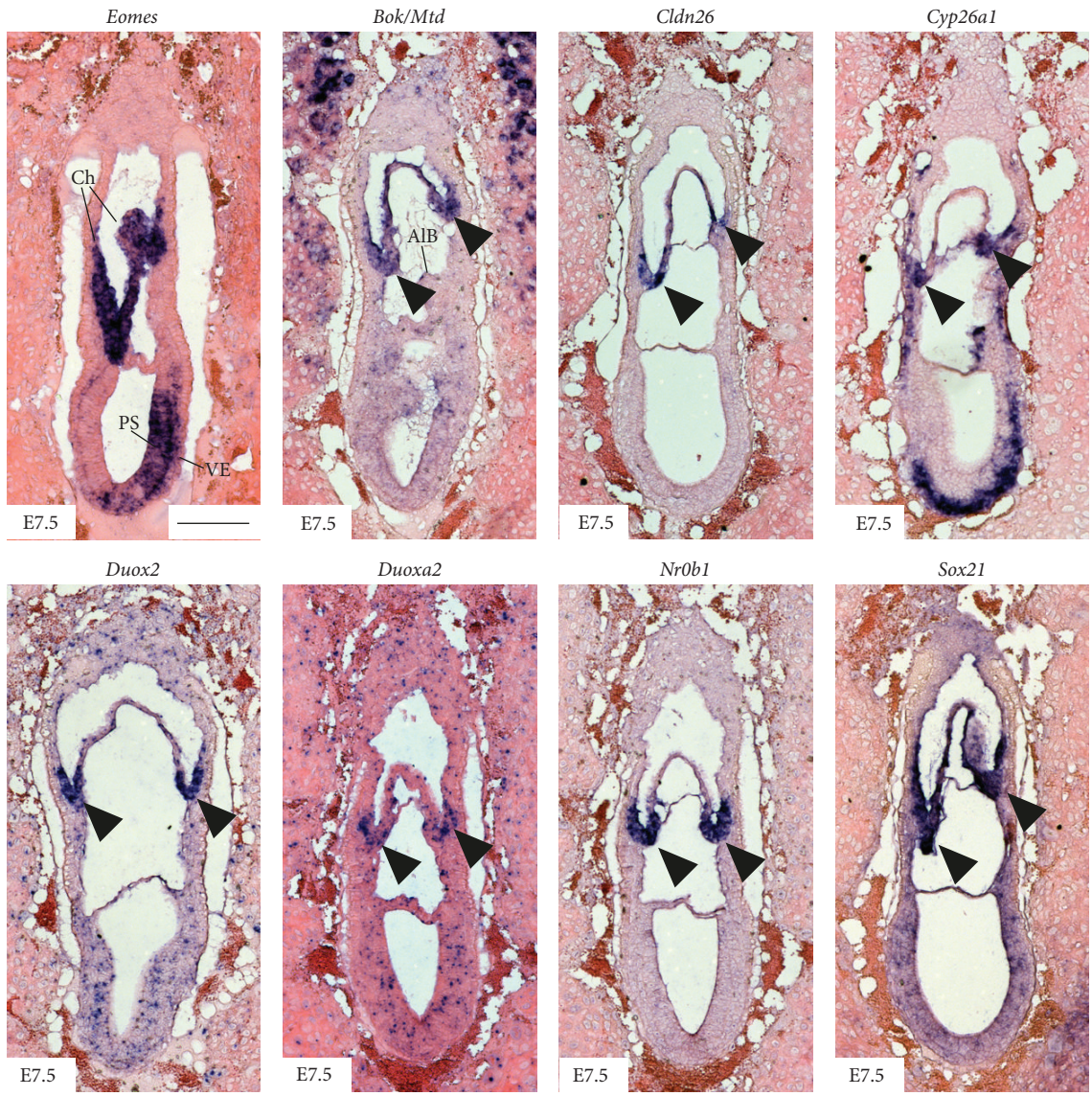

Figure 6: Differentially expressed genes show regional specific expression in the chorion of E7.5 embryos. *In situ* hybridisation analysis on sagittal sections of E7.5 mouse embryos reveals specific expression of *Eomes* as positive control and novel TSC marker genes *Bok/Mtd*, *Cldn26*, *Cyp26a1, Duox2*, *Duoxa2*, *Nr0b1*, and *Sox21*, in the entire chorion, or limited expression in the chorionic hinge (indicated by arrowheads). AlB, allantoic bud; Ch, chorion; PS, primitive streak; VE, visceral endoderm. Scale bar: 200 μM.

maintaining regulation of TSCs downstream of *Eomes* and *Cdx2*, followed by the assessment of transcriptional changes. The combined analysis of expression data resulted in a comprehensive list of candidate TSC marker genes, of which a handful were tested and positively validated for their specific expression in cultured undifferentiated TSCs and in the chorion of the gastrulating embryo. Thus, the presented expression data will serve as a valuable resource for further studies of stemness maintaining regulatory circuitries of TSCs.

Using TSCs that harbour the *Eomes*^{GFP} reporter allele allowed for the purification of GFP^{high} TSCs that by morphology and in their transcriptional signature likely resemble bona fide TSCs without contaminating early differentiating TSCs that are normally found in TSC cultures. Corresponding expression data of GFP^{high} TSCs thus resemble the actual signature of bona fide TSCs, underscored by the rapid, gross, and early changes in gene expression that we found during their differentiation. Expression profiles of TSCs in stemness maintaining conditions and during induced differentiation, either by removal of MCM and F4H or by genetic interference with the TSC regulatory circuitry, were previously reported and had revealed partially overlapping gene lists [53–55]. However, the validation of candidates from our comparative expression analysis identified several additional and novel TSC marker genes. Among those is the transcription factor *Sox21* that is strongly expressed in the chorion of the E7.5 embryo and is downregulated during differentiation of TSCs in culture. Interestingly, it was previously demonstrated that *Sox21* is induced by *Sox2*, and, unlike

Sox2 [53], *Sox21* negatively regulates transcription of *Cdx2* in mES and colon cancer cells [52]. This obvious difference in expression in mES cells and TSCs makes *Sox21* an interesting candidate that, like *Sox2* [53], might act differently in the circuitry of TSC and mES stemness factors. Functions of *Sox21* and other novel candidates in TSC biology and TE development will be addressed in ongoing studies.

The importance of *Cdx2* as lineage determining transcription factor was apparently demonstrated by the ability to convert mES cells to TSCs when overexpressed in mES cells [3], even though more recent studies suggest that this lineage conversion might not be complete at the phenotypic, transcriptional, and epigenetic level [56]. *Eomes* similarly has the capacity to induce TSC fate; however, *Eomes* seems less potent and possibly induces even less complete lineage conversion [3]. This notion is underscored by our datasets, which display more profound transcriptional responses following *Cdx2* in comparison to *Eomes* expression, when induced from the identical doxycycline-inducible locus. This difference might, at least partially, arise from the reduced induction of *Elf5* in *Eomes*-expressing mES cells which is known as a central component of a positive feed-forward regulation of the core TSC circuitry [25].

While both CDX2 and EOMES were previously used as markers for TSCs, coimmunofluorescence staining of cultured TSCs revealed a remarkable heterogeneity of labelling. Only a subset of TSCs that can be morphologically distinguished by a small cell and nucleus size consistently showed colabelling of CDX2 and EOMES, together with ELF5. We suspect that these cells resemble bona fide TSCs. It will require further fate analysis to reveal if the presence of individual key TSC factors primes future fate decisions, similar to lineage specifying roles of key pluripotency factors during embryonic development and in differentiating mES cells [50, 57]. It is noteworthy that EOMES is also detected in parietal trophoblast giant cells (pTGC) (Figure 1(e)) and thus it is tempting to speculate that differentiation towards the trophoblast giant cell lineage might be promoted by EOMES.

The immune-detection of EOMES, CDX2, and ELF5 in the chorion at late gastrulation stages revealed the presence of TSCs until E9.0–E9.5 in the remaining chorion, and the absence of EOMES-positive cells at later stages. These findings are in line with studies by Uy et al. that demonstrated the presence of TSCs that can be isolated and cultured until the 11-somite stage but not afterwards [31]. Another report that used an Eomes::GFP BAC-transgenic reporter [32] detected GFP positive cells in the margins of the E14.5 placenta. However, the nature of these cells was not defined in detail. We were unable to detect similar cells using EOMES-antibody staining. Thus, we conclude that TSCs are indeed only maintained until E9.5 in the remaining portions of the chorion from which they can be isolated as previously reported [31].

In summary, this study contributes to the characterisation of TSCs during early phases of placentogenesis and of TSCs in culture. We demonstrate that TSCs exhibit a remarkable degree of heterogeneity with respect to protein levels of key TSC transcription factors. TSCs are lost around E9.5 from their stem cell niche in the chorion. We used complementary genetic tools of cultured TSCs and ES cells to determine the transcriptional profile of TSCs in their fully undifferentiated and early differentiating state. Comparative analysis revealed several new TSC marker genes. Presented data can be used as a valuable resource for future studies of TSCs and the corresponding transcriptional regulatory network.

Conflict of Interests

The authors declare that there is no conflict of commercial interests.

Authors' Contribution

Sebastian J. Arnold conceived the study, and Georg Kuales and Sebastian J. Arnold performed experiments and analysed the data. Matthias Weiss and Oliver Sedelmeier assisted in and supervised some experiments. Dietmar Pfeifer performed microarray experiments and data analysis. Georg Kuales assembled the figures. Georg Kuales and Sebastian J. Arnold wrote and edited the paper.

Acknowledgments

The authors thank Klaus Geiger for FACS of *Eomes*^{GFP} cells, Marie Follo for supporting the qRT-PCR analysis, Michael Kyba for A2lox ES cells, Hynek Wichterle for the P2lox gateway cloning vector, and Gerd Walz for thoughtful discussion and generous support. This work was supported by an Exploration Grant from the Boehringer Ingelheim Foundation to Sebastian J. Arnold, a project grant (A03) of the Collaborative Research Centre 850 (SFB 850), and the Emmy Noether Programme (AR732/1-1) of the German Research Foundation (DFG) to Sebastian J. Arnold.

References

[1] S. J. Arnold and E. J. Robertson, "Making a commitment: cell lineage allocation and axis patterning in the early mouse embryo," *Nature Reviews Molecular Cell Biology*, vol. 10, no. 2, pp. 91–103, 2009.

[2] M. Zernicka-Goetz, S. A. Morris, and A. W. Bruce, "Making a firm decision: multifaceted regulation of cell fate in the early mouse embryo," *Nature Reviews Genetics*, vol. 10, no. 7, pp. 467–477, 2009.

[3] H. Niwa, Y. Toyooka, D. Shimosato et al., "Interaction between Oct3/4 and Cdx2 determines trophectoderm differentiation," *Cell*, vol. 123, no. 5, pp. 917–929, 2005.

[4] A. Ralston and J. Rossant, "Cdx2 acts downstream of cell polarization to cell-autonomously promote trophectoderm fate in the early mouse embryo," *Developmental Biology*, vol. 313, no. 2, pp. 614–629, 2008.

[5] K. Cockburn and J. Rossant, "Making the blastocyst: lessons from the mouse," *The Journal of Clinical Investigation*, vol. 120, no. 4, pp. 995–1003, 2010.

[6] M. Gasperowicz and D. R. C. Natale, "Establishing three blastocyst lineages-then what?" *Biology of Reproduction*, vol. 84, no. 4, pp. 621–630, 2011.

[7] R. Yagi, M. J. Kohn, I. Karavanova et al., "Transcription factor TEAD4 specifies the trophectoderm lineage at the beginning

of mammalian development," *Development*, vol. 134, no. 21, pp. 3827–3836, 2007.

[8] B. Zhao, X. Wei, W. Li et al., "Inactivation of YAP oncoprotein by the Hippo pathway is involved in cell contact inhibition and tissue growth control," *Genes and Development*, vol. 21, no. 21, pp. 2747–2761, 2007.

[9] M. Ota and H. Sasaki, "Mammalian Tead proteins regulate cell proliferation and contact inhibition as transcriptional mediators of Hippo signaling," *Development*, vol. 135, no. 24, pp. 4059–4069, 2008.

[10] N. Nishioka, S. Yamamoto, H. Kiyonari et al., "Tead4 is required for specification of trophectoderm in pre-implantation mouse embryos," *Mechanisms of Development*, vol. 125, no. 3-4, pp. 270–283, 2008.

[11] N. Nishioka, K.-I. Inoue, K. Adachi et al., "The Hippo signaling pathway components Lats and Yap pattern Tead4 activity to distinguish mouse trophectoderm from inner cell mass," *Developmental Cell*, vol. 16, no. 3, pp. 398–410, 2009.

[12] H. Sasaki, "Mechanisms of trophectoderm fate specification in preimplantation mouse development," *Development Growth and Differentiation*, vol. 52, no. 3, pp. 263–273, 2010.

[13] P. A. Latos and M. Hemberger, "Review: the transcriptional and signalling networks of mouse trophoblast stem cells," *Placenta*, vol. 35, pp. S81–S85, 2014.

[14] T. Rayon, S. Menchero, A. Nieto et al., "Notch and hippo converge on Cdx2 to specify the trophectoderm lineage in the mouse blastocyst," *Developmental Cell*, vol. 30, no. 4, pp. 410–422, 2014.

[15] Z. Cao, T. S. Carey, A. Ganguly, C. A. Wilson, S. Paul, and J. G. Knott, "Transcription factor AP-2 induces early Cdx2 expression and represses HIPPO signaling to specify the trophectoderm lineage," *Development*, vol. 142, no. 9, pp. 1606–1615, 2015.

[16] A. Ralston, B. J. Cox, N. Nishioka et al., "Gata3 regulates trophoblast development downstream of Tead4 and in parallel to Cdx2," *Development*, vol. 137, no. 3, pp. 395–403, 2010.

[17] S. Tanaka, T. Kunath, A.-K. Hadjantonakis, A. Nagy, and J. Rossant, "Promotion to trophoblast stem cell proliferation by FGF4," *Science*, vol. 282, no. 5396, pp. 2072–2075, 1998.

[18] M. Guzman-Ayala, N. Ben-Haim, S. Beck, and D. B. Constam, "Nodal protein processing and fibroblast growth factor 4 synergize to maintain a trophoblast stem cell microenvironment," *Proceedings of the National Academy of Sciences of the United States of America*, vol. 101, no. 44, pp. 15656–15660, 2004.

[19] D. G. Simmons and J. C. Cross, "Determinants of trophoblast lineage and cell subtype specification in the mouse placenta," *Developmental Biology*, vol. 284, no. 1, pp. 12–24, 2005.

[20] R. M. Roberts and S. J. Fisher, "Trophoblast stem cells," *Biology of Reproduction*, vol. 84, no. 3, pp. 412–421, 2011.

[21] D. J. Pearton, R. Broadhurst, M. Donnison, and P. L. Pfeffer, "*Elf5* regulation in the trophectoderm," *Developmental Biology*, vol. 360, no. 2, pp. 343–350, 2011.

[22] Q. Winger, J. Huang, H. J. Auman, M. Lewandoski, and T. Williams, "Analysis of transcription factor AP-2 expression and function during mouse preimplantation development," *Biology of Reproduction*, vol. 75, no. 3, pp. 324–333, 2006.

[23] P. Kuckenberg, S. Buhl, T. Woynecki et al., "The transcription factor TCFAP2C/AP-2γ cooperates with CDX2 to maintain trophectoderm formation," *Molecular and Cellular Biology*, vol. 30, no. 13, pp. 3310–3320, 2010.

[24] M. Donnison, A. Beaton, H. W. Davey, R. Broadhurst, P. L'Huillier, and P. L. Pfeffer, "Loss of the extraembryonic ectoderm in Elf5 mutants leads to defects in embryonic patterning," *Development*, vol. 132, no. 10, pp. 2299–2308, 2005.

[25] R. K. Ng, W. Dean, C. Dawson et al., "Epigenetic restriction of embryonic cell lineage fate by methylation of Elf5," *Nature Cell Biology*, vol. 10, no. 11, pp. 1280–1290, 2008.

[26] F. Wen, J. A. Tynan, G. Cecena et al., "Ets2 is required for trophoblast stem cell self-renewal," *Developmental Biology*, vol. 312, no. 1, pp. 284–299, 2007.

[27] P. Kuckenberg, C. Kubaczka, and H. Schorle, "The role of transcription factor Tcfap2c/TFAP2C in trophectoderm development," *Reproductive BioMedicine Online*, vol. 25, no. 1, pp. 12–20, 2012.

[28] F. Beck, T. Erler, A. Russell, and R. James, "Expression of Cdx-2 in the mouse embryo and placenta: possible role in patterning of the extra-embryonic membranes," *Developmental Dynamics*, vol. 204, no. 3, pp. 219–227, 1995.

[29] J. Luo, R. Sladek, J.-A. Bader, A. Matthyssen, J. Rossant, and V. Giguère, "Placental abnormalities in mouse embryos lacking the orphan nuclear receptor ERR-β," *Nature*, vol. 388, no. 6644, pp. 778–782, 1997.

[30] B. G. Ciruna and J. Rossant, "Expression of the T-box gene Eomesodermin during early mouse development," *Mechanisms of Development*, vol. 81, no. 1-2, pp. 199–203, 1999.

[31] G. D. Uy, K. M. Downs, and R. L. Gardner, "Inhibition of trophoblast stem cell potential in chorionic ectoderm coincides with occlusion of the ectoplacental cavity in the mouse," *Development*, vol. 129, no. 16, pp. 3913–3924, 2002.

[32] G. S. Kwon and A.-K. Hadjantonakis, "Eomes:GFP—a tool for live imaging cells of the trophoblast, primitive streak, and telencephalon in the mouse embryo," *Genesis*, vol. 45, no. 4, pp. 208–217, 2007.

[33] A. Erlebacher, K. A. Price, and L. H. Glimcher, "Maintenance of mouse trophoblast stem cell proliferation by TGF-β/activin," *Developmental Biology*, vol. 275, no. 1, pp. 158–169, 2004.

[34] A. P. Russ, S. Wattler, W. H. Colledge et al., "Eomesodermin is required for mouse trophoblast development and mesoderm formation," *Nature*, vol. 404, no. 6773, pp. 95–99, 2000.

[35] K. Chawiengsaksophak, R. James, V. E. Hammond, F. Köntgen, and F. Beck, "Homeosis and intestinal tumours in Cdx2 mutant mice," *Nature*, vol. 386, no. 6620, pp. 84–87, 1997.

[36] H. J. Auman, T. Nottoli, O. Lakiza, Q. Winger, S. Donaldson, and T. Williams, "Transcription factor AP-2gamma is essential in the extra-embryonic lineages for early postimplantation development," *Development*, vol. 129, no. 11, pp. 2733–2747, 2002.

[37] A. A. Avilion, S. K. Nicolis, L. H. Pevny, L. Perez, N. Vivian, and R. Lovell-Badge, "Multipotent cell lineages in early mouse development depend on SOX2 function," *Genes and Development*, vol. 17, no. 1, pp. 126–140, 2003.

[38] D. Zhu, S. Hölz, E. Metzger et al., "Lysine-specific demethylase 1 regulates differentiation onset and migration of trophoblast stem cells," *Nature Communications*, vol. 5, article 3174, 2014.

[39] M. Hemberger, W. Dean, and W. Reik, "Epigenetic dynamics of stem cells and cell lineage commitment: digging waddington's canal," *Nature Reviews Molecular Cell Biology*, vol. 10, no. 8, pp. 526–537, 2009.

[40] S. Roper and M. Hemberger, "Defining pathways that enforce cell lineage specification in early development and stem cells," *Cell Cycle*, vol. 8, no. 10, pp. 1515–1525, 2009.

[41] D. Strumpf, C.-A. Mao, Y. Yamanaka et al., "Cdx2 is required for correct cell fate specification and differentiation of trophectoderm in the mouse blastocyst," *Development*, vol. 132, no. 9, pp. 2093–2102, 2005.

[42] H. Yamamoto, M. L. Flannery, S. Kupriyanov et al., "Defective trophoblast function in mice with a targeted mutation of Ets2," *Genes and Development*, vol. 12, no. 9, pp. 1315–1326, 1998.

[43] P. Georgiades and J. Rossant, "Ets2 is necessary in trophoblast for normal embryonic anteroposterior axis development," *Development*, vol. 133, no. 6, pp. 1059–1068, 2006.

[44] T. Boroviak and J. Nichols, "The birth of embryonic pluripotency," *Philosophical Transactions of the Royal Society B: Biological Sciences*, vol. 369, no. 1657, 2014.

[45] S. J. Arnold, J. Sugnaseelan, M. Groszer, S. Srinivas, and E. J. Robertson, "Generation and analysis of a mouse line harboring GFP in the Eomes/Tbr2 locus," *Genesis*, vol. 47, no. 11, pp. 775–781, 2009.

[46] S. M. Gordon, J. Chaix, L. J. Rupp et al., "The transcription factors T-bet and Eomes control key checkpoints of natural killer cell maturation," *Immunity*, vol. 36, no. 1, pp. 55–67, 2012.

[47] S. J. Arnold, U. K. Hofmann, E. K. Bikoff, and E. J. Robertson, "Pivotal roles for eomesodermin during axis formation, epithelium-to-mesenchyme transition and endoderm specification in the mouse," *Development*, vol. 135, no. 3, pp. 501–511, 2008.

[48] E. O. Mazzoni, S. Mahony, M. Iacovino et al., "Embryonic stem cell-based mapping of developmental transcriptional programs," *Nature Methods*, vol. 8, no. 12, pp. 1056–1058, 2011.

[49] M. Kyba, R. C. R. Perlingeiro, and G. Q. Daley, "HoxB4 confers definitive lymphoid-myeloid engraftment potential on embryonic stem cell and yolk sac hematopoietic progenitors," *Cell*, vol. 109, no. 1, pp. 29–37, 2002.

[50] A. K. K. Teo, S. J. Arnold, M. W. B. Trotter et al., "Pluripotency factors regulate definitive endoderm specification through eomesodermin," *Genes & Development*, vol. 25, no. 3, pp. 238–250, 2011.

[51] I. Costello, I.-M. Pimeisl, S. Dräger, E. K. Bikoff, E. J. Robertson, and S. J. Arnold, "The T-box transcription factor Eomesodermin acts upstream of Mesp1 to specify cardiac mesoderm during mouse gastrulation," *Nature Cell Biology*, vol. 13, no. 9, pp. 1084–1092, 2011.

[52] A. N. Kuzmichev, S.-K. Kim, A. C. D'Alessio et al., "Sox2 acts through Sox21 to regulate transcription in pluripotent and differentiated cells," *Current Biology*, vol. 22, no. 18, pp. 1705–1710, 2012.

[53] K. Adachi, I. Nikaido, H. Ohta et al., "Context-dependent wiring of Sox2 regulatory networks for self-renewal of embryonic and trophoblast stem cells," *Molecular Cell*, vol. 52, no. 3, pp. 380–392, 2013.

[54] B. L. Kidder and S. Palmer, "Examination of transcriptional networks reveals an important role for TCFAP2C, SMARCA4, and EOMES in trophoblast stem cell maintenance," *Genome Research*, vol. 20, no. 4, pp. 458–472, 2010.

[55] D. J. Pearton, C. S. Smith, E. Redgate, J. van Leeuwen, M. Donnison, and P. L. Pfeffer, "Elf5 counteracts precocious trophoblast differentiation by maintaining Sox2 and 3 and inhibiting Hand1 expression," *Developmental Biology*, vol. 392, no. 2, pp. 344–357, 2014.

[56] F. Cambuli, A. Murray, W. Dean et al., "Epigenetic memory of the first cell fate decision prevents complete ES cell reprogramming into trophoblast," *Nature Communications*, vol. 5, p. 5538, 2014.

[57] M. Thomson, S. J. Liu, L.-N. Zou, Z. Smith, A. Meissner, and S. Ramanathan, "Pluripotency factors in embryonic stem cells regulate differentiation into germ layers," *Cell*, vol. 145, no. 6, pp. 875–889, 2011.

[58] M. Vooijs, J. Jonkers, and A. Berns, "A highly efficient ligand-regulated Cre recombinase mouse line shows that LoxP recombination is position dependent," *EMBO Reports*, vol. 2, no. 4, pp. 292–297, 2001.

[59] M. Iacovino, D. Bosnakovski, H. Fey et al., "Inducible cassette exchange: a rapid and efficient system enabling conditional gene expression in embryonic stem and primary cells," *Stem Cells*, vol. 29, no. 10, pp. 1580–1588, 2011.

[60] A. Nagy, M. Gertsenstein, K. Vintersten, and R. Behringer, *Manipulating the Mouse Embryo: A Laboratory Manual*, Cold Spring Harbor Laboratory Press, 3rd edition, 2003.